G
1046
.C1
N33
v.5

NOAA Atlas NESDIS 10

ATLAS OF SURFACE MARINE DATA 1994 VOLUME 5: ANOMALIES OF MISCELLANEOUS DERIVED QUANTITIES

Washington, D.C.
December 1994

U.S. DEPARTMENT OF COMMERCE
National Oceanic and Atmospheric Administration
National Environmental Satellite, Data, and Information Service

NOAA Atlas NESDIS 10

ATLAS OF SURFACE MARINE DATA 1994 VOLUME 5: ANOMALIES OF MISCELLANEOUS DERIVED QUANTITIES

Arlindo M. da Silva
Christine C. Young
University of Wisconsin-Milwaukee
Department of Geosciences

and

Sydney Levitus
National Oceanographic Data Center
Ocean Climate Laboratory

G
1046
.C1
N33
v.5

LIBRARY
MAY 29 2015
National Oceanic & Atmospheric Administration
U.S. Dept. of Commerce

Washington, D.C.
December 1994

U.S. DEPARTMENT OF COMMERCE
Ronald H. Brown, Secretary

National Oceanic and Atmospheric Administration
D. James Baker, Under Secretary

National Environmental Satellite, Data, and Information Service
Robert S. Winokur, Assistant Administrator

National Oceanographic Data Center
USER SERVICES

Additional copies of this publication, as well as information about NODC data holdings, products, and services, are available on request directly from the NODC. NODC information and data are also available over the Internet through the NODC Home Page on the World Wide Web and the NODC Gopher server.

National Oceanographic Data Center
User Services Branch
NOAA/NESDIS E/OC21
Washington, DC 20235

Telephone: (202) 606-4549

Fax: (202) 606-4586

E-mail: services@nodc.noaa.gov

NODC Home Page: http://www.nodc.noaa.gov/

NODC Gopher server: gopher.nodc.noaa.gov

Contents

Acknowledgements v

Abstract vii

1 Introduction vii

2 Data source and COADS quality control viii

3 Known biases in COADS ix
3.1 Sea surface temperature ix
3.2 Air temperature ix
3.3 Dew point temperature ix
3.4 Wind speed x

4 Bias corrections x
4.1 Wind speed x

5 Parameterizations xi
5.1 Air-sea difference and moisture terms xi
5.2 Stability parameter xi
5.3 Surface atmospheric fluxes xii

6 Computation of monthly statistics and objective analysis xii

7 Results xiii

8 Limitations and shortcomings of the data sets xiv

9 Summary and plans for future work xv

References xvi

10 Sea minus air temperature maps 1
10.1 Seasonal observation density 3
10.2 Decadal observation density 4
10.3 Seasonal climatology 5
10.4 Interannual standard deviation 6
10.5 Seasonal standard deviation 7
10.6 Seasonal anomalies 8

11 Relative humidity maps 53
11.1 Seasonal observation density 55
11.2 Decadal observation density 56
11.3 Seasonal climatology 57
11.4 Interannual standard deviation 58
11.5 Seasonal standard deviation 59
11.6 Seasonal anomalies 60

12 Sea minus air humidity maps 105
12.1 Seasonal observation density 107
12.2 Decadal observation density 108
12.3 Seasonal climatology 109
12.4 Interannual standard deviation 110
12.5 Seasonal standard deviation 111
12.6 Seasonal anomalies 112

13 Sea level specific humidity maps 157
13.1 Seasonal observation density . . . 159
13.2 Decadal observation density . . . 160
13.3 Seasonal climatology . . . 161
13.4 Interannual standard deviation . . . 162
13.5 Seasonal standard deviation . . . 163
13.6 Seasonal anomalies . . . 164

14 Vapor pressure maps 209
14.1 Seasonal observation density . . . 211
14.2 Decadal observation density . . . 212
14.3 Seasonal climatology . . . 213
14.4 Interannual standard deviation . . . 214
14.5 Seasonal standard deviation . . . 215
14.6 Seasonal anomalies . . . 216

15 Zonal heat flux maps 261
15.1 Seasonal observation density . . . 263
15.2 Decadal observation density . . . 264
15.3 Seasonal climatology . . . 265
15.4 Interannual standard deviation . . . 266
15.5 Seasonal standard deviation . . . 267
15.6 Seasonal anomalies . . . 268

16 Meridional heat flux maps 313
16.1 Seasonal observation density . . . 315
16.2 Decadal observation density . . . 316
16.3 Seasonal climatology . . . 317
16.4 Interannual standard deviation . . . 318
16.5 Seasonal standard deviation . . . 319
16.6 Seasonal anomalies . . . 320

17 Z/L (10m/Monin Obukov length) maps 365
17.1 Seasonal observation density . . . 367
17.2 Decadal observation density . . . 368
17.3 Seasonal climatology . . . 369
17.4 Interannual standard deviation . . . 370
17.5 Seasonal standard deviation . . . 371
17.6 Seasonal anomalies . . . 372

Acknowledgments

The work described in this atlas series would not be possible without the phenomenal work of the people in the COADS Project (Slutz *et al.* 1985; Woodruff *et al.* 1987) and the dedicated work of the observers on the many ships of the Voluntary Observing Fleet. We are particularly grateful to Scott Woodruff for long phone conversations and electronic mail messages which helped clarify many questions we had along the way. We also would like to thank Hans-Jörg Isemer for discussions regarding our wind speed correction. Special thanks go to D. Adamec and C. Deser for reviewing the manuscript. Most of the calculations reported here were conducted at the Department of Geosciences of the University of Wisconsin-Milwaukee (UWM). The support of Associate Dean Robert Hall and the UWM Geosciences Faculty is greatly appreciated. This work was concluded after A. da Silva joined the Data Assimilation Office of NASA's Goddard Space Flight Center; the support of R. Rood is acknowledged. At the later stages of this work C. Young has joined Systems Engineering and Security. This research has been supported by NSF grant ATM 9215811 (AMdS/CCY) and by NOAA's Climate and Global Change Program (SL/CCY). The data sets and products represented by this atlas are for distribution internationally, without restriction.

Atlas of Surface Marine Data 1994
Vol. 5: Anomalies of Miscellaneous Derived Quantities

ARLINDO M. DA SILVA AND CHRISTINE C. YOUNG
Department of Geosciences, University of Wisconsin–Milwaukee
AND
SYDNEY LEVITUS
NOAA/National Oceanographic Data Center

Abstract

This atlas presents objectively analyzed fields of surface marine climatology and anomalies of sea minus air temperature, relative humidity, sea level minus air specific humidity, sea level specific humidity, vapor pressure, atmospheric zonal and meridional heat transport at the surface, and a stability parameter (10m/Monin-Obukhov length) over most of the global ocean. These revised monthly mean fields are derived from individual observations in the Comprehensive Ocean-Atmosphere Data Set (COADS) from January 1945 to December 1989 and are analyzed on a 1-degree by 1-degree global grid. Corrections have been made to reduce wind speed bias associated with an erroneous Beaufort equivalent scale. In addition to seasonal anomalies, maps of seasonal climatology, standard deviations, and the number of observations are presented for each quantity.

1 Introduction

The compilation of the Comprehensive Ocean-Atmosphere Data Set (COADS) as documented by Slutz *et al.* (1985) and Woodruff *et al.* (1987) has provided climate researchers with the most complete record of surface marine climate to date. The availability of this data set has contributed significantly to advancing our understanding of the atmosphere-ocean climate system. In addition to observational studies based on COADS, atmospheric and oceanic modelers have relied on this data set for boundary conditions in long-term integrations of atmospheric and oceanic circulation models.

One of the main contributions of the COADS project was to unify several historical data sets in a single, consistent format, and to subject the ship reports to the same quality control procedure. This homogenized data set is available in two forms: as monthly mean summaries in 2 by 2-degree boxes over the global oceans, and as raw individual observations. Due to the massive number of individual ship reports, the majority of researchers have used the monthly mean summaries.

In addition to the directly observed quantities (sea surface temperature, surface air temperature, etc.), COADS monthly mean summaries include a wealth of derived quantities such as moisture and pseudo oceanic fluxes, in which transfer coefficients have been ignored. In an attempt to extend and improve the oceanic fluxes in COADS, a collaborative project between the Department of Geosciences of the University of Wisconsin-Milwaukee (UWM) and the National Oceanographic Data Center/NOAA was initiated. The main goal of this project was to produce high resolution (1-degree by 1-degree), stability dependent heat and momentum fluxes, as well as evaporation, precipitation and radiational fluxes which were absent from the COADS monthly mean summaries. In addition to improved resolution and boundary layer parameterizations, a new scientific Beaufort equivalent scale was developed which reduces wind speed bias and artificial wind speed trends in the post World War II period.

Our revised monthly mean summaries (henceforth referred to as UWM/COADS monthly mean summaries) are available in the form of raw monthly means, standard deviations, and number of observations in 1 by 1-degree boxes over the global oceans, from 1945 to 1989. These raw data are made available for those users desiring to perform their own objective analysis. In addition, the monthly mean fields have

been objectively analyzed with essentially the same successive correction scheme used by Levitus (1982). It is important to note that although the analyzed fields are given with a 1-degree grid spacing, only wavelengths greater than about 770 km remain due to the smoothing effects of the analysis. Climatological half-degree by half-degree analyses have also been produced; these results will be discussed elsewhere.

In this atlas series, we present objectively analyzed seasonal mean anomalies along with climatology, standard deviations, standard error and observation density. In order to conserve space, we show seasonal averaged anomalies computed from the monthly anomalies. This volume documents the anomaly structure of miscellaneous derived quantities for the period 1945–1989. Volume 1 describes all the computations in detail. The directly observed quantities are presented in Volume 2. Volume 3 deals with heat and momentum fluxes at the ocean surface. The buoyancy and fresh water fluxes are presented in Volume 4.

2 Data source and COADS quality control

The primary data source for this study is Release 1 of COADS which covers the period 1854–1979. For the 1980's we rely on an interim data product that preceded COADS Release 1A (recently made available). Release 1A adds more observations to the interim data base and extends it to 1992. This improved data base, which was not available in time for our calculations, will be used in future versions of our analyses.

As described below, our detailed calculations require the consideration of individual ship reports. Product 10 of COADS, the *Compressed Marine Reports* (CMR-5), contains individual reports of surface marine and atmospheric observations from merchant vessels, research vessels, buoys, and bathythermographs (Woodruff *et al.* 1987). The reports in CMR-5 include the following directly reported quantities:

- zonal and meridional wind components
- air temperature
- sea surface temperature
- sea level pressure
- dew point depression
- cloudiness
- present weather

along with quality control indicators which are briefly described next. The interested reader should consult the original COADS documentation (Slutz *et al.* 1985) for a detailed description of the quality control procedure. Note that wind, dew point depression and sea level pressure are not directly observed but rather calculated by ship personnel. When measured, the reported wind speed and direction are computed from the anemometer reading taking in consideration the ship velocity, a procedure that often introduces errors. Dew point depression is computed from the measured dry and wet bulb temperatures. Sea level pressure is computed from the measured pressure with a height correction to reduce it to sea level. WMO Publication No. 47 (e.g., WMO 1990), available yearly since 1955 (in digital form since 1973), lists all the Ships of the Voluntary Observing Fleet along with the ship instrumentation and routes. Kent and Taylor (1991) describes in some detail observing practice by VOS and the instruments they used during the VSOP-NA project (May/88 to September/90).

Quality control in COADS is implemented by means of a multiple step statistical procedure to identify "outliers." The first step is to generate *Decadal Summary Untrimmed Limits* for six variables: sea surface temperature, air temperature, air pressure, zonal wind, meridional wind, and humidity. Sextiles are calculated for each variable in every 2° box for each decade and month. Next, the first, third (the median), and fifth sextiles are averaged across latitude, longitude, month, and decade. Averaging is done for three non-overlapping periods (1854–1909, 1910–1949, 1950–79) in an attempt to separate possible climatic epochs or observational discontinuities. Further smoothing is done for the resulting 216 sets of sextile triplets (6 variables × 3 periods × 12 months). The result is three sets of smoothed lower and upper limits (σ_1, σ_5) around the smoothed mean ($\overline{x}$) for each variable, month, and 2° box. These means and limits are used to create trimming bounds for the variables. A detailed description of the statistical process can be found in Slutz *et al.* (1985), section C. Trimming flags for sea surface temperature, air temperature, humidity, wind and sea level pressure are included in CMR-5 for each observation. Note that trimming does not take into account different methods of observation within the same period, nor were bias corrections applied when the limits were generated.

We have used the COADS/CMR-5 flags to perform quality control on the data used as input to our 1-degree statistics and analysis. Table 1 summarizes the possible values of the quality control flags in COADS/CMR-5. In general, an observation is rejected if it differs from the smoothed median by more

than 3.5 "standard deviations" (flag value equal to 2) or the smoothed limits are not available (flag value equal to -999). However, over the regions climatologically covered by sea ice, this trimming procedure still yields very noisy fields. This is due to the irregular coverage of observations in ice-covered regions in both area and time. In an effort to generate smoother fields in regions where sea ice is common, a more stringent trimming criterion is used. If an observation occurs in a climatologically ice-covered region, the observation is trimmed if it differs from the smoothed median by more than 2.8 "standard deviations" (flag value equal to 1 or 2).

Table 1: Quality control flags in COADS/CMR-5, where x is is an individual observation of the variable under scrutiny, $\overline{x}$ is the smoothed median and σ_1 and σ_5 are the smoothed lower and upper median deviation. See text for details.

Flag Value	Trimming Limits	Trim?
0	$\overline{x} - 2.8\sigma_1 \leq x \leq \overline{x} + 2.8\sigma_5$	no
1	$\overline{x} - 3.5\sigma_1 \leq x < \overline{x} - 2.8\sigma_1$	if obs.
	or $\overline{x} + 2.8\sigma_5 < x \leq \overline{x} + 3.5\sigma_5$	over ice
2	$x < \overline{x} - 3.5\sigma_1$ or $x > \overline{x} + 3.5\sigma_5$	yes
-999	missing	yes

3 Known biases in COADS

The purpose of this section is to discuss some of the known biases and other problems in COADS surface marine reports. In subsequent sections, we describe our bias correction scheme for wind speed.

3.1 Sea surface temperature

Biases in sea surface temperature are associated with different methods of measurements (basically *bucket* and *intake*), which also respond in different ways to atmospheric conditions. On average, measurement with an uninsulated canvas bucket introduces an error of about 0.5°C due to evaporative cooling. Folland and Hsiung (1986) [see also Folland 1991] have developed a physical model for a typical canvas bucket that predicts the amount of evaporative cooling as a function of the atmospheric conditions and exposure time of the bucket. This model has been used effectively to correct the bias in bucket observations (Farmer *et al.* 1989). However, Farmer *et al.* (1989) have used the bucket correction method only for pre-World War II observations. Observations after that time were assumed to be almost exclusively measured by intake or by insulated buckets. This is consistent with the fact that the largest discontinuity in SST due to changes in measurement procedure (approximately one-half degree rise in SST around 1940) took place prior to our analysis period (Bottomley *et al.* 1990, Kushnir 1994).

Recently, the *Voluntary Observing Ships Special Observing Program for the North Atlantic* (VSOP-NA, Kent *et al.* 1993a) has found that observations of SST from insulated buckets and hull contact sensors are reliable. A constant bias of 0.35°C was found in observations from ships' intake thermometers compared to those measured by bucket.

The unreliability of the bucket/intake indicator in COADS and the lack of reliable information about the kind of bucket used make this correction impractical from individual observations. Therefore, we do not include a sea surface temperature correction in this version of our calculations.

3.2 Air temperature

Systematic errors in air temperature are believed to be caused primarily by the heating of the ship superstructure, causing biases of 0.4°–0.8°C in some regions of the tropics (Isemer and Hasse 1987 and references within). In view of this, some authors (Folland *et al.* 1984) have preferred to discard daytime observations. Although night time observations may be adequate to study long term trends in air temperature, we feel that it significantly reduces the number of observations and tends to bias the data toward a generally lower night time temperature.

Kent *et al.* (1993b) devised a method of correction for daytime surface air temperature based on wind speed and the incoming short wave radiation. Preliminary calculations by these authors indicate correcting daytime air temperature results in increases in mean sensible and latent heat fluxes of 3.3 and 1.0 W/m^2, respectively, in the North Atlantic Ocean (Kent and Taylor 1995). We intend to include such a correction in future versions of our data set, but we do not do so at this time.

3.3 Dew point temperature

Biases in dew point temperature are generally associated with contamination of the wet bulb thermometer by salt or insufficient moistening of the wet bulb thermometer wick. These instrumentation problems lead to a systematically higher value of the specific humidity. On average, the dew point temperature is biased about 0.5°C (Isemer and Hasse 1987 and references within). Since this bias is due mainly to human errors for which no record is available, it is very difficult to devise a correction.

Kent *et al.* (1993a) have found that dew point temperature measured by psychrometers were on average lower than those reported from ships using screens. By considering the many factors that might have contributed to this discrepancy, Kent *et al.* (1993a) concluded that psychrometer observations were more reliable and a simple regression equation was devised to correct screen-measured dew point temperatures. Because of inadequate metadata in COADS/CMR-5 (there is no indicator of the method of measurement for dew point temperature) this correction could not be implemented at the present time.

3.4 Wind speed

Because wind is a key parameter for the determination of the air-sea fluxes at the ocean surface, a great deal of effort has been devoted to sort out the problems with ship winds. Wind speeds reported by ships are either directly measured with anemometers or are estimated from the *sea state*. Instrumentation problems with anemometers are believed (or better, assumed) to be non-systematic and are expected to cancel out when spatial/temporal averages are taken. Estimated winds are somewhat subjective and depend on the skill of the observer. But even when a correct identification of the sea state is made, it still needs to be converted to wind speed through a Beaufort equivalent scale.

Since 1946, a Beaufort equivalent scale developed by Simpson (1906), combined with a well defined sea state devised by Petersen (1927), has been used by meteorological weather services (Roll 1965; Isemer and Hasse 1991). This scale is known as Code 1100 and is sometimes referred to as the *old* WMO scale. It is now widely accepted that the old WMO Beaufort equivalent scale results in systematic biases when compared to anemometer measured winds. There are a few alternative Beaufort equivalent scales (WMO 1970; Cardone 1969; Kaufeld 1981), and they all suggest that the old WMO scale underestimates the winds for Beaufort numbers less than about 6 and overestimates winds for Beaufort numbers greater than about 6. As pointed out by Isemer and Hasse (1991), this systematic error causes climatological wind speeds to be underestimated, and climatological wind speed standard deviation to be overestimated in the North Atlantic Ocean. Concerning long term variability, Cardone *et al.* (1990) have shown that a Beaufort scale correction, ship anemometer height adjustment, and stability correction strongly reduce artificial trends in wind speed, and drastically improve the agreement between measured and estimated winds.

Finally, most definitions of transfer coefficients are calibrated to work with winds from a reference level of 10 m above the ocean surface. Cardone *et al.* (1990) suggest that the average ship anemometer height is actually 20 m. Kent *et al.* (1993a) shows that during VSOP-NA a typical anemometer height is in the range 15–20 m, but on modern container ships the anemometer heights are about 30 m. A common approximation is to take the 20 m wind in place of the required 10 m. Since virtually all ship anemometers are higher than 10 m, this approximation introduces a systematic error. Isemer and Hasse (1991) estimated that the 10 m wind speed is on average 93% of the wind speed at 20 m. Calculations by the authors show that for light winds under stable conditions, the surface layer has strong shear and the wind at 10 m can be as low as 40% of the wind speed at 20 m. This result suggests that a careful stability dependent correction is warranted.

The ship type indicator, however, is often incorrect or missing in COADS/CMR-5. This is particularly significant in the 1980's when large numbers of drifting buoys were placed in the southern oceans. We have found that nearly all buoy observations in the COADS/CMR-5 1980's interim product are not identified correctly. The result is that a wind observation measured at 5 m is treated as if it were taken at 20 m. Winds in regions sampled mainly by drifting buoys will be biased toward lower values. This problem has apparently been fixed in COADS Release 1A and the correct identification of buoys will be included in future analyses.

4 Bias corrections

This section documents our bias correction procedures for wind speed. No additional correction is applied to the other directly observed quantities.

4.1 Wind speed

Several scientific Beaufort equivalent scales have been developed to correct WMO Code 1100 (WMO 1970; Cardone 1969; Kaufeld 1981). Data used to generate these scales have mainly been limited to the North Atlantic and North Pacific oceans. In Vol. 1, we have examined the performance of several Beaufort equivalent scales by comparing monthly mean estimated and anemometer measured wind speeds in the Northern Hemisphere oceans. The analysis was conducted for the two decades from 1970 to 1989, a period which has a good mix of estimated and measured wind observations. Taking the wind speed measurement indicator (flag WI in COADS/CMR-5) at face value, all available Beaufort equivalent scales showed climatological biases in at least some part of the wind speed range. This fact prompted the authors to empirically

derive a Beaufort equivalent scale which attempts to reduce the climatological wind speed bias in COADS. After much experimentation we derived a wind speed correction of the form

$$W_{\text{new}} = x_1 W_{\text{old}} + x_2 \sqrt{W_{\text{old}}} \qquad (1)$$

where W_{old} is the WMO Code 1100 speed of the estimated wind and W_{new} is the corrected wind speed. We find that this functional form fits the relationship between measured and estimated winds reasonably well and can also accurately express the other alternative Beaufort equivalent scales. In particular, it is shown in Vol. 1 that this method also produces consistent measured/estimated wind speed standard deviations. It is important to note that the formula above is valid only for individual observations and should not be used to correct monthly mean quantities. The factors x_1 and x_2 were determined for several averaging periods (annual and monthly means), and for several regions of the world oceans by means of a least squares fit. After examining the seasonal/regional sensitivity of the correction, it was concluded that a single set of parameters x_1,x_2 based on Northern Hemisphere January data was sufficient. The chosen values are

$$x_1 = 0.7870, \qquad x_2 = 0.9547. \qquad (2)$$

This choice of parameters gives mean measured/estimated wind speeds with regression slopes within 5% of 1 and standard deviations less than 0.4 m/s (see Vol. 1). Table 2 lists equivalent wind speed for WMO Code 1100 and our new Beaufort equivalent scale. It is important to realize that this new Beaufort equivalent scale produces wind speeds valid at a 20 meter reference level. Whenever 10 meter wind speed is required, the proper conversion from 20 meters should be performed using stability dependent surface layer similarity theory. For additional details on this wind speed correction procedure, the reader is referred to Vol. 1.

Table 2: WMO Code 1100 and the revised Beaufort equivalent scale. The equivalent wind speed is given in m/s.

Beaufort Number	**Equivalent Wind Speed** Code 1100	Revised Scale
0	0	0
1	0.8	1.5
2	2.4	3.4
3	4.3	5.4
4	6.7	7.7
5	9.4	10.4
6	12.3	13.0
7	15.5	16.0
8	18.9	19.0
9	22.6	22.4
10	26.4	25.7
11	30.6	29.3
12	34.9	33.1

5 Parameterizations

This section describes the parameterizations used in the production of the data set. The thermodynamic quantities described below (e.g., specific humidity, vapor pressure, etc.) are computed as in COADS (Slutz *et al.* 1985) using the software documented in Schlatter *et al.* (1981).

Symbols

q	specific humidity (g kg^{-1} or unitless)
q_s	saturation specific humidity at the surface (g kg^{-1})
L	Monin-Obukhov length (m)
T_a	surface air temperature (° C or K)
T_s	sea surface temperature (° C or K)

5.1 Air-sea difference and moisture terms

The air-sea difference terms are ΔT and Δq. These are given by

$$\Delta T = T_s - T_a \qquad (3)$$

$$\Delta q = q_s - q\,. \qquad (4)$$

The saturation specific humidity at the surface, q_s, is calculated based on the sea surface temperature. The value is decreased by 2% to compensate for the lower evaporation rate of salt water: $q_s = 0.98 q_{satur.}(T_s)$. The specific humidity, q, is calculated based on the air temperature and therefore valid at the height of the ship's or buoy's observation platform. The other humidity terms, relative humidity (rh) and vapor pressure (e) are also valid at the height of the observation platform.

5.2 Stability parameter

The stability parameter Z/L is calculated at a 10 m reference level resulting in $Z/L = 10/L$. The complete derivation of Z/L can be found in Volume 1.

5.3 Surface atmospheric fluxes

The surface zonal and meridional transports of atmospheric heat and moisture are estimated along the surface by uT_a, vT_a, uq, and vq. The zonal and meridional wind speed used in these terms, u and v, are corrected as discussed previously and adjusted to a reference height of 10 m. In the calculation of ua and va, the wind components are multiplied by the air temperature measured in Kelvins. In the calculation of zonal and meridional moisture flux, each wind component is multiplied by the specific humidity, measured in grams per gram (yielding units of m/s). Notice that (uq,vq) is not the vertical flux of moisture and therefore is not sufficient to quantitatively close the atmospheric moisture budget and provide a check on E-P. However, at the tropics the surface moisture divergence can be used to qualitatively assess the patterns of E-P.

6 Computation of monthly statistics and objective analysis

The raw monthly fields are computed from the individual observations in the following manner:

1. The world oceans are divided into boxes with constant grid spacing in latitude and longitude. The grid we consider here is 1-degree latitude by 1-degree longitude (the same as Levitus [1982]).

2. All available (quality controlled) observations are averaged in each box for each month during the 45 year period, and the standard deviation and number of observations recorded. Bias corrections, if applicable, are made to each individual observation before averaging.

The raw monthly mean fields are then objectively analyzed to filter out spatial noise and interpolate to gridpoints where data are missing. The objective analysis scheme used is essentially the same scheme described by Levitus (1982). This is an iterative difference-correction scheme (Cressman 1959) with a weight function developed by Barnes (1964). The procedure can be summarized as follows:

1. Determine a first guess F (see below).

2. Compute the difference between the raw observed data (O) and the first guess (F),

$$Q_{ij} = O_{ij} - F_{ij},$$

at grid point (i, j).

3. Compute the smoothed analysis increments

$$C_{ij} = \frac{\sum_{s=1}^{n} W_s Q_{i_s,j_s}}{\sum_{s=1}^{n} W_s} \tag{5}$$

where W_s is the Barnes weight function: $W_s = \exp(-4r^2R^{-2})$ for $r \leq \mathcal{R}$ where r is the distance between the sth gridpoint (i_s, j_s) and the analysis gridpoint (i, j). The sum on the RHS is over the region of influence, i.e., those points that are at a distance less than $\mathcal{R}$, the radius of influence.

4. Update the first guess

$$F_{ij} := F_{ij} + C_{ij}\,. \tag{6}$$

5. Apply a 5–point nonlinear median filter to F_{ij} (Beaton and Tukey 1974; Rabiner *et al.* 1975) followed by two passes of a 5–point linear filter (Shapiro 1970). It was found that this combination effectively filters out noise with scales of the mesh-size. The two filters are applied as follows:

   (a) Non-linear. The smoothed value at the grid point (i, j) is simply the *median* value of the nine grid points in the 3 by 3 box centered at the grid point (i, j). The filter is not applied to grid points located over or adjacent to land. The median filter is used to remove noise from the data while preserving sharp gradients (Reynolds 1988; Rabiner *et al.* 1975).

   (b) Linear. The smoothed value S_{ij} at grid point (i, j) of a grid G is

$$\begin{aligned} S_{ij} &= G_{ij} + \frac{\alpha}{4}(G_{i-1,j} + G_{i+1,j} \\ &+ G_{i,j-1} + G_{i,j+1} - 4G_{ij}) \end{aligned}$$

   where α is a smoothing parameter. Two passes of the Shapiro filter are performed with $\alpha = 0.5$ for the first pass and $\alpha = -0.5$ for the second pass. The second pass is intended to restore the amplitude of the large scales which were slightly damped in the first pass (Shapiro 1970). The filter is not applied to the grid point if it is located over land or if any of the four adjacent grid points (north, south, east, and west) are located over land.

6. Repeat steps 2–5 with a different radius of influence R.

The radius of influence is decreased with each pass in order to analyze smaller scale features with each

successive iteration (Cressman 1959). In practice, the smallest wavelengths are noisy. Therefore, the smallest radius of influence needs to be at least seven to eight times the average separation distance (Levitus 1982). The smallest radius of influence we use, 771 km, is over seven times the average separation distance of a 1- by 1-degree grid.

For climatologies and anomalies, 4 passes of the analysis scheme are performed with radii of influence equal to 1541 km, 1211 km, 881 km, and 771 km, as in Levitus (1982). These radii correspond to 14°, 11°, 8°, and 7° in latitude and longitude at the Equator. At 60° latitude North or South, the radii correspond to 28°, 22°, 16°, and 14° longitude. Below 40°S only the first two passes of the analysis are used in an effort to smooth the noisy data in these latitudes. The standard deviation and standard error fields are also noisy. In order to smooth them sufficiently, only two passes of the analysis are applied to those fields, using the two largest radii.

Table 3: Response function for objective analysis with and without linear Shapiro filter.

wavelength	no filter	with filter	
(km)	4 passes	4 passes	2 passes
3300	1.00	1.01	0.90
2640	0.99	1.00	0.77
2200	0.97	0.98	0.65
1980	0.95	0.95	0.56
1650	0.87	0.88	0.36
1320	0.70	0.69	0.14
1100	0.49	0.49	0.07
990	0.37	0.36	0.04
880	0.23	0.22	0.01
660	0.05	0.05	0.01
550	0.02	0.02	0.01

The response function for the objective analysis using four passes with radii of 1541, 1211, 881, and 771 km, but without any linear or nonlinear filter, is given in the second column of Table 3 (from Levitus 1982). As expected, the short wavelengths are damped severely while the intermediate and longer wavelengths receive moderate and little damping, respectively. Table 3 also shows the response function of the analysis including the linear filter, for both four passes and two passes of the analysis. Notice that the damping is much greater for all but the smallest wavelengths with two passes of the analysis compared to that with four passes. For extremely long wavelengths (not shown), the damping from two passes of the analysis is nearly identical to the damping from four passes.

Finally, the first guess for the analysis depends on the kind of data being analyzed:

Annual Mean Climatology:
Individual raw monthly means are averaged to produce the raw monthly mean climatologies. These monthly climatologies are averaged to produce the raw annual climatology. The first guess for the annual climatology analysis is the zonal average for the individual ocean basins, following Levitus (1982).

Monthly Mean Climatologies:
The first guess for the analysis of a raw monthly climatology is the analyzed annual mean climatology.

Monthly Mean Anomalies:
From the observed raw monthly mean fields, the monthly mean analyzed climatology is subtracted to produce observed *raw* anomalies. A zero field is used as first guess in the analysis scheme.

Monthly Standard Deviation/Error:
The first guess for the analysis of the raw monthly standard deviation or standard error is the zonal average for the individual ocean basins.

7 Results

Table 4 lists the eight derived quantities presented in this volume. Although all the analyses have been performed globally, in order to conserve space we only present maps from 40°S to 80°N, eliminating the less observed and noisier Southern and Arctic oceans. For each quantity the following information is displayed:

Seasonal density of observations:
These maps document the average data coverage for each season, clearly indicating the well traveled shipping lanes. The density of observations η is defined as the mean number of observations per month per 1°× 1° box. The size of each black square is related to the value of η in each 5°box (see scale on top of page).

Decadal density of observations:
These maps document the increase in data coverage in the last 3 decades. The density of observations η is defined as the mean number of observations per month per 1°× 1° box. The size of each black square is related to the value of η in each 5°box (see scale on top of page). A much more detailed description of the data coverage evolution in the period 1945-89 can be

Table 4: Derived quantities presented in this atlas.

Parameter	Description	Units
dT	sea minus air temperature	°C
rh	relative humidity	%
dq	qs minus q	g/kg
qs	surface saturation specific humidity	g/kg
e	vapor pressure	hPa
ua	zonal heat flux	K m/s
va	meridional heat flux	K m/s
Z/L	stability parameter	none

found in Young *et al.* (1993) where the location of each sea surface temperature observation is displayed for each month from January/45 to December/89.

Seasonal climatology:
Computed from monthly mean analyzed climatology. Units are given in Table 4.

Seasonal interannual standard deviation:
Computed from the analyzed monthly anomalies and averaged seasonally. The interannual standard deviation for a 1° × 1° box for a particular month is given by

$$\sigma_{\text{int}} = \sqrt{\frac{\sum_{y=1}^{N}(a_y)^2}{N-1}} \qquad (7)$$

where a_y is the anomaly value for year number y and N is the total number of years (45 in this case).

Seasonal standard deviation:
The total standard deviation for a month in a single 1° × 1° box with more than one observation is given by

$$\sigma = \sqrt{\frac{\sum_{i=1}^{n}(x_i - \bar{x})^2}{n-1}} \qquad (8)$$

where x_i is the value for observation number i during the desired month and $\bar{x}$ is the average of all x_i's for that particular month. The total number of observations over the 45–year period for that month and box is n. The *seasonal standard deviation* fields are computed by objectively analyzing these total standard deviation fields for each month and then averaging seasonally. Units are given in Table 4.

Seasonal anomalies:
Computed from analyzed monthly mean anomalies. The anomalies are computed from the analyzed 45-year climatology for each month. Units are given in Table 4.

The contour interval ("ci" for short) along with units and season information (DJF for December-January-February, MAM for March-April-May, etc.) are displayed in a box on the continent of Asia for each map.

A detailed exposition of the spatial and temporal structure of the anomaly fields is beyond the scope of this atlas. In particular, study of the impact of our bias corrections and comparison with other authors is underway and will be reported elsewhere. Several other projects are in progress to document the decadal/interannual variability of the atmosphere-ocean system which in turn will provide guidance regarding the quality of the data set and hopefully point to ways to improve it in future releases. The maps presented here are intended to serve as a reference for researchers engaged in observational or modeling studies using our revised data sets.

8 Limitations and shortcomings of the data sets

A description of surface marine data sets could not be complete without a discussion of the remaining problems and limitations for which solutions may never be found. Because ship reports are probably the only comprehensive observational record available of the surface marine climate, this data source will undoubtedly continue to be used in studies of the ocean-atmosphere system. As large uncertainties are present, it is imperative that researchers remember that an analysis of surface marine data is an evolving process. Continual improvement will be necessary as more data or metadata become available, physical parameterizations are improved, and advances in data assimilation techniques become available. The corrections we have reported here are, at best, a step in the right direction, but much remains to be done. In the remainder of this section, we discuss some of the remaining problems. This list is by no means exhaustive.

The first, and most uncontrollable, errors exist in the ship reports themselves. Marine and atmospheric measurement techniques and the recording of these observations are not perfect. Some errors are introduced through poor instrumentation. Surface air temperature can be biased due to heating of a ship's superstructure during the day and inadequate shelter ventilation (Isemer and Hasse 1987; Ramage 1984; Kent *et al.* 1993a,b). Sea surface temperature observations taken via ship intake will be biased compared to those taken by insulated bucket or hull sensors.

Many of the biases are impossible to correct due to the lack of instrumentation information as discussed in section 3. A proper homogenization of the measured wind speeds requires the knowledge of the precise anemometer height information which is not included in COADS/CMR-5 at the present time; an average anemometer height of 20 m has been assumed in our calculations. In addition, the flag WI in COADS/CMR-5, which allows the discrimination between measured and estimated winds, is not reliable (Slutz *et al.* 1985, Cardone *et al.* 1990). Our wind speed bias correction procedure takes the WI flag at face value and consequently is affected by this uncertainty. Any systematic bias in the anemometer winds remains to be evaluated.

Even when an observation is considered accurate and unbiased, the recording stage may result in errors (Slutz *et al.* 1985). Some observations are taken in different units (such as Fahrenheit vs. Celsius) without documentation. Coding practices change but are not implemented by all observers on the same date. Ship positions may be erroneous. The transfer of written records to digital form can also introduce error. Some recording errors were repaired by the compilers of COADS, but some miscoded errors undoubtedly remain. The tendency for ships to avoid stormy weather also introduces a fair weather bias into the observations when considered as a whole, although this bias is less problematic in the tropics.

After we deal with the correctable biases and calculate raw fields, error can be introduced by the analysis scheme as well. One problem with the successive correction method used in our analysis is the introduction of unrealistic features (Levitus 1982). Objective analysis of the sort used here fills in the gaps by interpolating/extrapolating smoothed data from remote regions, but cannot compensate entirely for poor sampling. This effect is particularly troublesome in the tropics and southern oceans where observations are clumped along ship tracks with data void areas in between. As a result, bull's eye type features often remain in analyzed fields, particularly in anomaly fields.

The analysis of anomaly values rather than the observed data can result in spurious extrema. For example, the analysis has problems handling positive definite quantities such as fractional cloud cover which only take values between 0 and 1. The analysis procedure can produce full field values (climatology plus anomalies) less than 0 in broad clear areas or values greater than 1 in broad overcast regions. The climatology fields in the data set have been corrected so that positive definite quantities (cloudiness, relative and specific humidity, vapor pressure, precipitation, etc.) have a minimum value of zero. Maximum limits have not been applied to the climatology, however, nor have the full field values been corrected to their valid ranges. The only additional correction made to the anomaly fields was to force the 45-year mean monthly anomaly to equal zero at each grid point.

It should always be kept in mind that although the analyzed fields are given on a $1° \times 1°$ grid, only features with wavelength greater than 770 km (1300 km or greater for regions below 40°S and for standard deviation fields) are retained. The reader is referred to Levitus (1982) or Daley (1991) for additional discussions of the limitations of the objective analysis technique. A higher resolution climatological analysis has been performed on a half-degree by half-degree grid where features with wavelength greater than 386 km are retained. These results will be presented elsewhere.

In contrast to our analysis method, modern data assimilation techniques are assisted by some sort of dynamic constraint: a model is used to provide a first guess for the analysis or to ensure a proper balance of the analyzed fields (Daley 1991). In this first version of our analysis, we concentrated on bias corrections and calculations from individual observations, using a successive correction method to grid the data. Current four dimensional atmospheric reanalysis efforts (Schubert *et al.* 1993; Kalnay and Jenne 1991; Bengtsson and Shukla 1988) will provide several estimates of surface marine fields which would prove useful to validate and assess the limitations of our approach. We are also making available the raw, unanalyzed fields to allow researchers to develop their own objective analyses/data assimilation system from the monthly mean data.

9 Summary and plans for future work

We have described the results of a collaborative project between the Department of Geosciences of the University of Wisconsin-Milwaukee and the National Oceanographic Data Center to produce high resolution analyses of surface marine fields for climate variability studies. Our work is based on individual surface marine reports prepared by the COADS project (Slutz *et al.* 1985). We have corrected wind speed and cloudiness biases in the original COADS reports and produced monthly means and other statistics on 1° boxes over the global oceans. Although we have attempted to create objectively analyzed fields that can be used as is, we have documented several shortcomings and limitations of the data sets which we hope will be taken into consideration by the careful researcher. Analyzed fields of this sort are es-

timates of the *true* surface marine climate, and we hope to improve these estimates by inclusion of additional data/metadata and overall improvements in our analysis system.

An immediate improvement concerns the use of COADS Release 1A (COADS/1A) which was not available at the time of this calculation. For the 1980's, our analysis is based on the so-called *interim* product. COADS/1A includes several delayed ship and buoy sources in the 1980's, and other sources not included in the interim product. COADS/1A contains more elaborate duplicate elimination, some corrections to the data, and more quality control flags. Furthermore, COADS/1A adopts a more complete report format including ship ID call sign, buoy number and identification of platform type whenever feasible (S. Woodruff, personal communication). All these extra data and metadata should improve our analysis significantly. In addition, the dew point and air temperature corrections proposed by Kent *et al.* (1993a,b) will be implemented, as metadata permit.

Ultimately, the use of these data to address scientific issues in the dynamics of the ocean-atmosphere climate system will establish the strengths and weaknesses of the data sets and hopefully provide clues for further improvements. For this reason, and to ensure the widest possible distribution, the objective analyses as well as the raw monthly means on which they are based are being made available internationally, without restriction, on various magnetic media as well as CD-ROM.

References

Barnes, S. L., 1964: A technique for maximizing details in numerical weather map analysis. *J. Appl. Meteor.*, **3**, 396–409.

Beaton, A. E., and J. W. Tukey, 1974: The fitting of power series, meaning polynomials, illustrated on band-spectroscopic data. *Technometrics*, **16**, 147–185.

Bengtsson, L., and J. Shukla, 1988: Integration of space and in situ observations to study global climate change. *Bull. Amer. Meteor. Soc.*, **69**, 1130–1143.

Bottomley, M., C. K. Follund, J. Hsiung, R. E. Newell and D. E. Parker, 1990: *Global Ocean Surface Temperature Atlas.* Joint Meteorol. Off./Mass. Inst. Techno. Proj., supported by U. S. Dept. of Energy, U. S. Natl. Sci. Found., and U. S. Off. of Nav. Res., funded by U. K. Depts. of Energy and Environ., Her Majesty's Stationery Office, London, 20 pp., 313 plates.

Cardone, V. J., 1969: Specification of the wind distribution in the marine boundary layer for wave forecasting. Report TR69-1, New York University, New York, NY, 131 pp. [NTIS AD 702 490].

Cardone, V. J., J. G. Greenwood and M. Cane, 1990: On trends in historical marine wind data. *J. Climate*, **3**, 113–127.

Cressman, G. P., 1959: An operational objective analysis scheme. *Mon. Wea. Rev.*, **87**, 329–340.

Daley, R., 1991: *Atmospheric Data Analysis.* Cambridge University Press, Cambridge, 457pp.

Farmer, G., T. M. L. Wigley, P. D. Jones and M. Salmon, 1989: Documenting and explaining recent global-mean temperature changes. *Final Report to Natural Environment Research Council.*, Climate Research Unit, University of East Anglia, U. K.

Folland, C. K., 1991: Sea temperature bucket models used to correct historical SST data in the Meteorological Office. Climate Research Technical Note No. 14, British Meteorological Office, England.

Folland, C. K., and J. Hsiung, 1986: Correction of seasonally varying biases in uninsulated bucket sea surface temperature data using a physical model. Met. Office Synoptic Climatology Branch Memo No. 154.

Folland, C. K., D. E. Parker and F. E. Kates, 1984: World wide marine temperature fluctuations 1856–1981. *Nature*, **310**, 670–673.

Isemer, H.-J. and L. Hasse, 1987: *The Bunker Atlas of the North Atlantic Ocean. Vol. 2: Air–sea interactions.* Springer Verlag, 252 pp.

———, 1991: The scientific Beaufort equivalent scale: Effects on wind statistics and climatological air–sea flux estimates in the North Atlantic ocean. *J. Climate*, **4**, 819–836.

Kalnay, E., and R. Jenne, 1991: Summary of the NMC/NCAR reanalysis workshop of April 1991. *Bull. Amer. Meteor. Soc.*, **72**, 1897–1904.

Kaufeld, L., 1981: The development of a new Beaufort equivalent scale. *Meteor. Rundsch.*, **34**, 17–23.

Kent, E. C. and P. K. Taylor, 1991: Ships observing marine climate: a catalogue of the Voluntary Observing Ships Participating in the VSOP-NA. *Marine and Oceanographic Activities Report 25*, WMO, Geneva, 123pp.

Kent, E. C. and P. K. Taylor, 1995: A comparison of heat flux estimates for the North Atlantic ocean. *J. Phys. Oceanogr.*. In press.

Kent, E. C., P. K. Taylor, B. S. Truscott and J. S. Hopkins, 1993a: The accuracy of voluntary observing ships' meteorological observations – Results of the VSOP-NA. *J. Atmos. & Oceanic Tech.*, **10**, 591–608.

Kent, E. C., R. J. Tiddy and P. K. Taylor, 1993b: Correction of marine daytime air temperature observations for radiation effects. *J. Atmos. & Oceanic Tech.*, **10**, 900–906.

Kushnir, Y., 1994: Interdecadal variations in North Atlantic sea surface temperature and associated atmospheric conditions. *J. Climate*, **7**, 141–157.

Levitus, S., 1982: Climatological Atlas of the World Ocean, NOAA Prof. Paper No. 13, U. S. Government Printing Office, Washington D. C., 17 fiches, 173 pp.

Petersen, P., 1927: Zur Bestimmung der Windstärke auf See. *Ann. Hydrogr.*, **55**, 69–72.

Rabiner, L. R., M. R. Sambur and C. E. Schmidt, 1975: Applications of a nonlinear smoothing algorithm to speech processing. *IEEE Transactions on Acoustics, Speech, and Signal Processing*, **ASSP–23**, 552–557.

Ramage, C. S., 1984: Can shipboard measurements reveal secular changes in tropical air–sea heat flux? *J. Climate Appl. Meteor.*, **23**, 187–193.

Reynolds, R. W., 1988: A real–time global sea surface temperature analysis. *J. Climate*, **1**, 75–86.

Roll, H. U., 1965: *Physics of the Marine Atmosphere.* Int. Geophys. Ser., Vol. 7, 426 pp.

Schlatter, T. W., and D. V. Baker, 1981: Algorithms for thermodynamic calculations. NOAA/ERL PROFS Program Office, Boulder, CO, 34 pp.

Schubert, S. D., R. B. Rood and J. Pfaendtner, 1993: An assimilated dataset for earth sciences applications. *Bull. Amer. Meteor. Soc.*, **74**, 2331–2342.

Shapiro, R., 1970: Smoothing, filtering, and boundary effects. *Rev. of Geophys. and Space Phys.*, **8**, 359–387.

Simpson, G. C., 1906: The velocity equivalents of the Beaufort scale. Rep. of Director of Meteorological Office No. 180, London.

Slutz, R. J., S. J. Lubker, J. D. Hiscox, S. D. Woodruff, R. L. Jenne, D. H. Joseph, P. M. Steurer and J. D. Elms, 1985: COADS, Comprehensive Ocean–Atmosphere Data Set, Release 1. Climate Research Program, Environmental Research Laboratory, Boulder, CO, 262 pp.

Woodruff, S. D., R. J. Slutz, R. L. Jenne and P. M. Steurer, 1987: A comprehensive ocean–atmosphere data set. *Bull. Amer. Meteor. Soc.*, **68**, 1239–1250.

World Meteorological Organization (WMO), 1970: Reports on marine science affairs. Rep. No. 3: The Beaufort scale of wind force. WMO, Geneva, Switzerland, 22pp.

World Meteorological Organization (WMO), 1990: International list of selected, suplementary and auxiliary ships. *WMO Publ. No. 47*, World Meteorological Organization, Geneva.

Young, C. C., A. M. da Silva and S. Levitus, 1993: Monthly Distribution of SST Observations in COADS: 1945-89. *Tech. Rep. Geosci. 93.01*, University of Wisconsin-Milwaukee, 275pp.

10 Sea minus air temperature

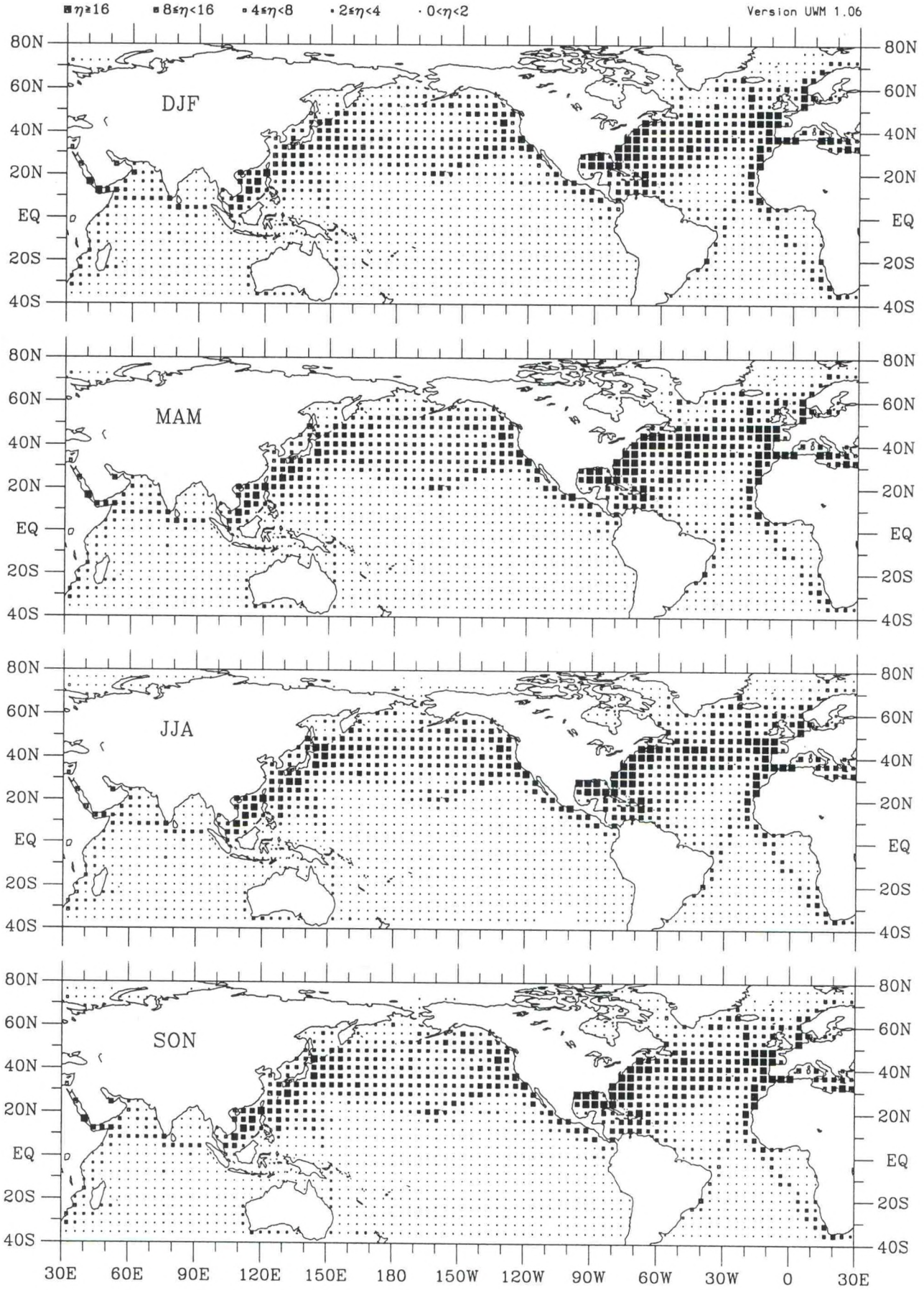

Figure dT-1. sst minus sat seasonal observation density (1945-89).

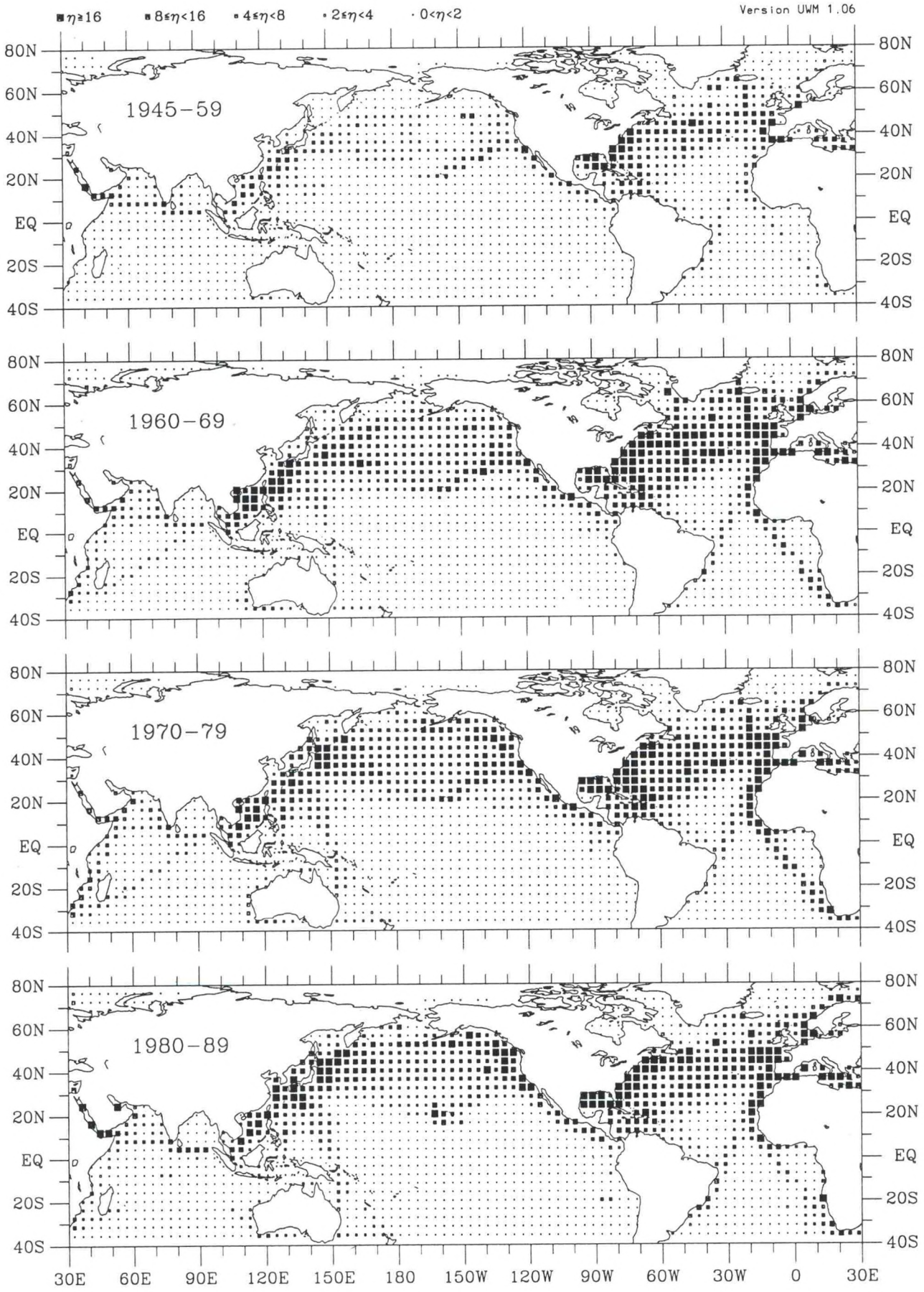

Figure dT-2. sst minus sat decadal observation density.

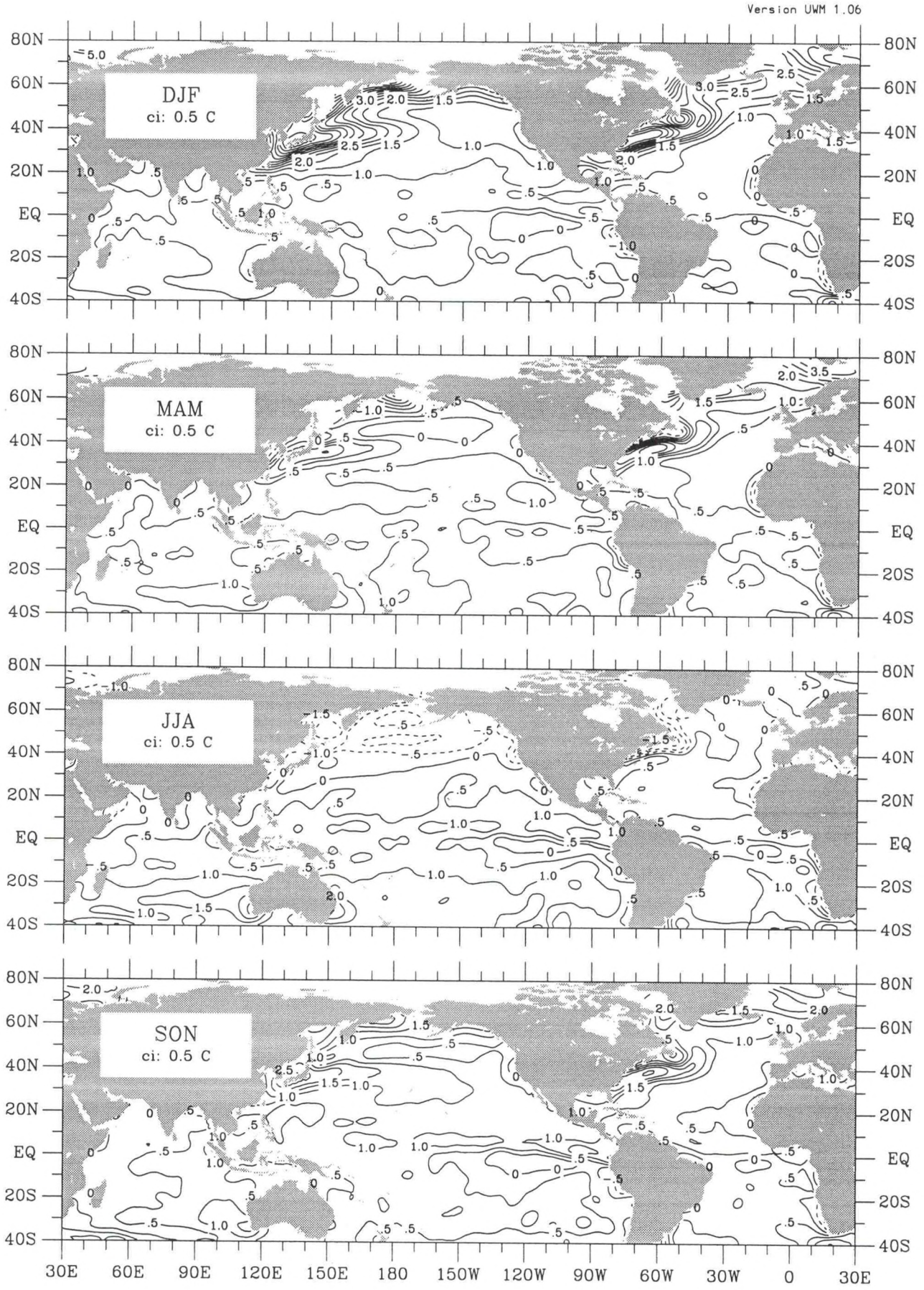

Figure dT-3. sst minus sat seasonal climatology (1945-89).

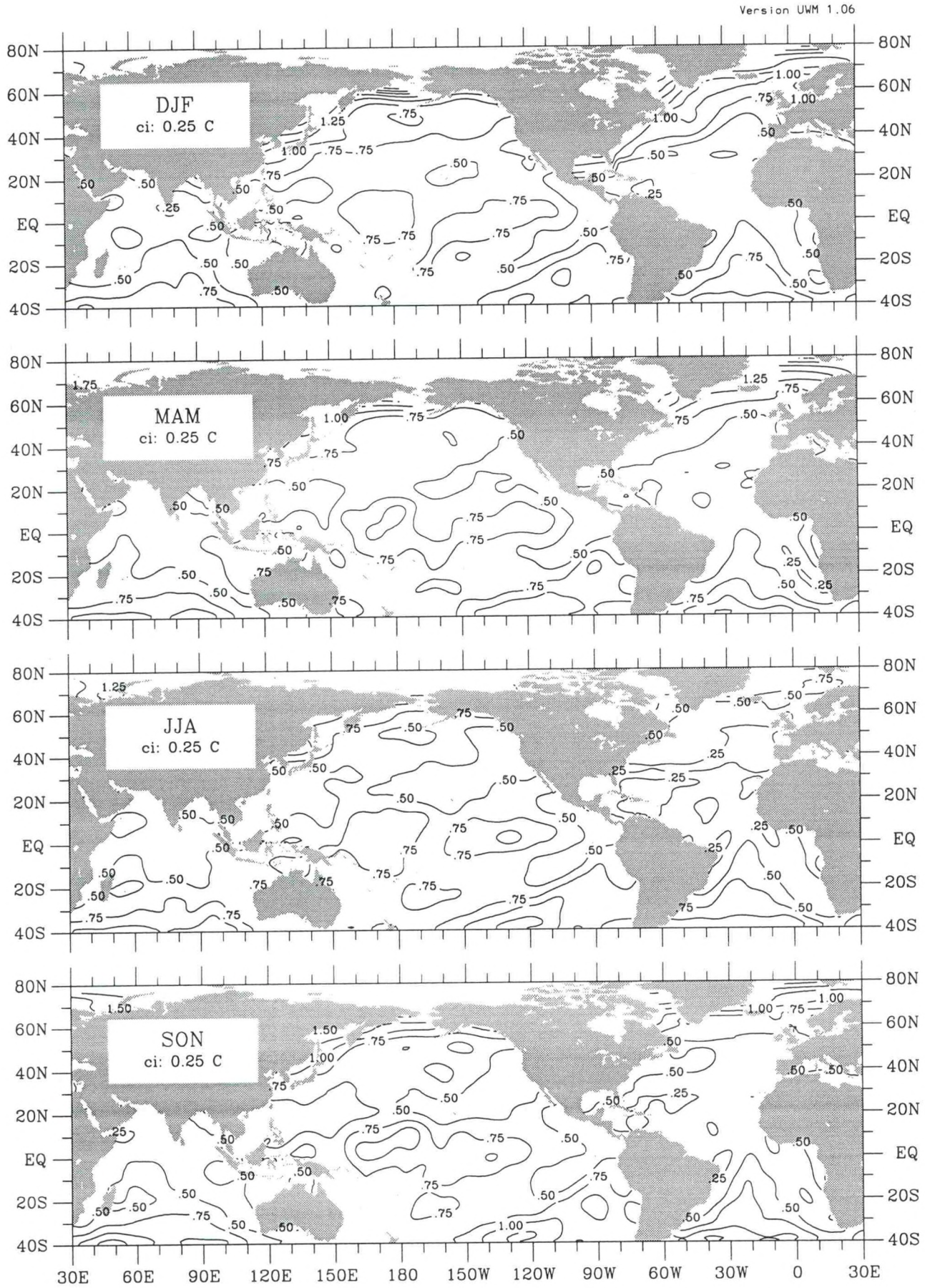

Figure dT-4. sst minus sat seasonal interannual std dev (1945-89).

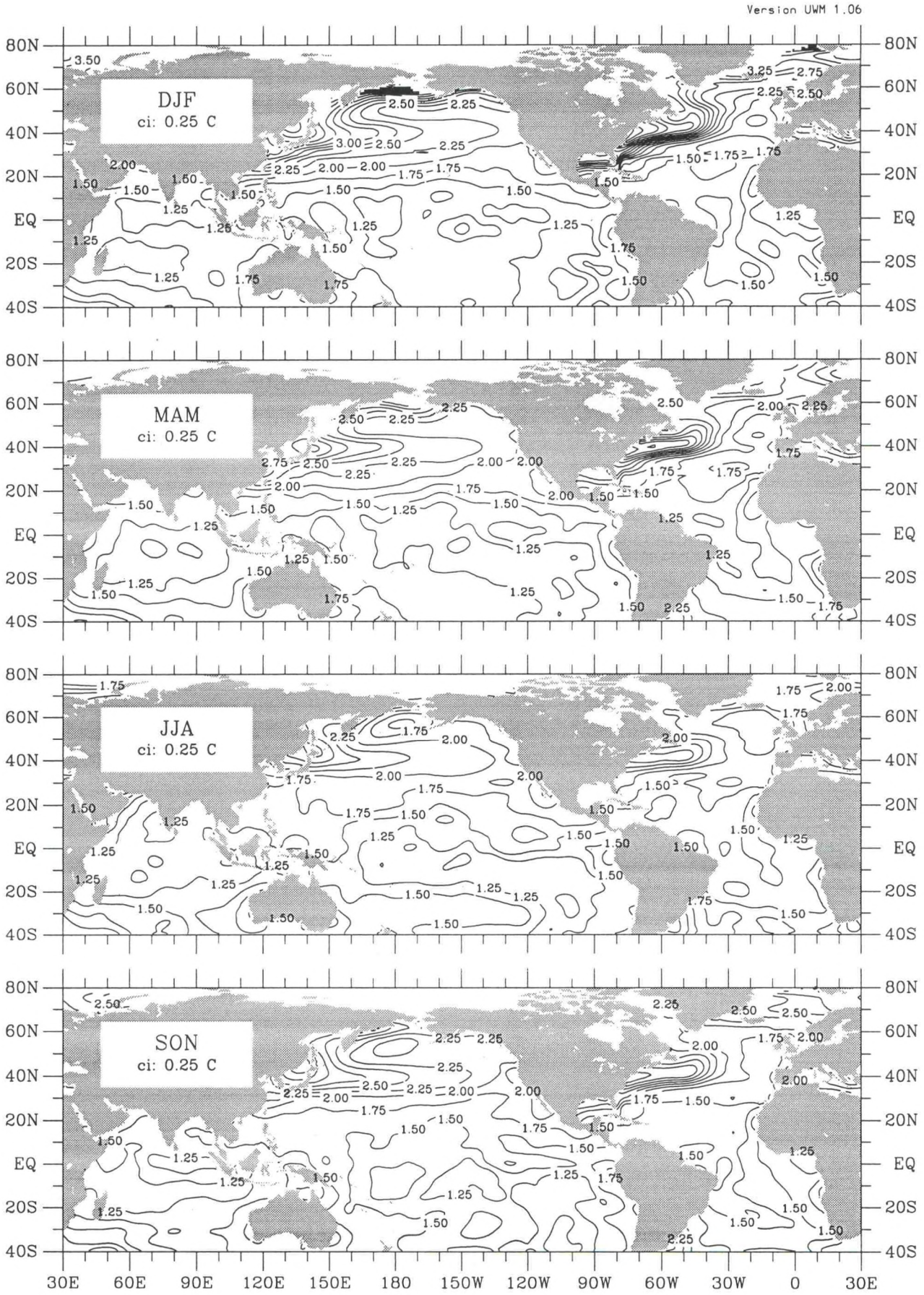

Figure dT-5. sst minus sat seasonal standard deviation (1945-89).

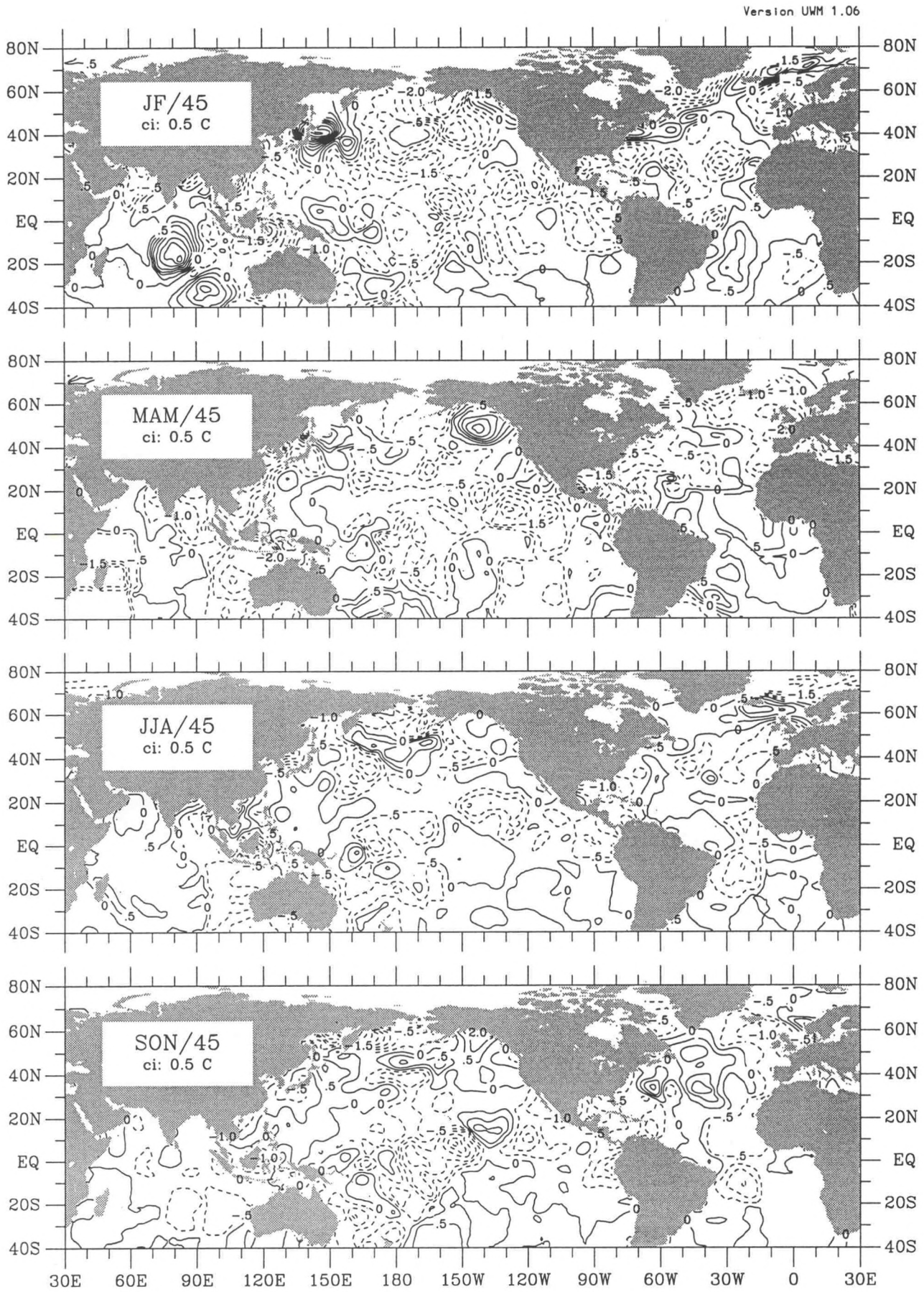

Figure dT-6. sst minus sat seasonal anomaly for 1945.

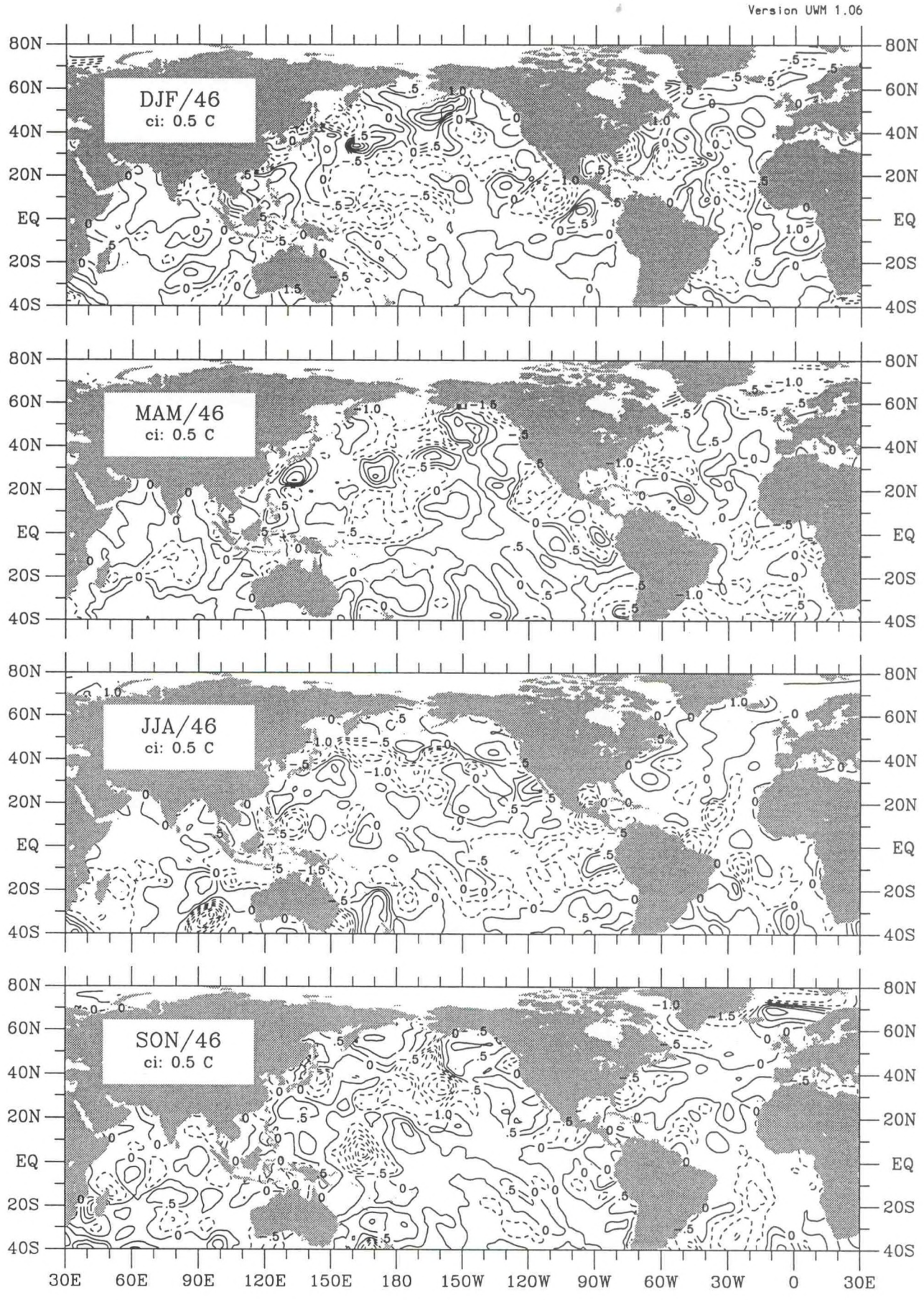

Figure dT-7. sst minus sat seasonal anomaly for 1946.

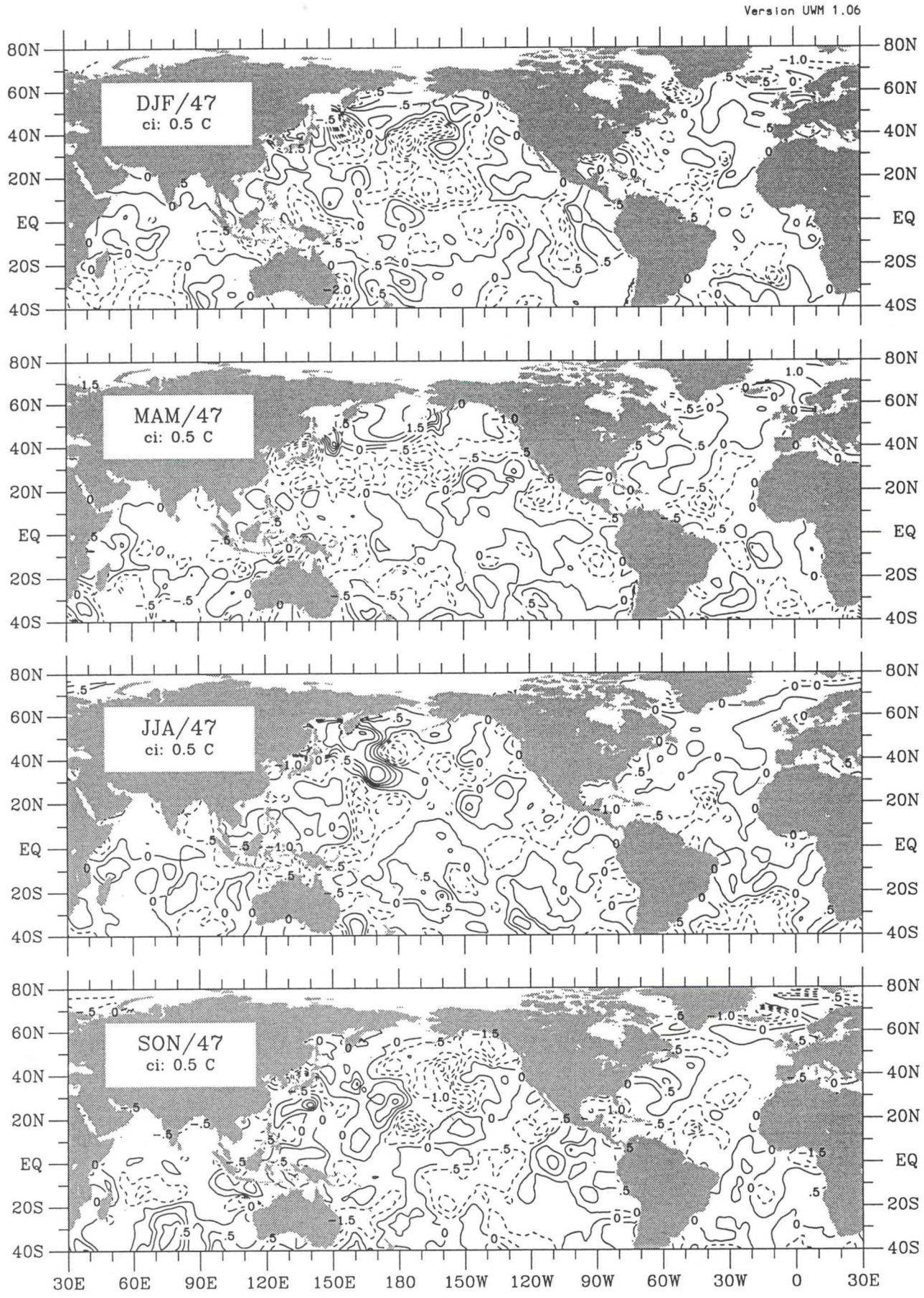

Figure dT–8. sst minus sat seasonal anomaly for 1947.

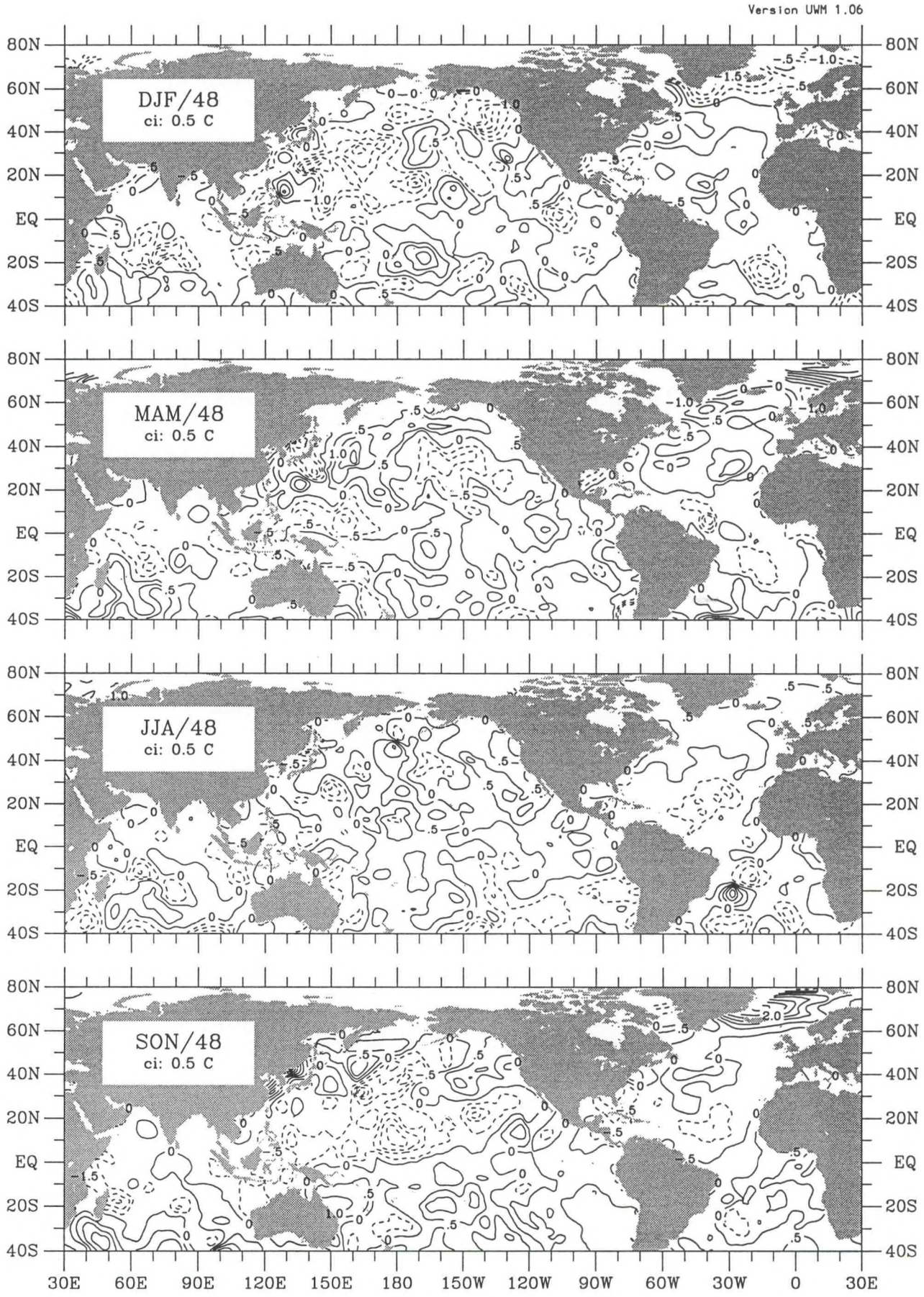

Figure dT–9. sst minus sat seasonal anomaly for 1948.

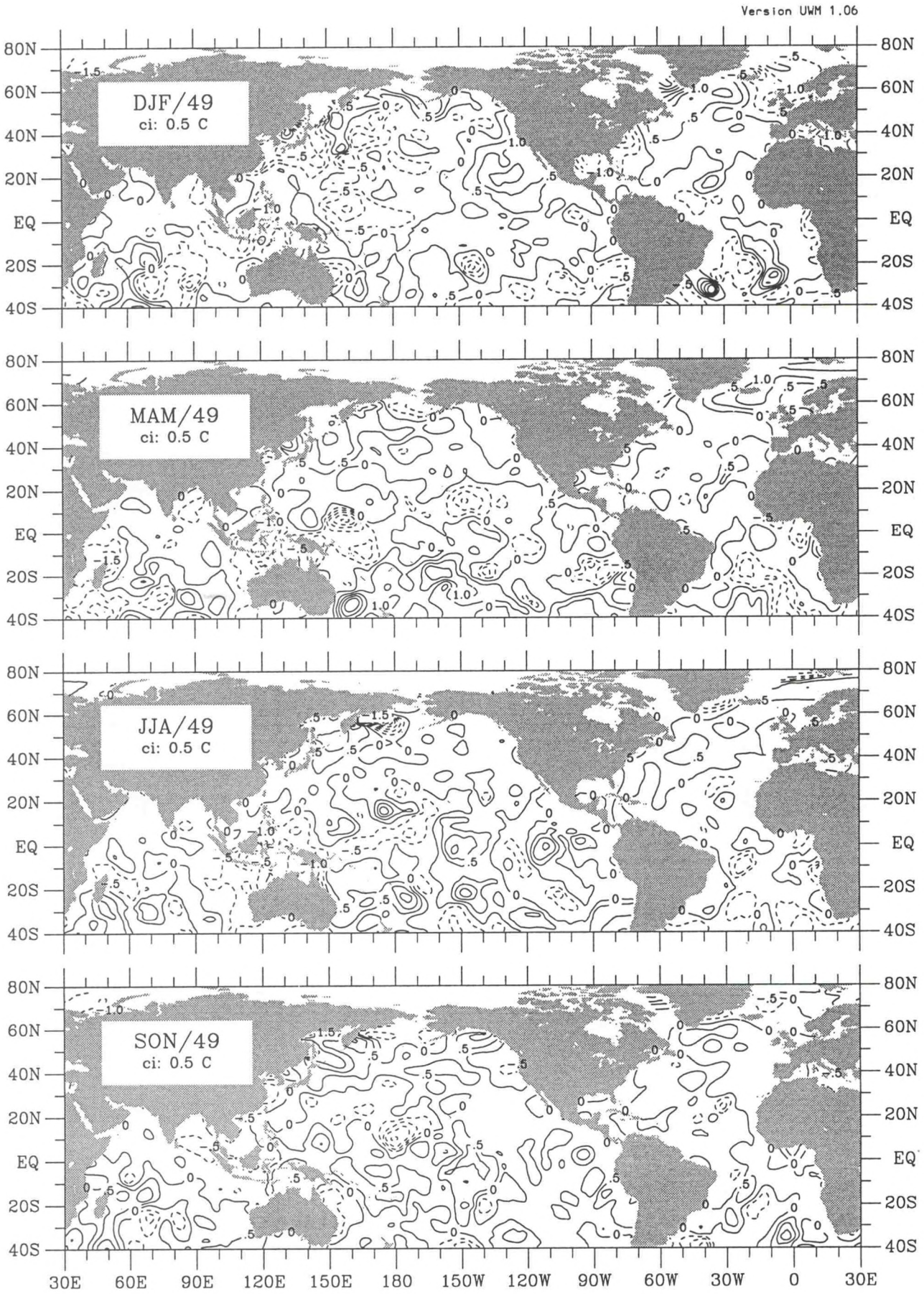

Figure dT-10. sst minus sat seasonal anomaly for 1949.

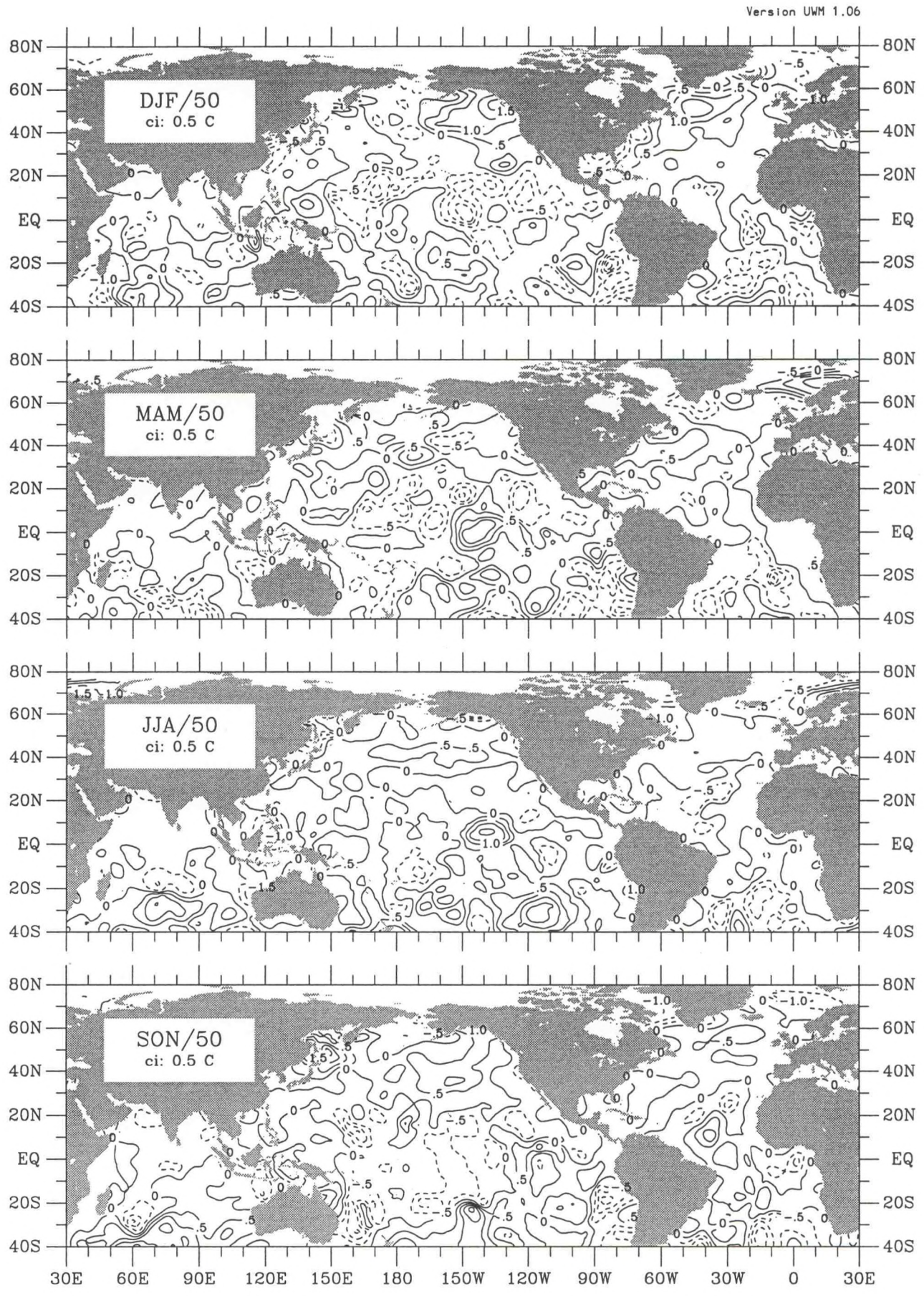

Figure dT-11. sst minus sat seasonal anomaly for 1950.

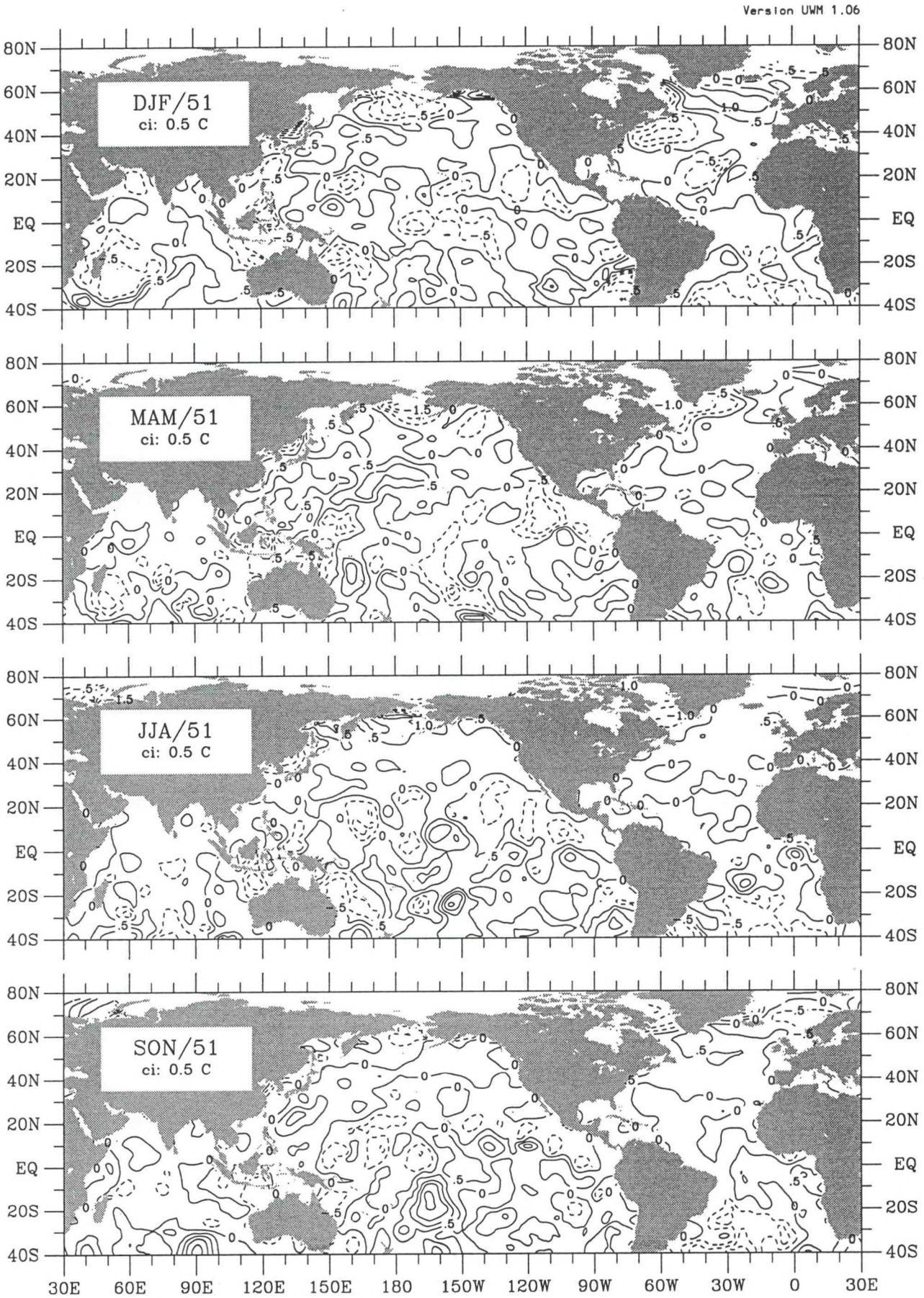

Figure dT-12. sst minus sat seasonal anomaly for 1951.

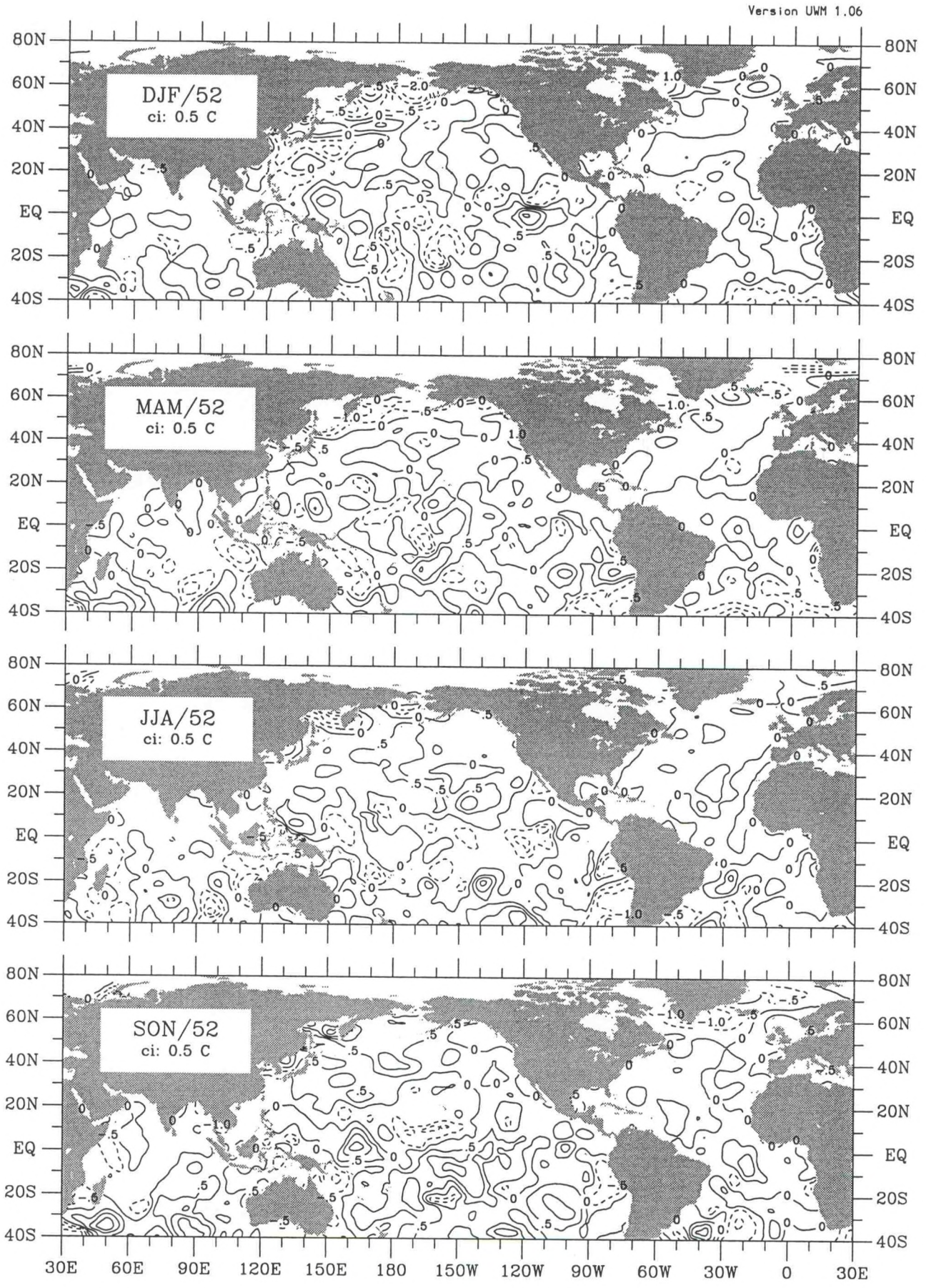

Figure dT-13. sst minus sat seasonal anomaly for 1952.

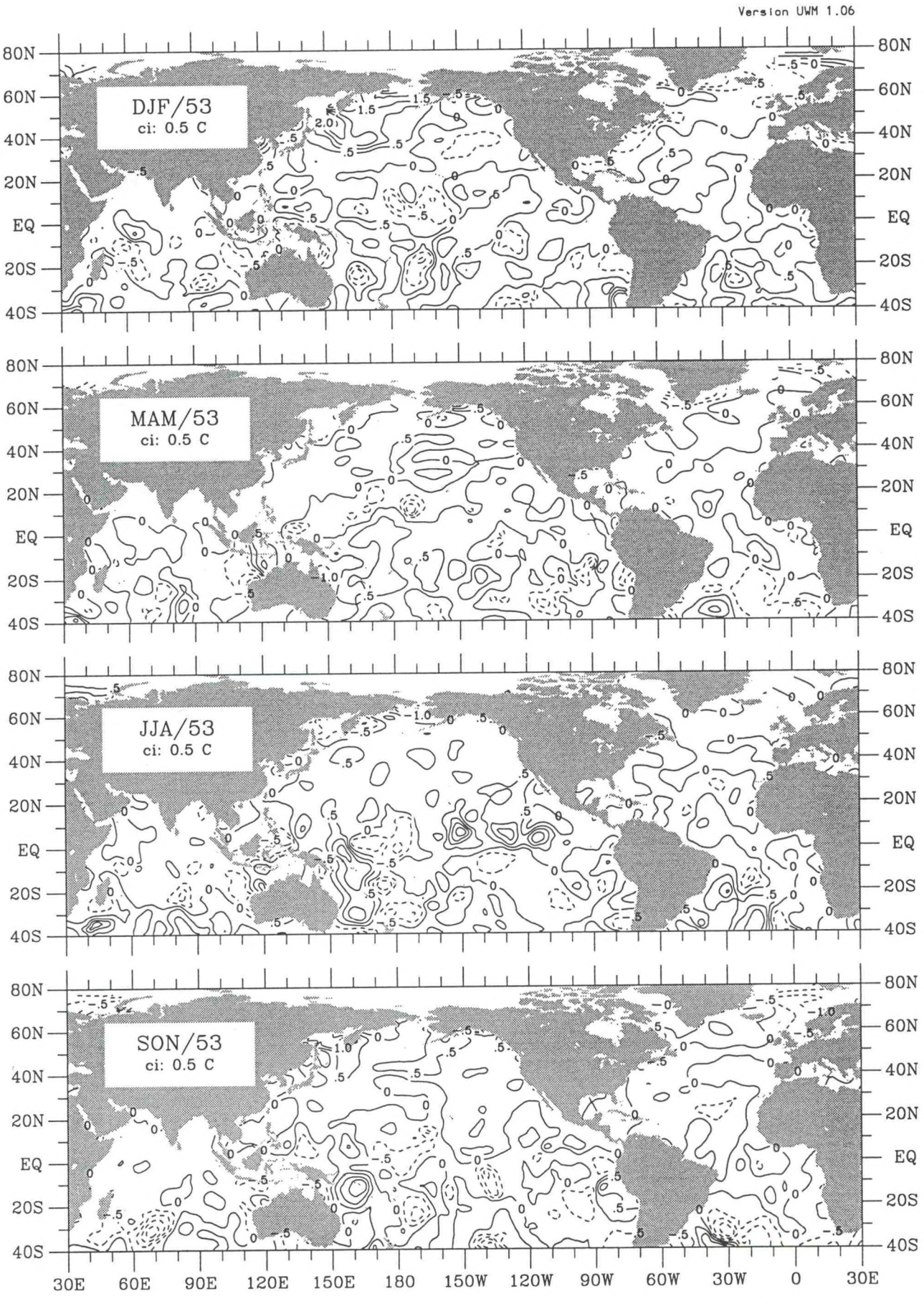

Figure dT-14. sst minus sat seasonal anomaly for 1953.

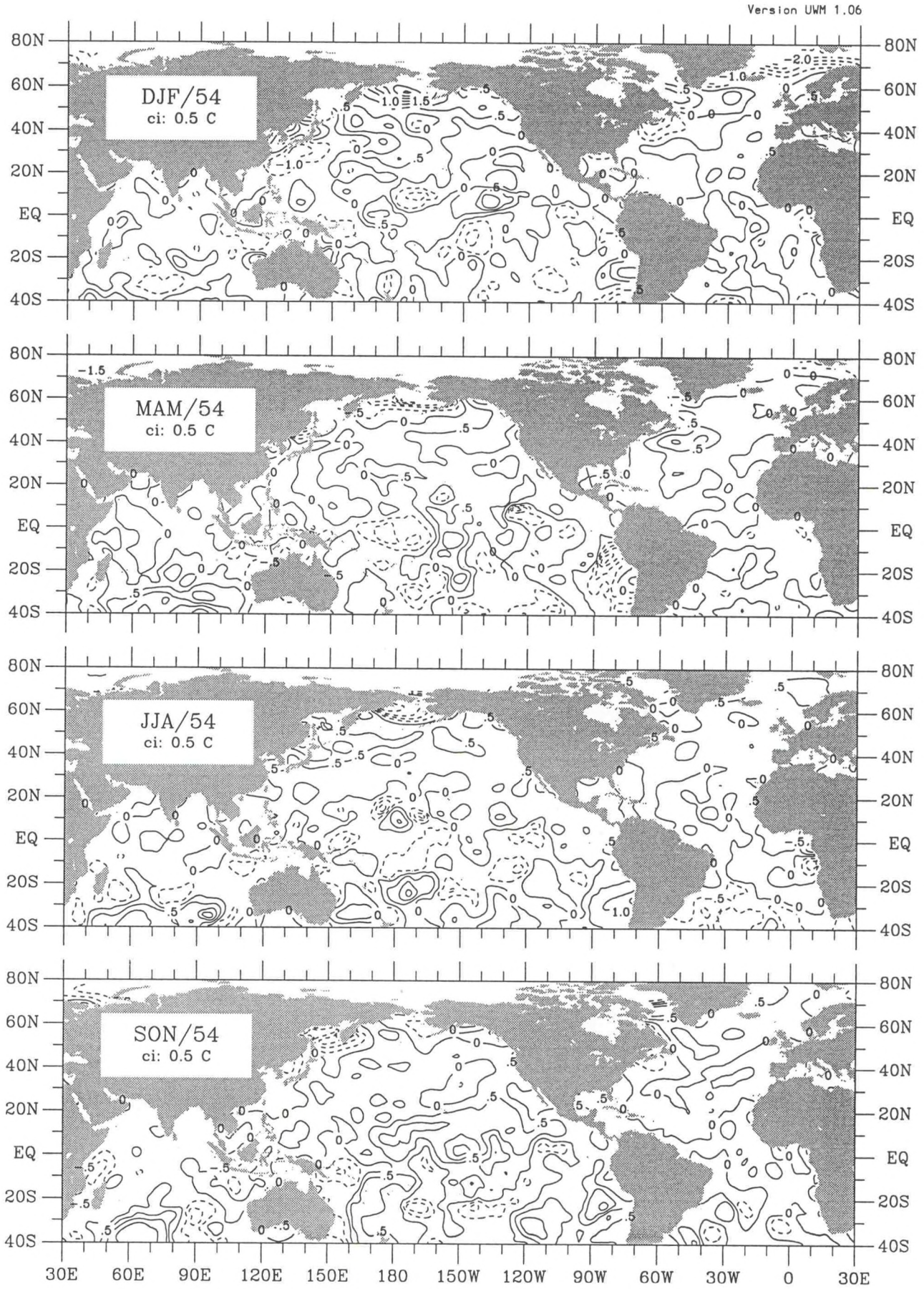

Figure dT-15. sst minus sat seasonal anomaly for 1954.

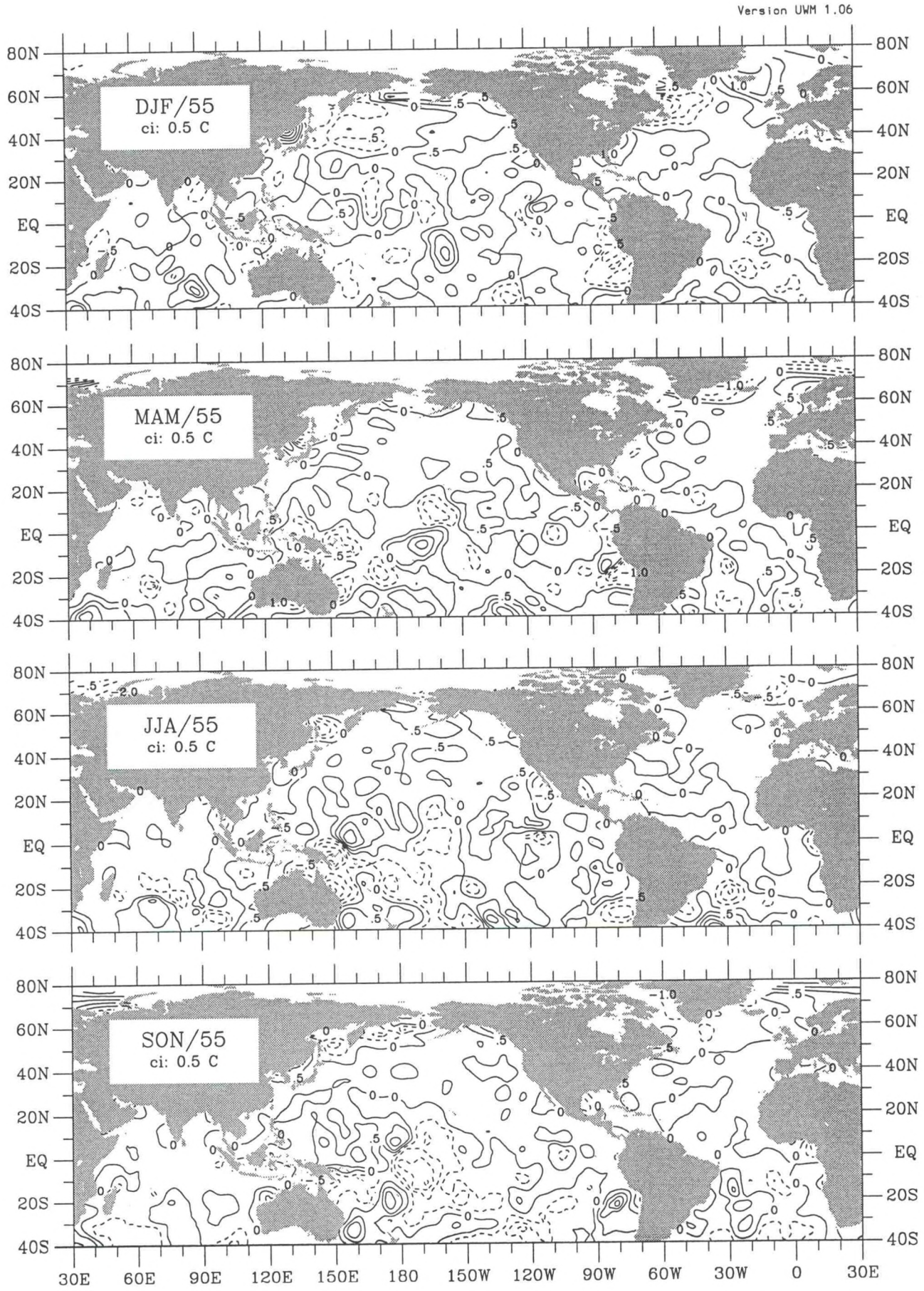

Figure dT-16. sst minus sat seasonal anomaly for 1955.

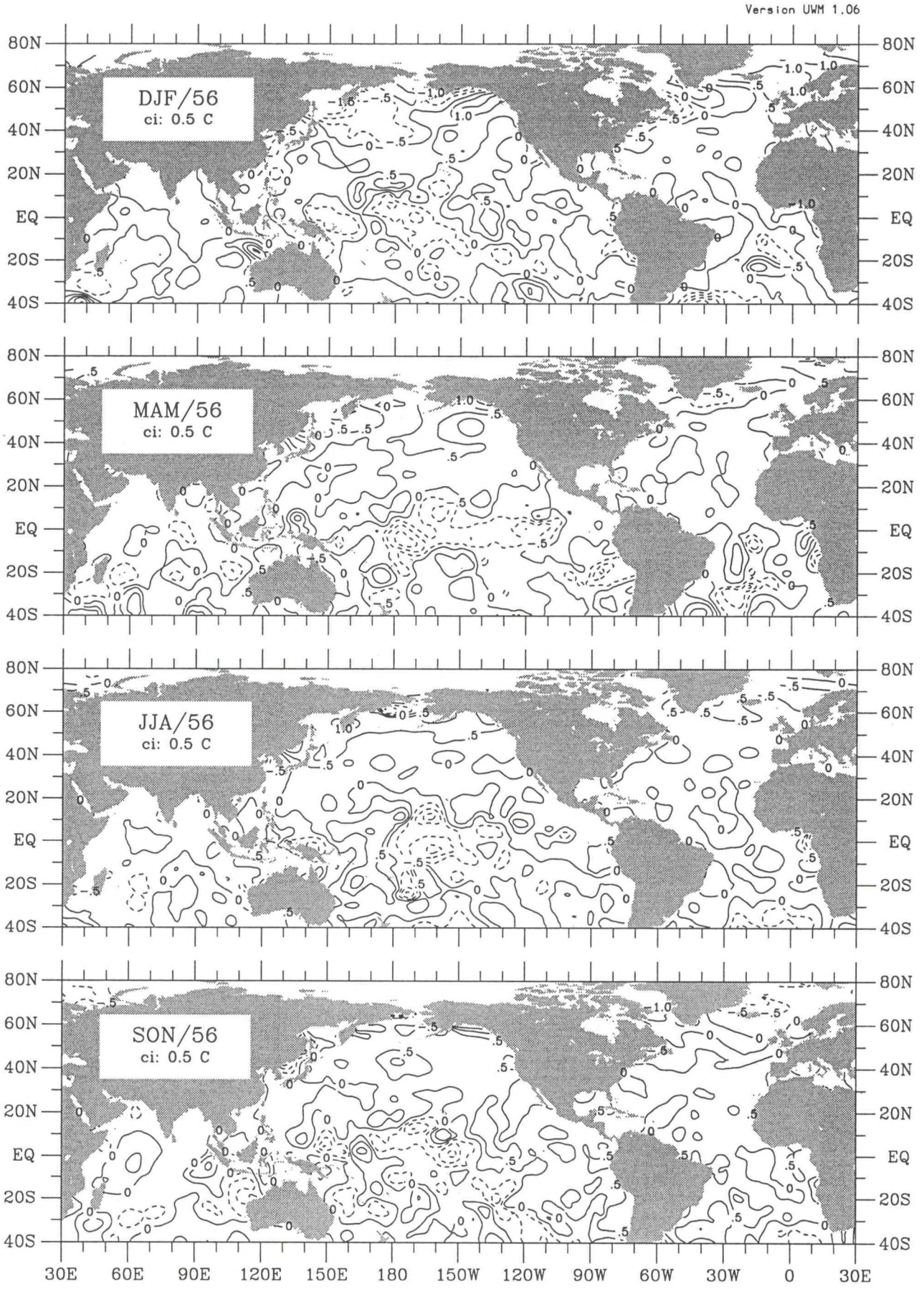

Figure dT-17. sst minus sat seasonal anomaly for 1956.

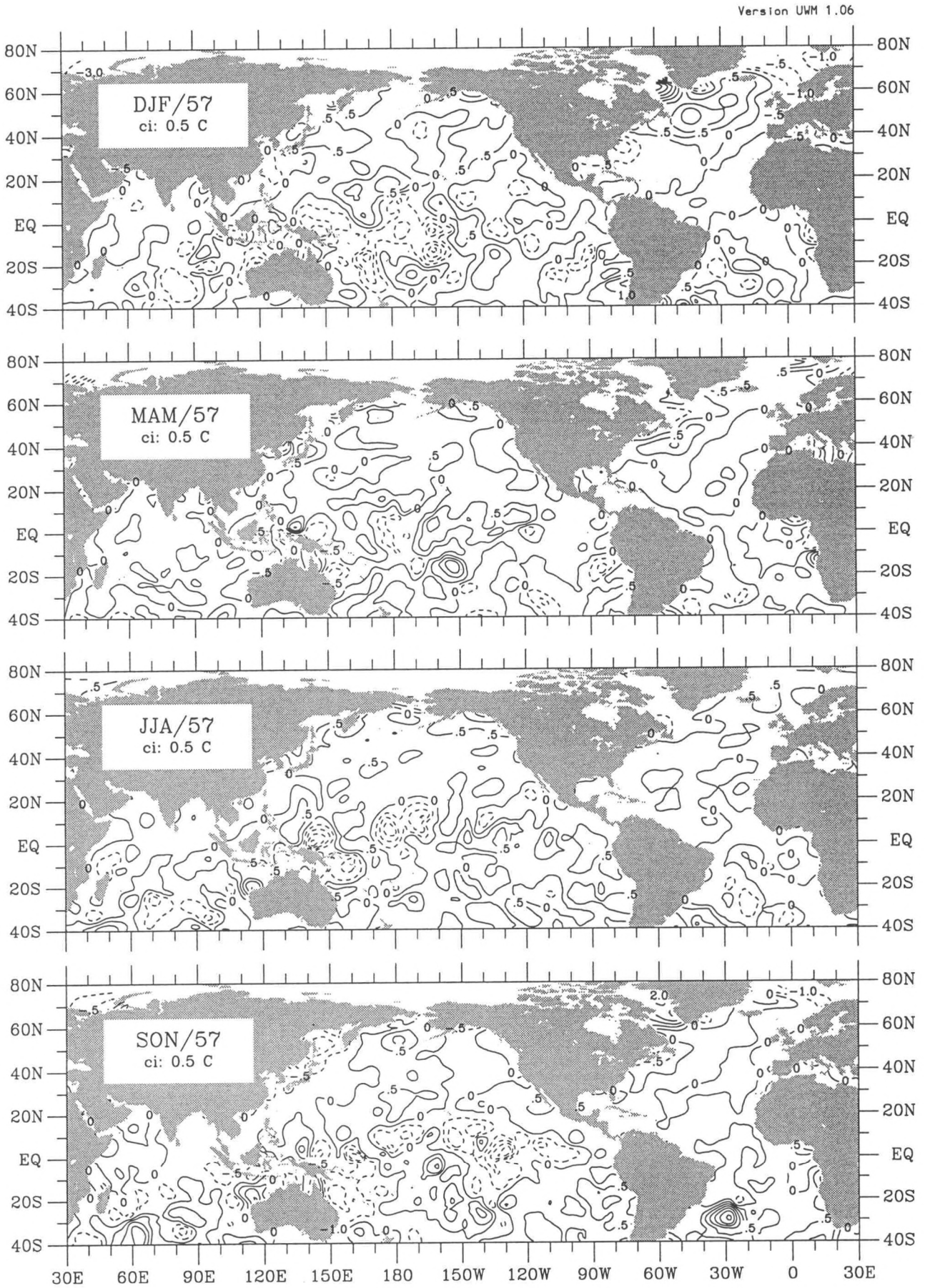

Figure dT-18. sst minus sat seasonal anomaly for 1957.

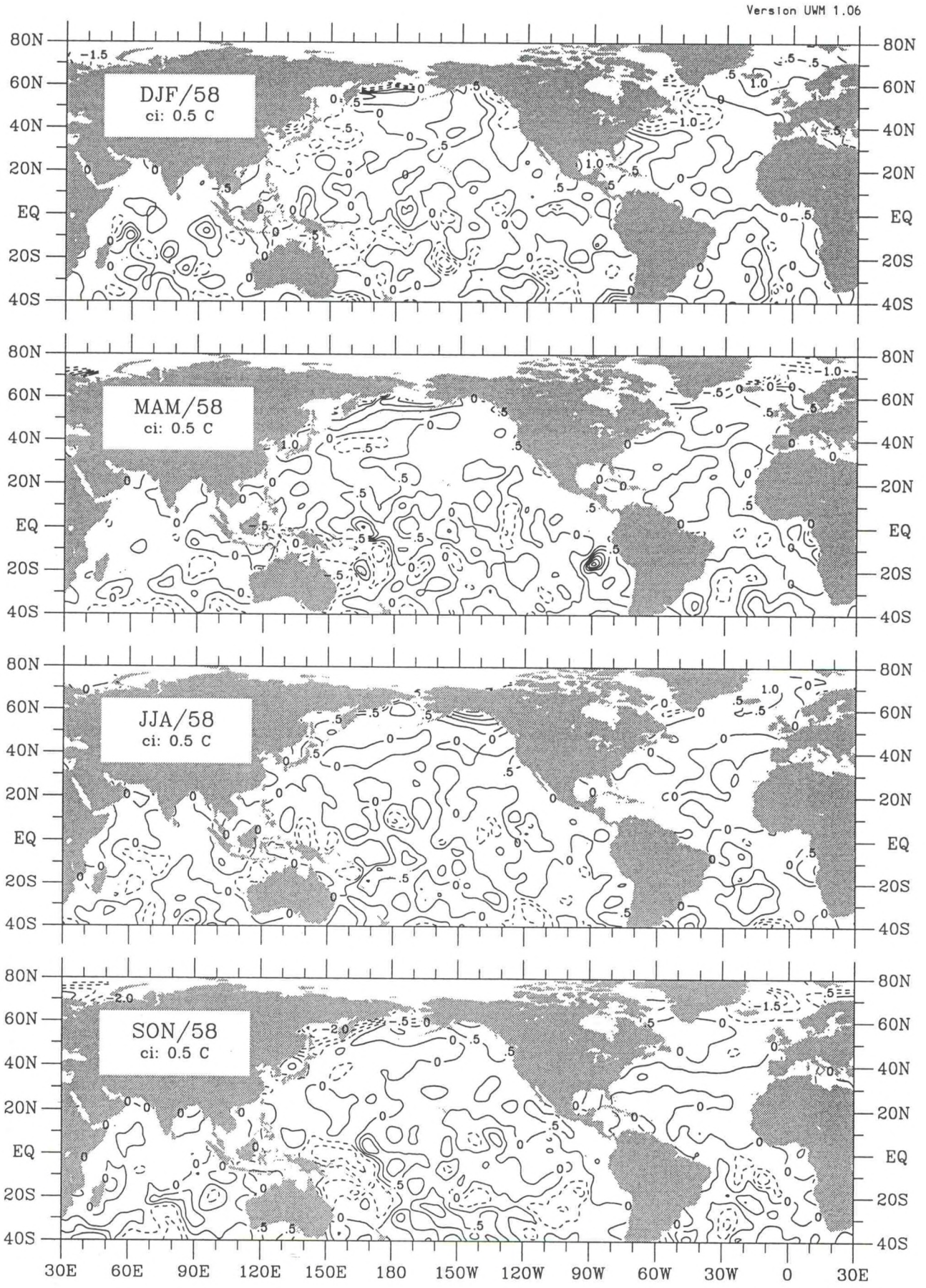

Figure dT-19. sst minus sat seasonal anomaly for 1958.

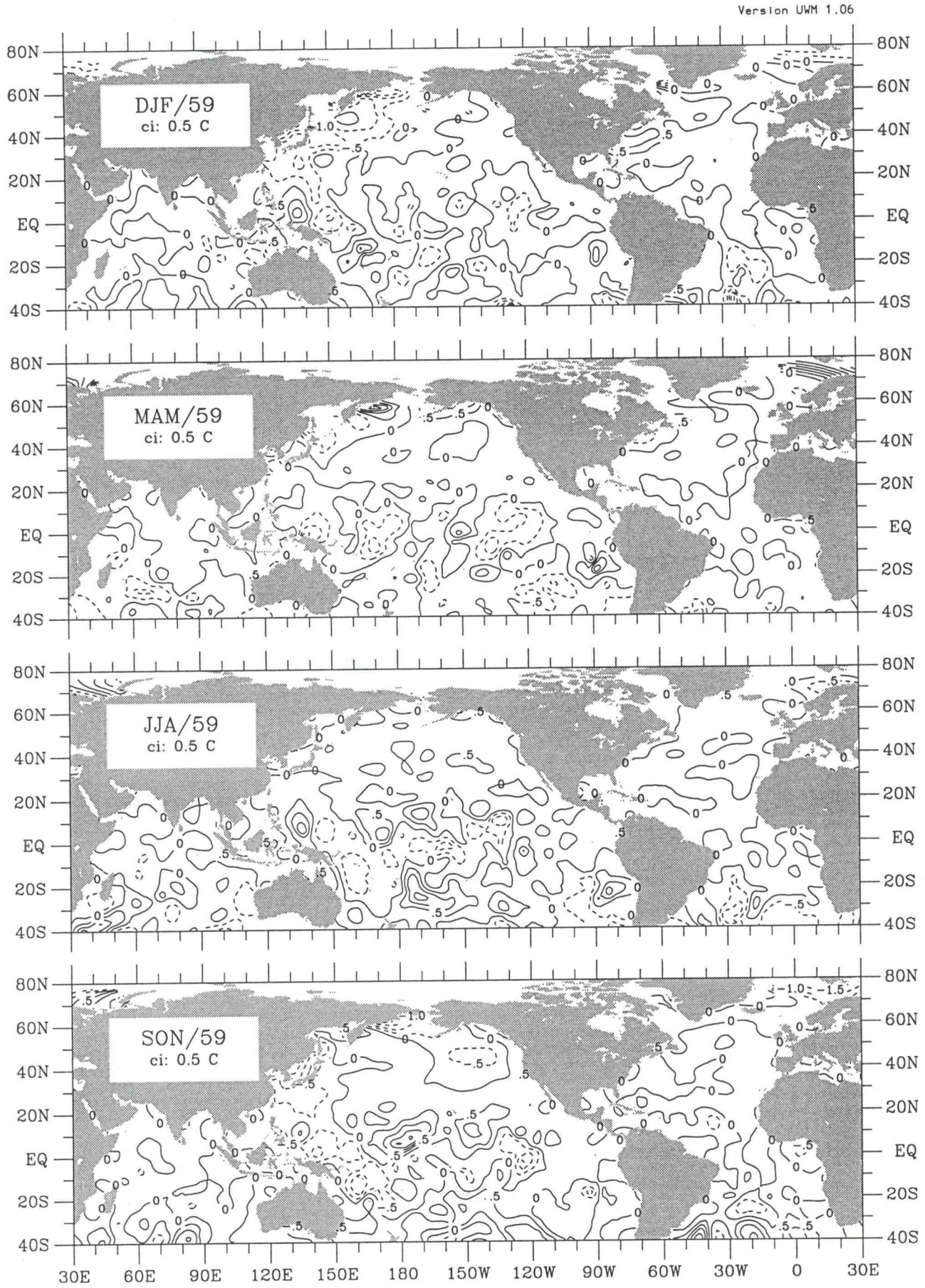

Figure dT-20. sst minus sat seasonal anomaly for 1959.

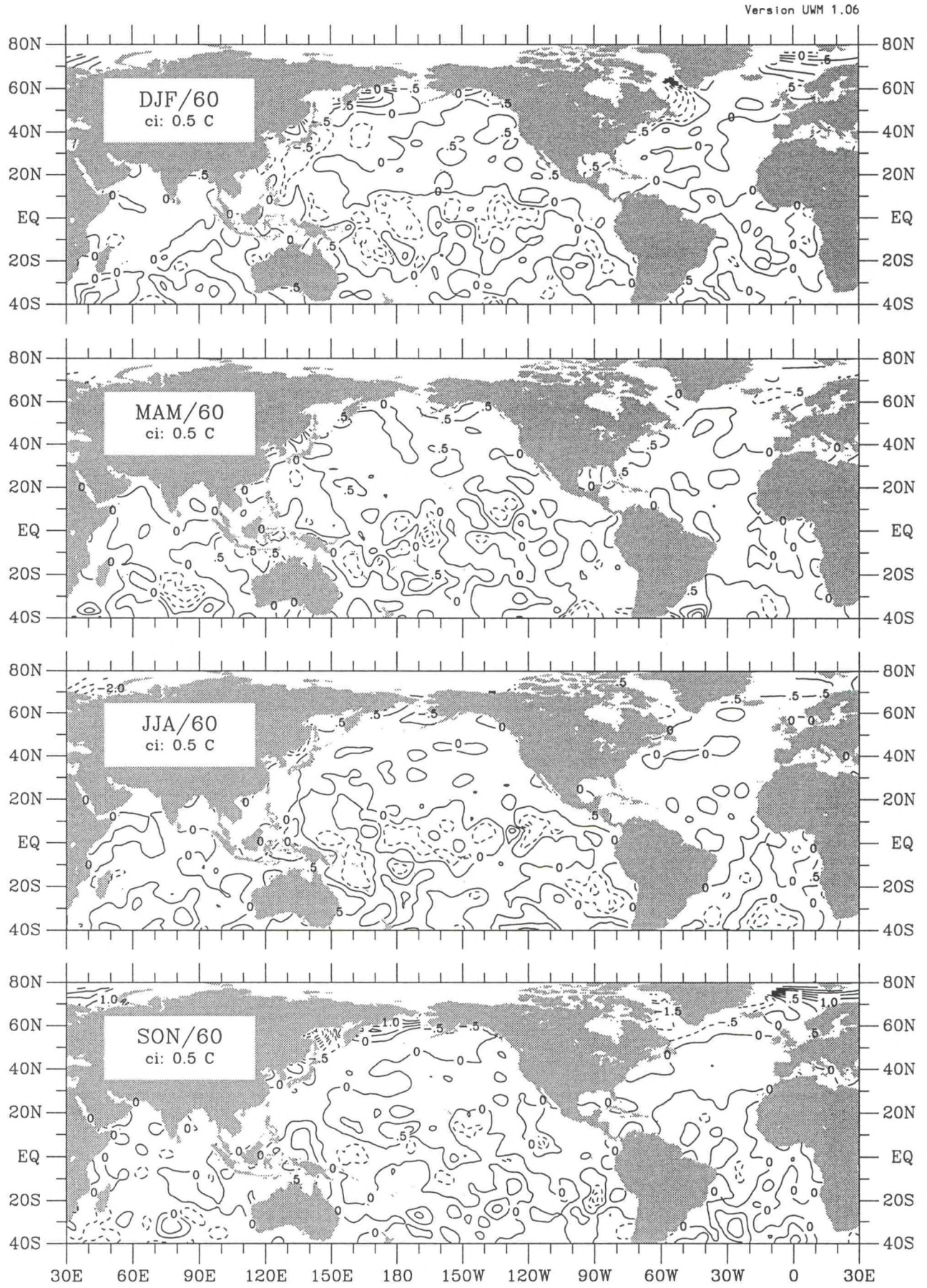

Figure dT-21. sst minus sat seasonal anomaly for 1960.

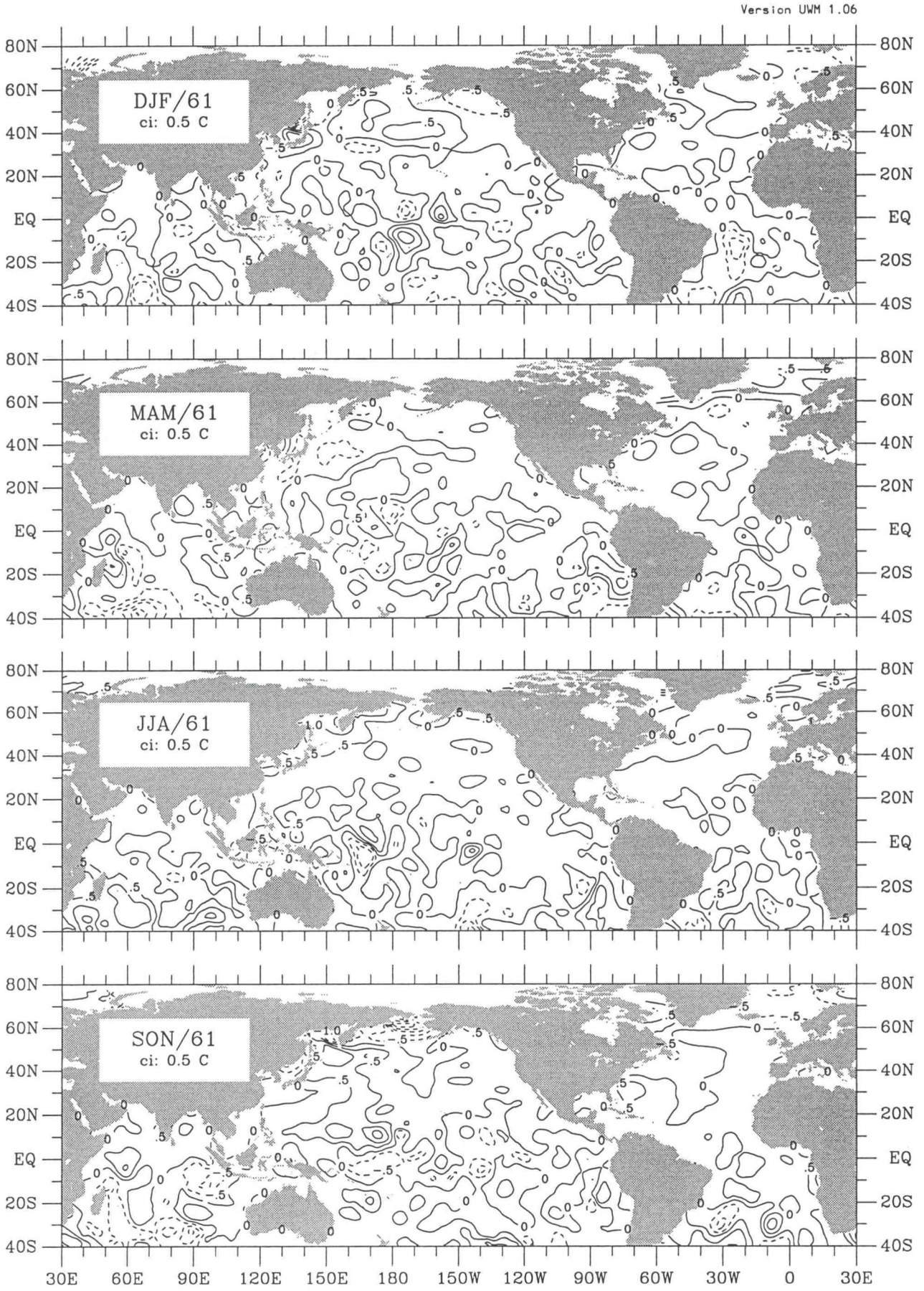

Figure dT-22. sst minus sat seasonal anomaly for 1961.

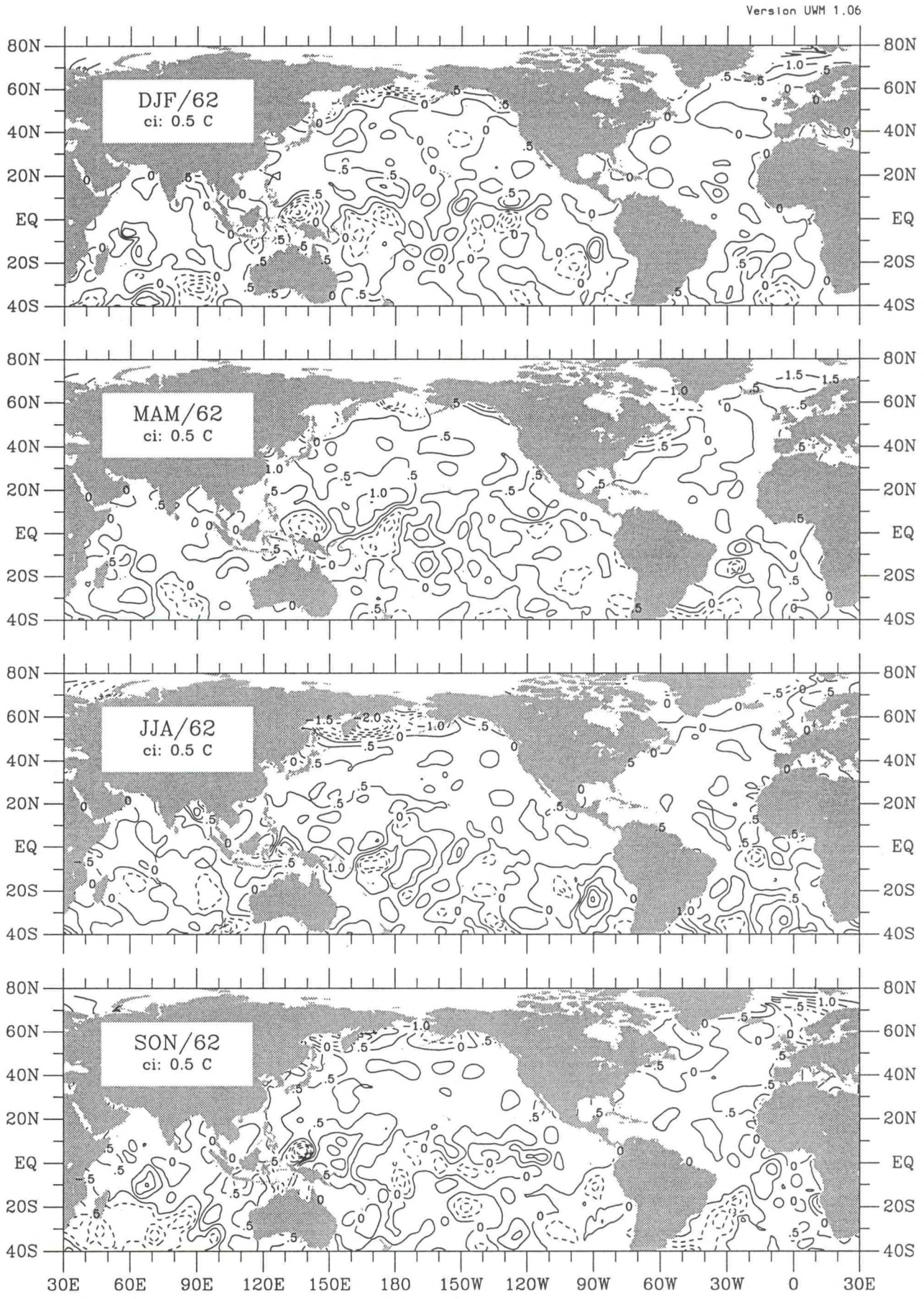

Figure dT-23. sst minus sat seasonal anomaly for 1962.

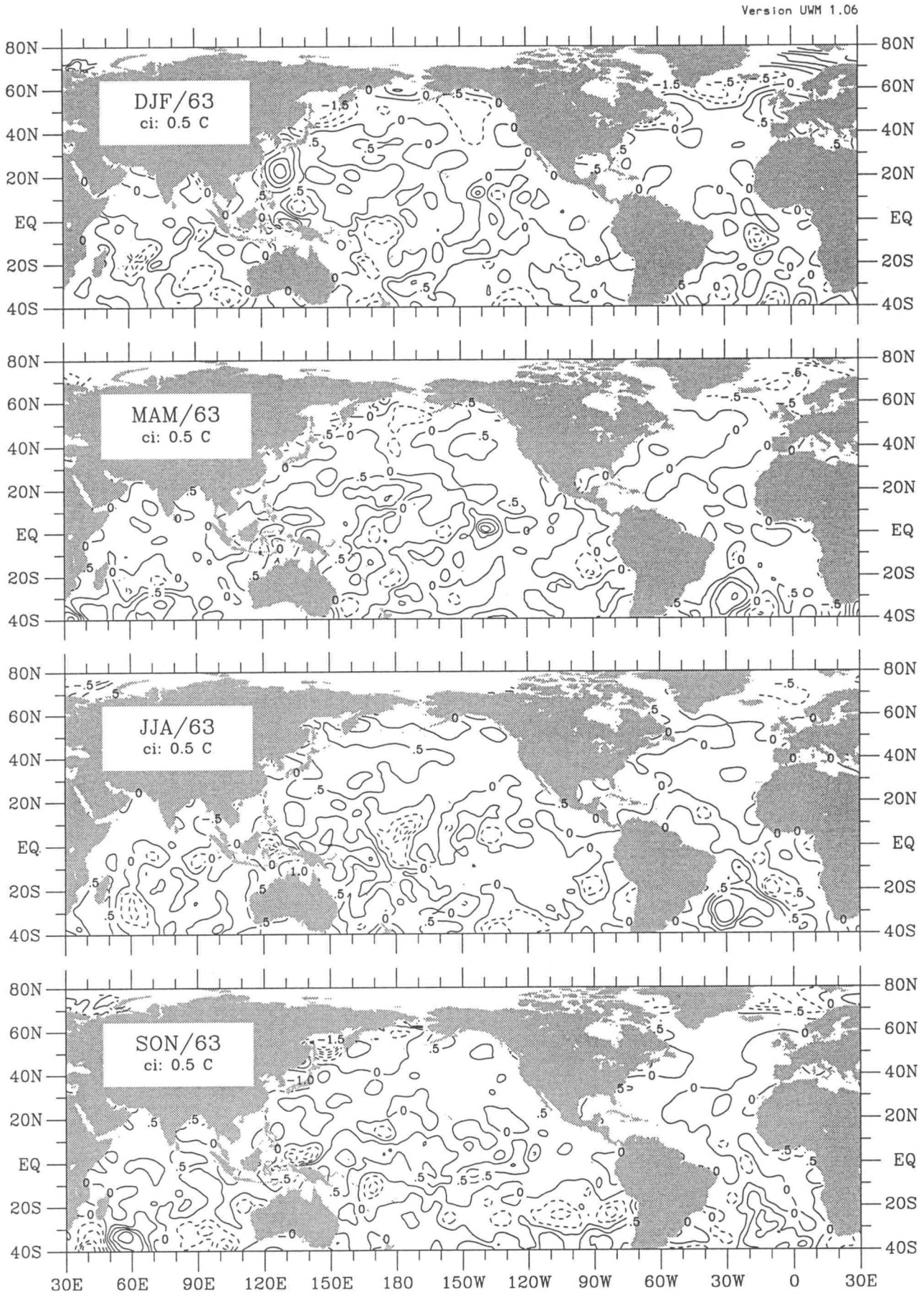

Figure dT-24. sst minus sat seasonal anomaly for 1963.

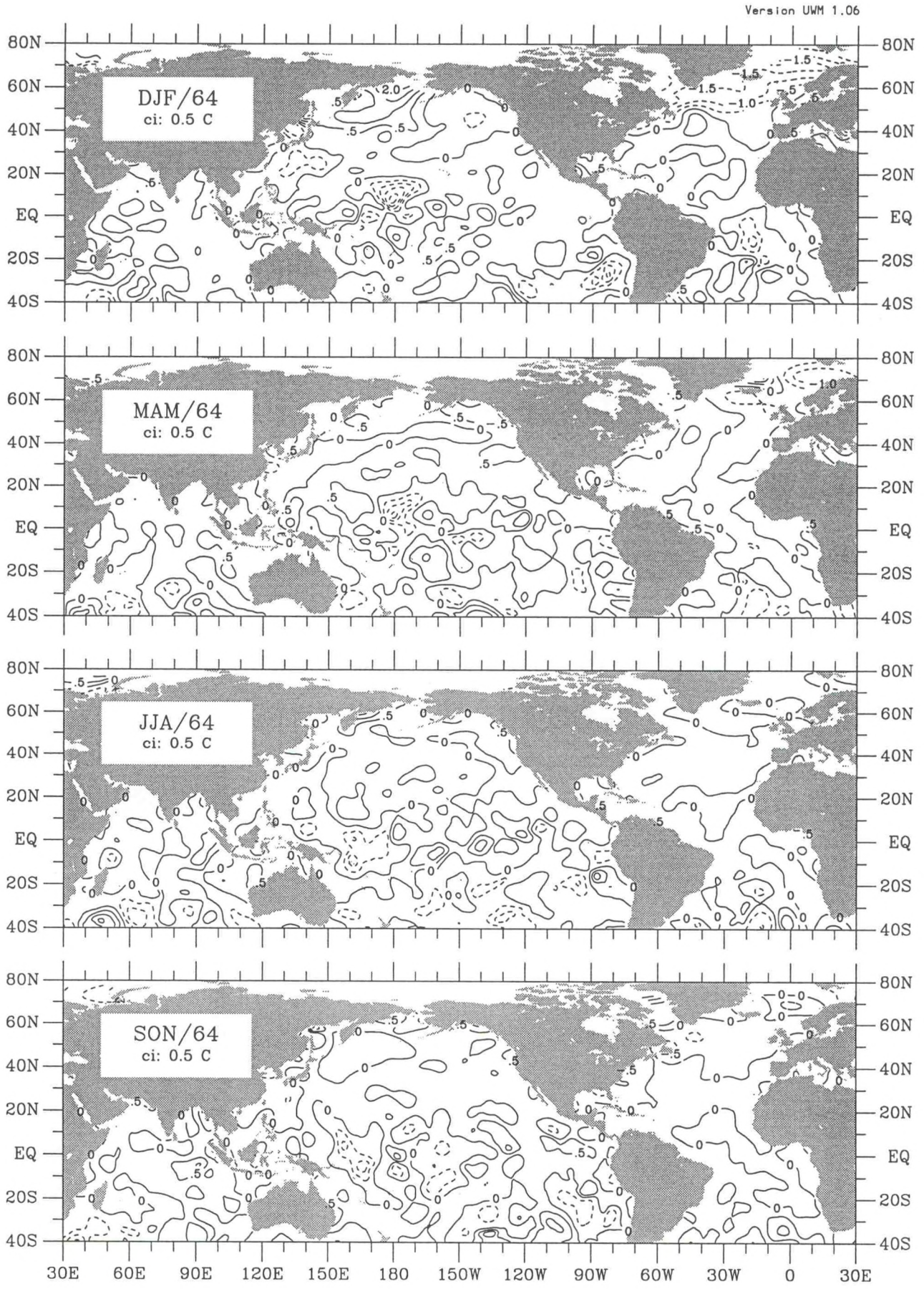

Figure dT-25. sst minus sat seasonal anomaly for 1964.

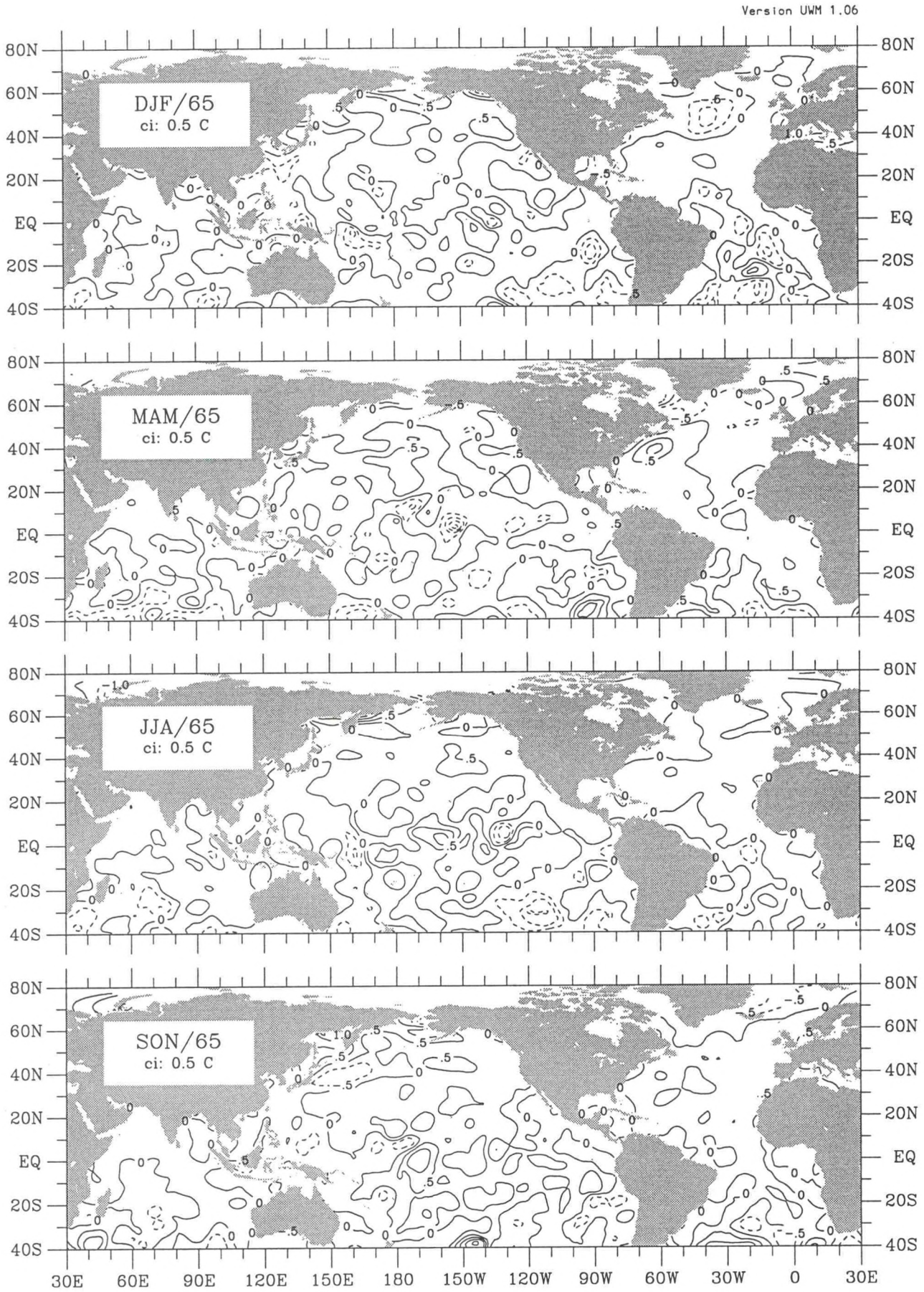

Figure dT-26. sst minus sat seasonal anomaly for 1965.

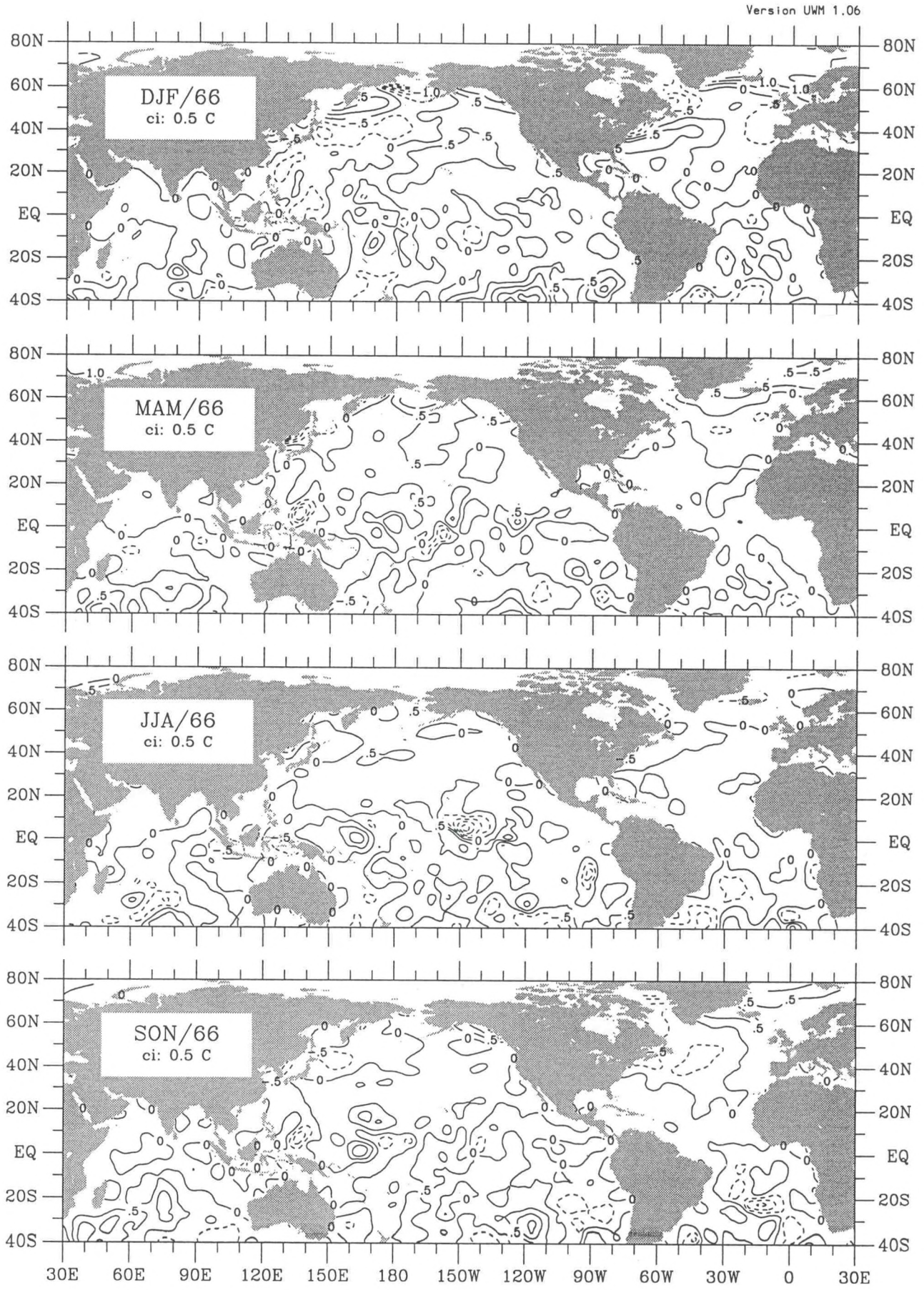

Figure dT-27. sst minus sat seasonal anomaly for 1966.

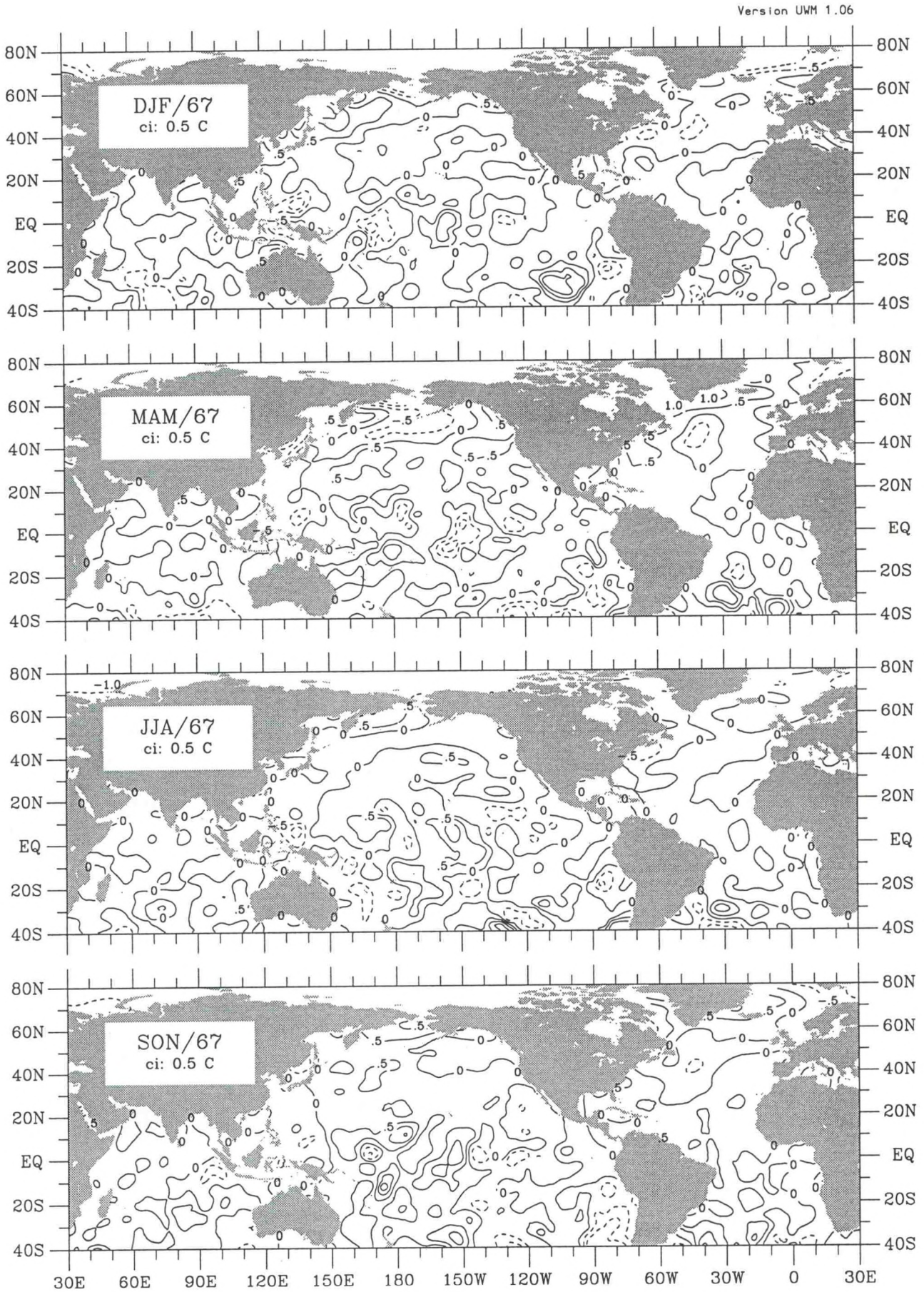

Figure dT-28. sst minus sat seasonal anomaly for 1967.

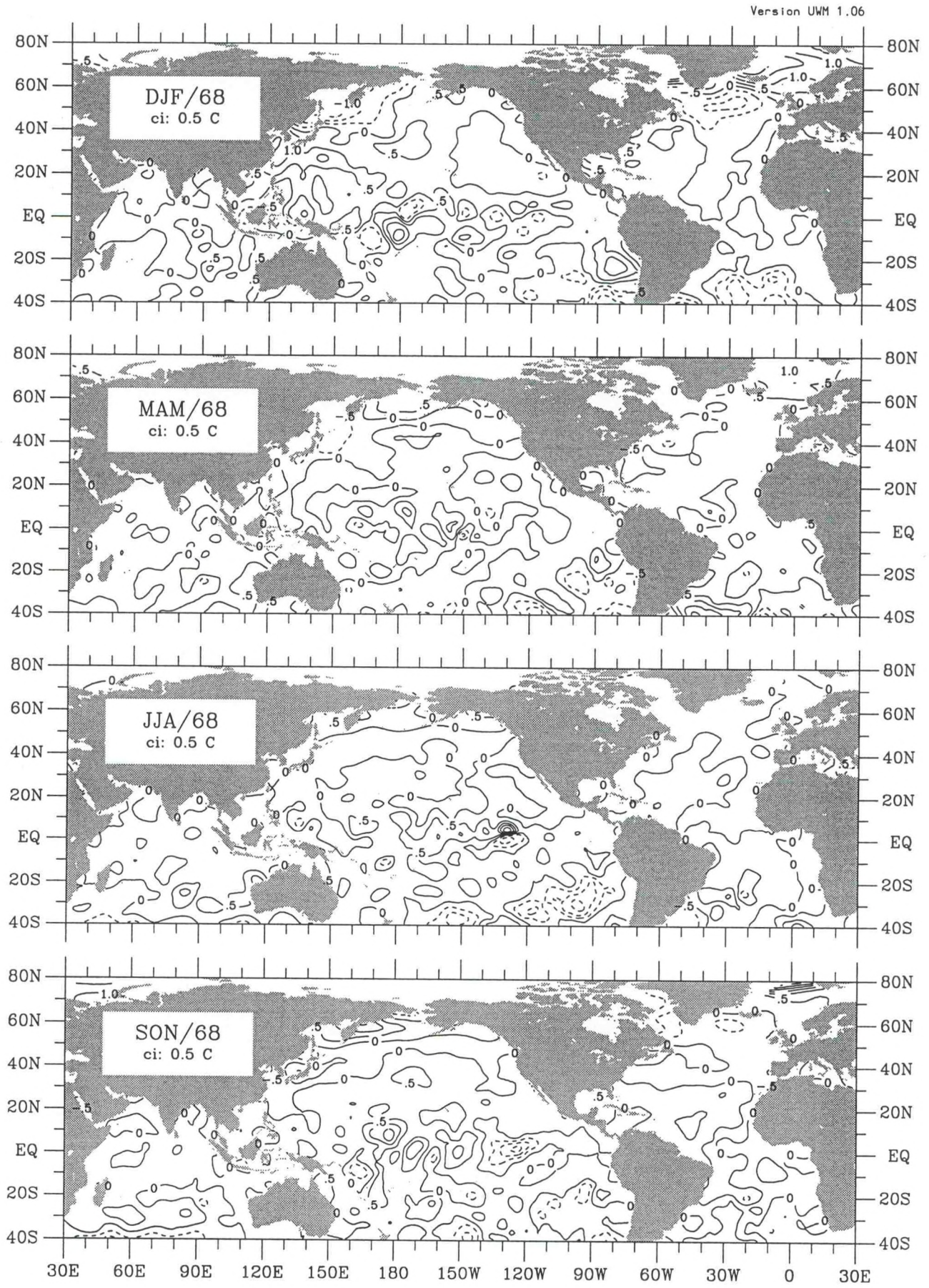

Figure dT-29. sst minus sat seasonal anomaly for 1968.

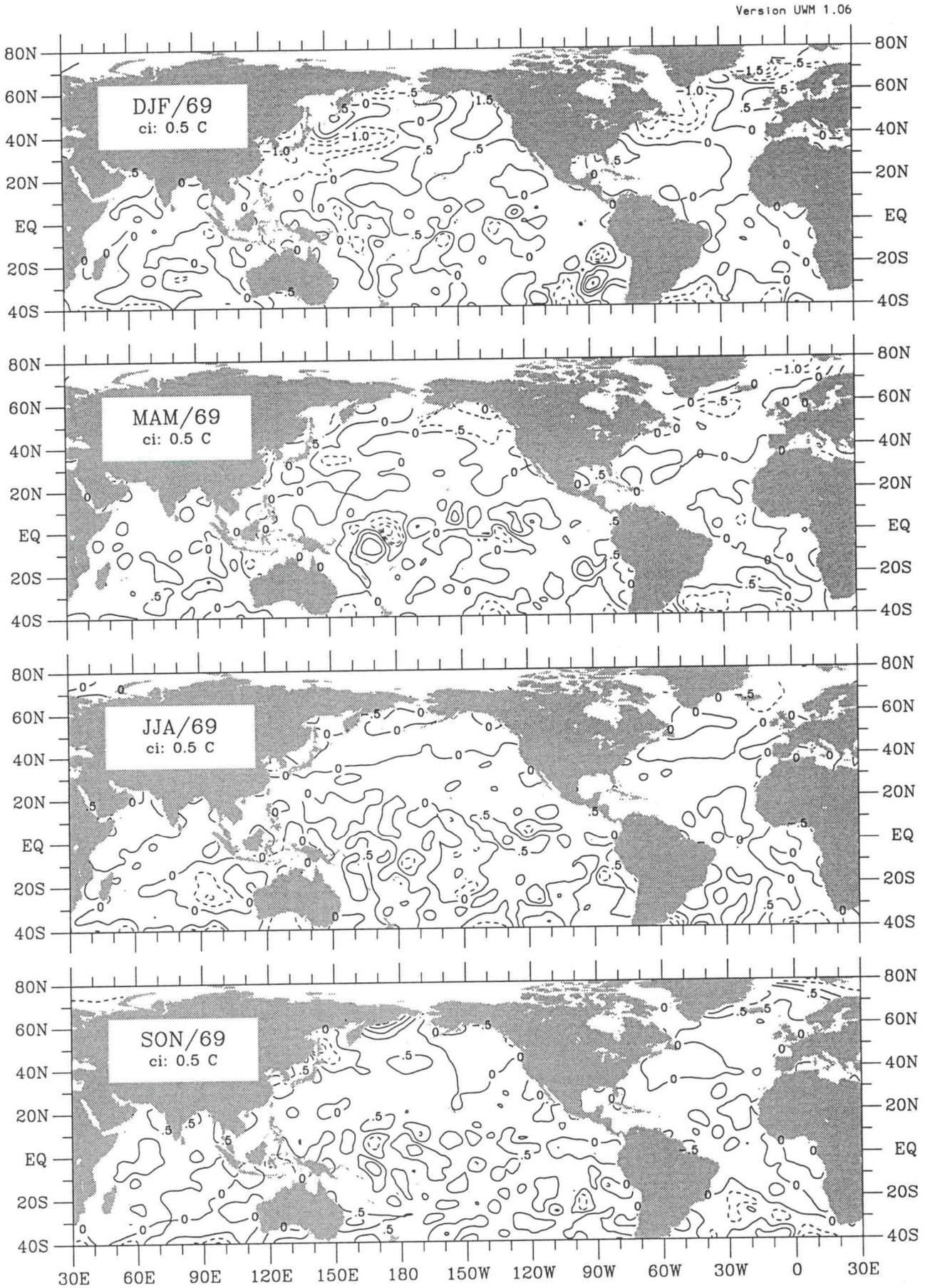

Figure dT-30. sst minus sat seasonal anomaly for 1969.

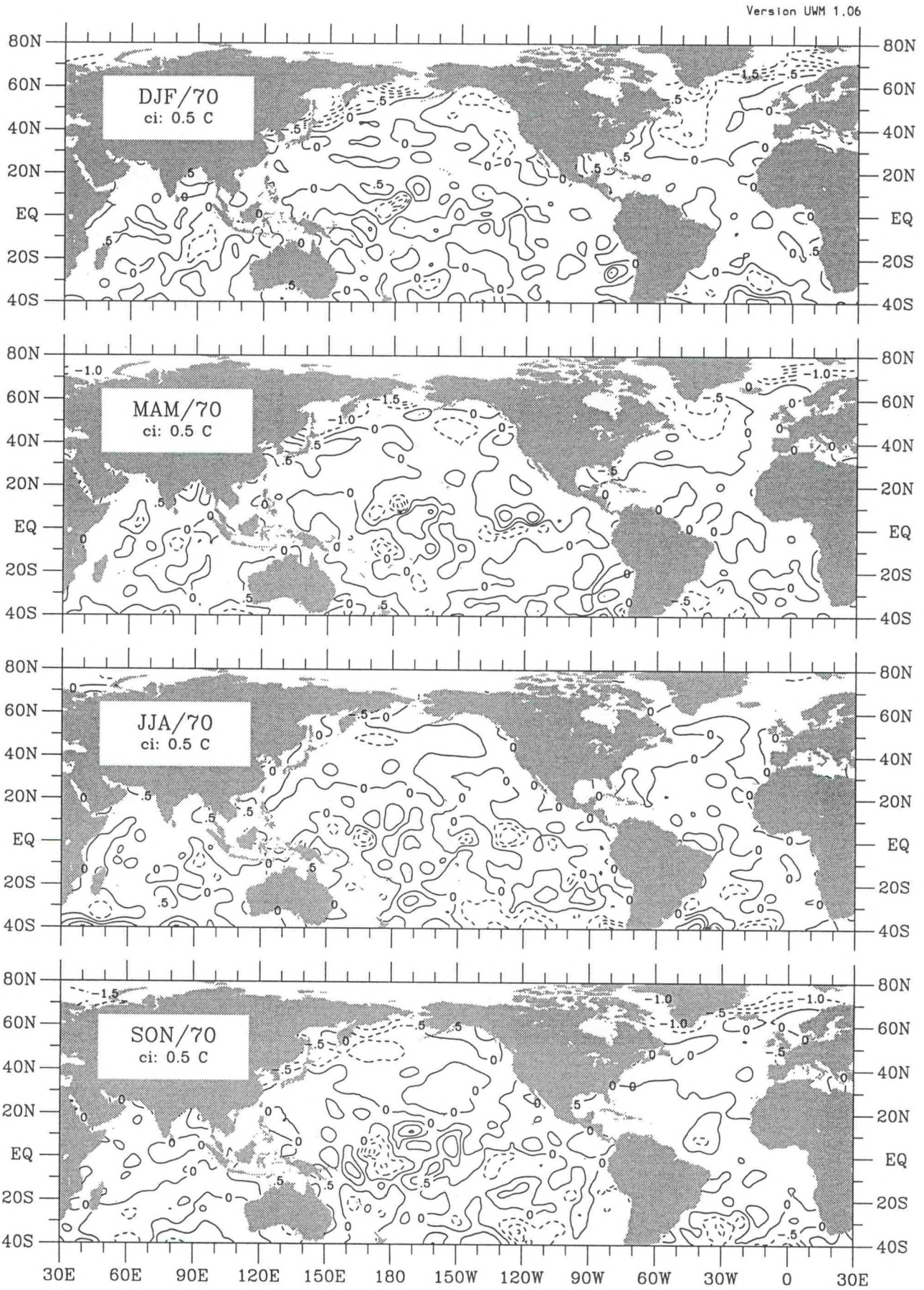

Figure dT-31. sst minus sat seasonal anomaly for 1970.

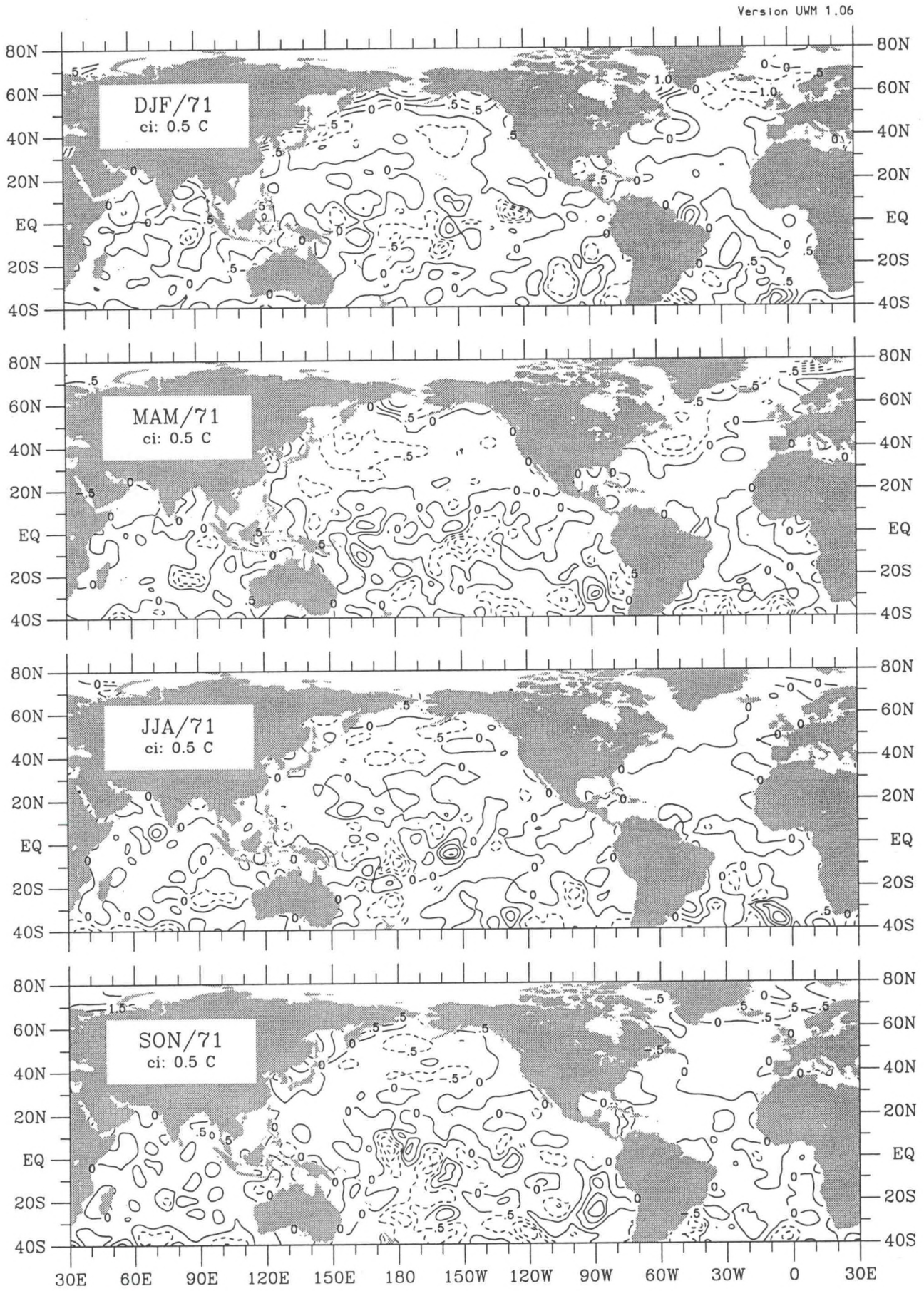

Figure dT-32. sst minus sat seasonal anomaly for 1971.

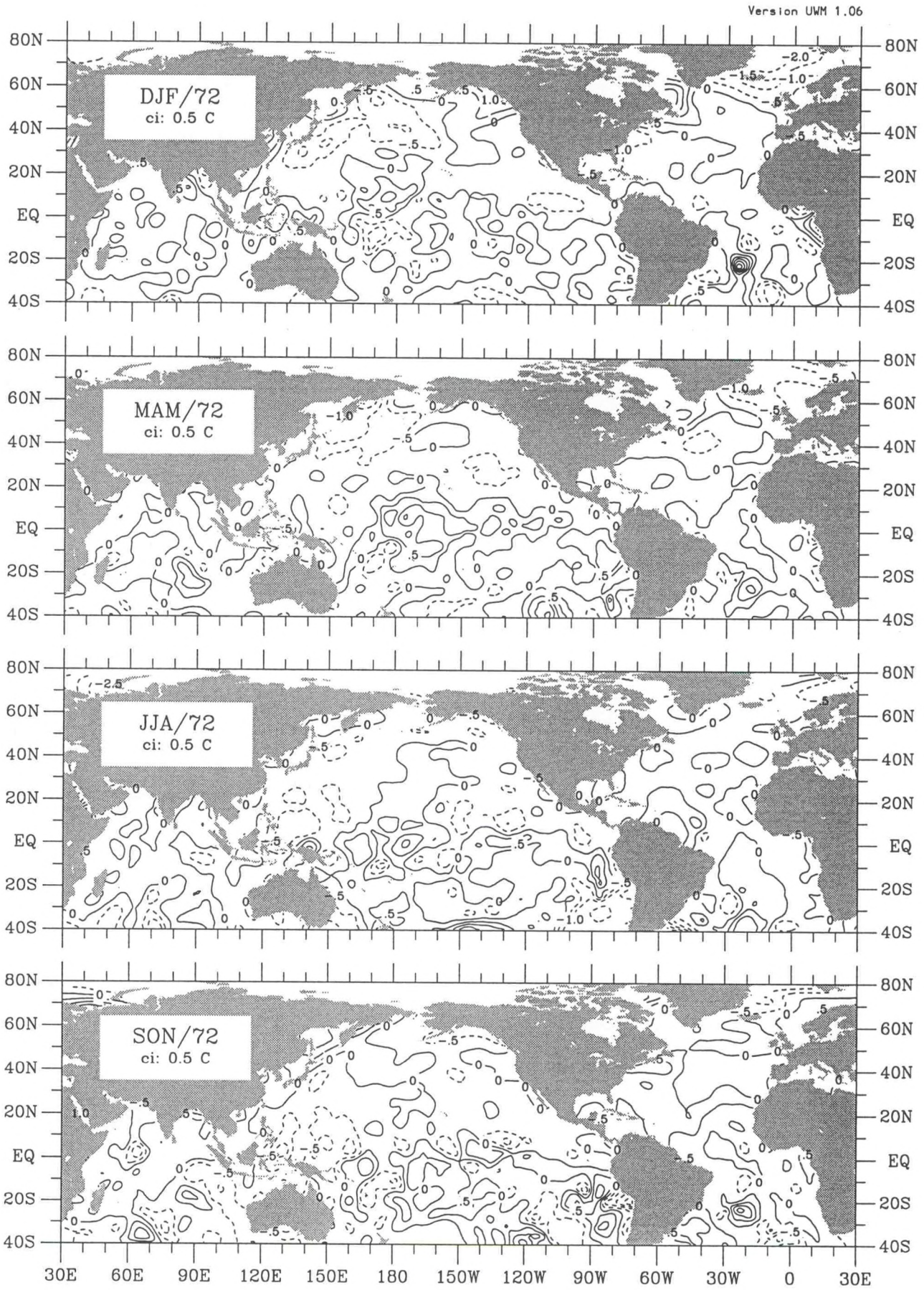

Figure dT-33. sst minus sat seasonal anomaly for 1972.

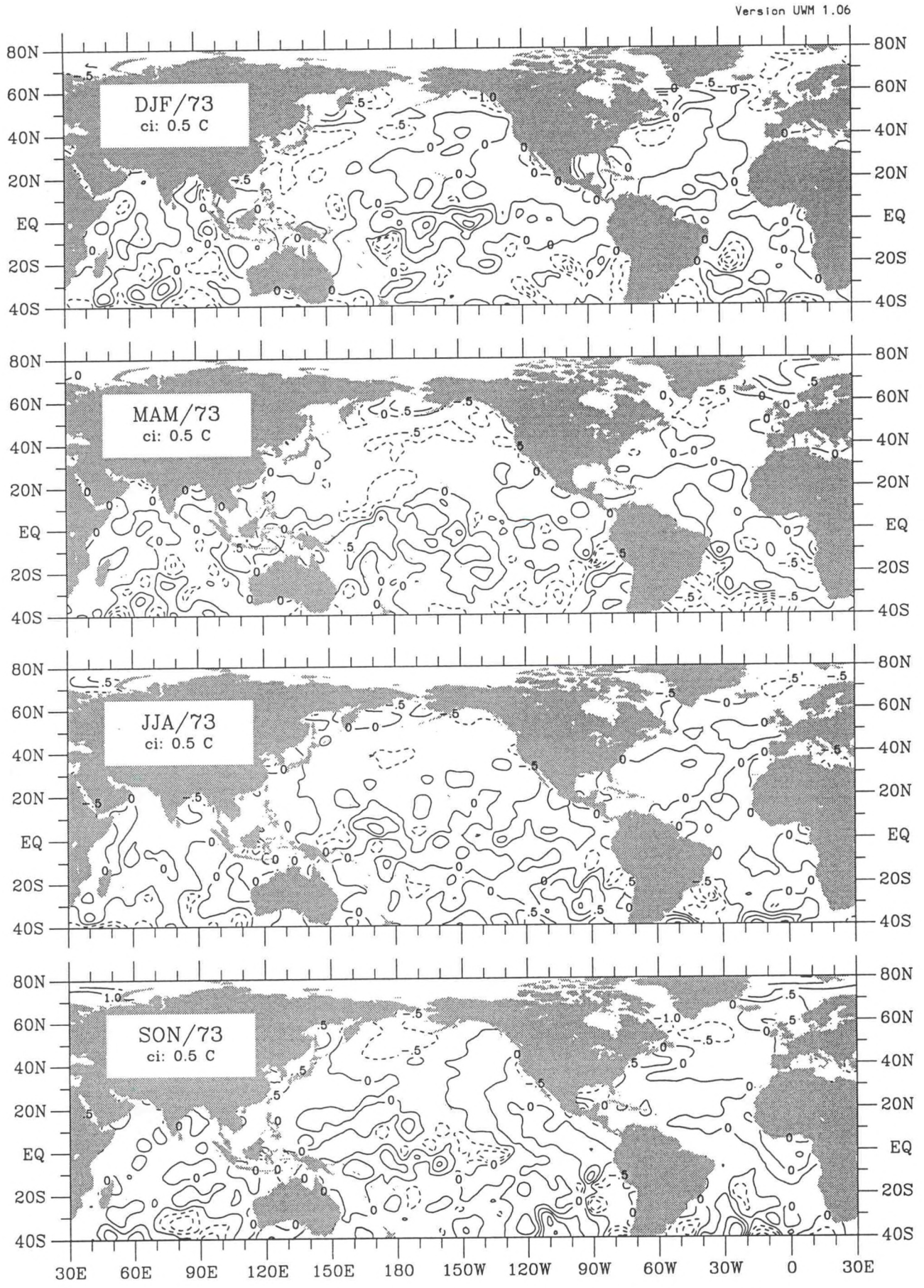

Figure dT-34. sst minus sat seasonal anomaly for 1973.

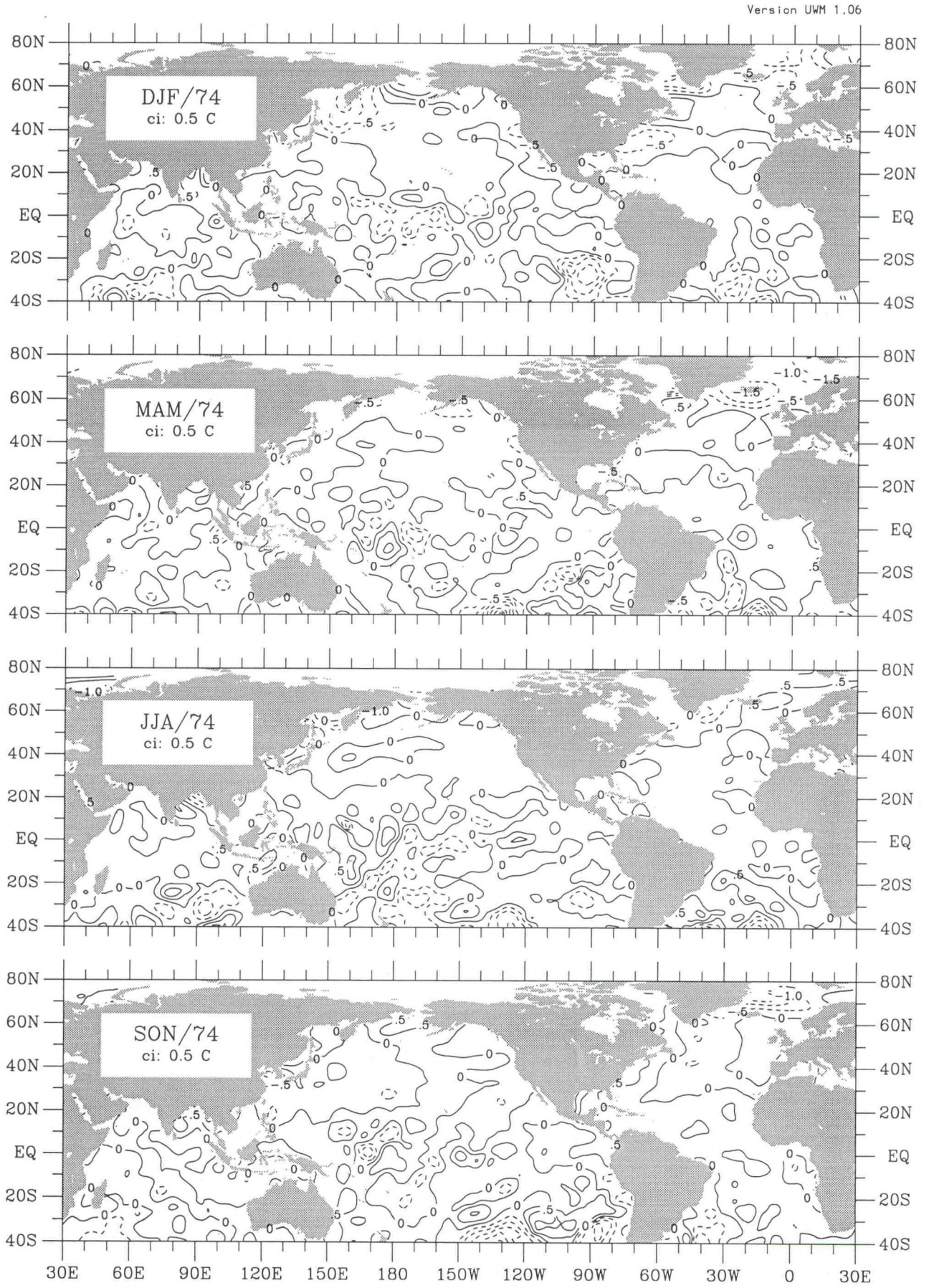

Figure dT-35. sst minus sat seasonal anomaly for 1974.

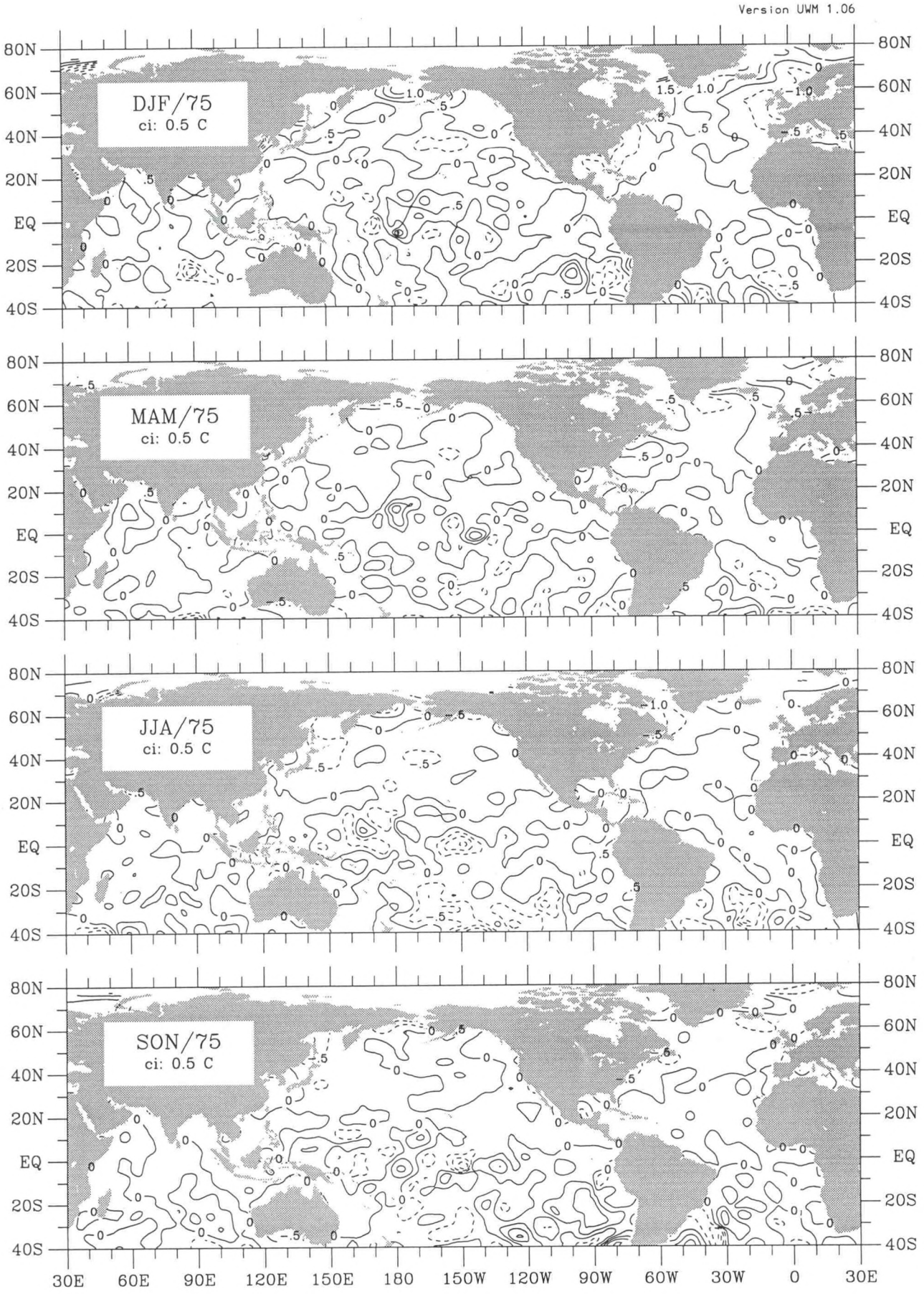

Figure dT-36. sst minus sat seasonal anomaly for 1975.

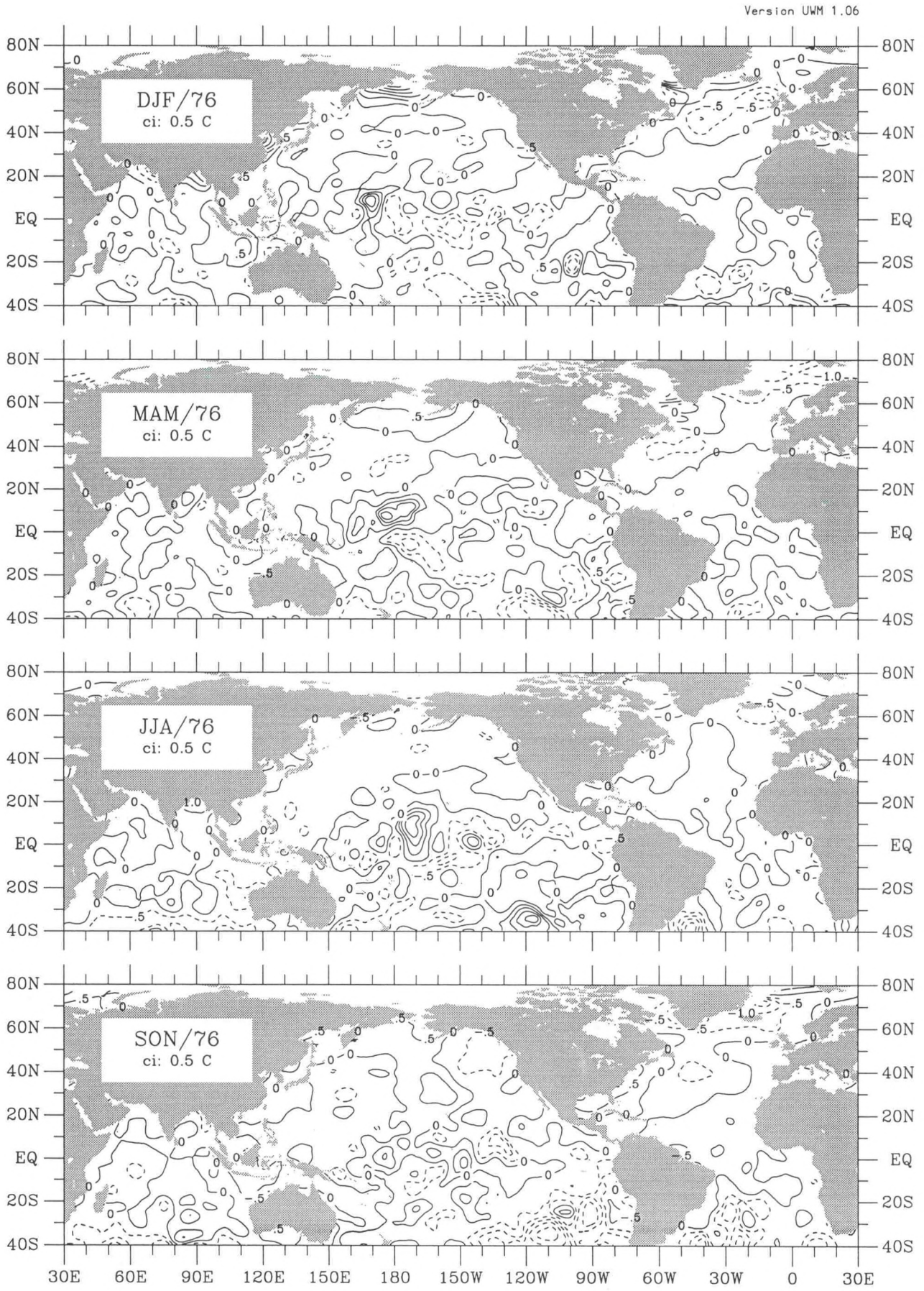

Figure dT-37. sst minus sat seasonal anomaly for 1976.

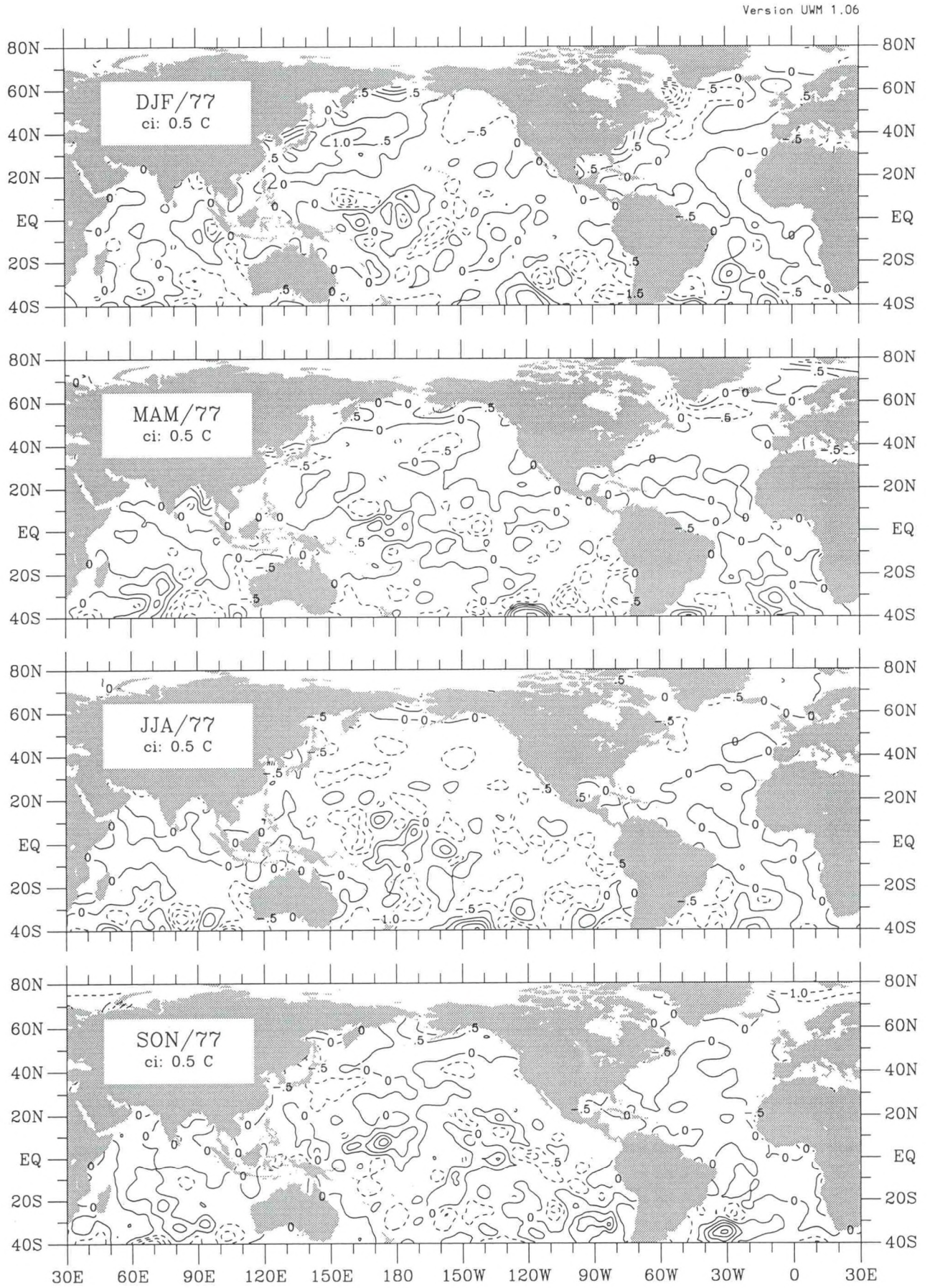

Figure dT-38. sst minus sat seasonal anomaly for 1977.

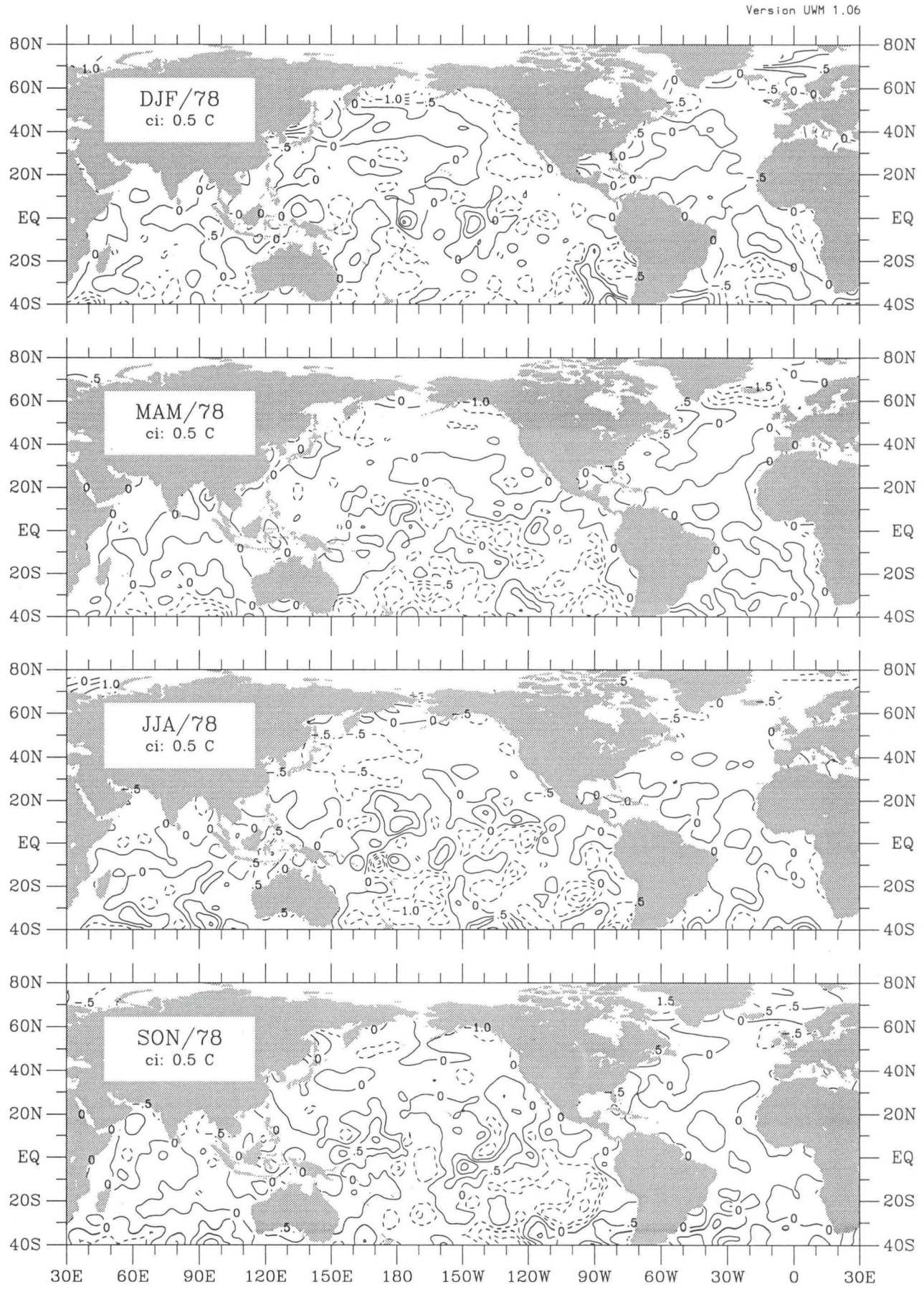

Figure dT-39. sst minus sat seasonal anomaly for 1978.

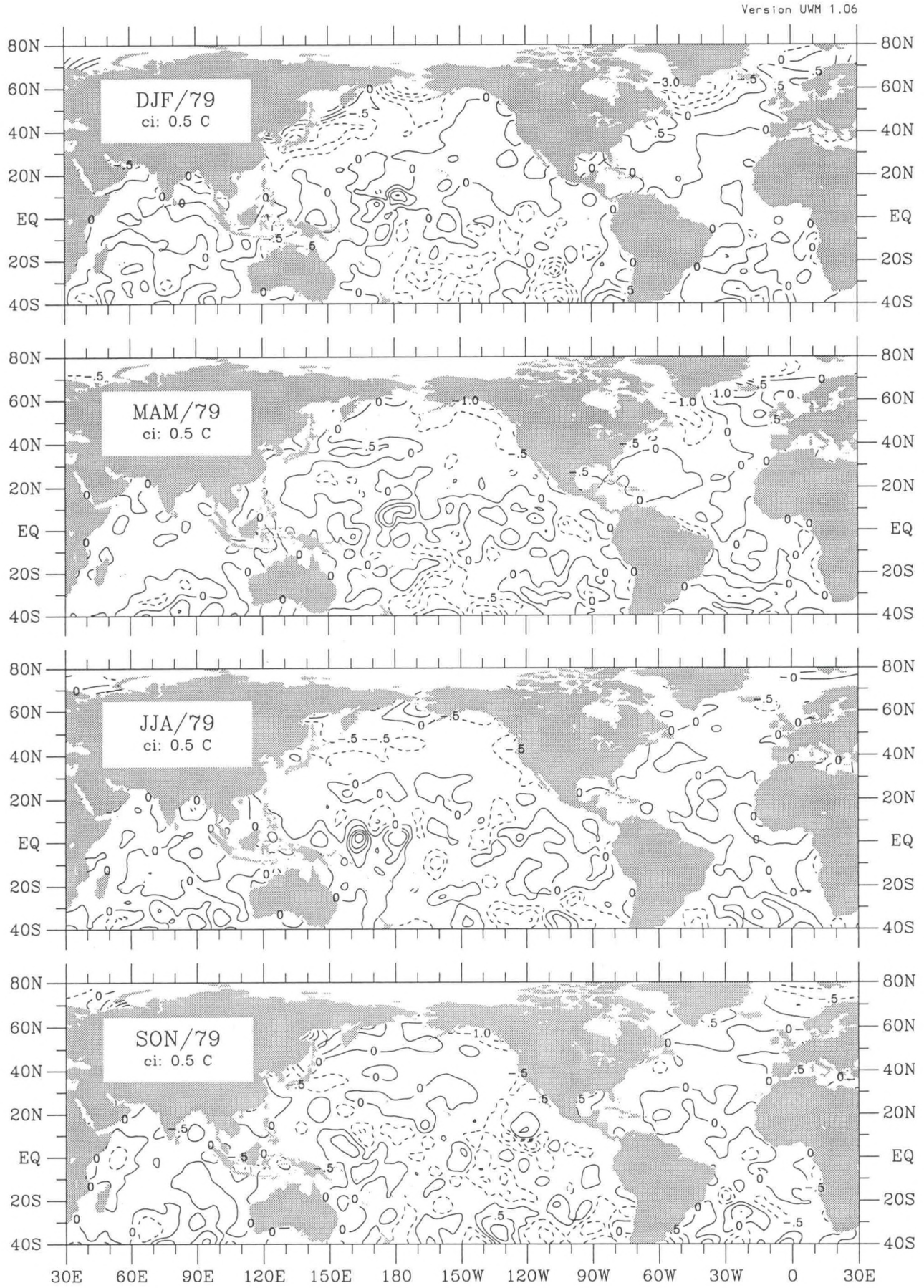

Figure dT-40. sst minus sat seasonal anomaly for 1979.

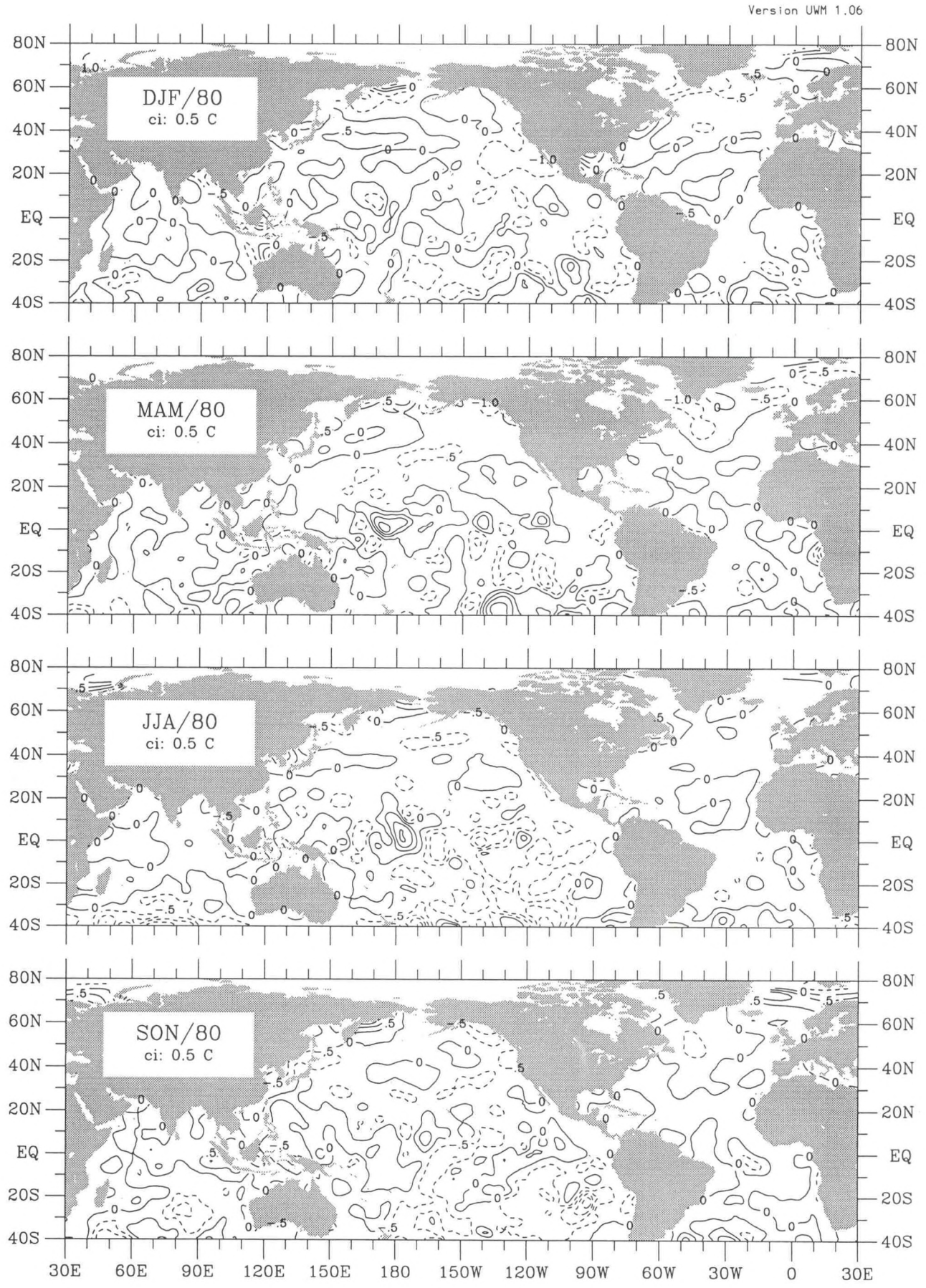

Figure dT-41. sst minus sat seasonal anomaly for 1980.

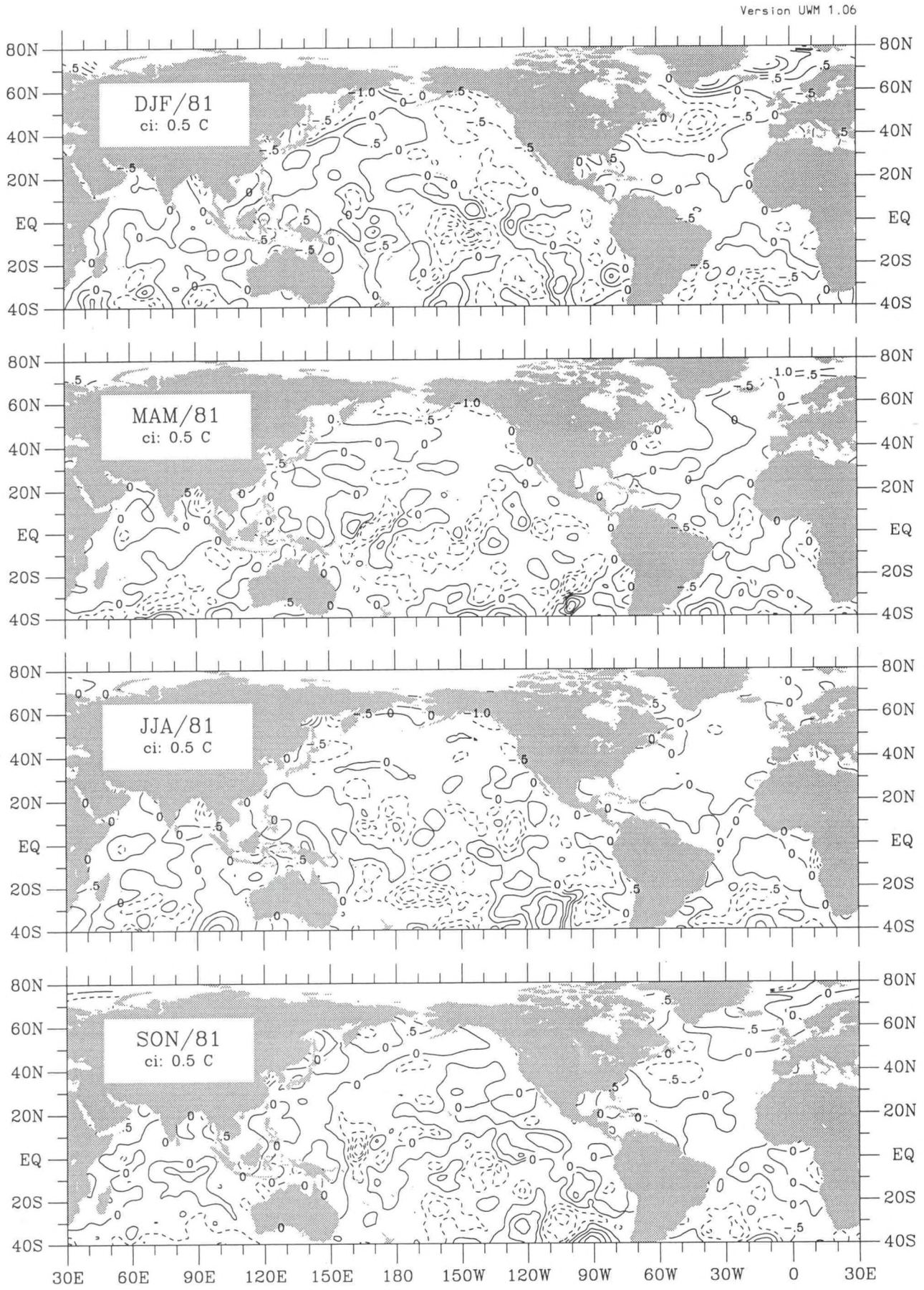

Figure dT-42. sst minus sat seasonal anomaly for 1981.

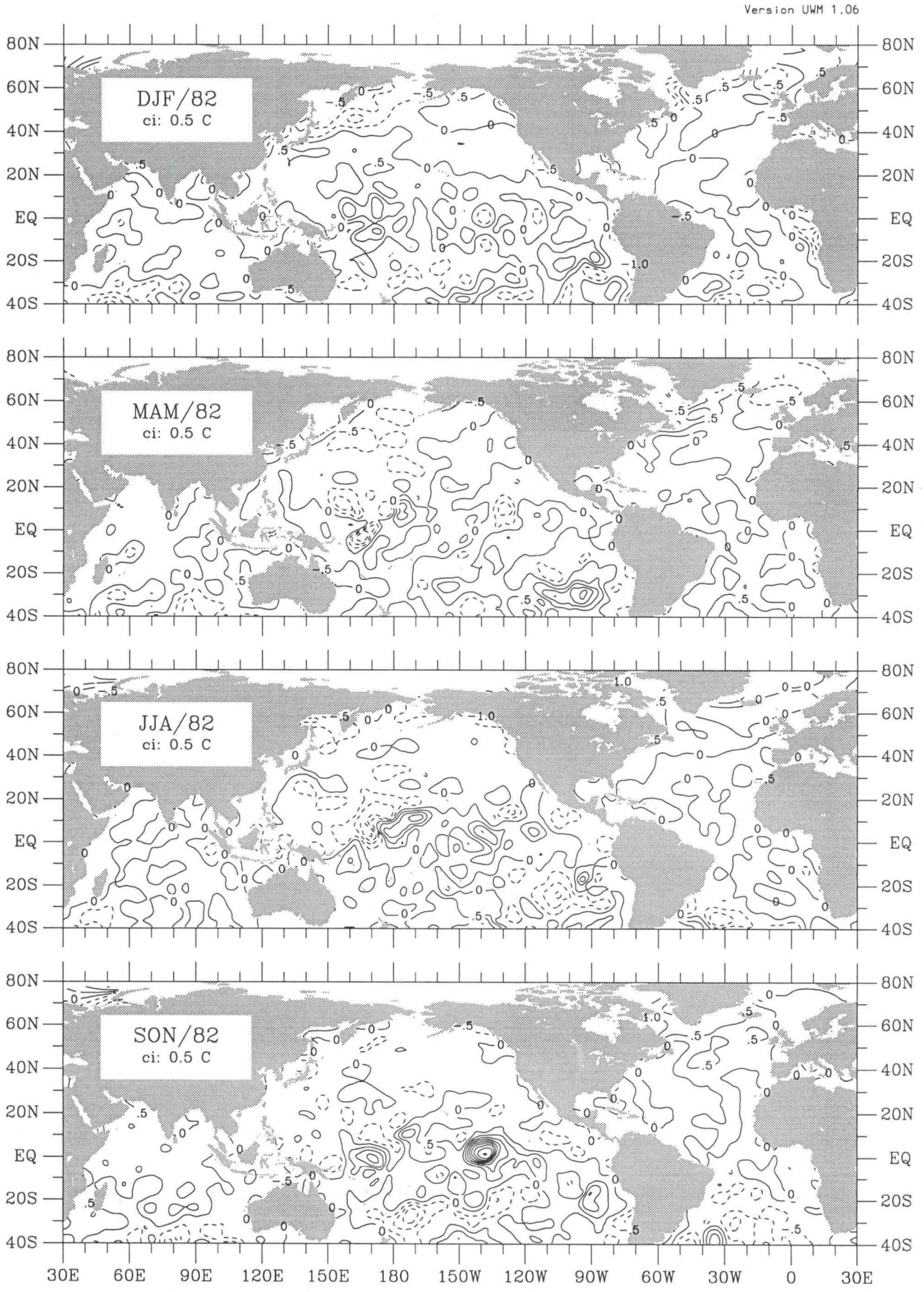

Figure dT-43. sst minus sat seasonal anomaly for 1982.

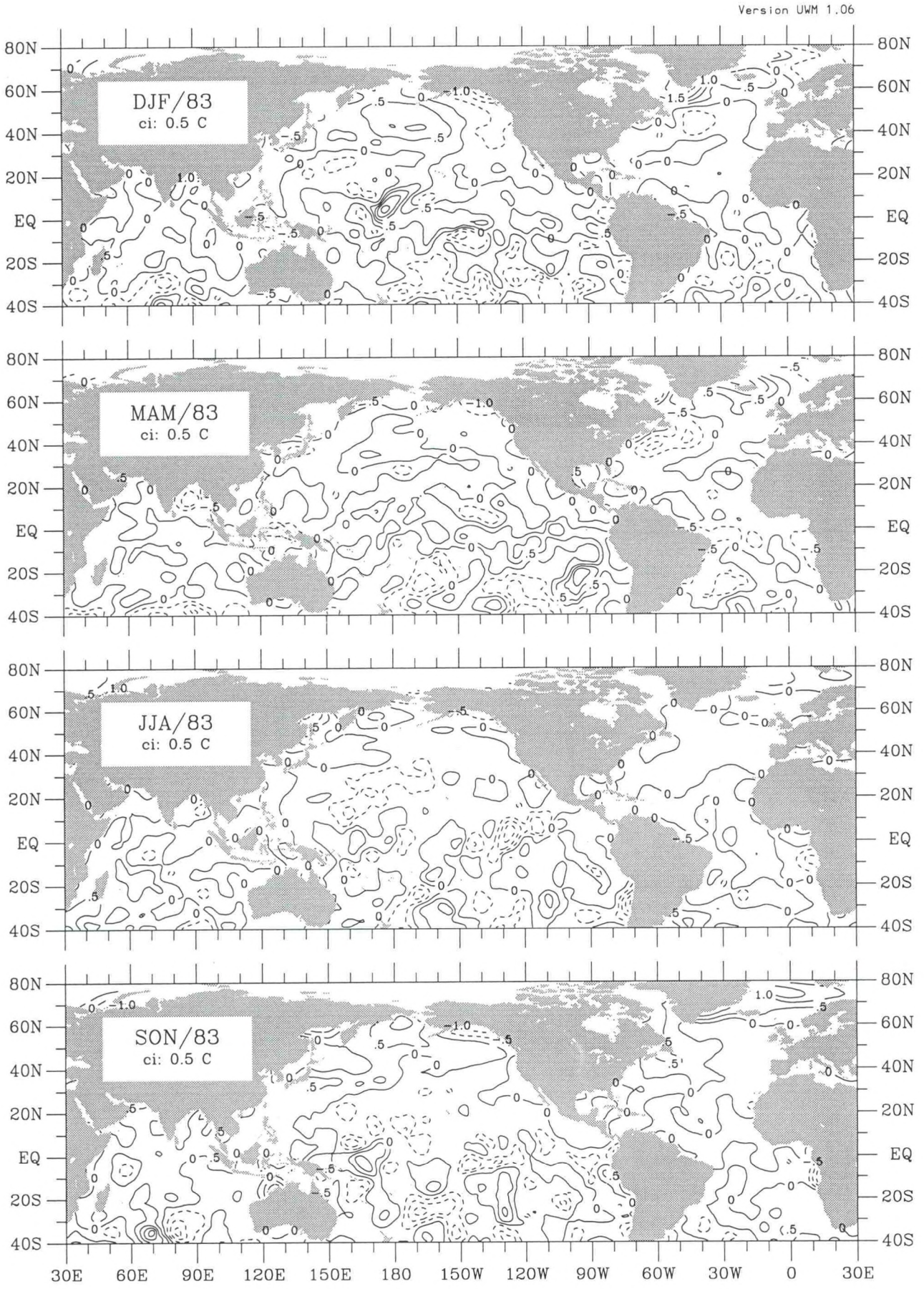

Figure dT-44. sst minus sat seasonal anomaly for 1983.

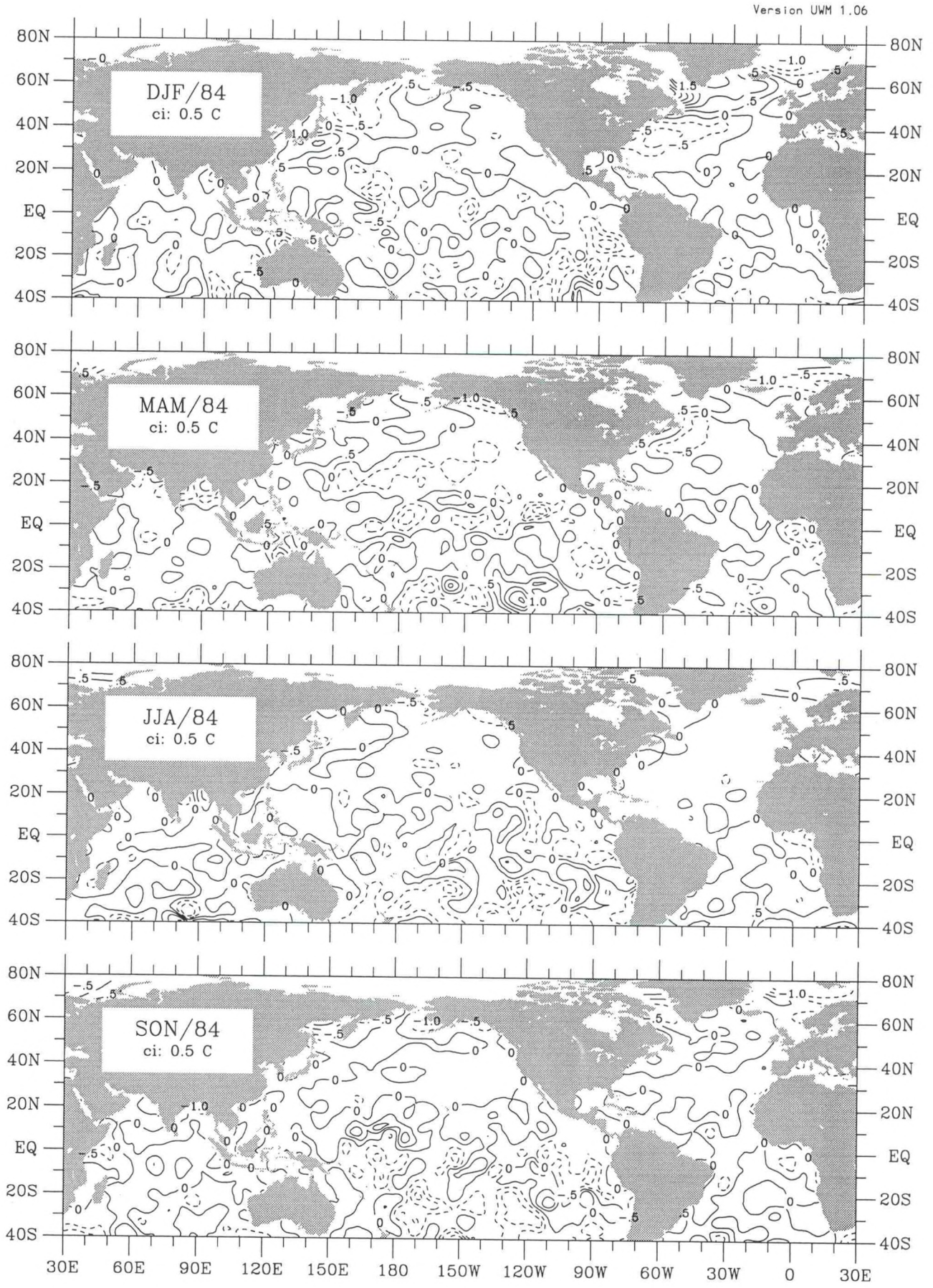

Figure dT-45. sst minus sat seasonal anomaly for 1984.

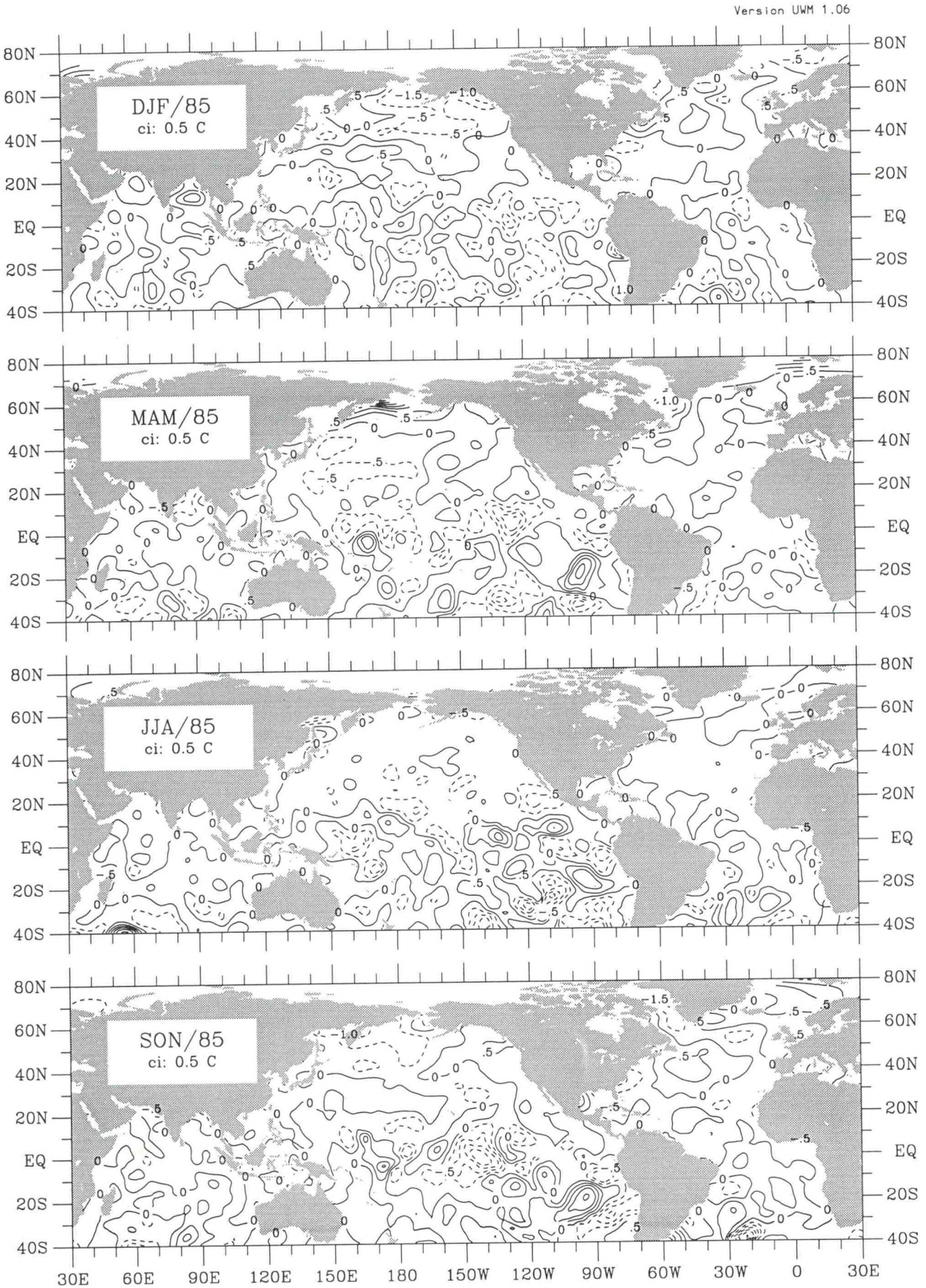

Figure dT-46. sst minus sat seasonal anomaly for 1985.

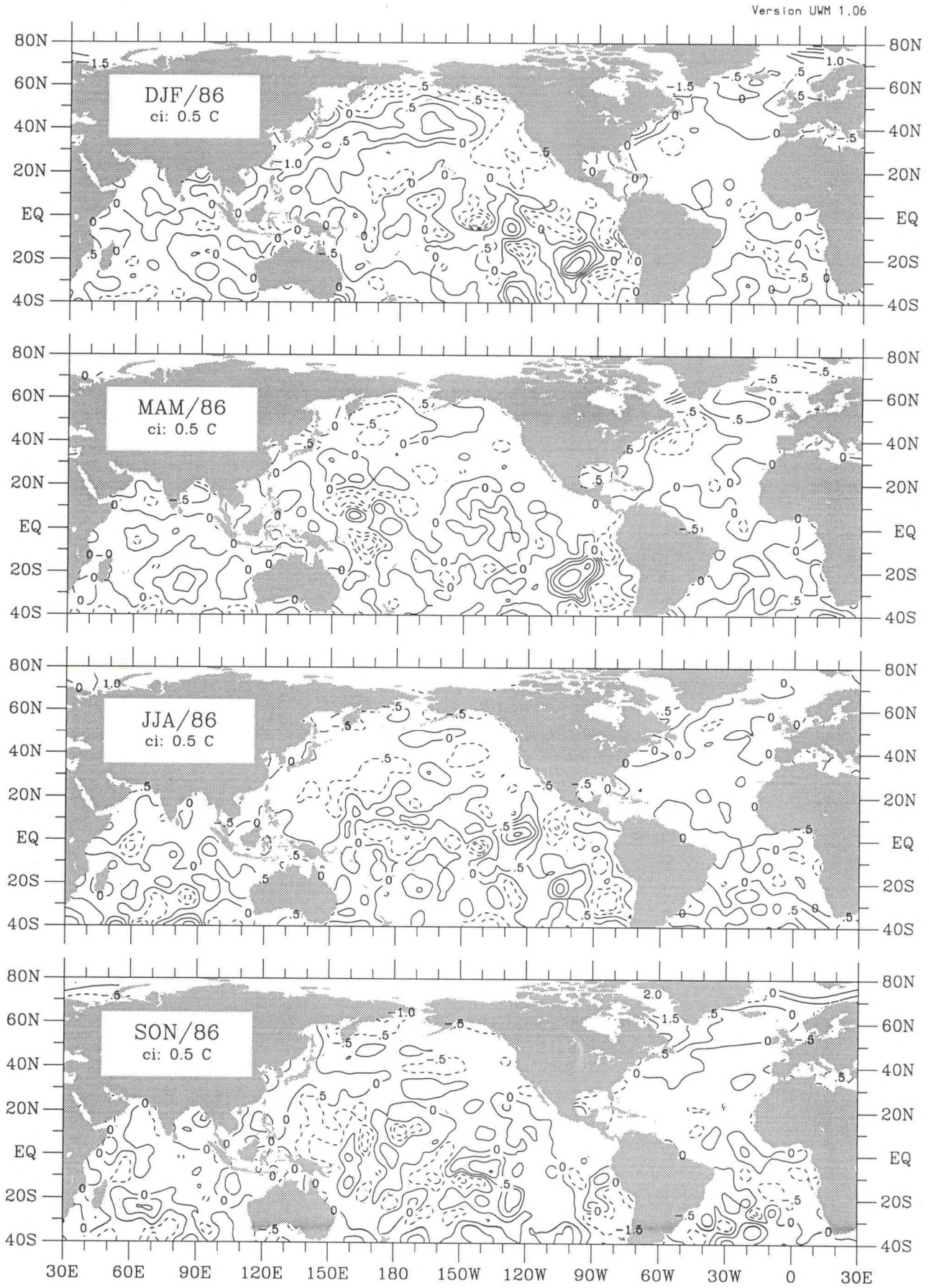

Figure dT-47. sst minus sat seasonal anomaly for 1986.

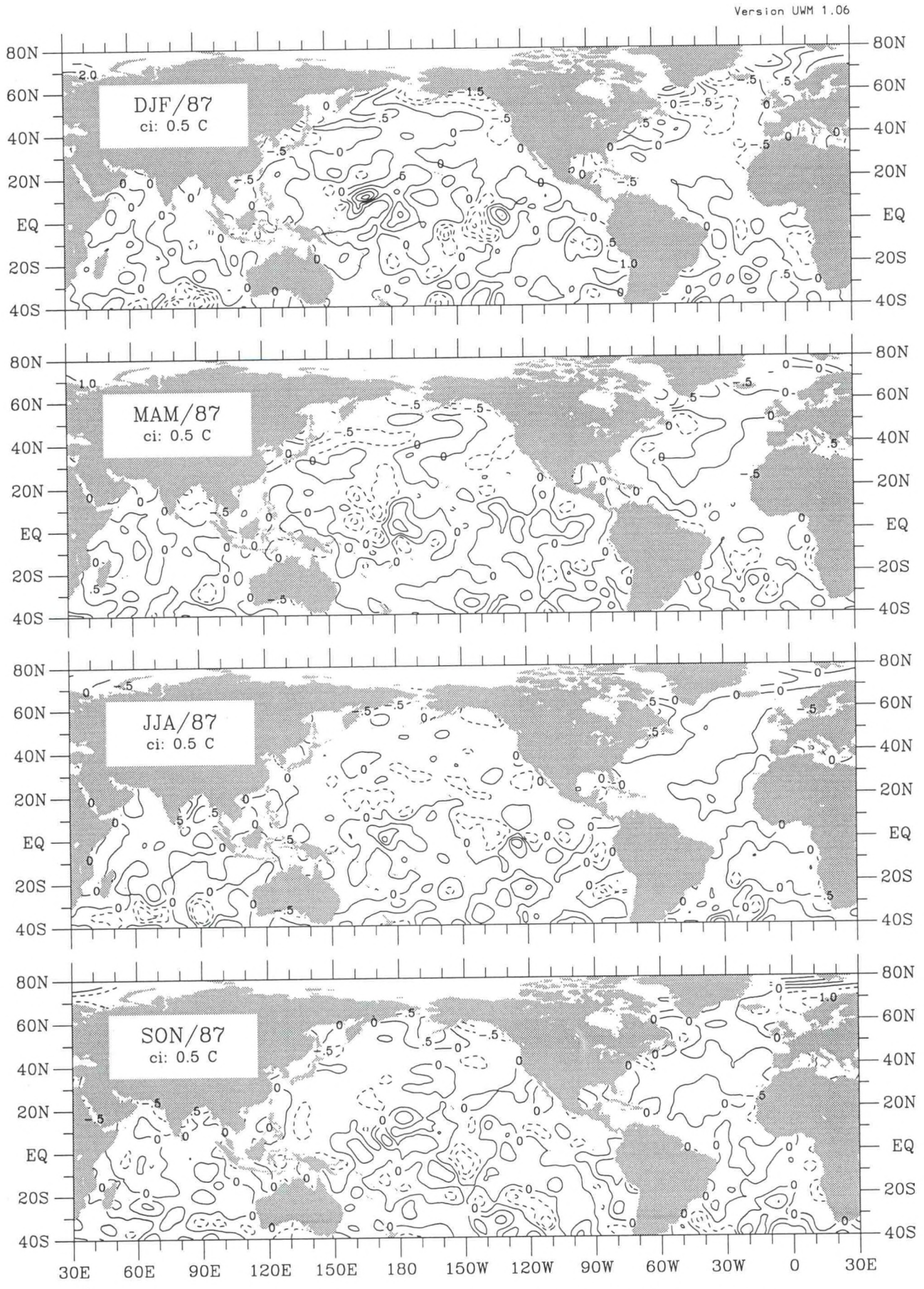

Figure dT-48. sst minus sat seasonal anomaly for 1987.

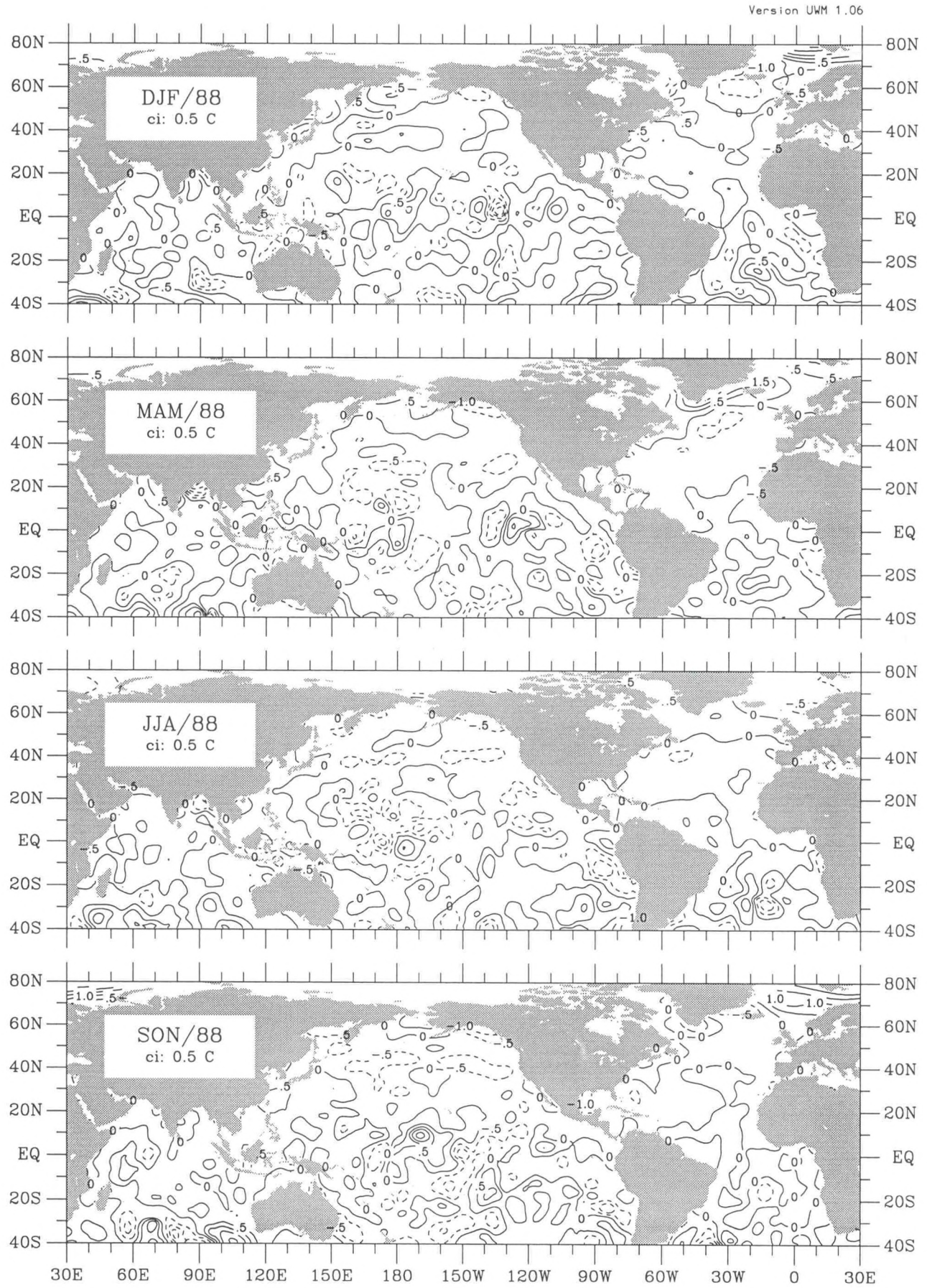

Figure dT-49. sst minus sat seasonal anomaly for 1988.

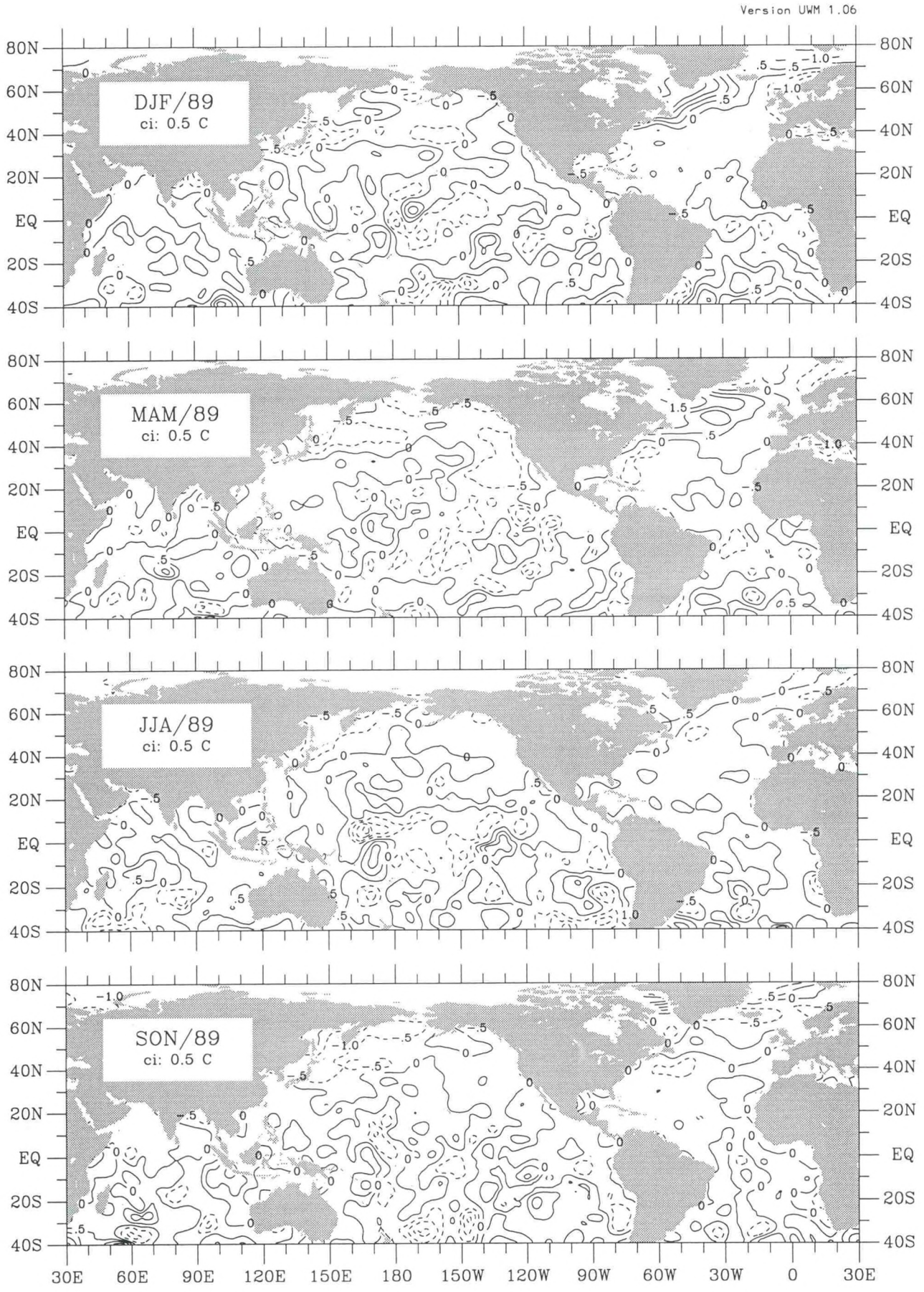

Figure dT-50. sst minus sat seasonal anomaly for 1989.

11 Relative humidity

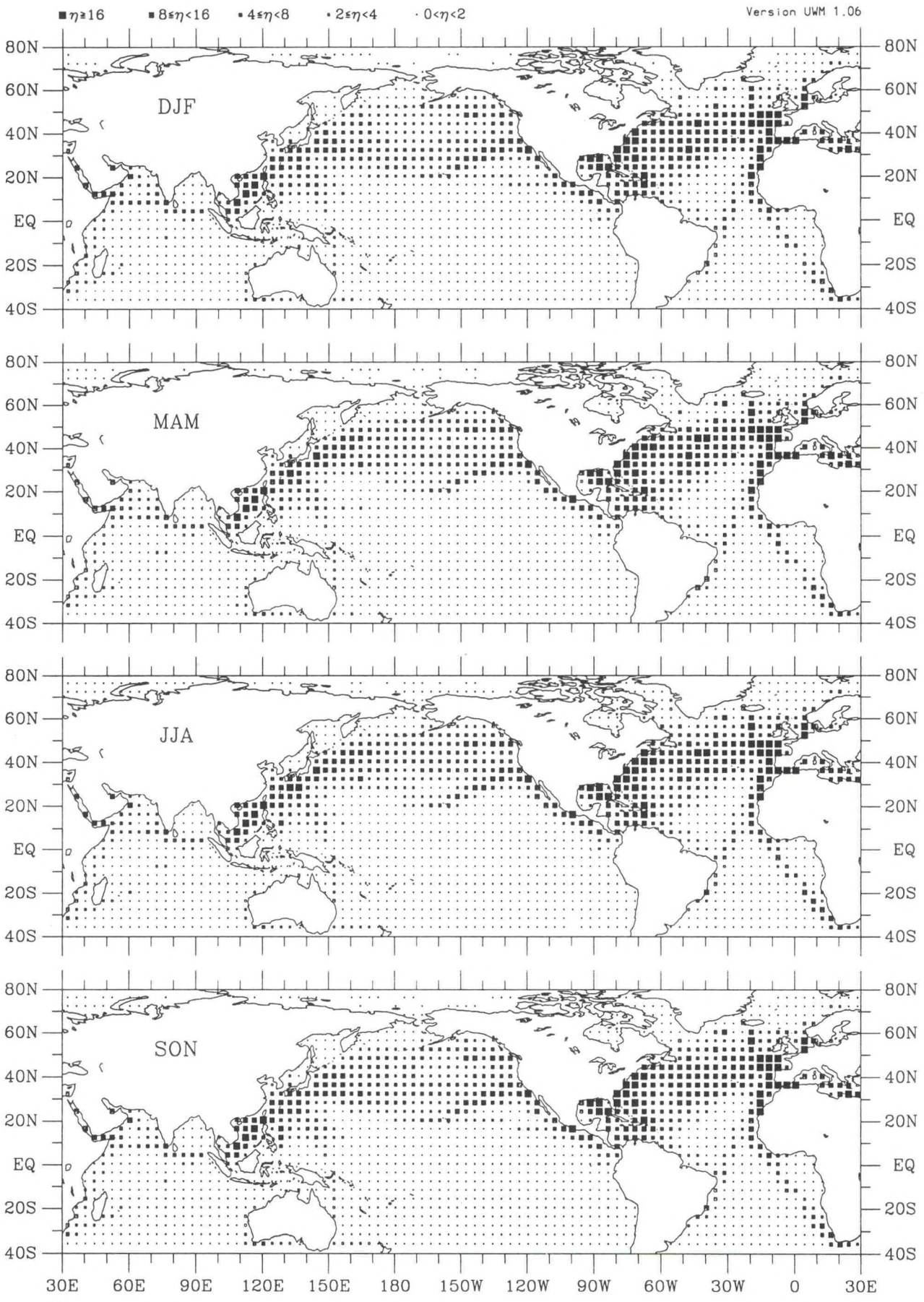

Figure rh-1. Relative humidity seasonal observation density (1945-89).

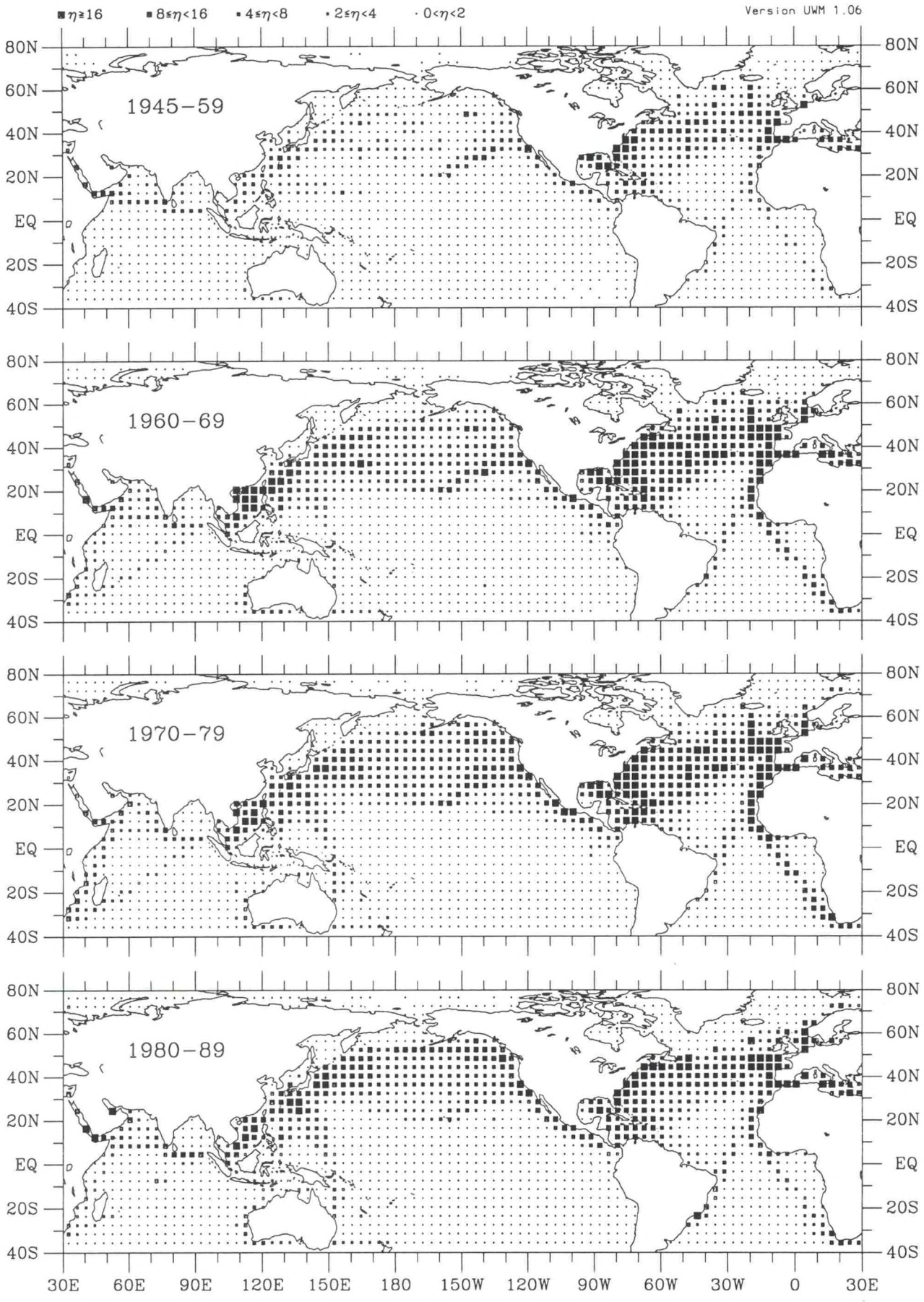

Figure rh-2. Relative humidity decadal observation density.

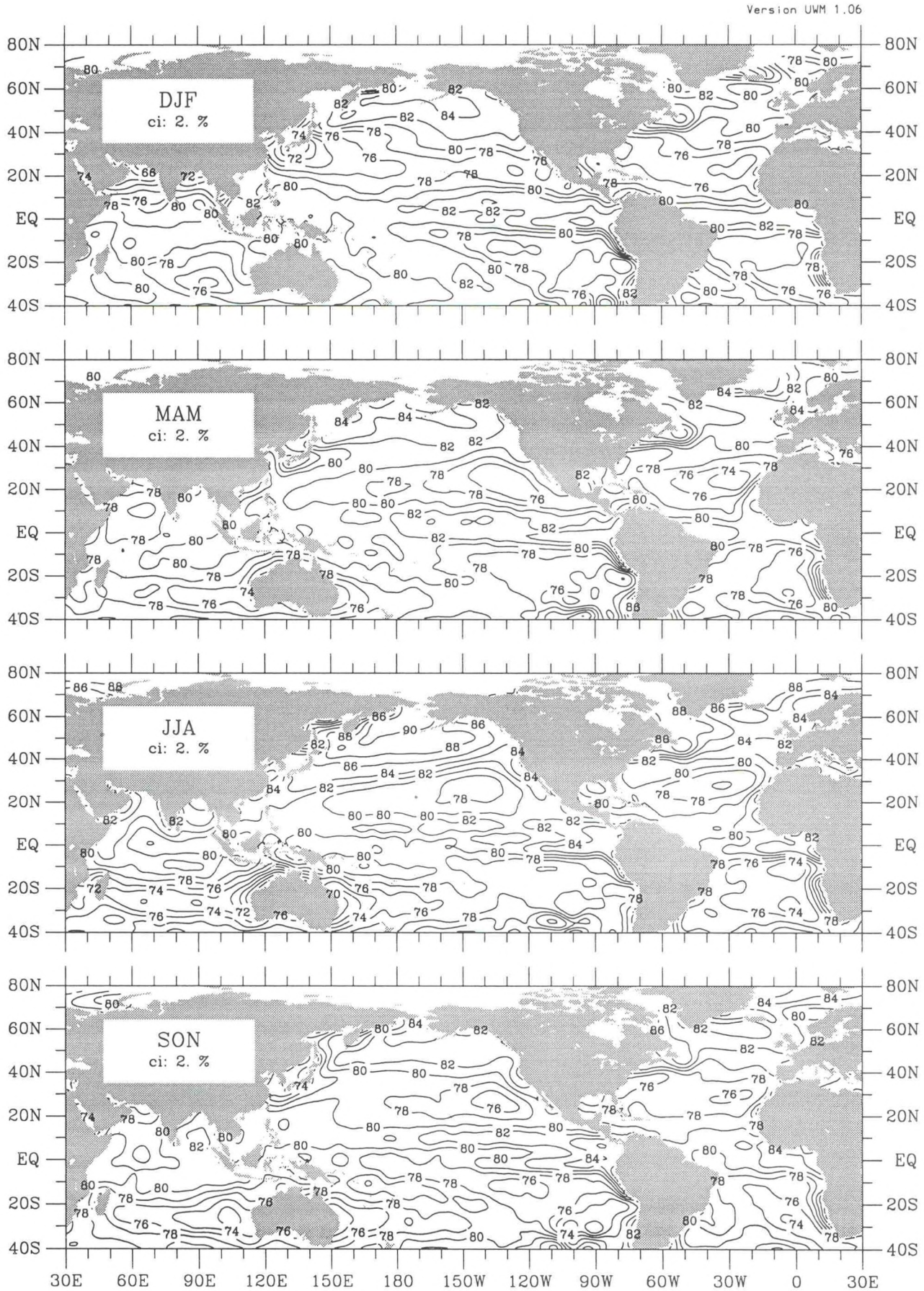

Figure rh-3. Relative humidity seasonal climatology (1945-89).

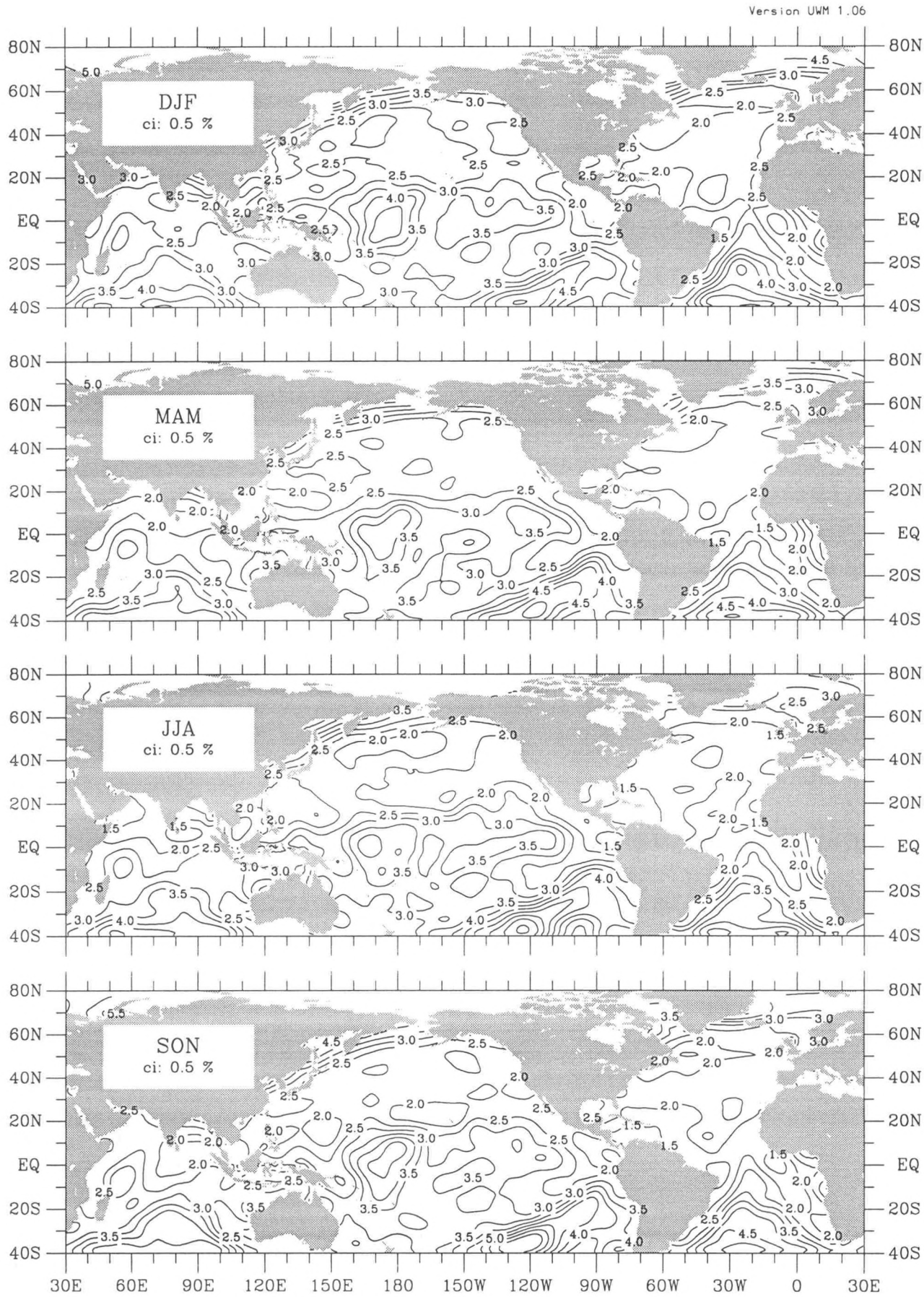

Figure rh-4. Relative humidity seasonal interannual std dev (1945-89).

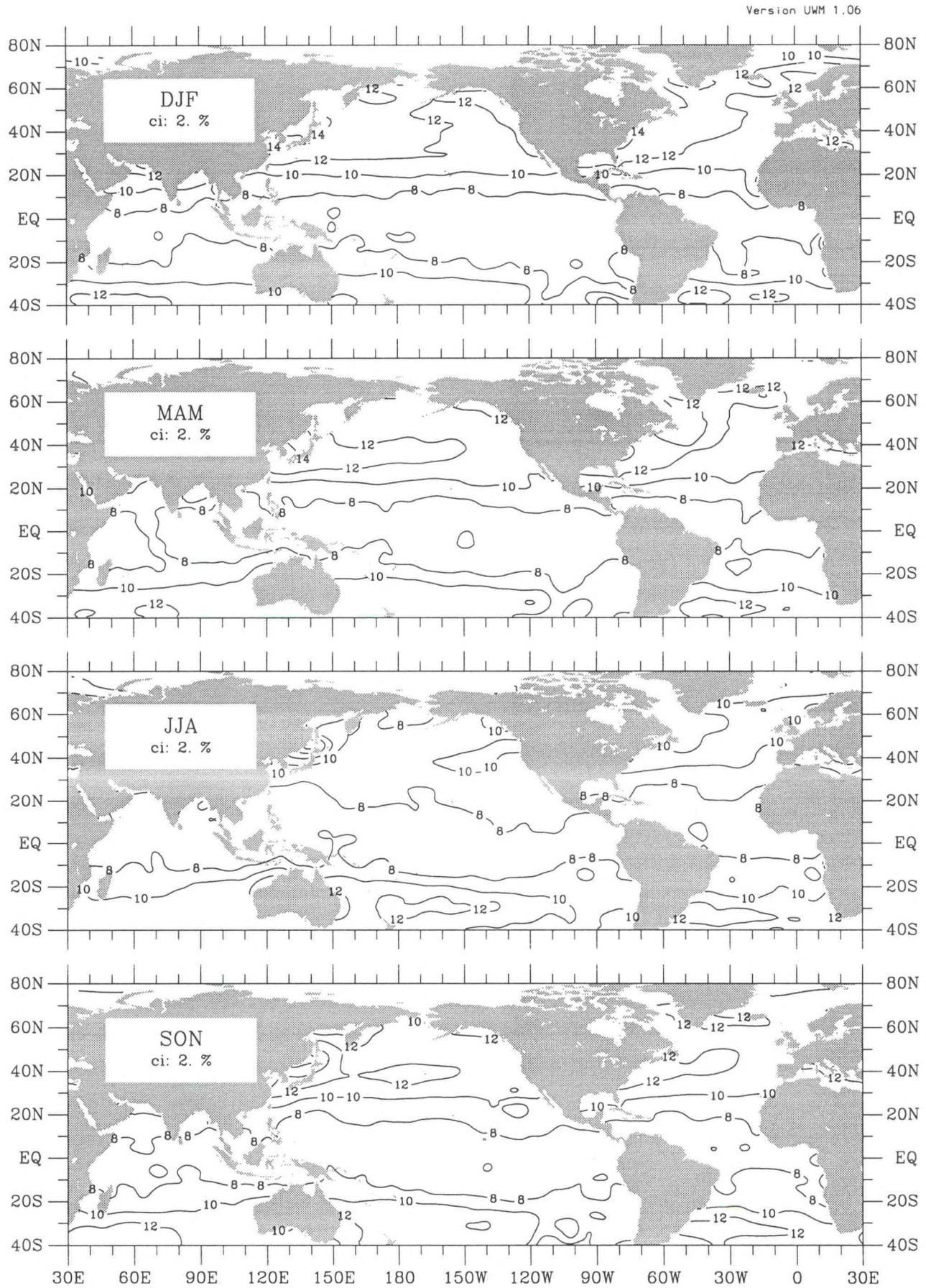

Figure rh-5. Relative humidity seasonal standard deviation (1945-89).

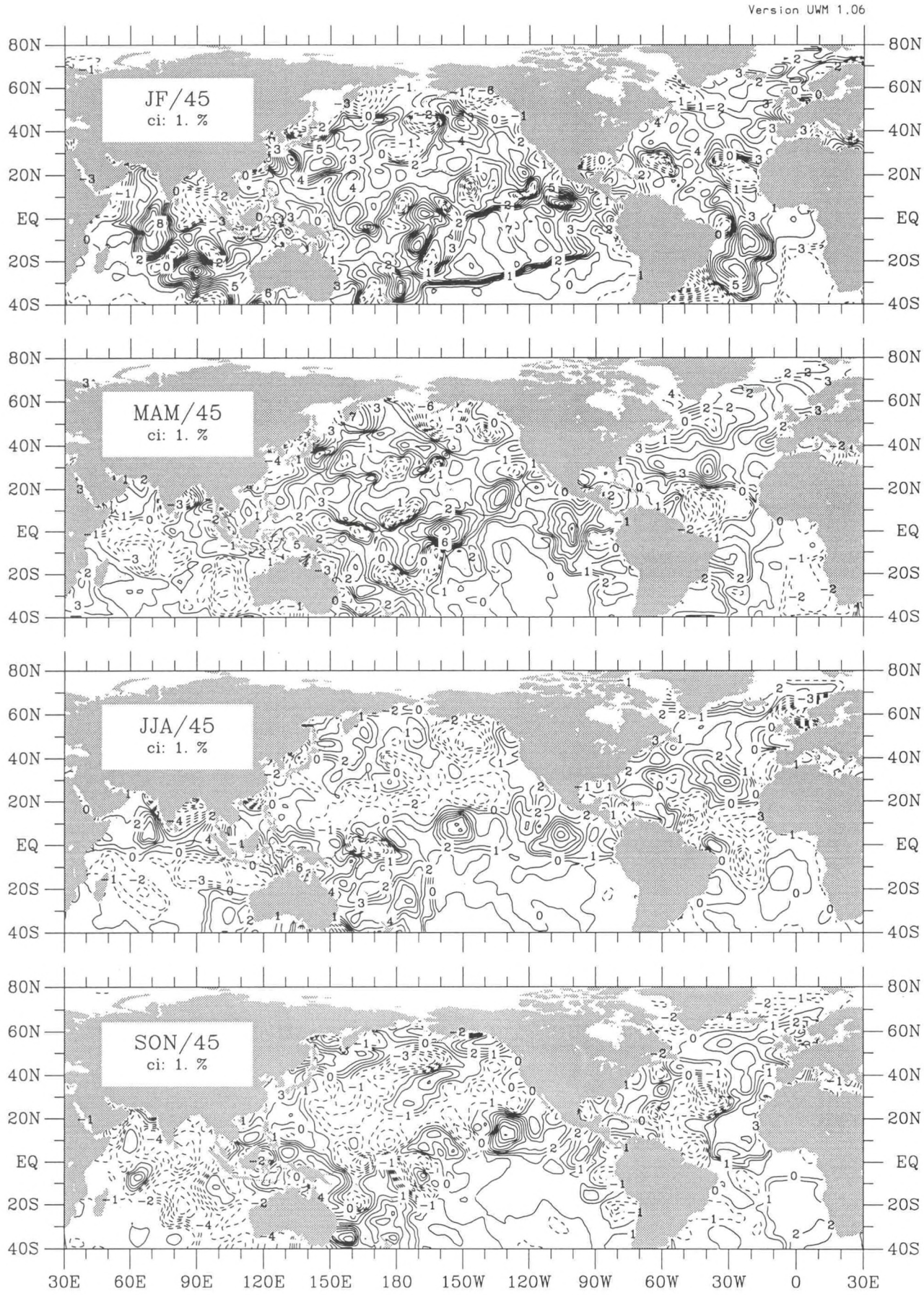

Figure rh-6. Relative humidity seasonal anomaly for 1945.

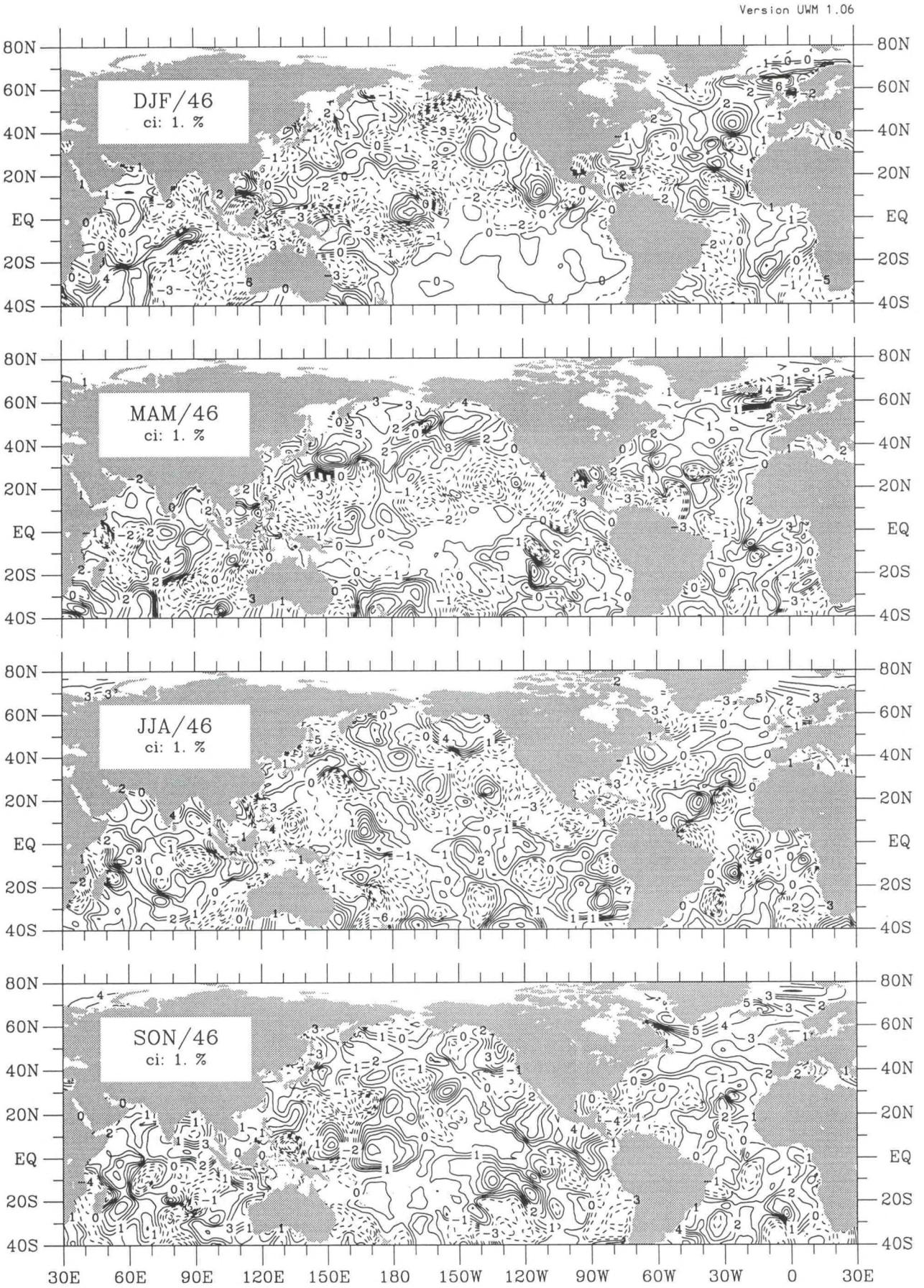

Figure rh-7. Relative humidity seasonal anomaly for 1946.

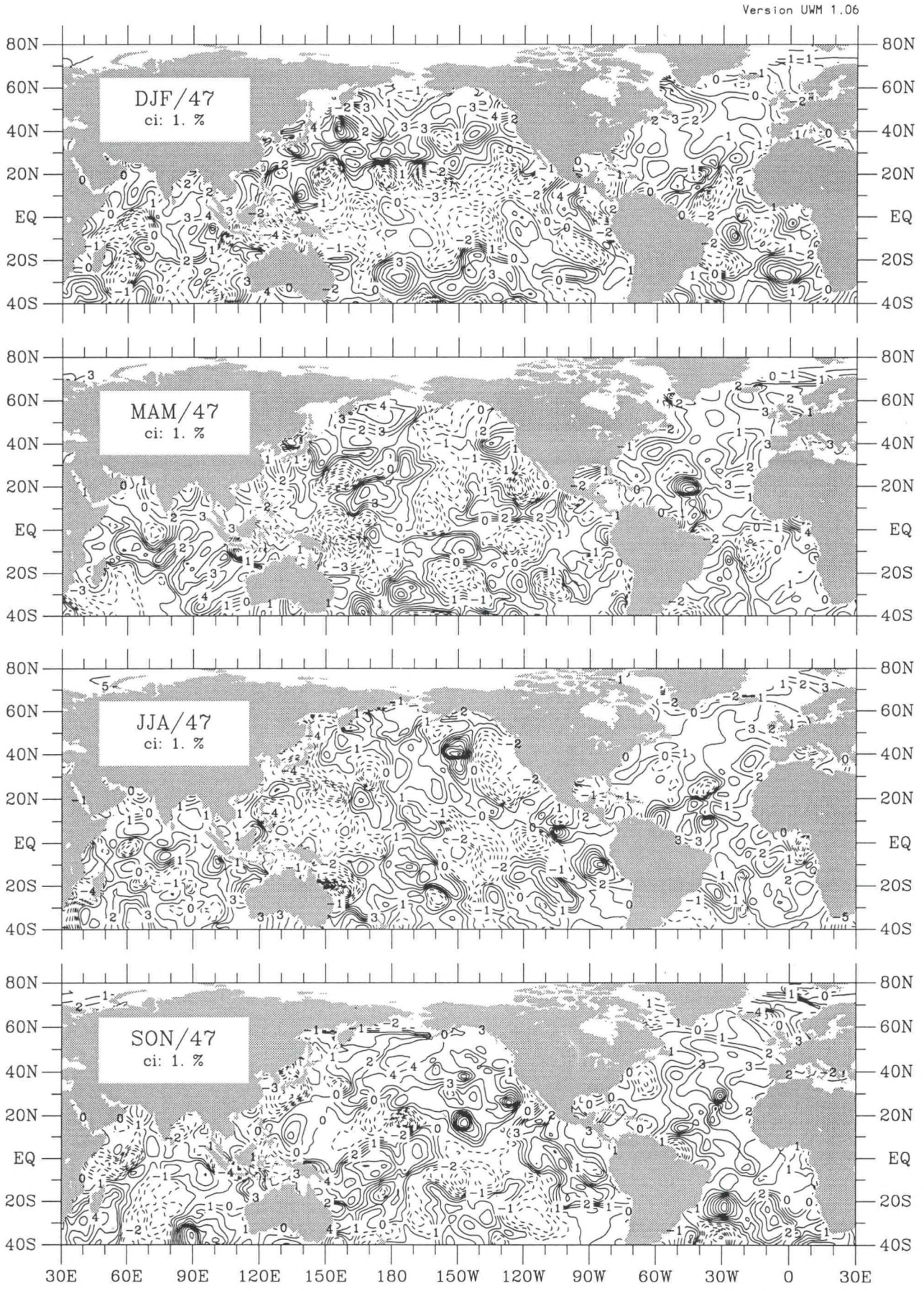

Figure rh-8. Relative humidity seasonal anomaly for 1947.

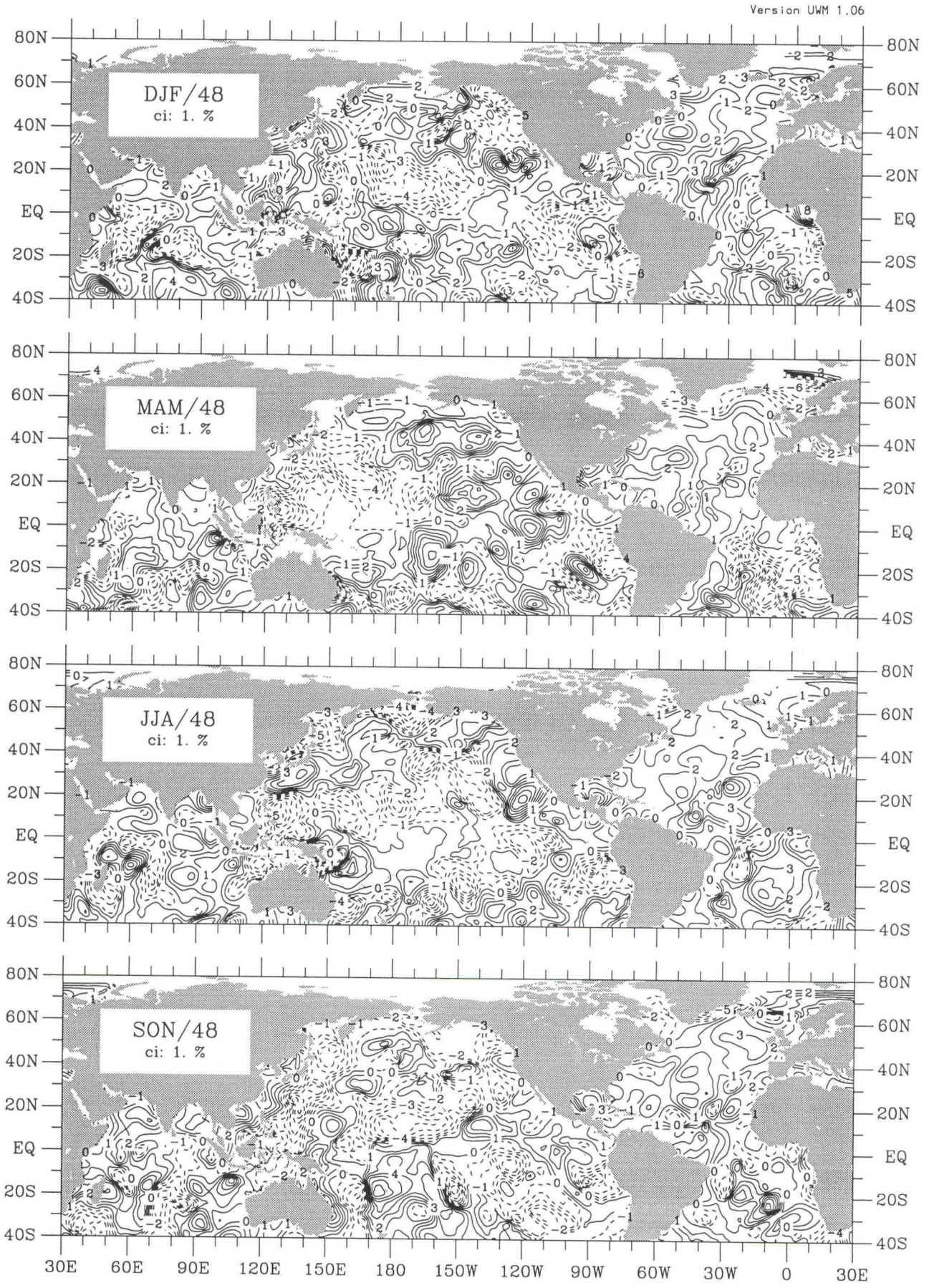

Figure rh-9. Relative humidity seasonal anomaly for 1948.

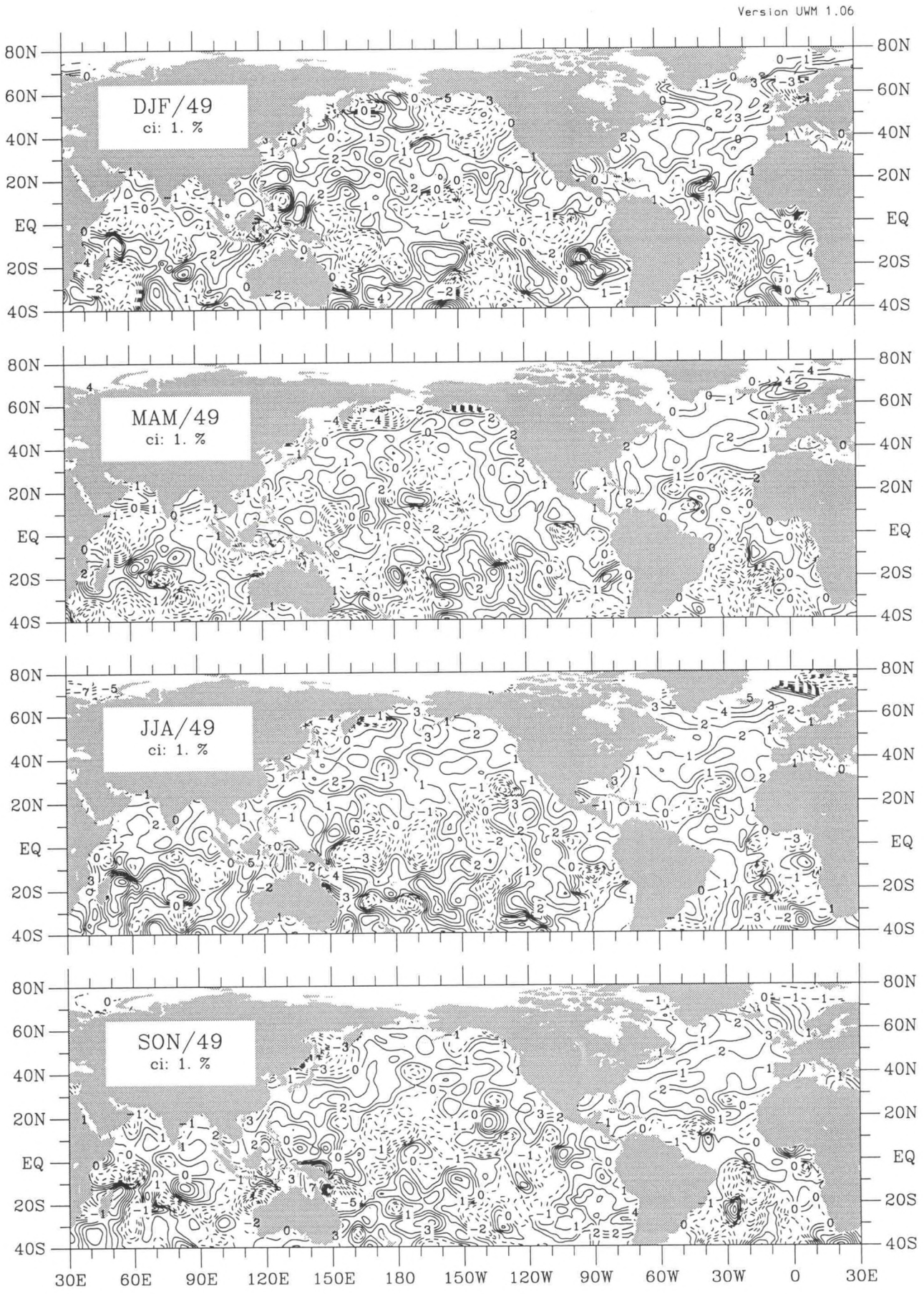

Figure rh-10. Relative humidity seasonal anomaly for 1949.

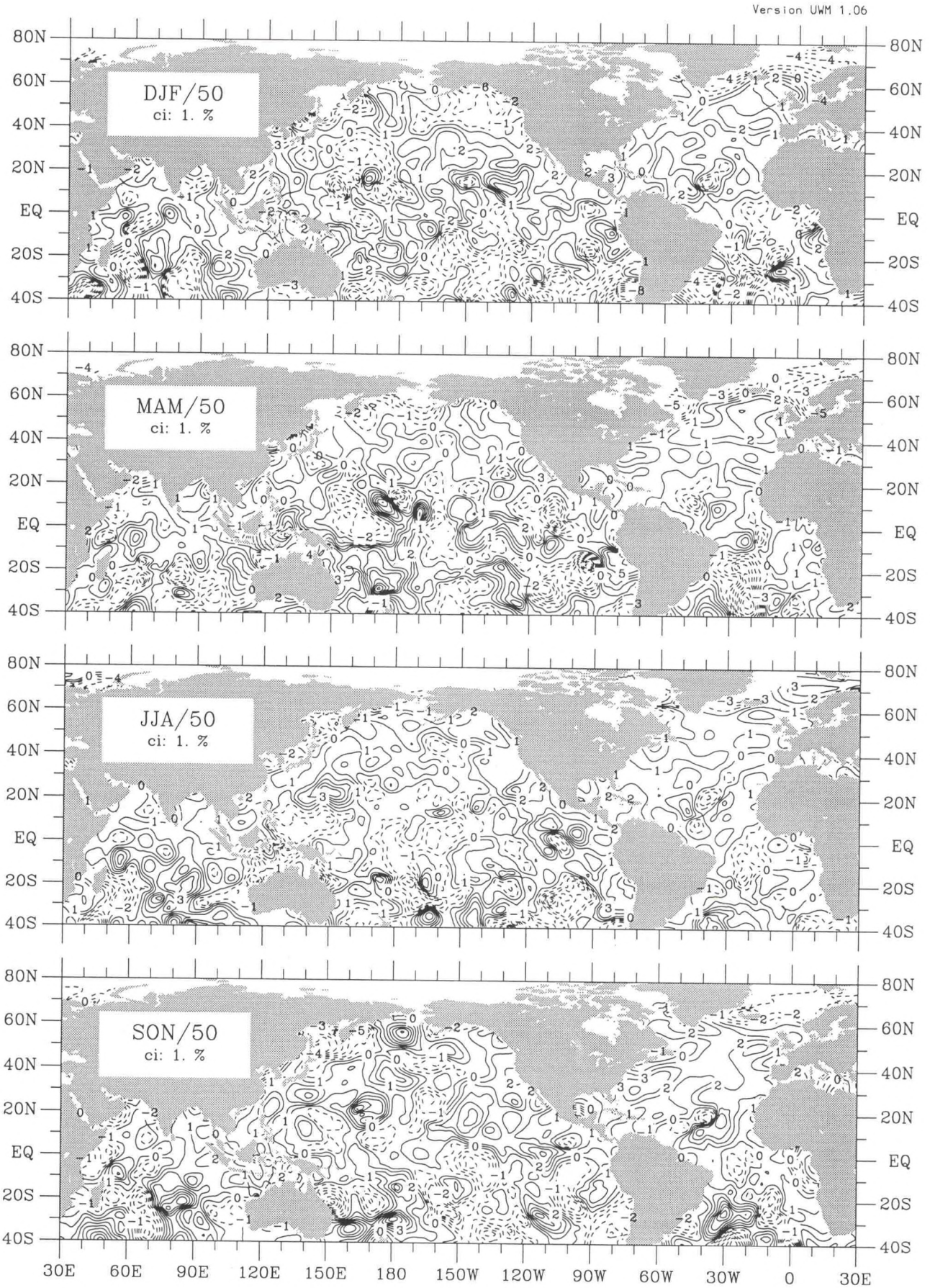

Figure rh-11. Relative humidity seasonal anomaly for 1950.

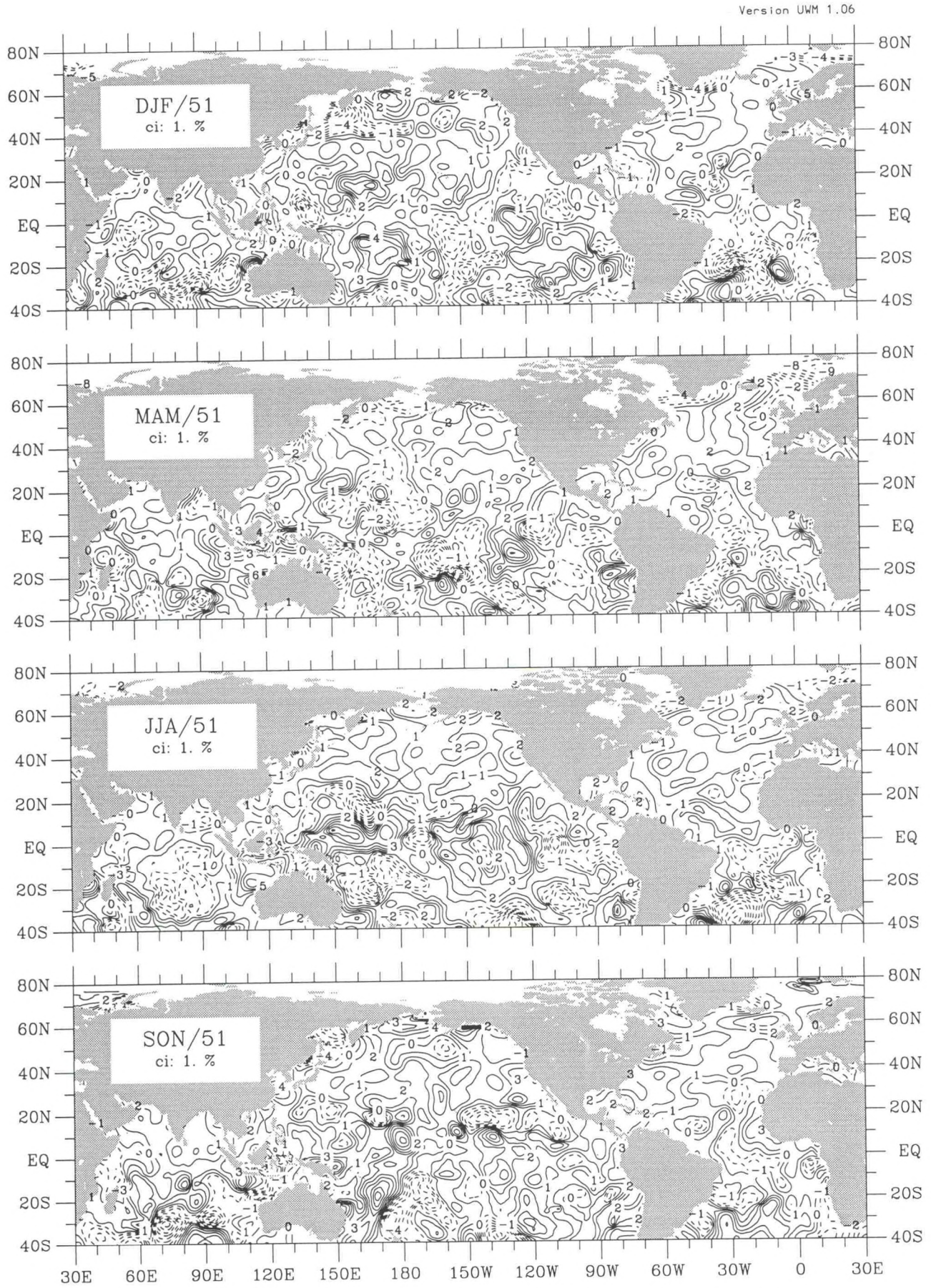

Figure rh-12. Relative humidity seasonal anomaly for 1951.

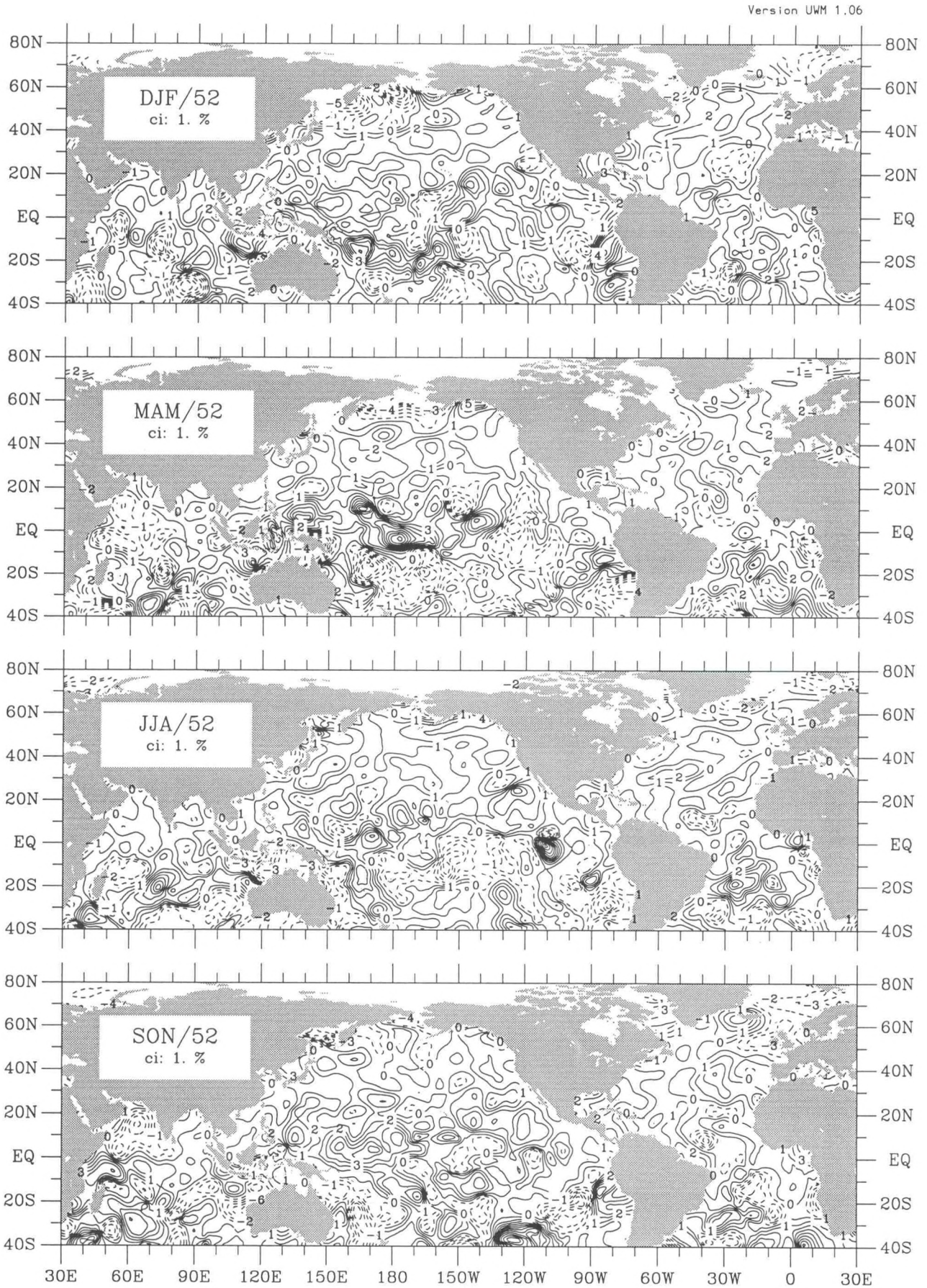

Figure rh-13. Relative humidity seasonal anomaly for 1952.

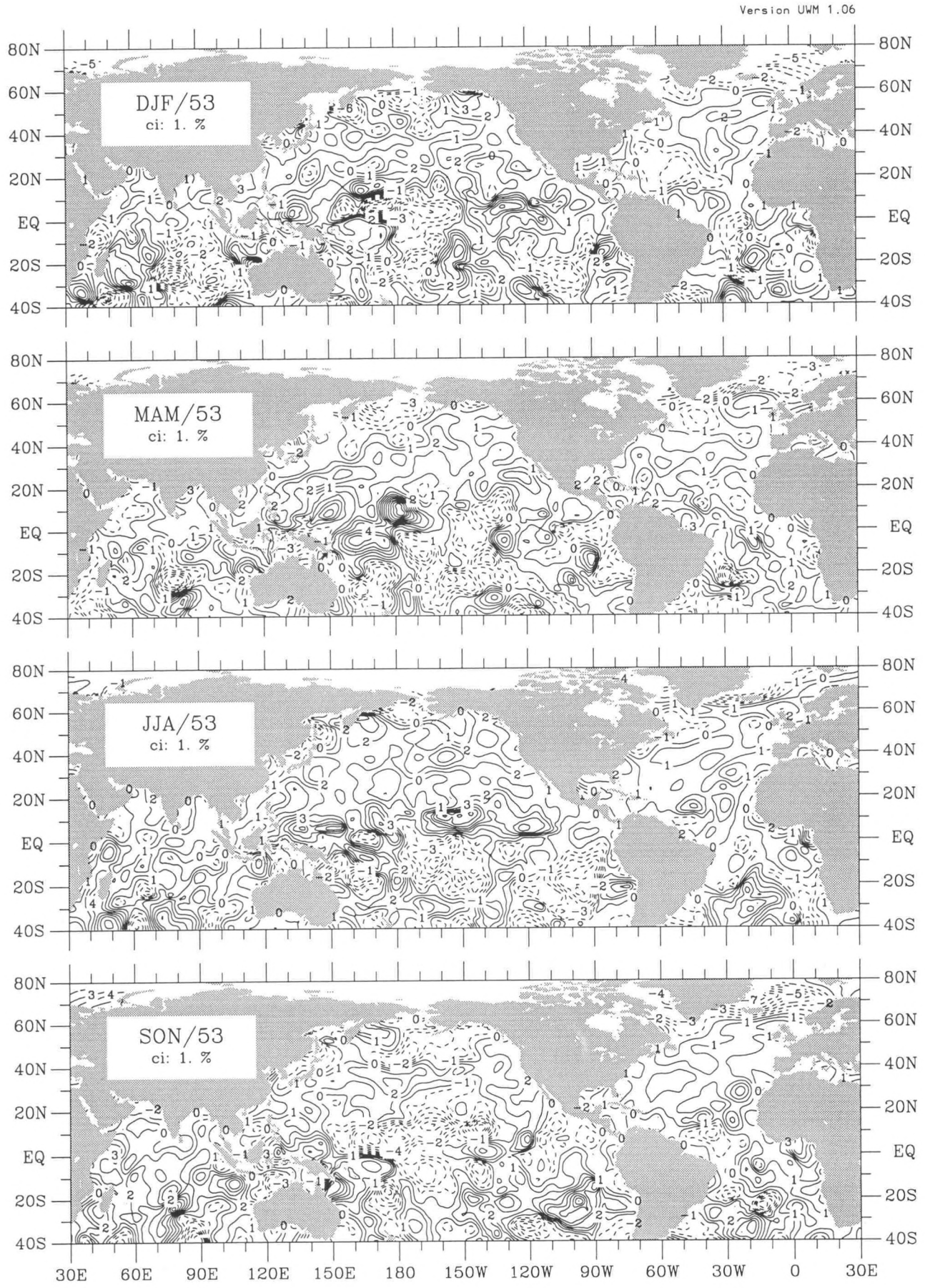

Figure rh-14. Relative humidity seasonal anomaly for 1953.

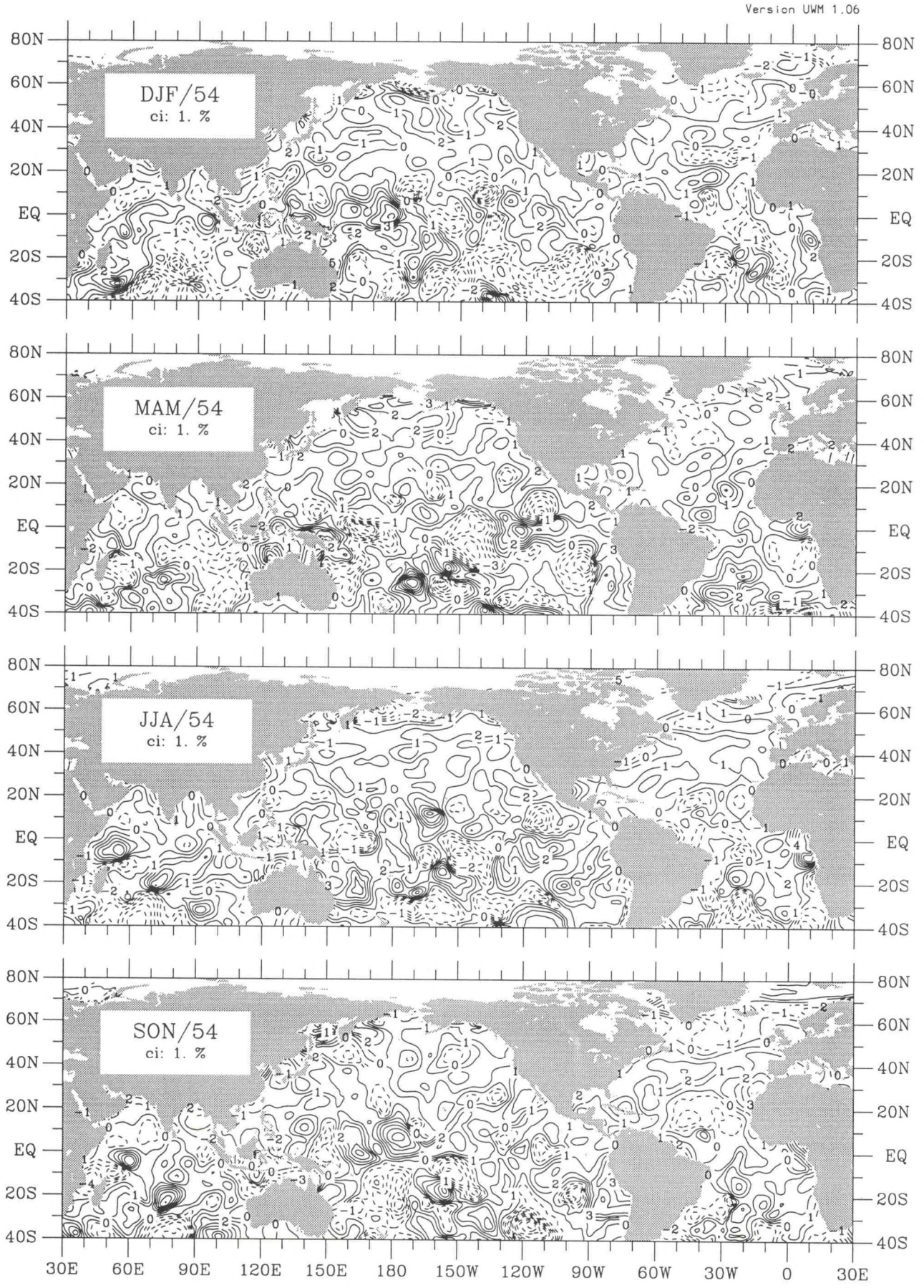

Figure rh-15. Relative humidity seasonal anomaly for 1954.

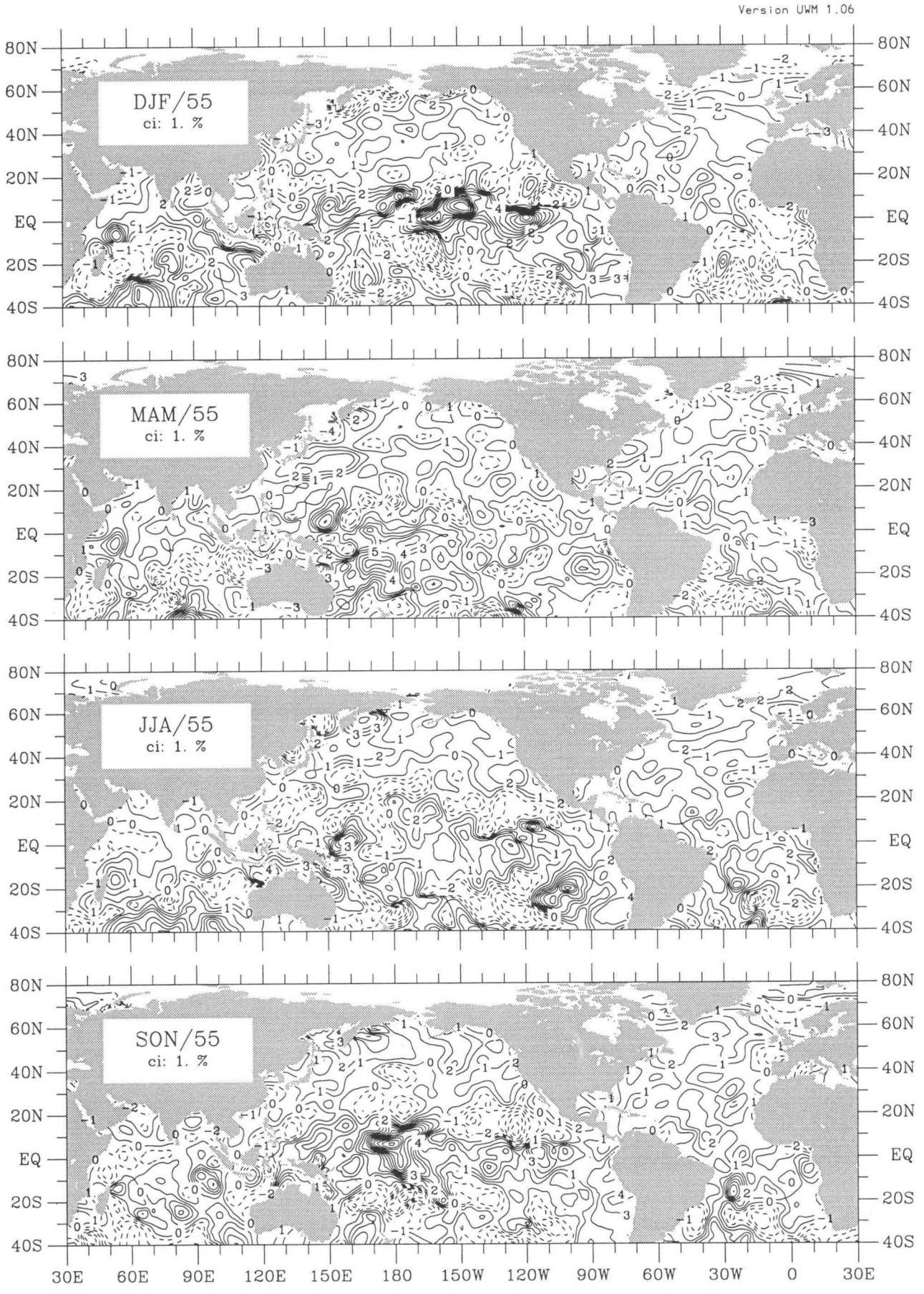

Figure rh-16. Relative humidity seasonal anomaly for 1955.

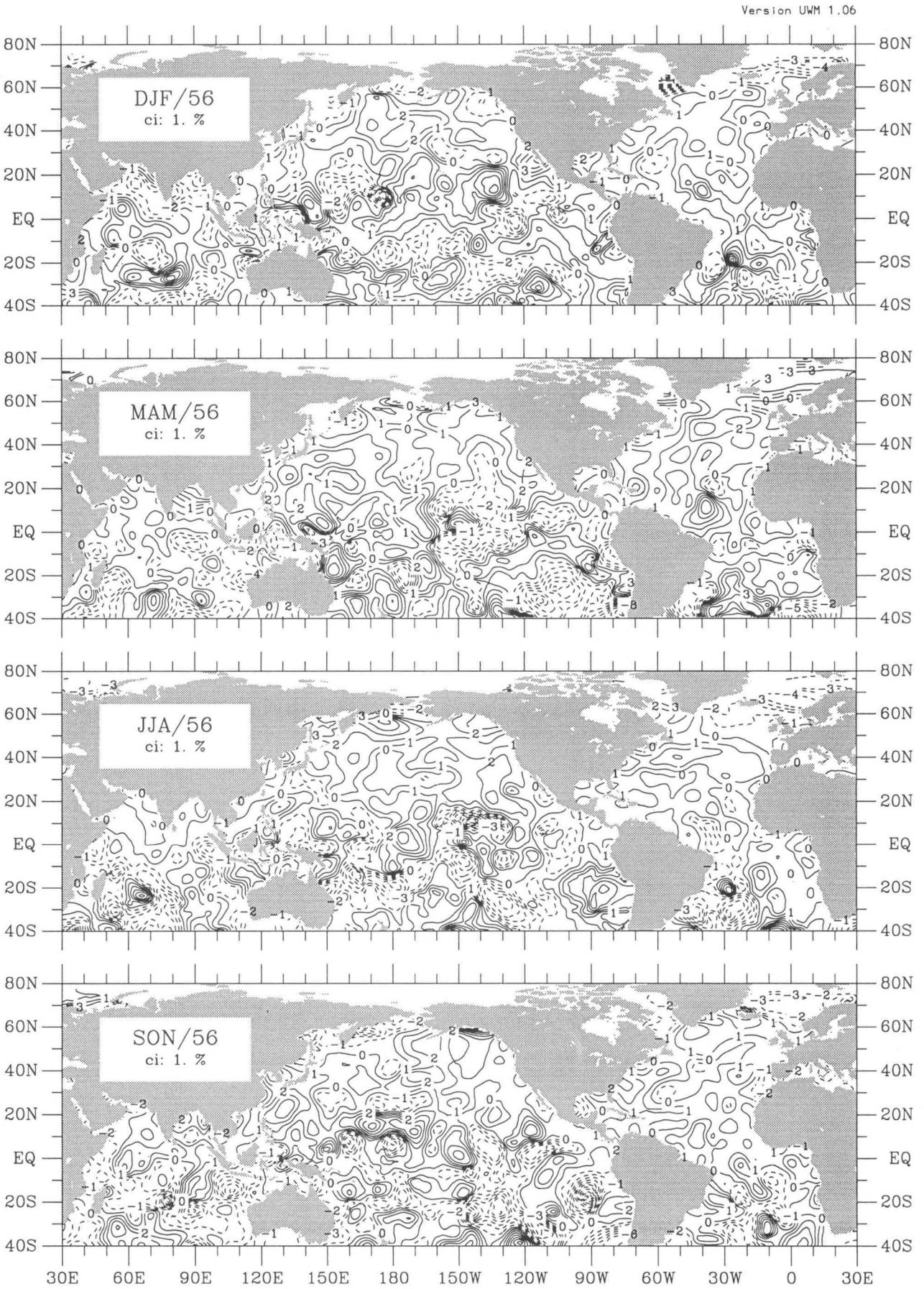

Figure rh-17. Relative humidity seasonal anomaly for 1956.

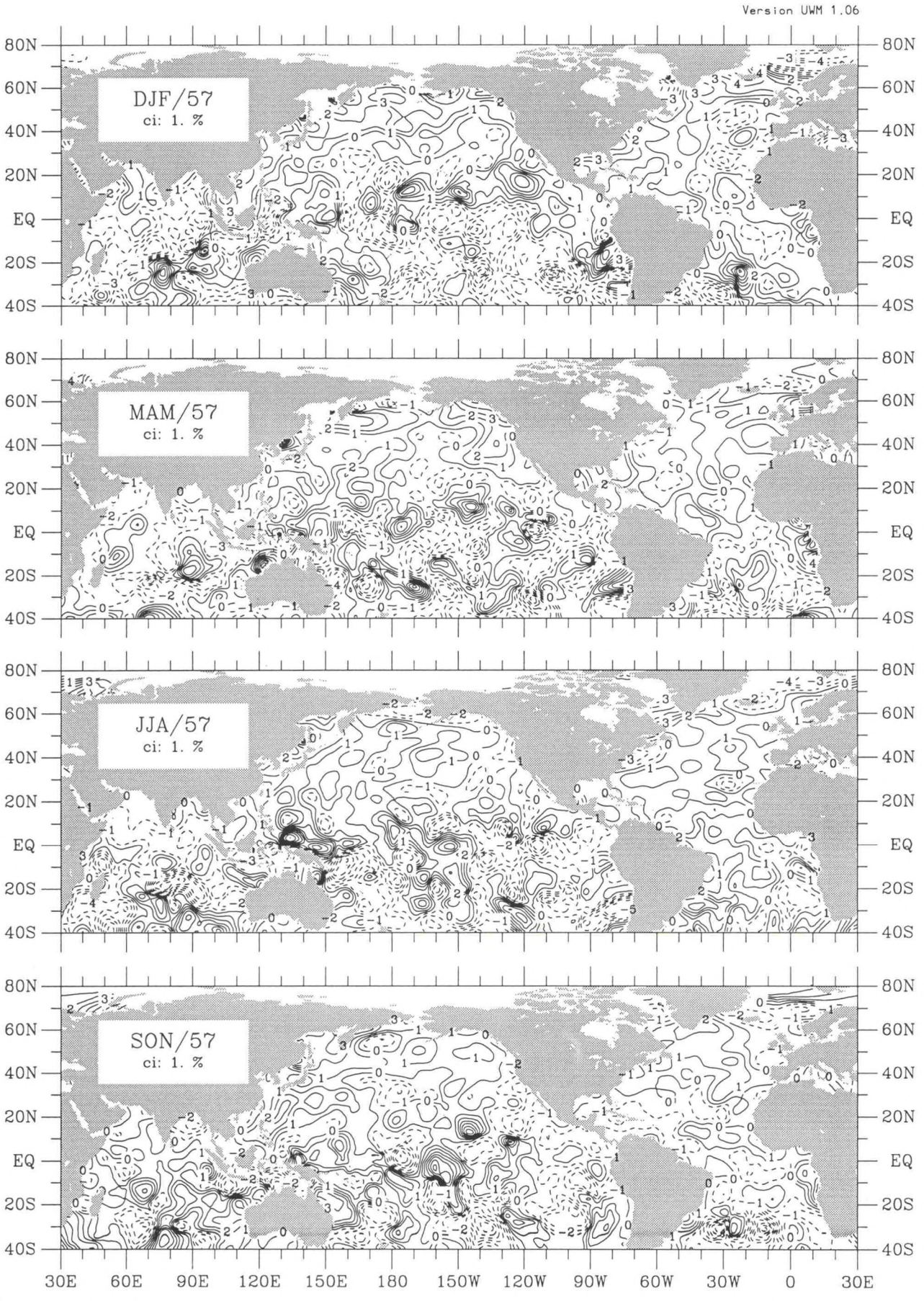

Figure rh-18. Relative humidity seasonal anomaly for 1957.

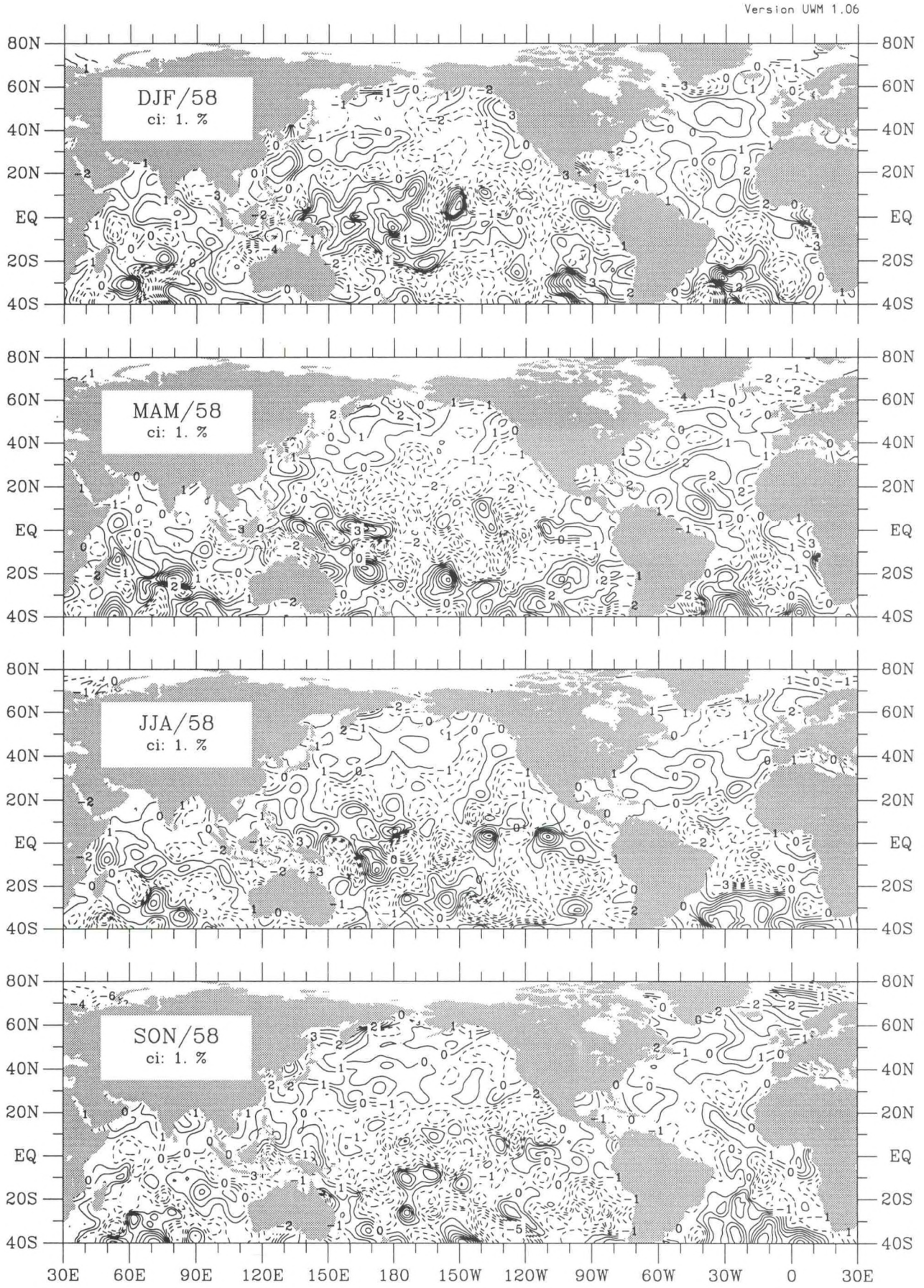

Figure rh-19. Relative humidity seasonal anomaly for 1958.

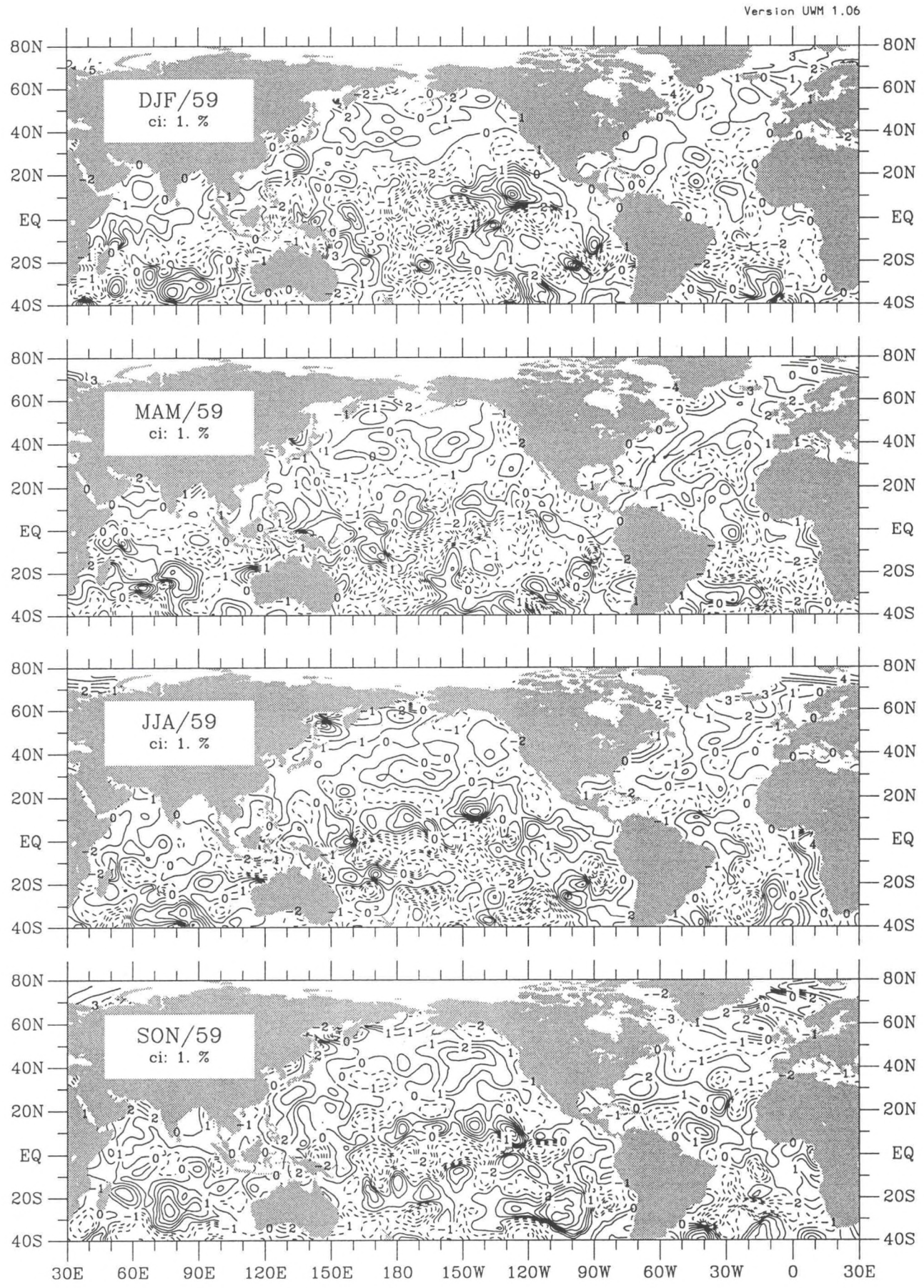

Figure rh-20. Relative humidity seasonal anomaly for 1959.

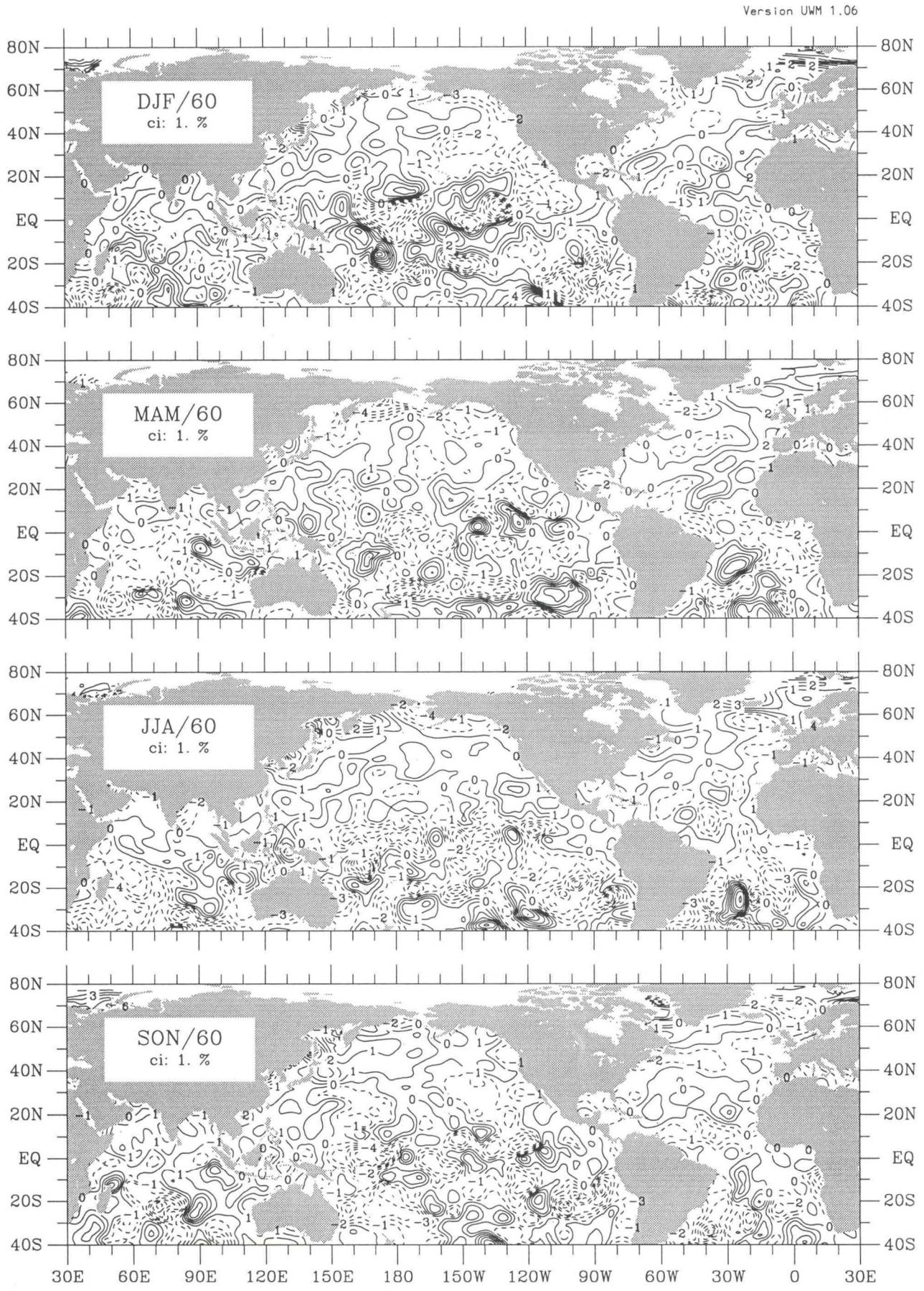

Figure rh-21. Relative humidity seasonal anomaly for 1960.

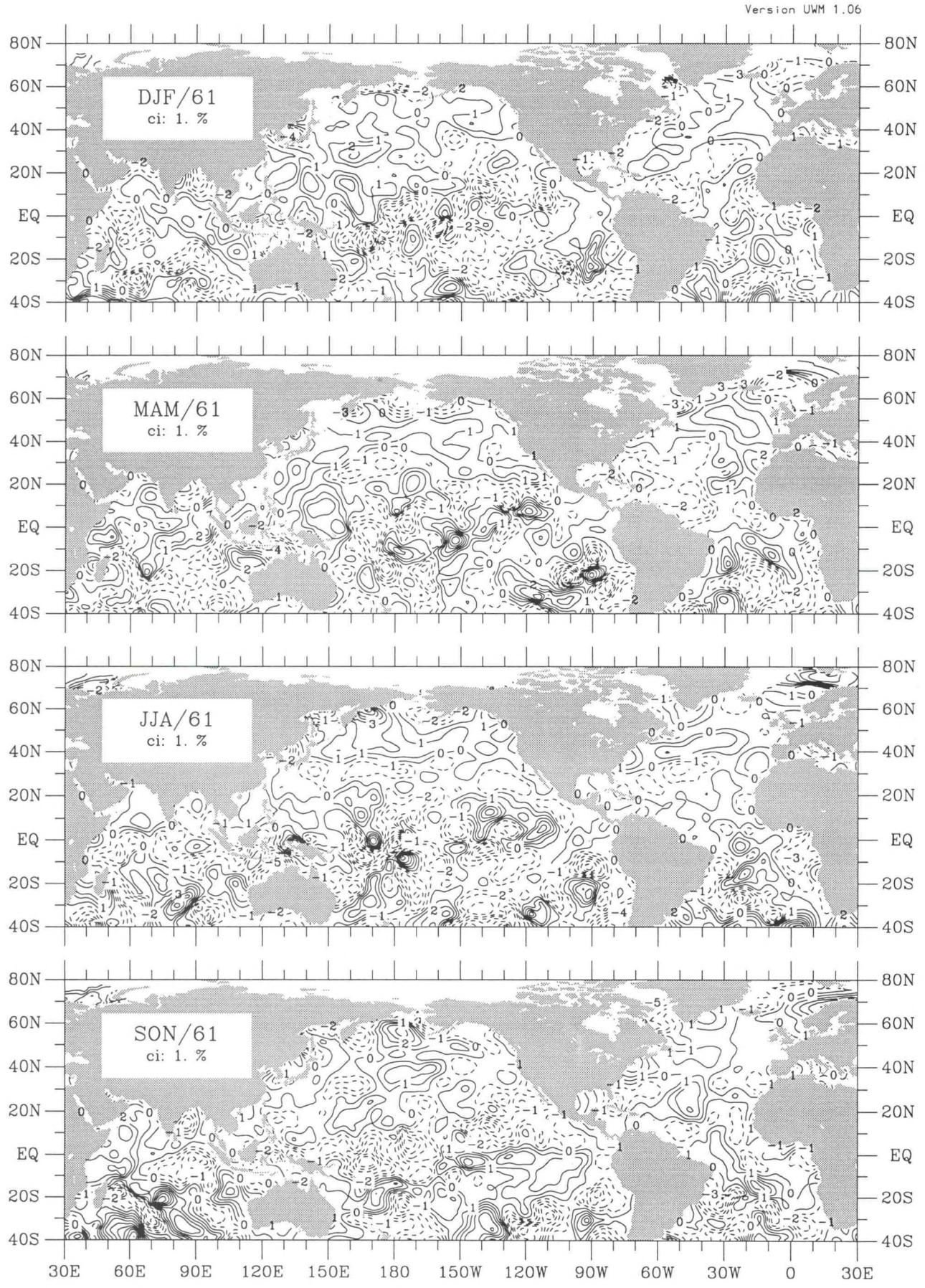

Figure rh-22. Relative humidity seasonal anomaly for 1961.

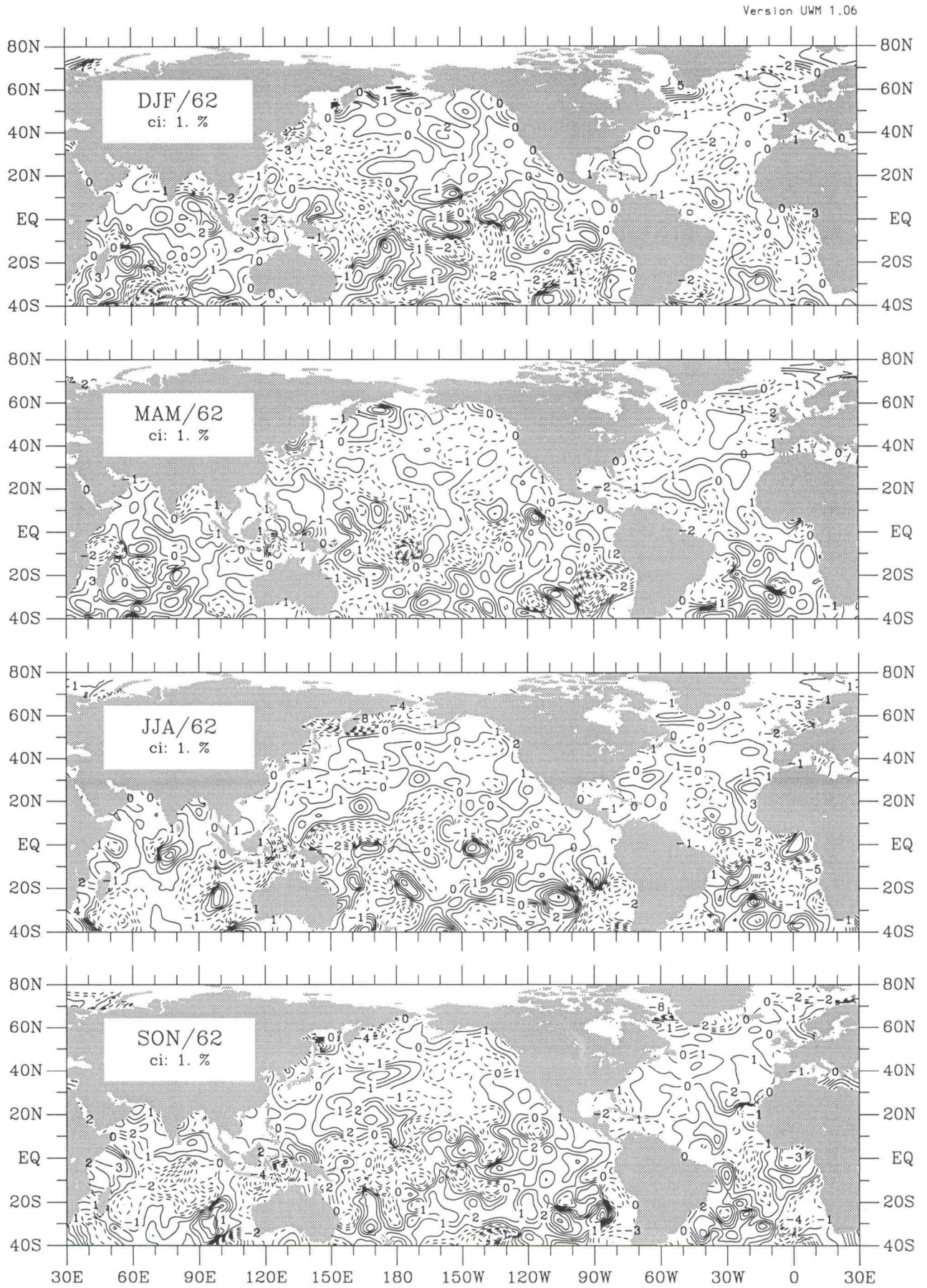

Figure rh-23. Relative humidity seasonal anomaly for 1962.

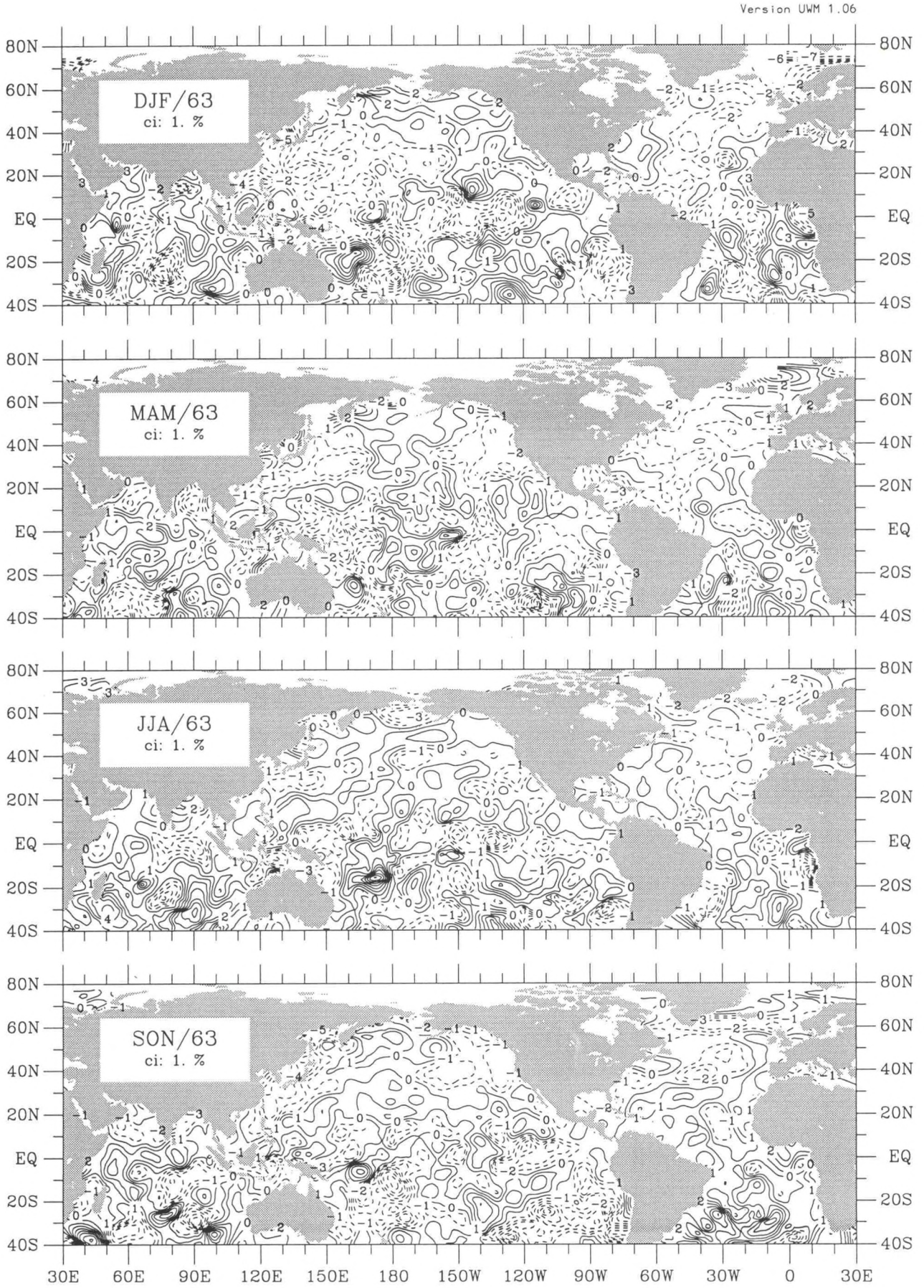

Figure rh-24. Relative humidity seasonal anomaly for 1963.

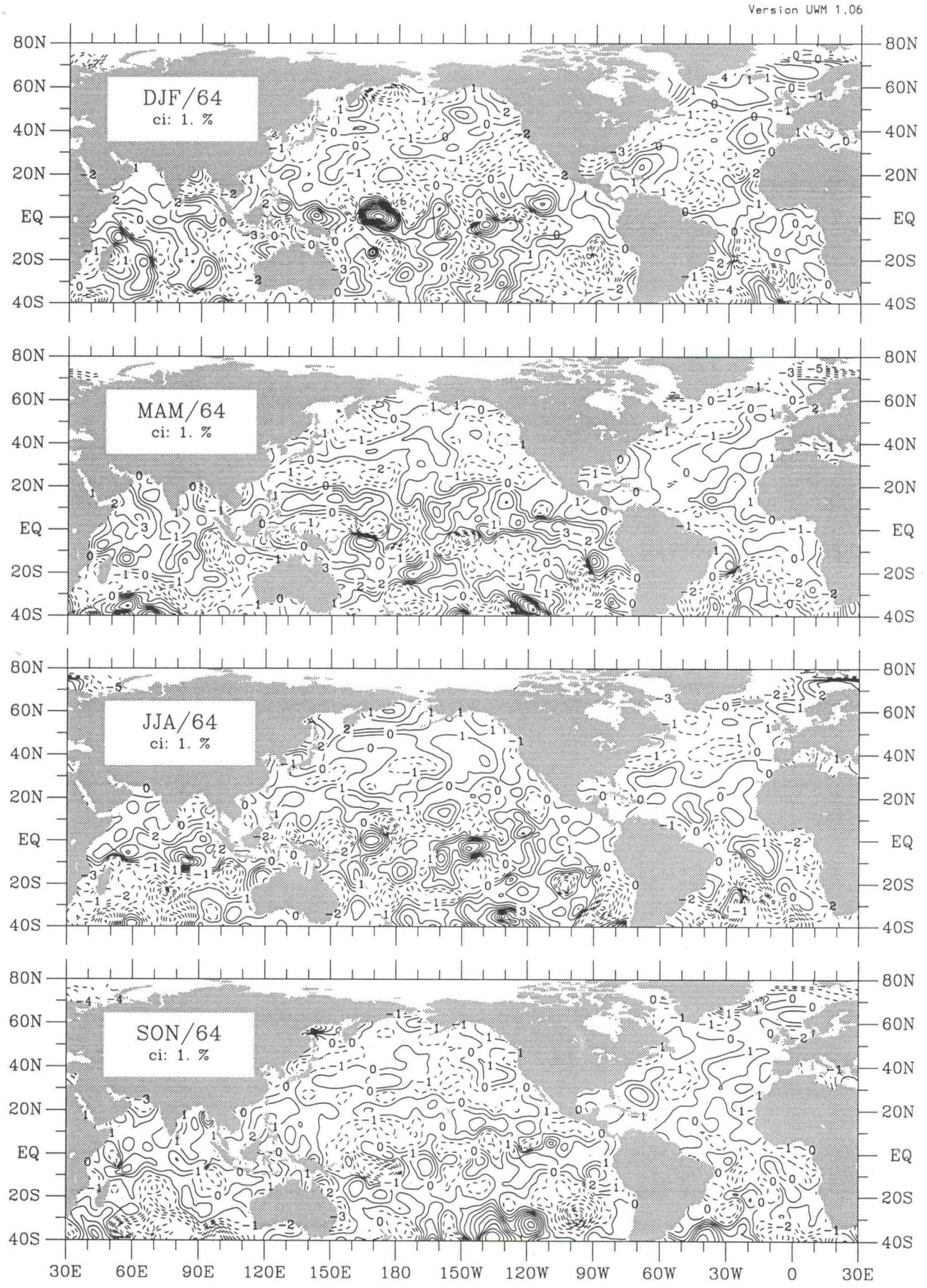

Figure rh-25. Relative humidity seasonal anomaly for 1964.

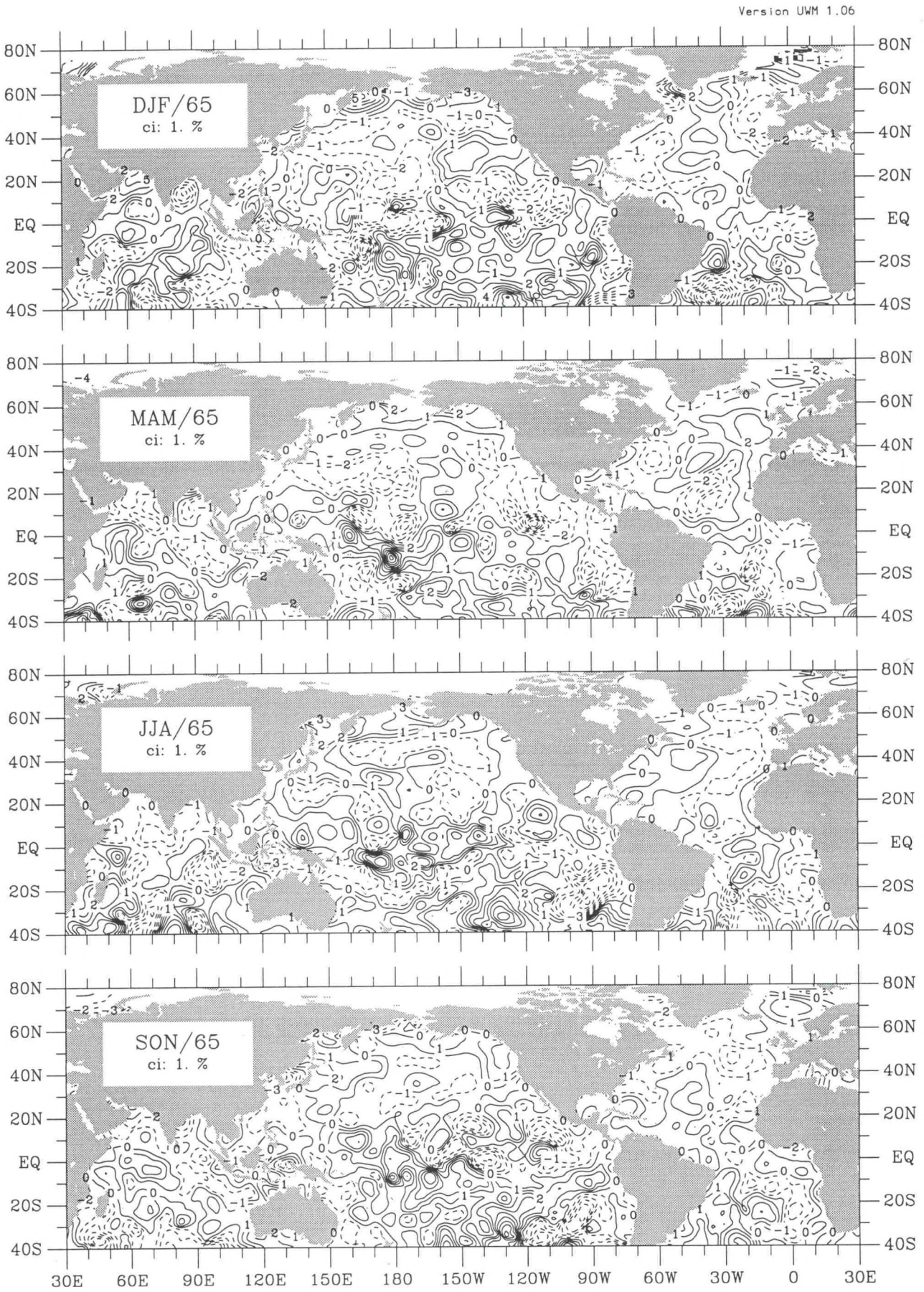

Figure rh-26. Relative humidity seasonal anomaly for 1965.

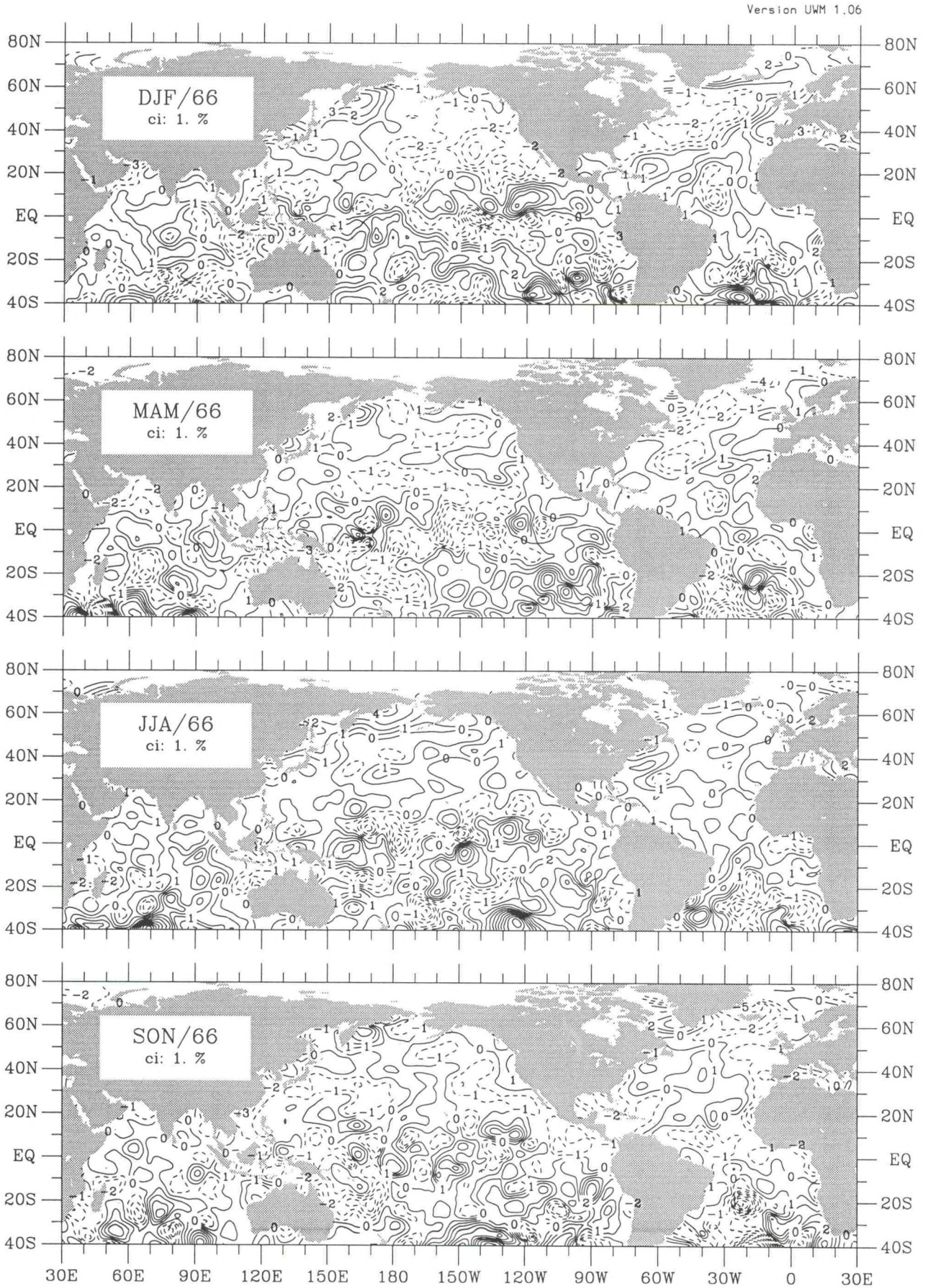

Figure rh-27. Relative humidity seasonal anomaly for 1966.

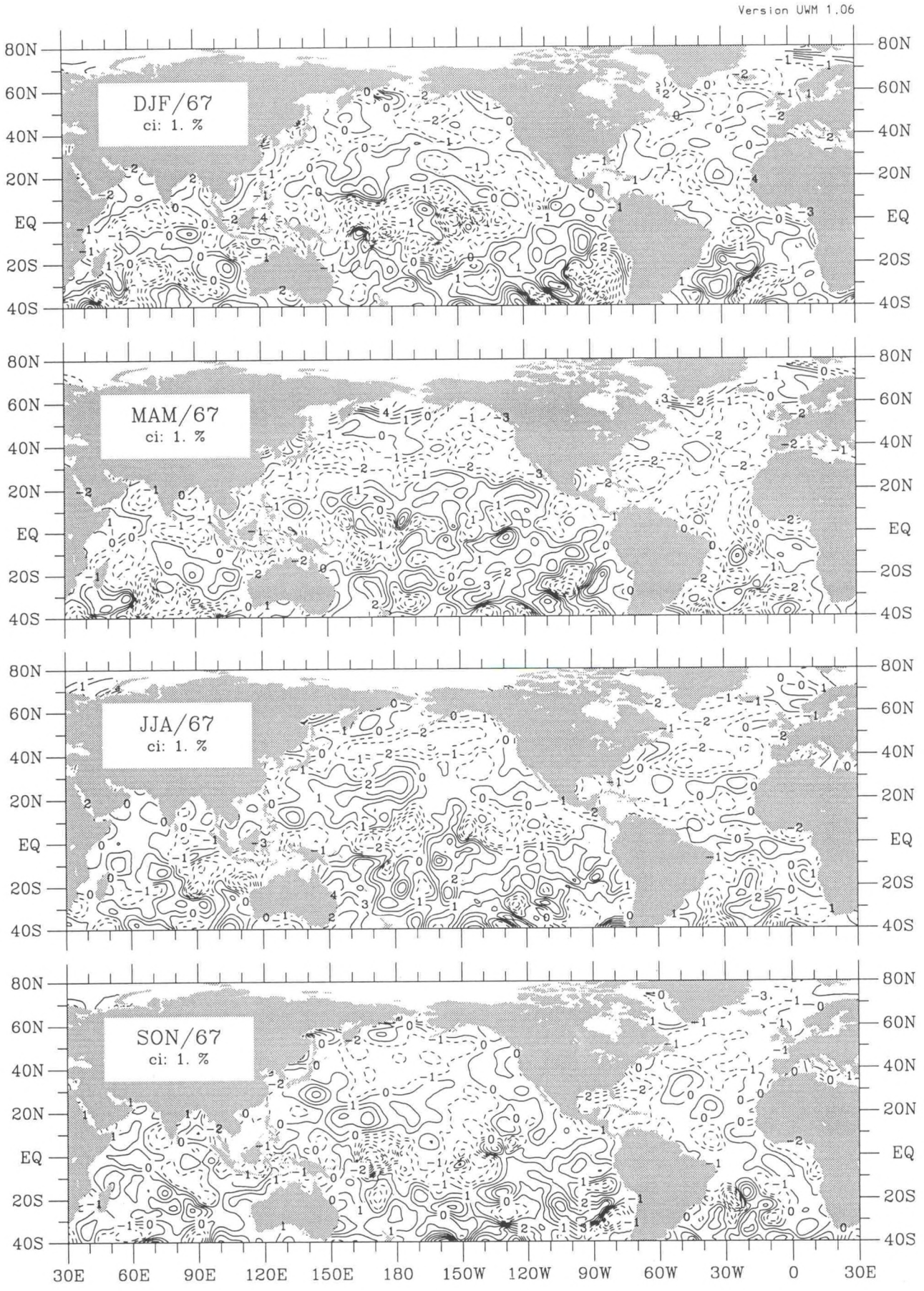

Figure rh-28. Relative humidity seasonal anomaly for 1967.

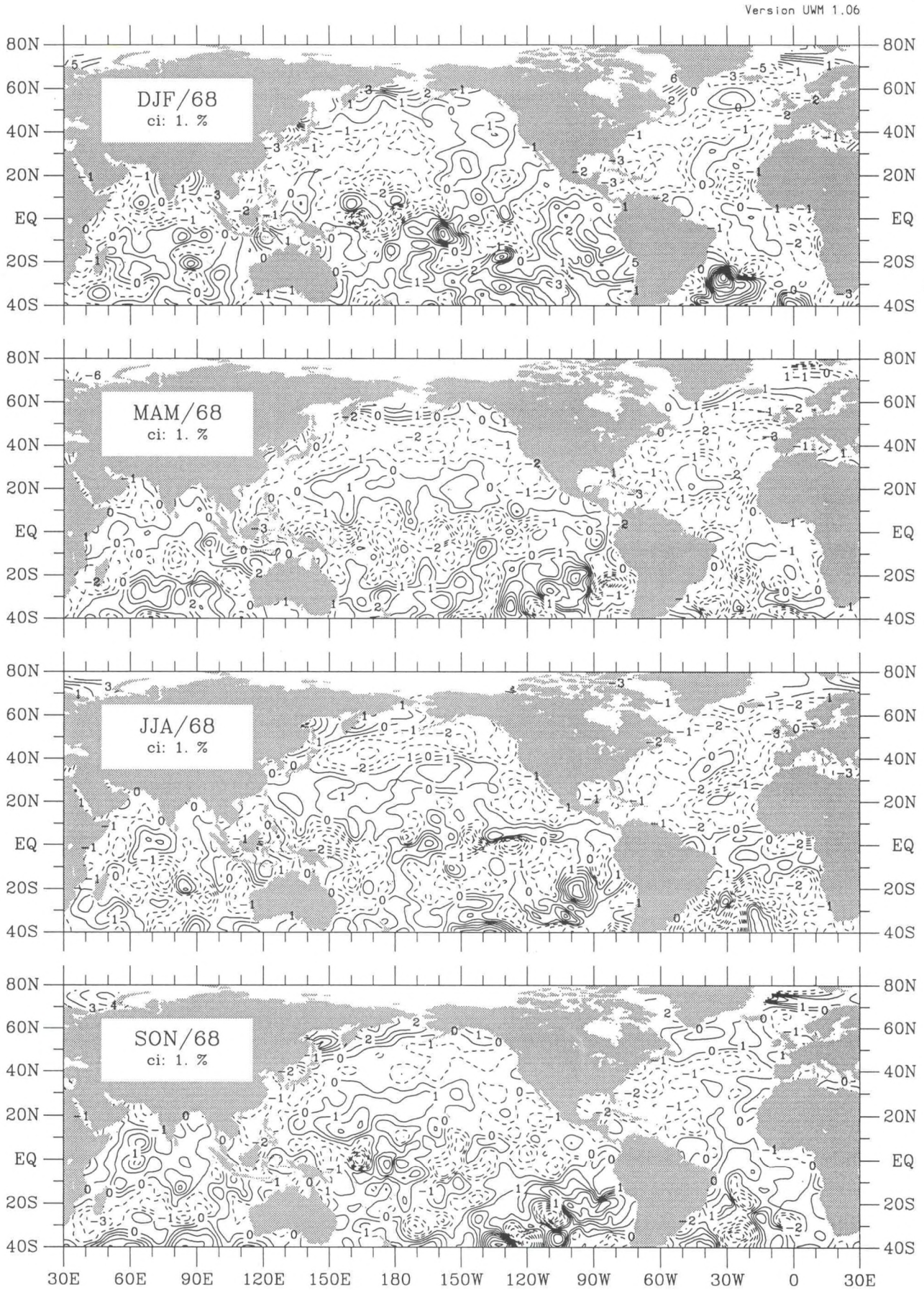

Figure rh-29. Relative humidity seasonal anomaly for 1968.

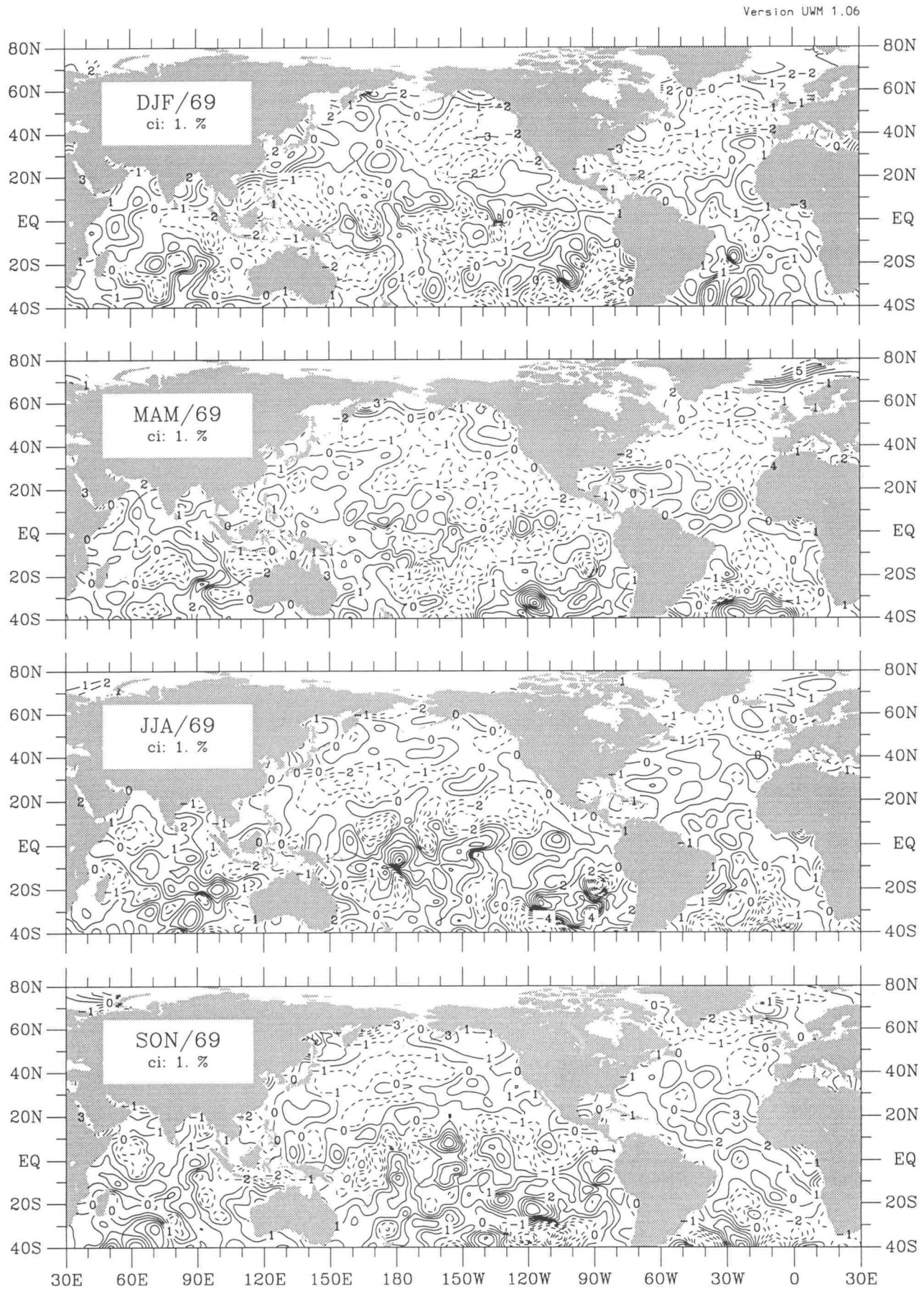

Figure rh-30. Relative humidity seasonal anomaly for 1969.

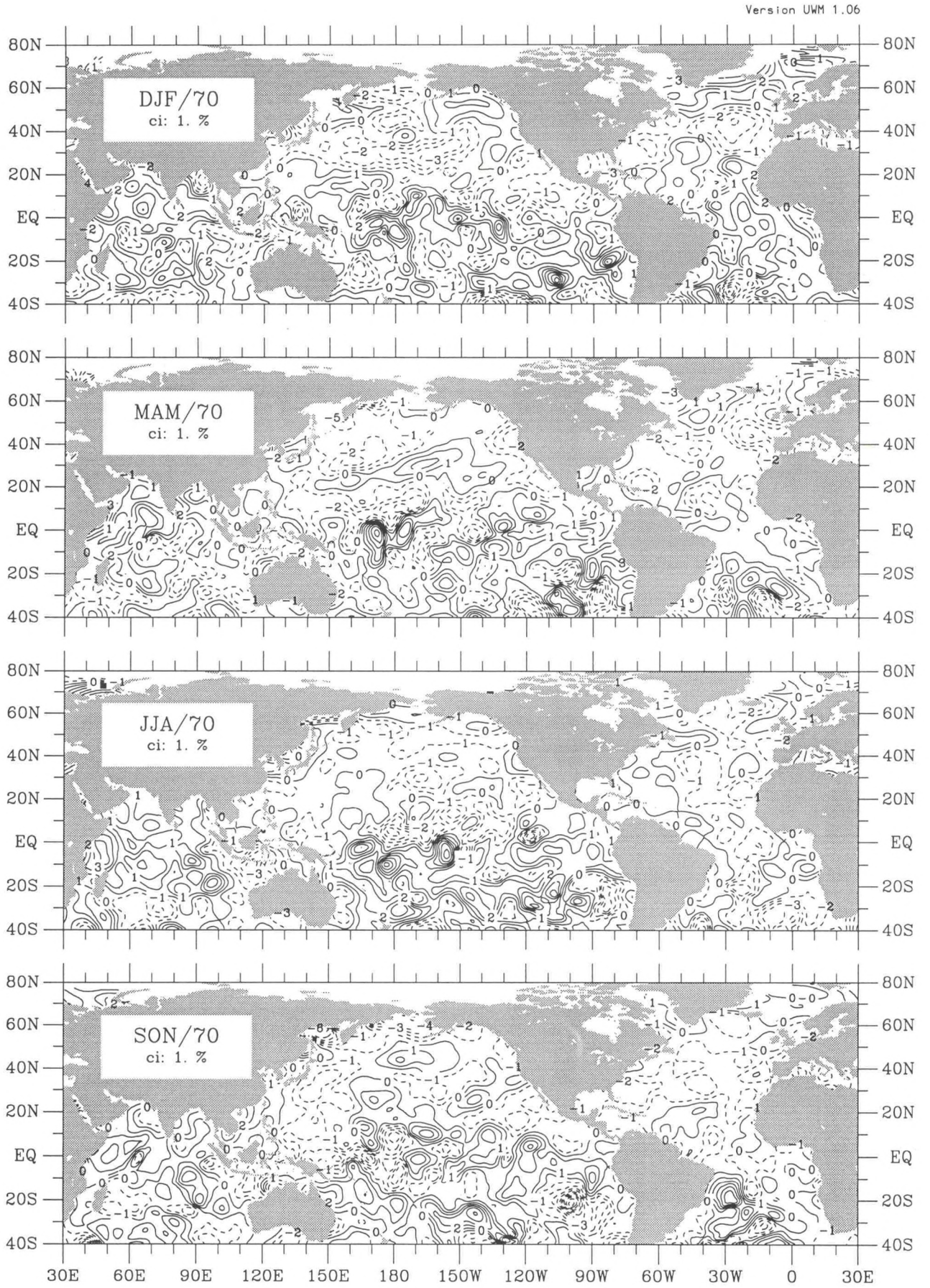

Figure rh-31. Relative humidity seasonal anomaly for 1970.

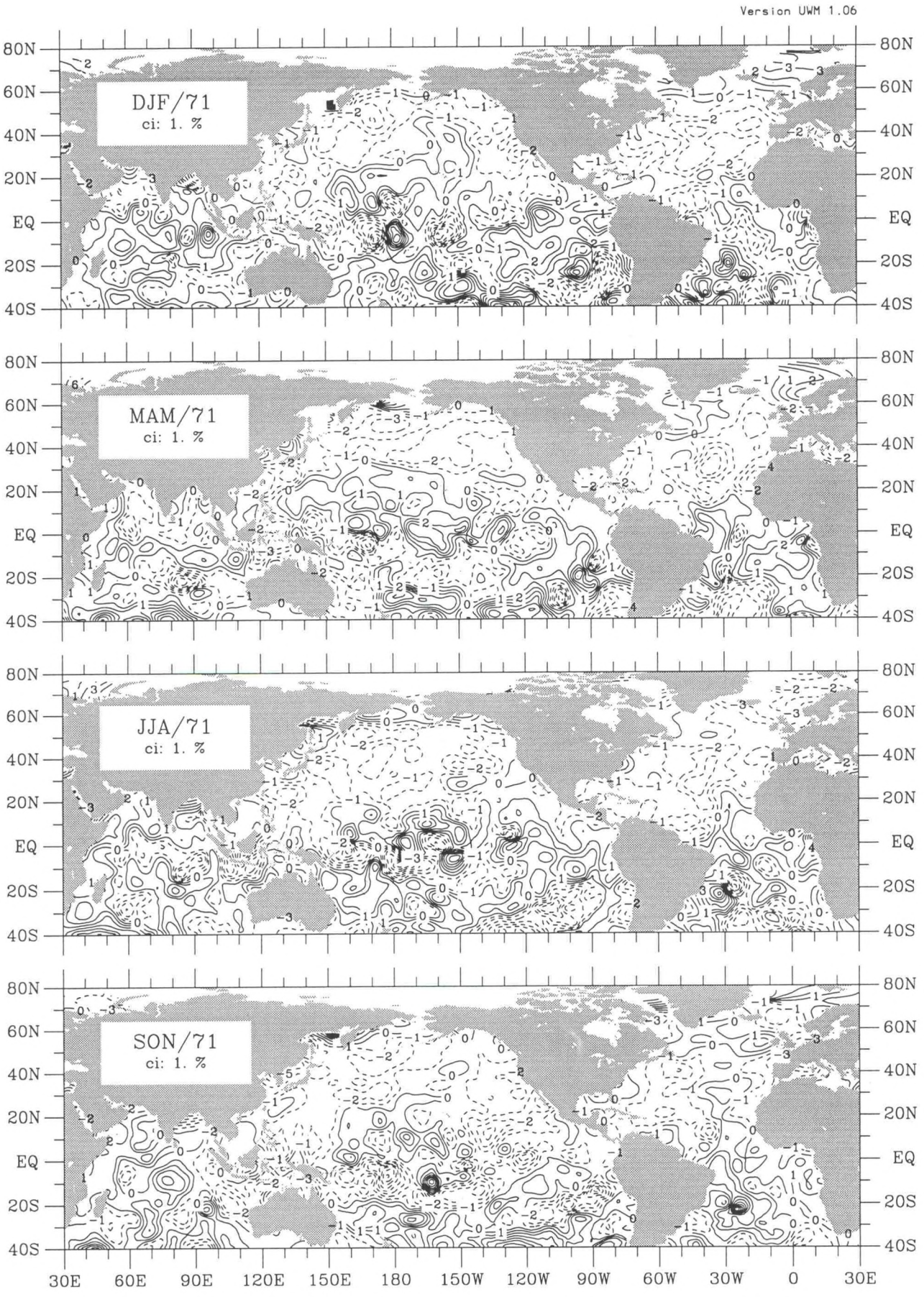

Figure rh-32. Relative humidity seasonal anomaly for 1971.

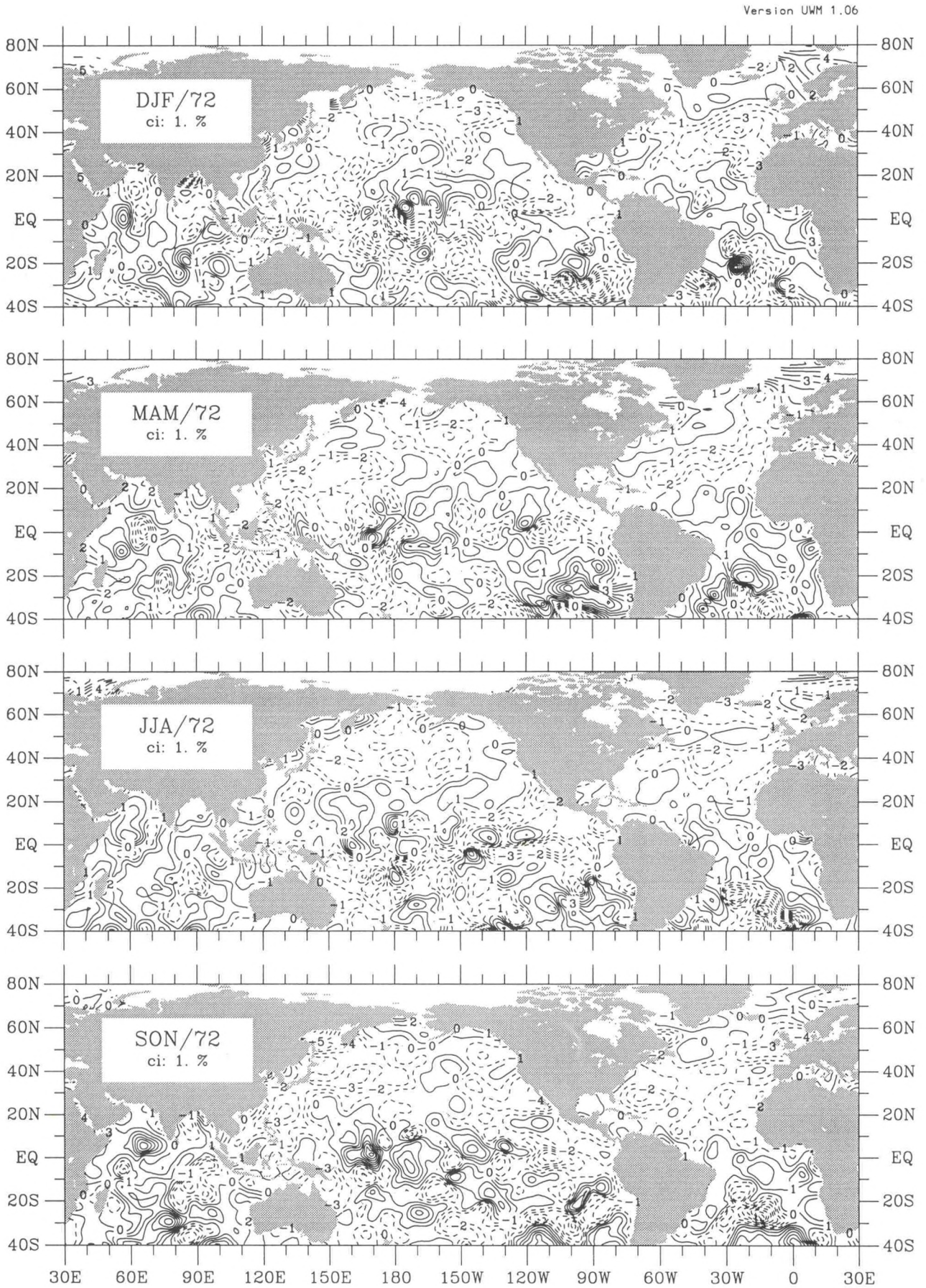

Figure rh-33. Relative humidity seasonal anomaly for 1972.

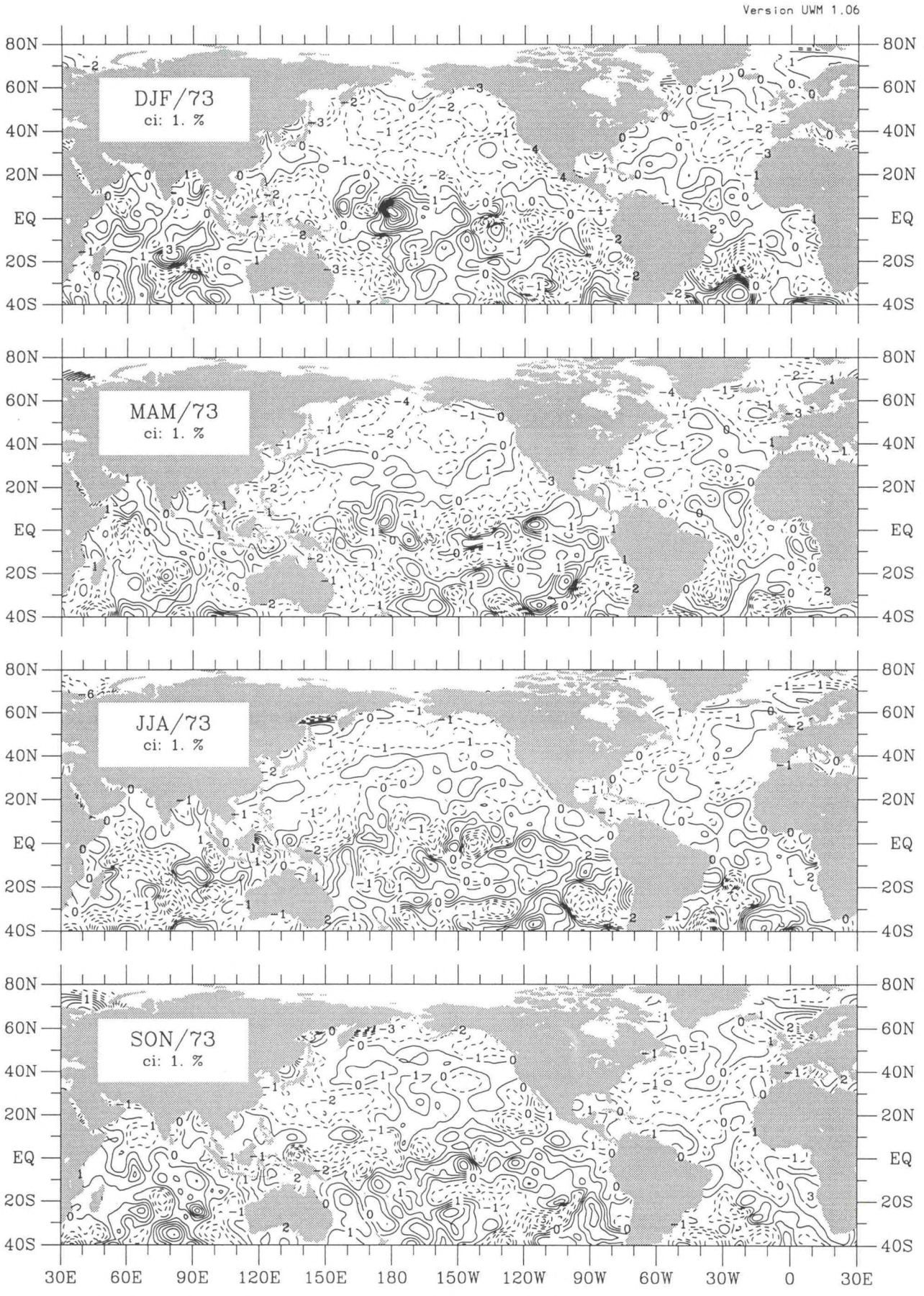

Figure rh-34. Relative humidity seasonal anomaly for 1973.

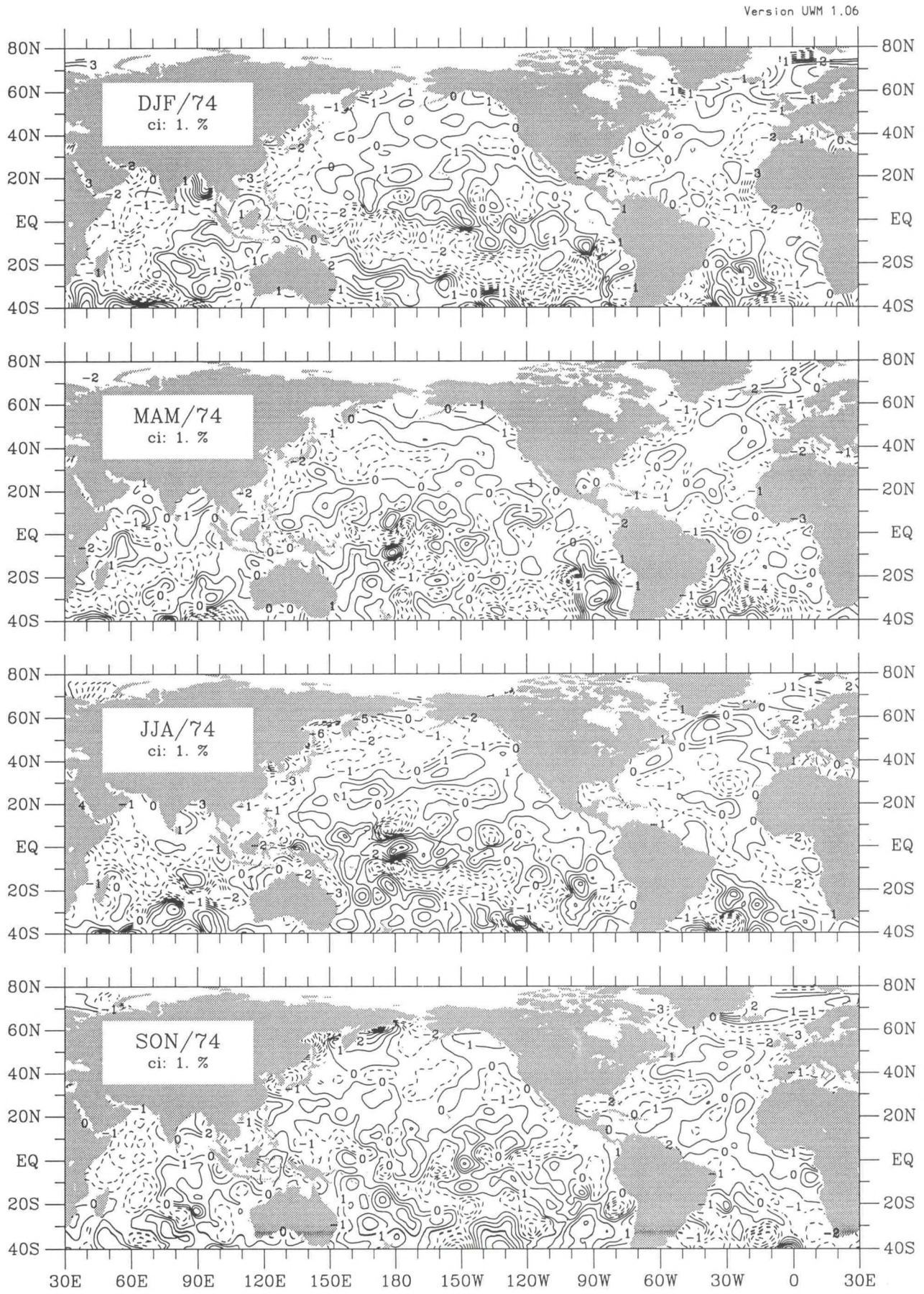

Figure rh-35. Relative humidity seasonal anomaly for 1974.

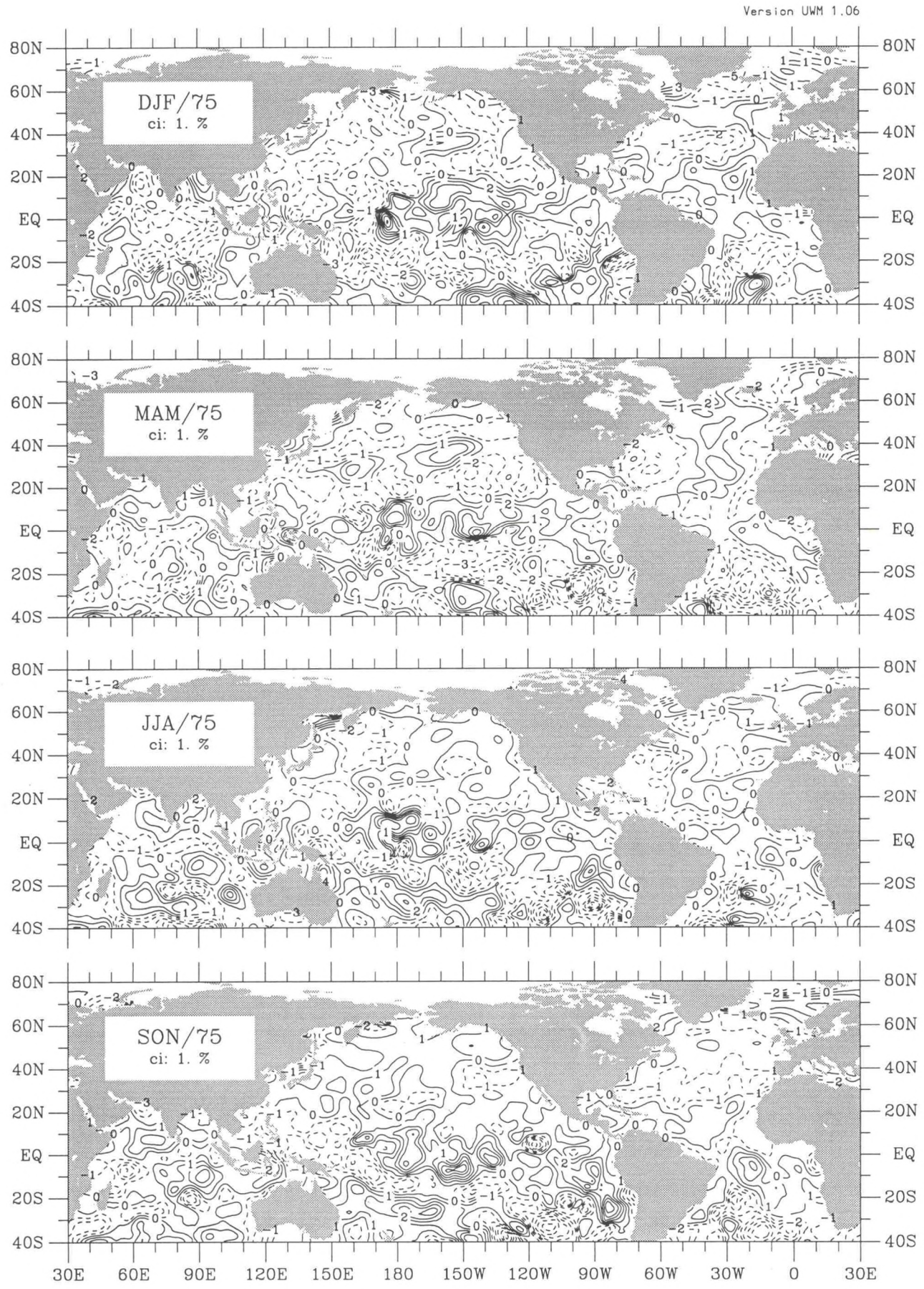

Figure rh-36. Relative humidity seasonal anomaly for 1975.

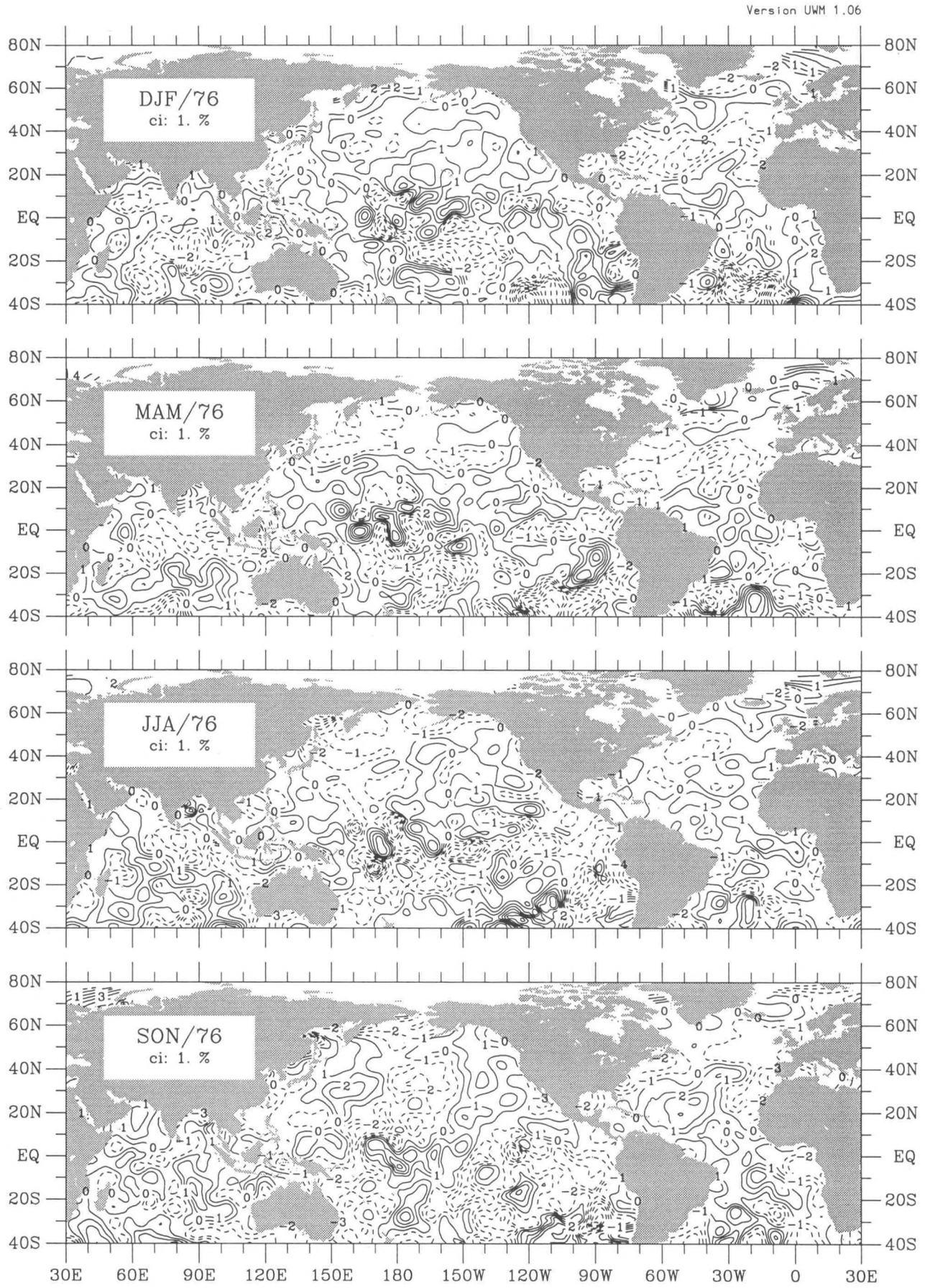

Figure rh-37. Relative humidity seasonal anomaly for 1976.

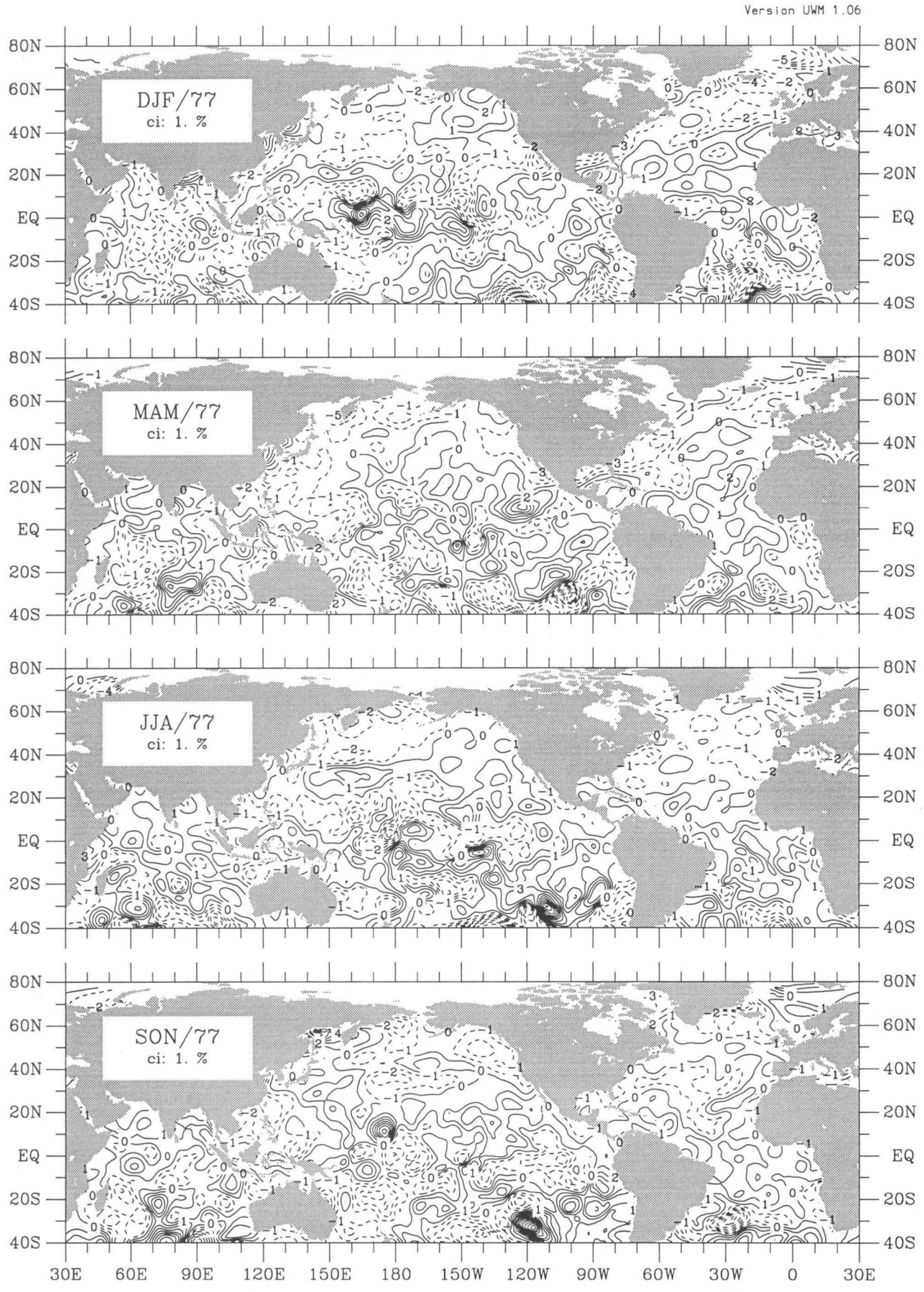

Figure rh-38. Relative humidity seasonal anomaly for 1977.

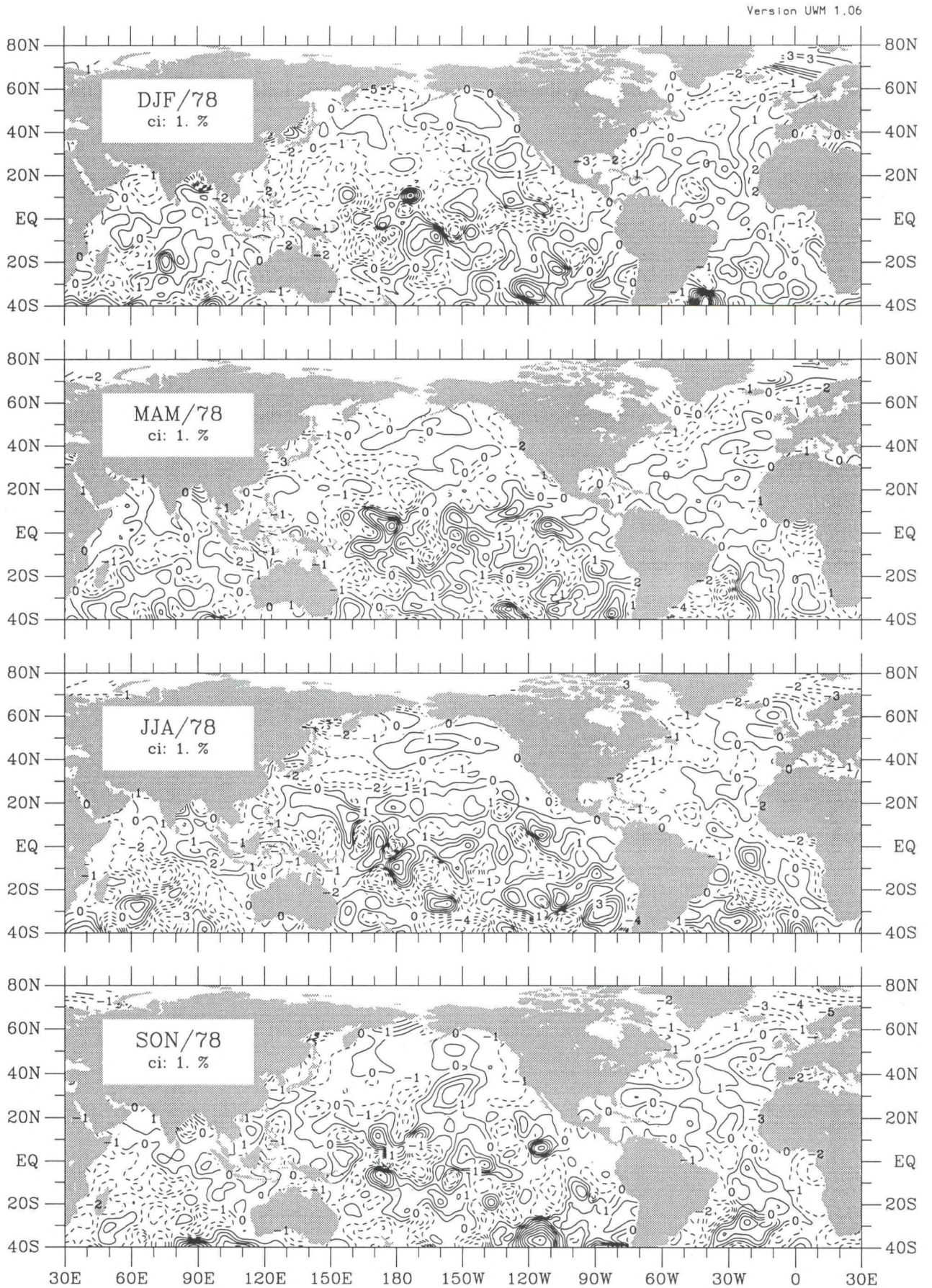

Figure rh-39. Relative humidity seasonal anomaly for 1978.

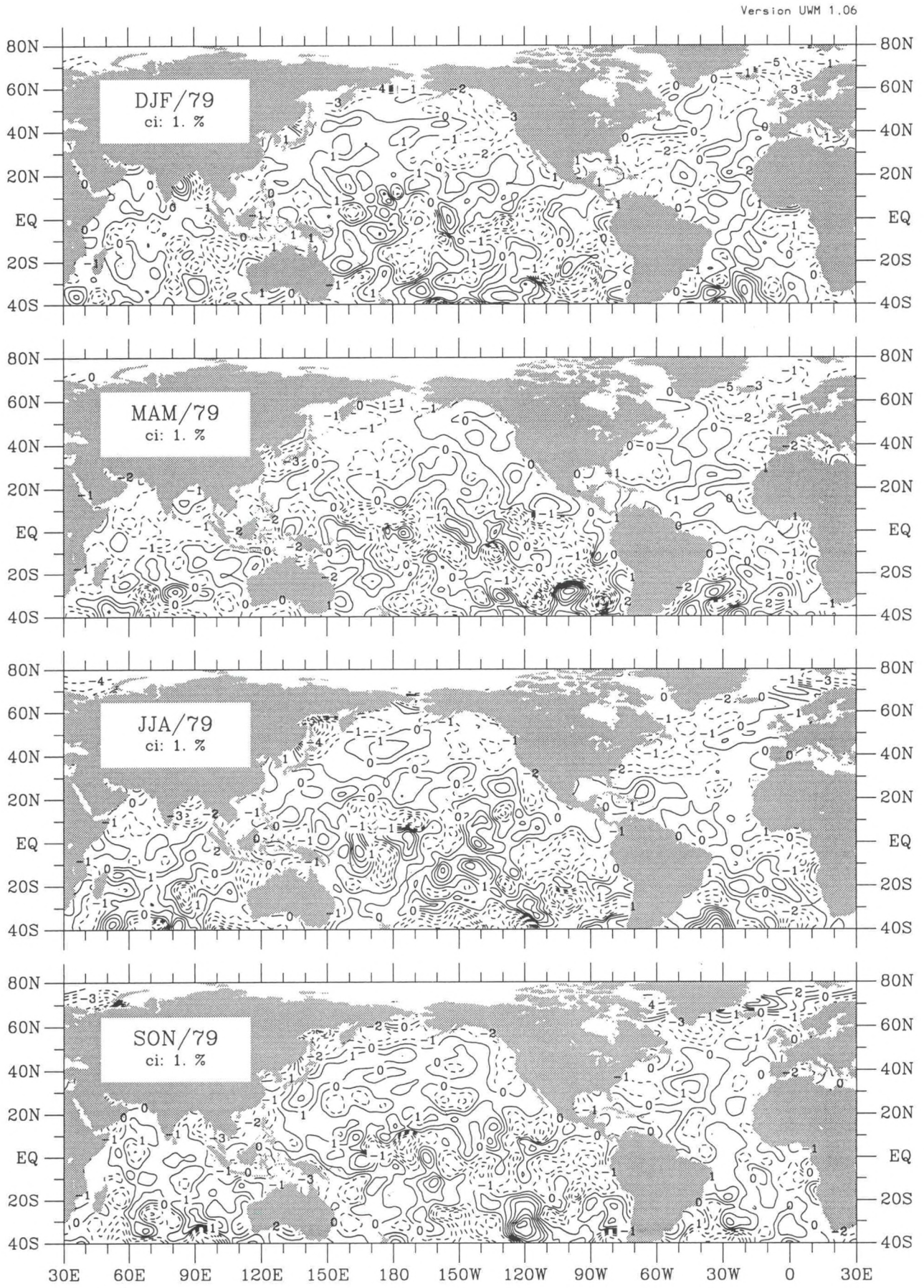

Figure rh-40. Relative humidity seasonal anomaly for 1979.

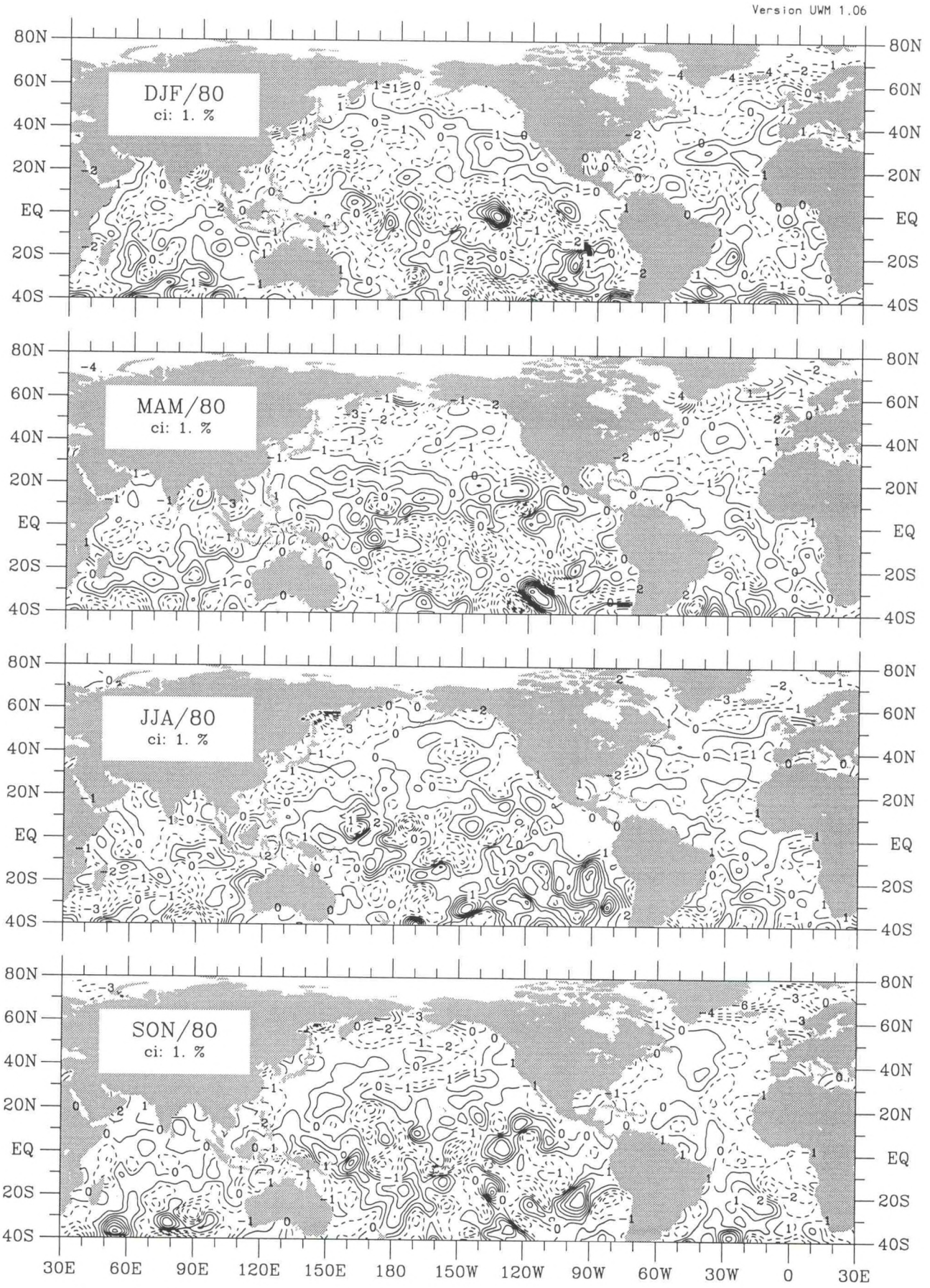

Figure rh-41. Relative humidity seasonal anomaly for 1980.

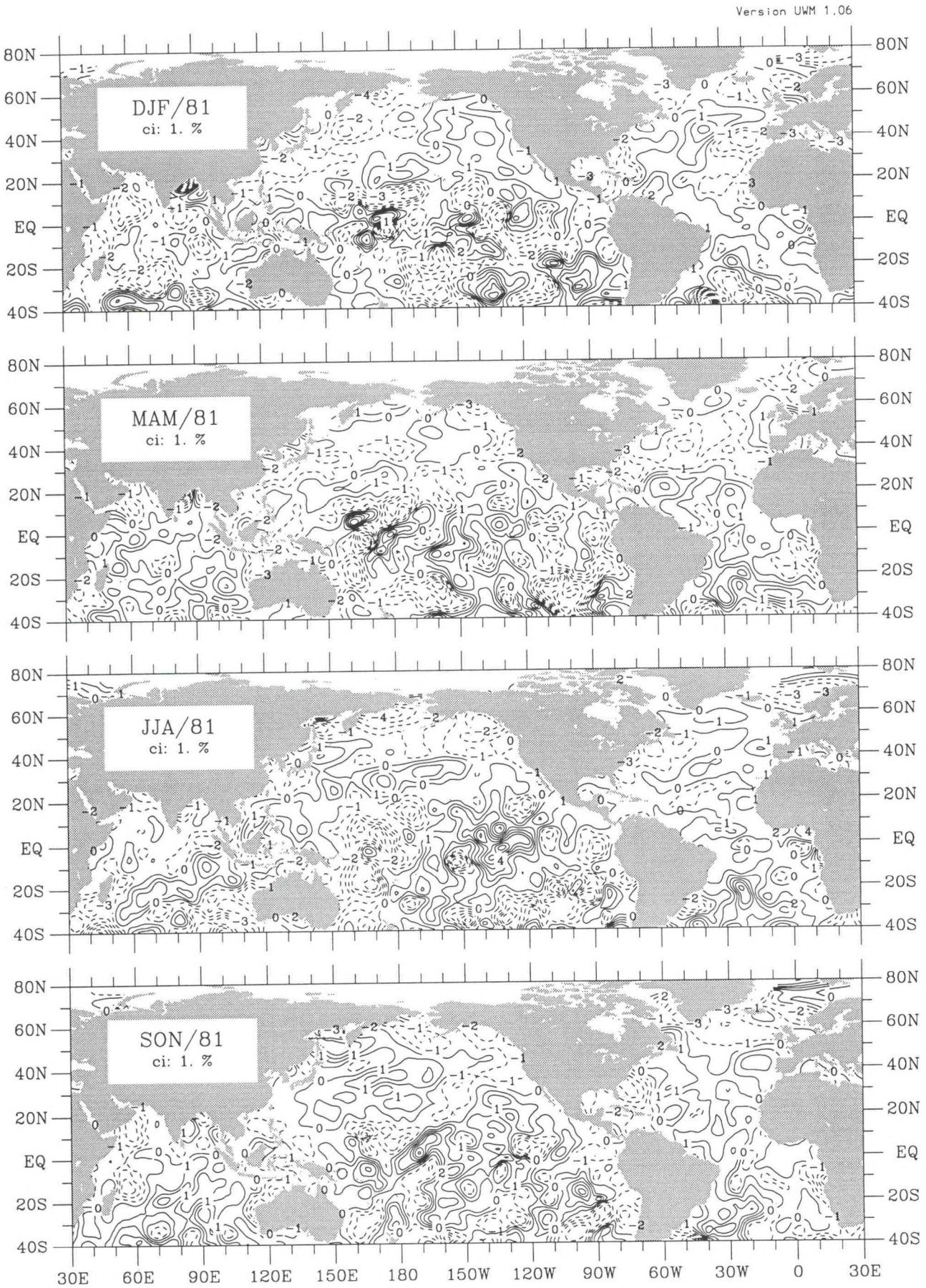

Figure rh-42. Relative humidity seasonal anomaly for 1981.

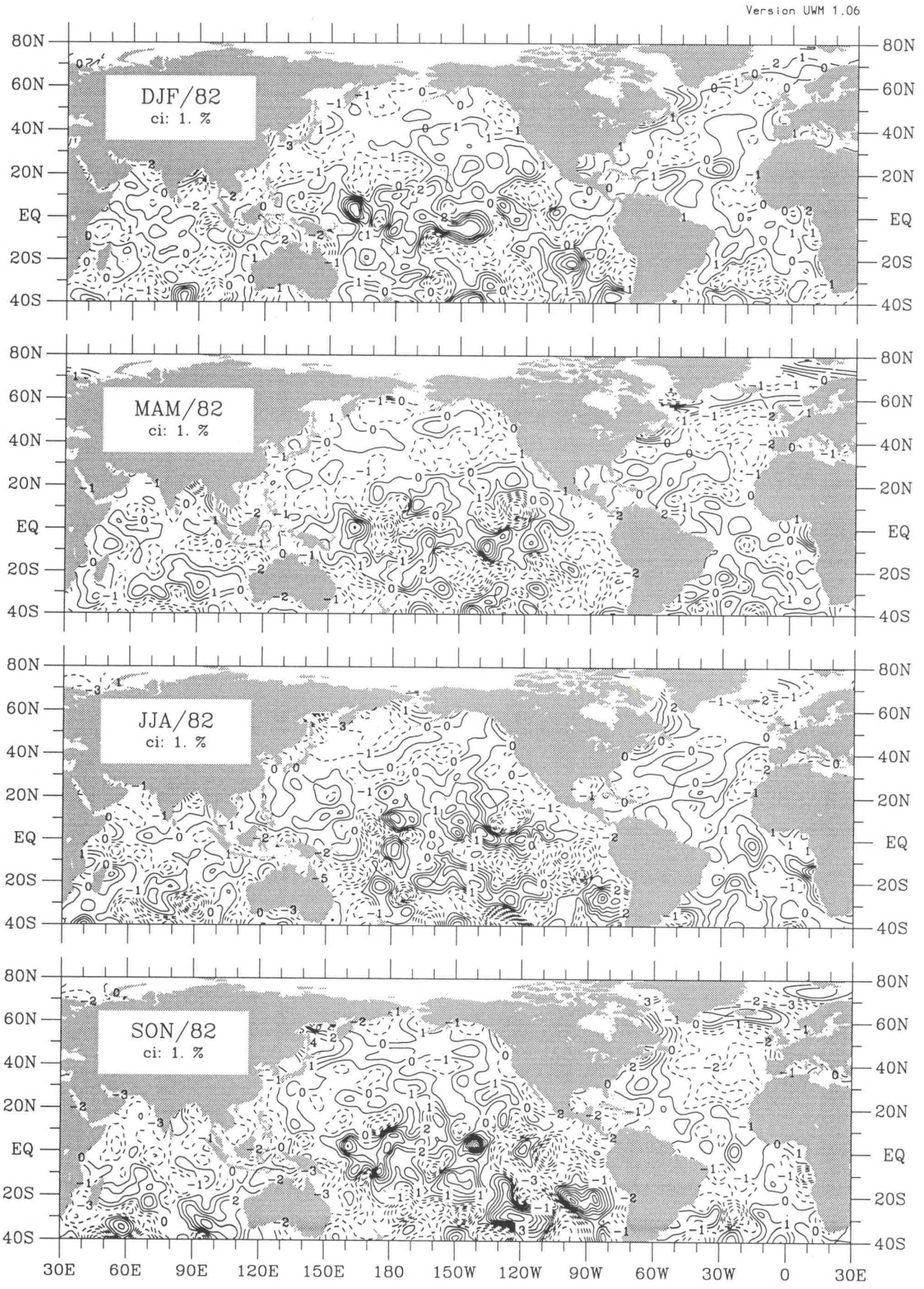

Figure rh-43. Relative humidity seasonal anomaly for 1982.

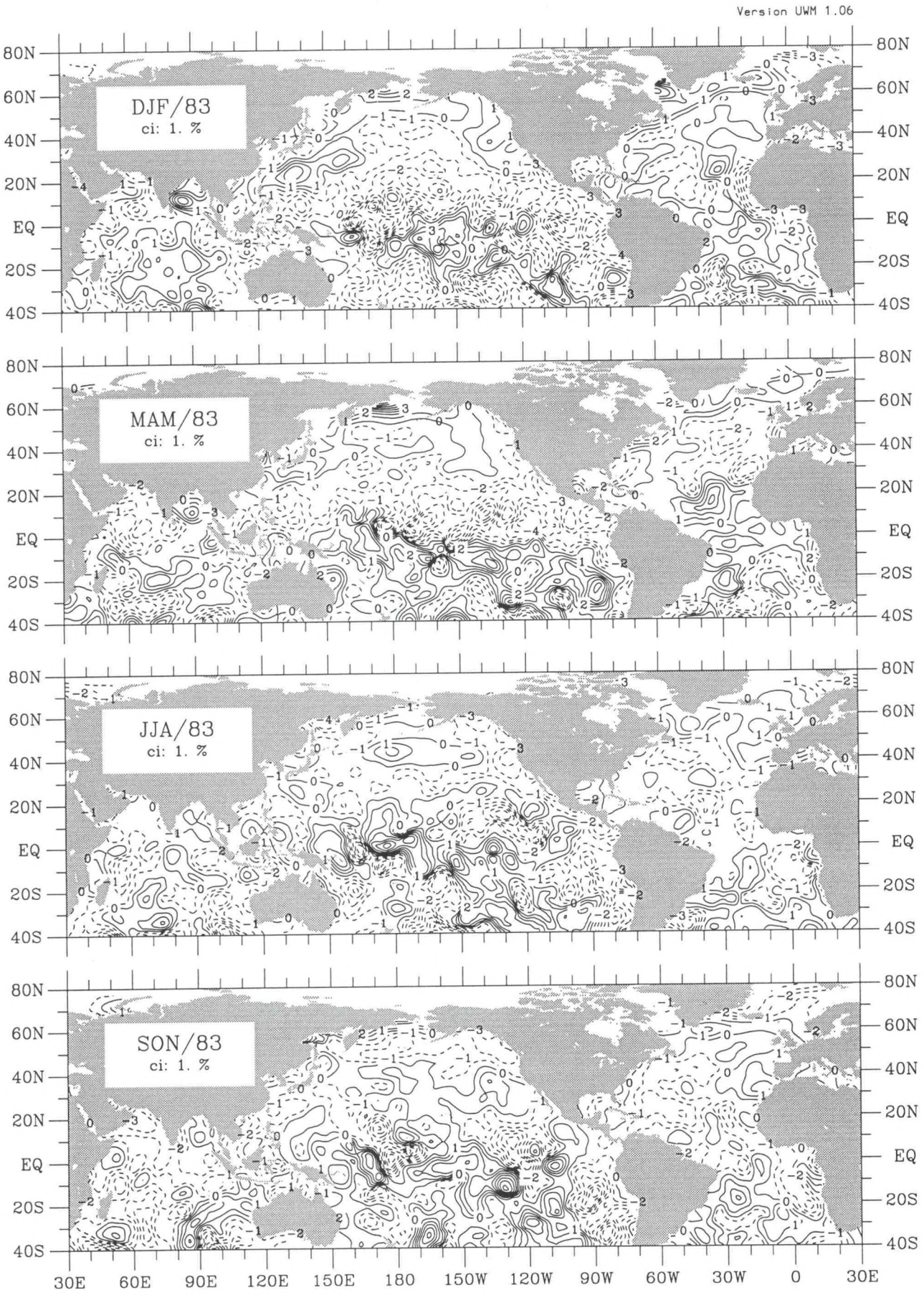

Figure rh-44. Relative humidity seasonal anomaly for 1983.

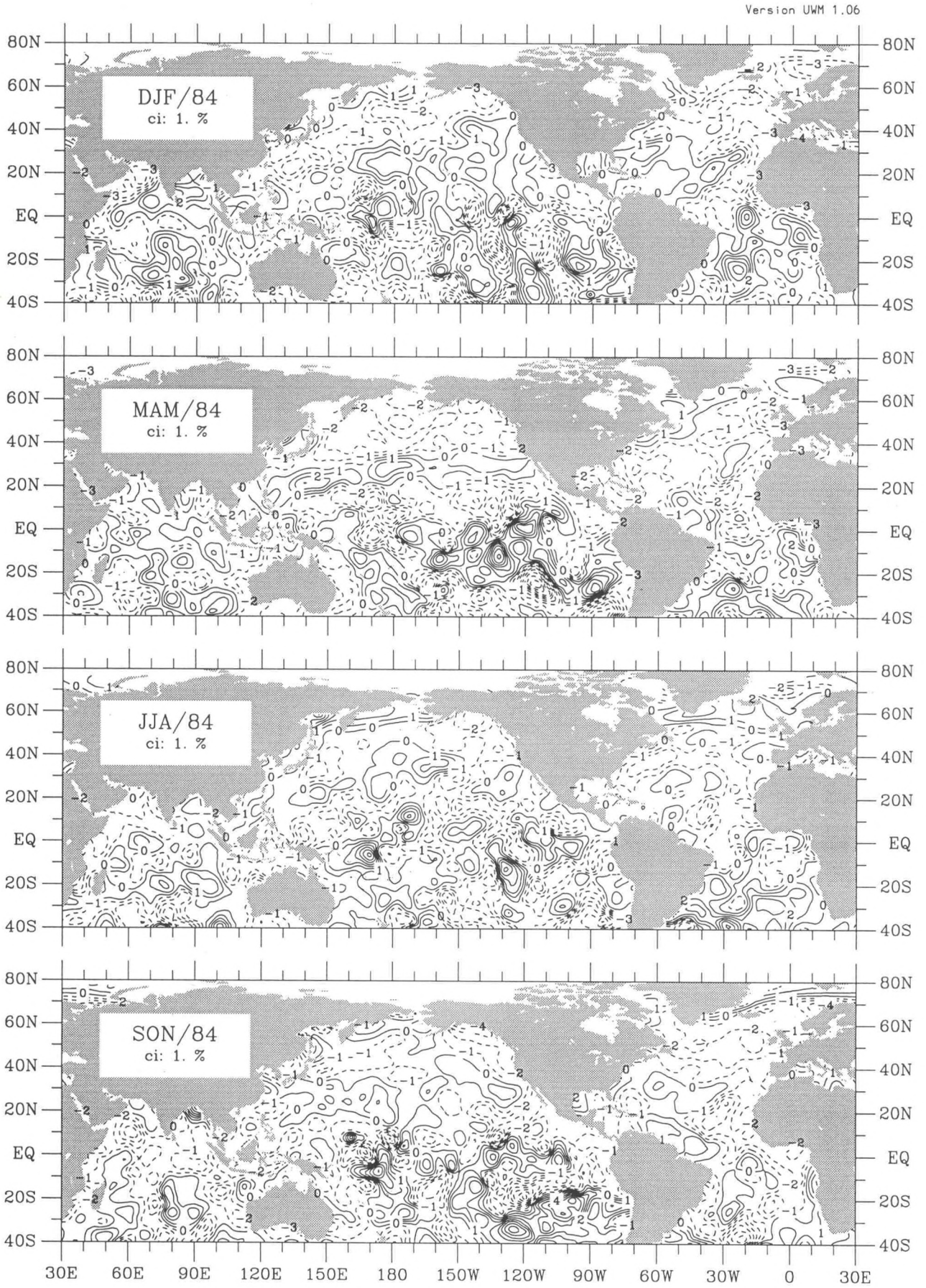

Figure rh-45. Relative humidity seasonal anomaly for 1984.

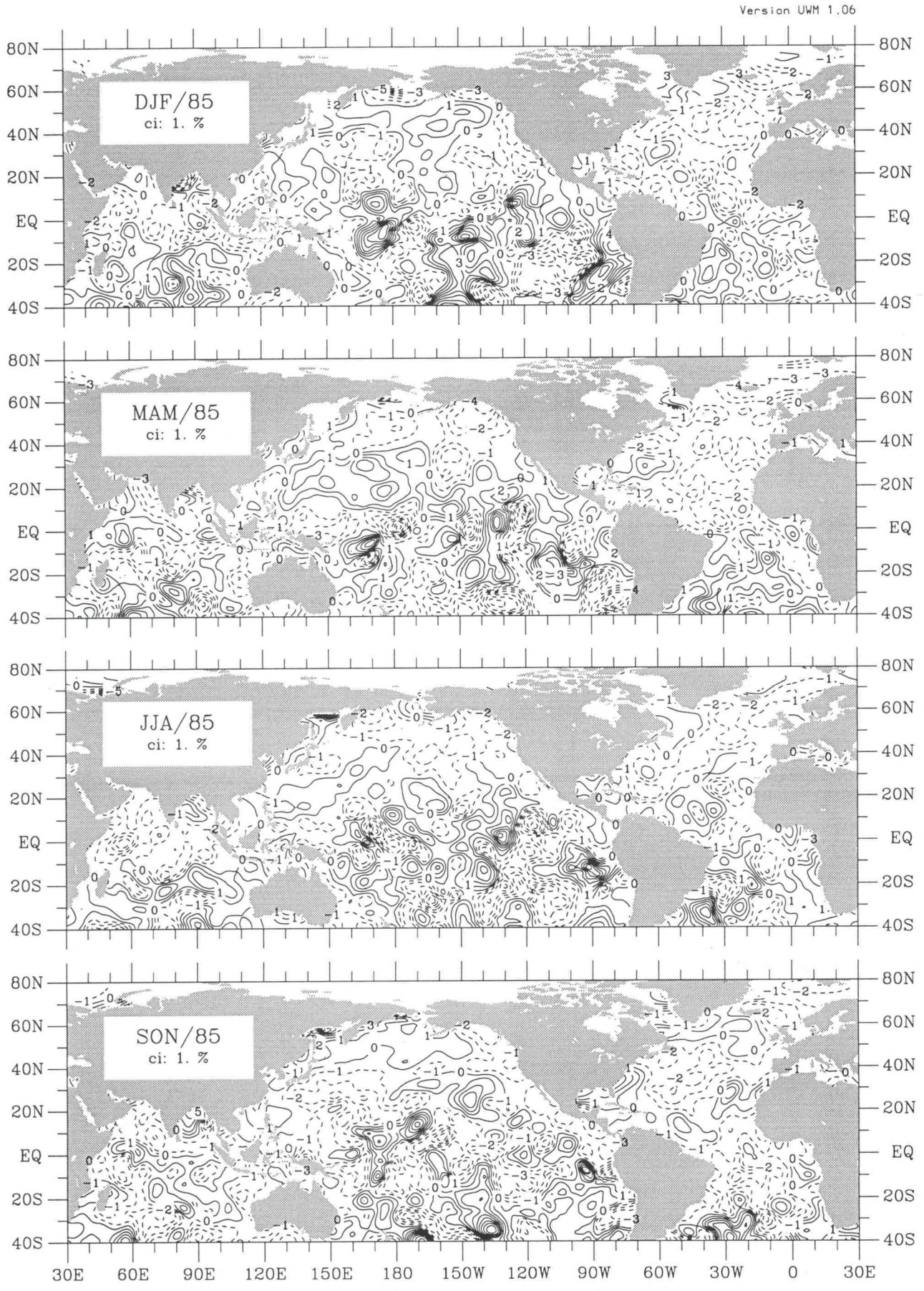

Figure rh-46. Relative humidity seasonal anomaly for 1985.

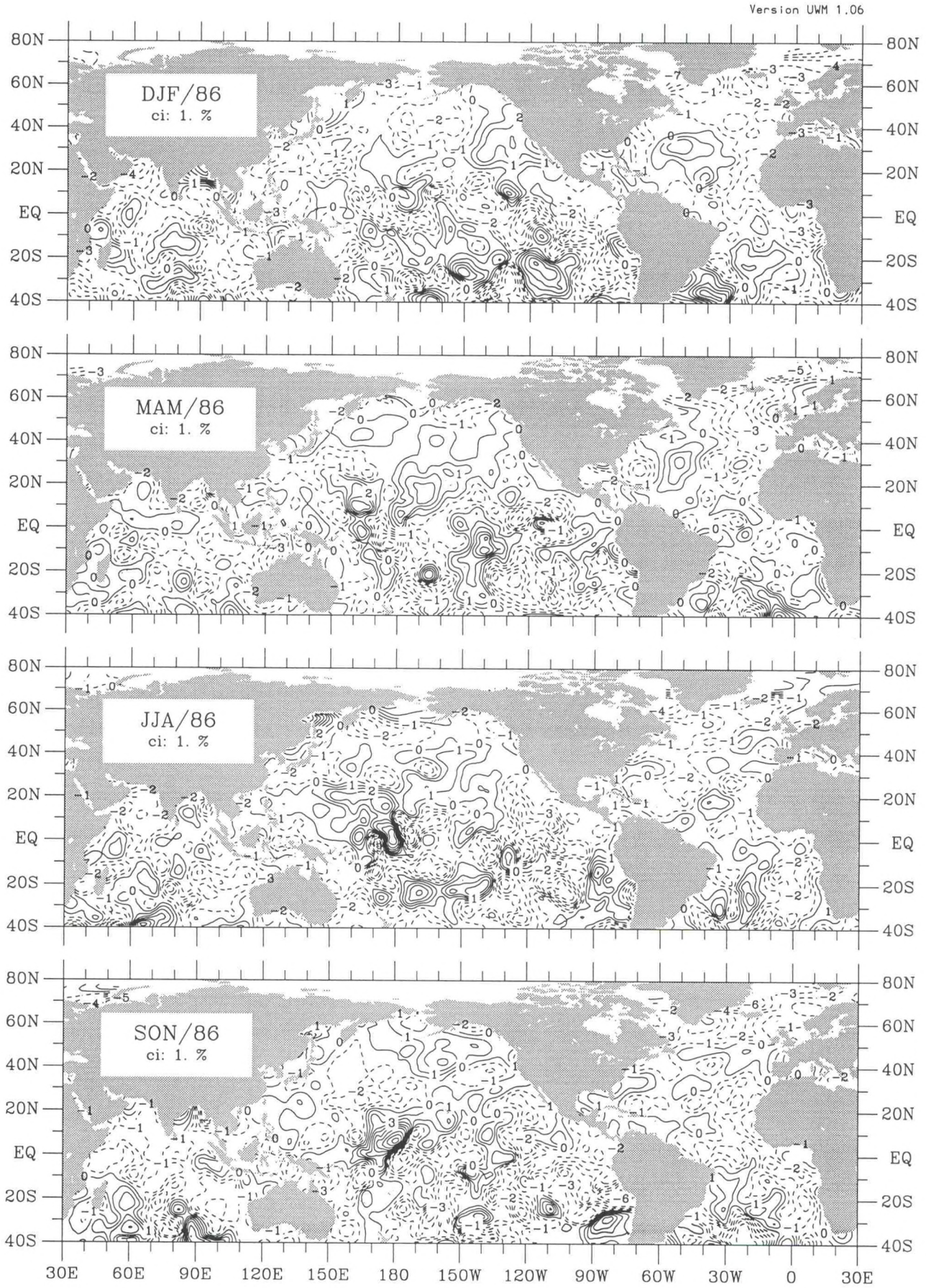

Figure rh-47. Relative humidity seasonal anomaly for 1986.

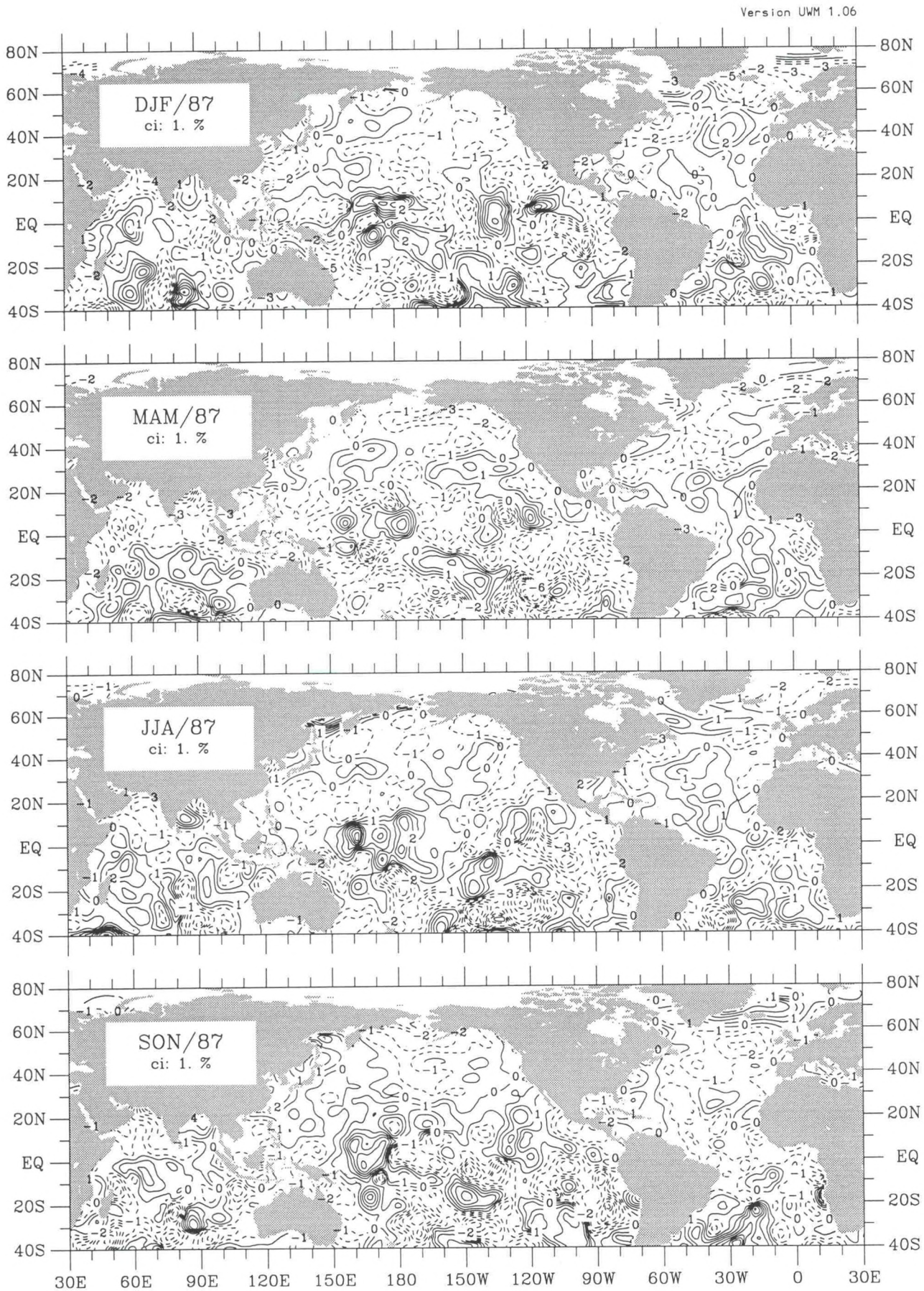

Figure rh-48. Relative humidity seasonal anomaly for 1987.

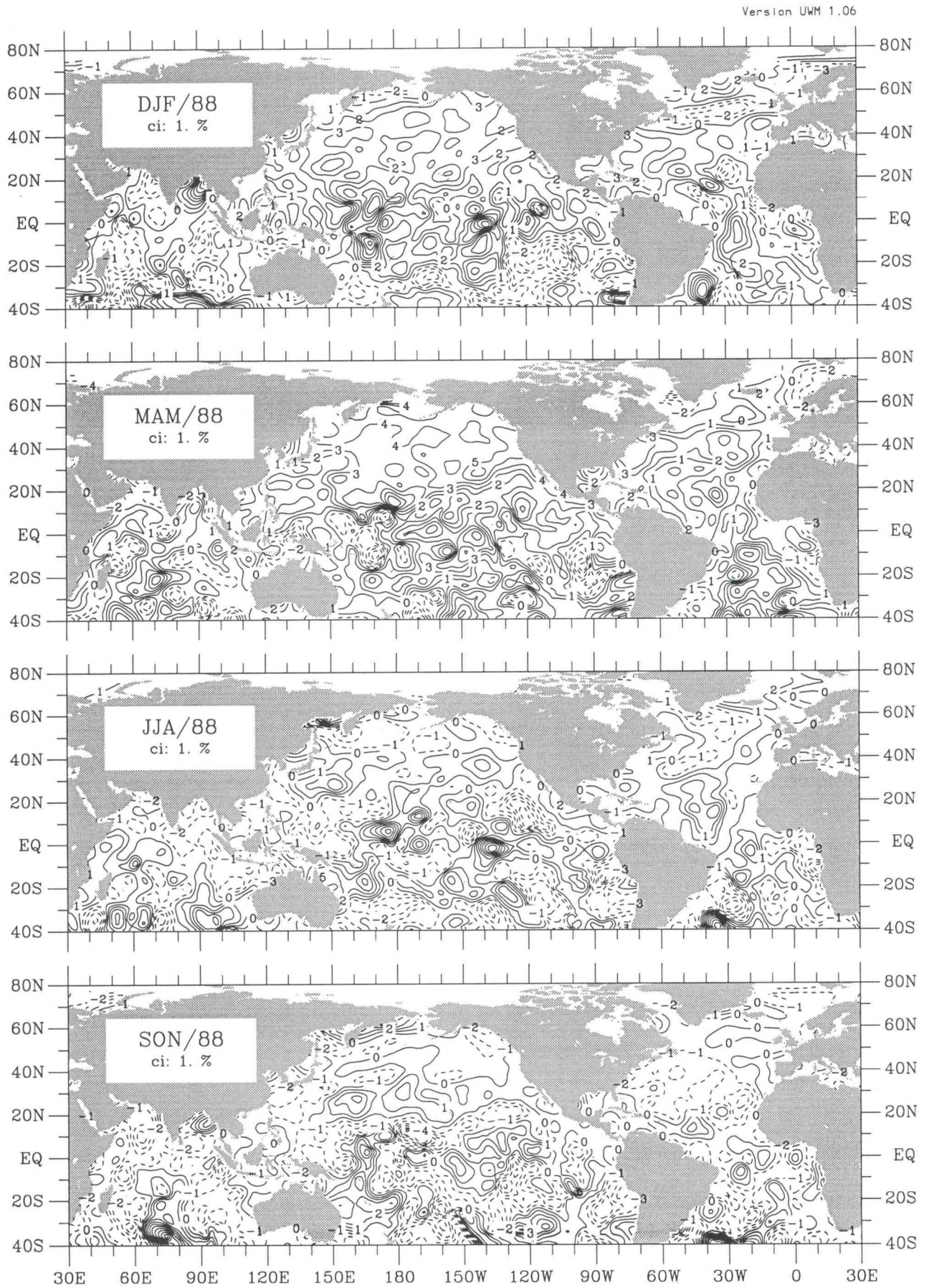

Figure rh-49. Relative humidity seasonal anomaly for 1988.

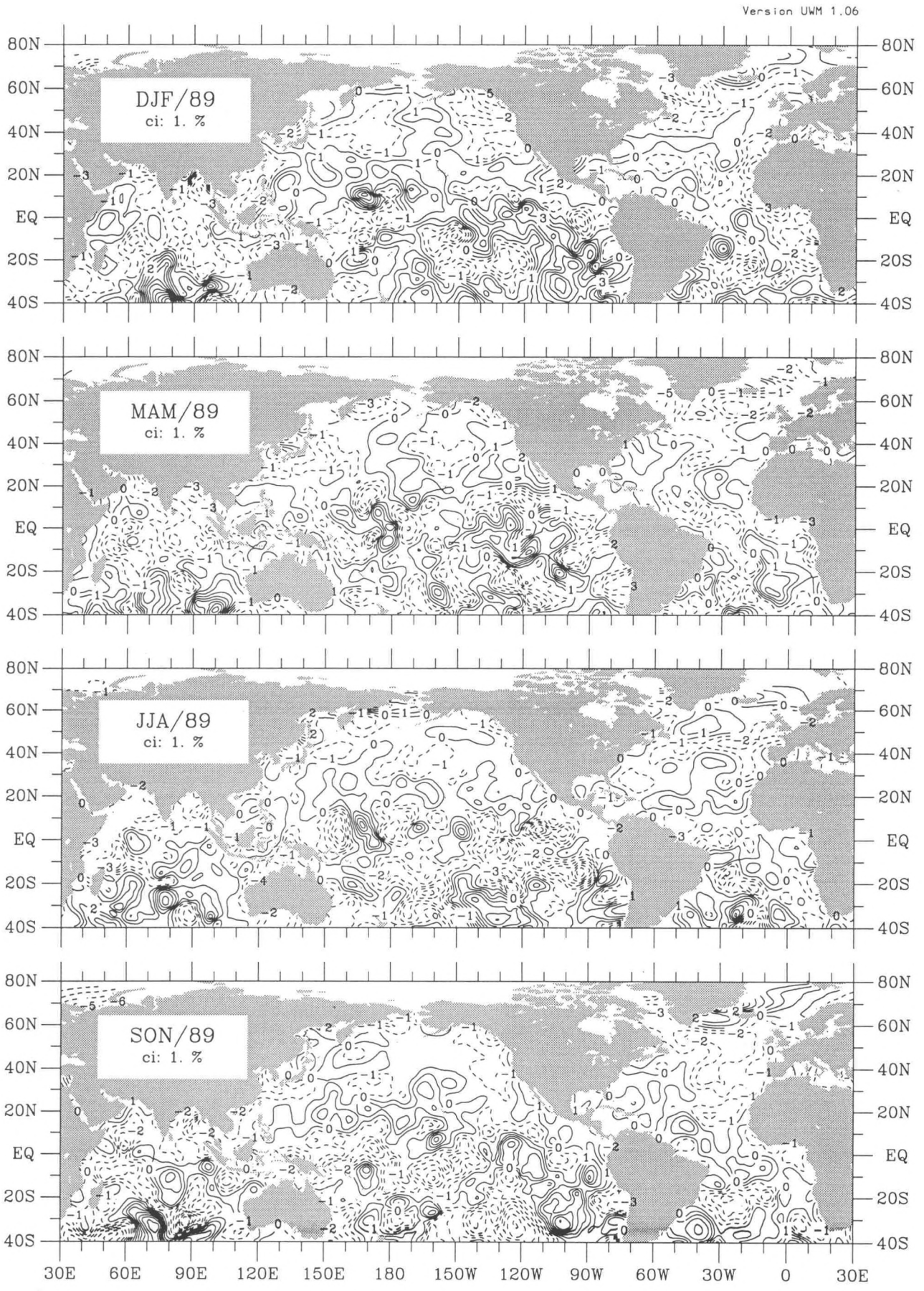

Figure rh-50. Relative humidity seasonal anomaly for 1989.

12 Sea minus air humidity

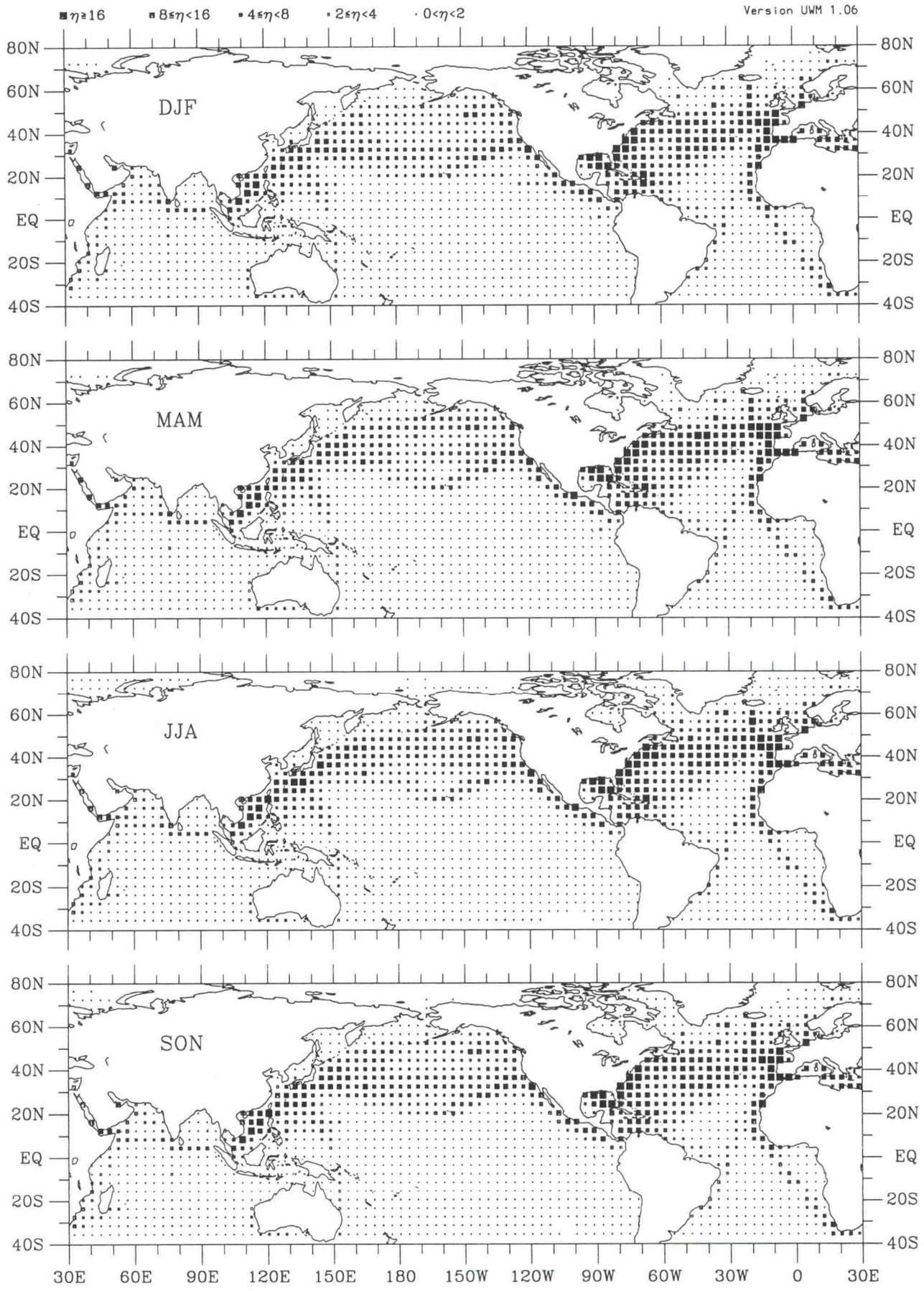

Figure dq-1. qs minus q seasonal observation density (1945-89).

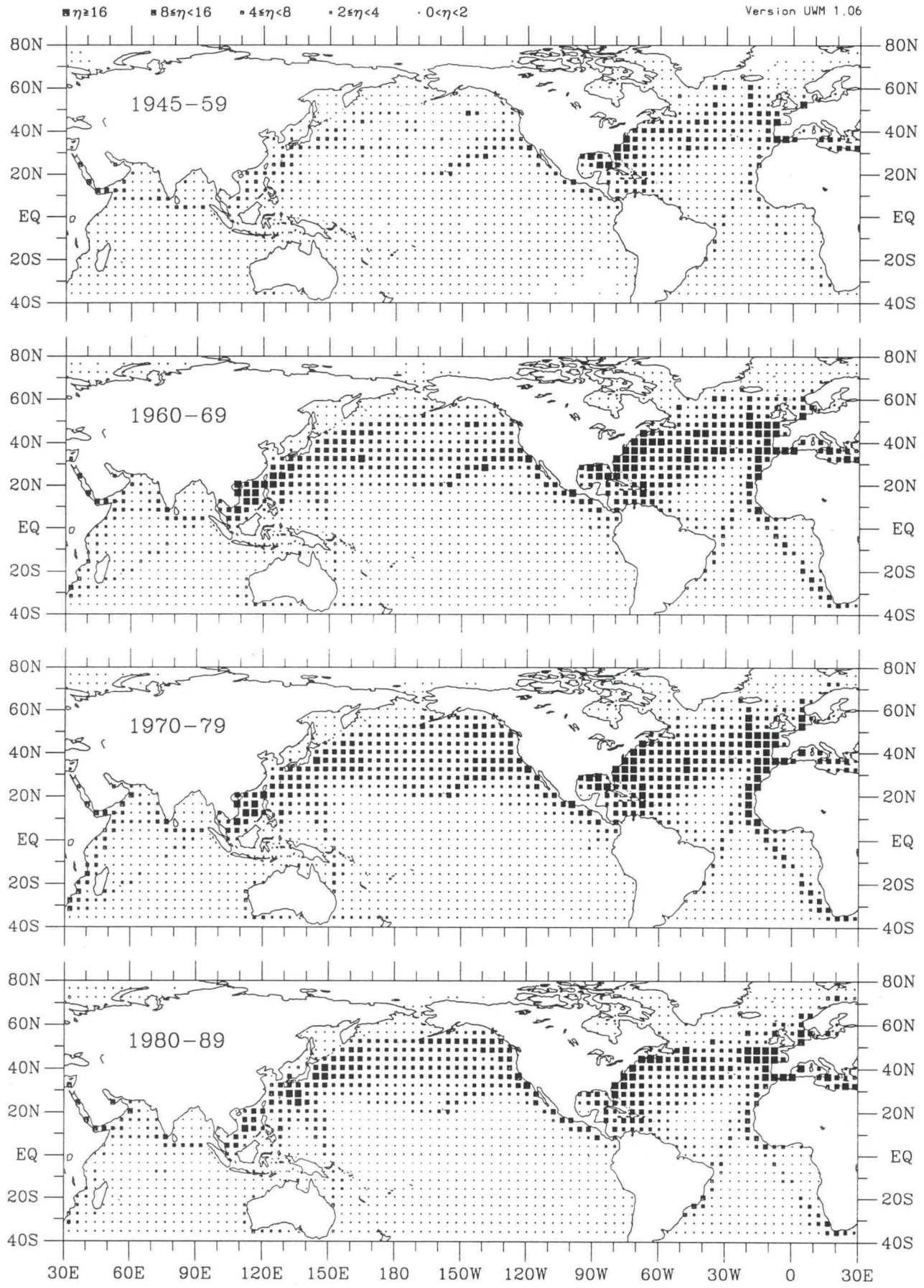

Figure dq-2. qs minus q decadal observation density.

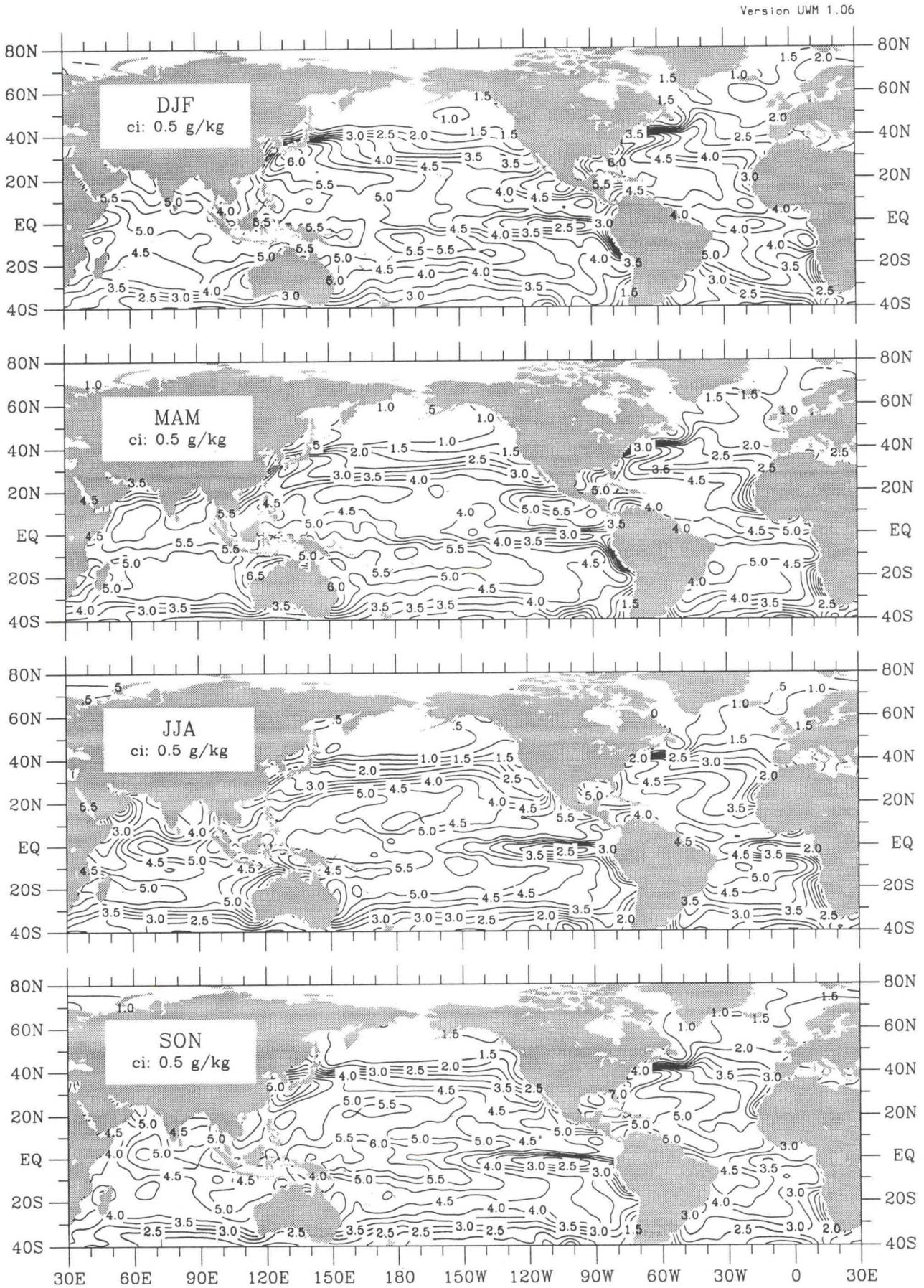

Figure dq-3. qs minus q seasonal climatology (1945-89).

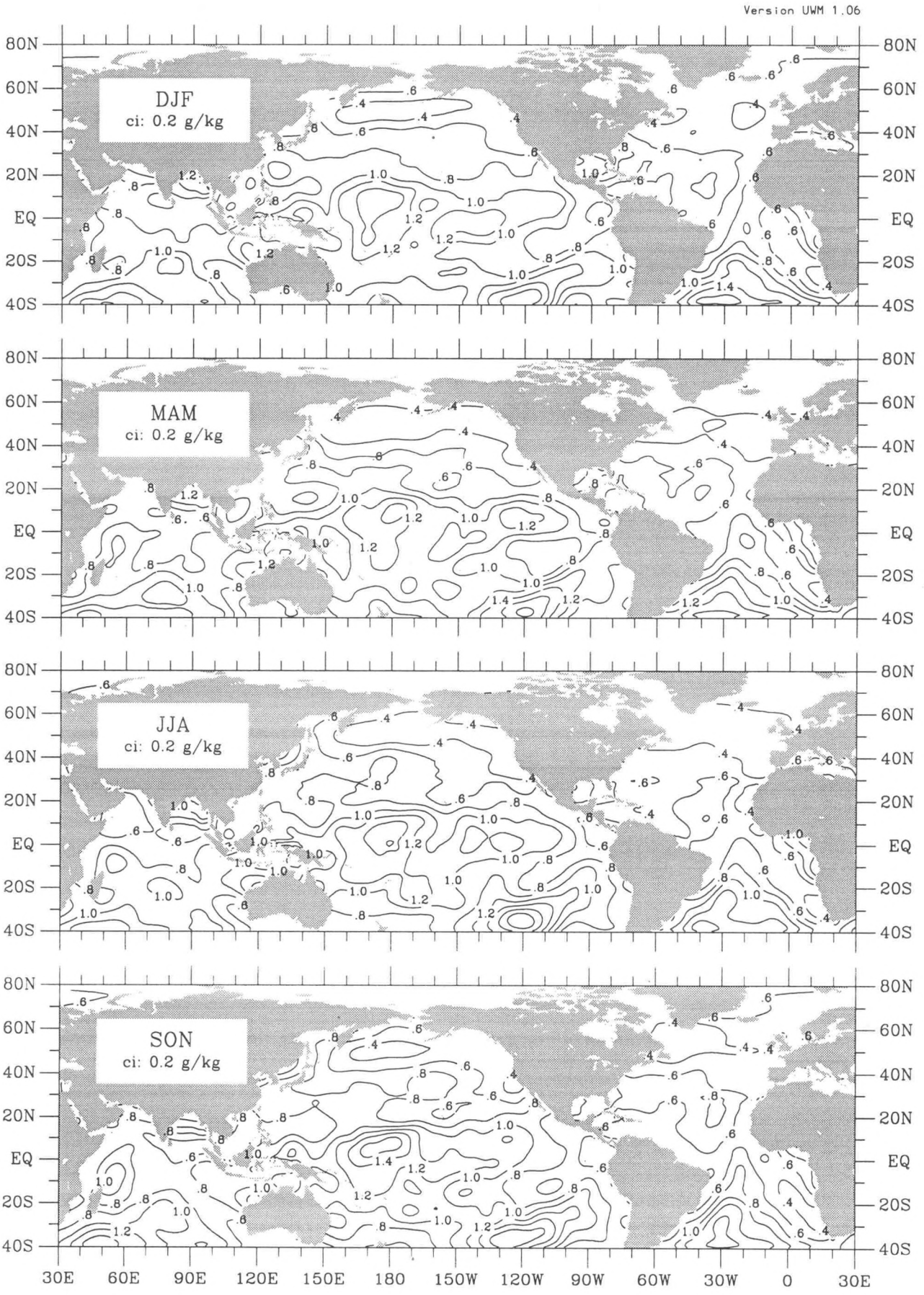

Figure dq-4. qs minus q seasonal interannual std dev (1945-89).

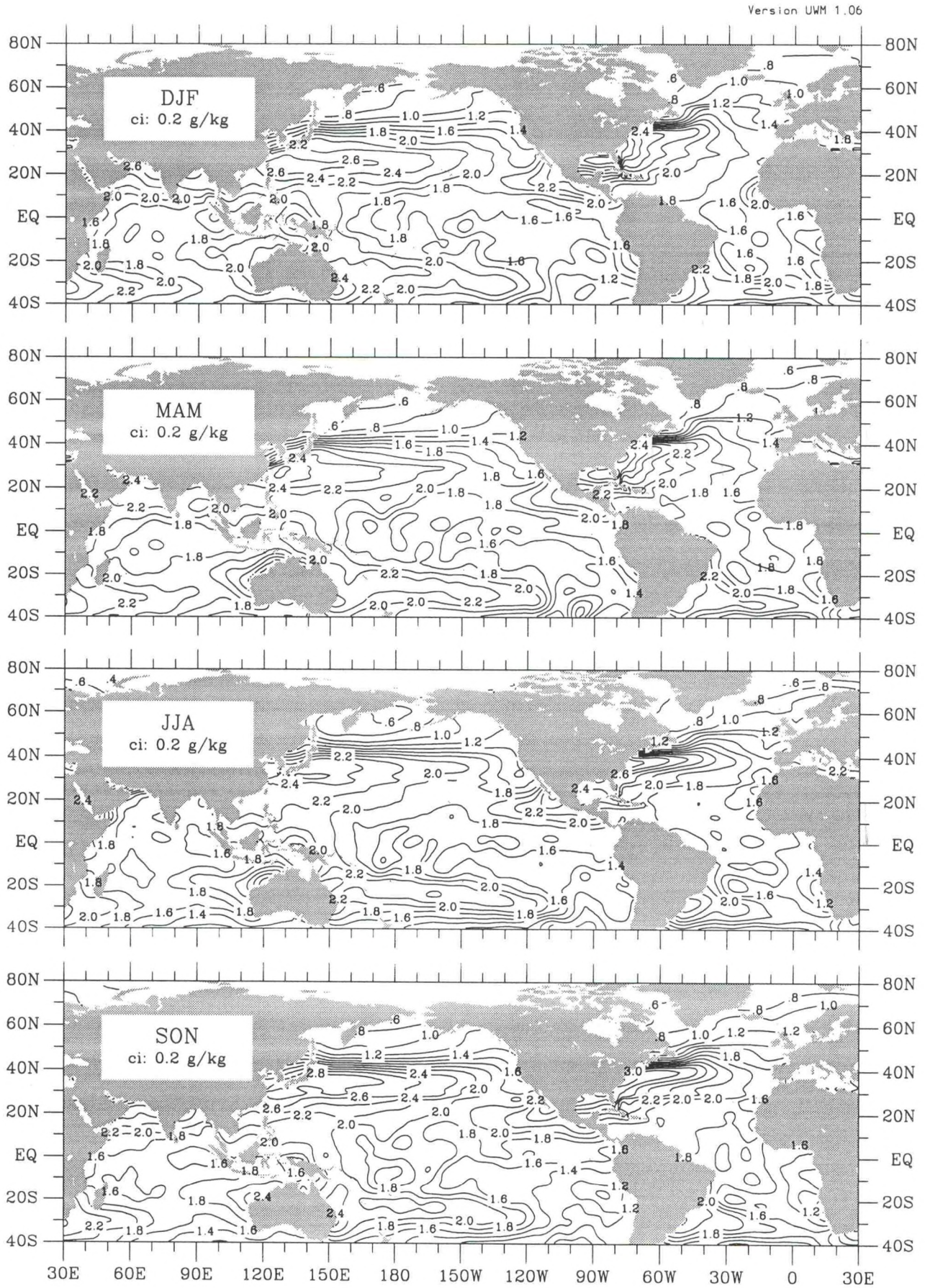

Figure dq–5. qs minus q seasonal standard deviation (1945–89).

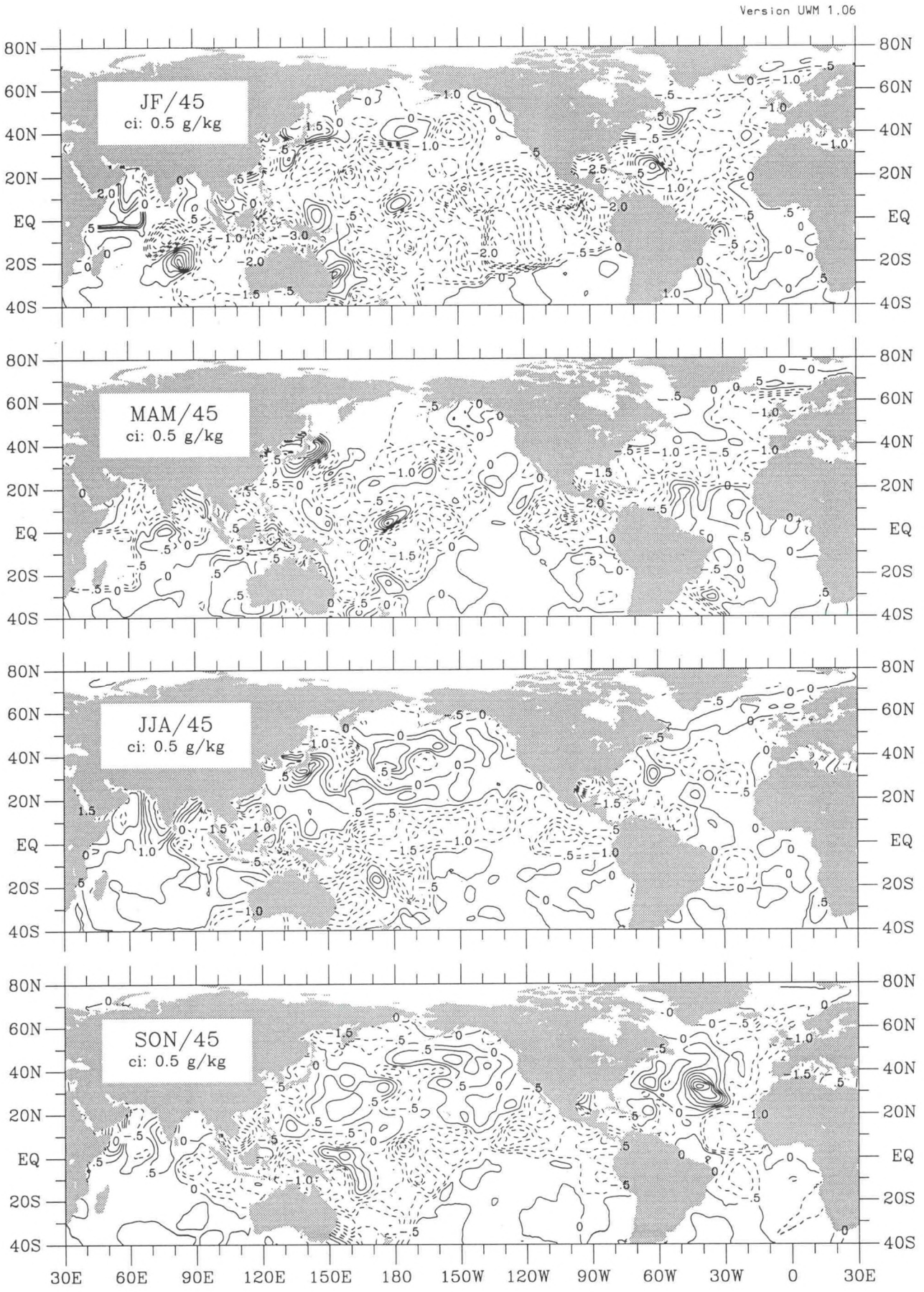

Figure dq-6. qs minus q seasonal anomaly for 1945.

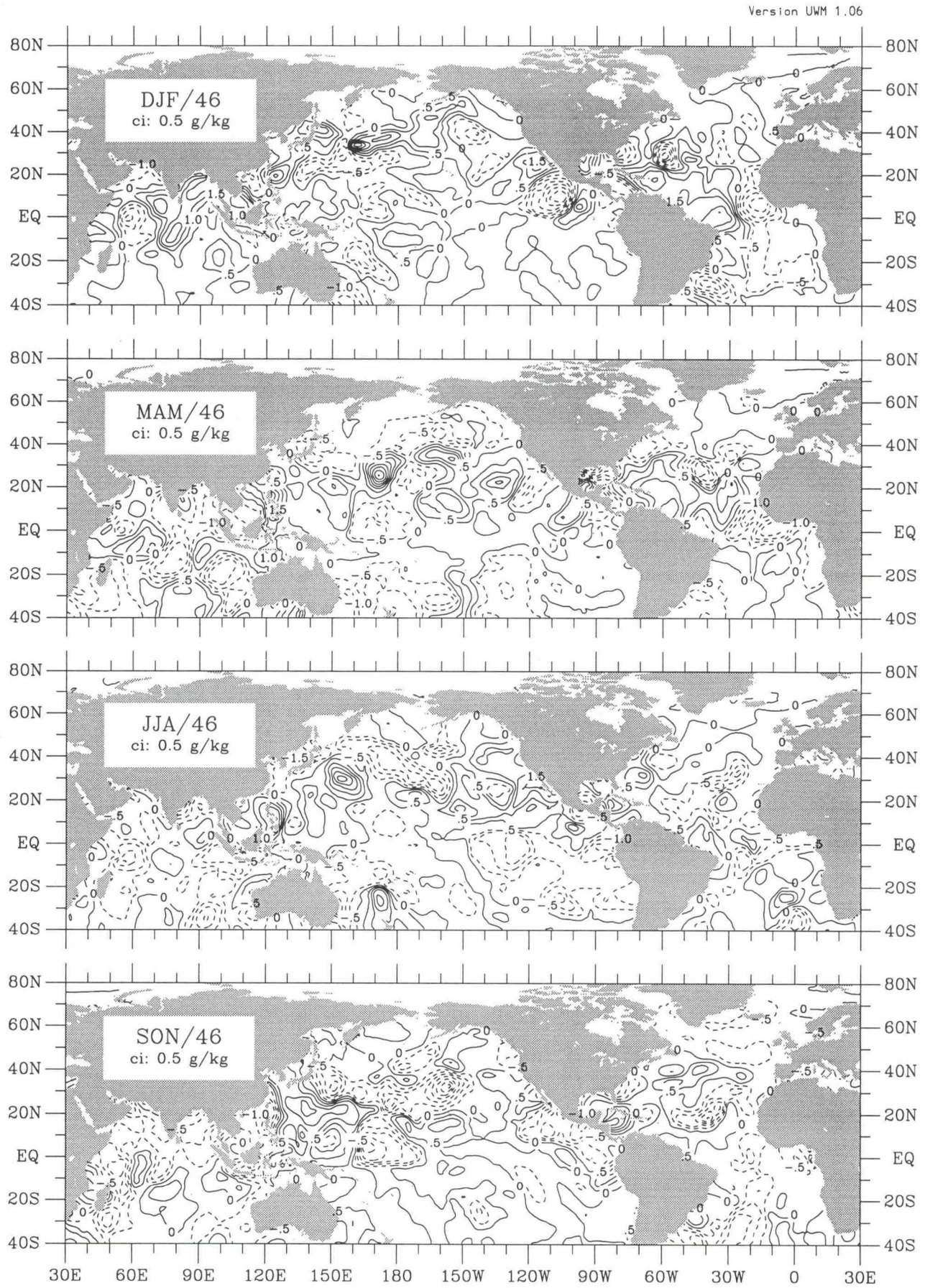

Figure dq-7. qs minus q seasonal anomaly for 1946.

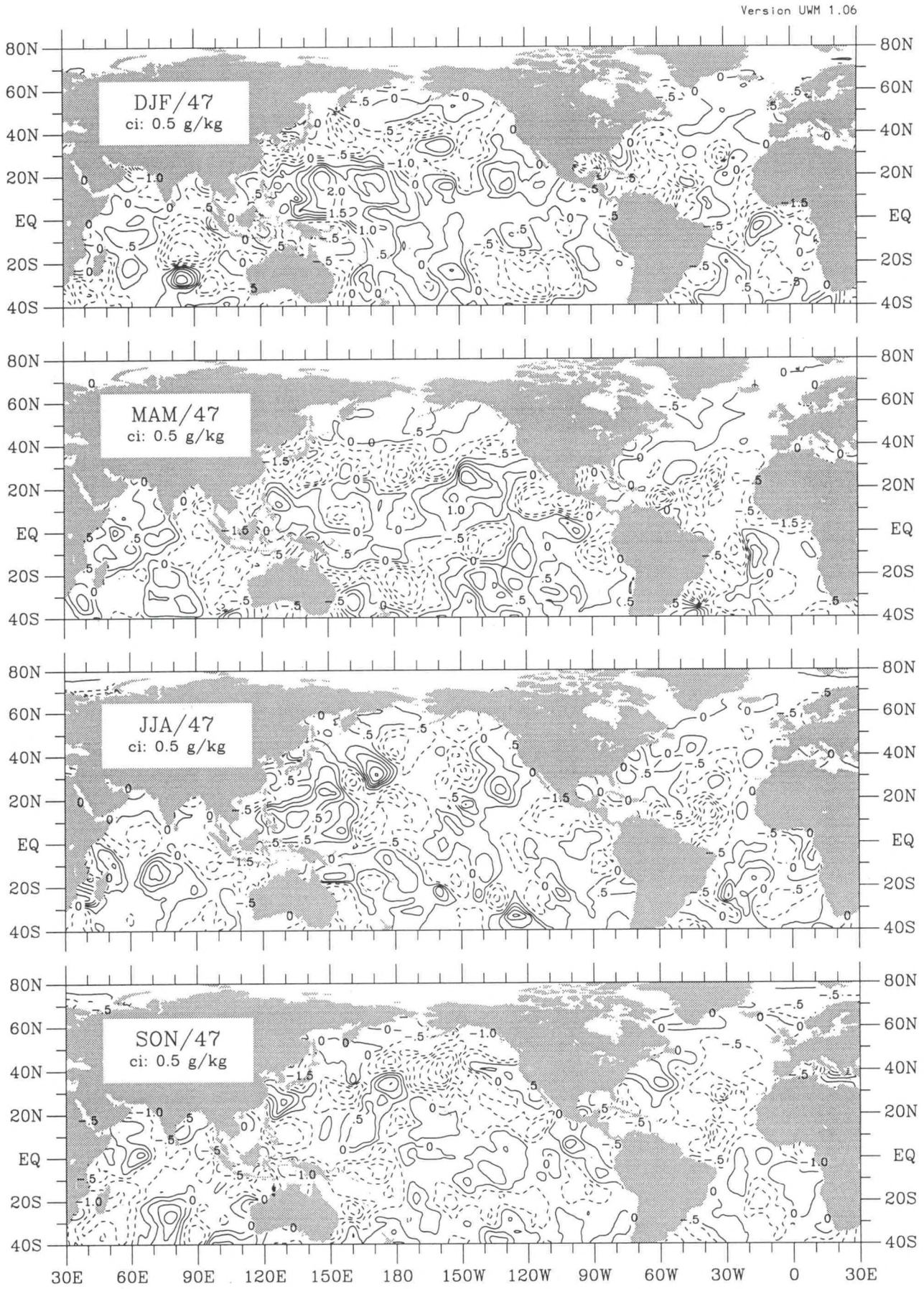

Figure dq-8. qs minus q seasonal anomaly for 1947.

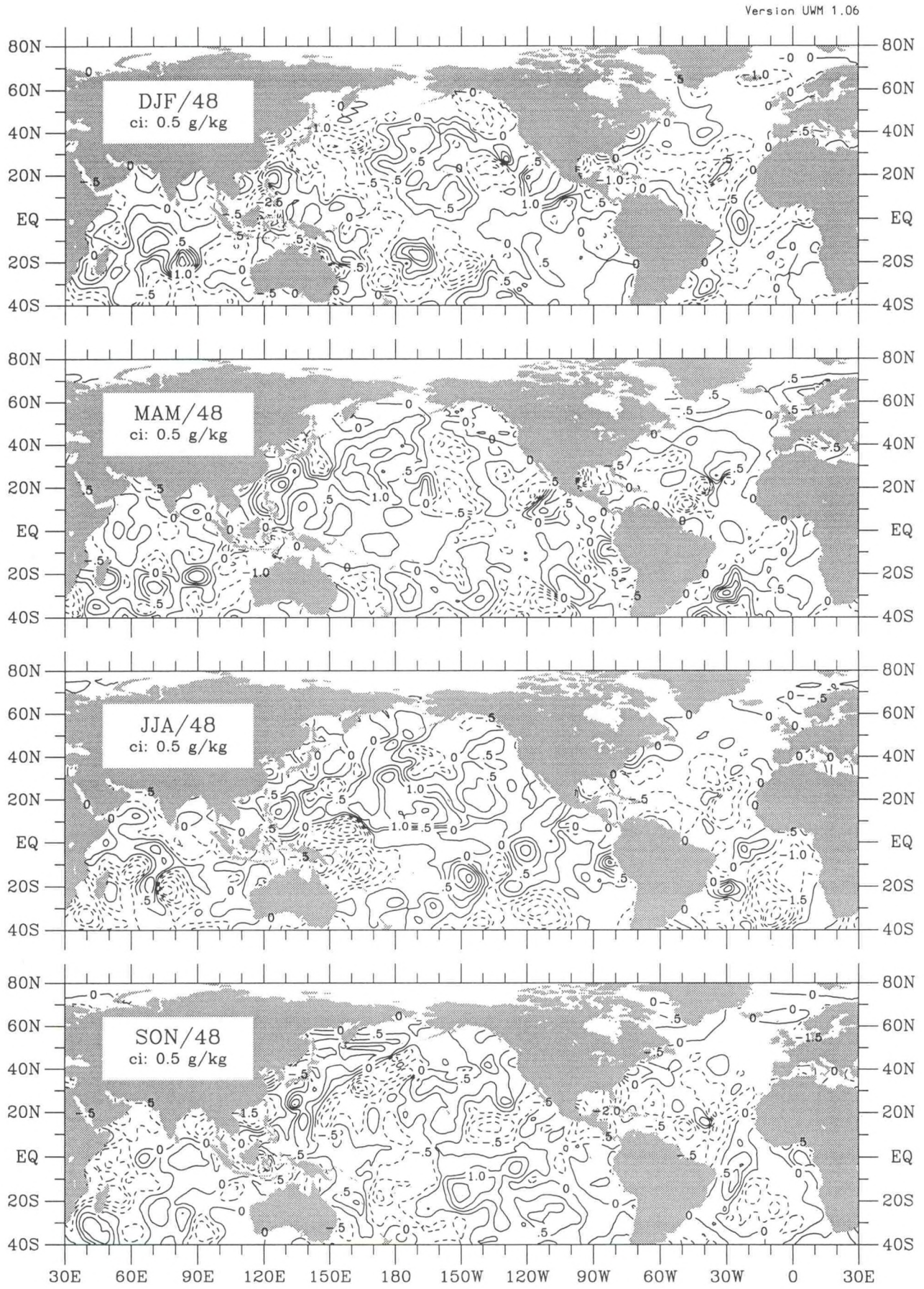

Figure dq-9. qs minus q seasonal anomaly for 1948.

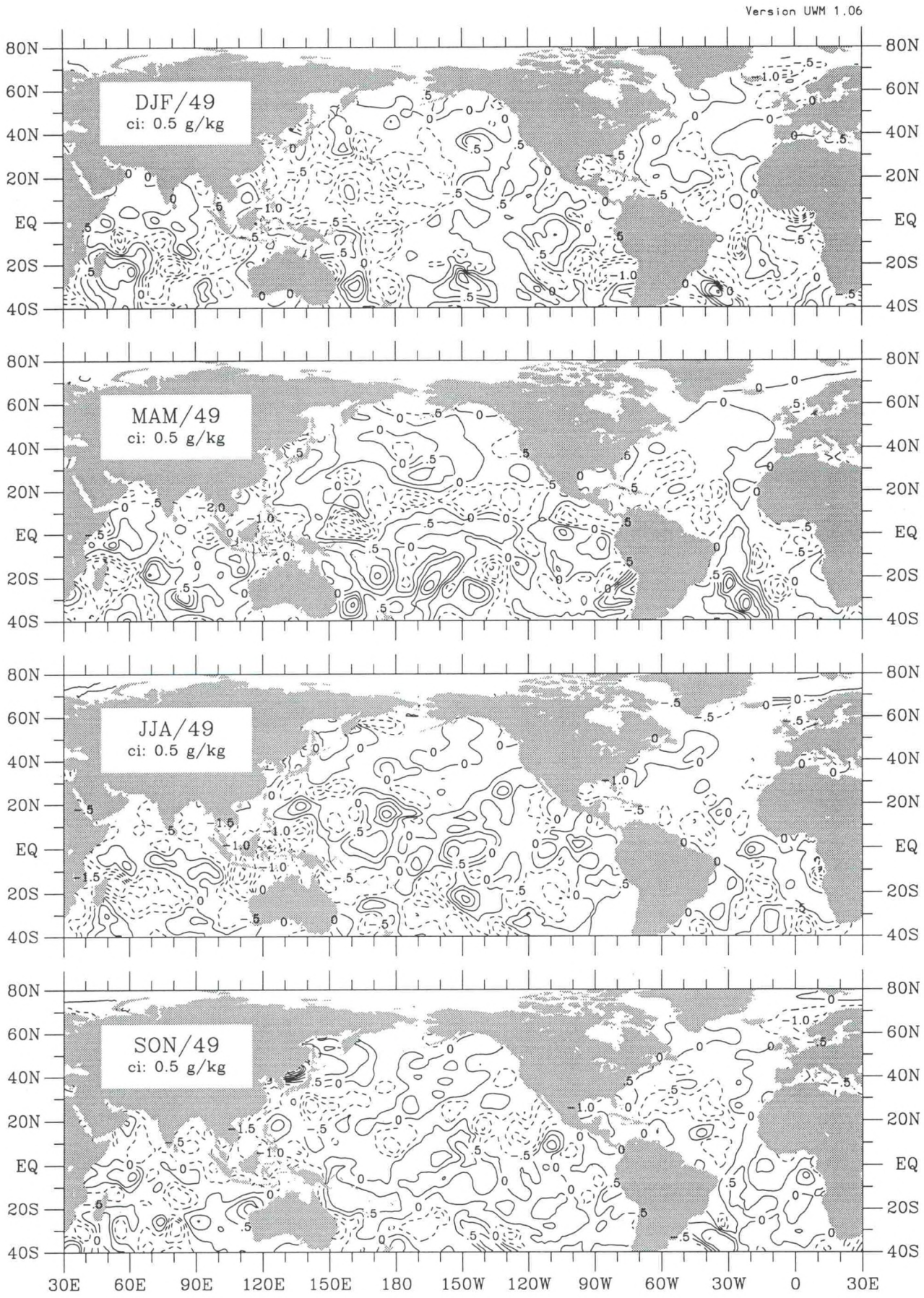

Figure dq-10. qs minus q seasonal anomaly for 1949.

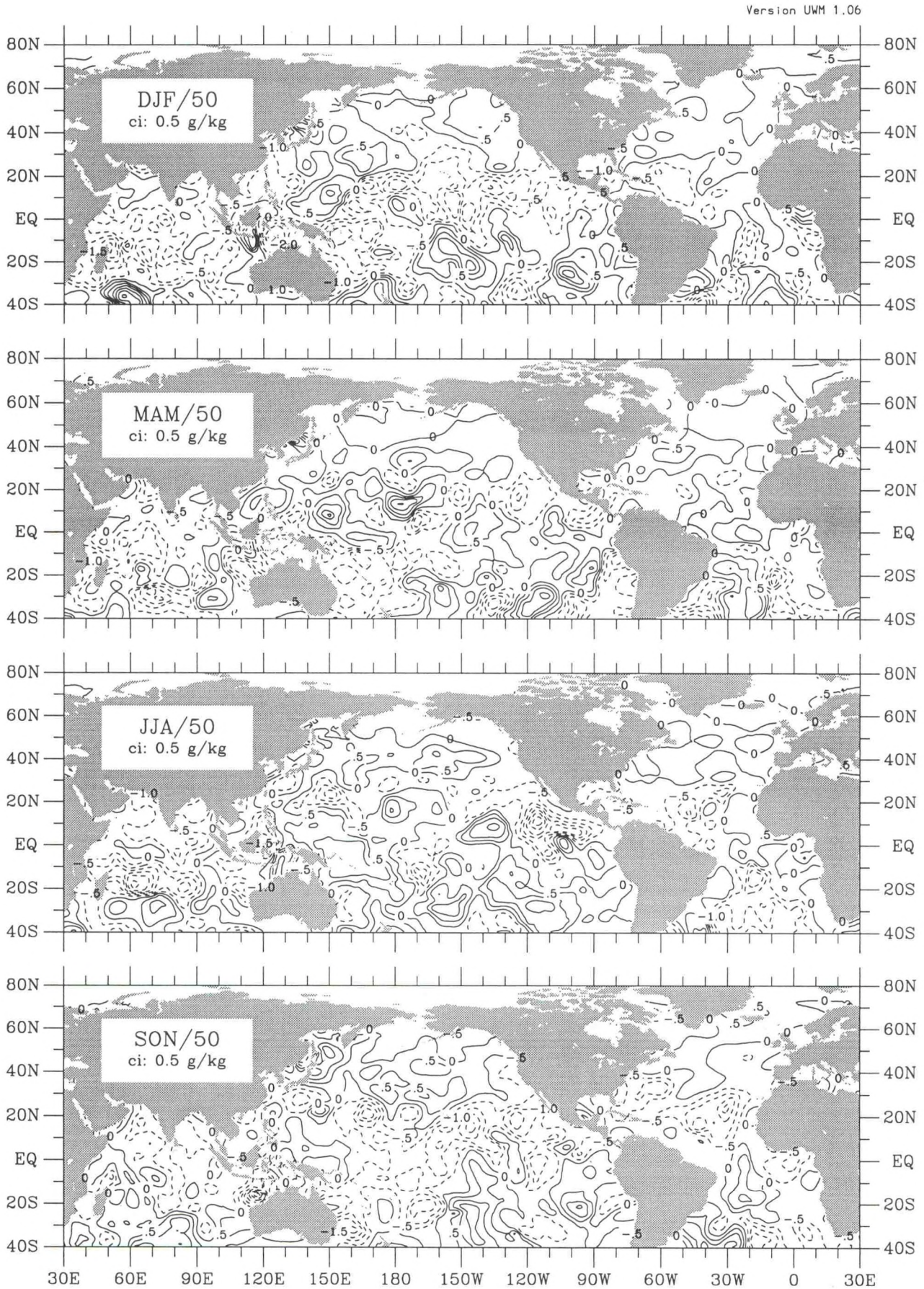

Figure dq-11. qs minus q seasonal anomaly for 1950.

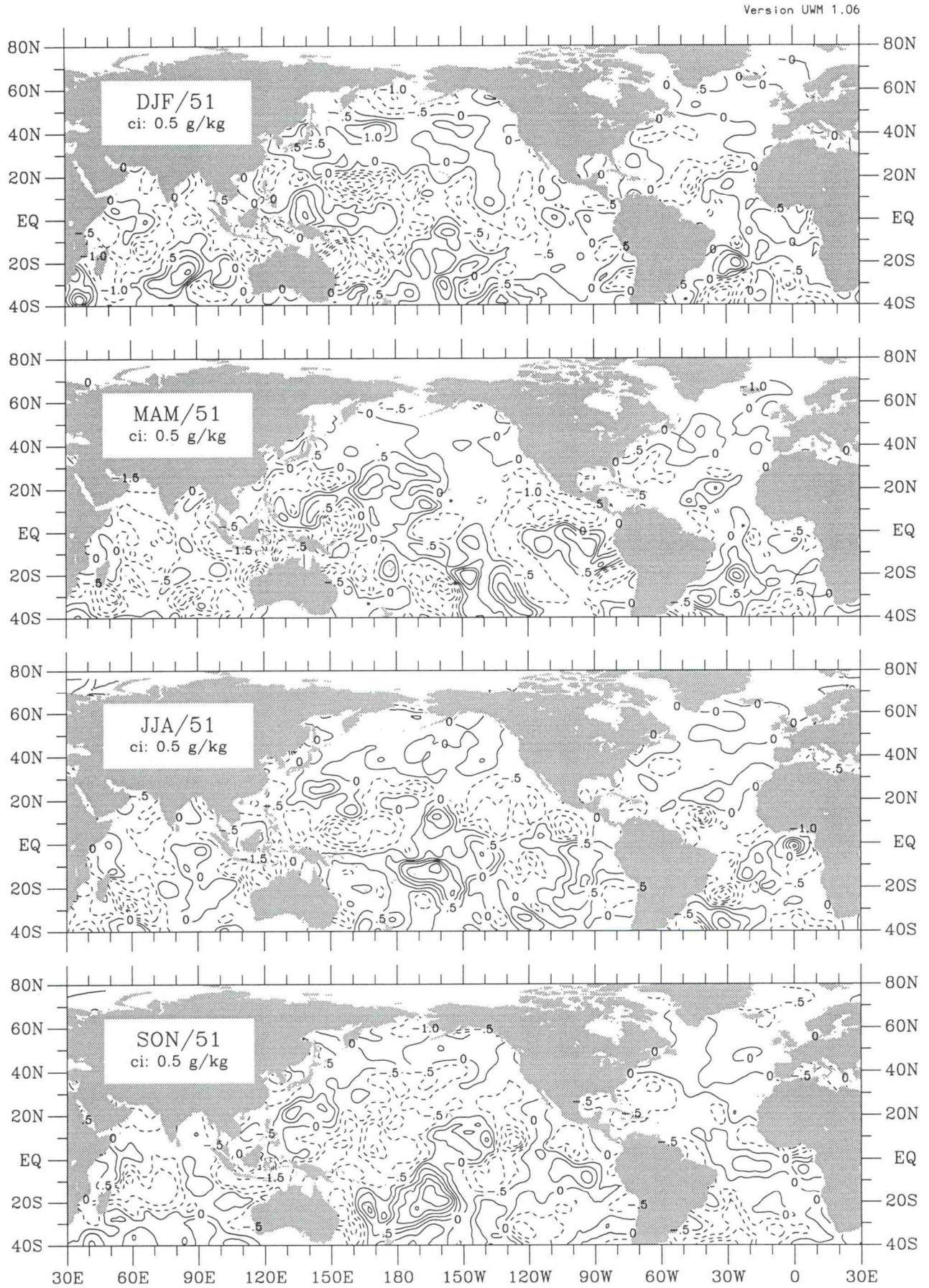

Figure dq-12. qs minus q seasonal anomaly for 1951.

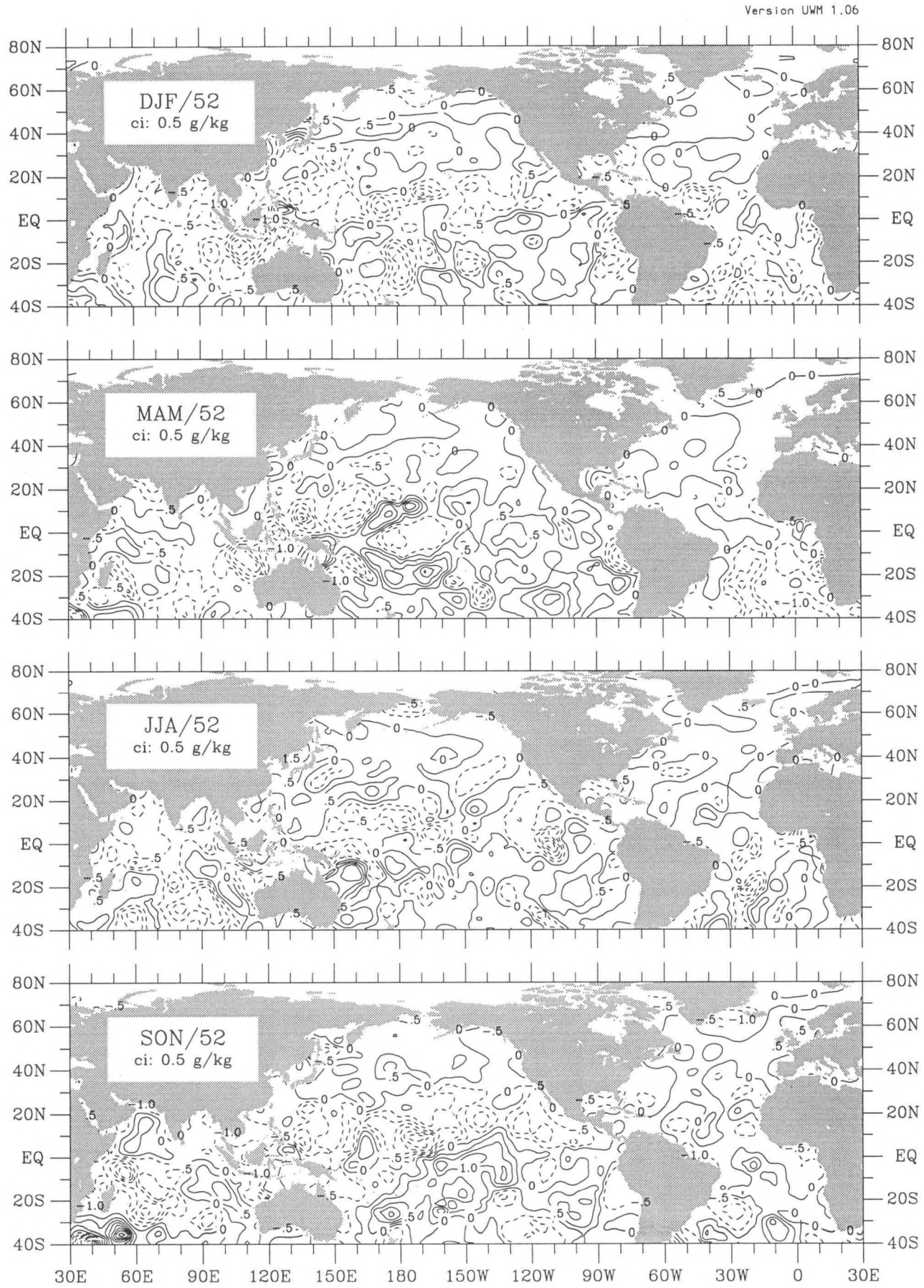

Figure dq-13. qs minus q seasonal anomaly for 1952.

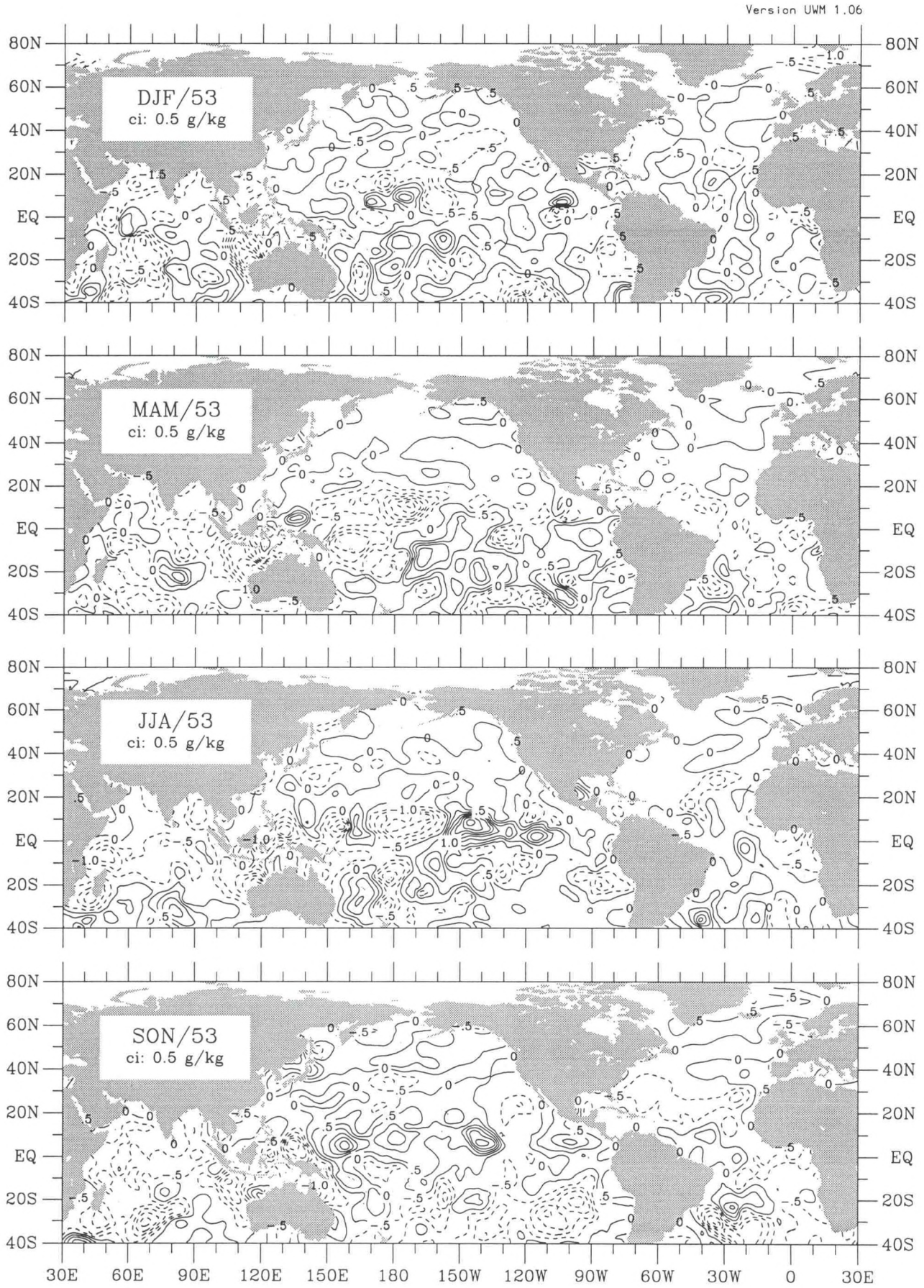

Figure dq-14. qs minus q seasonal anomaly for 1953.

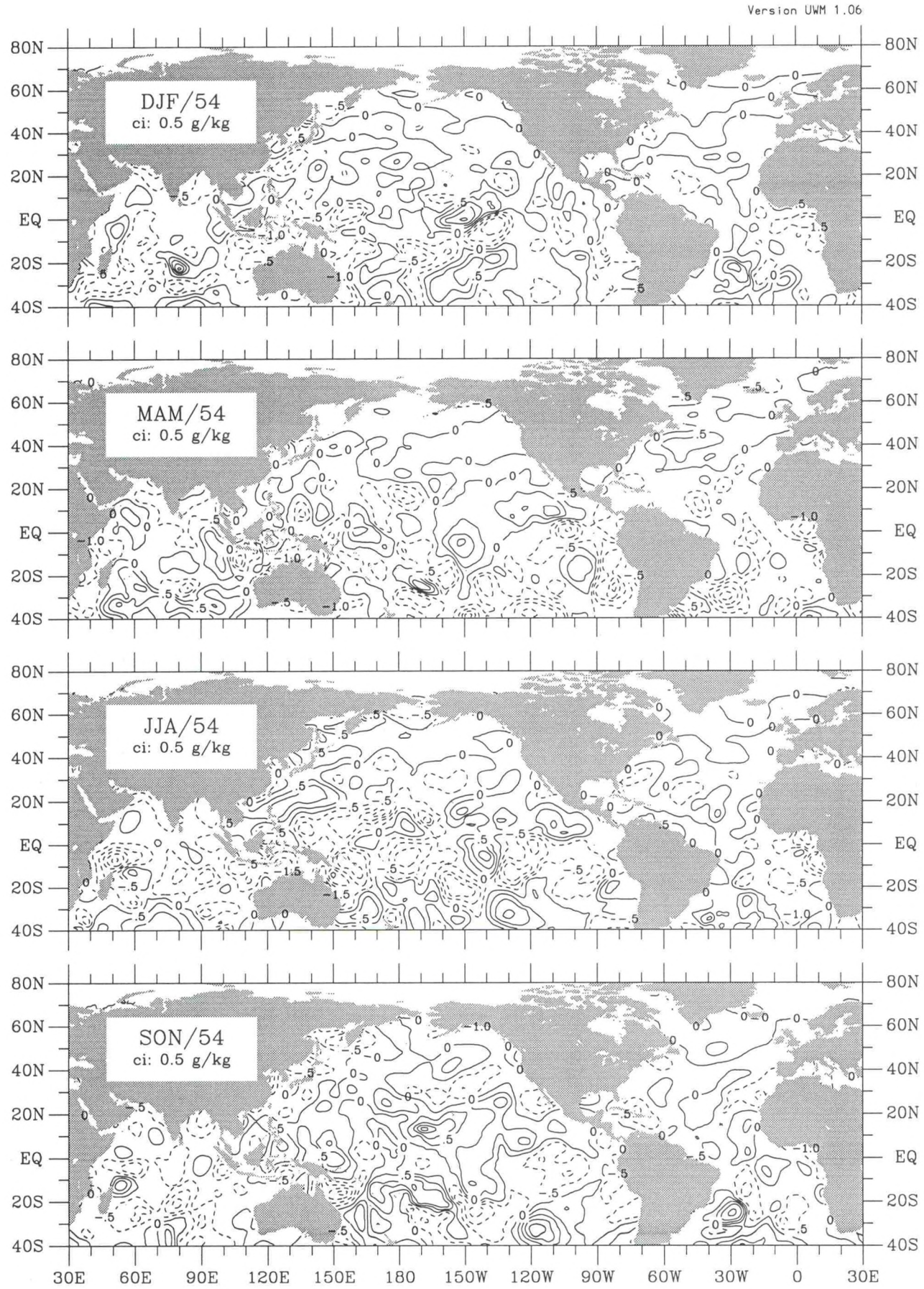

Figure dq-15. qs minus q seasonal anomaly for 1954.

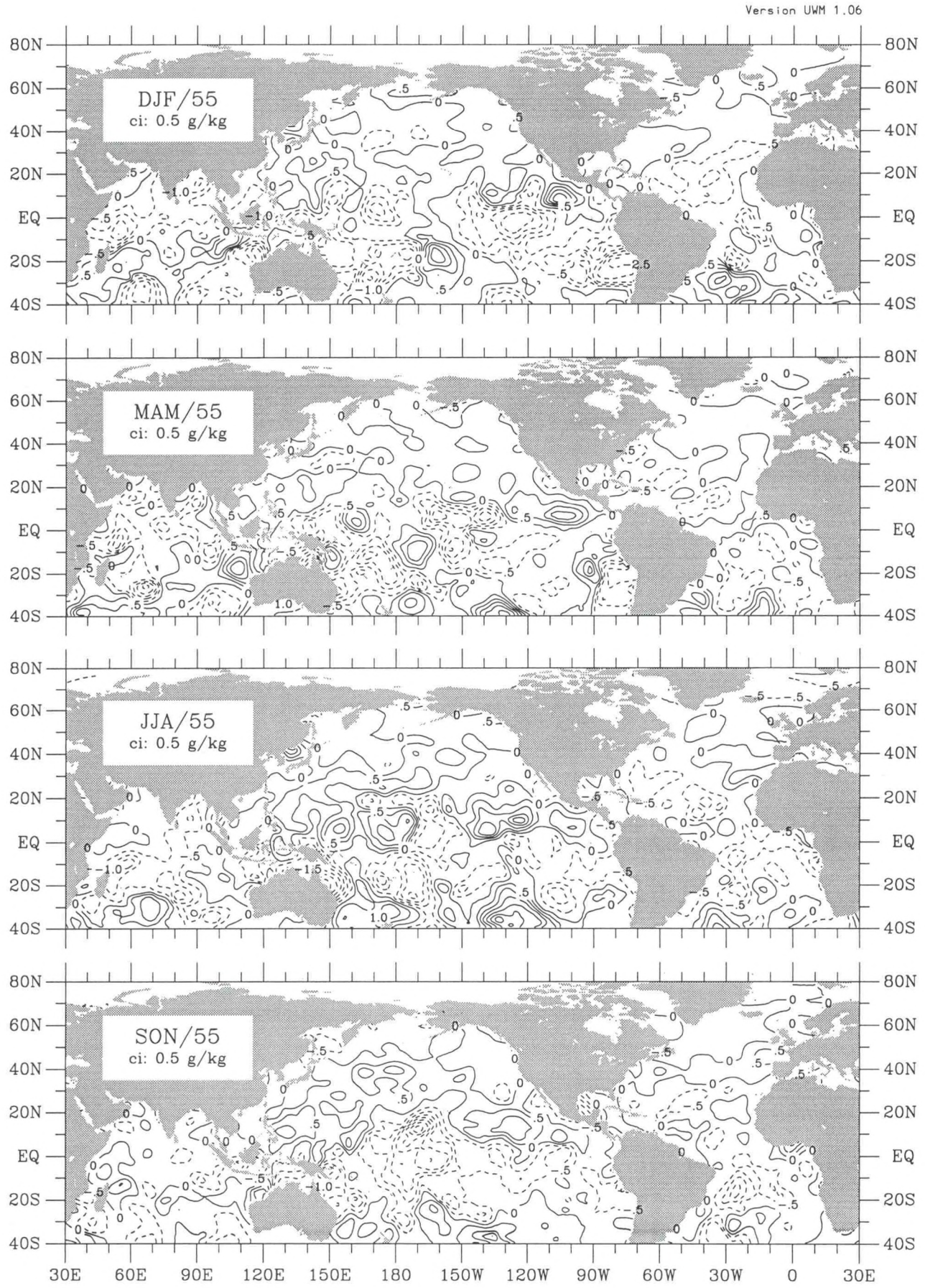

Figure dq-16. qs minus q seasonal anomaly for 1955.

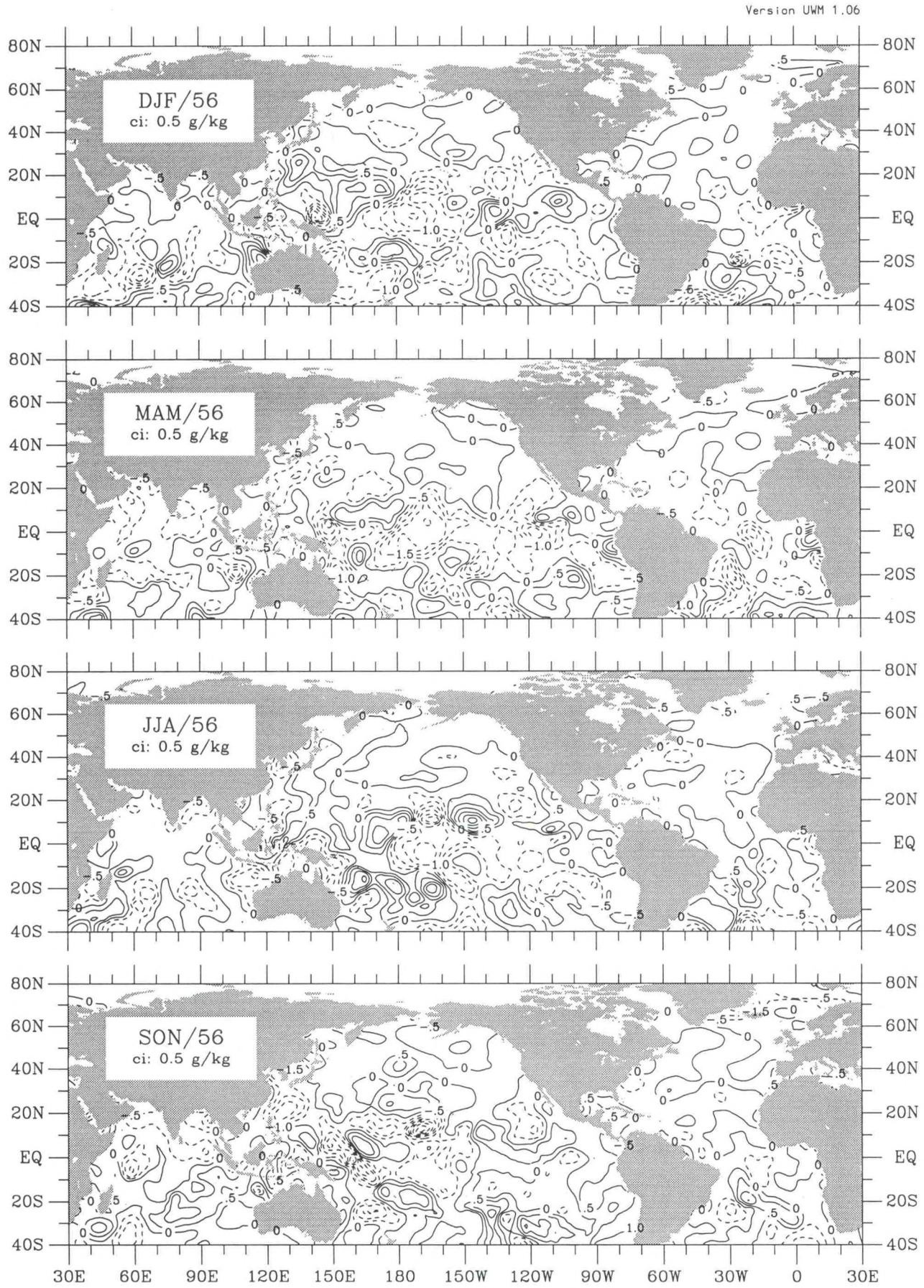

Figure dq-17. qs minus q seasonal anomaly for 1956.

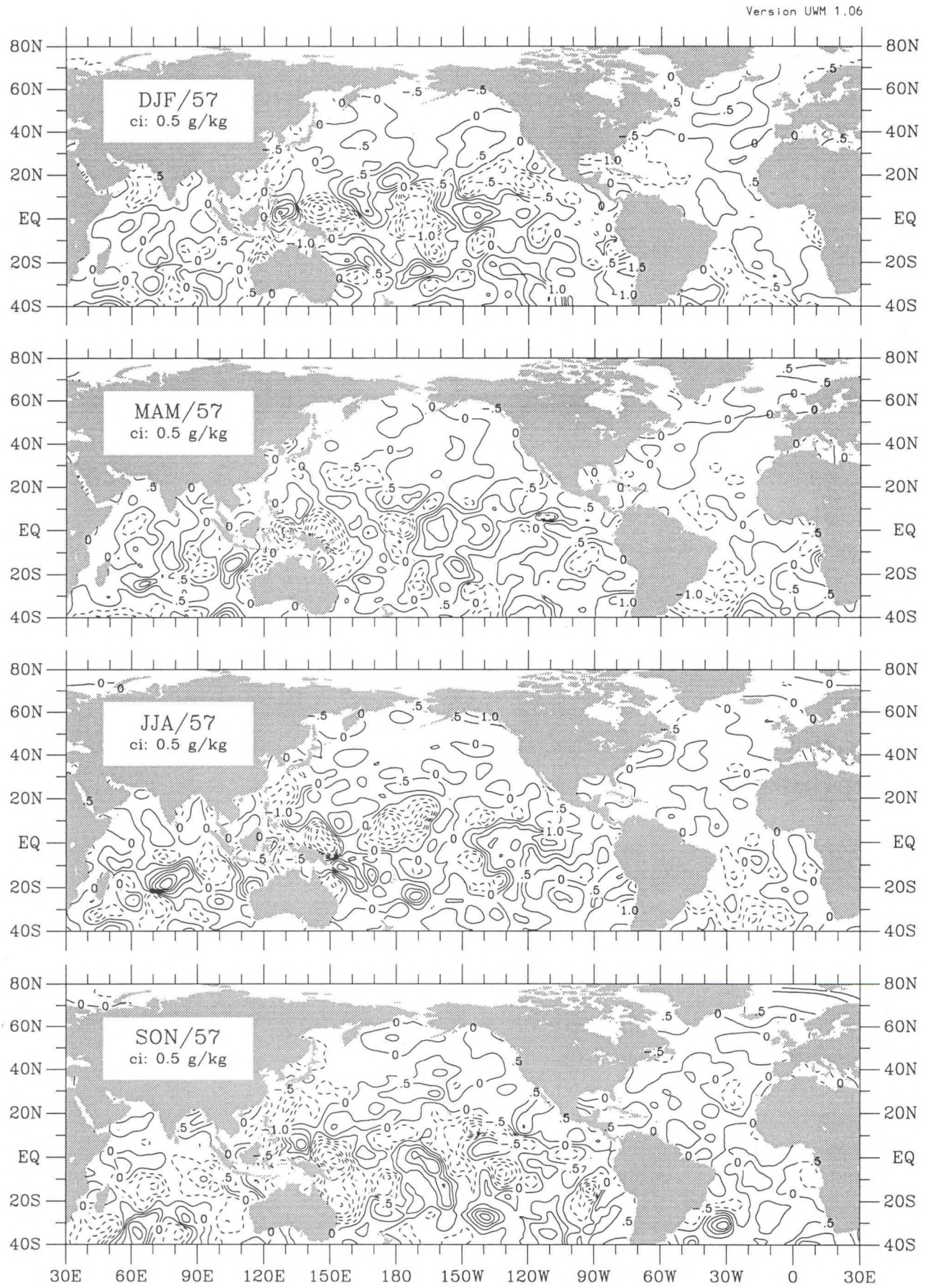

Figure dq-18. qs minus q seasonal anomaly for 1957.

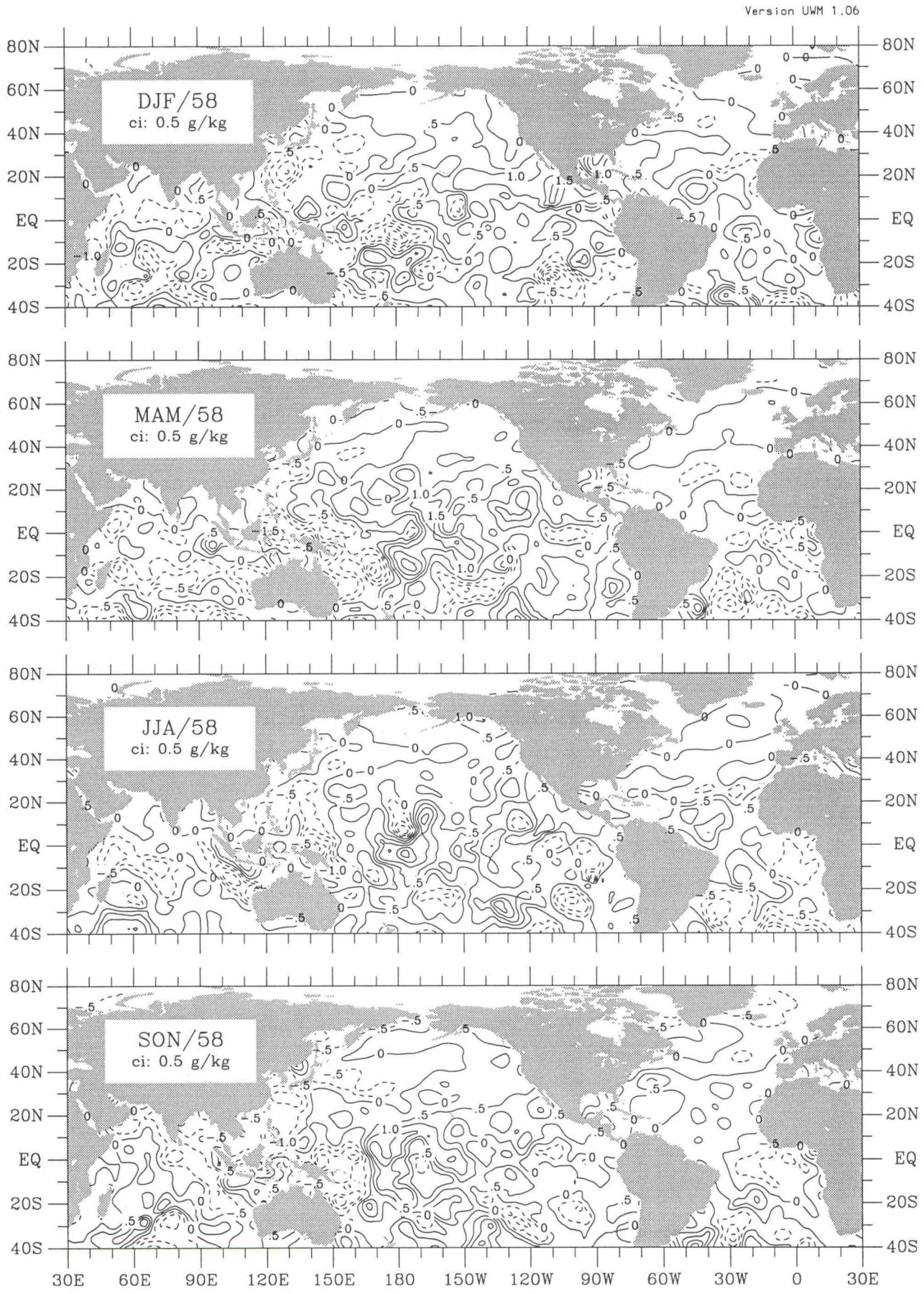

Figure dq-19. qs minus q seasonal anomaly for 1958.

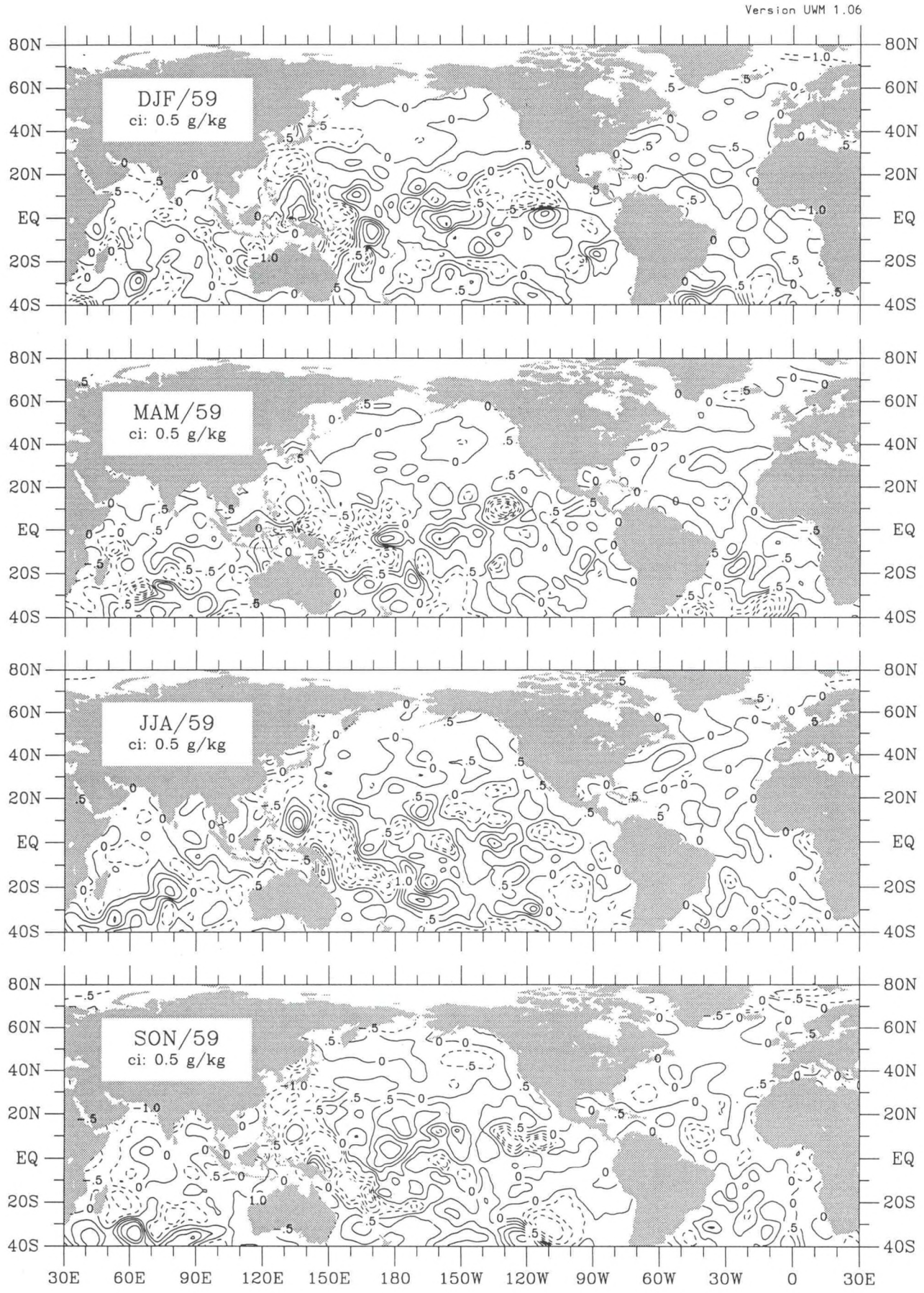

Figure dq-20. qs minus q seasonal anomaly for 1959.

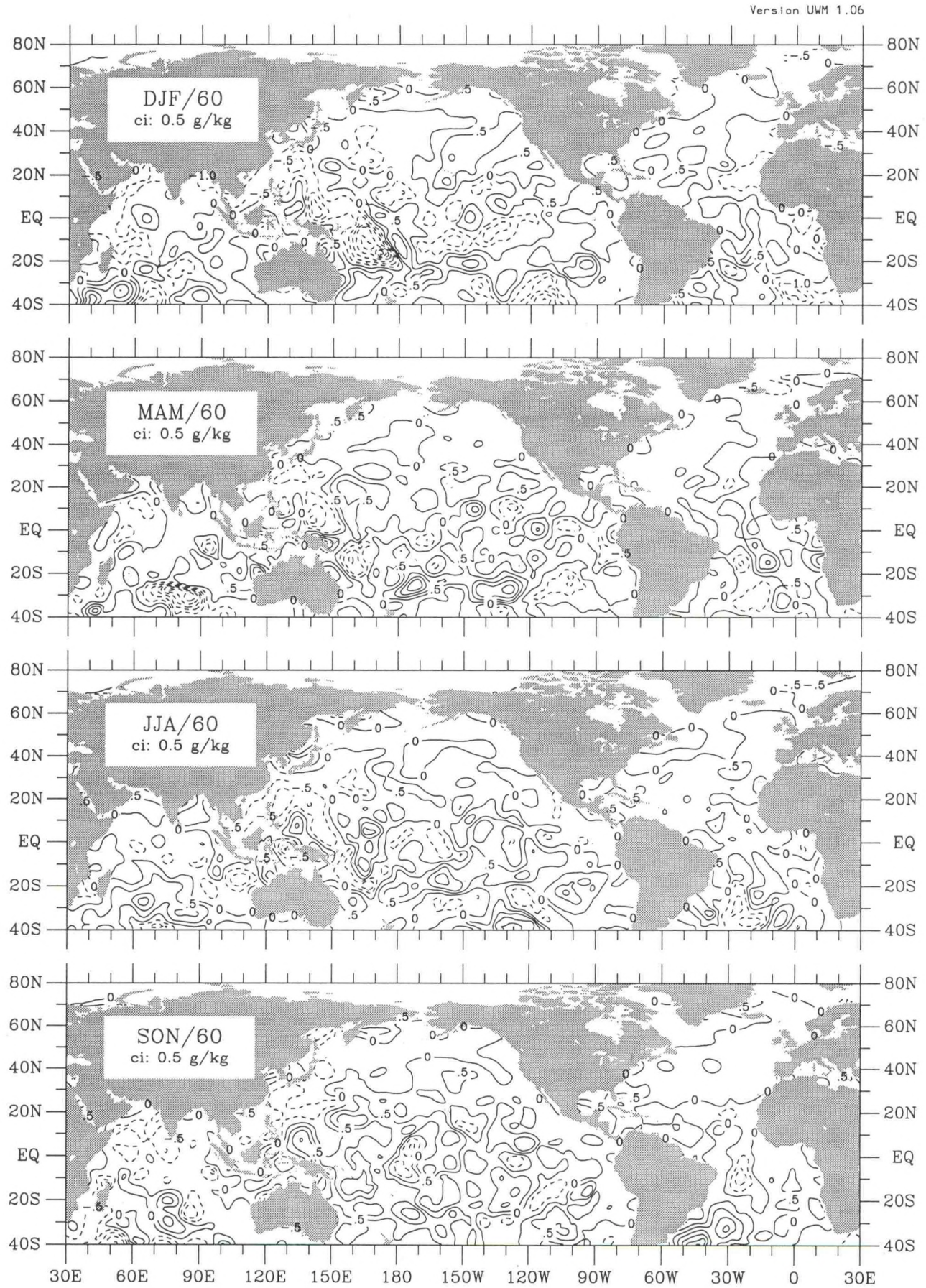

Figure dq-21. qs minus q seasonal anomaly for 1960.

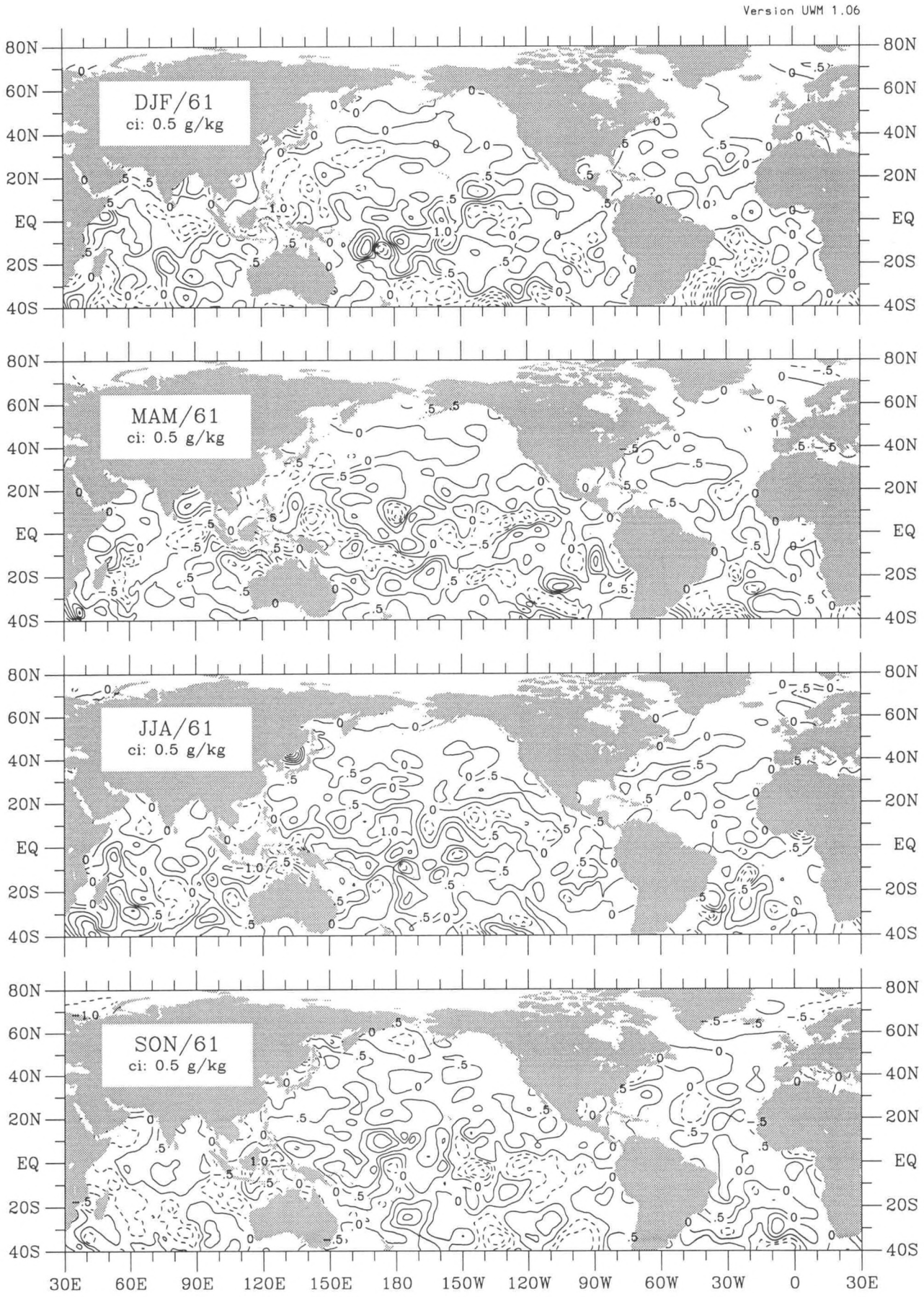

Figure dq-22. qs minus q seasonal anomaly for 1961.

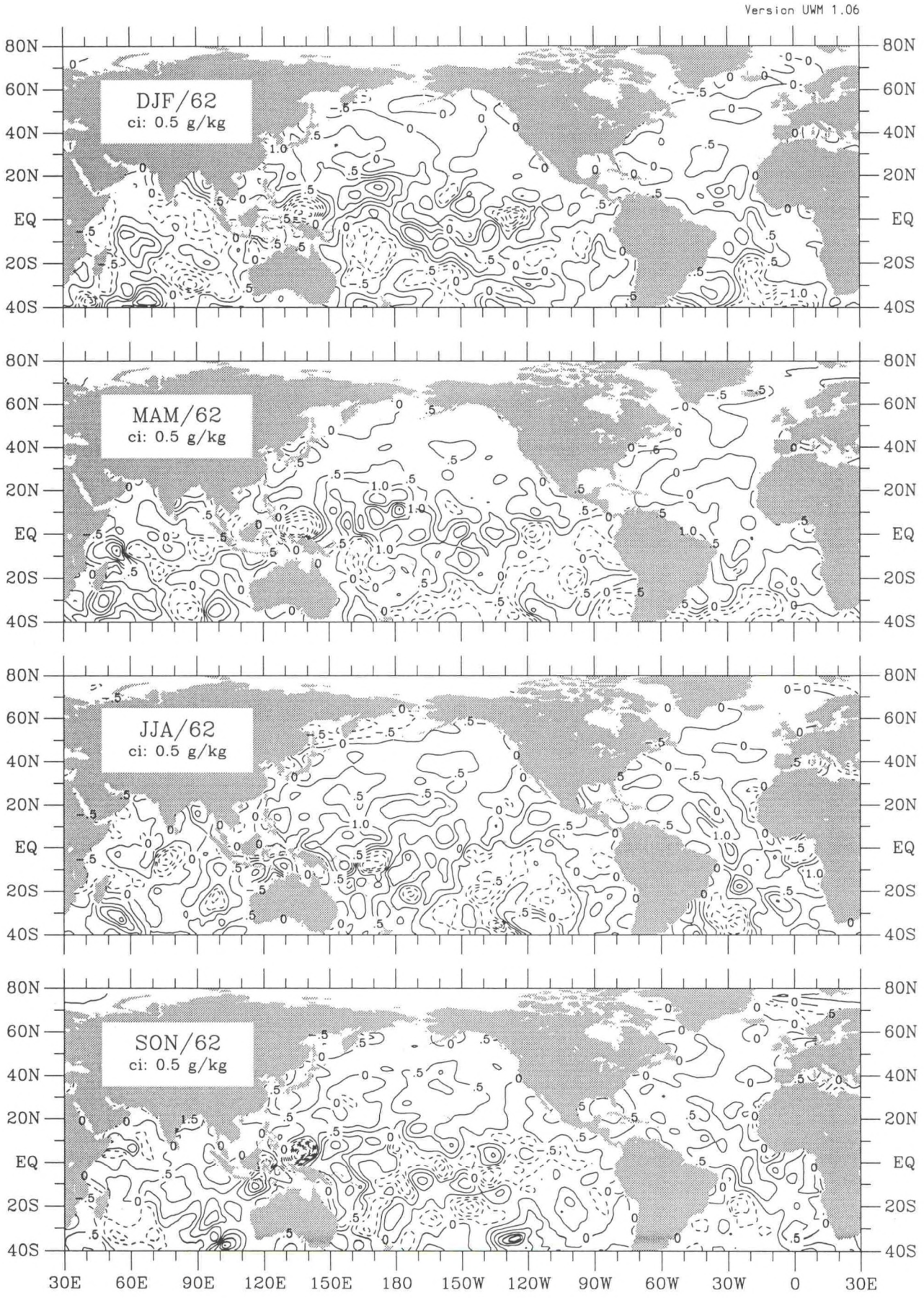

Figure dq-23. qs minus q seasonal anomaly for 1962.

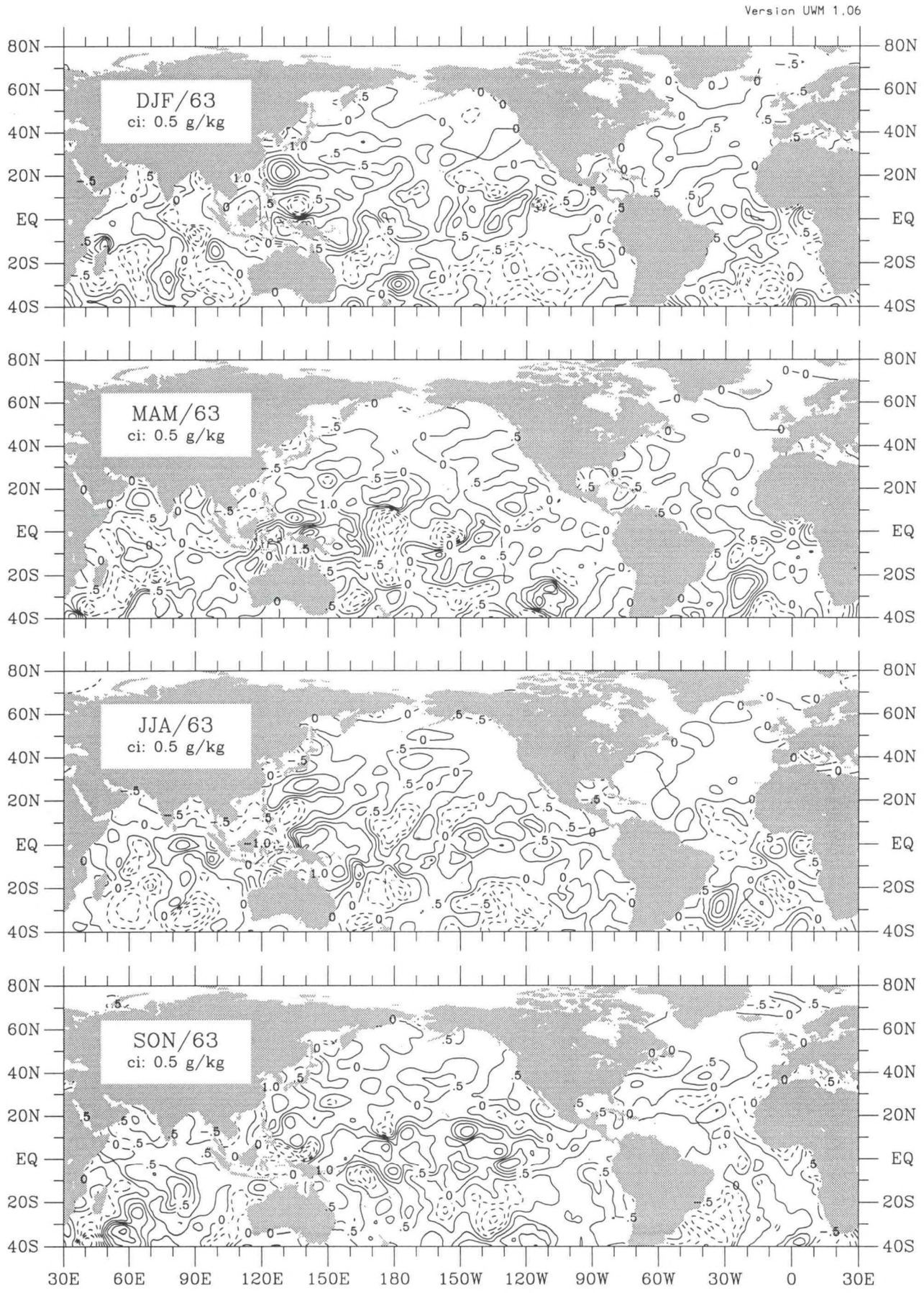

Figure dq-24. qs minus q seasonal anomaly for 1963.

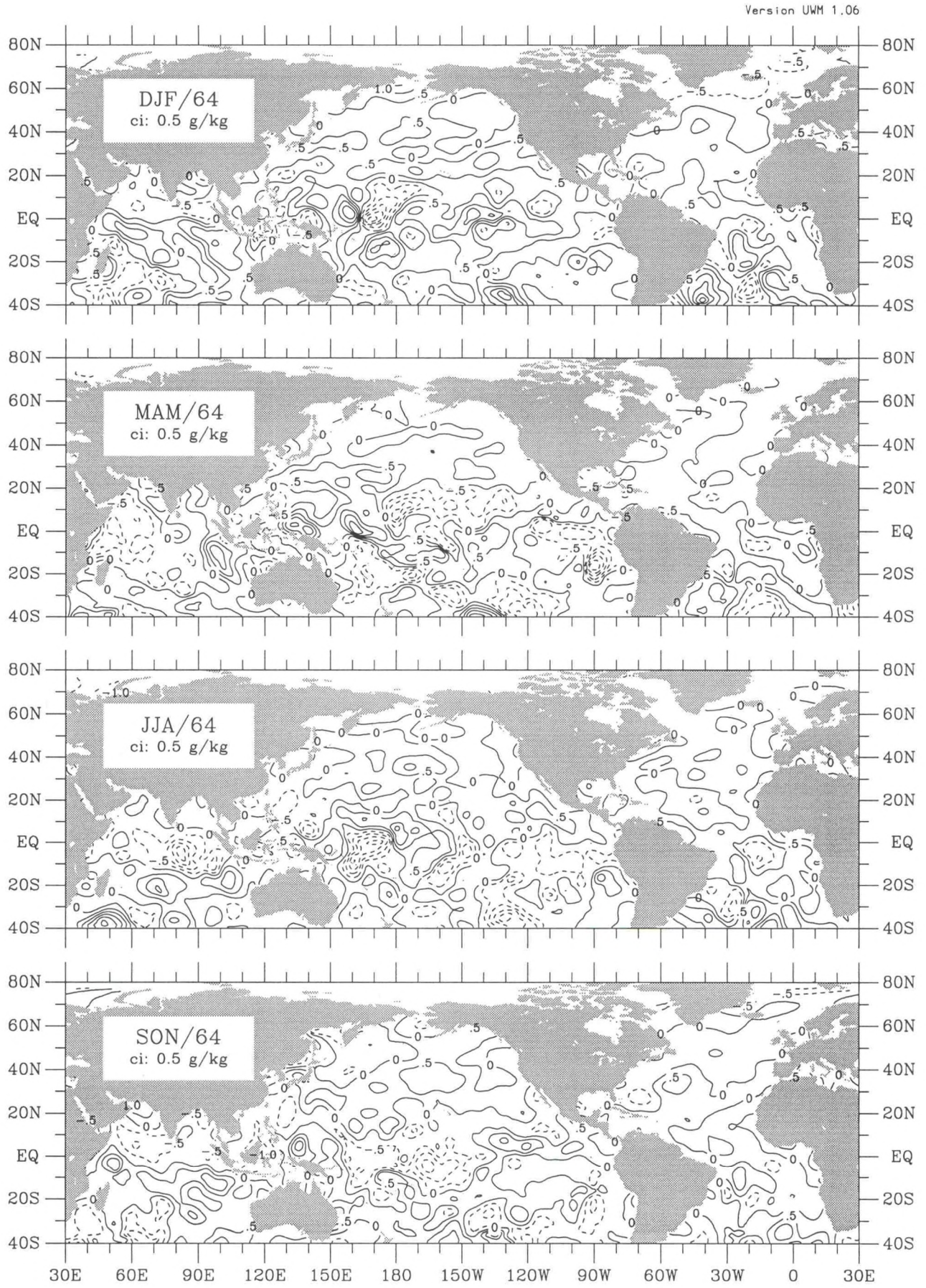

Figure dq-25. qs minus q seasonal anomaly for 1964.

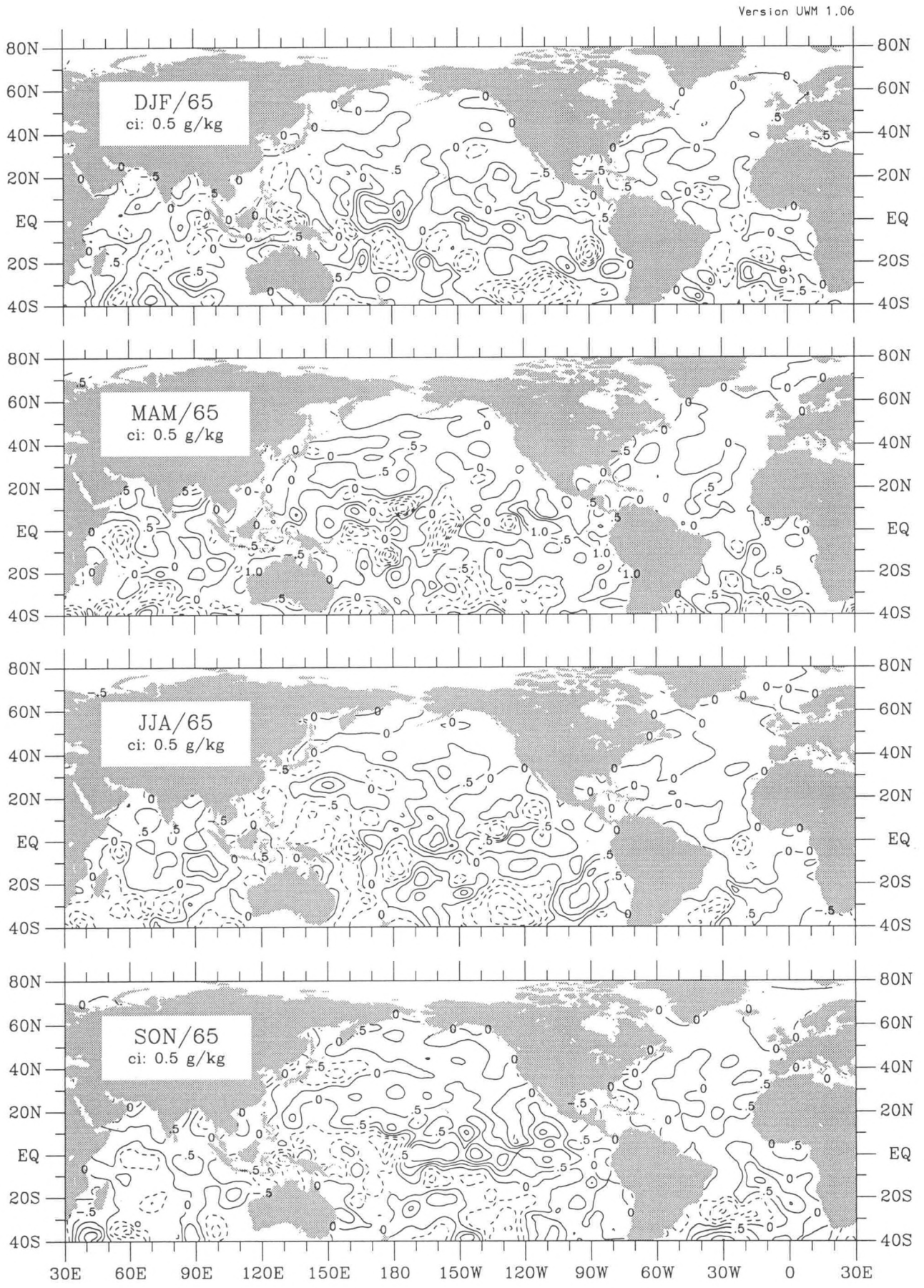

Figure dq-26. qs minus q seasonal anomaly for 1965.

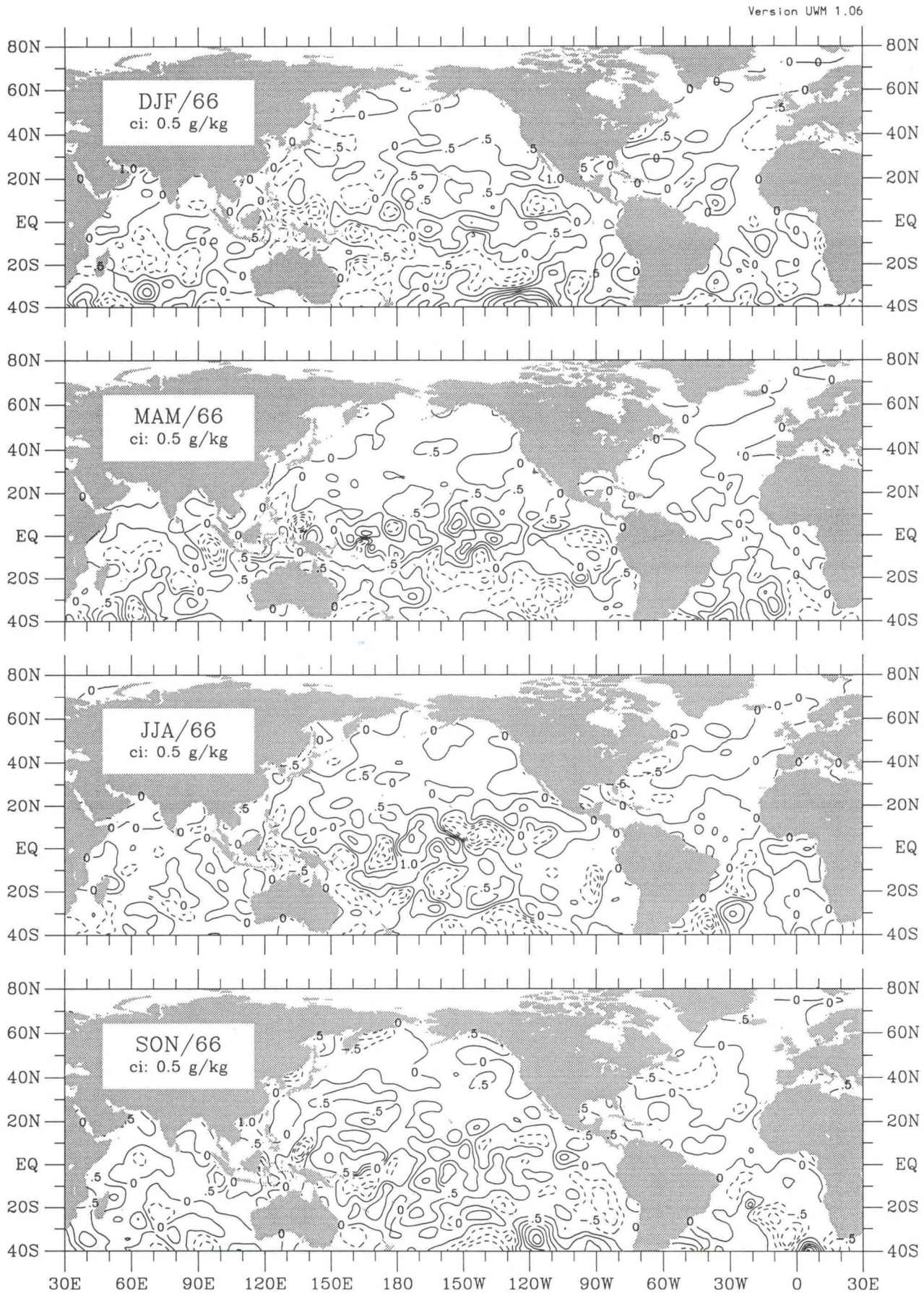

Figure dq-27. qs minus q seasonal anomaly for 1966.

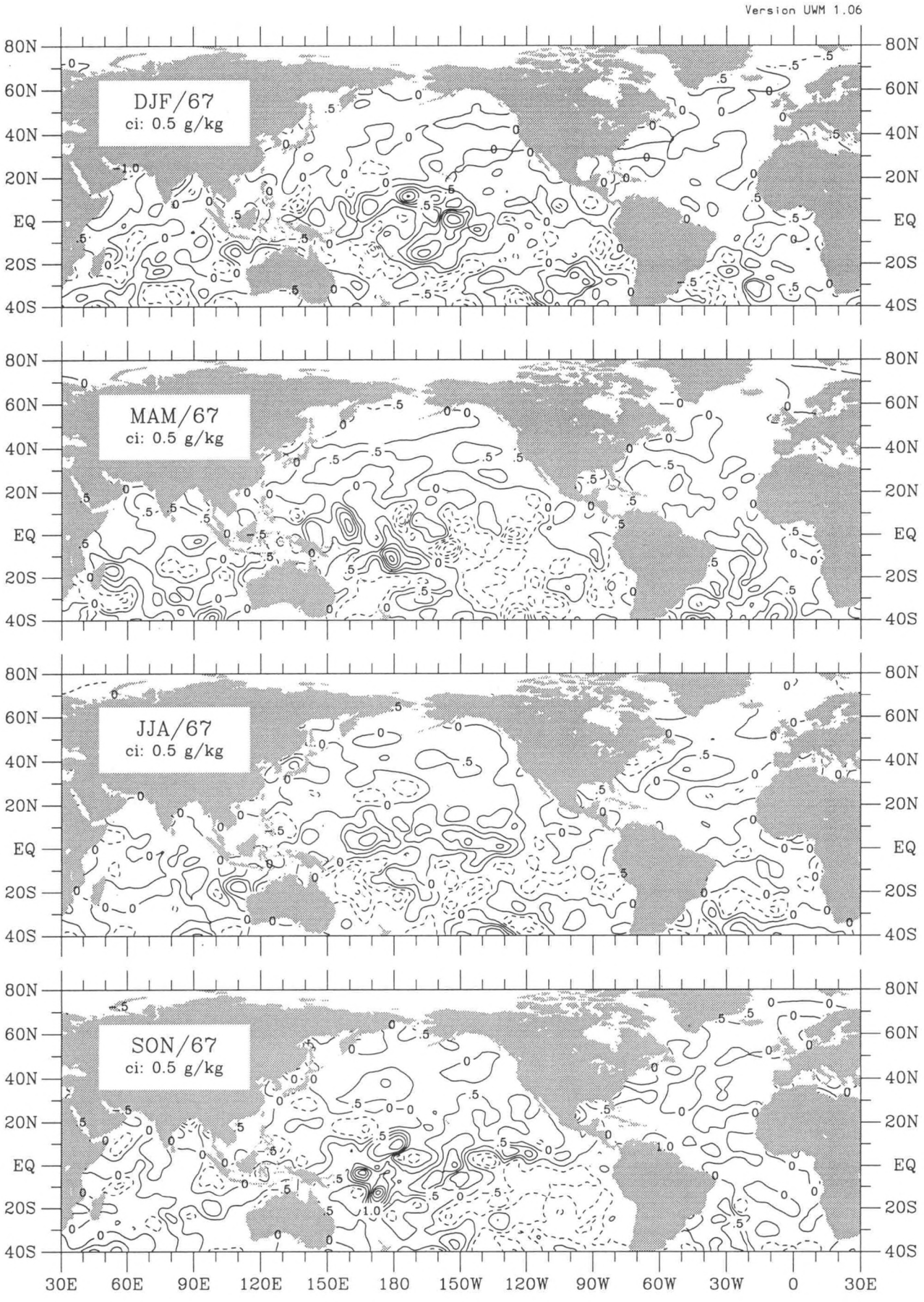

Figure dq-28. qs minus q seasonal anomaly for 1967.

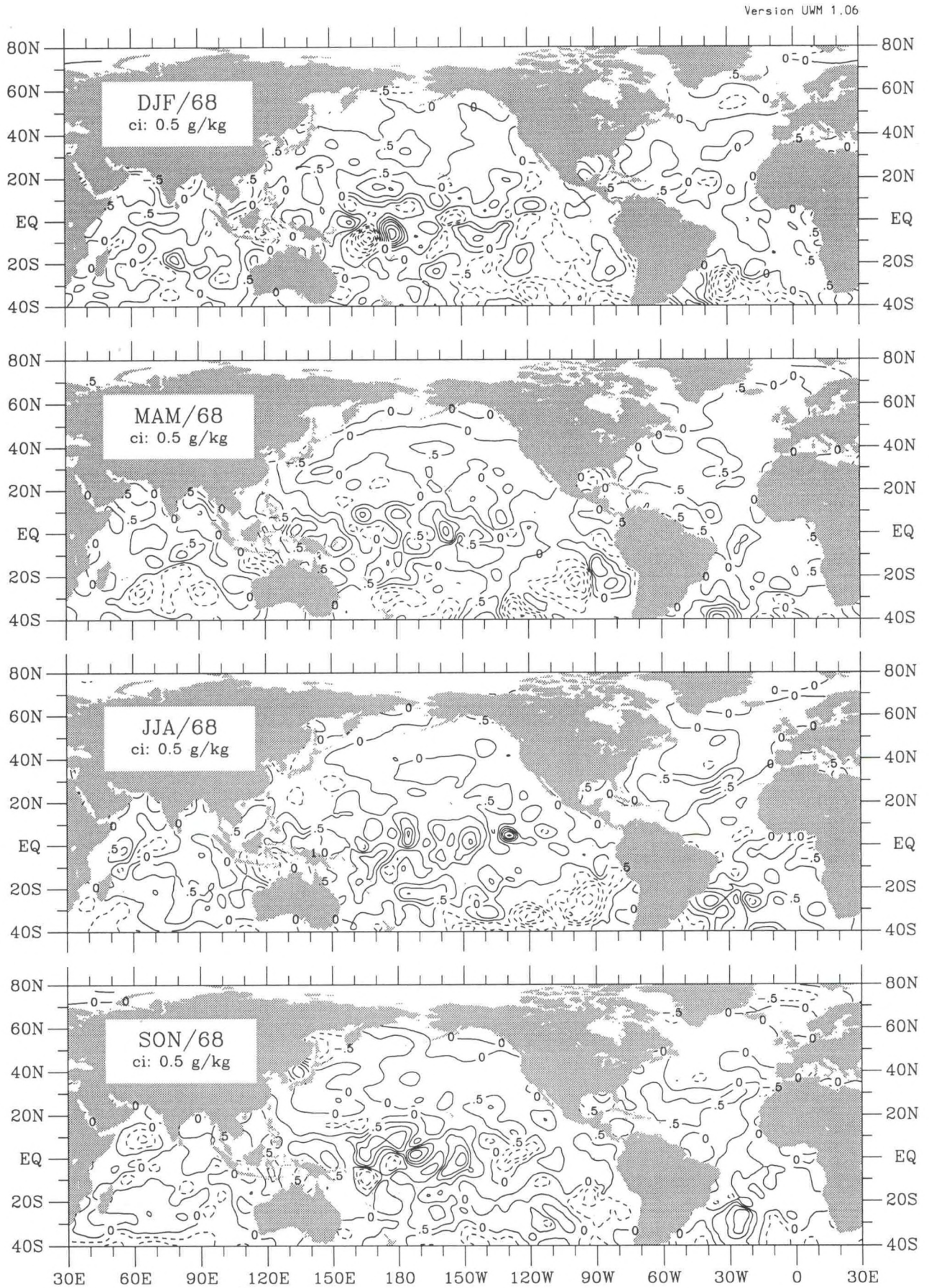

Figure dq-29. qs minus q seasonal anomaly for 1968.

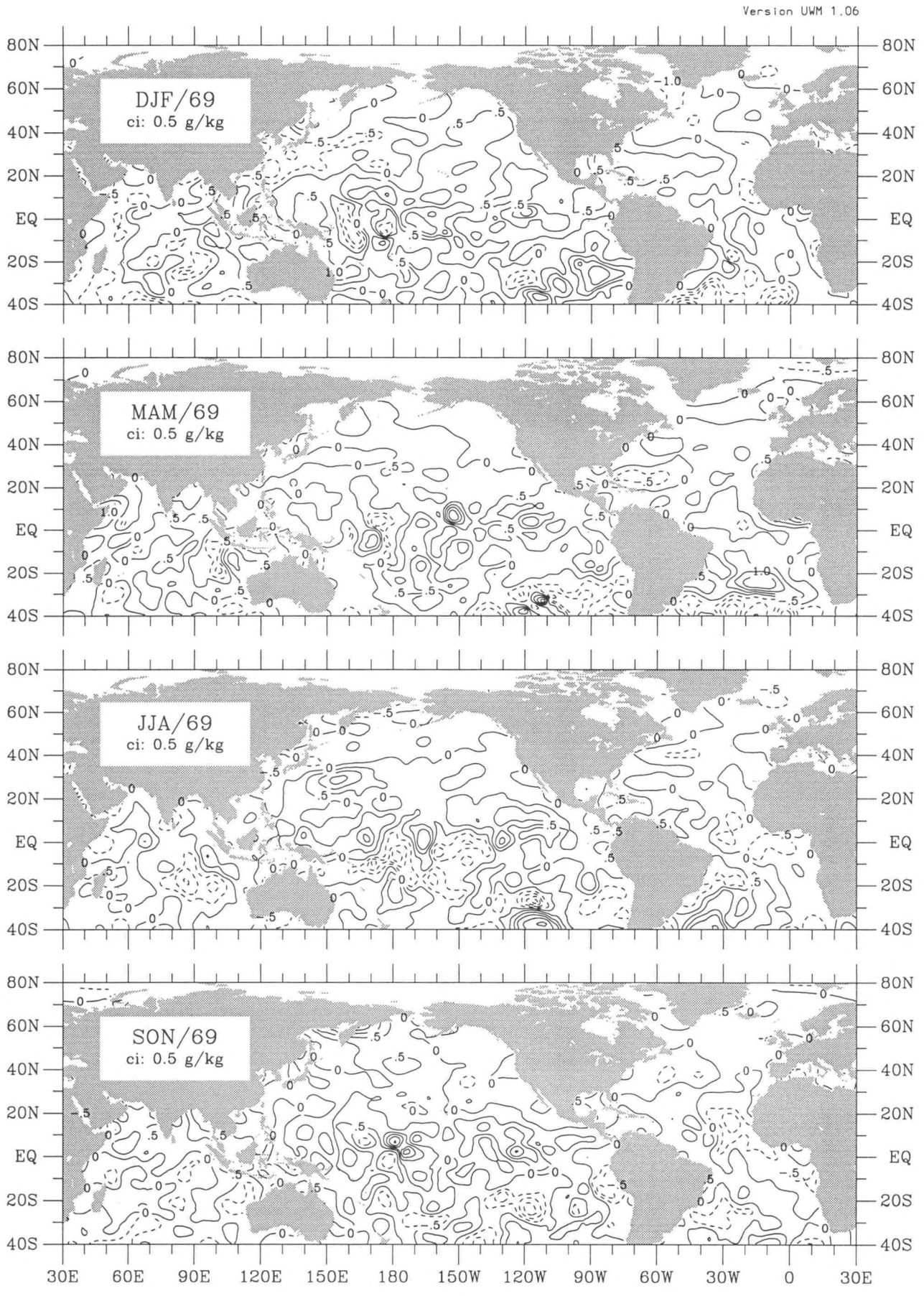

Figure dq-30. qs minus q seasonal anomaly for 1969.

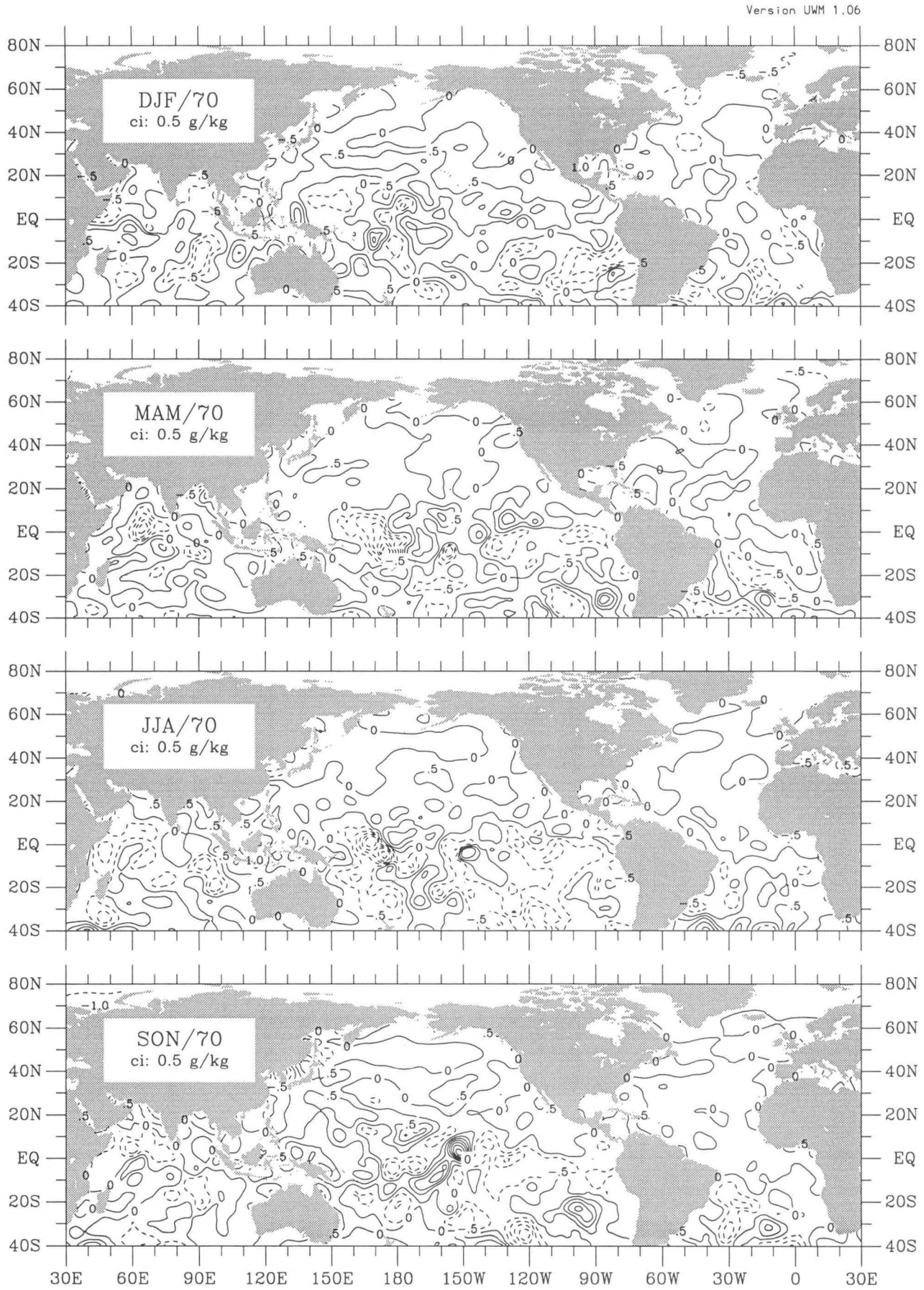

Figure dq-31. qs minus q seasonal anomaly for 1970.

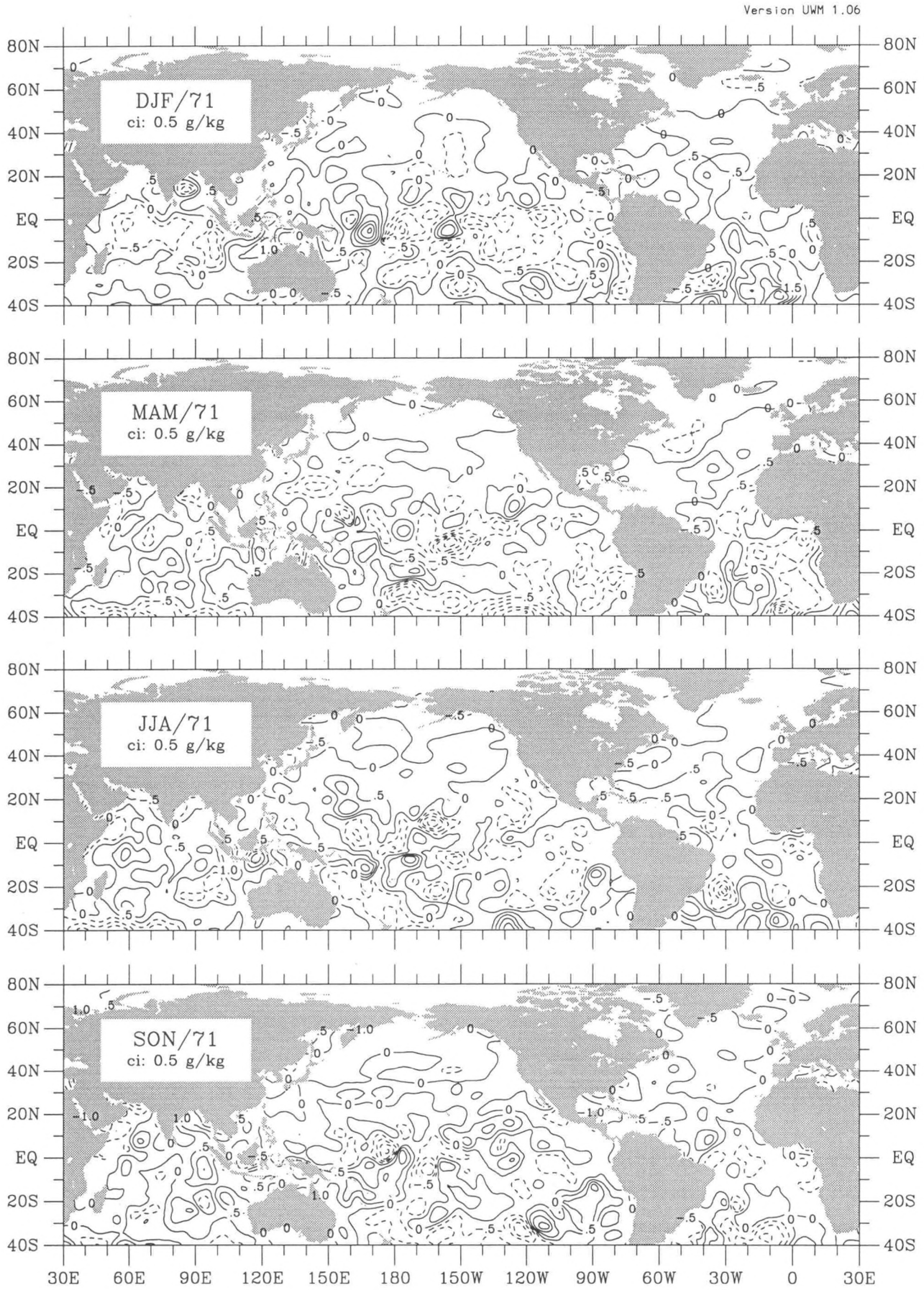

Figure dq-32. qs minus q seasonal anomaly for 1971.

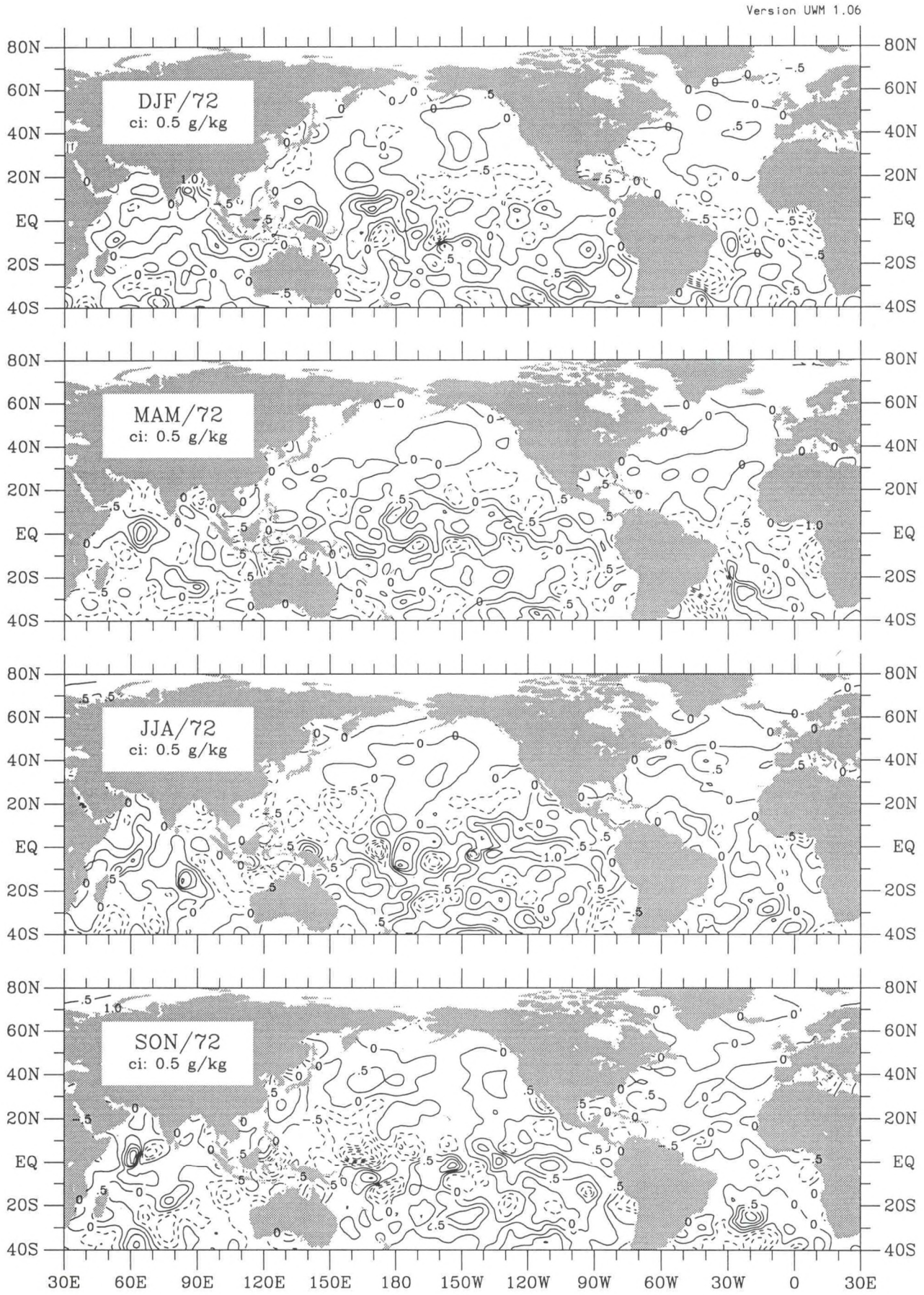

Figure dq-33. qs minus q seasonal anomaly for 1972.

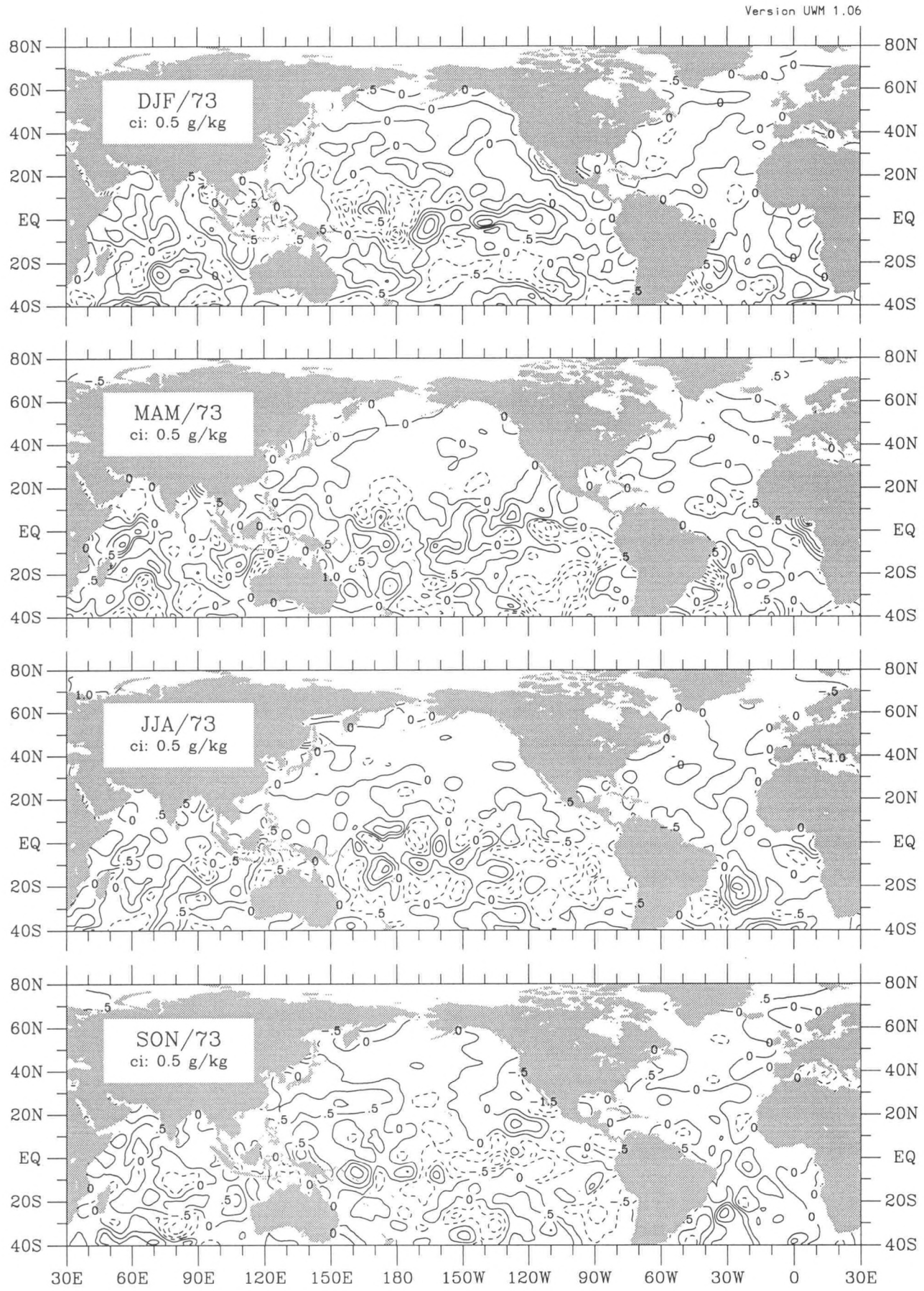

Figure dq-34. qs minus q seasonal anomaly for 1973.

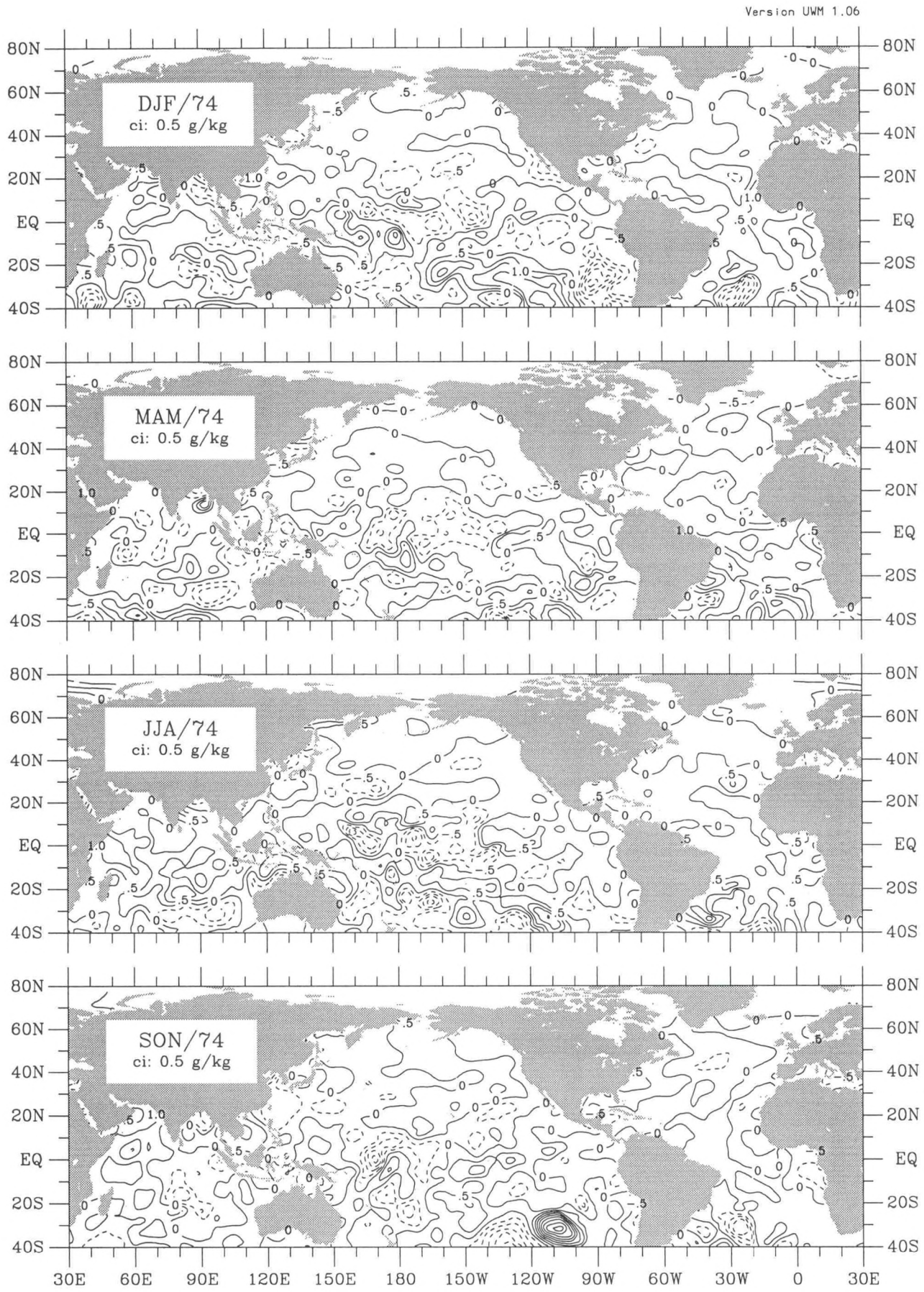

Figure dq-35. qs minus q seasonal anomaly for 1974.

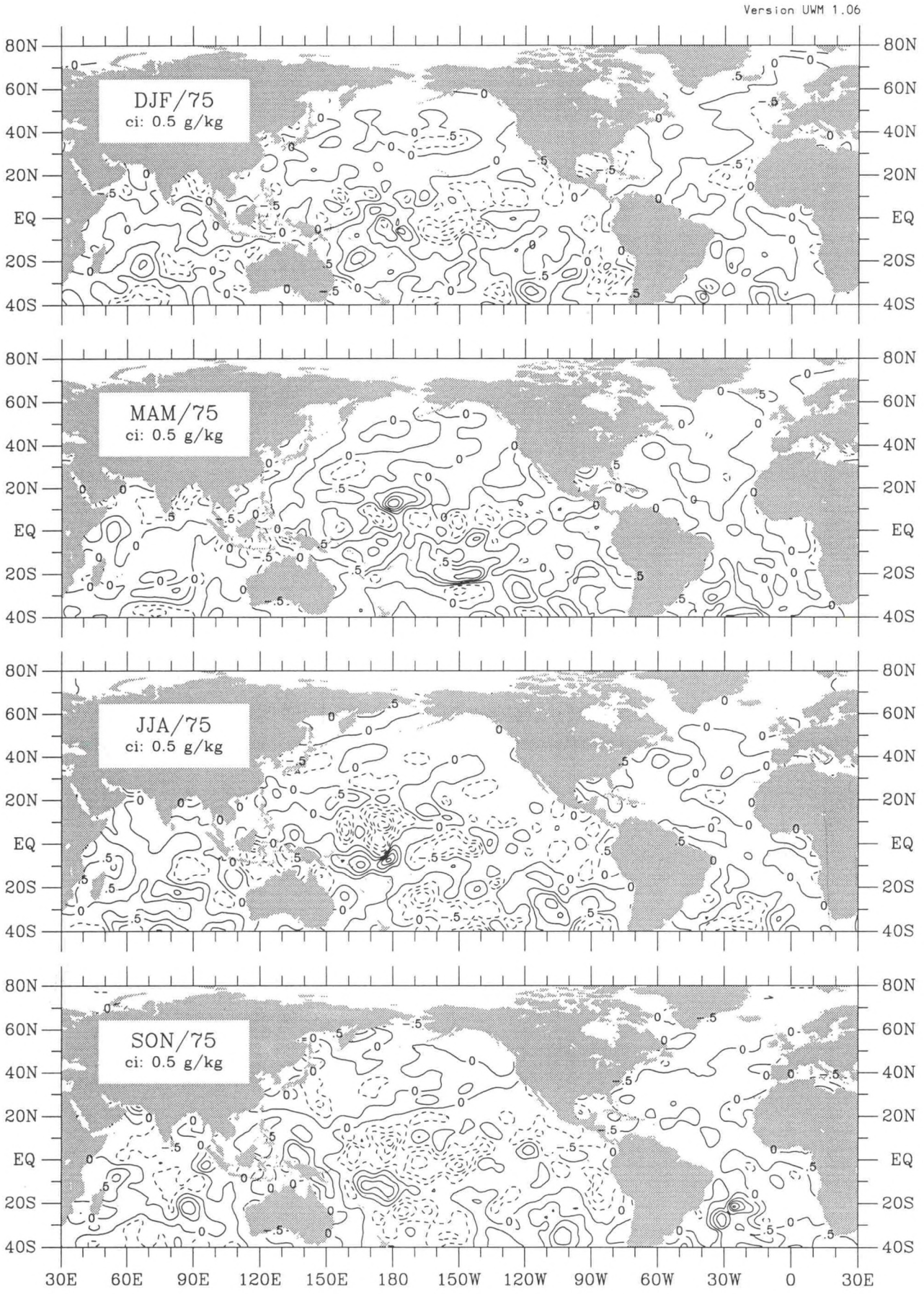

Figure dq-36. qs minus q seasonal anomaly for 1975.

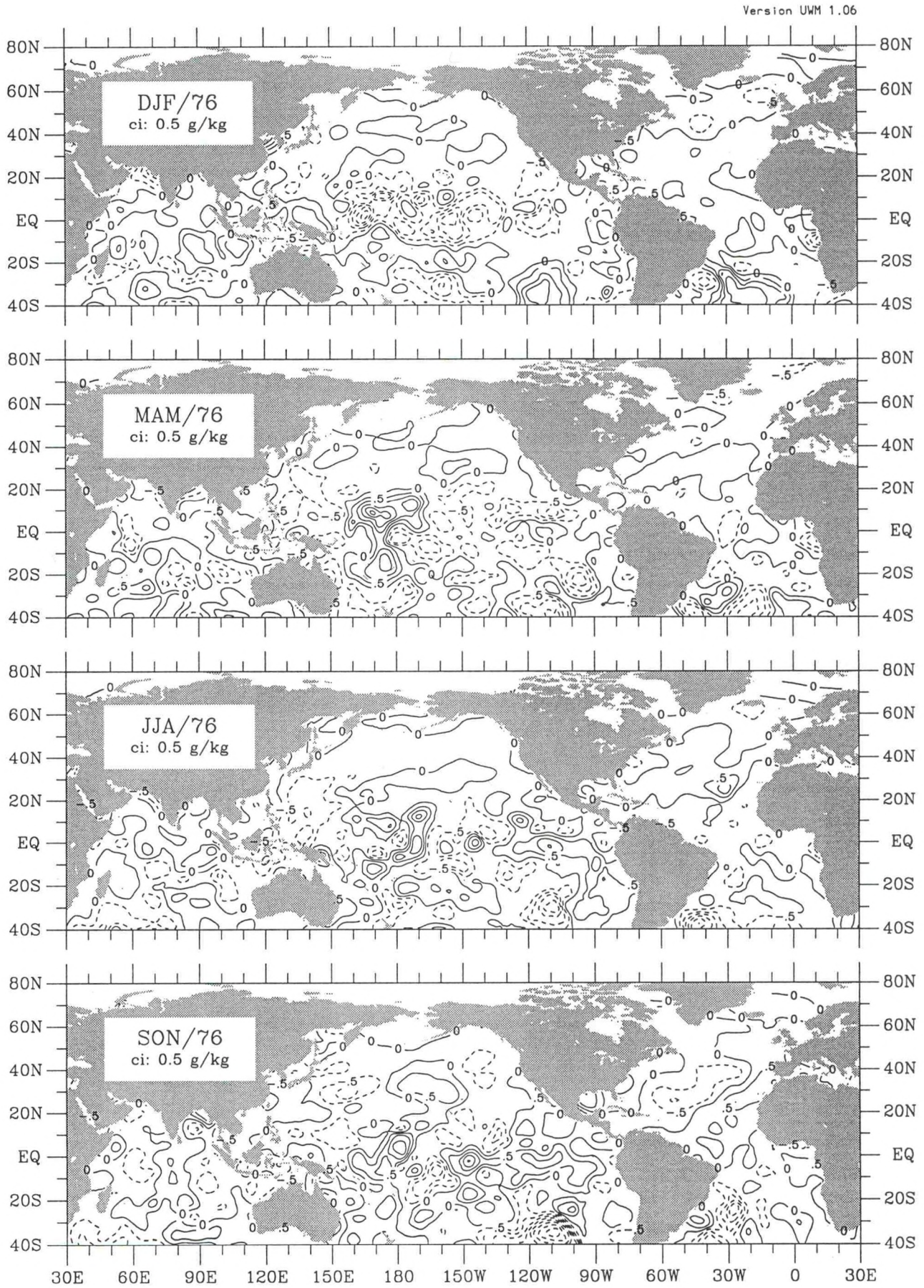

Figure dq-37. qs minus q seasonal anomaly for 1976.

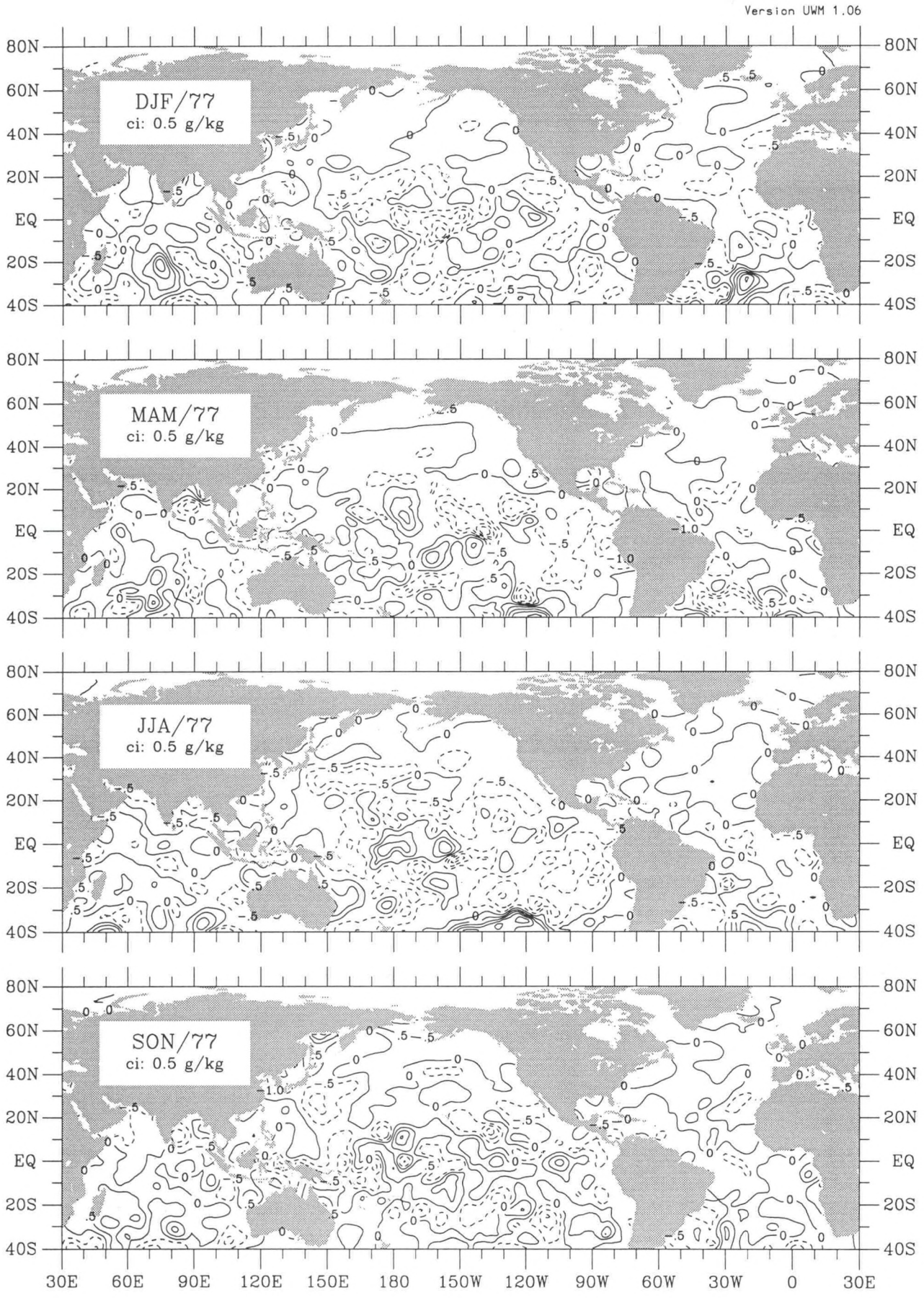

Figure dq-38. qs minus q seasonal anomaly for 1977.

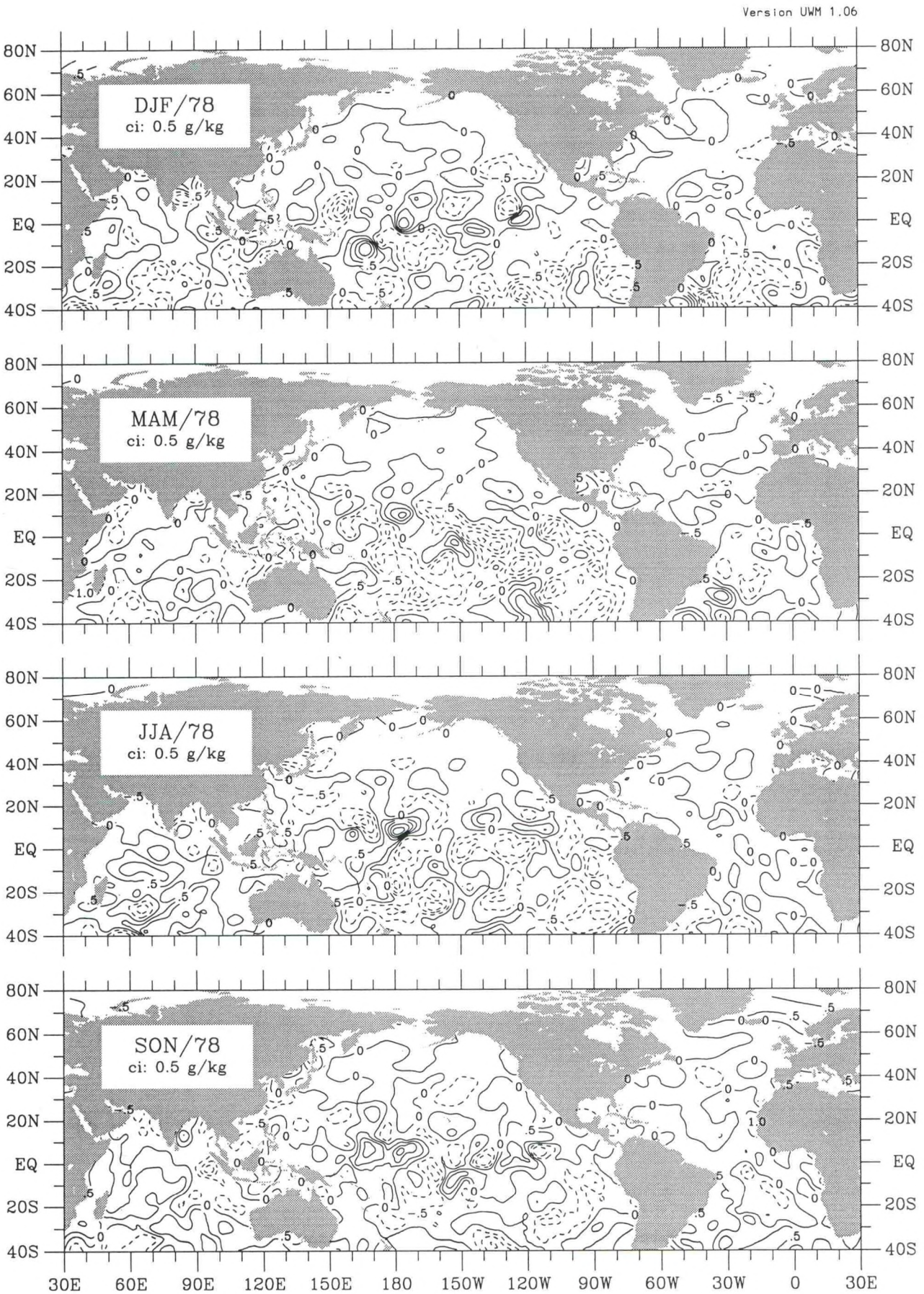

Figure dq-39. qs minus q seasonal anomaly for 1978.

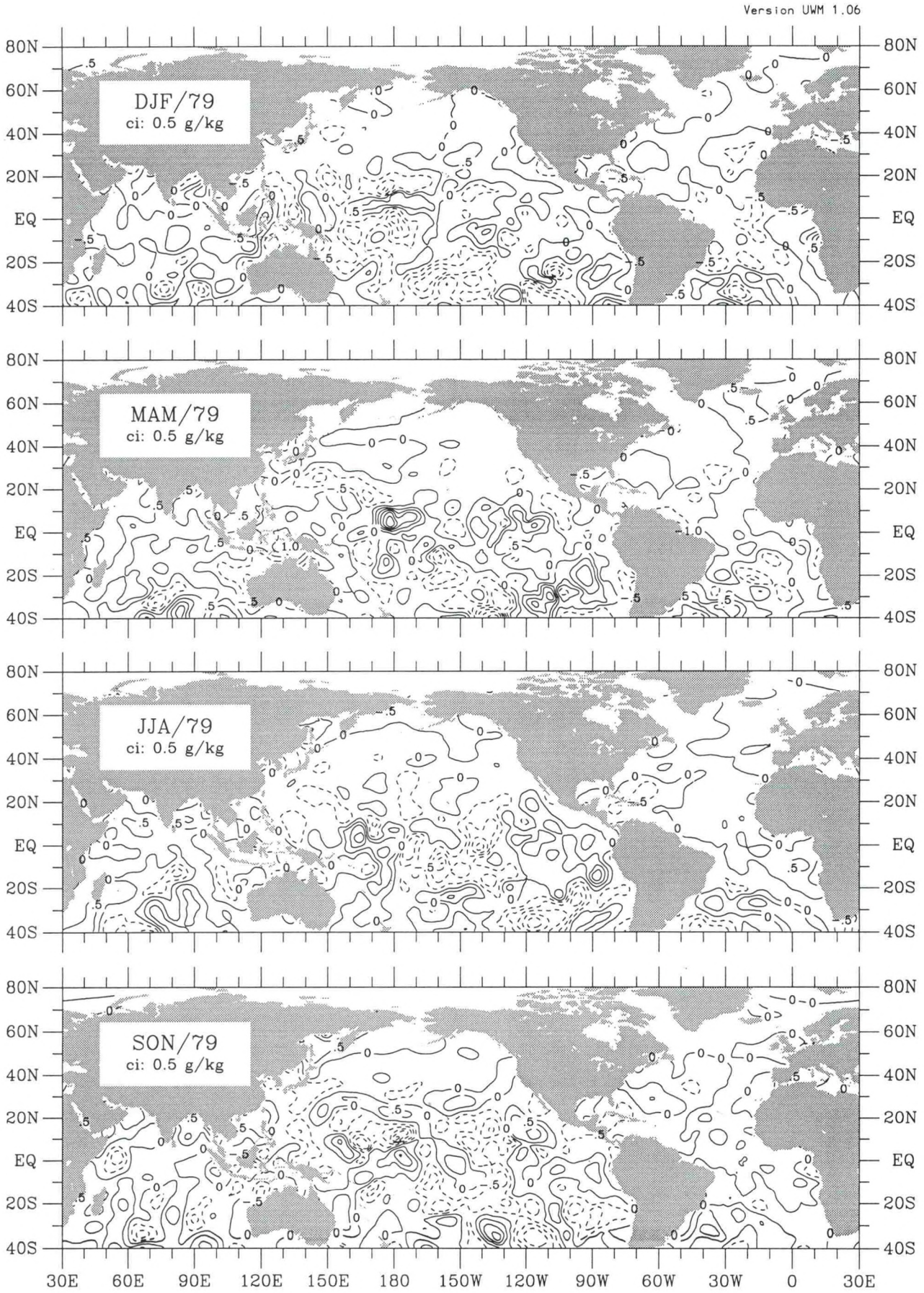

Figure dq-40. qs minus q seasonal anomaly for 1979.

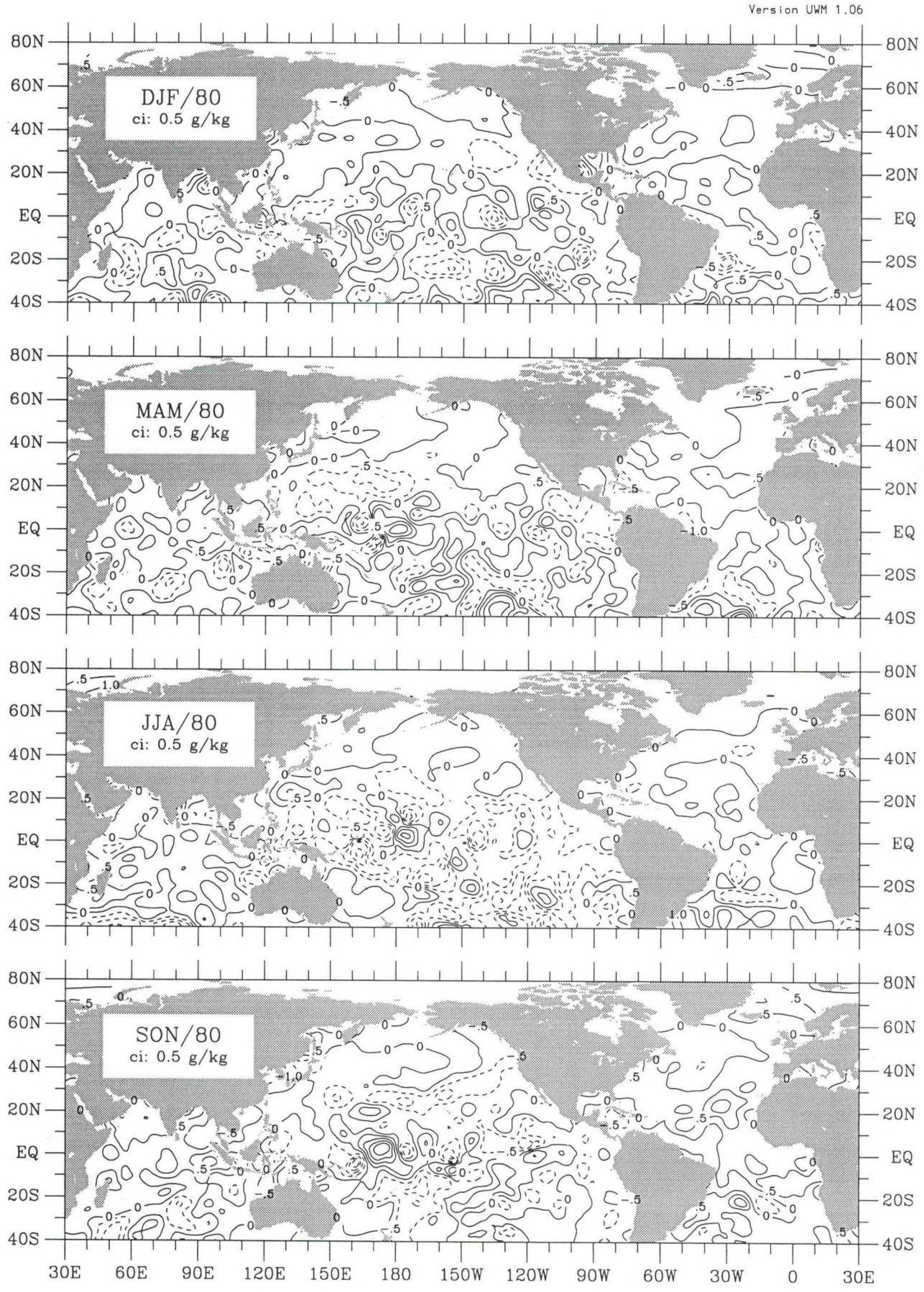

Figure dq-41. qs minus q seasonal anomaly for 1980.

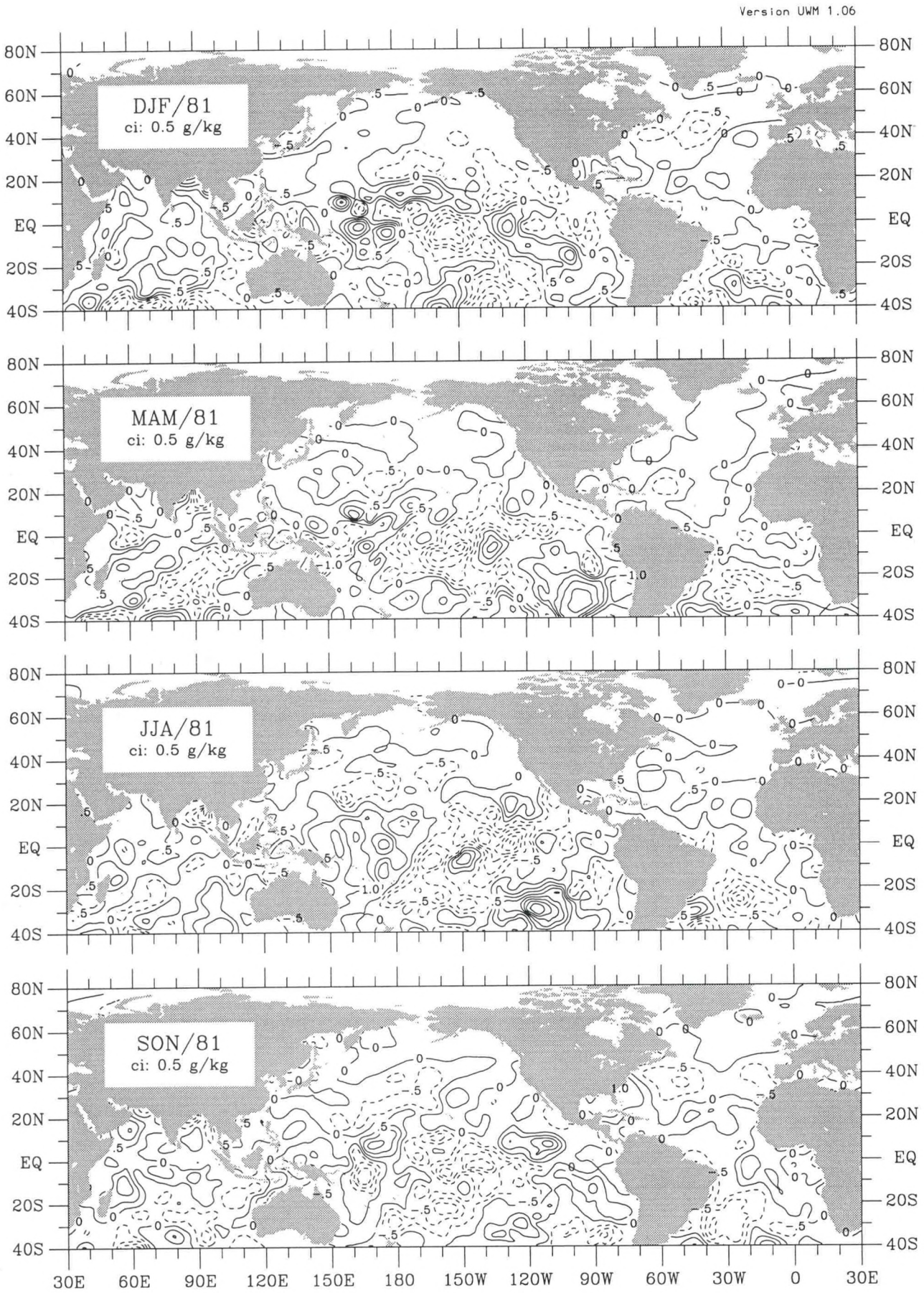

Figure dq-42. qs minus q seasonal anomaly for 1981.

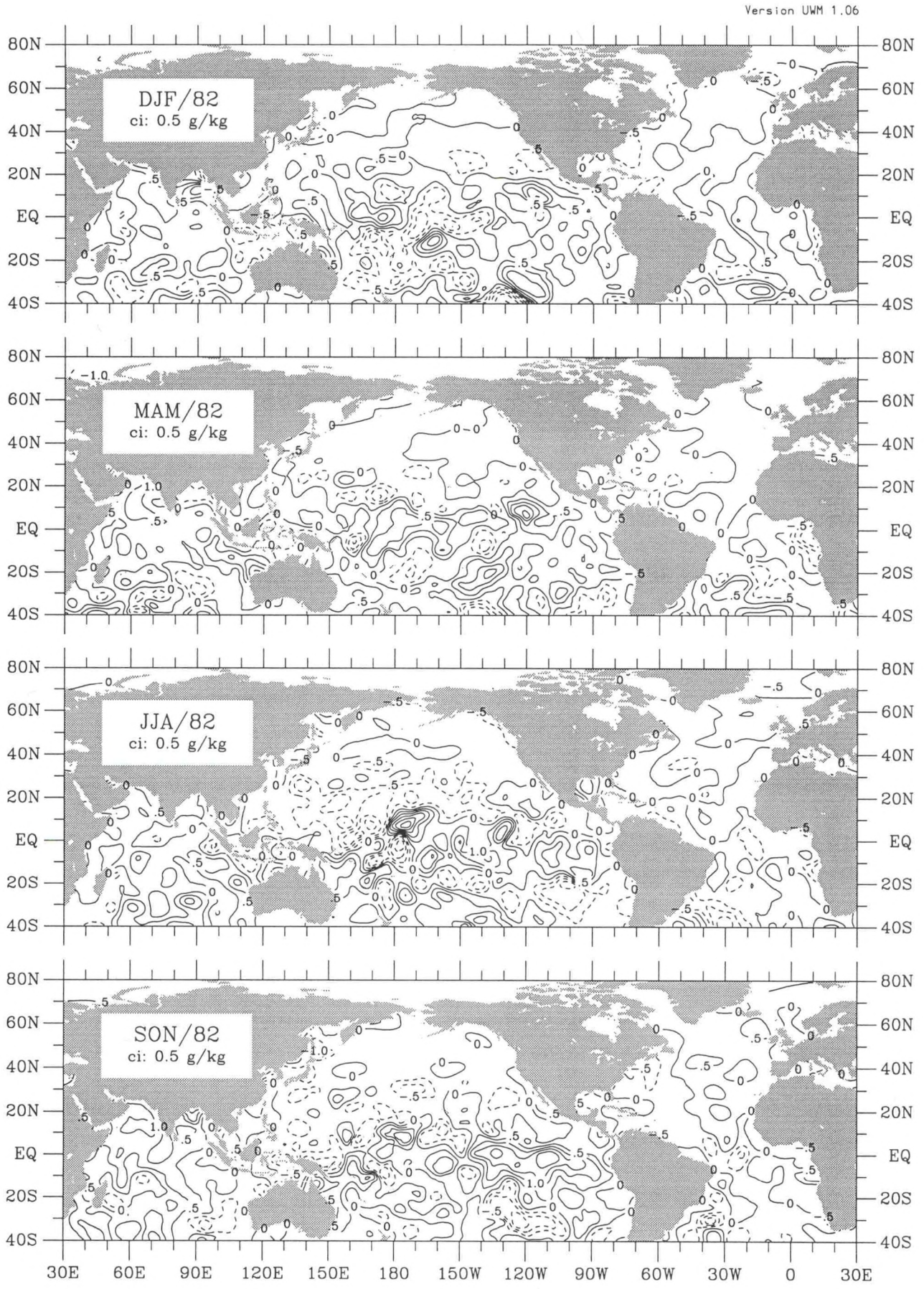

Figure dq-43. qs minus q seasonal anomaly for 1982.

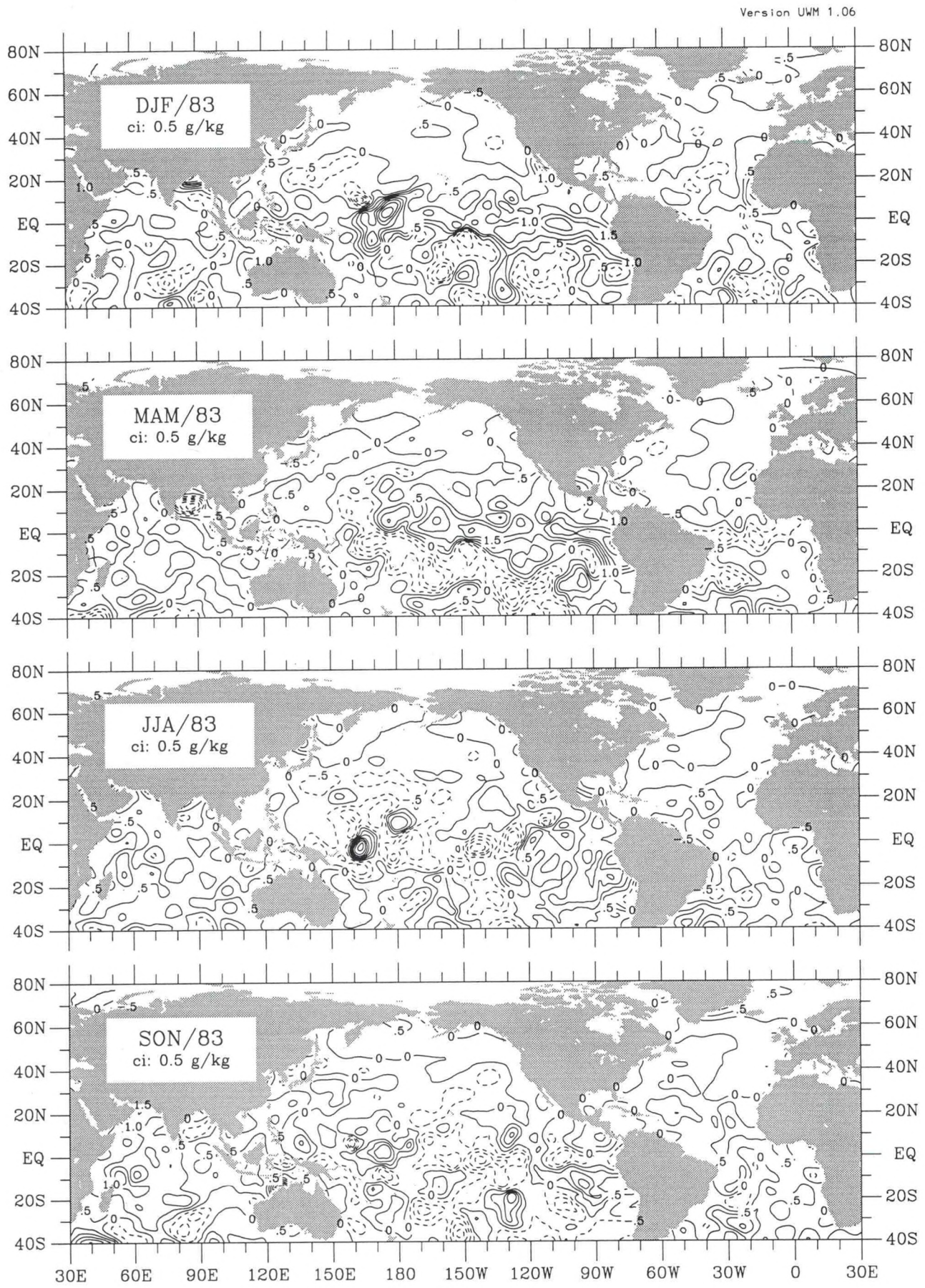

Figure dq-44. qs minus q seasonal anomaly for 1983.

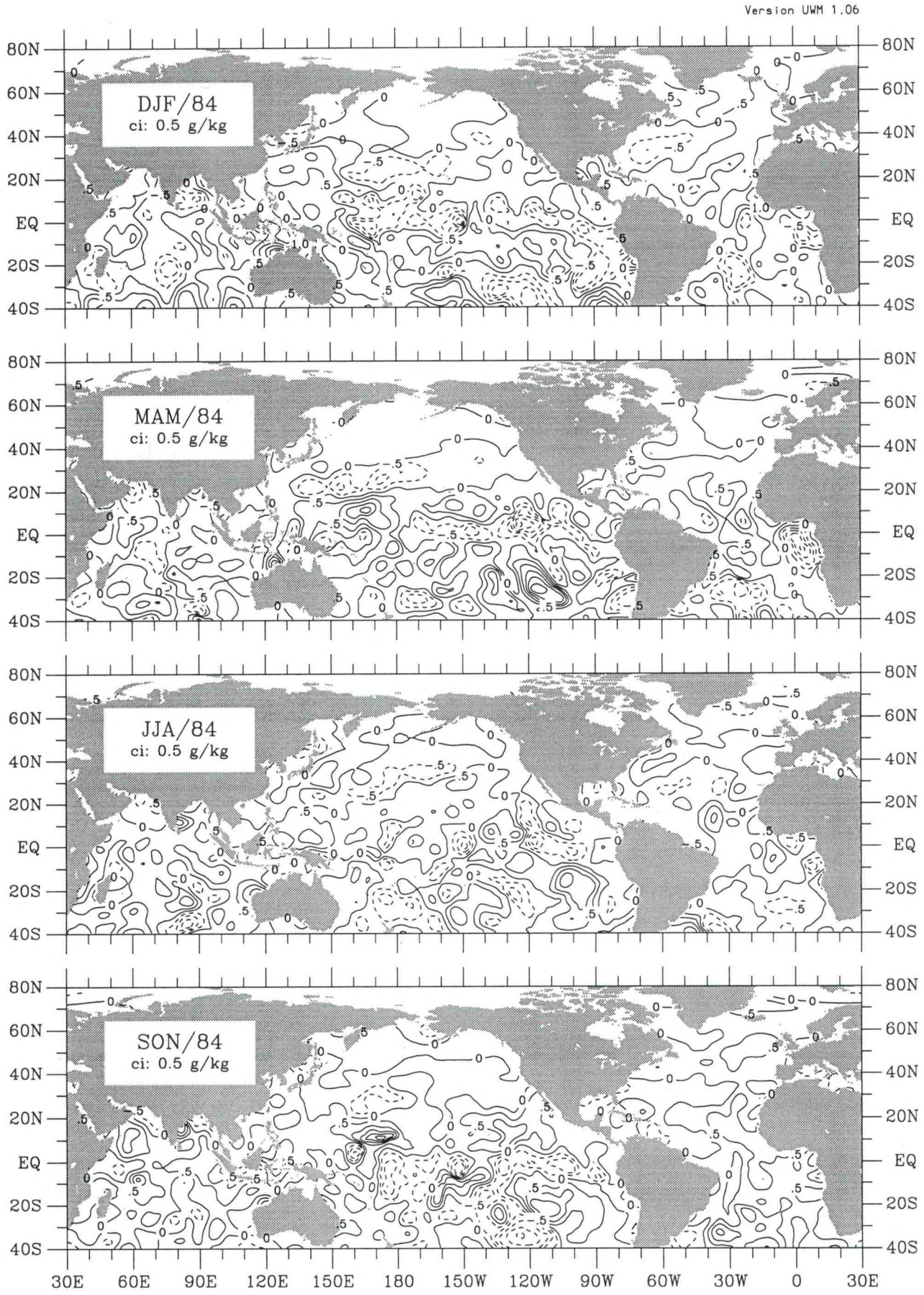

Figure dq-45. qs minus q seasonal anomaly for 1984.

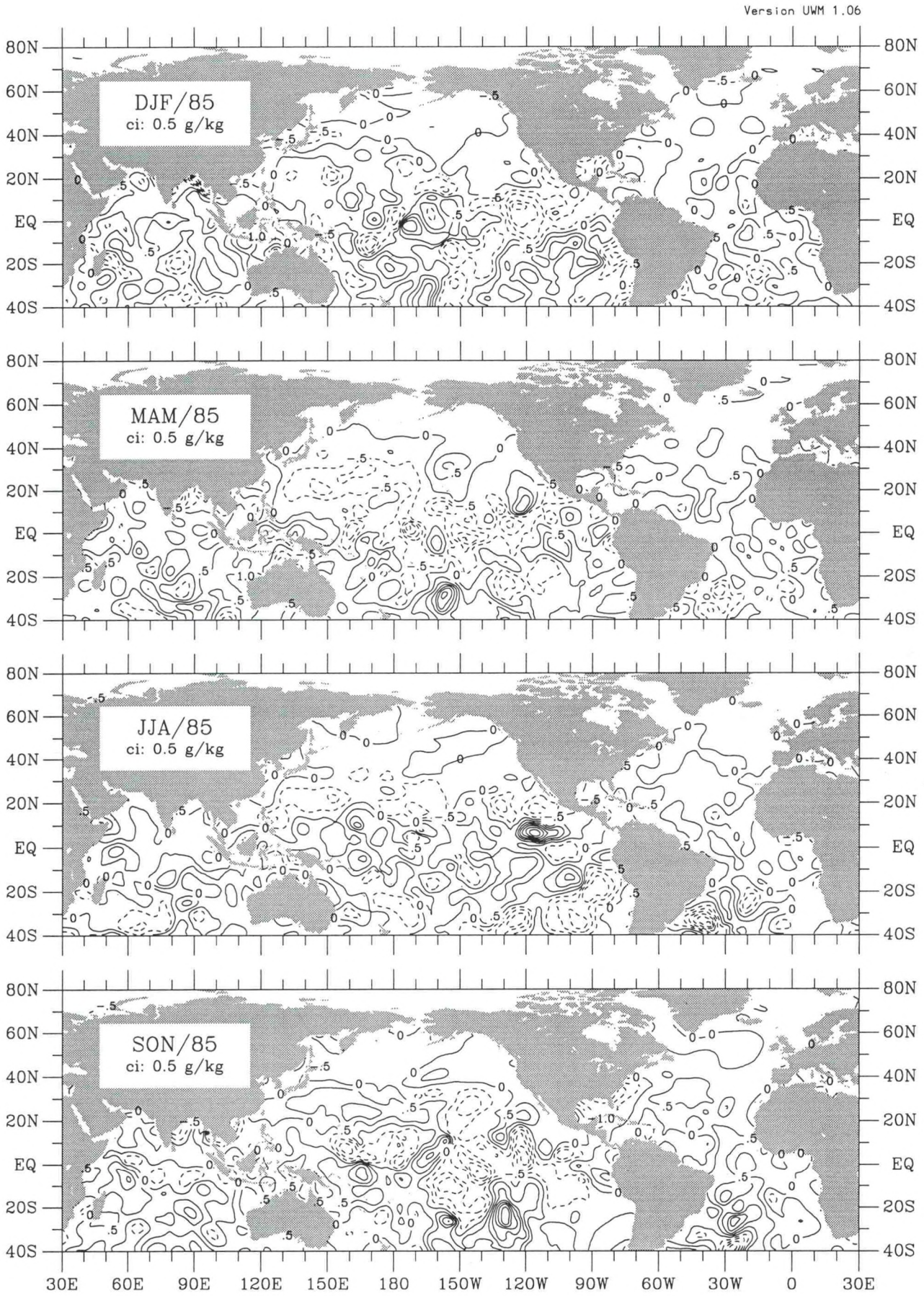

Figure dq-46. qs minus q seasonal anomaly for 1985.

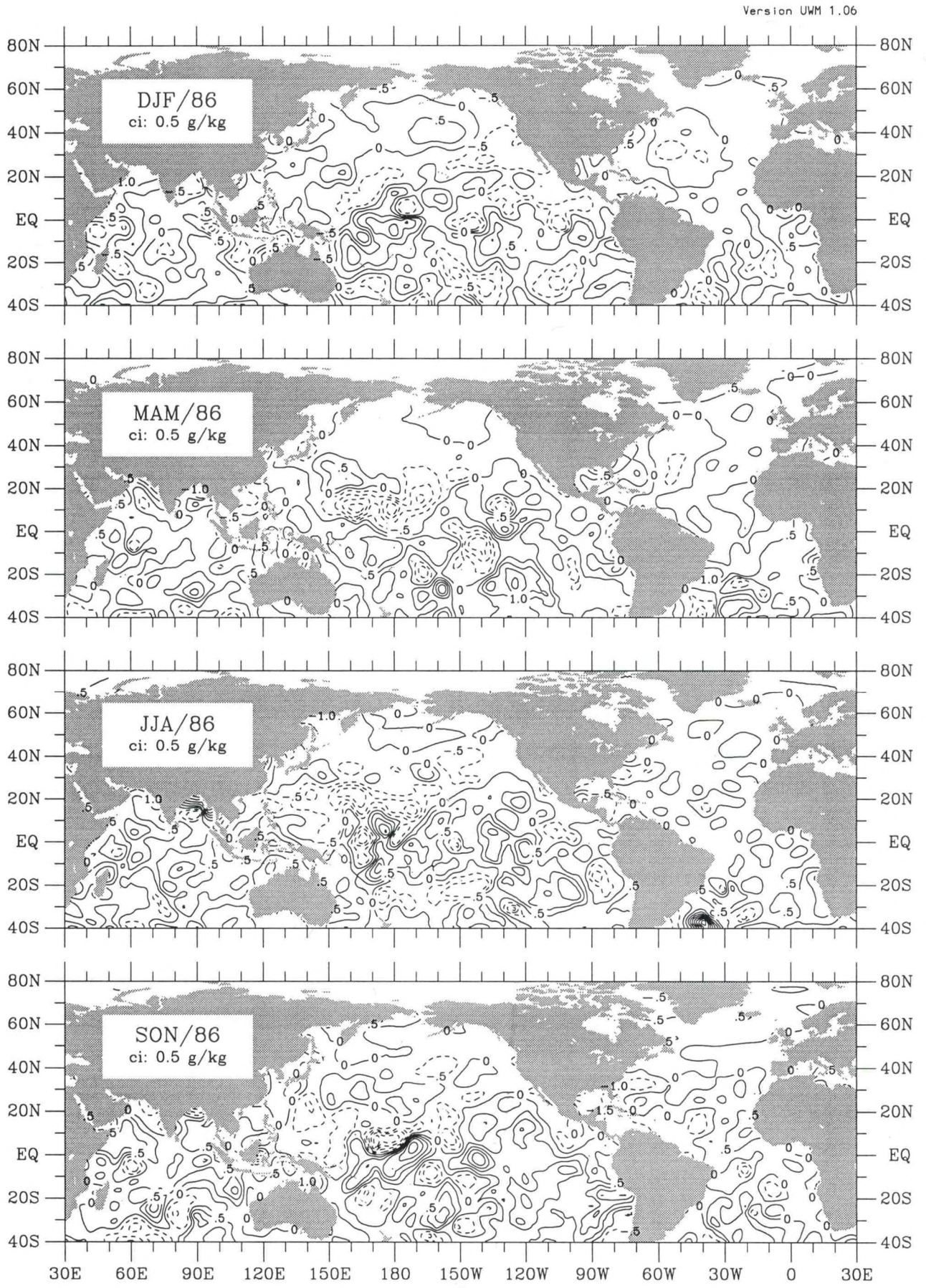

Figure dq-47. qs minus q seasonal anomaly for 1986.

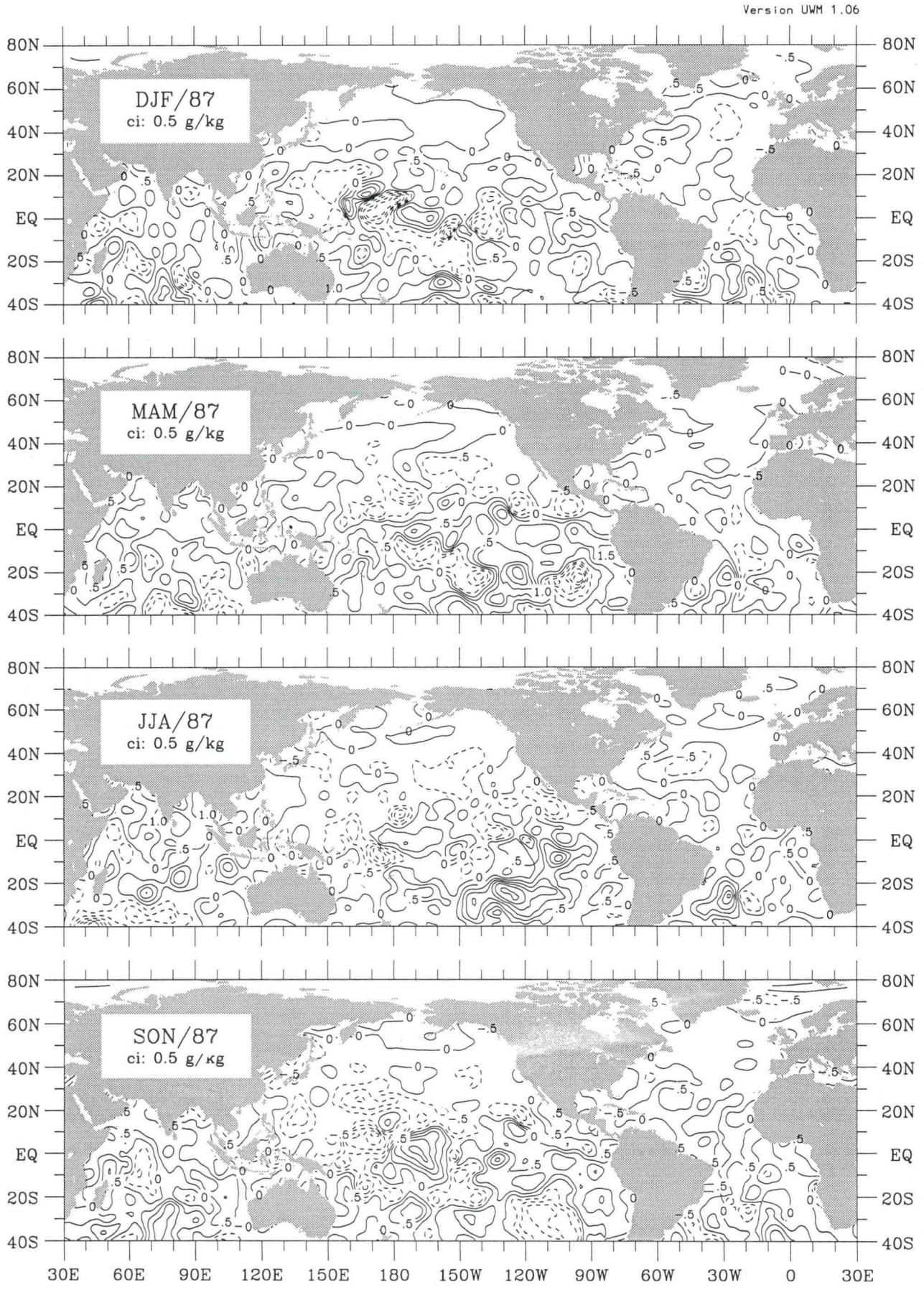

Figure dq-48. qs minus q seasonal anomaly for 1987.

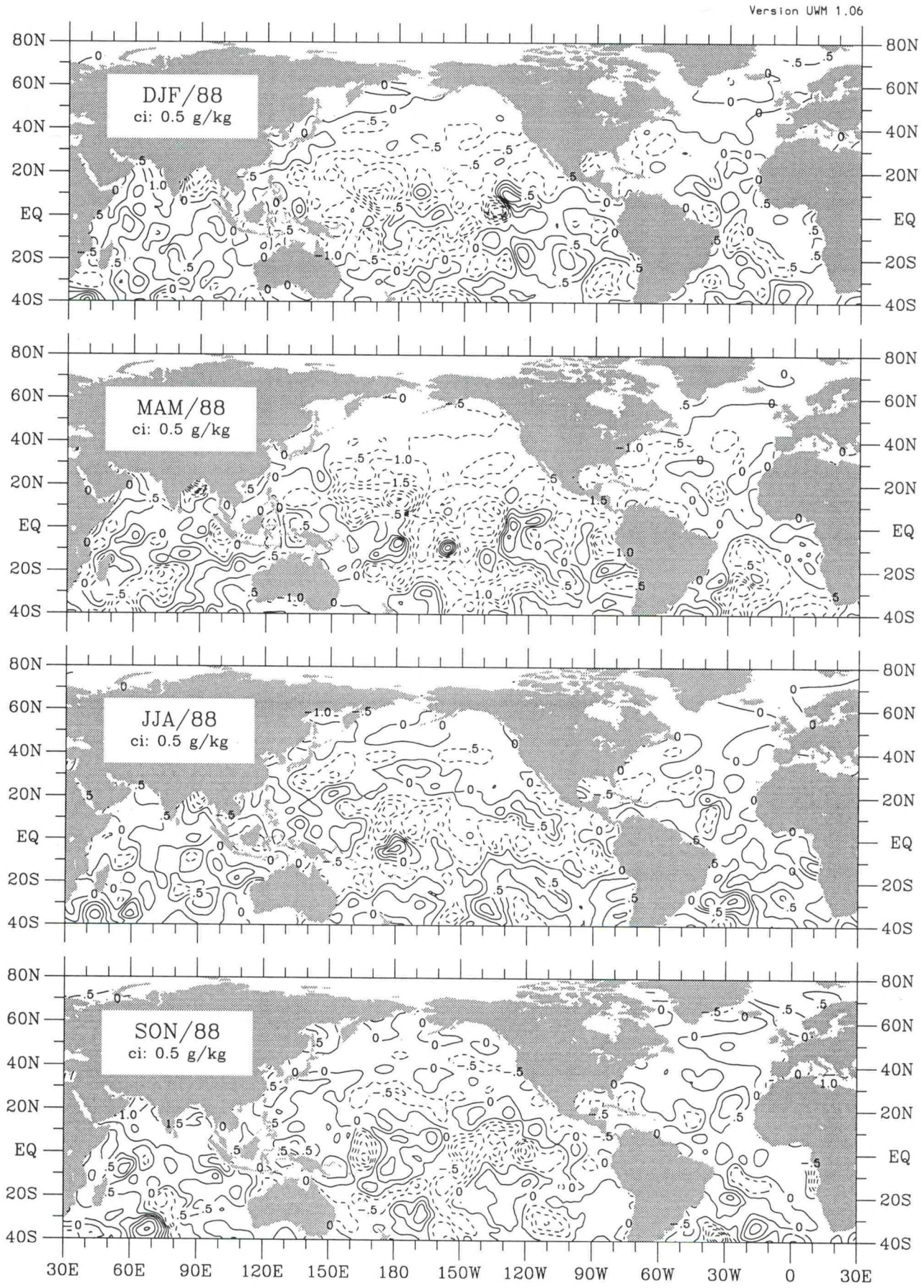

Figure dq-49. qs minus q seasonal anomaly for 1988.

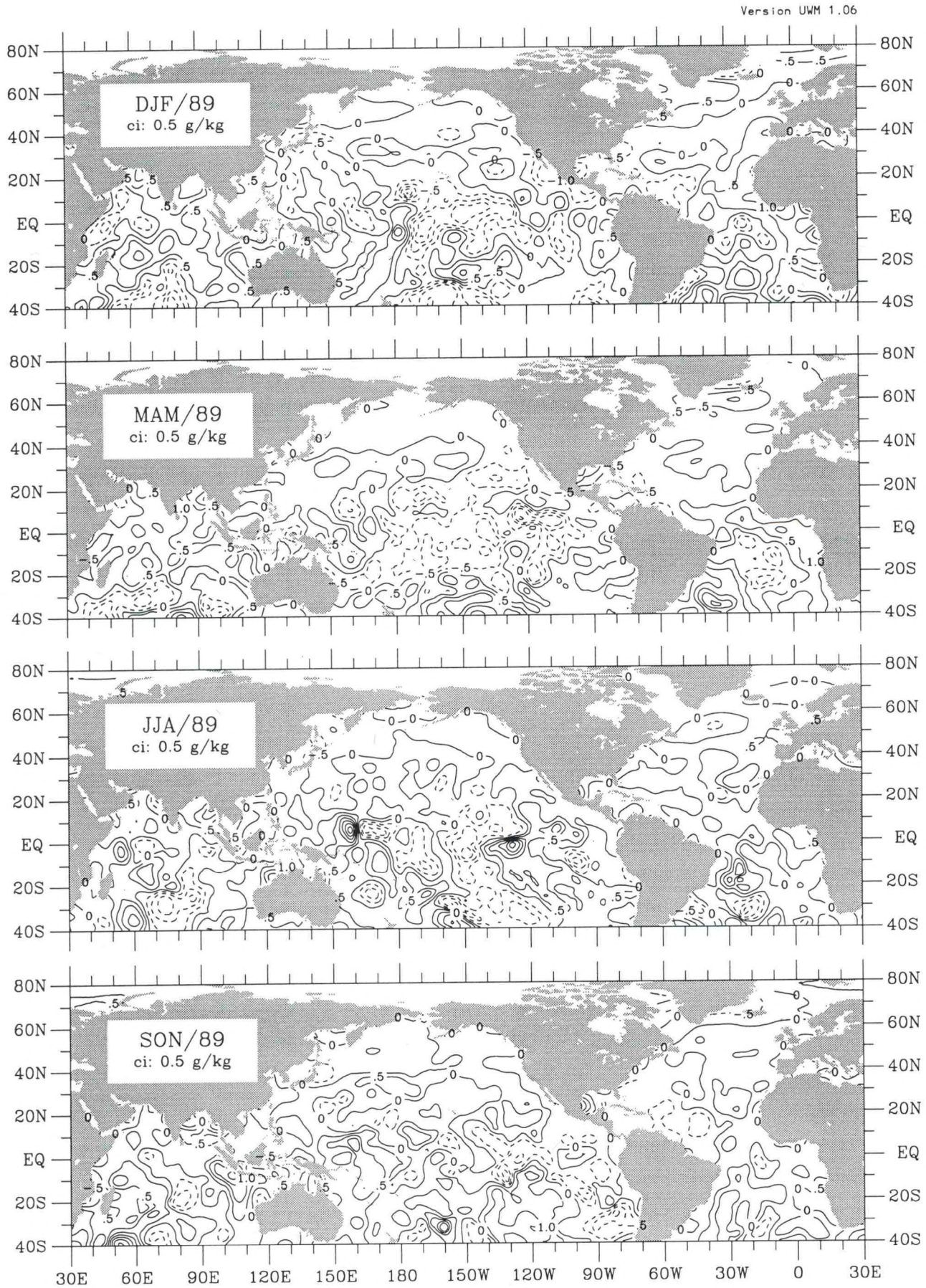

Figure dq-50. qs minus q seasonal anomaly for 1989.

13 Sea level specific humidity

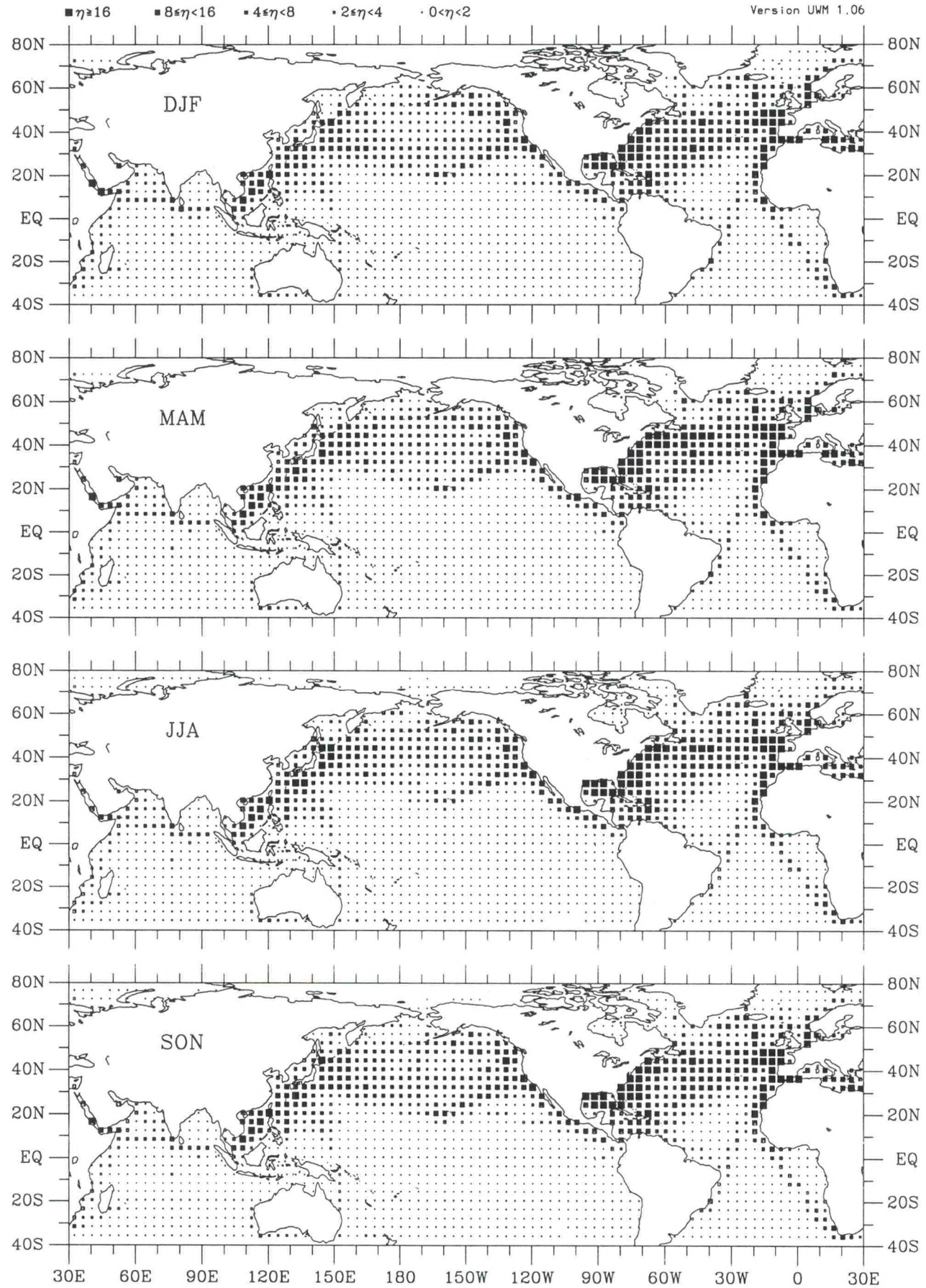

Figure qs-1. Sea level humidity seasonal observation density (1945-89).

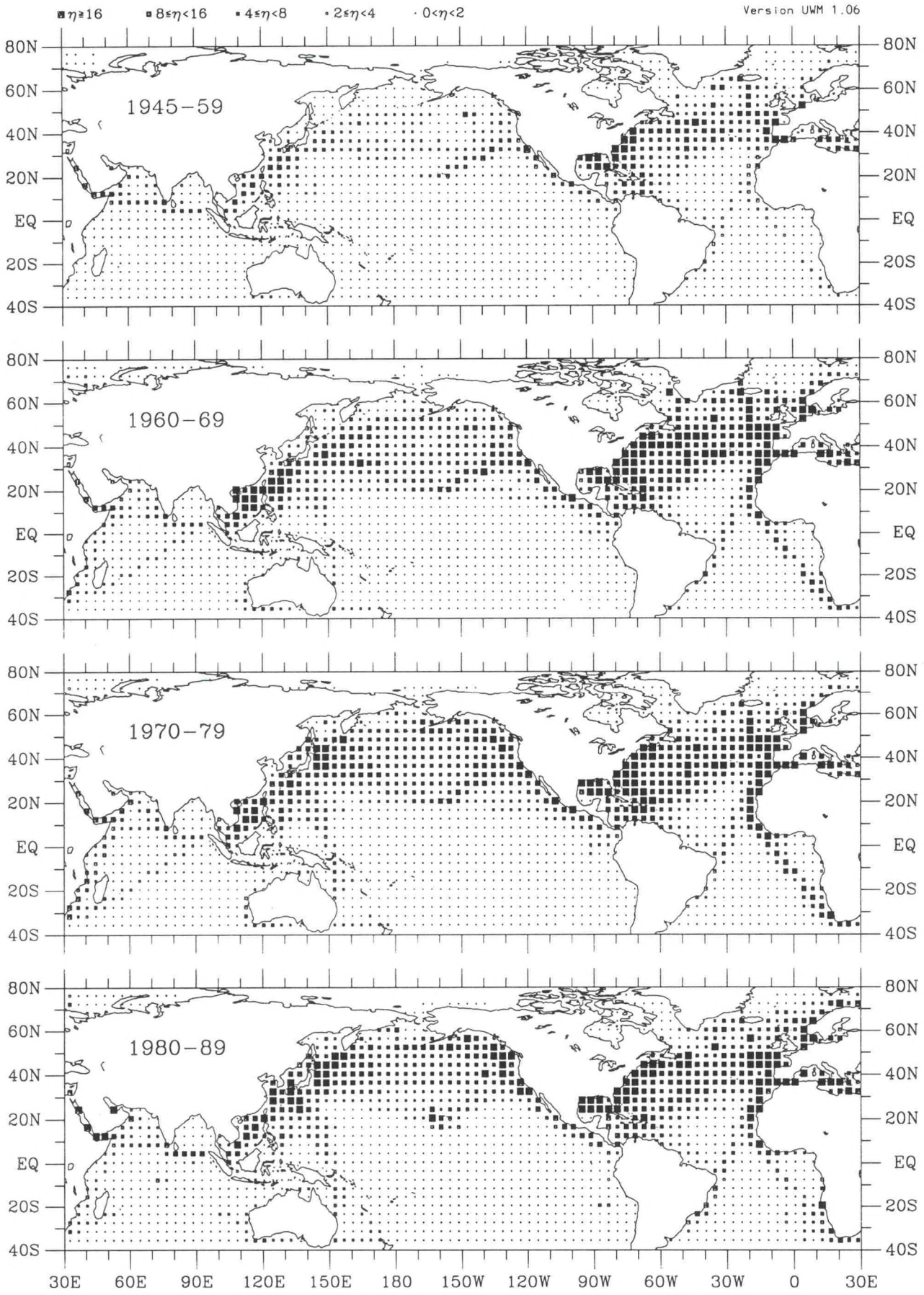

Figure qs-2. Sea level humidity decadal observation density.

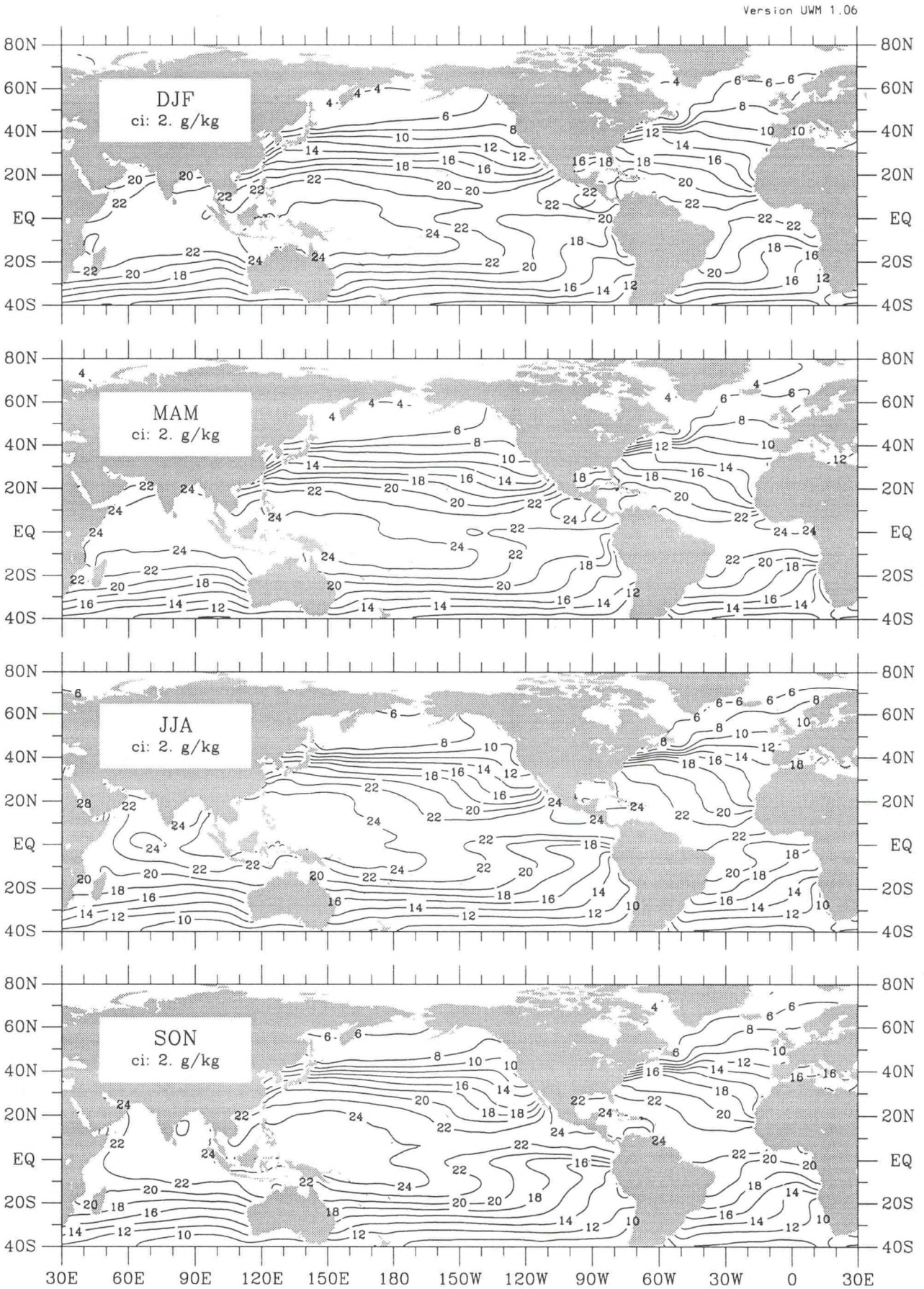

Figure qs-3. Sea level humidity seasonal climatology (1945-89).

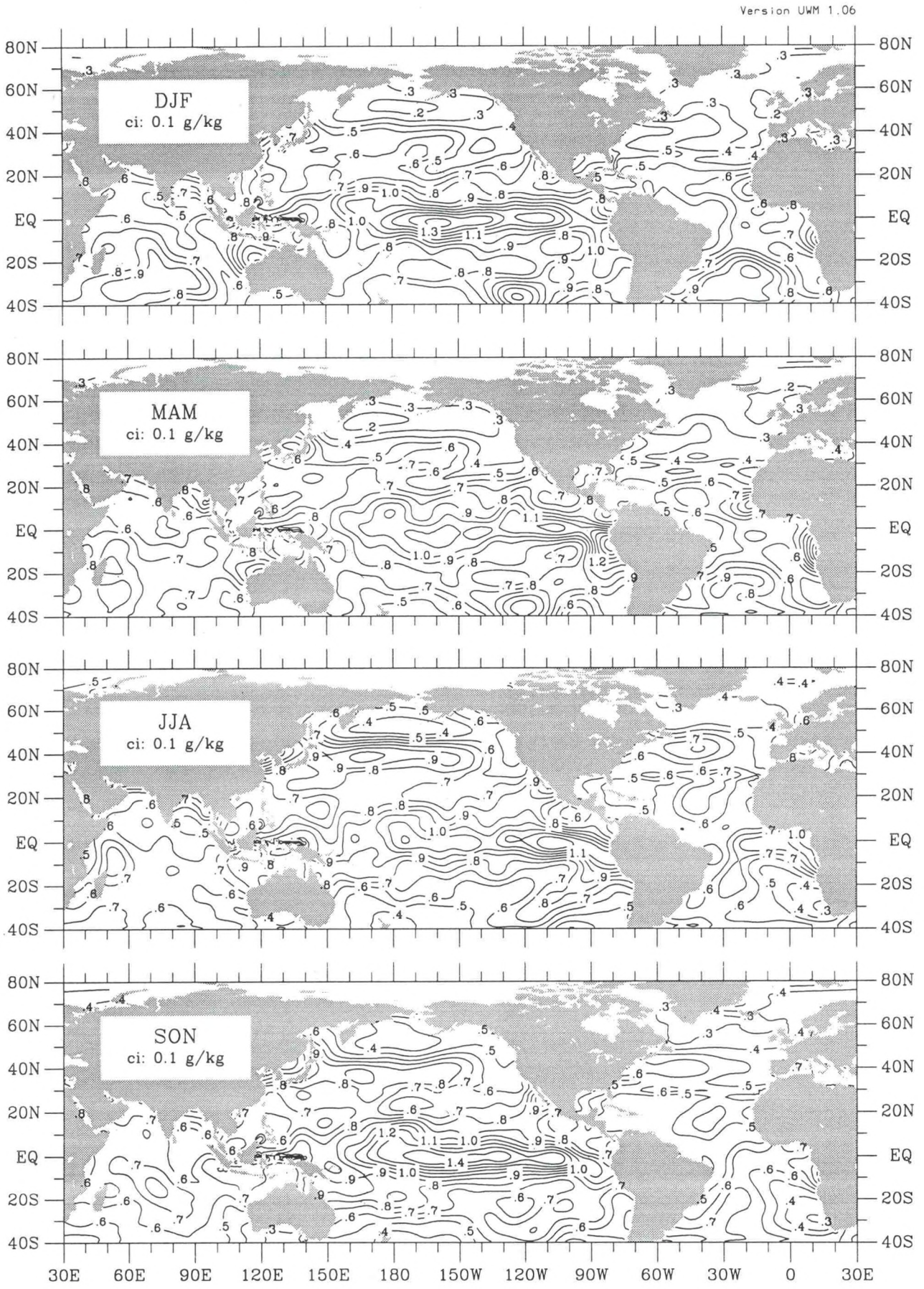

Figure qs-4. Sea level humidity seasonal interannual std dev (1945-89).

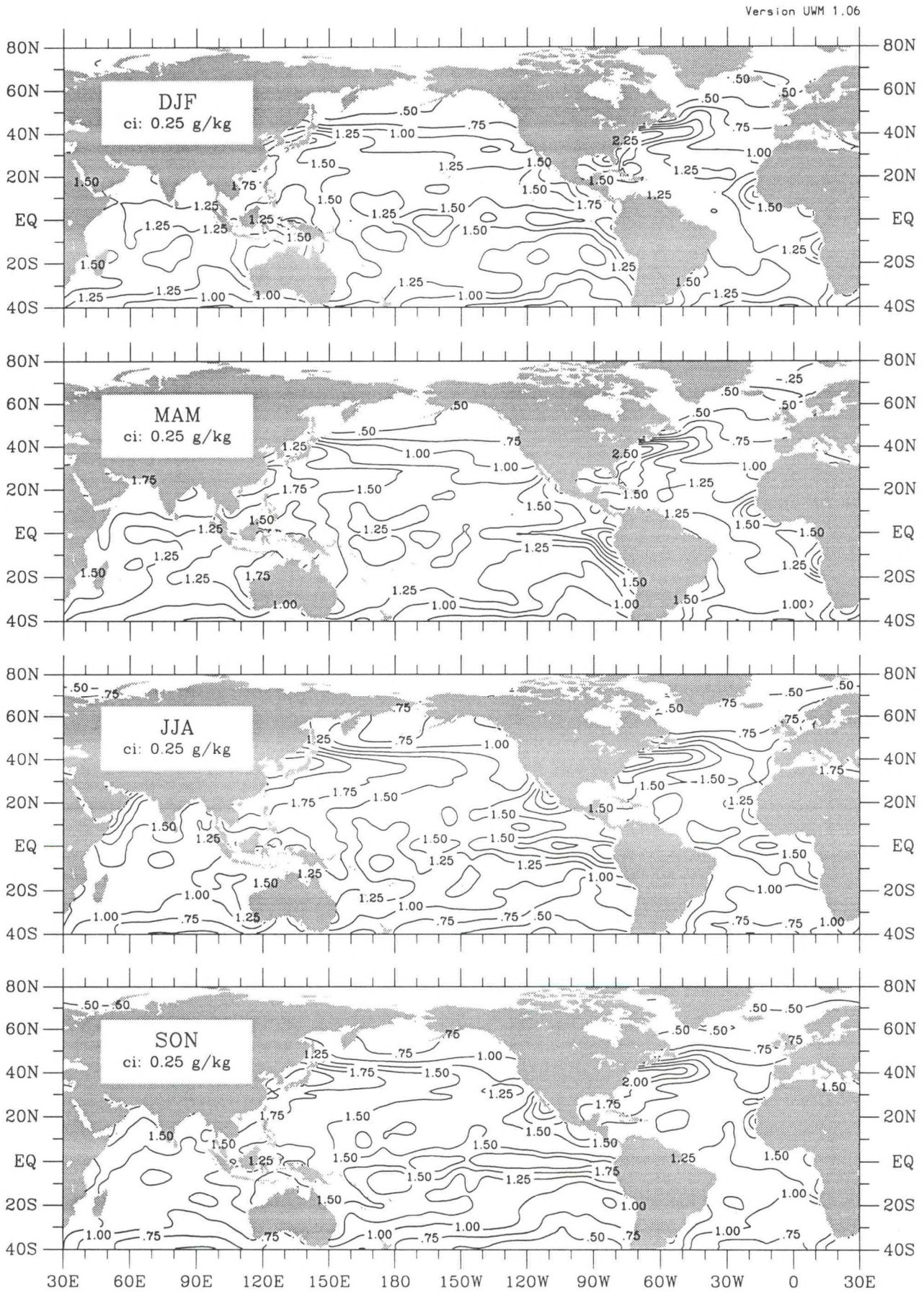

Figure qs-5. Sea level humidity seasonal standard deviation (1945-89).

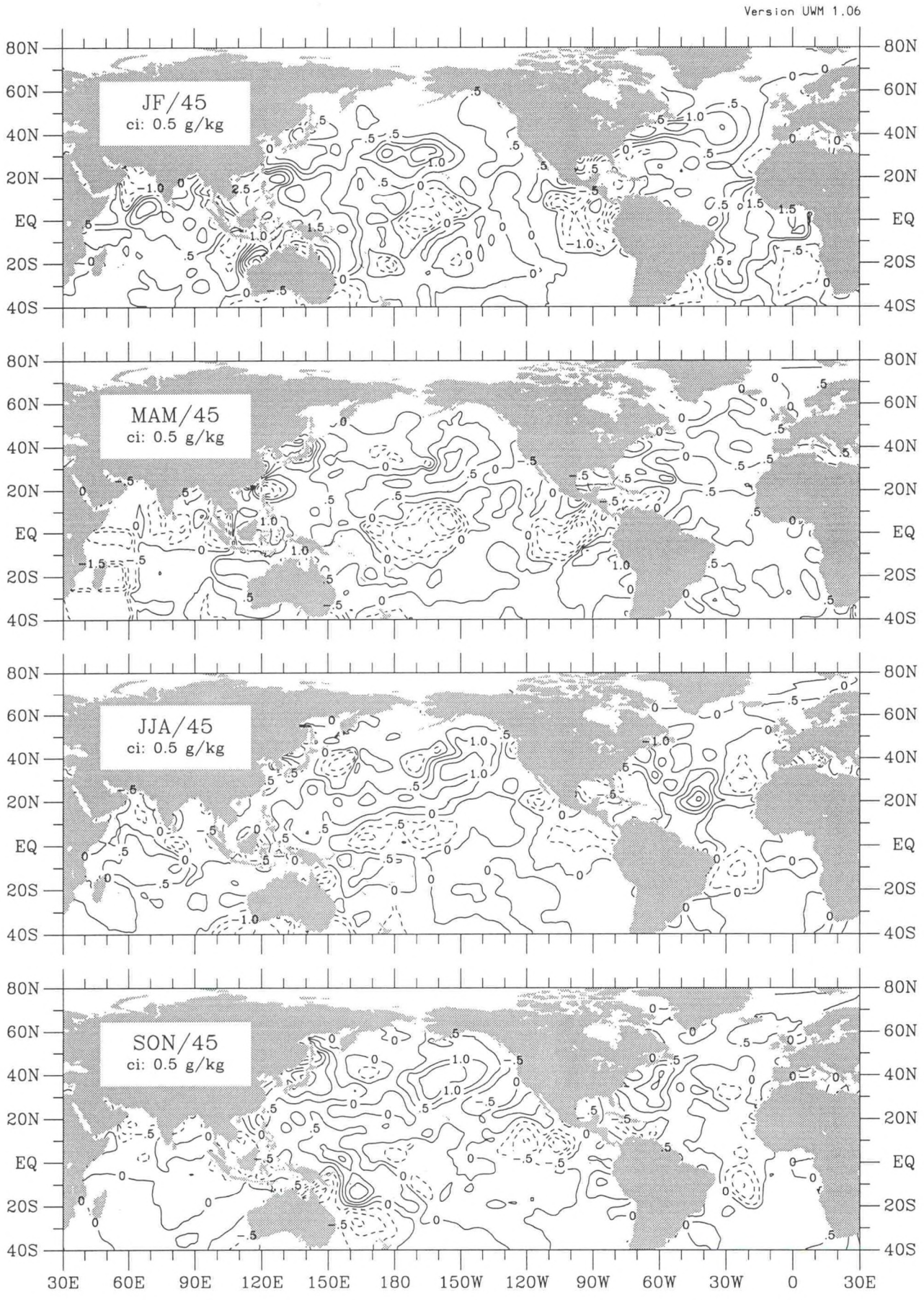

Figure qs-6. Sea level humidity seasonal anomaly for 1945.

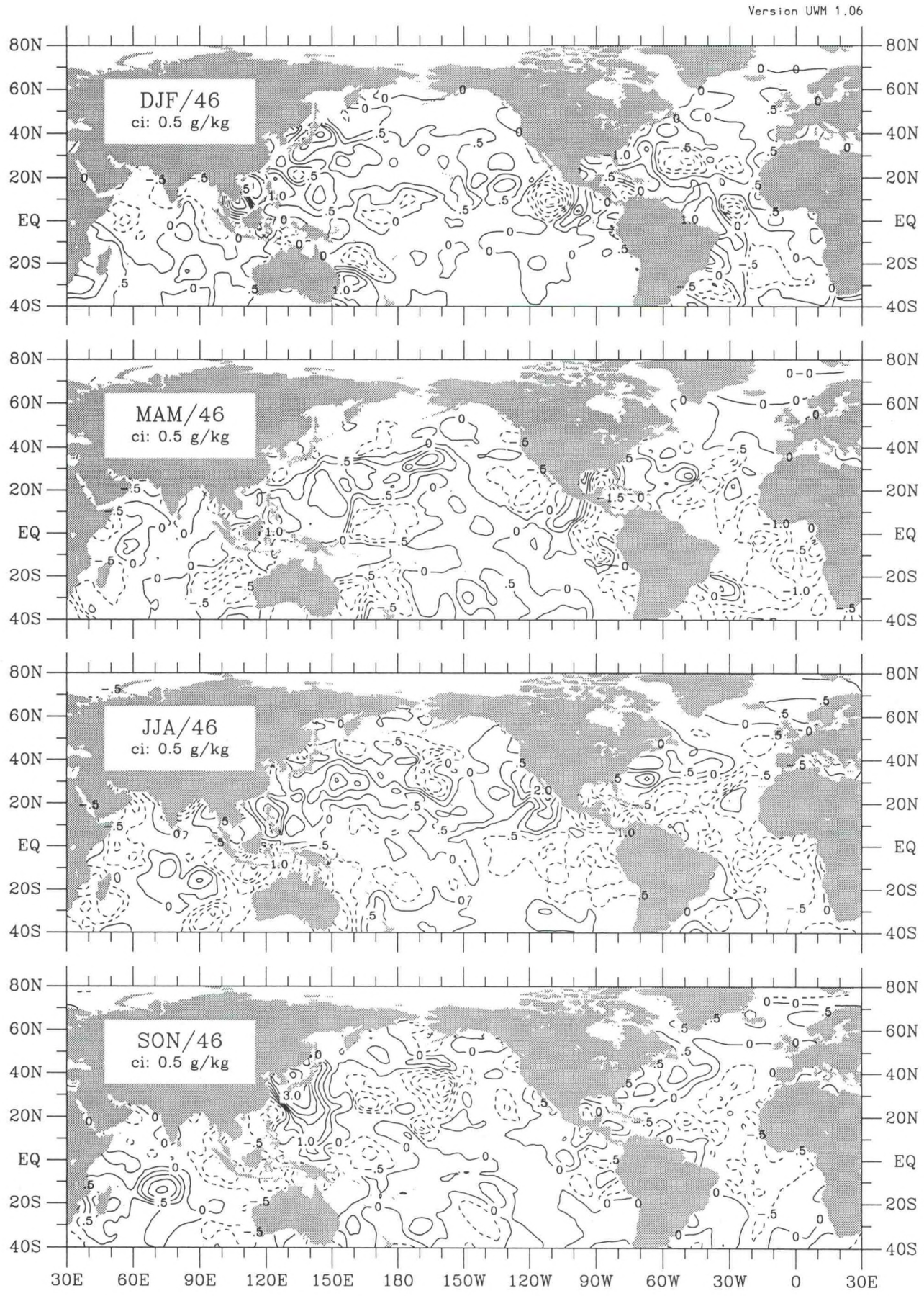

Figure qs-7. Sea level humidity seasonal anomaly for 1946.

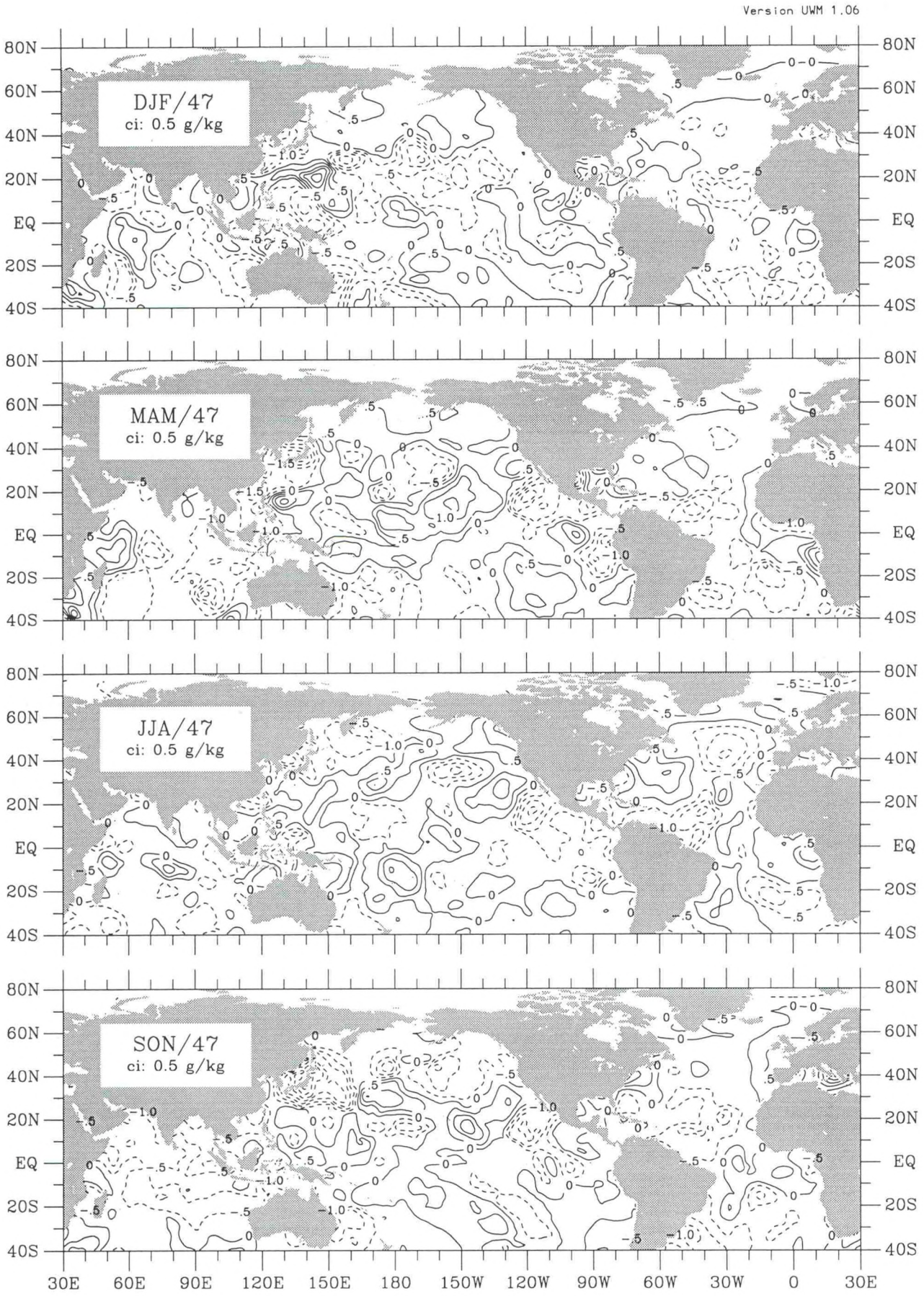

Figure qs-8. Sea level humidity seasonal anomaly for 1947.

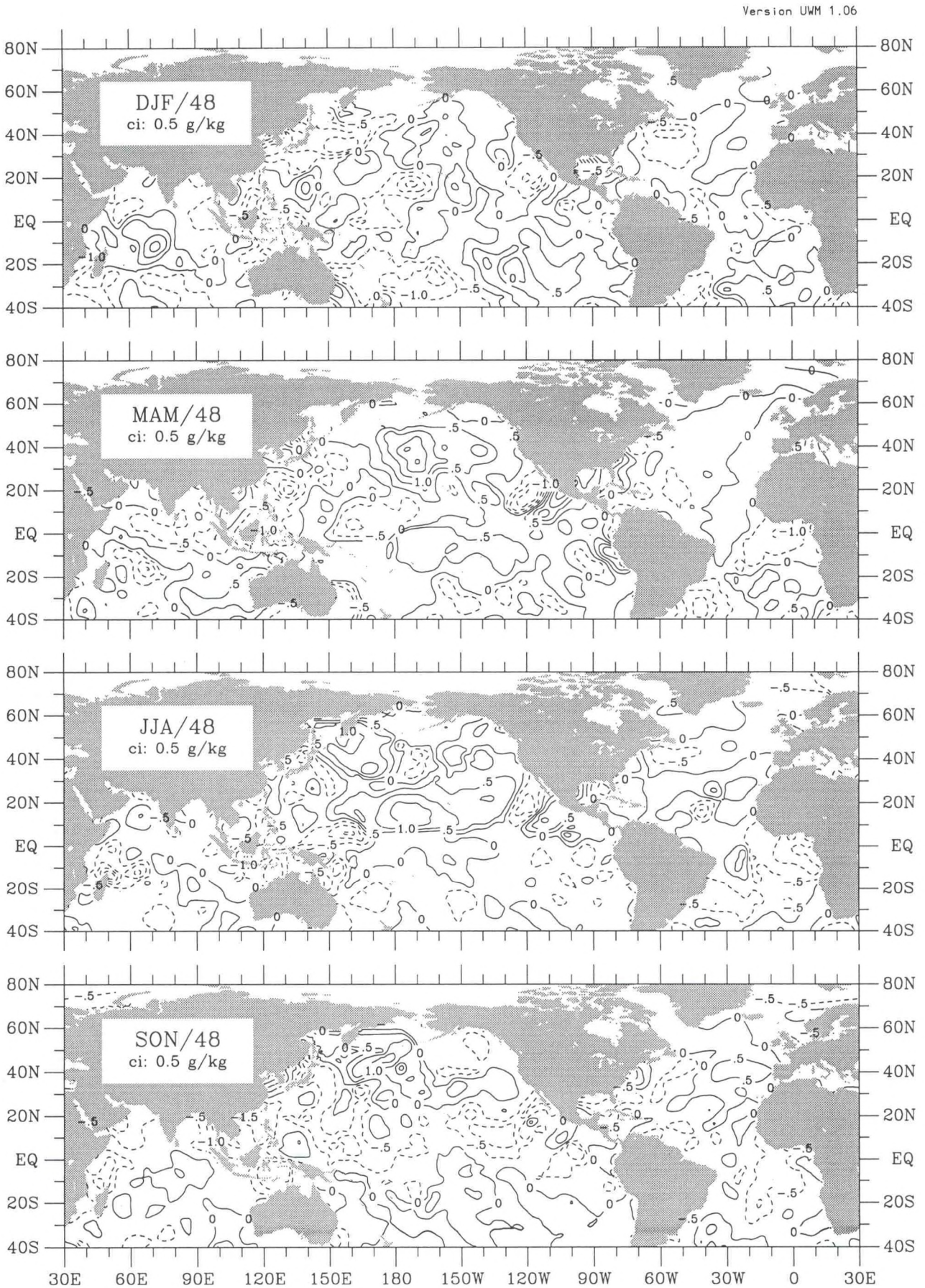

Figure qs-9. Sea level humidity seasonal anomaly for 1948.

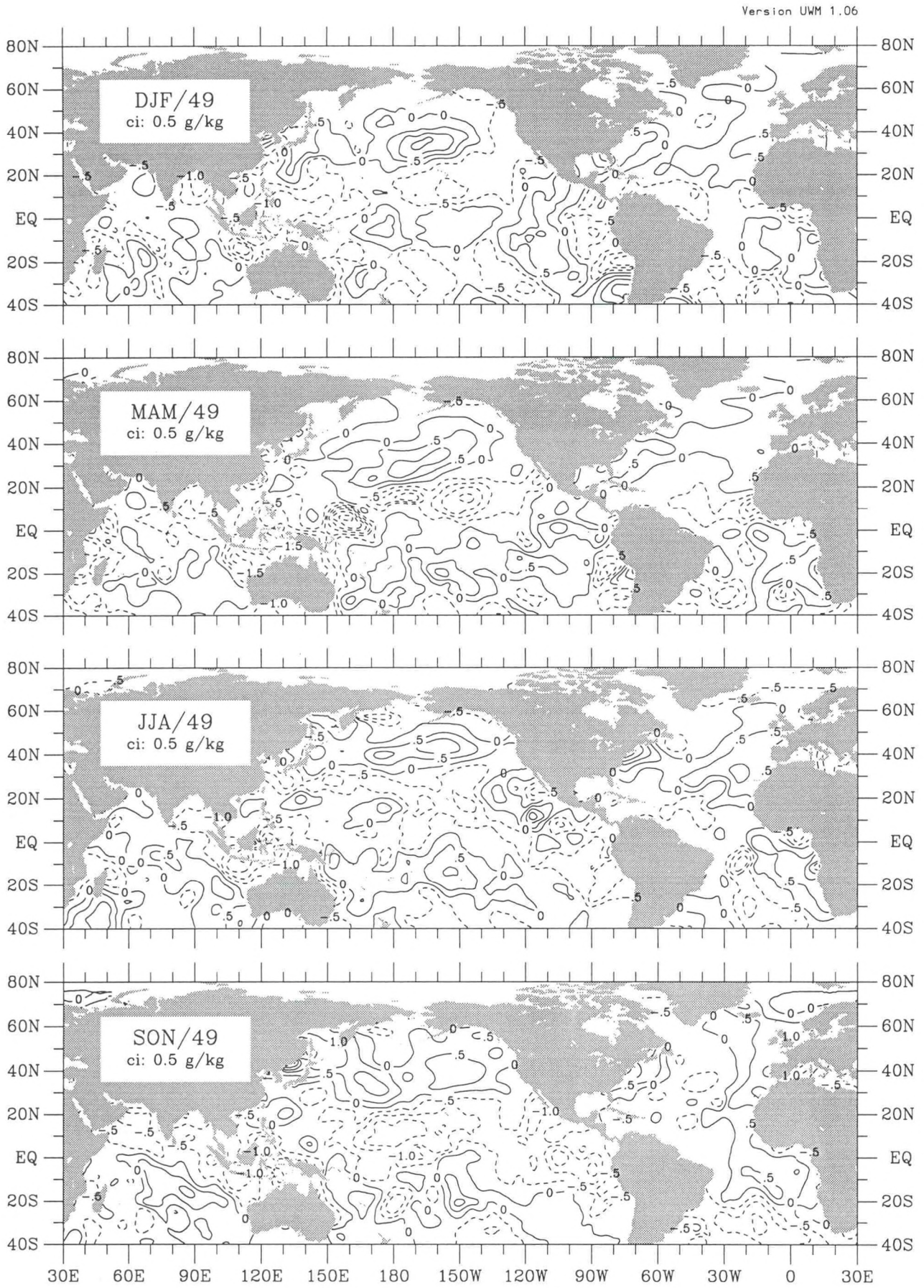

Figure qs-10. Sea level humidity seasonal anomaly for 1949.

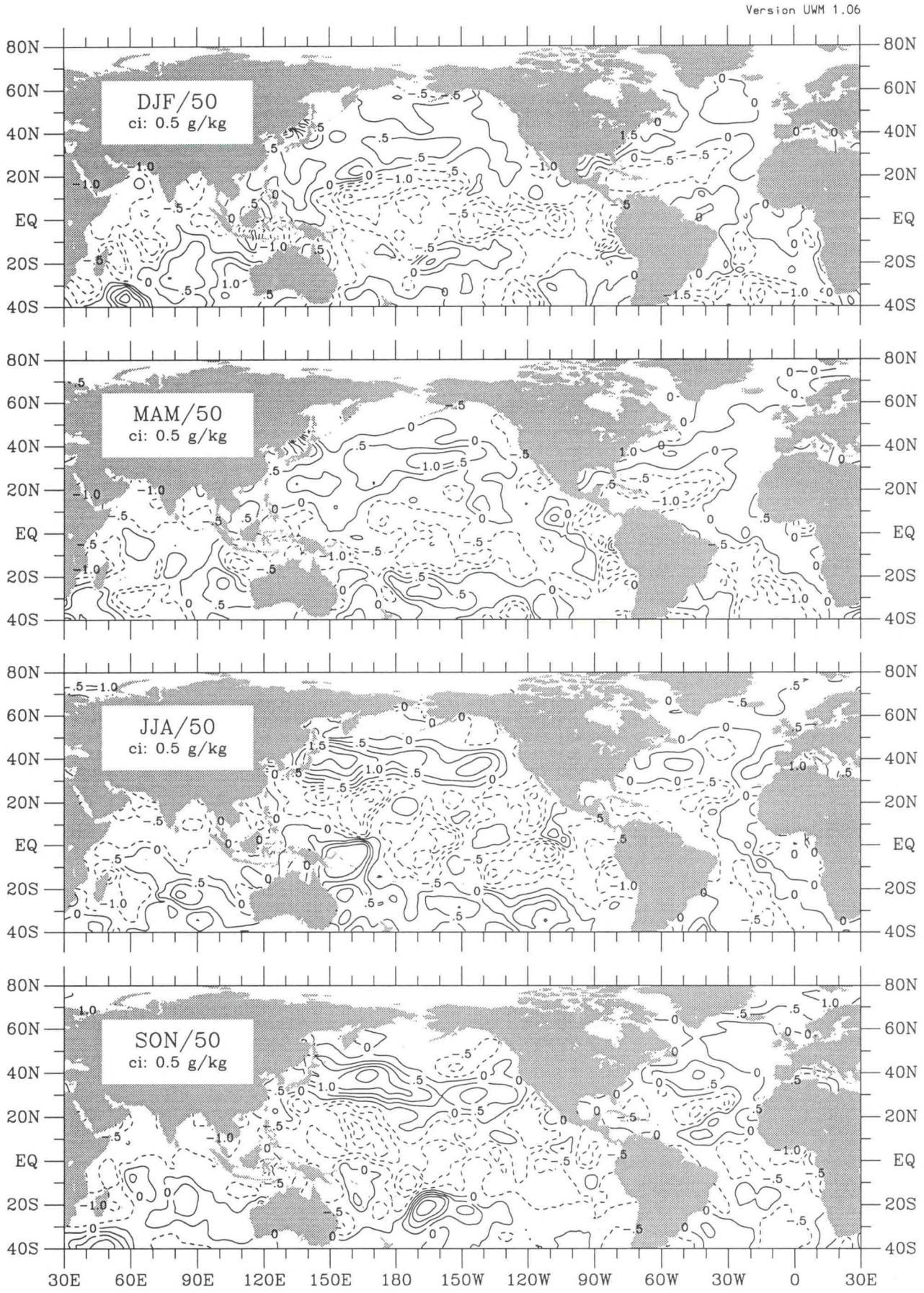

Figure qs-11. Sea level humidity seasonal anomaly for 1950.

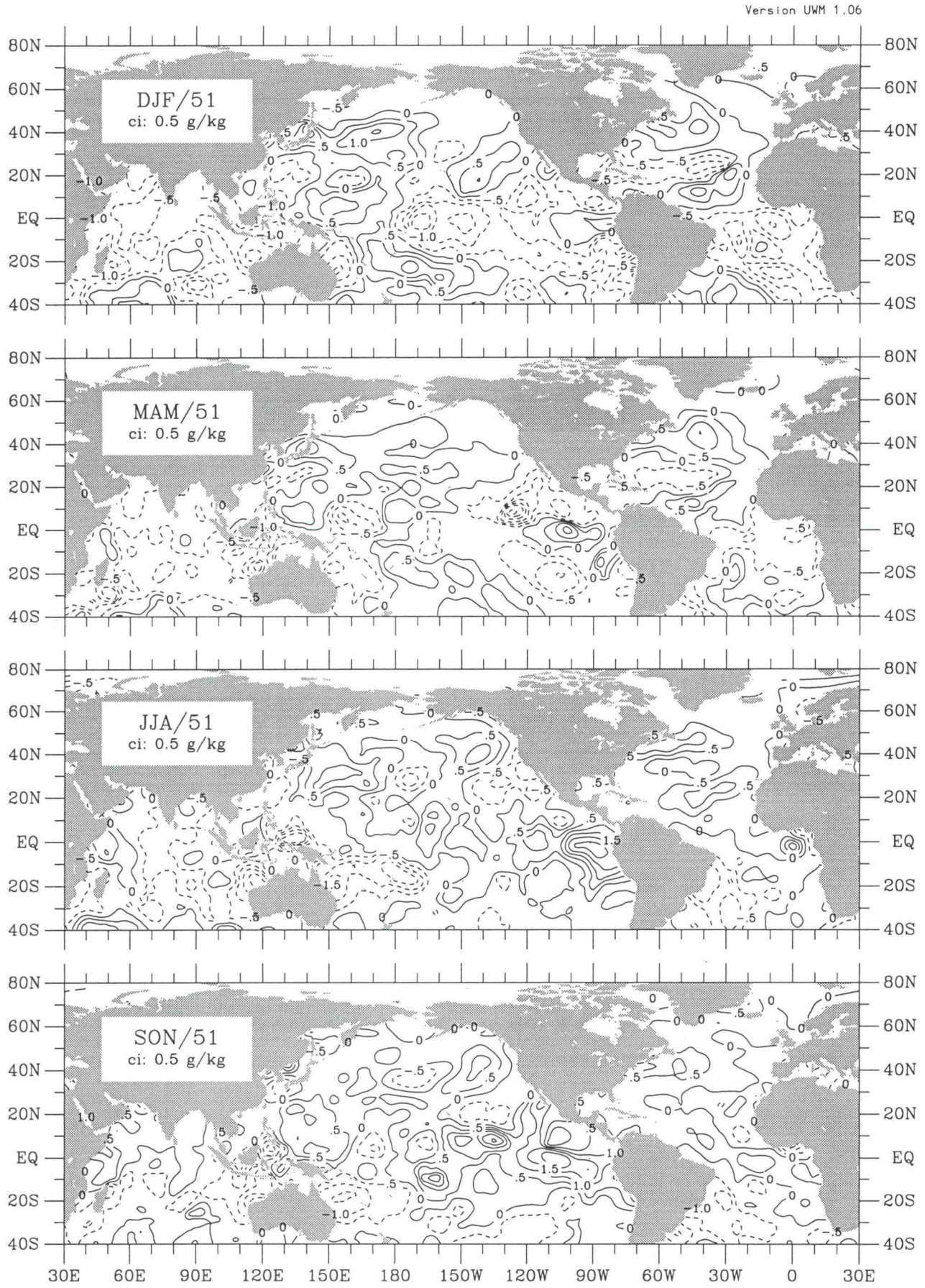

Figure qs-12. Sea level humidity seasonal anomaly for 1951.

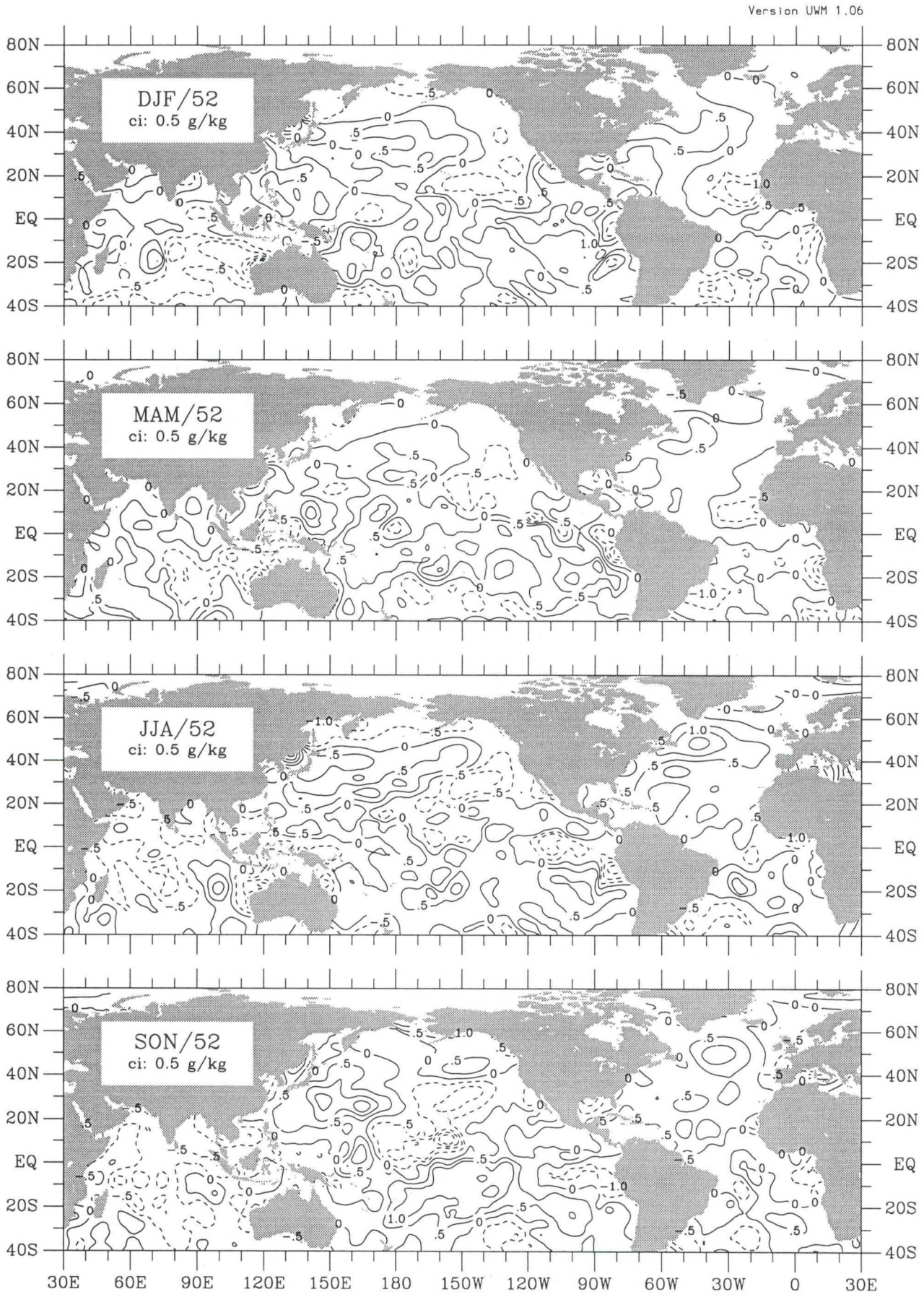

Figure qs-13. Sea level humidity seasonal anomaly for 1952.

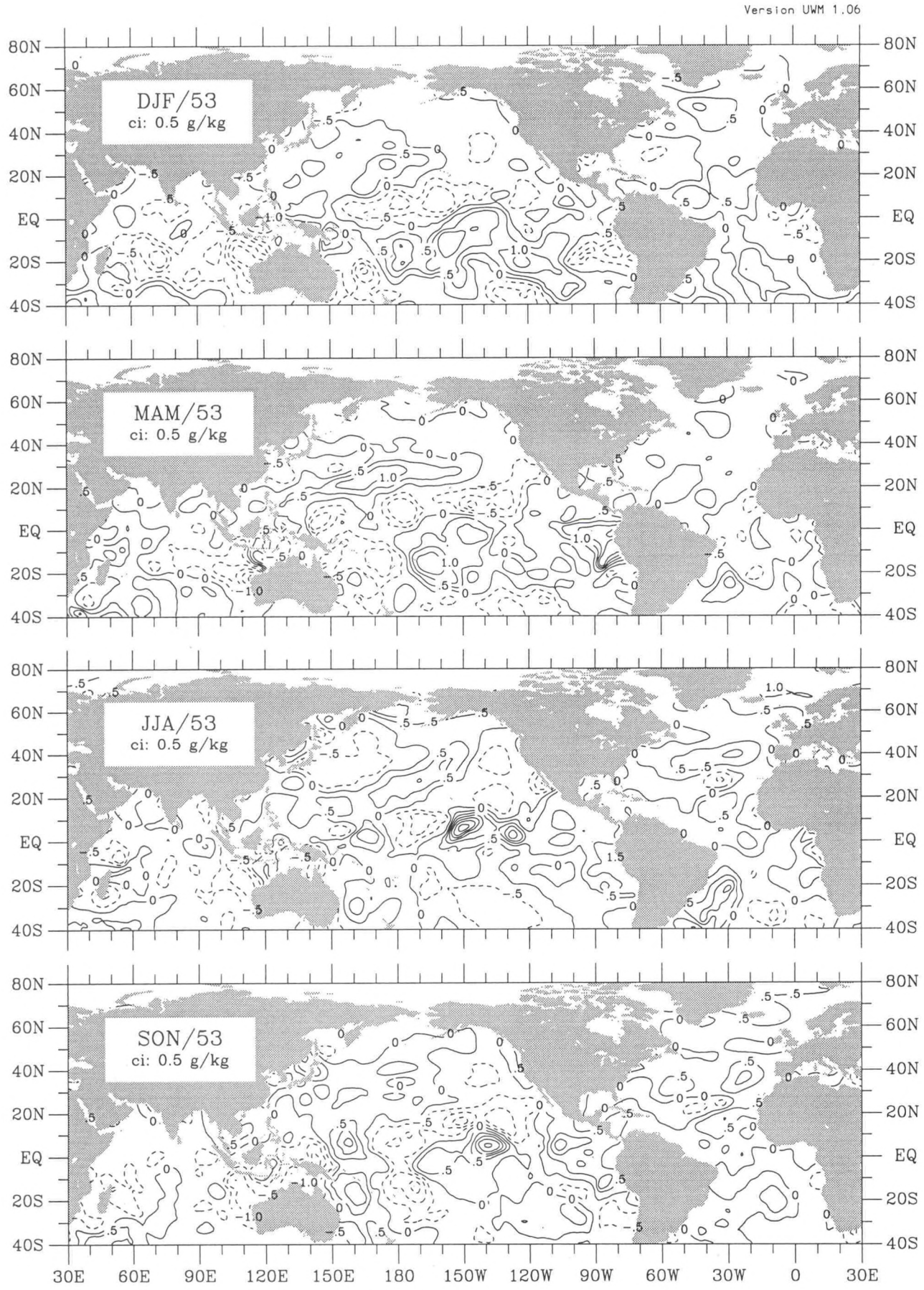

Figure qs-14. Sea level humidity seasonal anomaly for 1953.

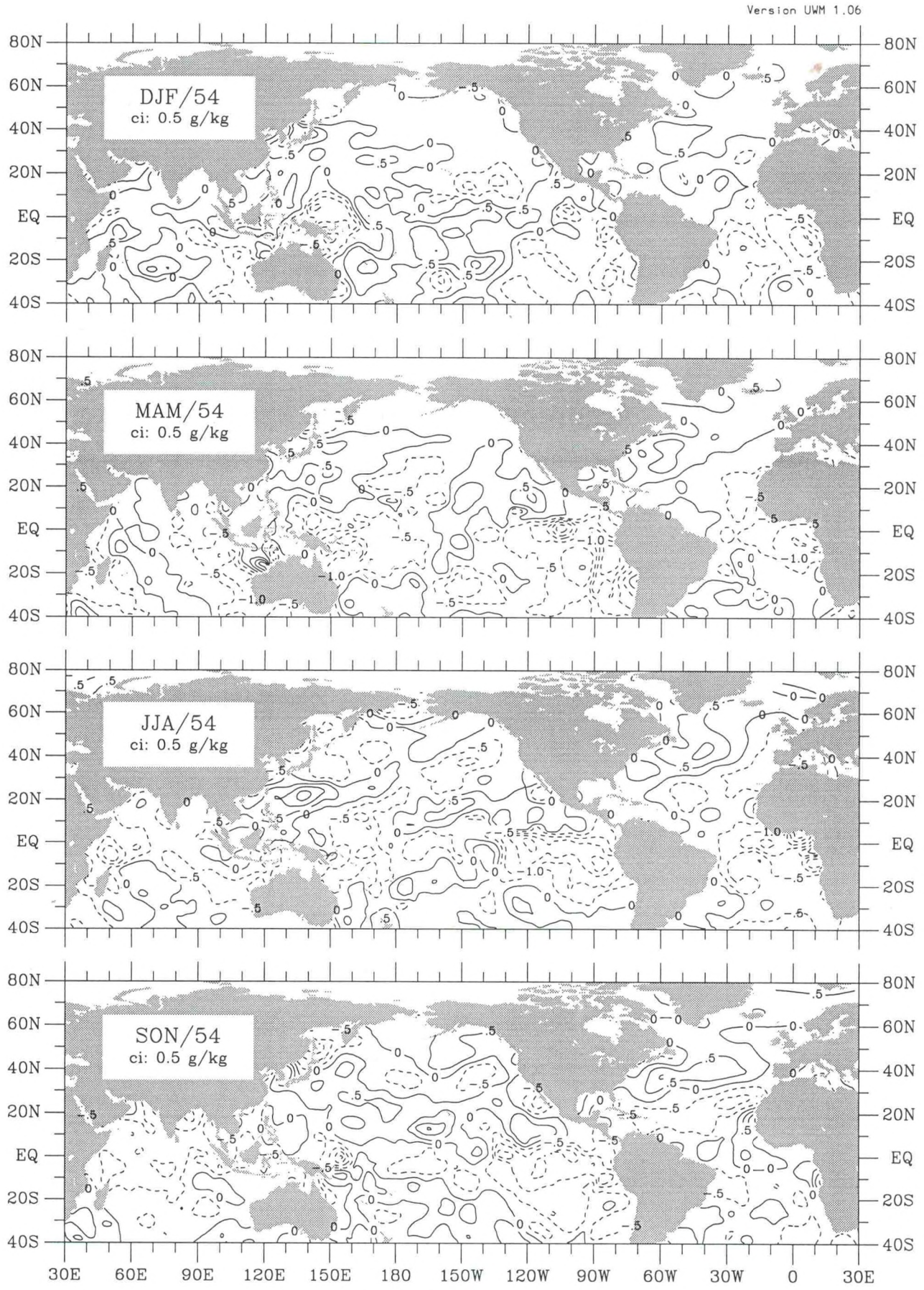

Figure qs-15. Sea level humidity seasonal anomaly for 1954.

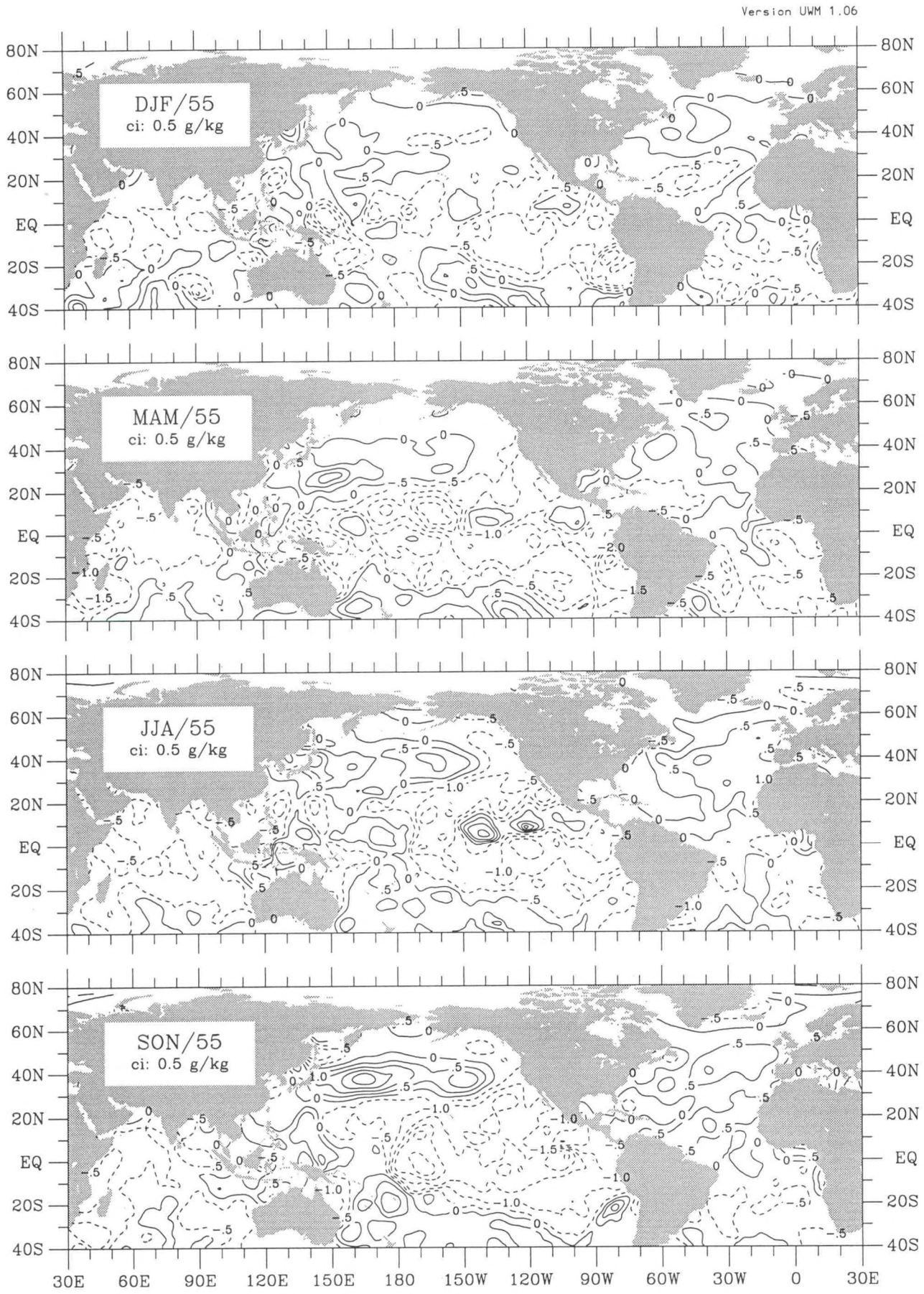

Figure qs-16. Sea level humidity seasonal anomaly for 1955.

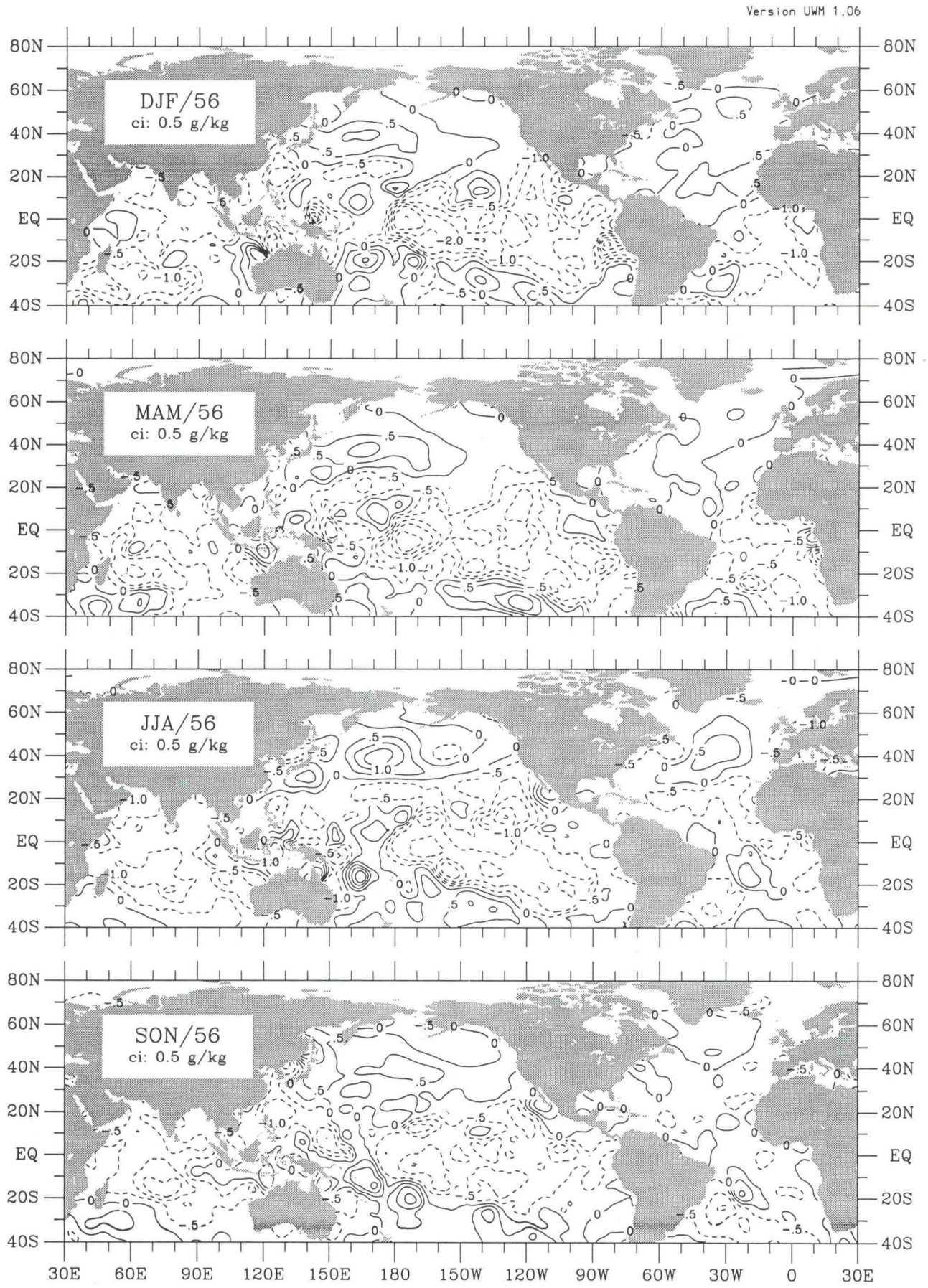

Figure qs-17. Sea level humidity seasonal anomaly for 1956.

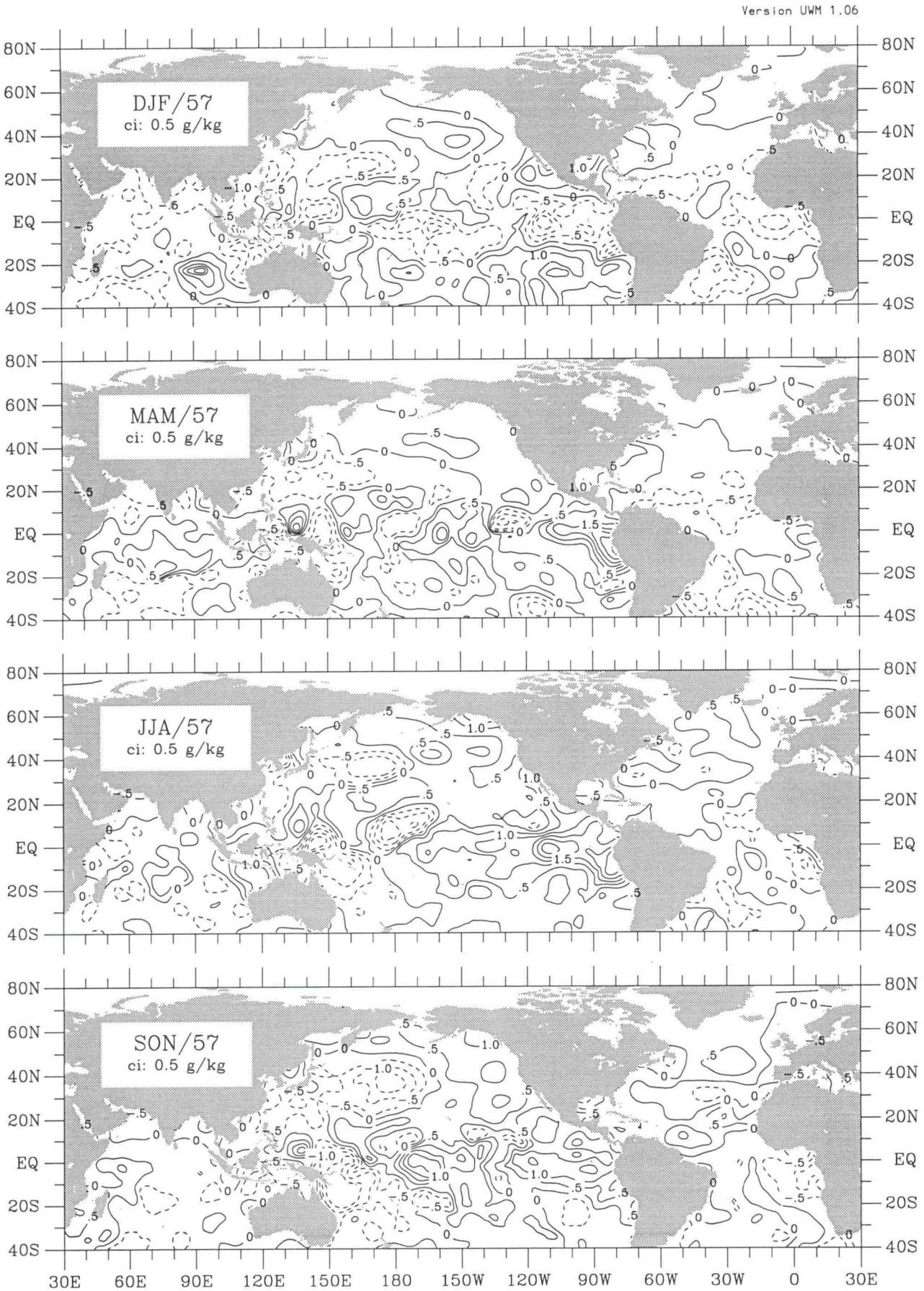

Figure qs-18. Sea level humidity seasonal anomaly for 1957.

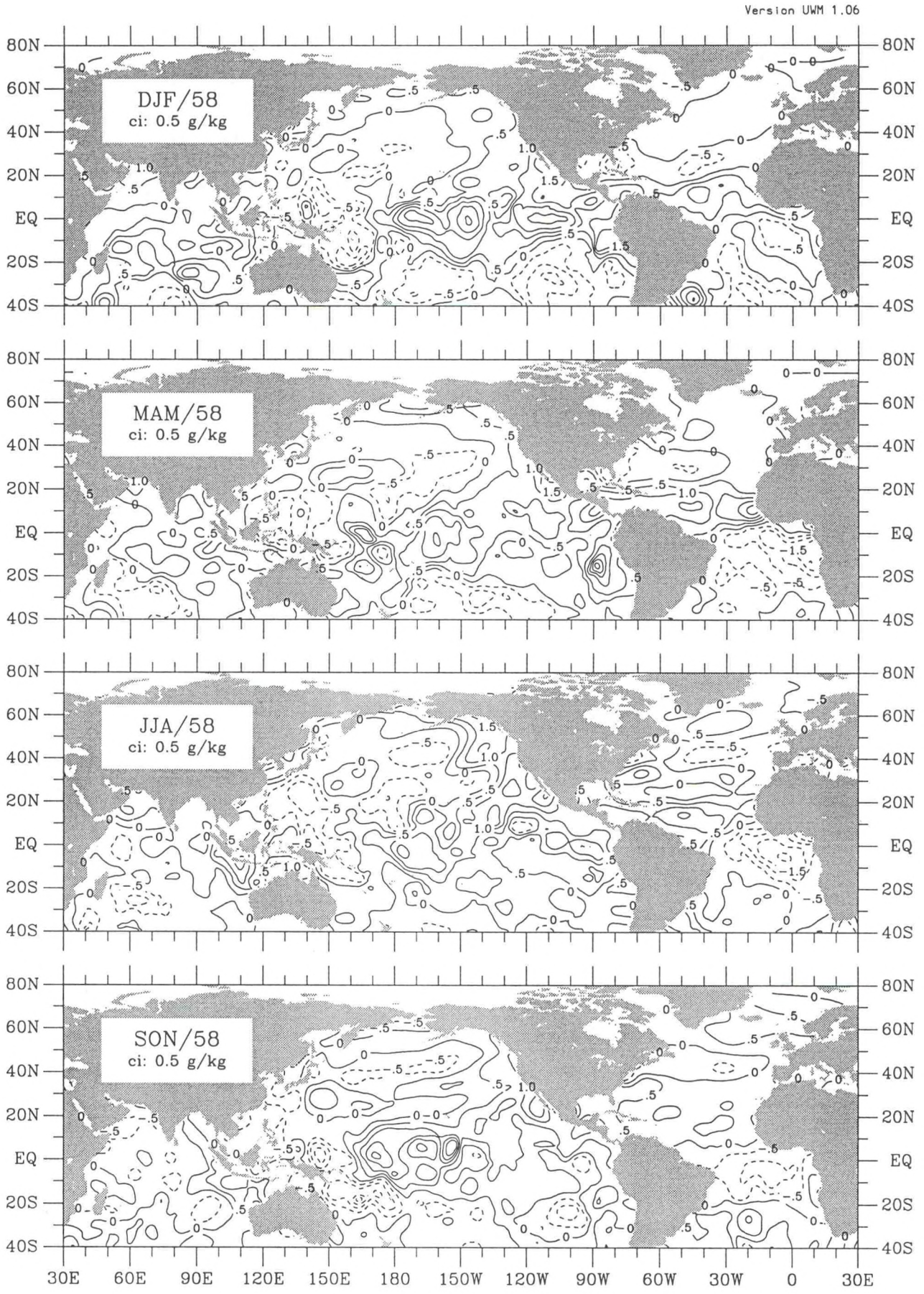

Figure qs-19. Sea level humidity seasonal anomaly for 1958.

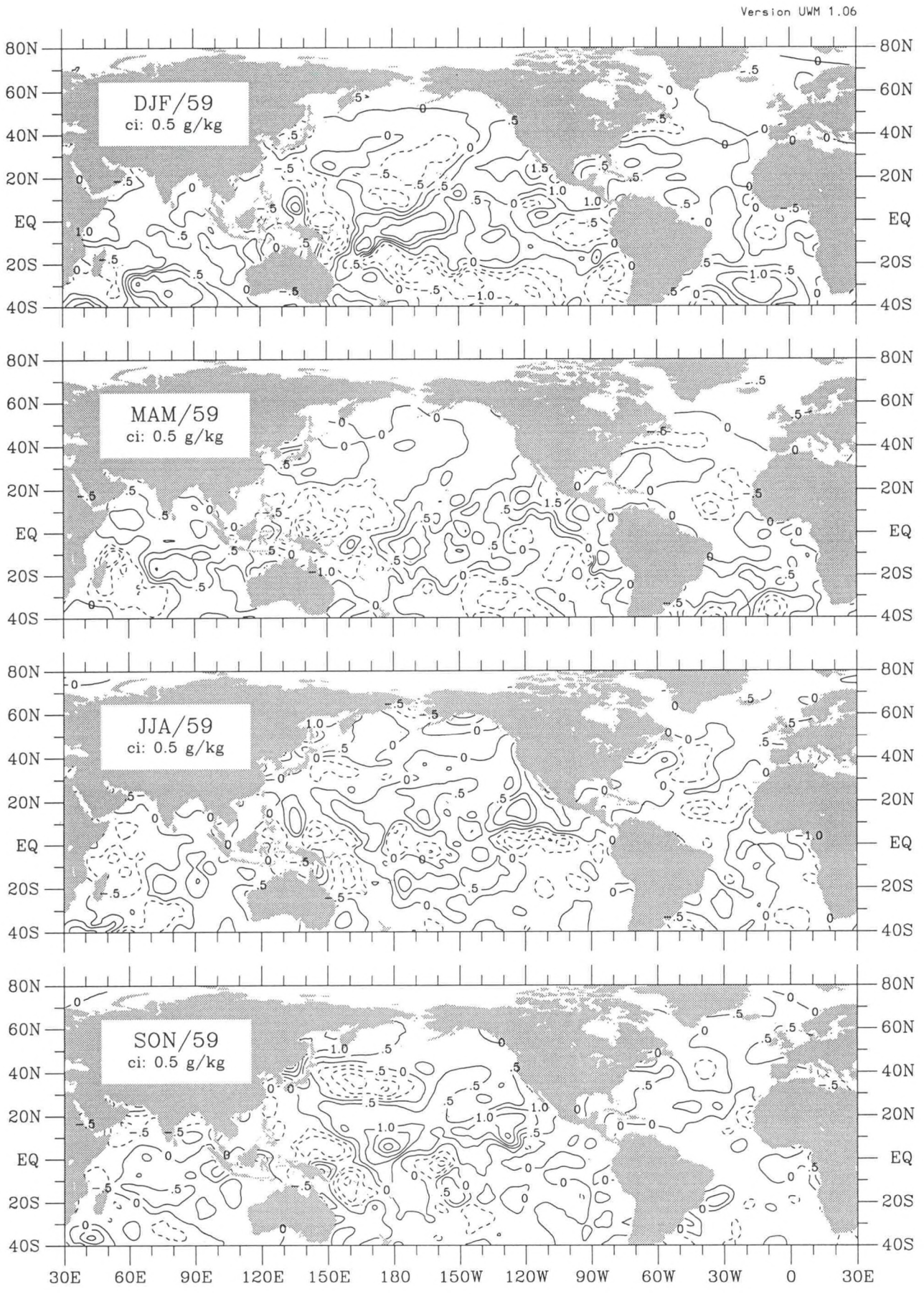

Figure qs-20. Sea level humidity seasonal anomaly for 1959.

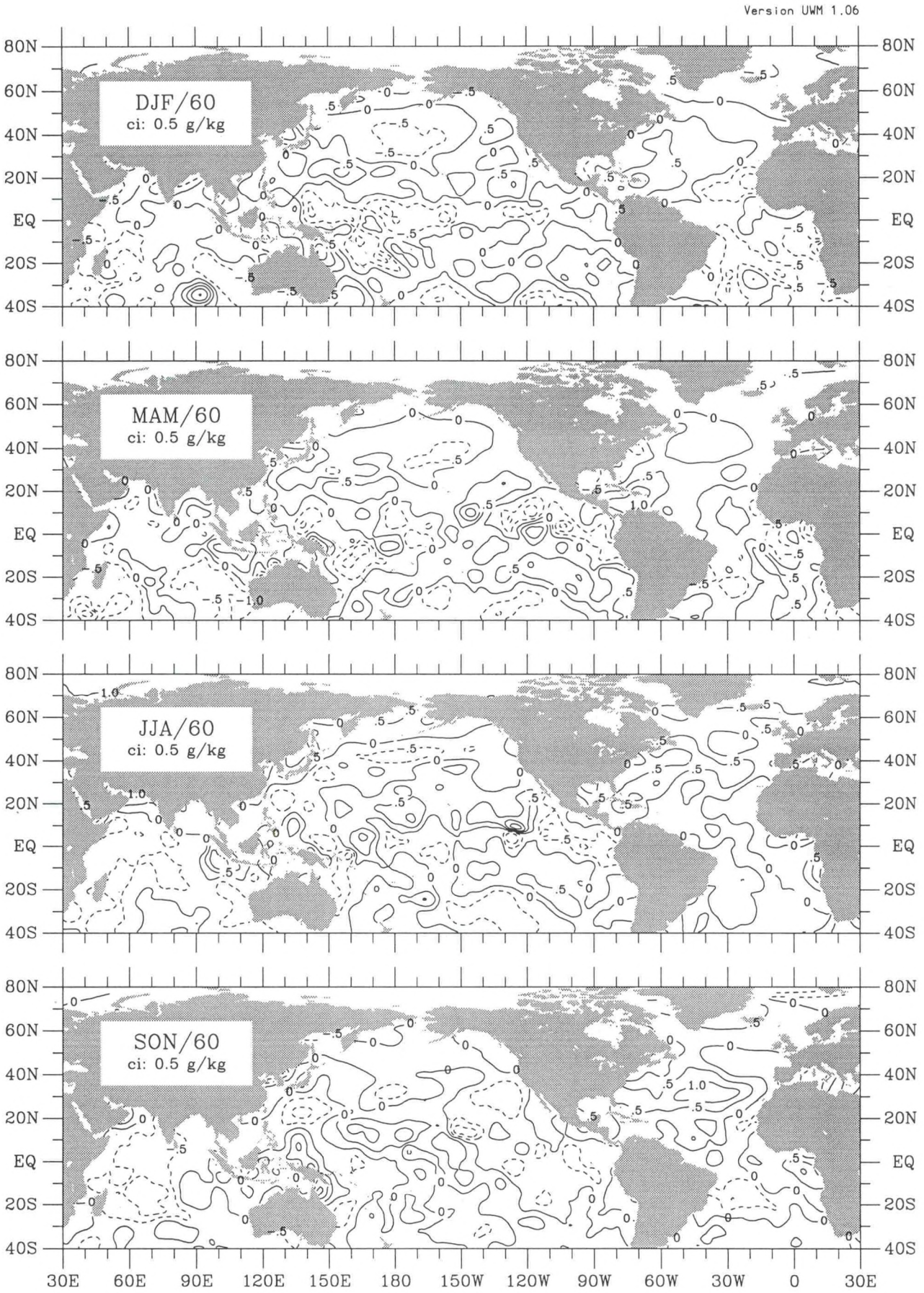

Figure qs-21. Sea level humidity seasonal anomaly for 1960.

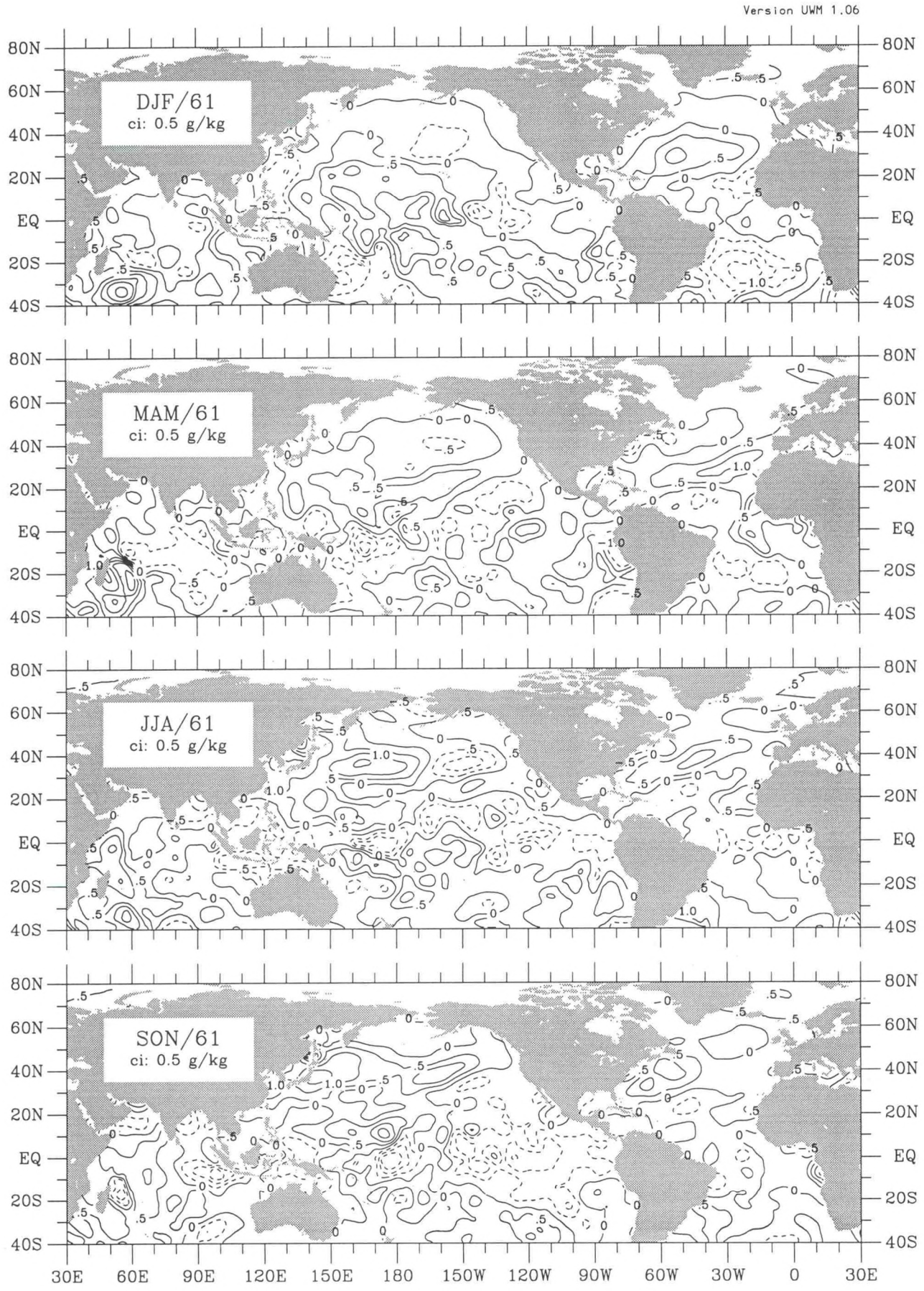

Figure qs-22. Sea level humidity seasonal anomaly for 1961.

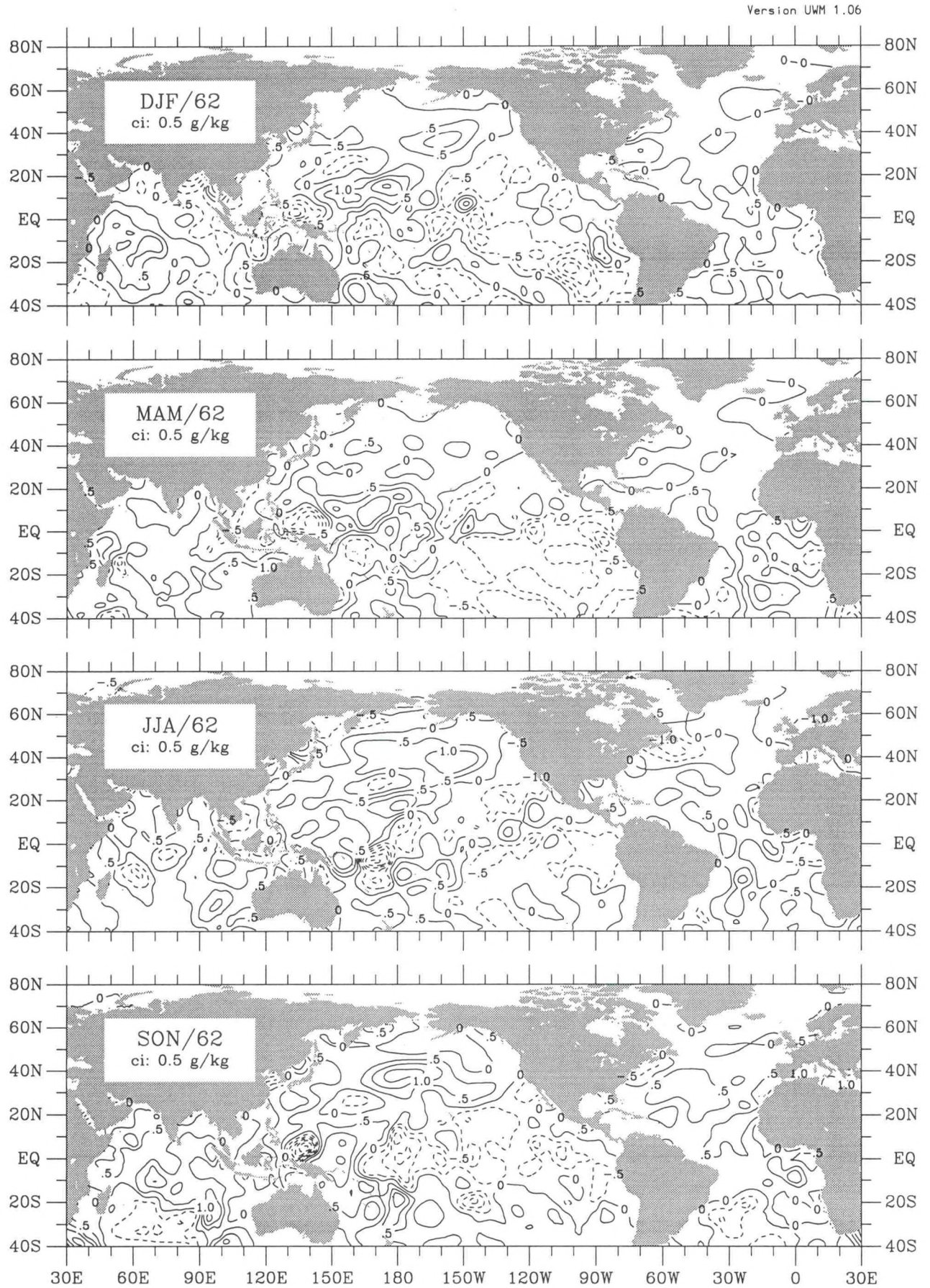

Figure qs-23. Sea level humidity seasonal anomaly for 1962.

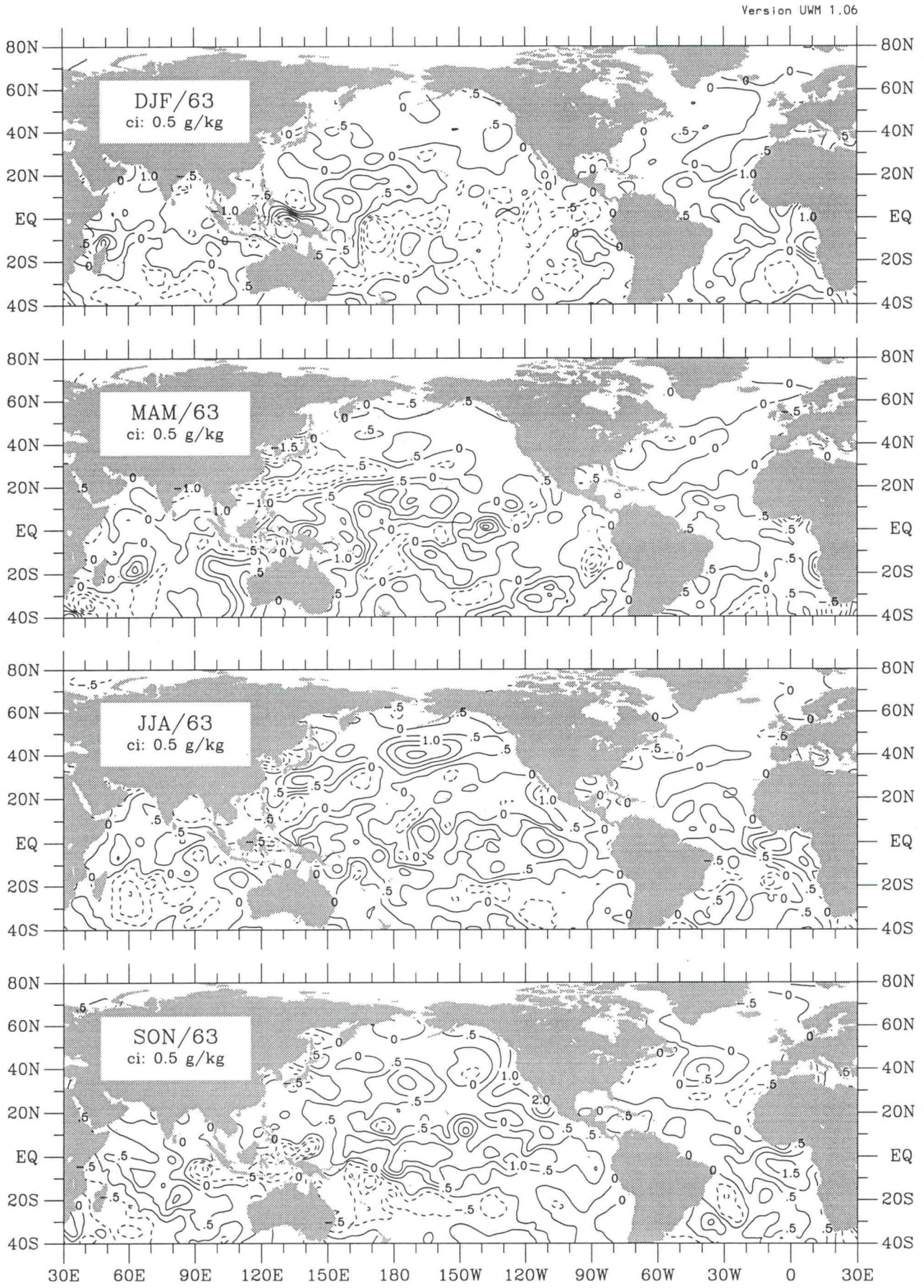

Figure qs-24. Sea level humidity seasonal anomaly for 1963.

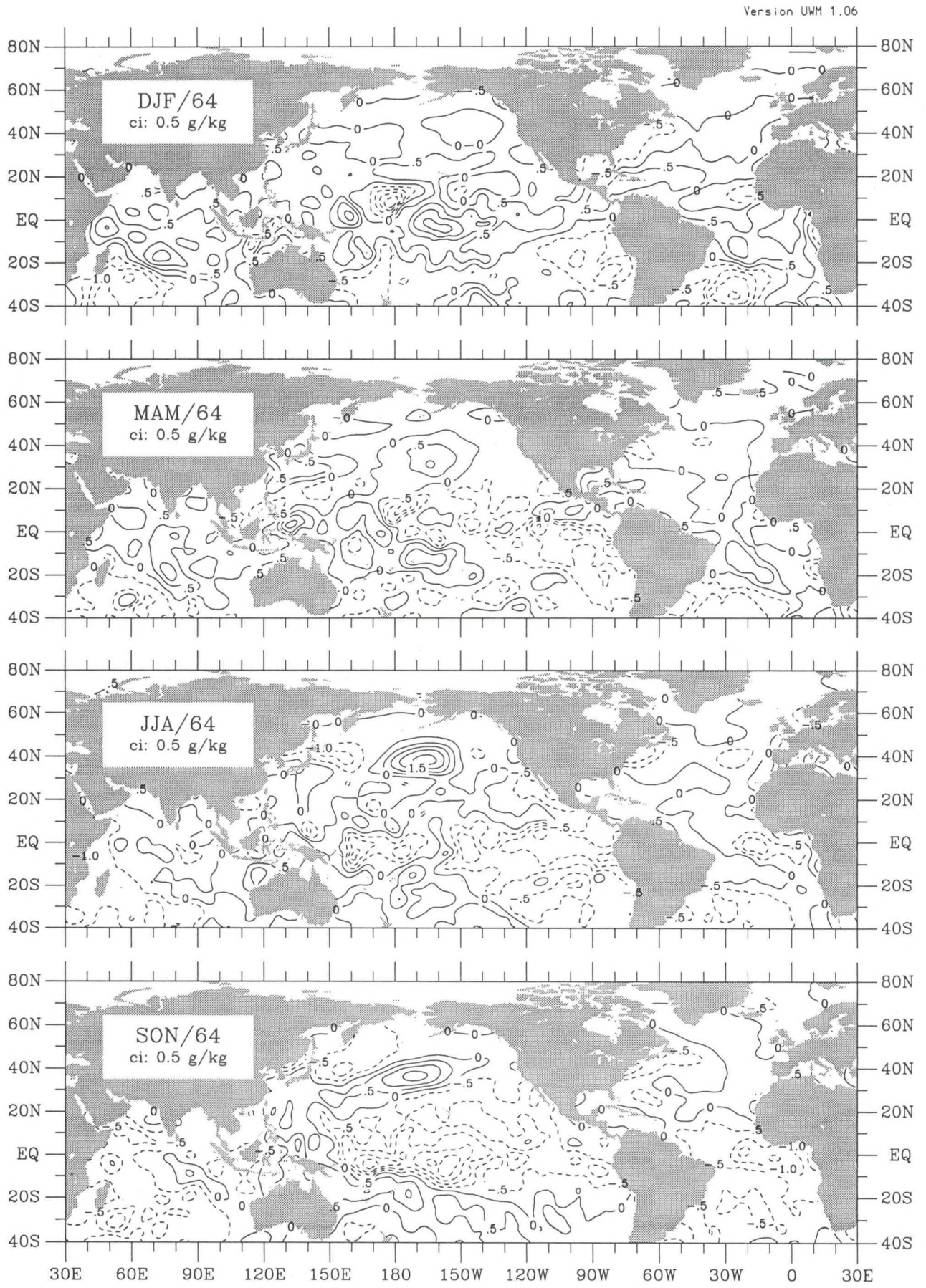

Figure qs-25. Sea level humidity seasonal anomaly for 1964.

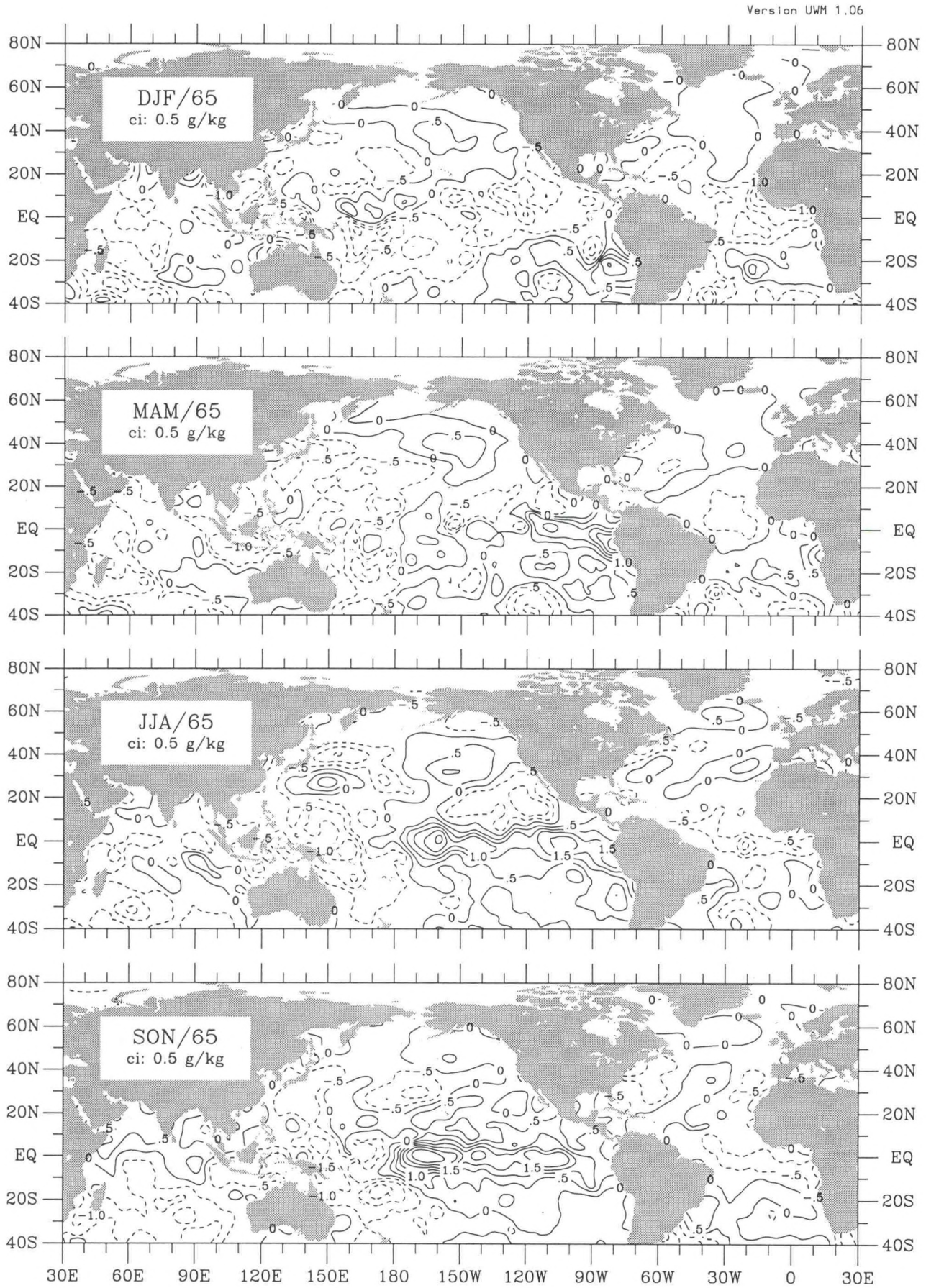

Figure qs-26. Sea level humidity seasonal anomaly for 1965.

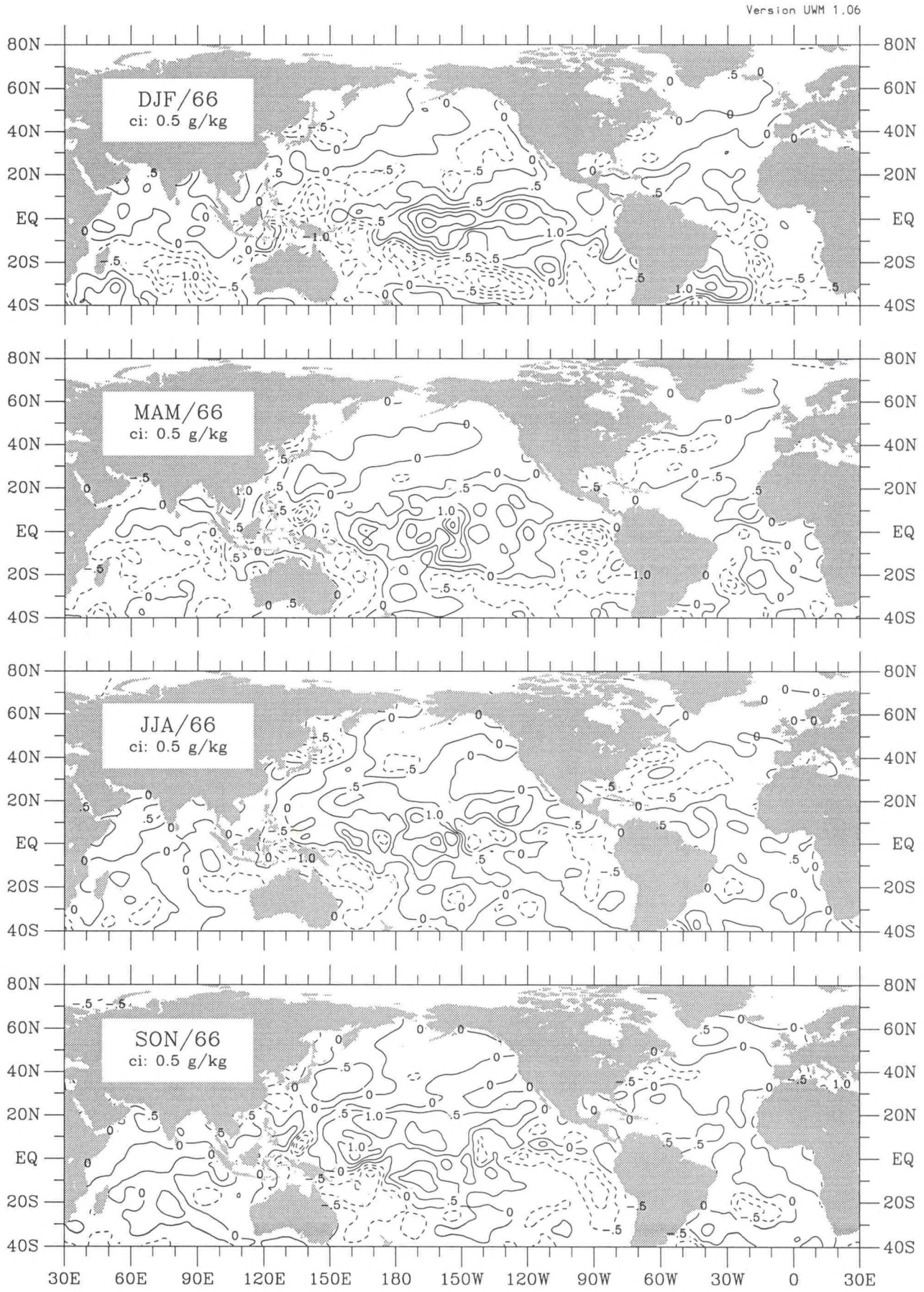

Figure qs-27. Sea level humidity seasonal anomaly for 1966.

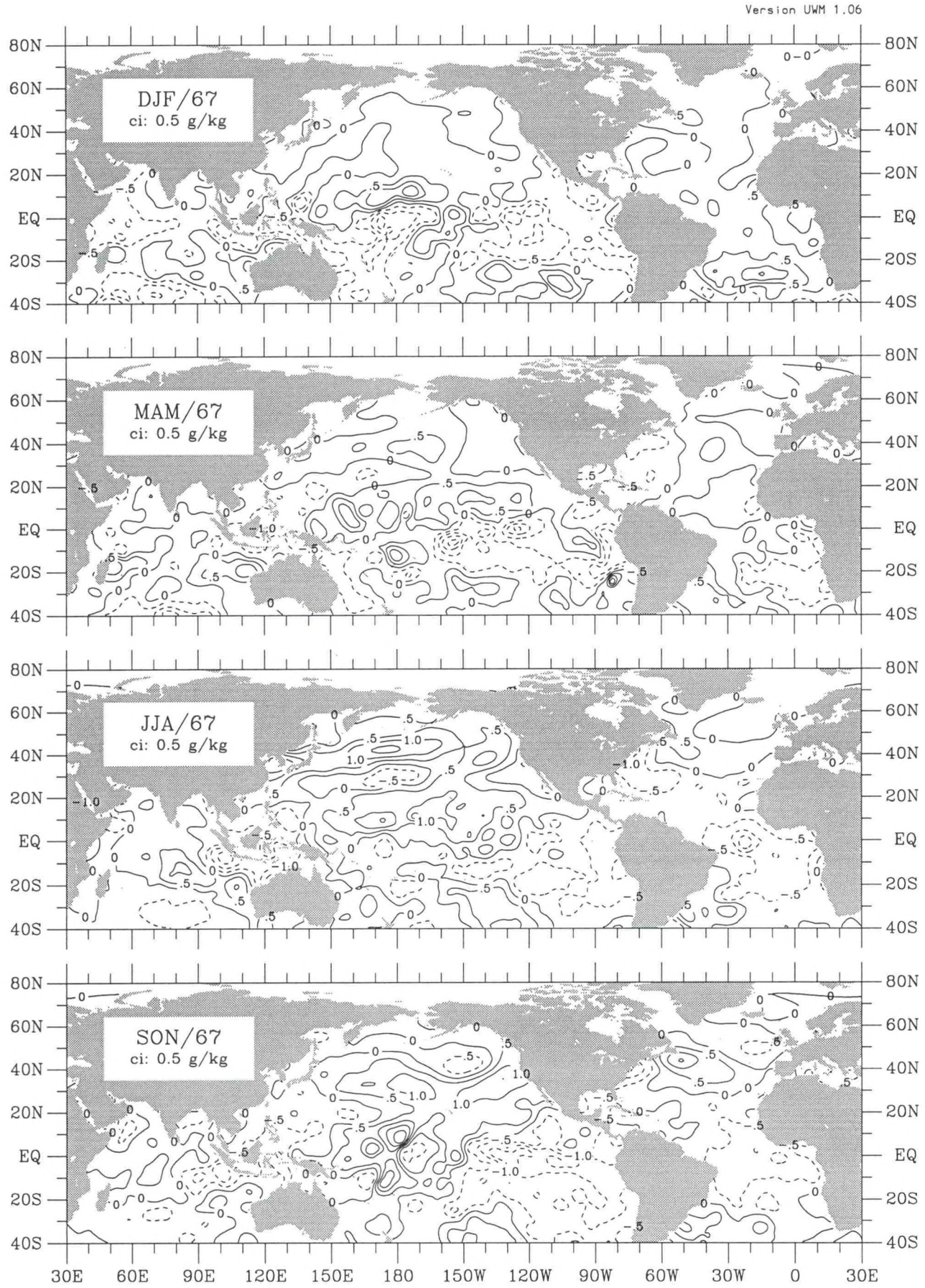

Figure qs-28. Sea level humidity seasonal anomaly for 1967.

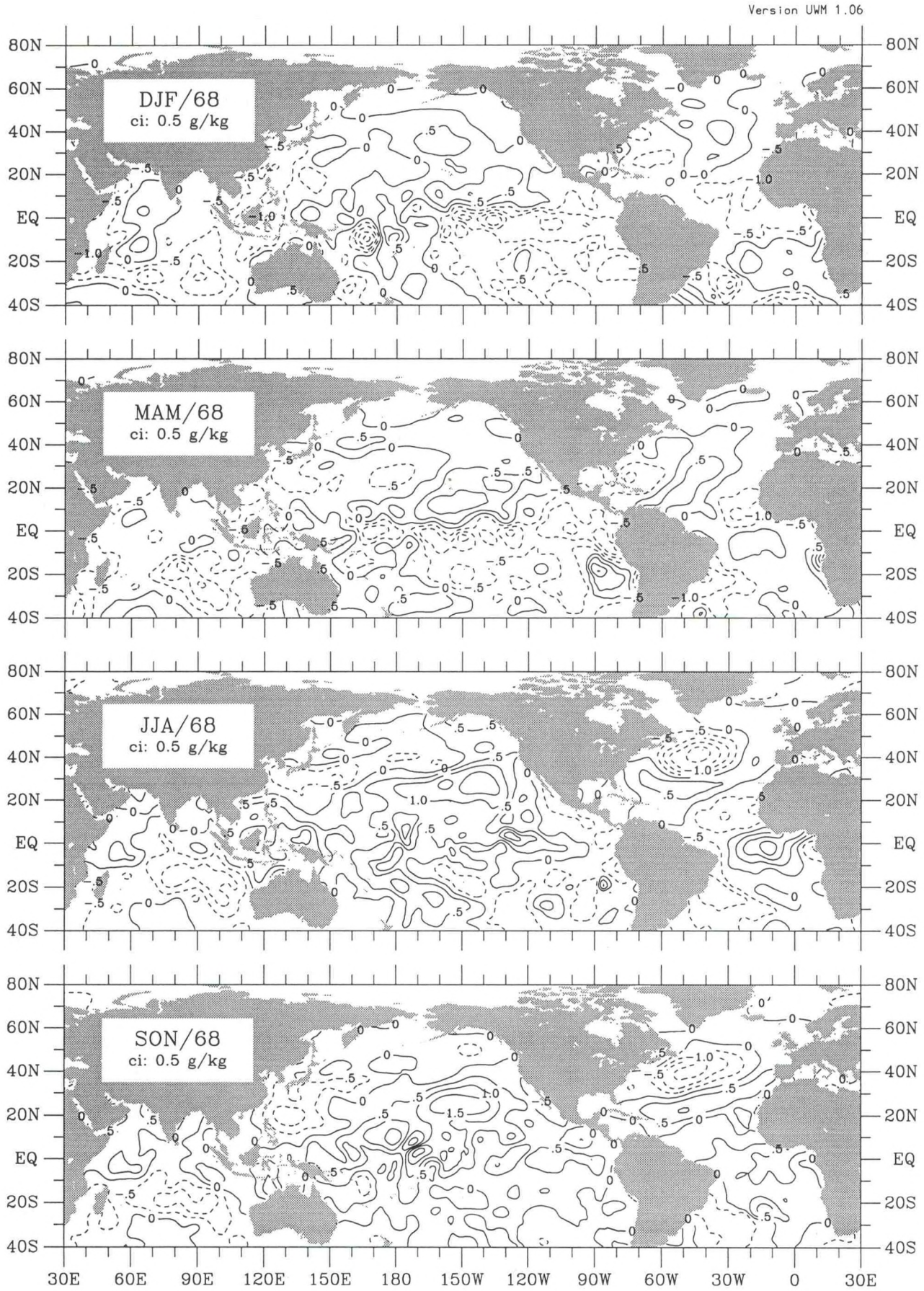

Figure qs-29. Sea level humidity seasonal anomaly for 1968.

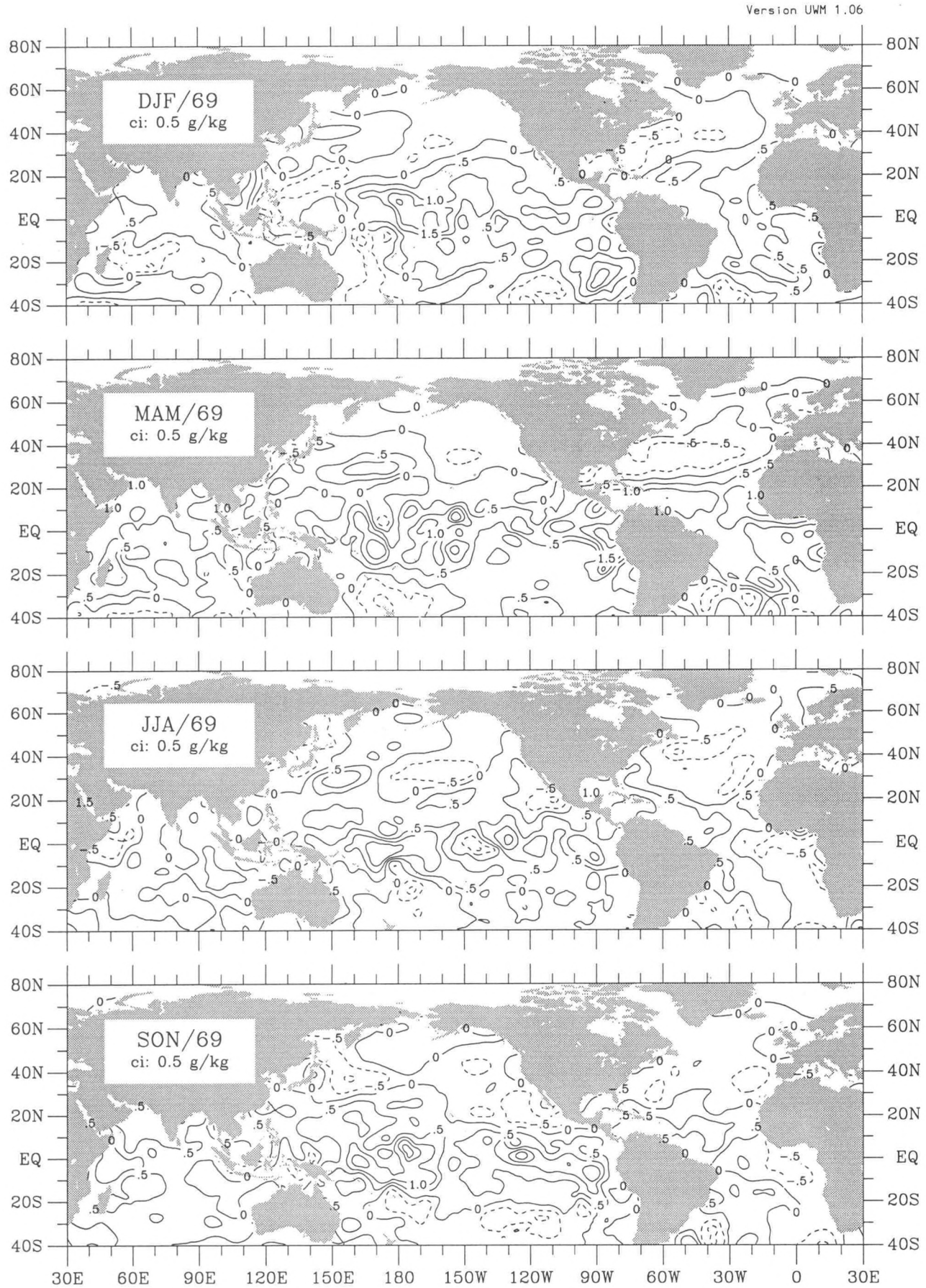

Figure qs-30. Sea level humidity seasonal anomaly for 1969.

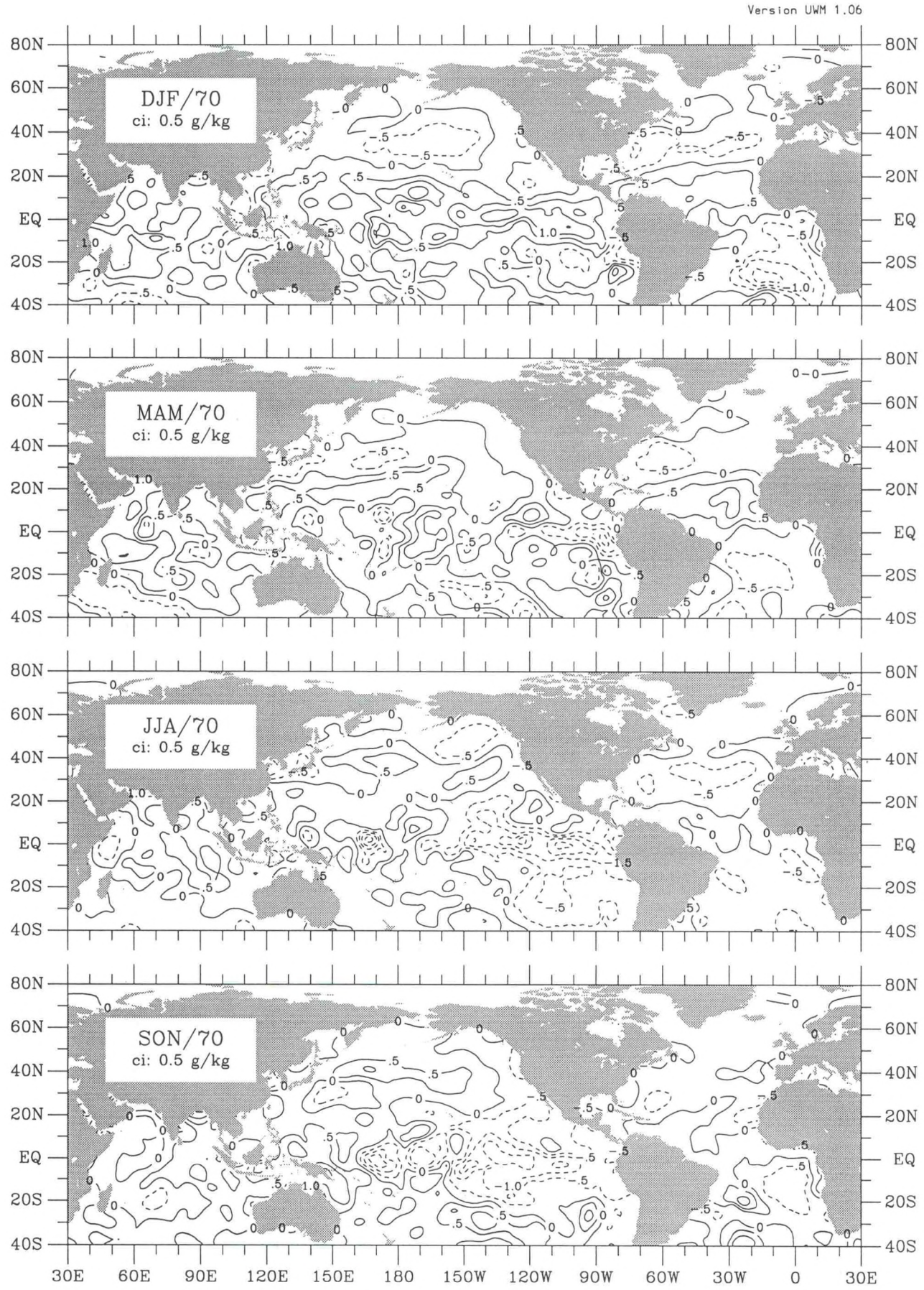

Figure qs-31. Sea level humidity seasonal anomaly for 1970.

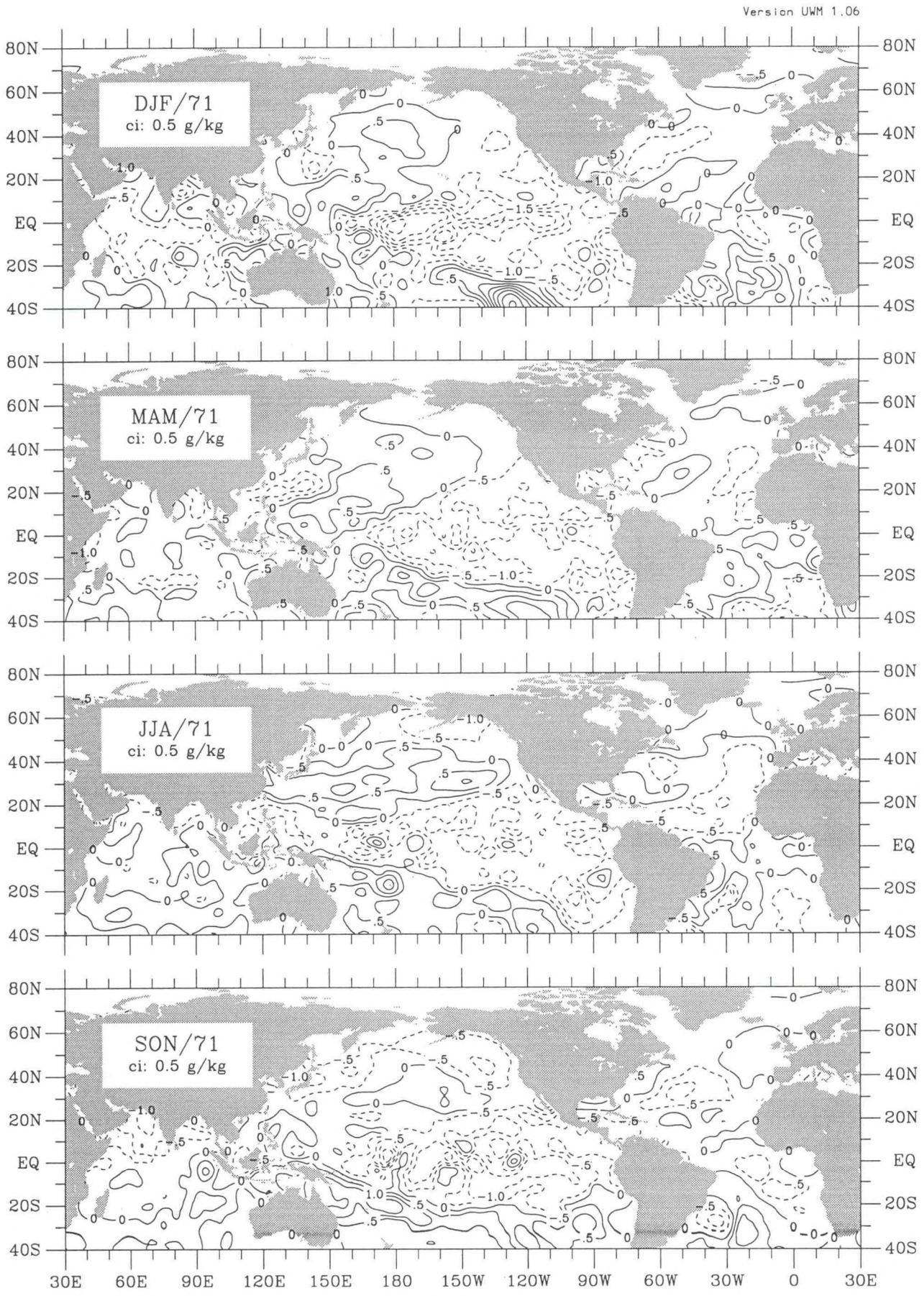

Figure qs-32. Sea level humidity seasonal anomaly for 1971.

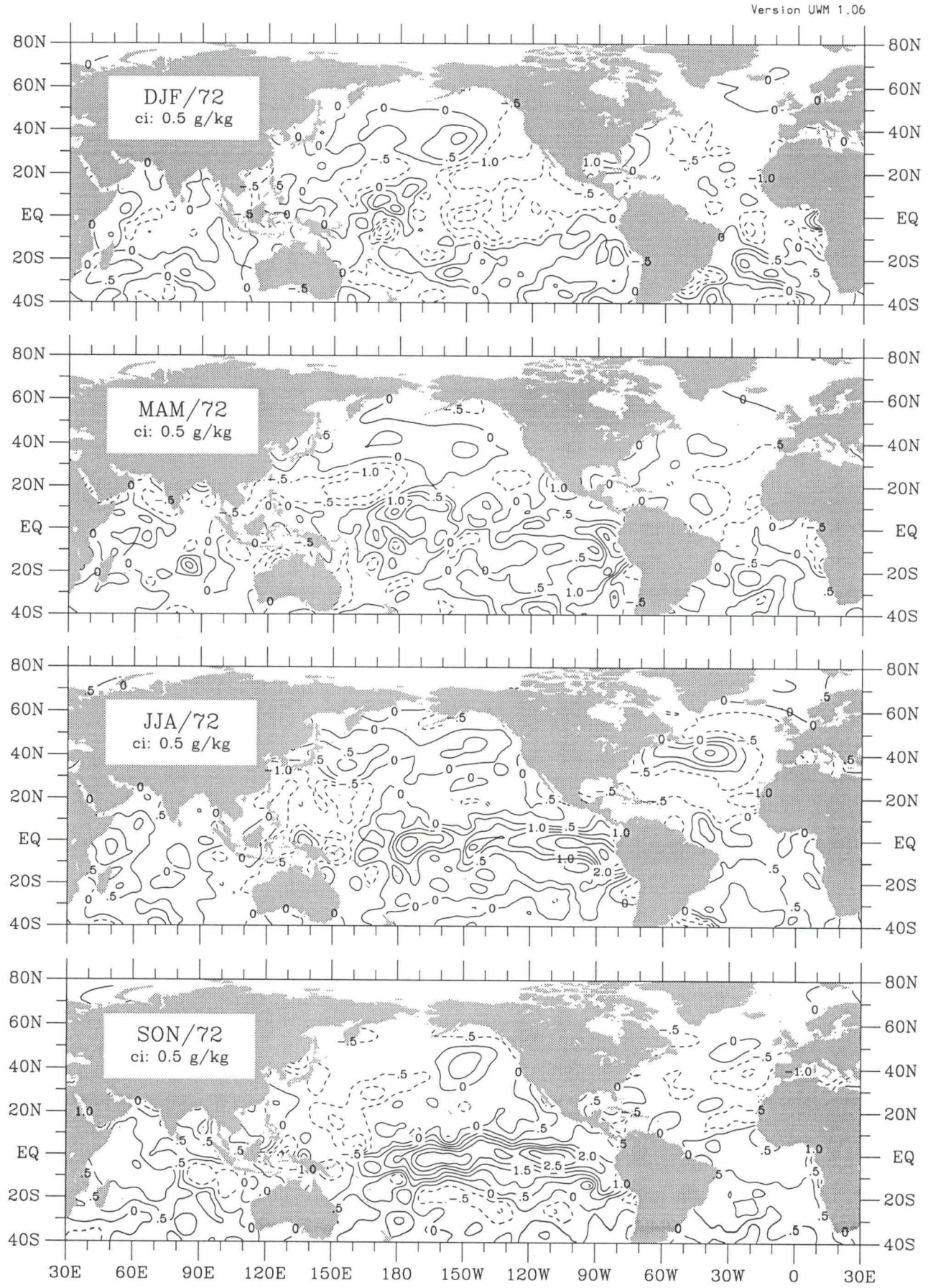

Figure qs-33. Sea level humidity seasonal anomaly for 1972.

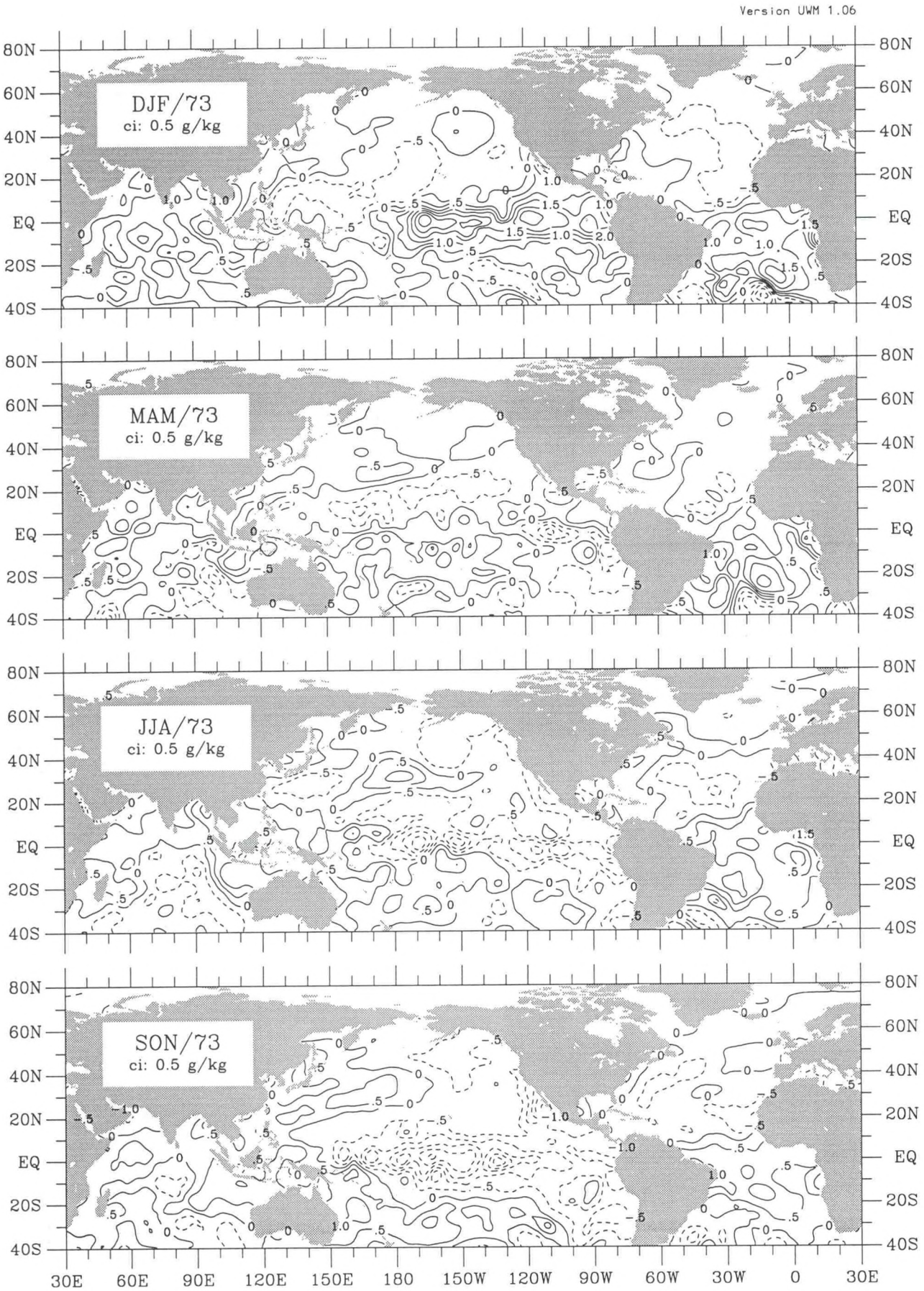

Figure qs-34. Sea level humidity seasonal anomaly for 1973.

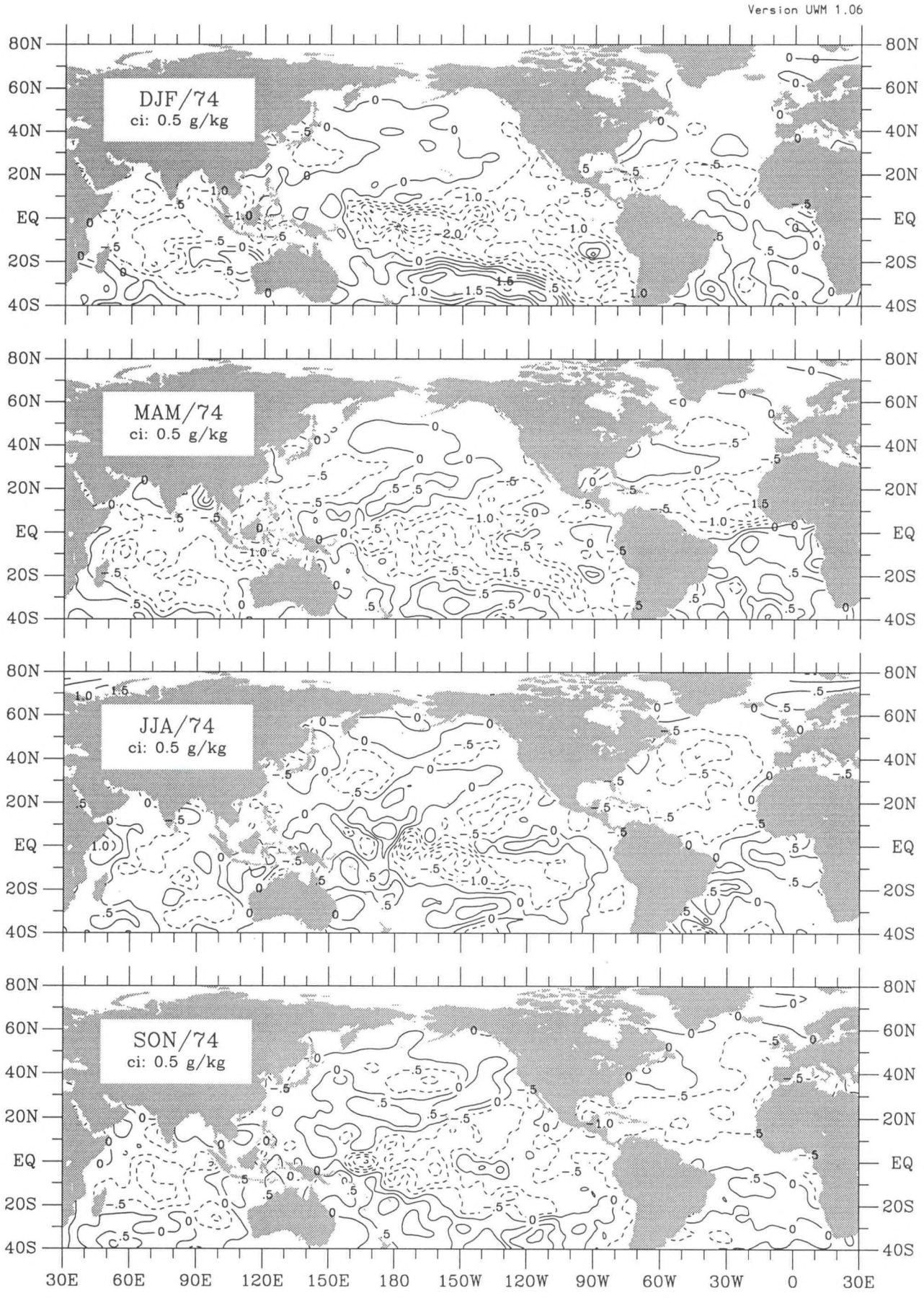

Figure qs–35. Sea level humidity seasonal anomaly for 1974.

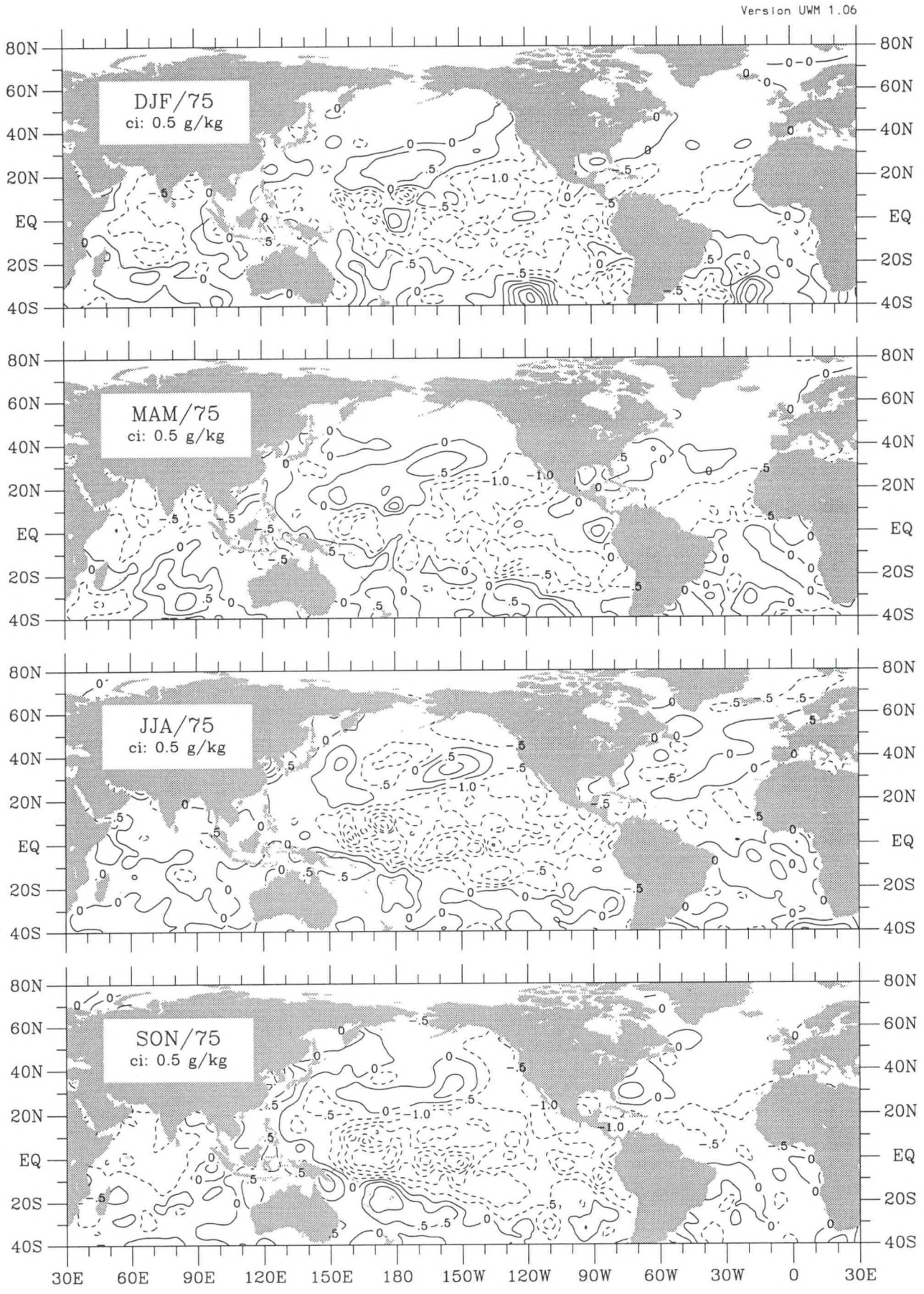

Figure qs-36. Sea level humidity seasonal anomaly for 1975.

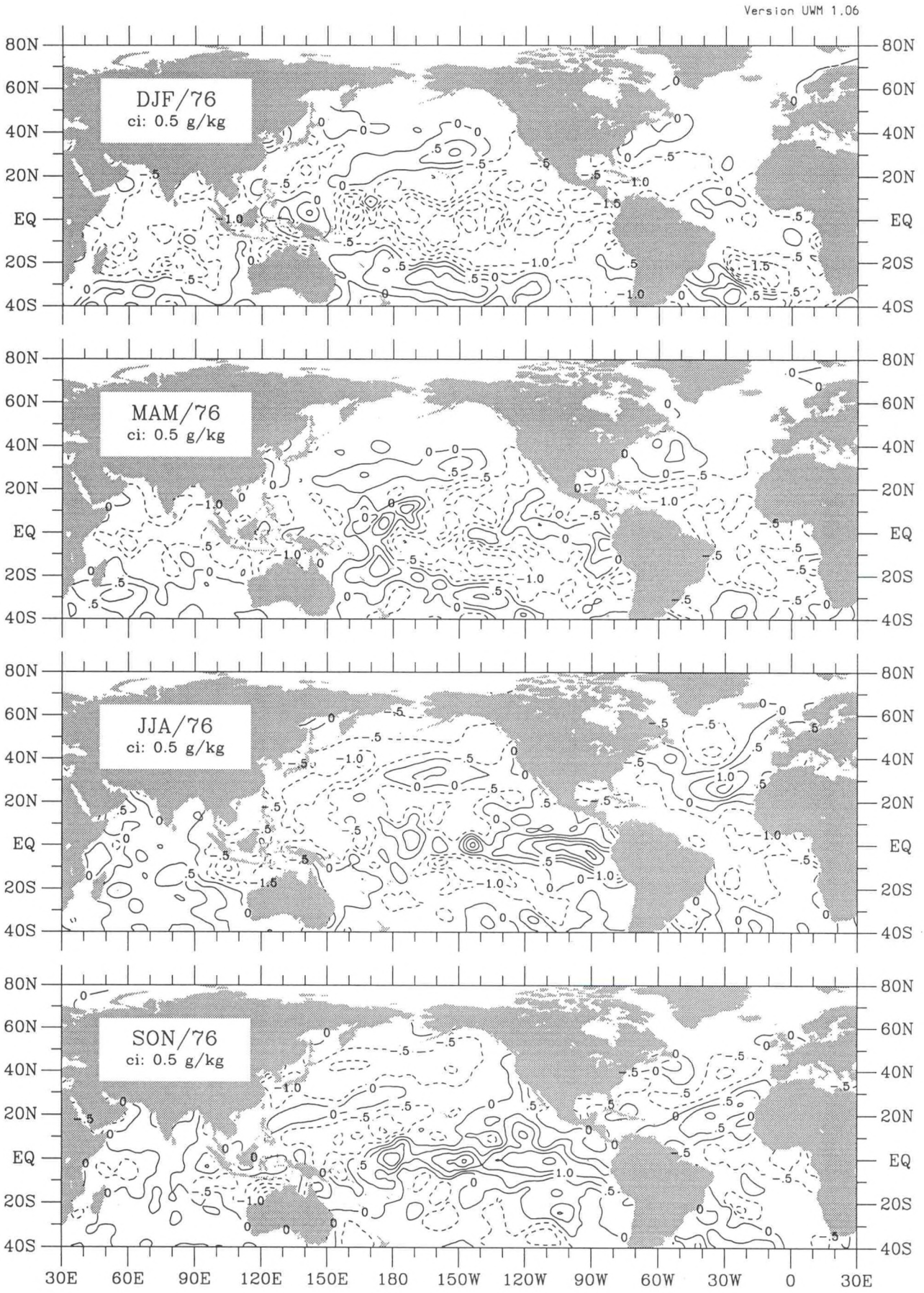

Figure qs-37. Sea level humidity seasonal anomaly for 1976.

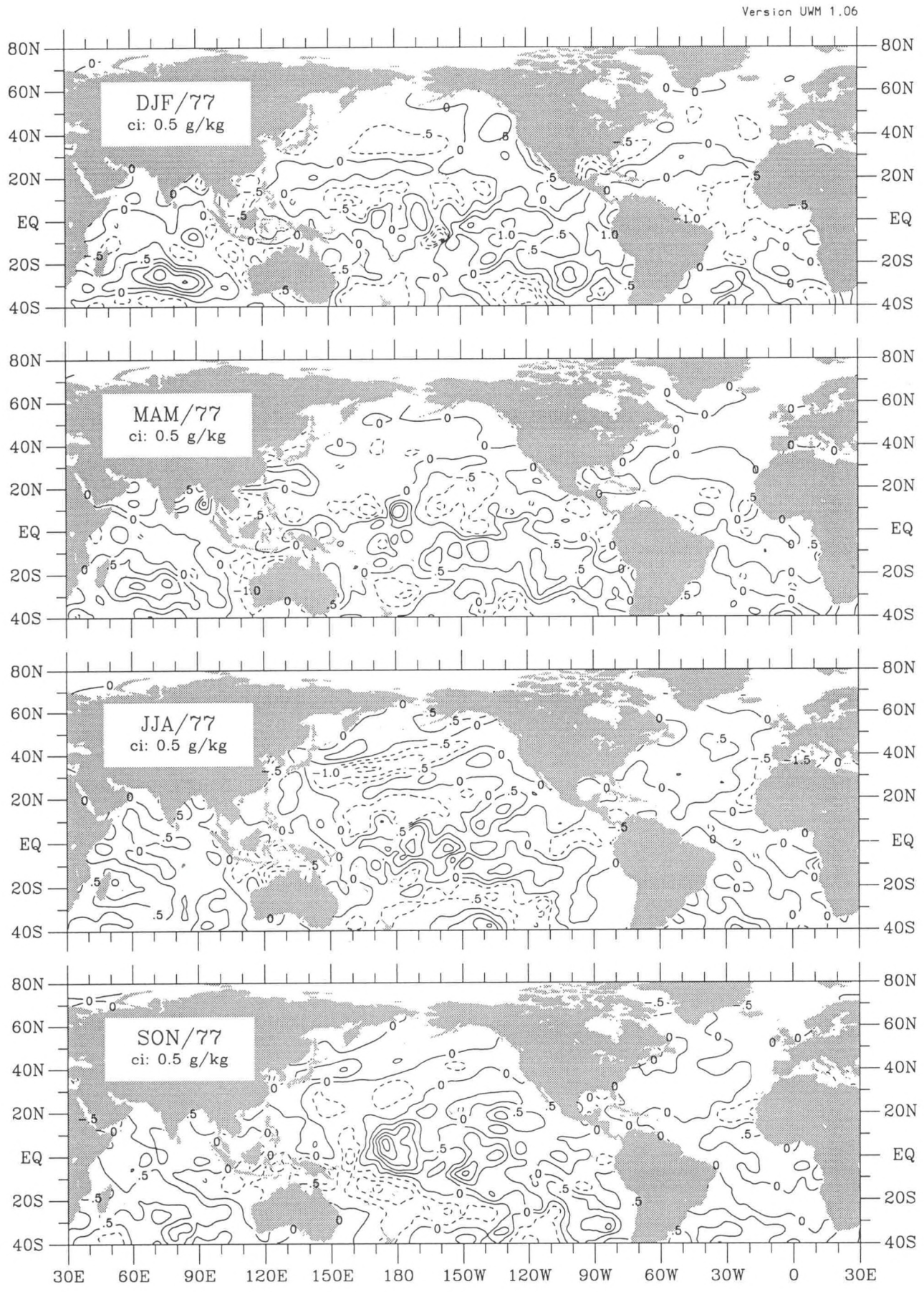

Figure qs-38. Sea level humidity seasonal anomaly for 1977.

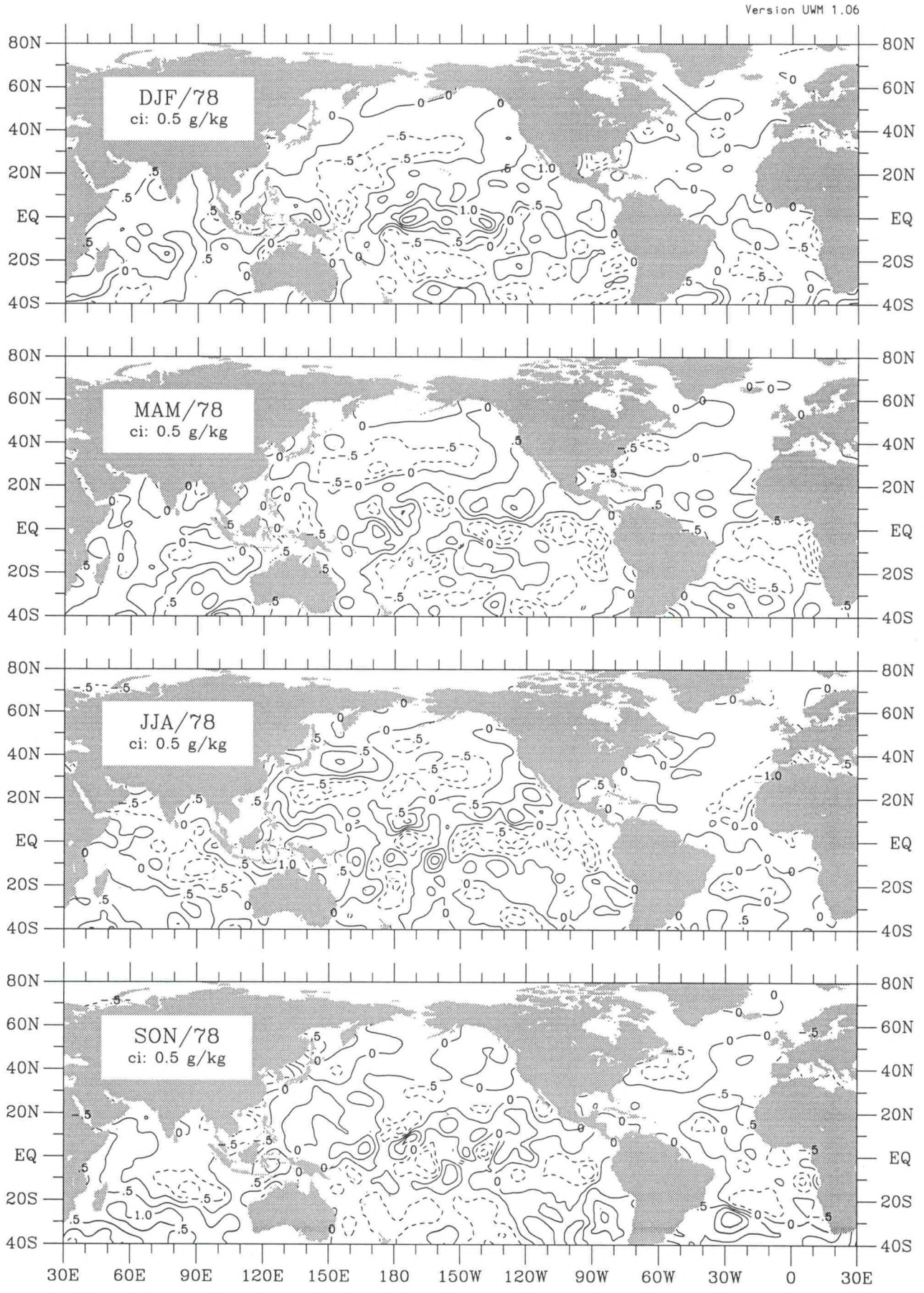

Figure qs-39. Sea level humidity seasonal anomaly for 1978.

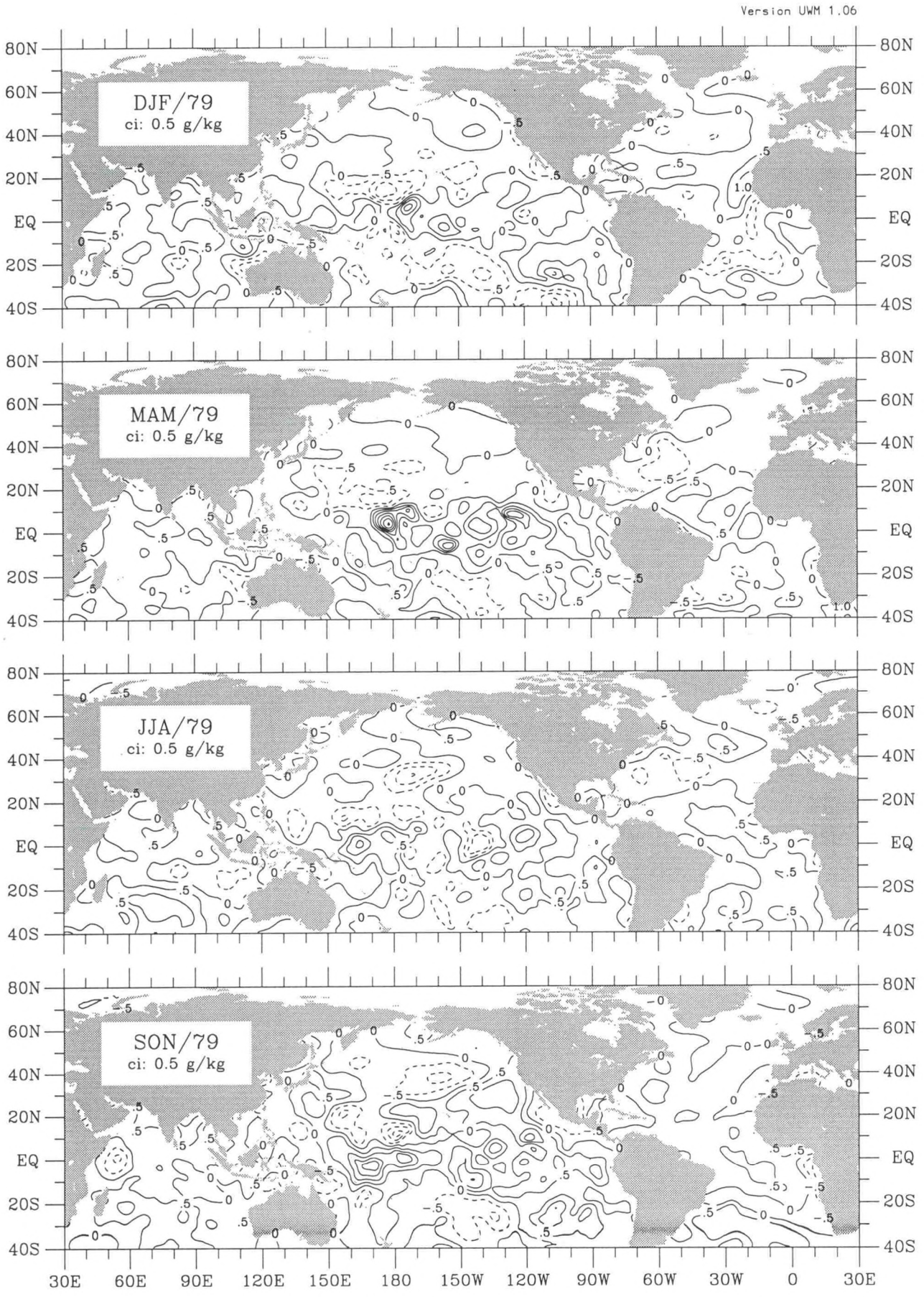

Figure qs-40. Sea level humidity seasonal anomaly for 1979.

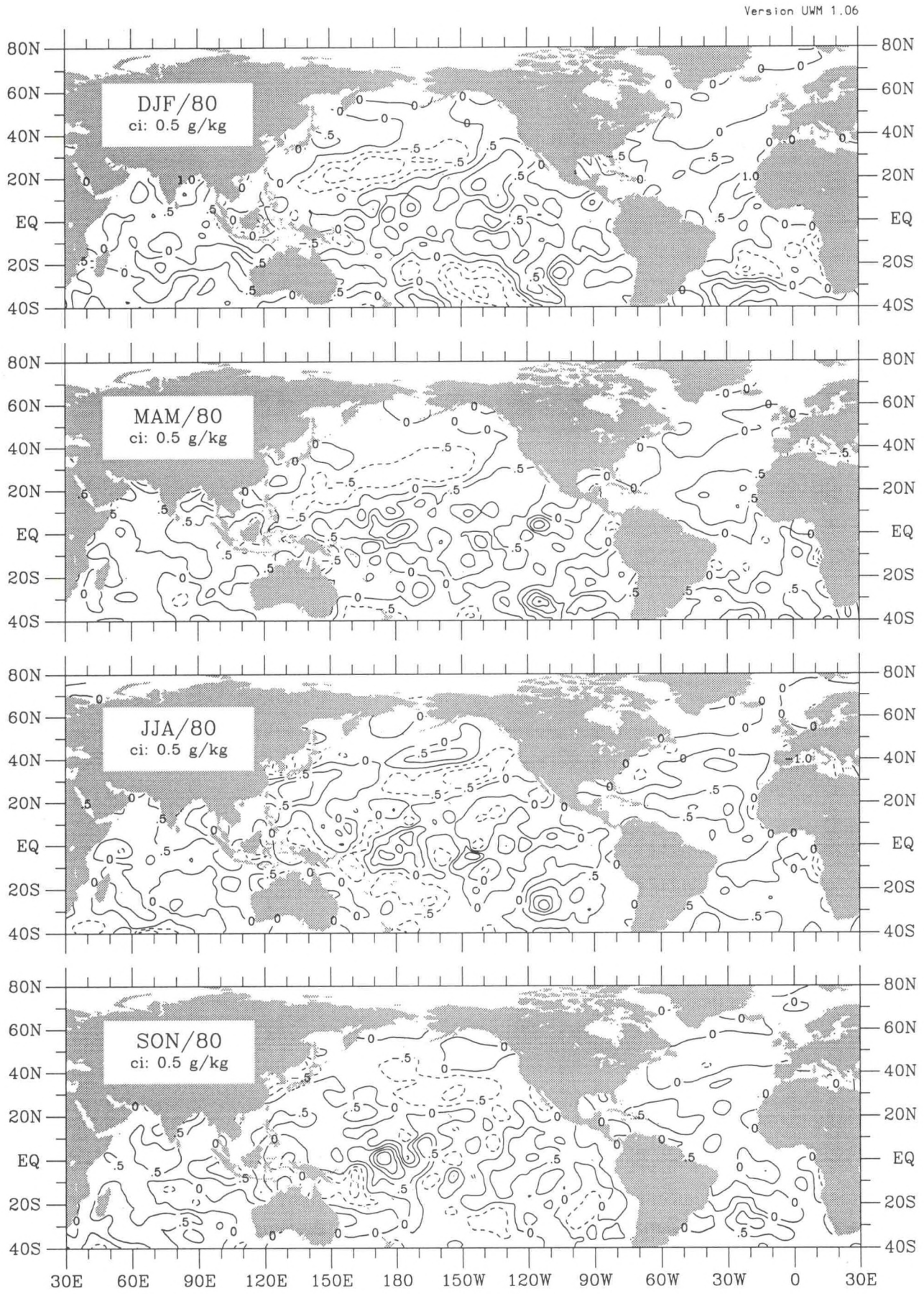

Figure qs-41. Sea level humidity seasonal anomaly for 1980.

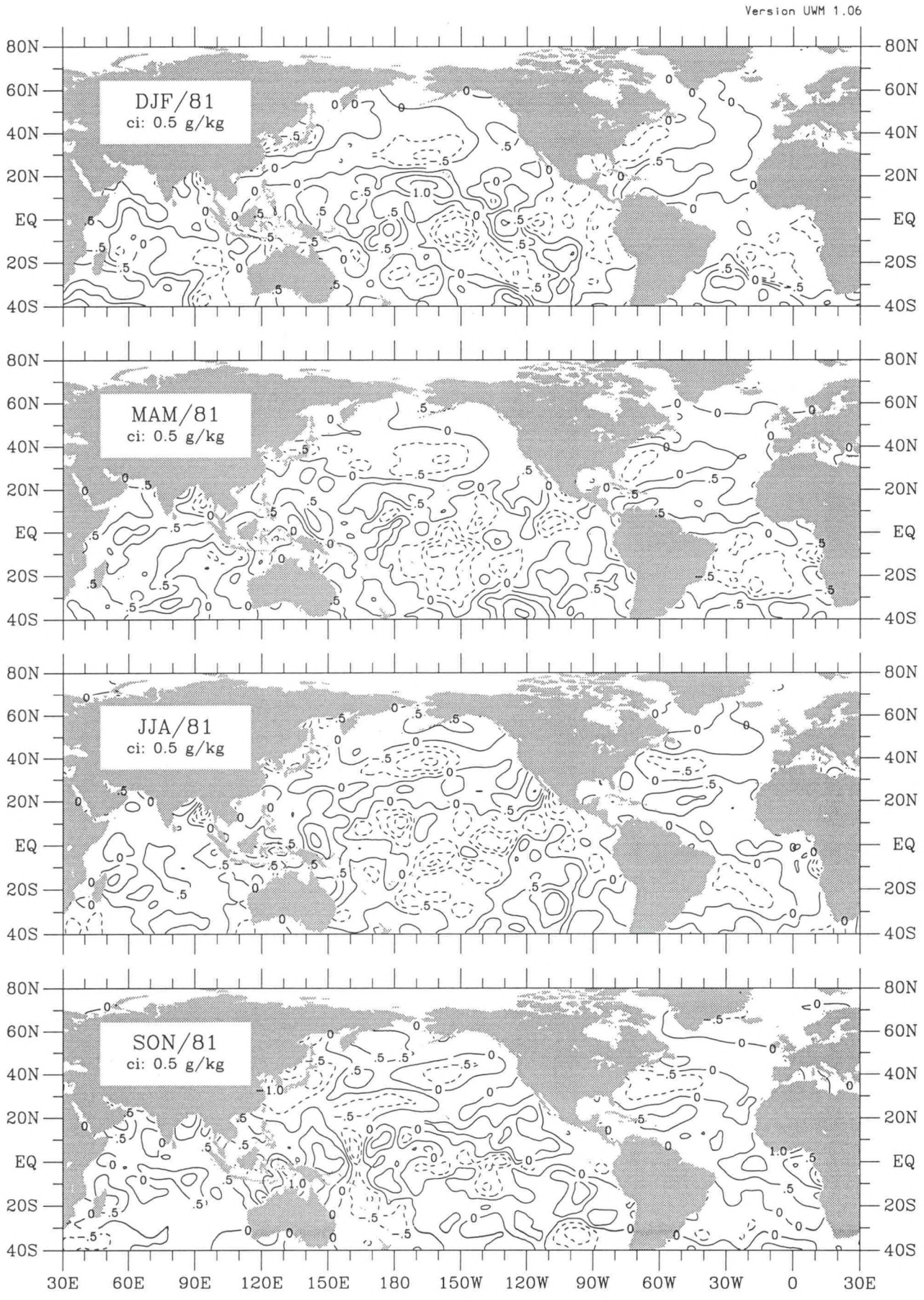

Figure qs-42. Sea level humidity seasonal anomaly for 1981.

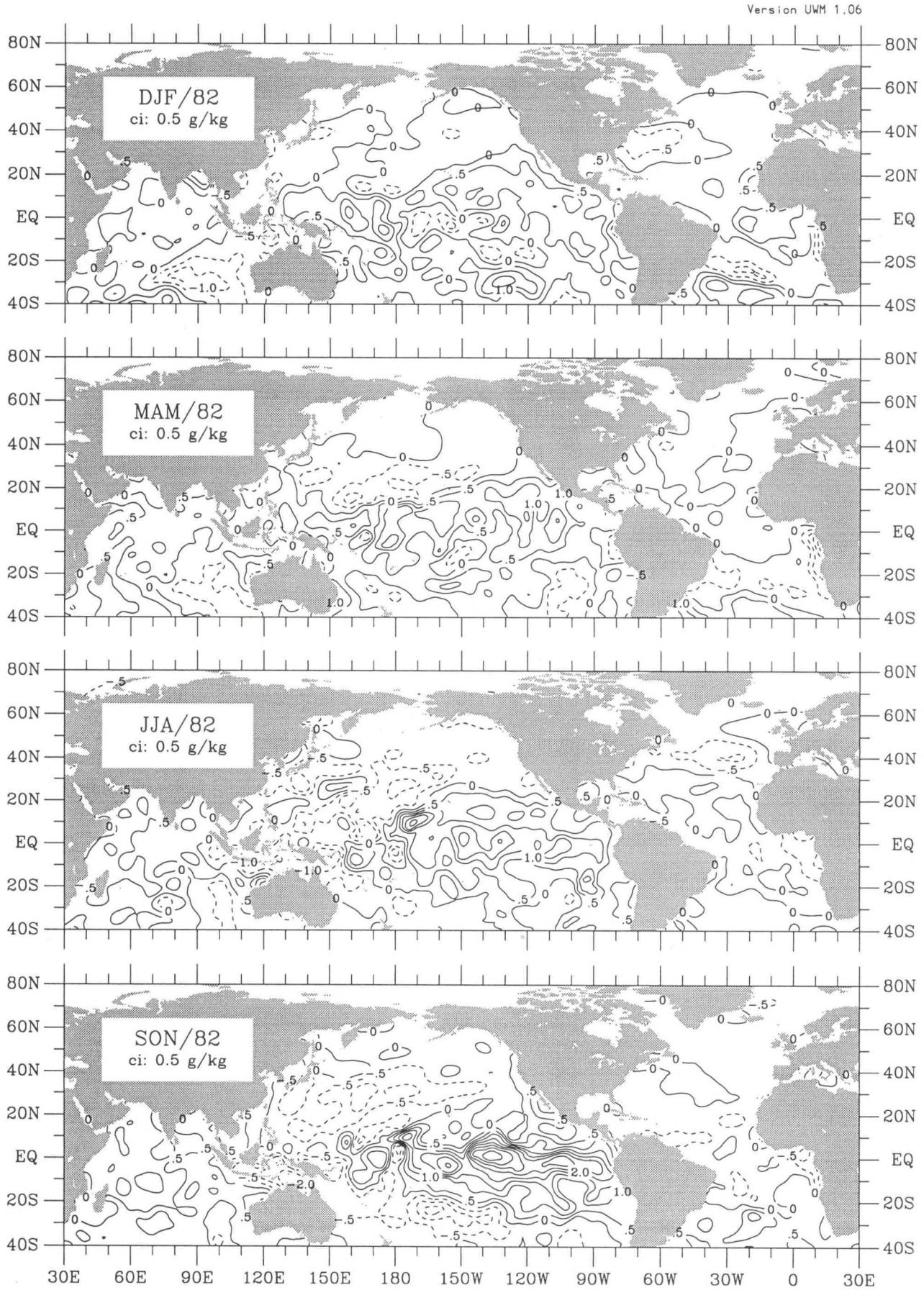

Figure qs-43. Sea level humidity seasonal anomaly for 1982.

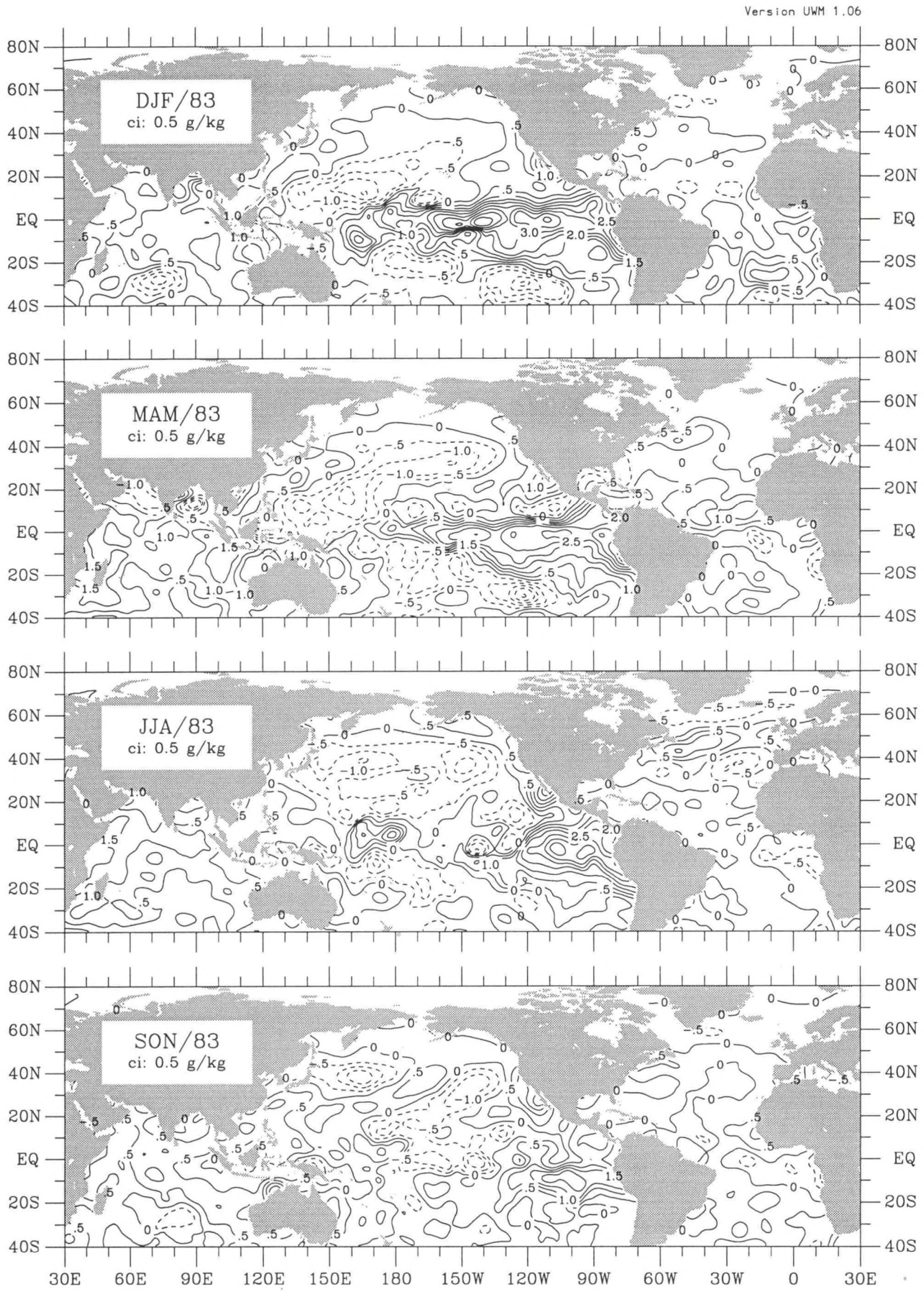

Figure qs-44. Sea level humidity seasonal anomaly for 1983.

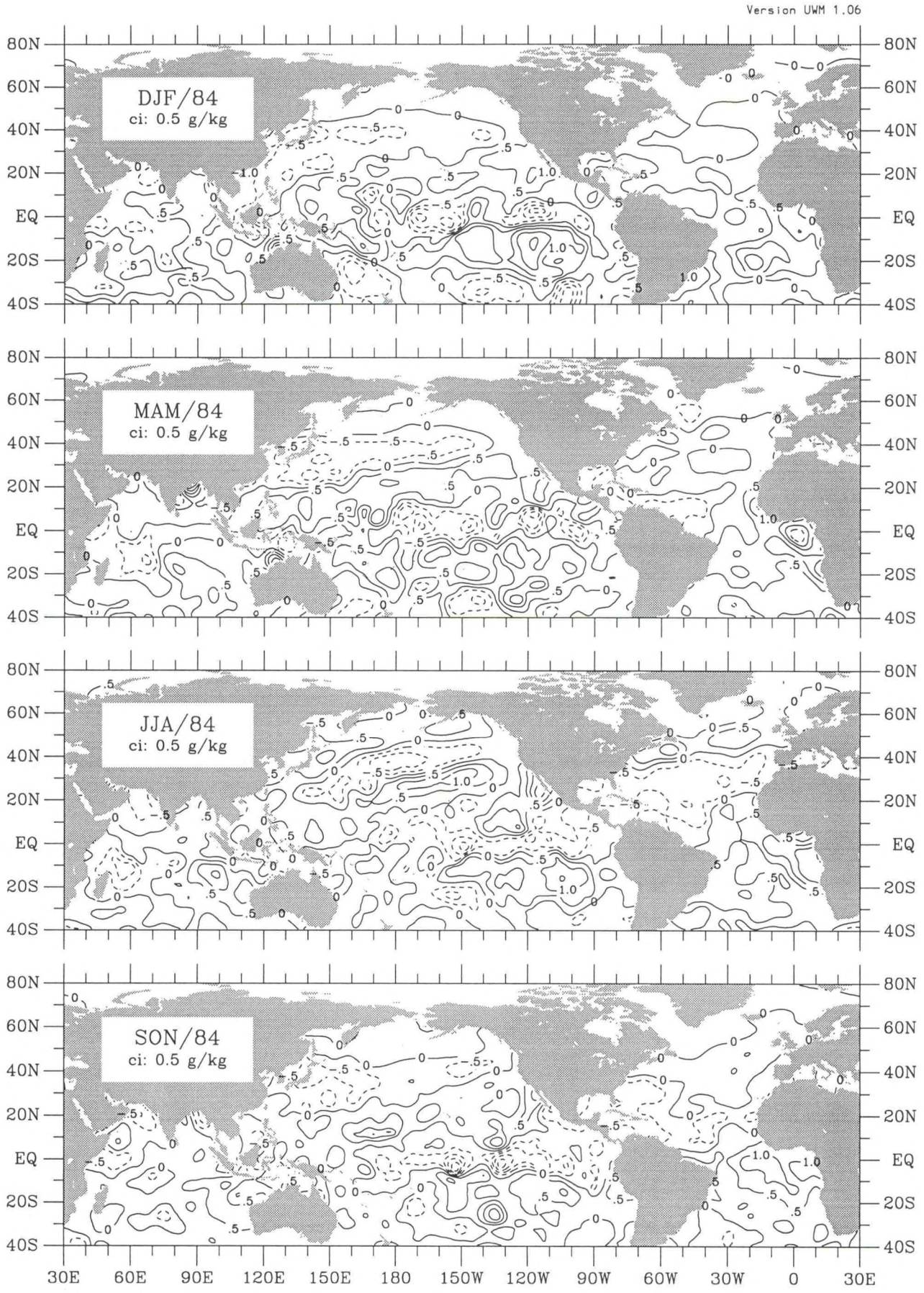

Figure qs-45. Sea level humidity seasonal anomaly for 1984.

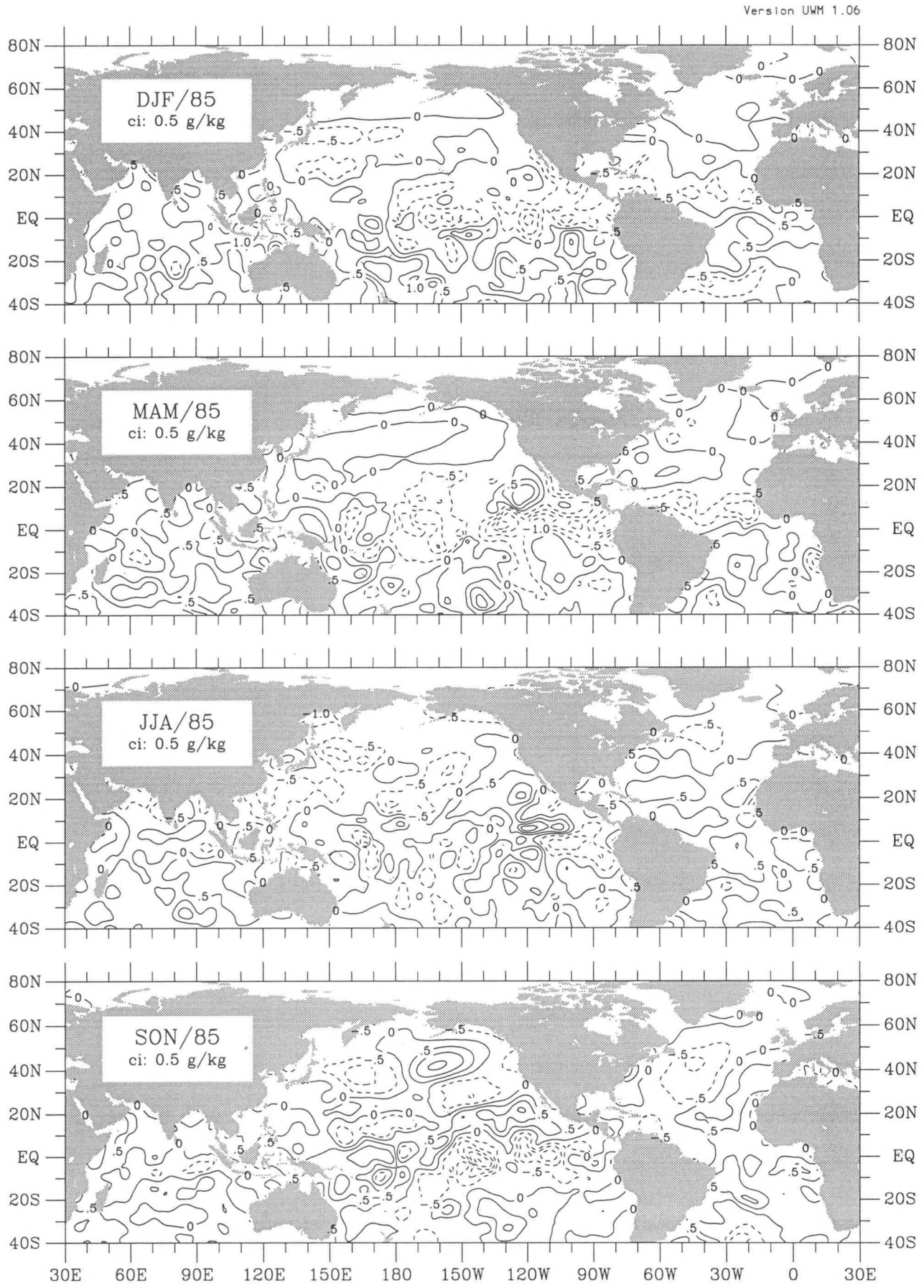

Figure qs-46. Sea level humidity seasonal anomaly for 1985.

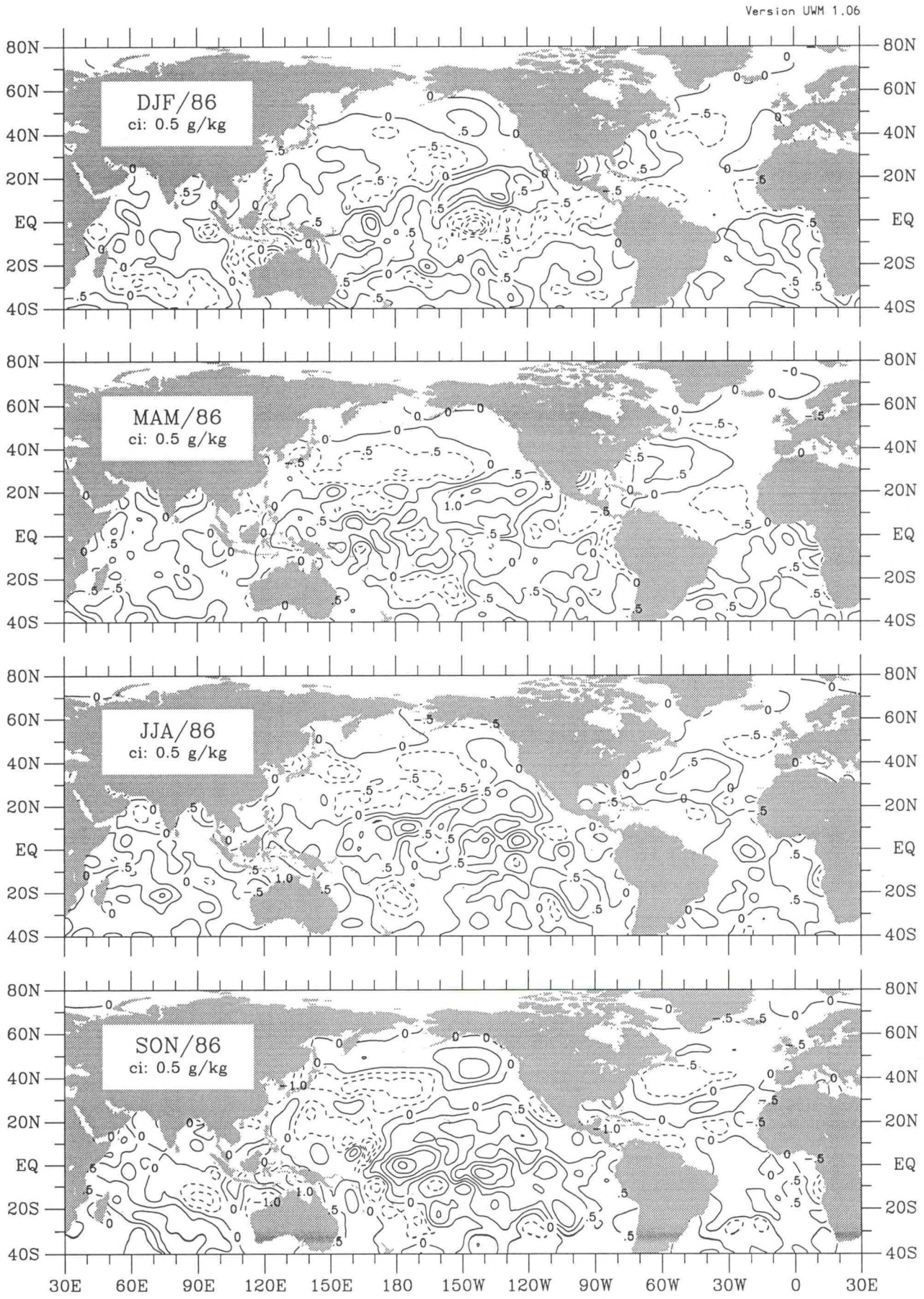

Figure qs-47. Sea level humidity seasonal anomaly for 1986.

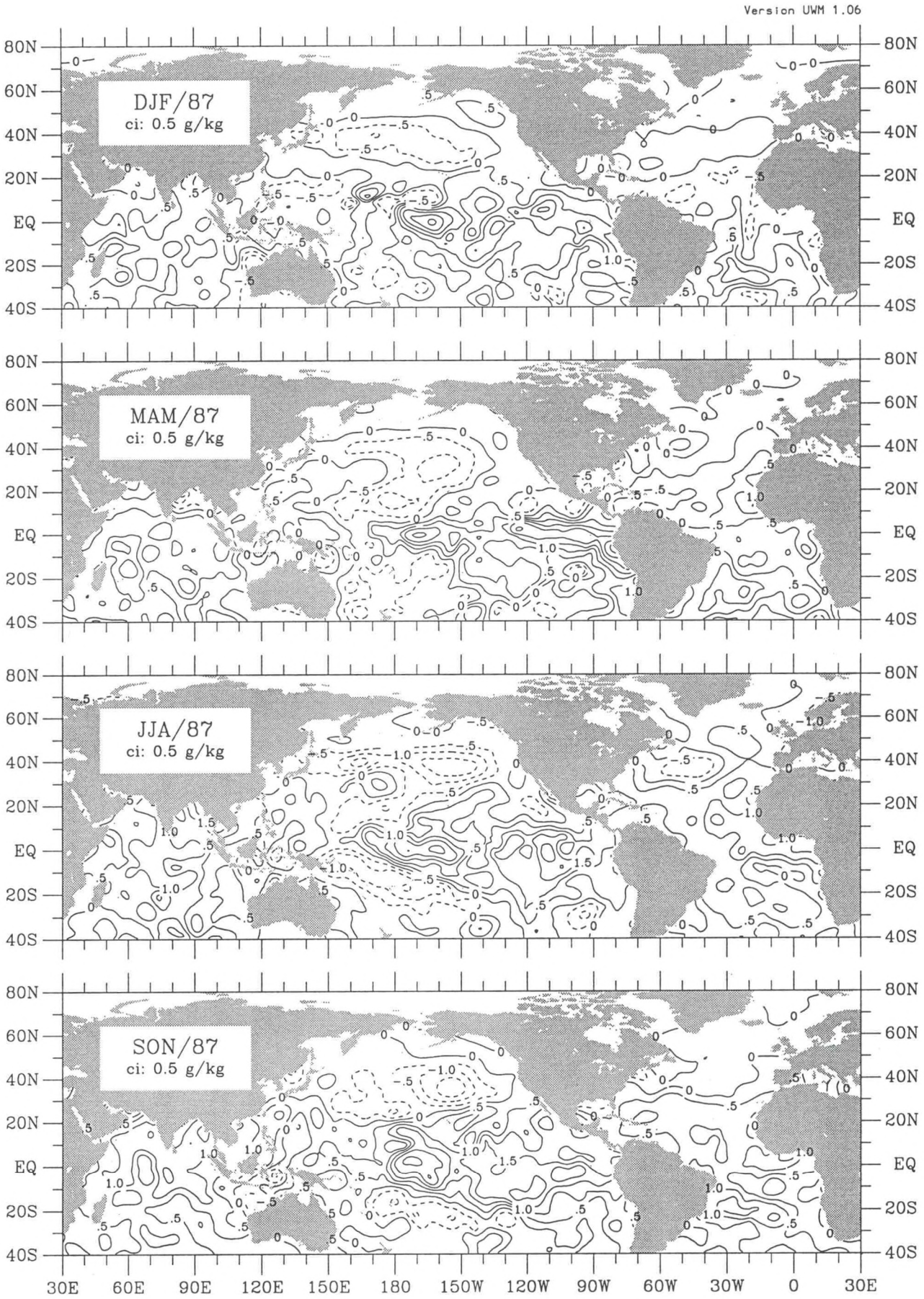

Figure qs-48. Sea level humidity seasonal anomaly for 1987.

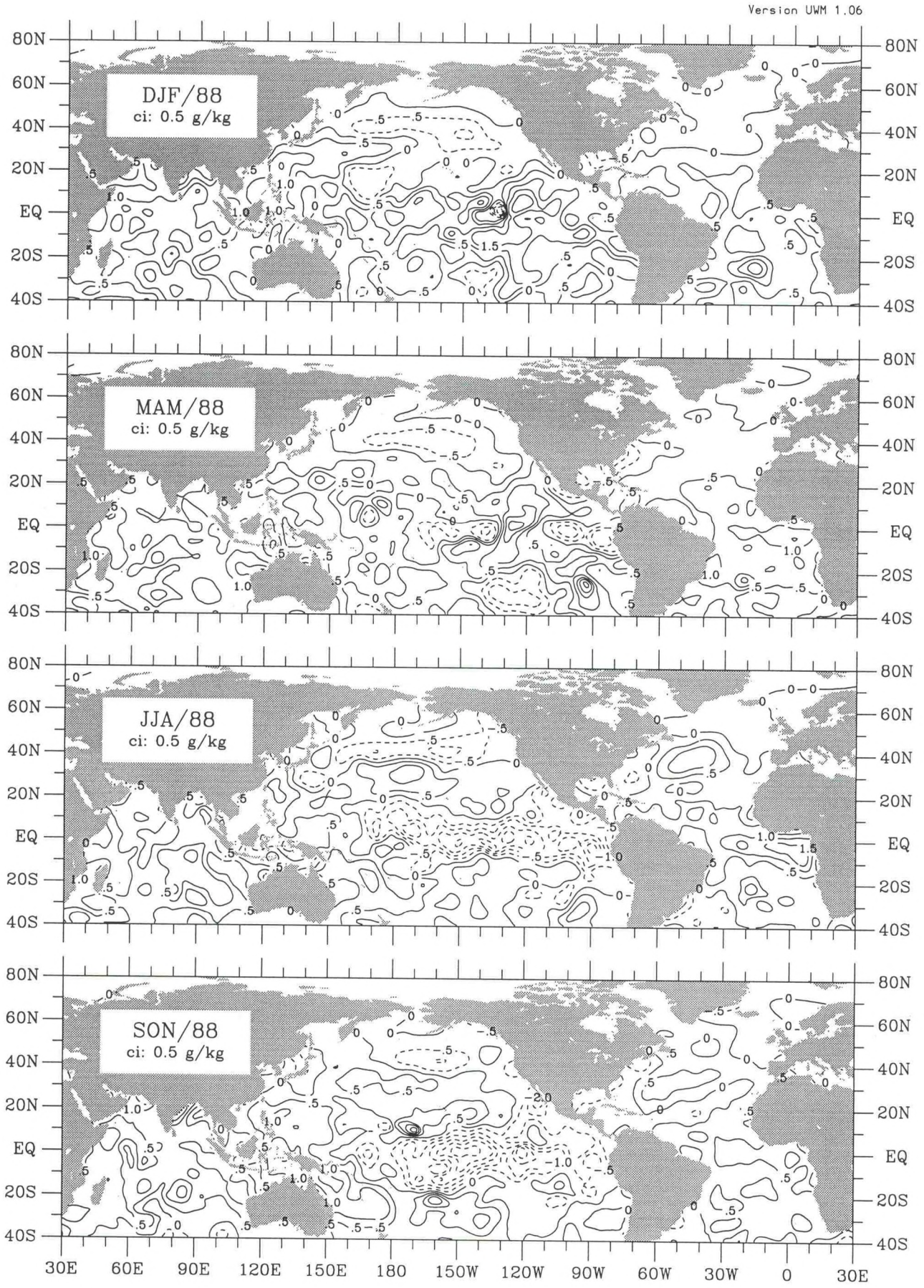

Figure qs-49. Sea level humidity seasonal anomaly for 1988.

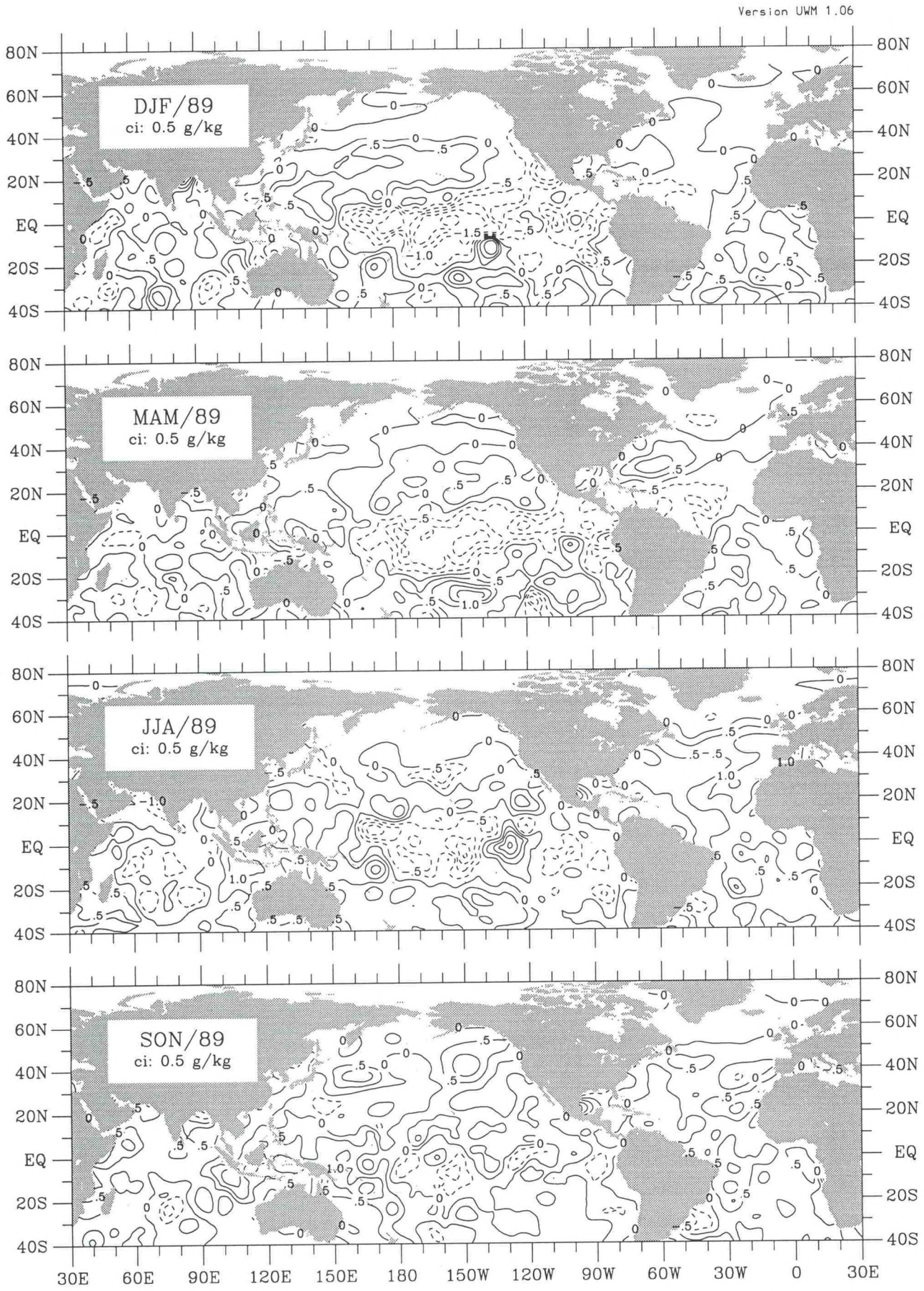

Figure qs-50. Sea level humidity seasonal anomaly for 1989.

14 Vapor pressure

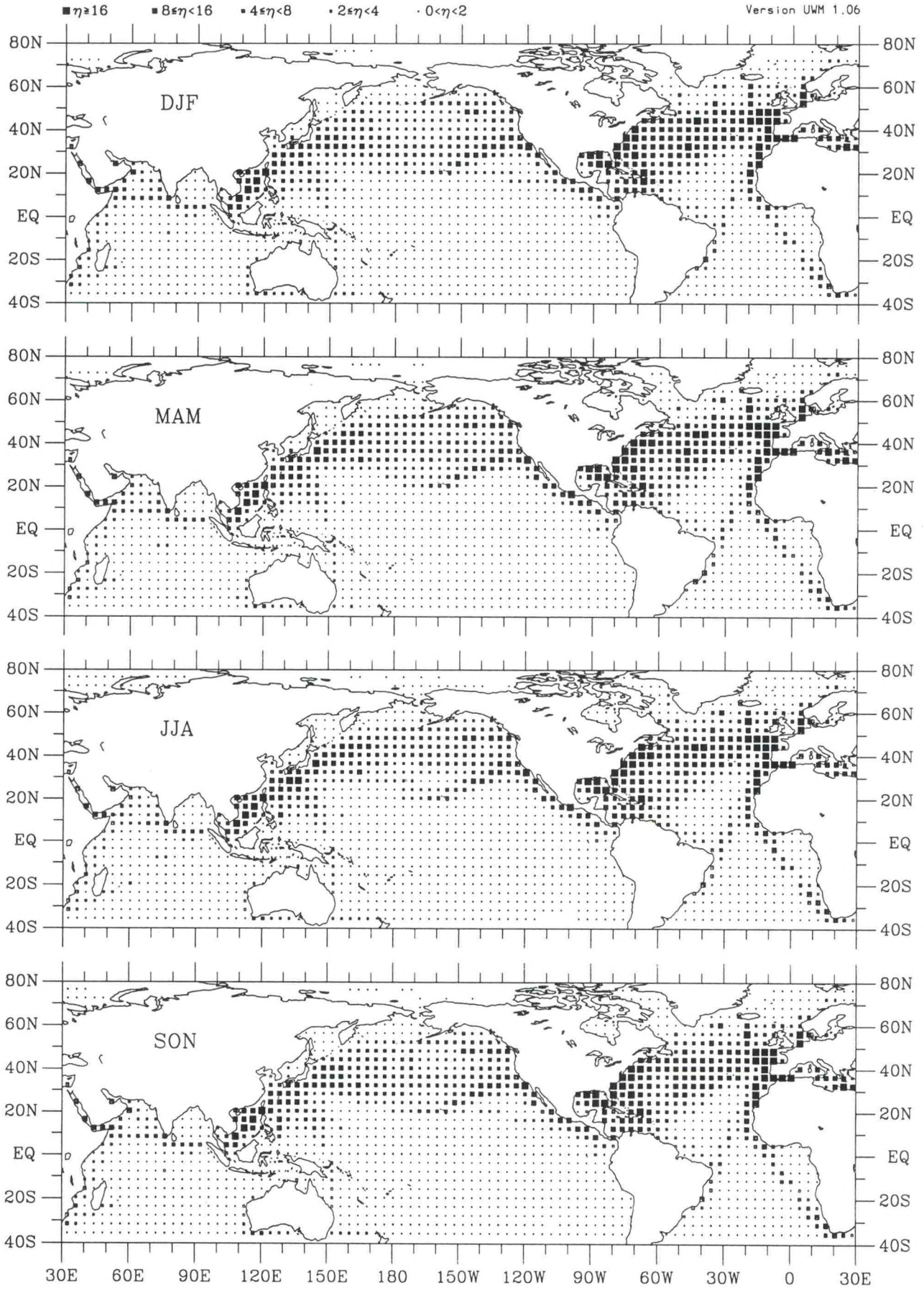

Figure e-1. Vapor pressure seasonal observation density (1945-89).

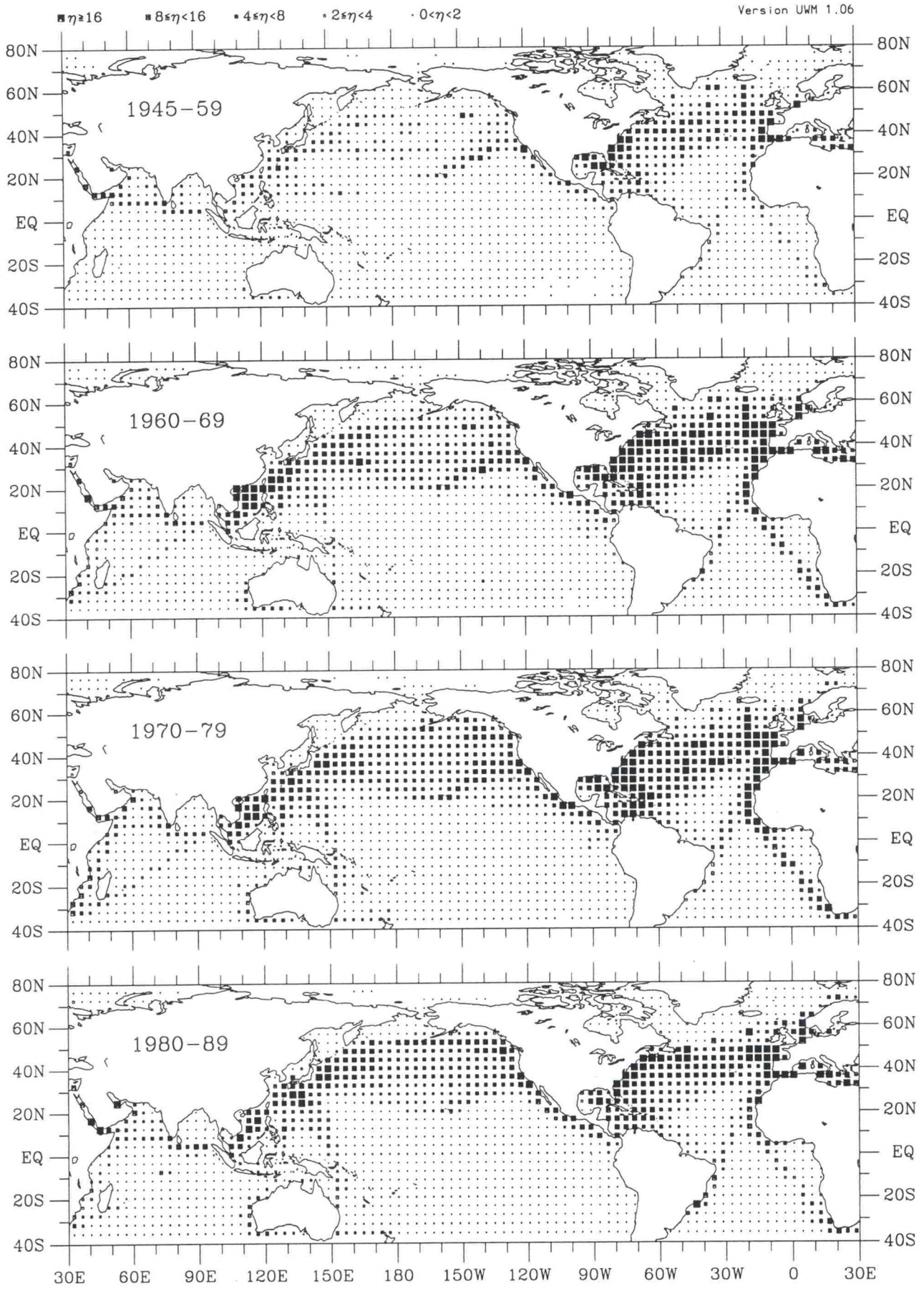

Figure e-2. Vapor pressure decadal observation density.

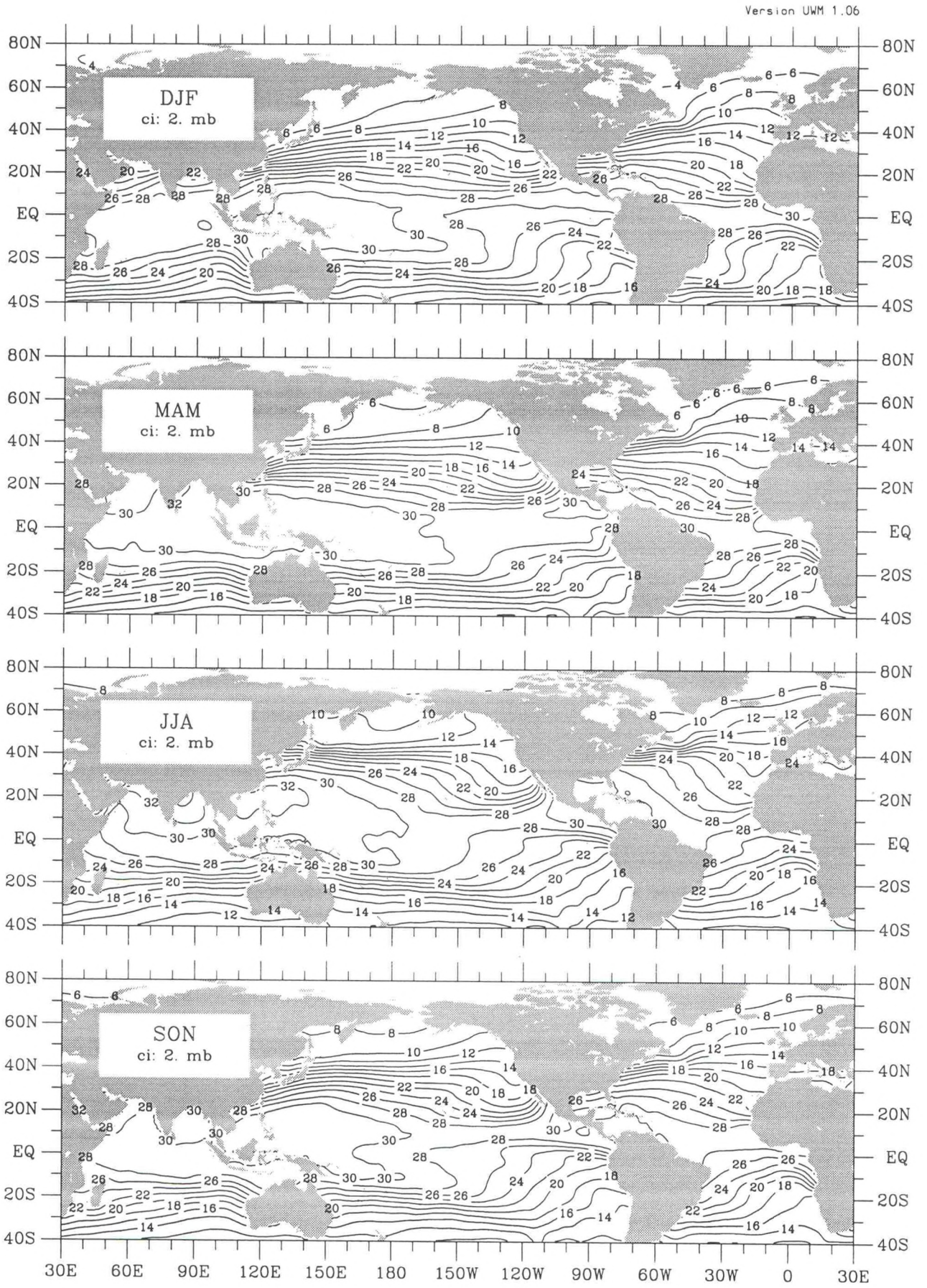

Figure e-3. Vapor pressure seasonal climatology (1945-89).

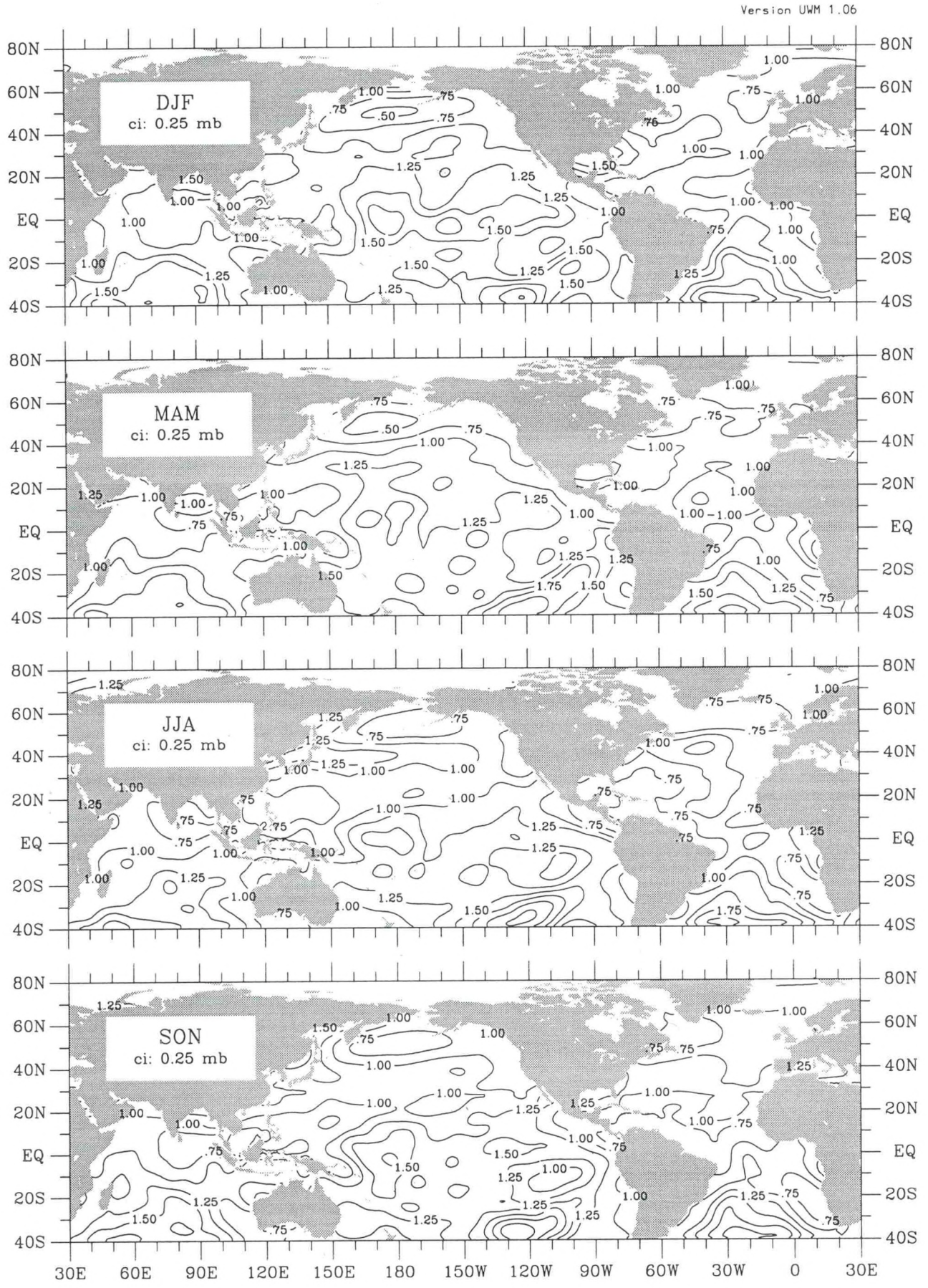

Figure e-4. Vapor pressure seasonal interannual std dev (1945-89).

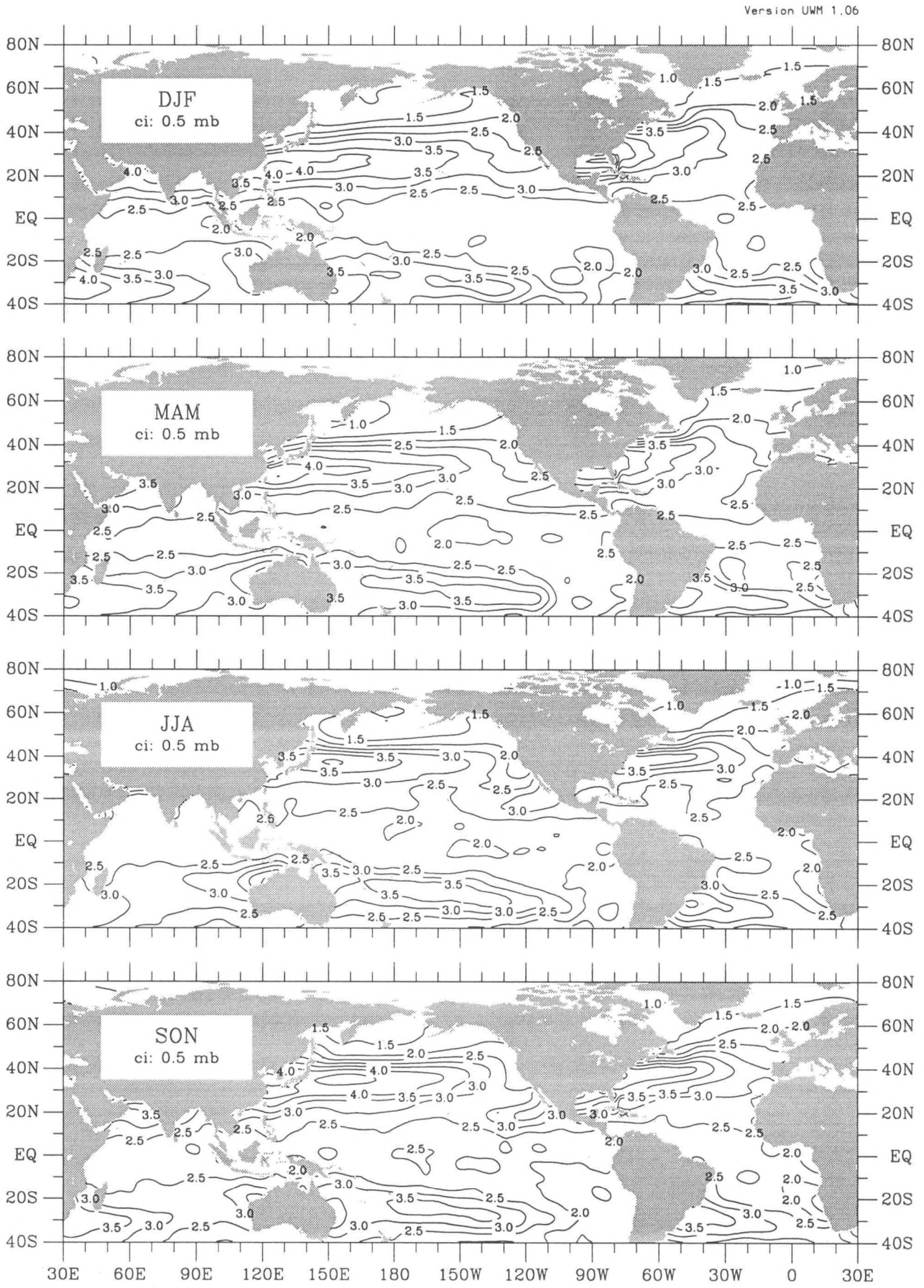

Figure e-5. Vapor pressure seasonal standard deviation (1945-89).

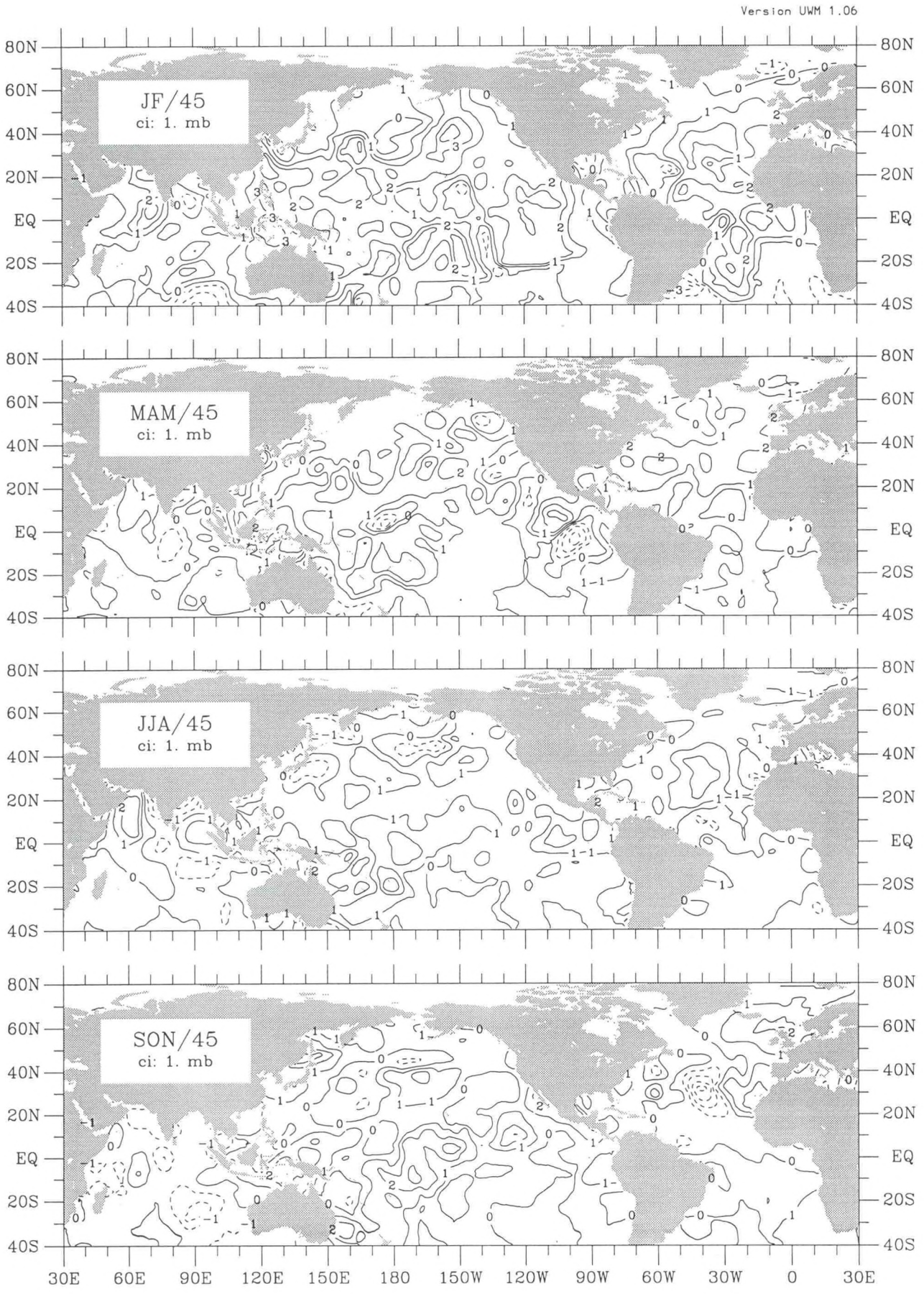

Figure e-6. Vapor pressure seasonal anomaly for 1945.

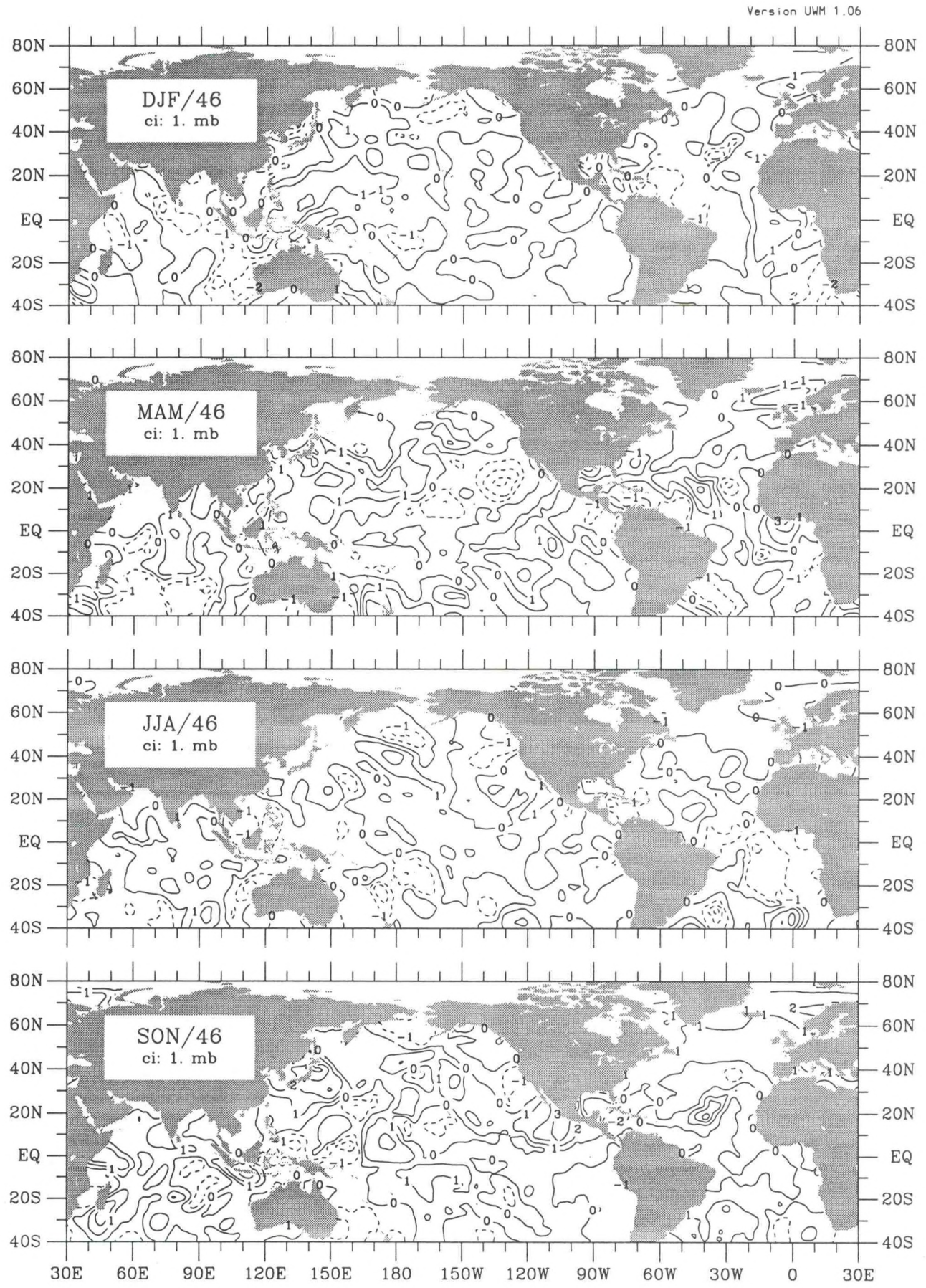

Figure e-7. Vapor pressure seasonal anomaly for 1946.

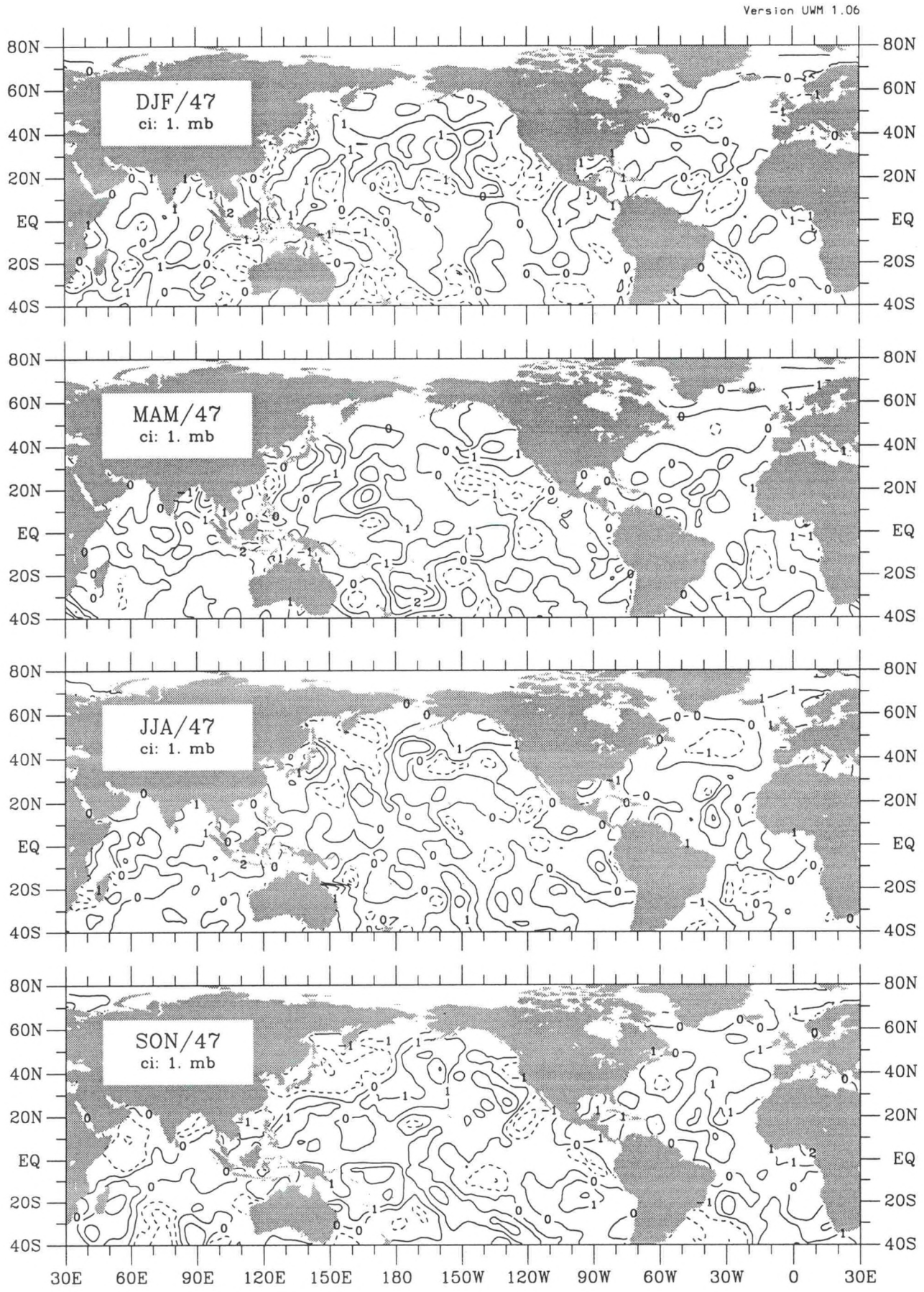

Figure e-8. Vapor pressure seasonal anomaly for 1947.

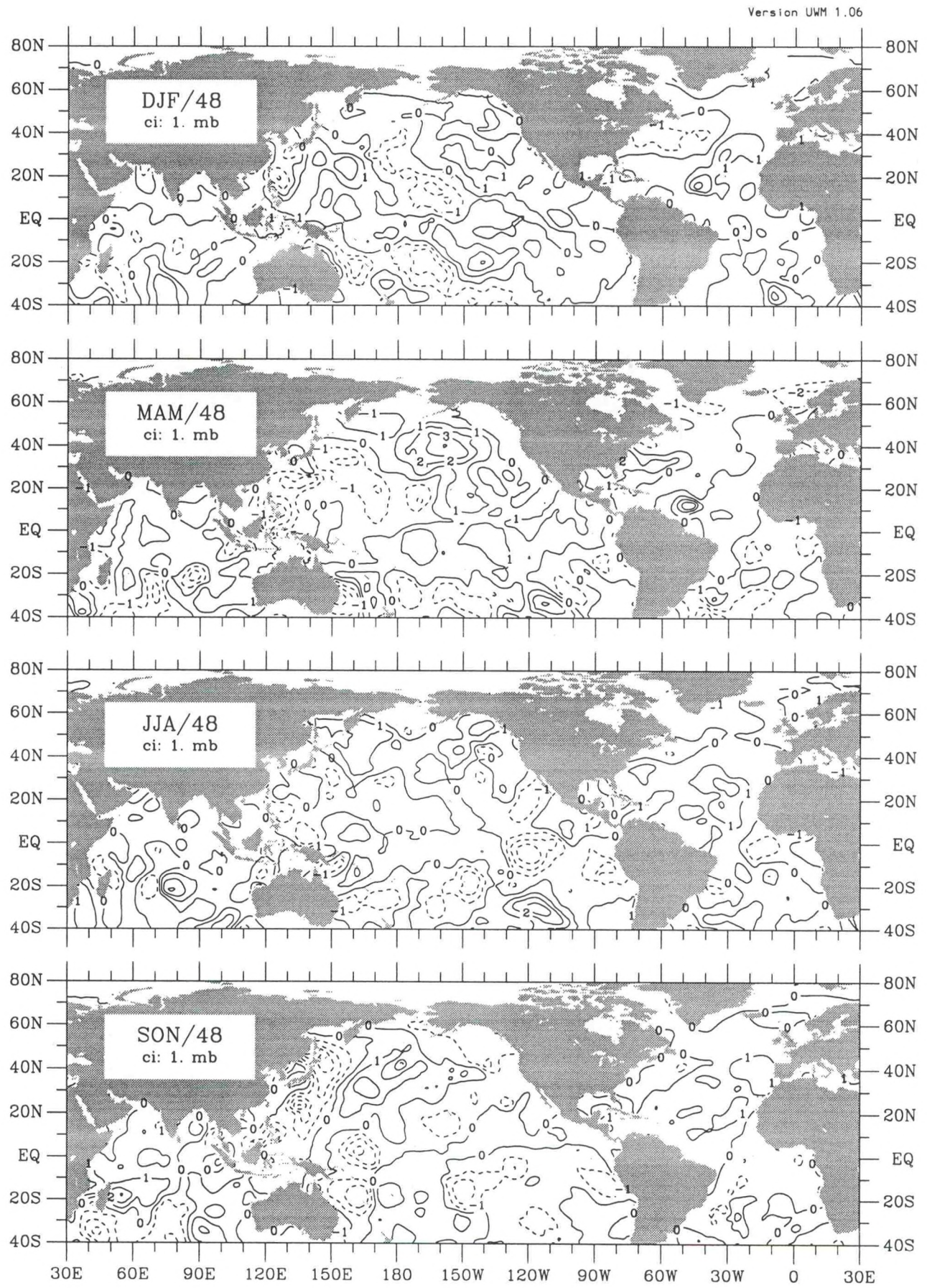

Figure e-9. Vapor pressure seasonal anomaly for 1948.

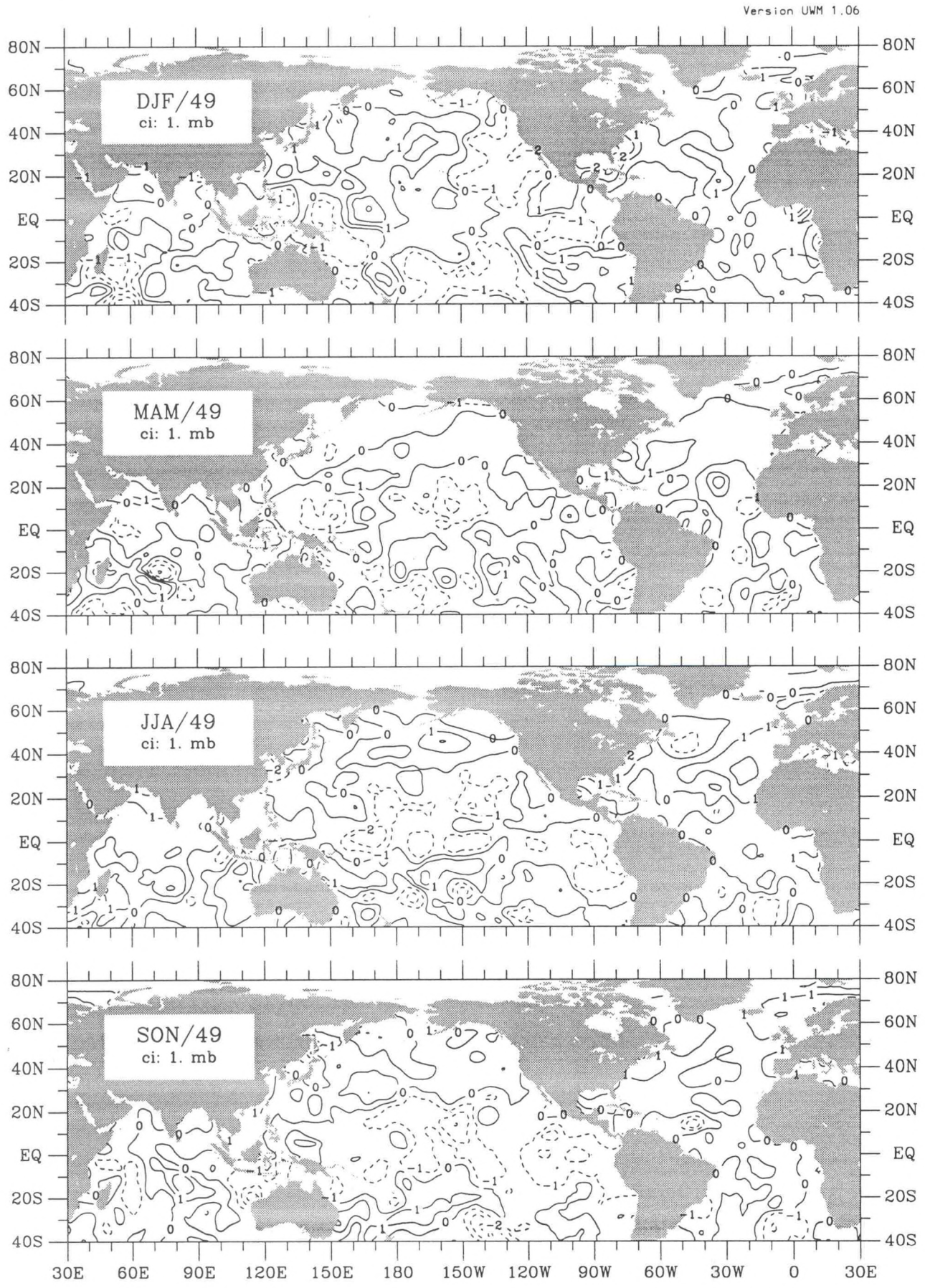

Figure e-10. Vapor pressure seasonal anomaly for 1949.

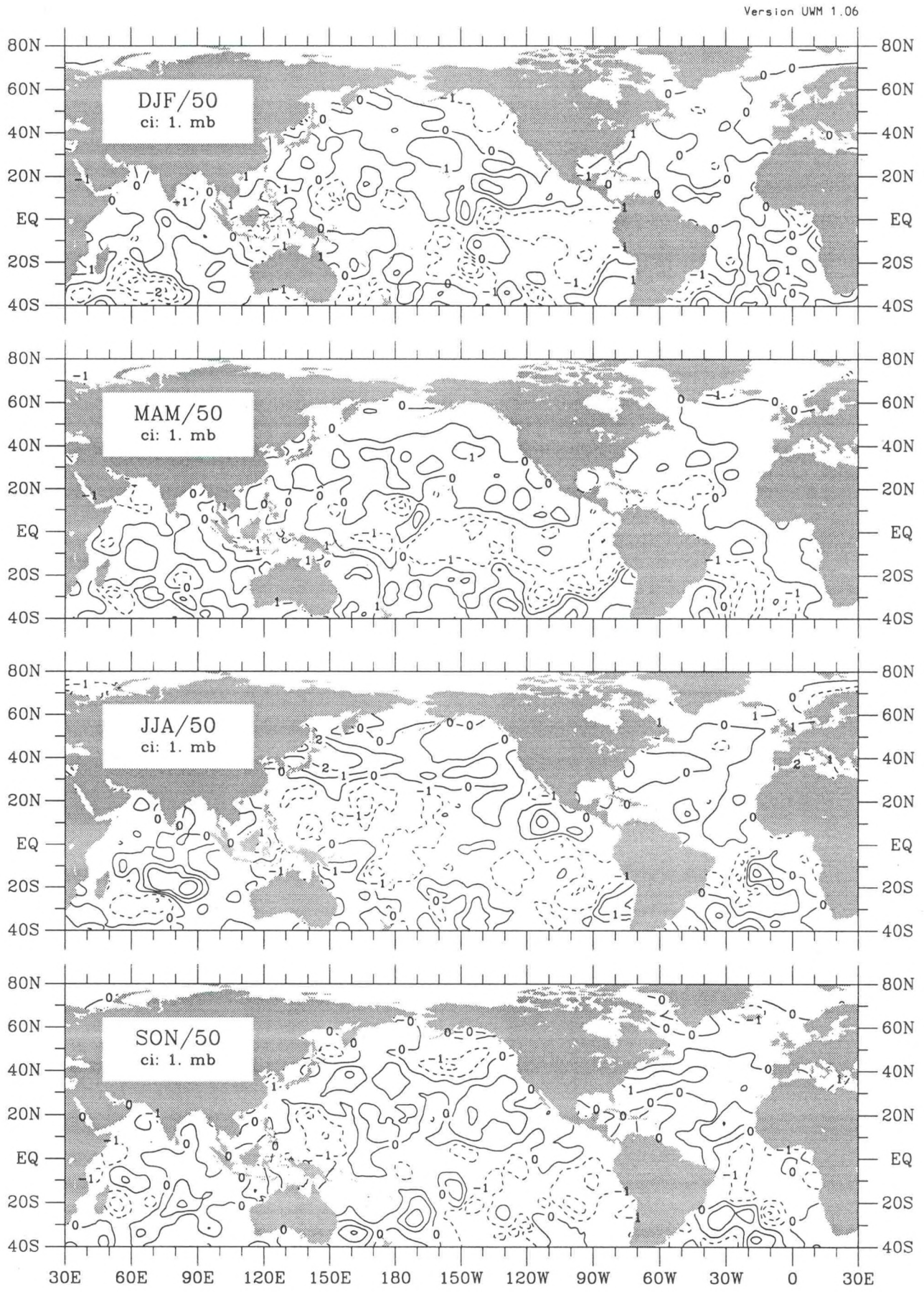

Figure e-11. Vapor pressure seasonal anomaly for 1950.

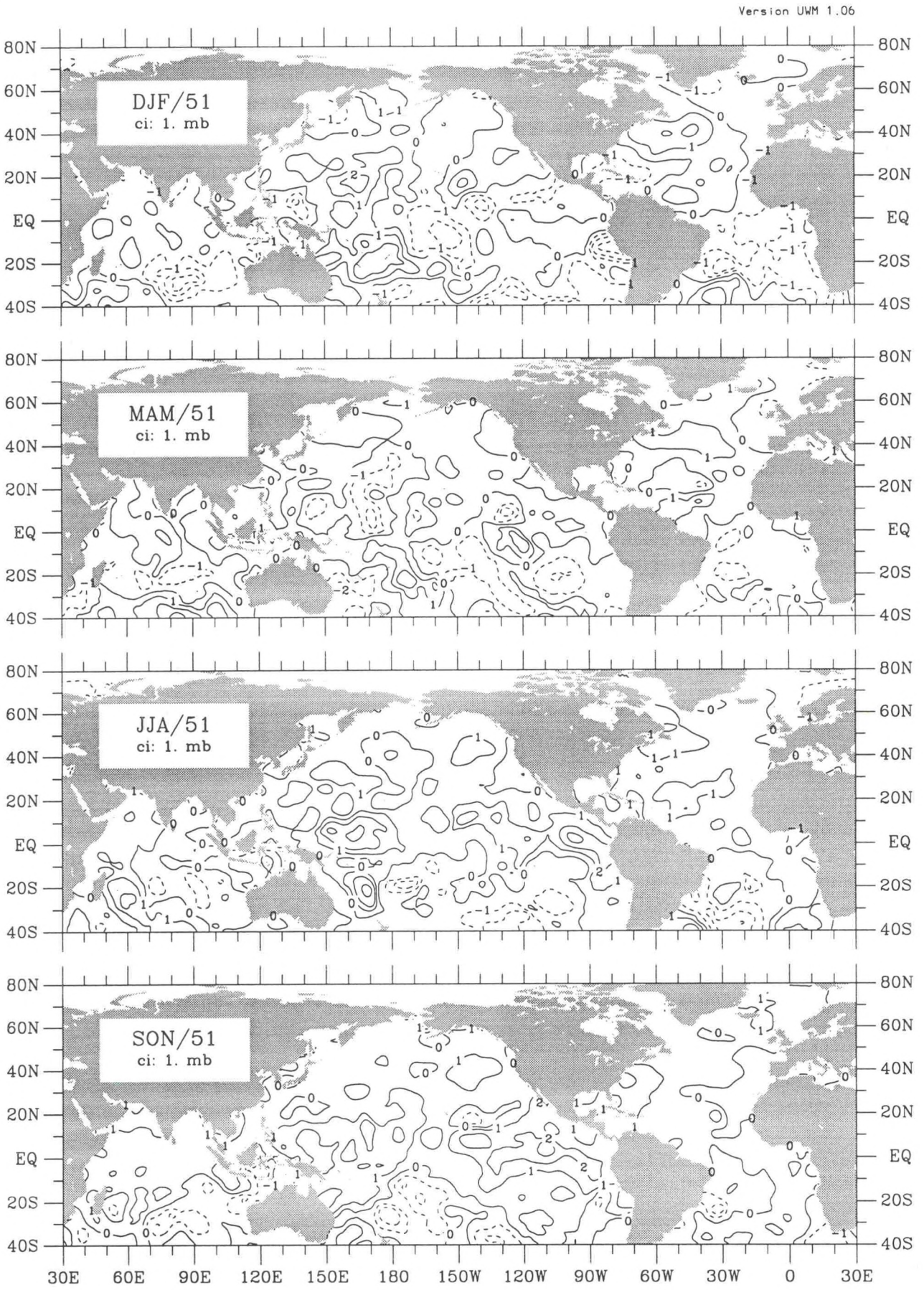

Figure e-12. Vapor pressure seasonal anomaly for 1951.

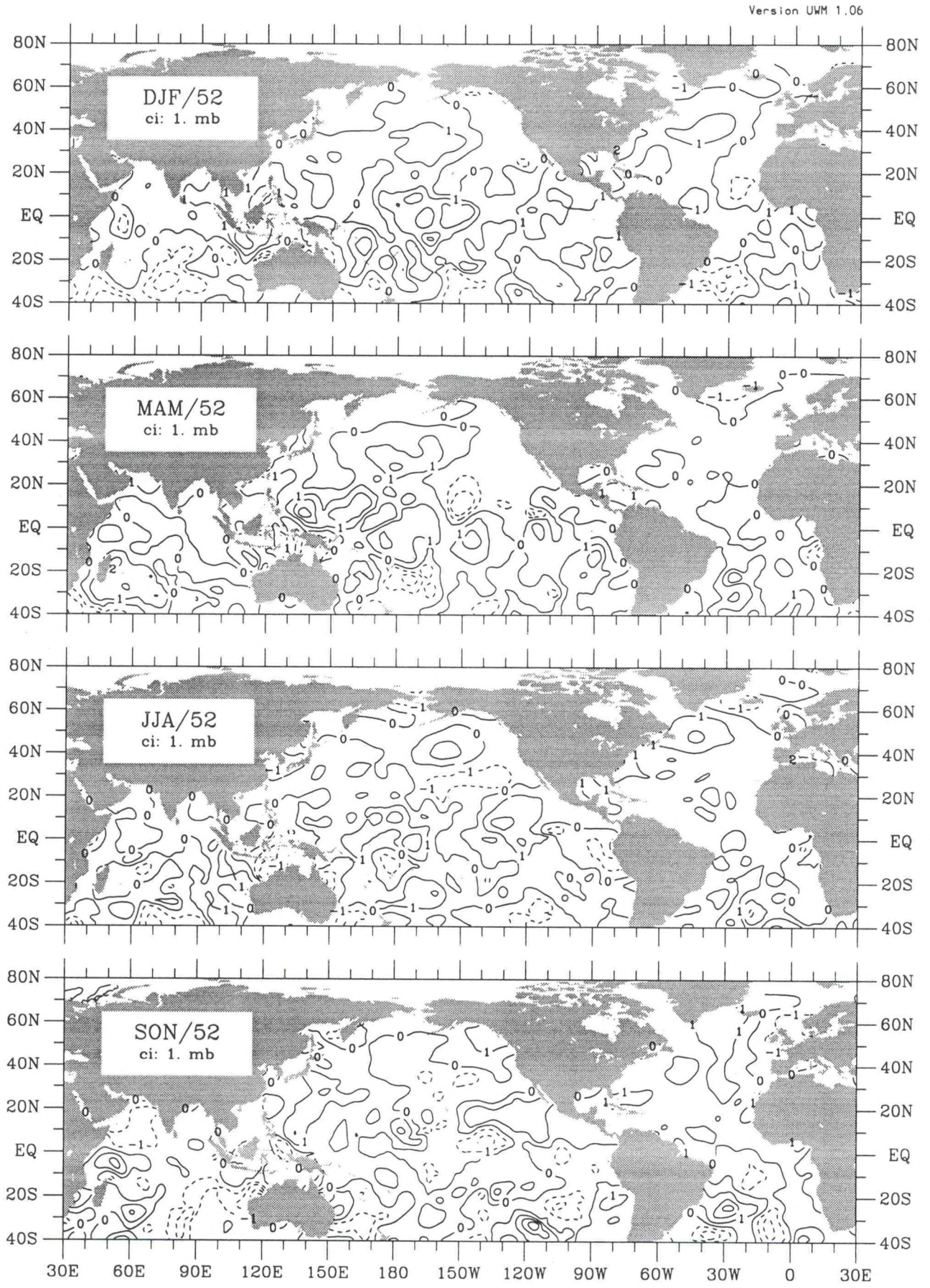

Figure e-13. Vapor pressure seasonal anomaly for 1952.

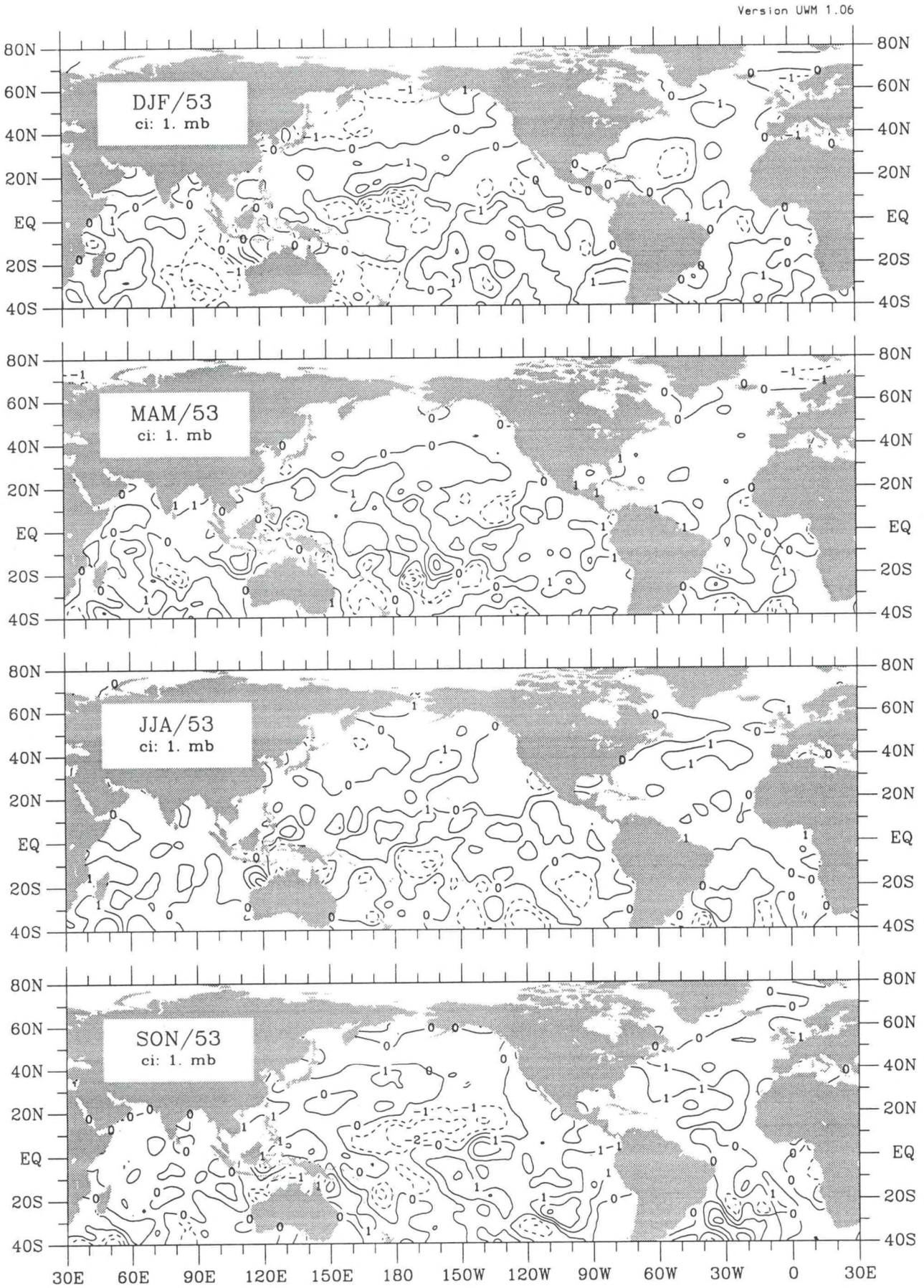

Figure e-14. Vapor pressure seasonal anomaly for 1953.

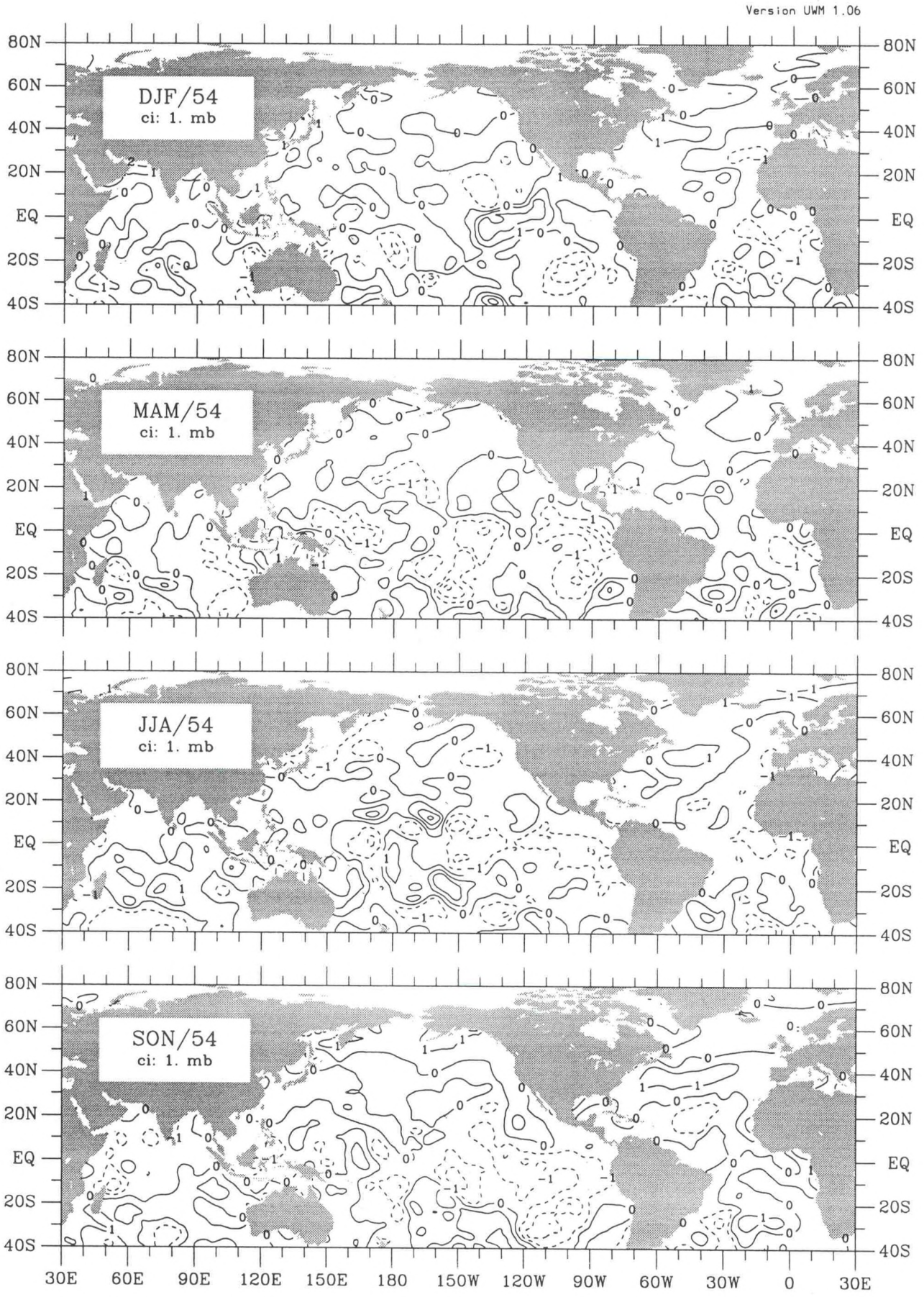

Figure e-15. Vapor pressure seasonal anomaly for 1954.

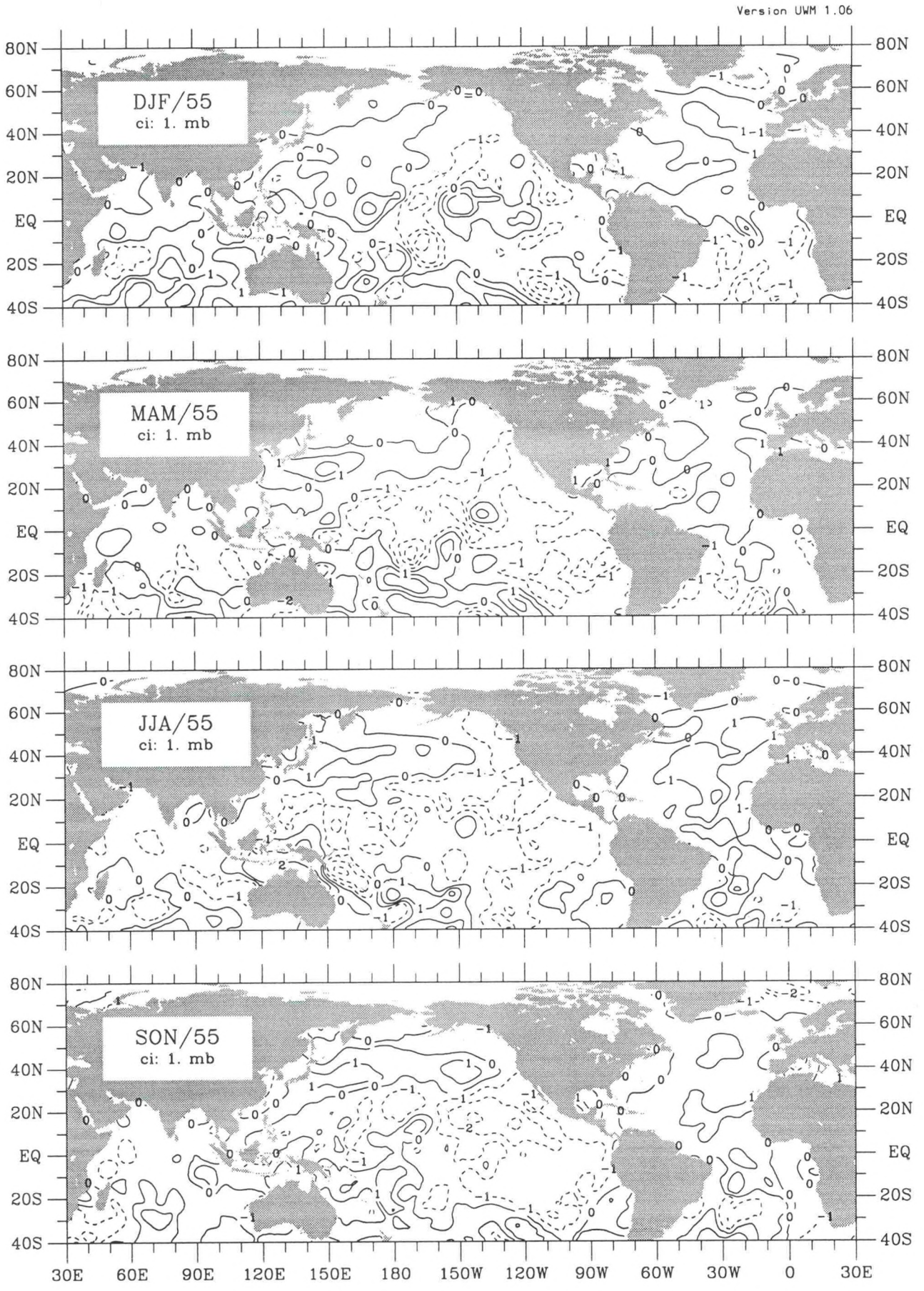

Figure e-16. Vapor pressure seasonal anomaly for 1955.

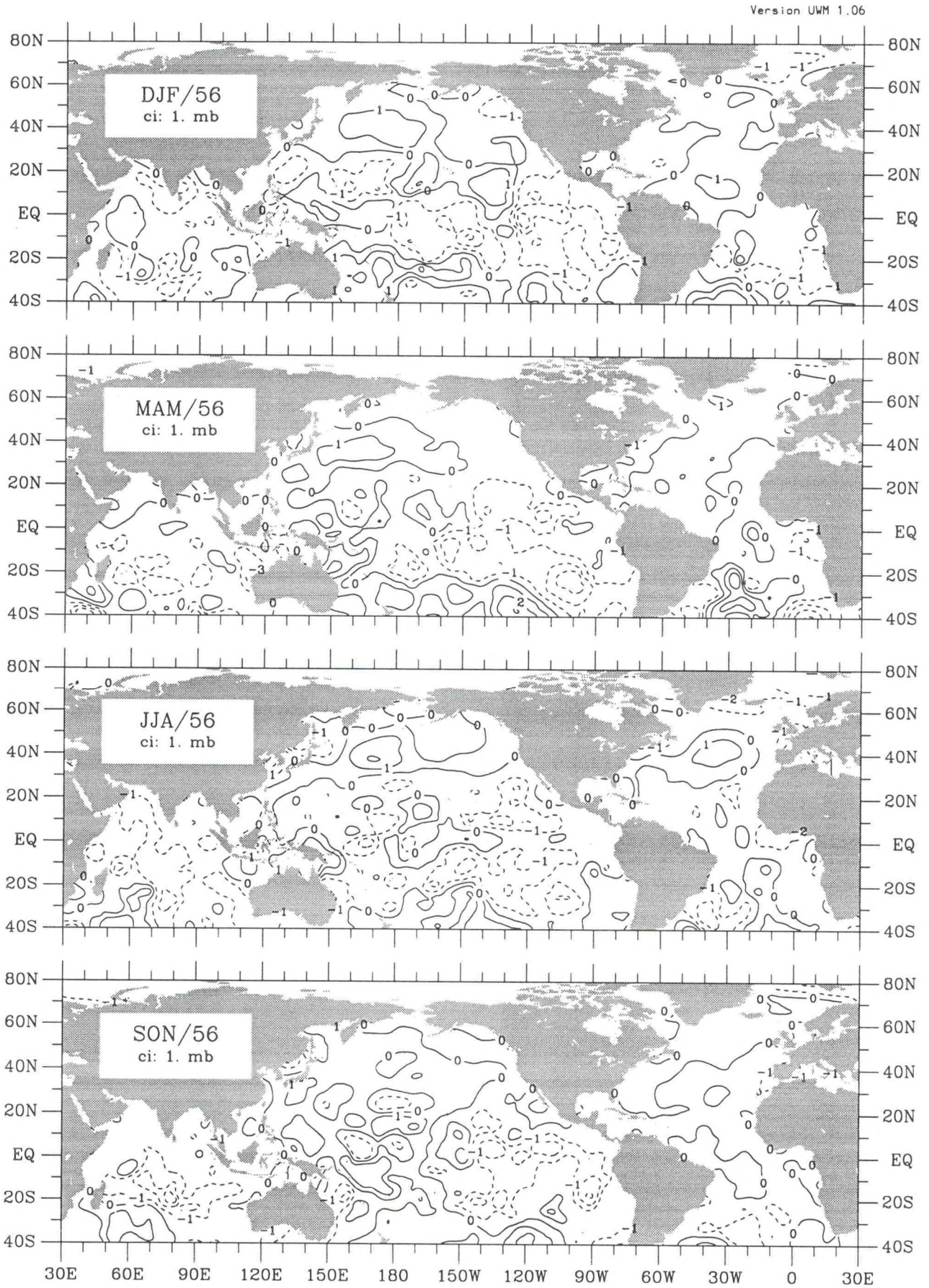

Figure e-17. Vapor pressure seasonal anomaly for 1956.

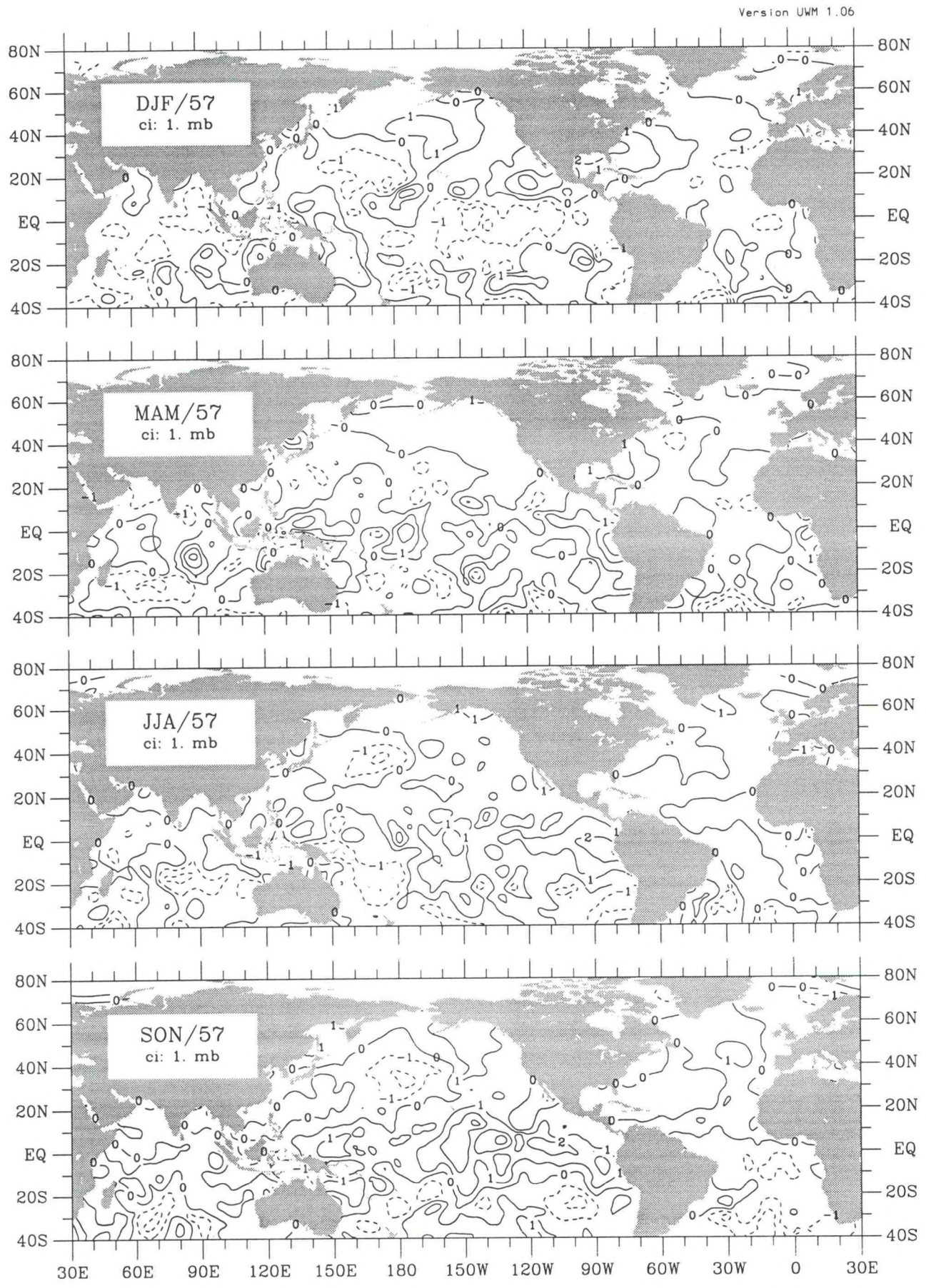

Figure e-18. Vapor pressure seasonal anomaly for 1957.

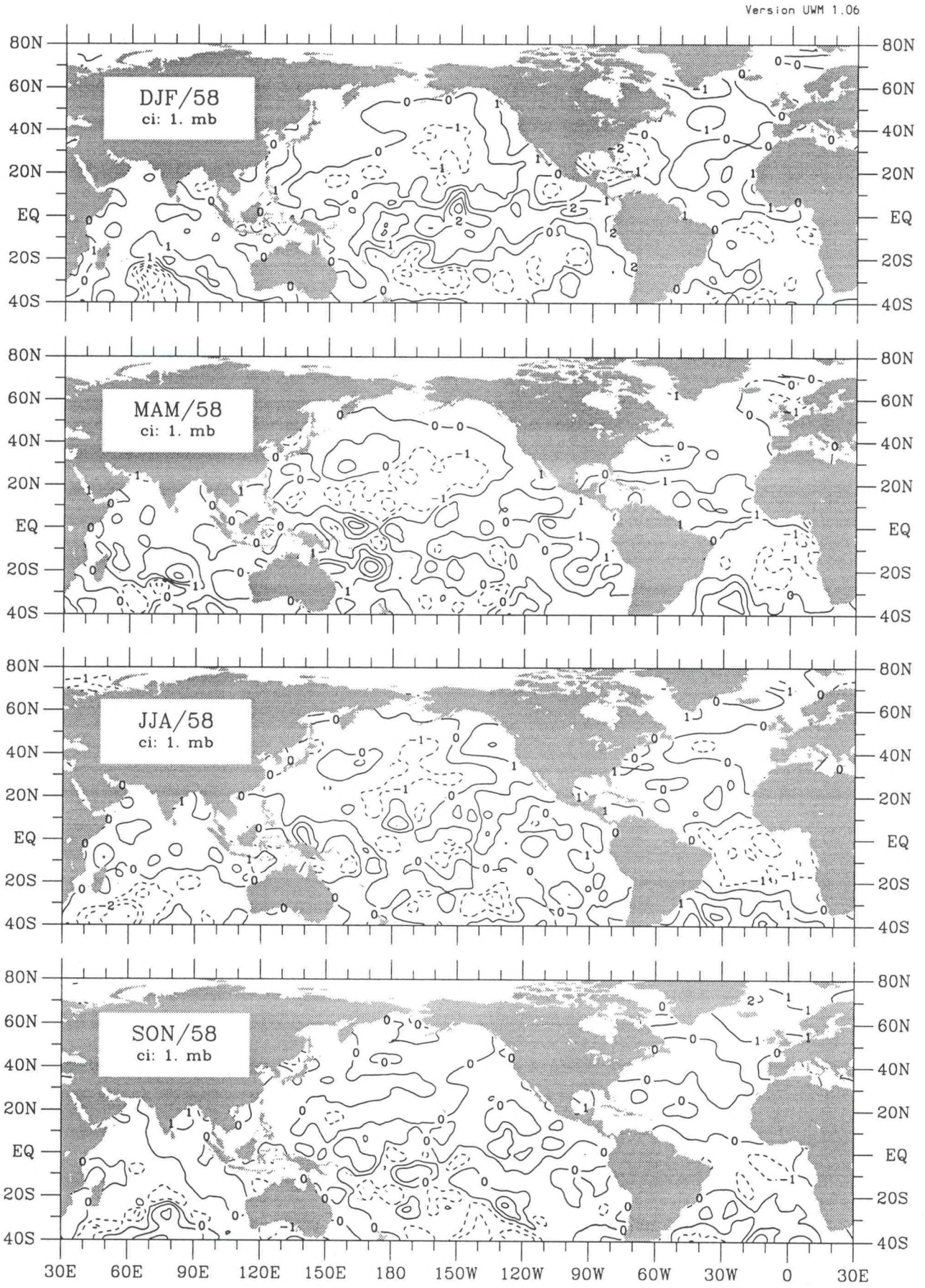

Figure e-19. Vapor pressure seasonal anomaly for 1958.

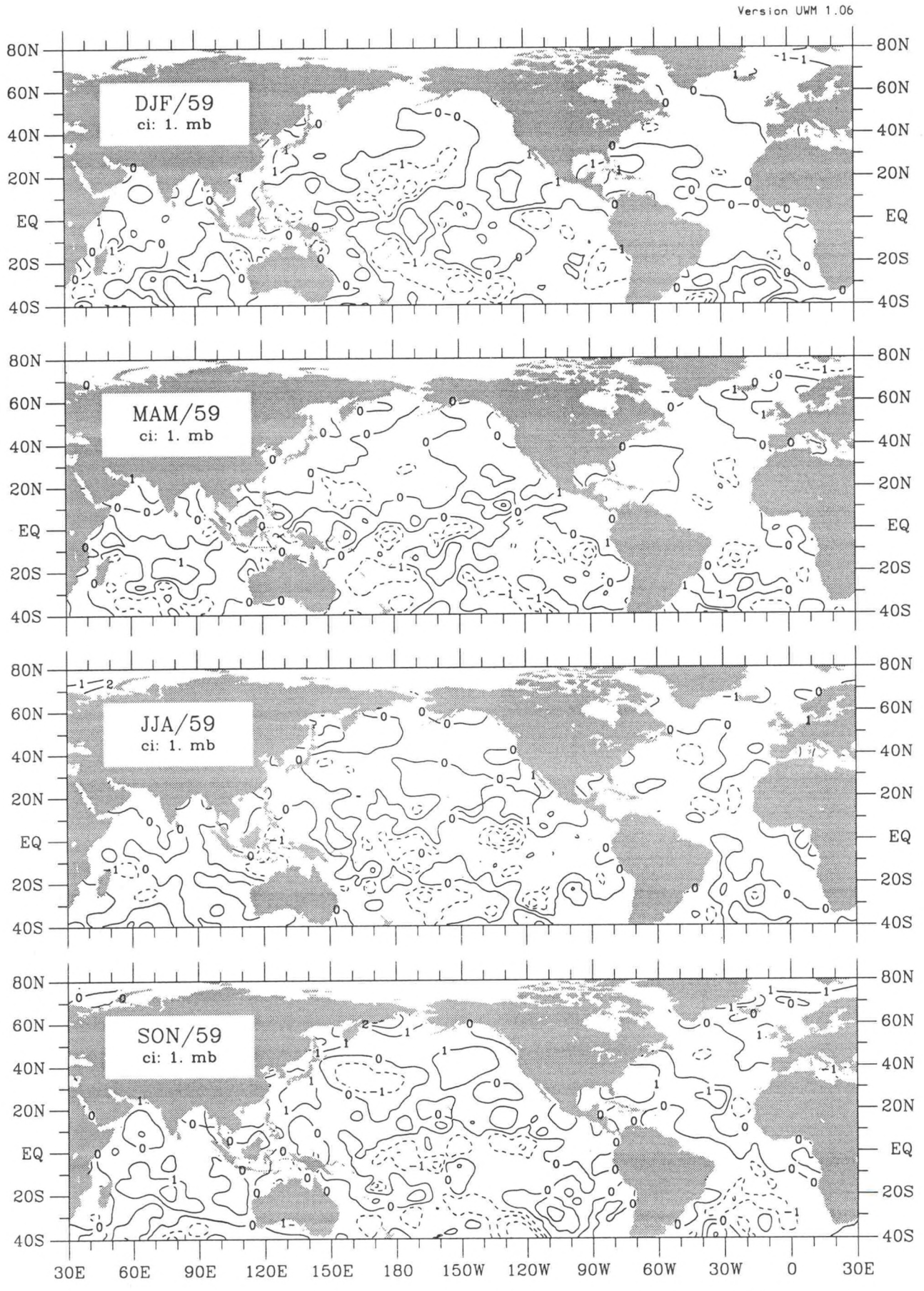

Figure e-20. Vapor pressure seasonal anomaly for 1959.

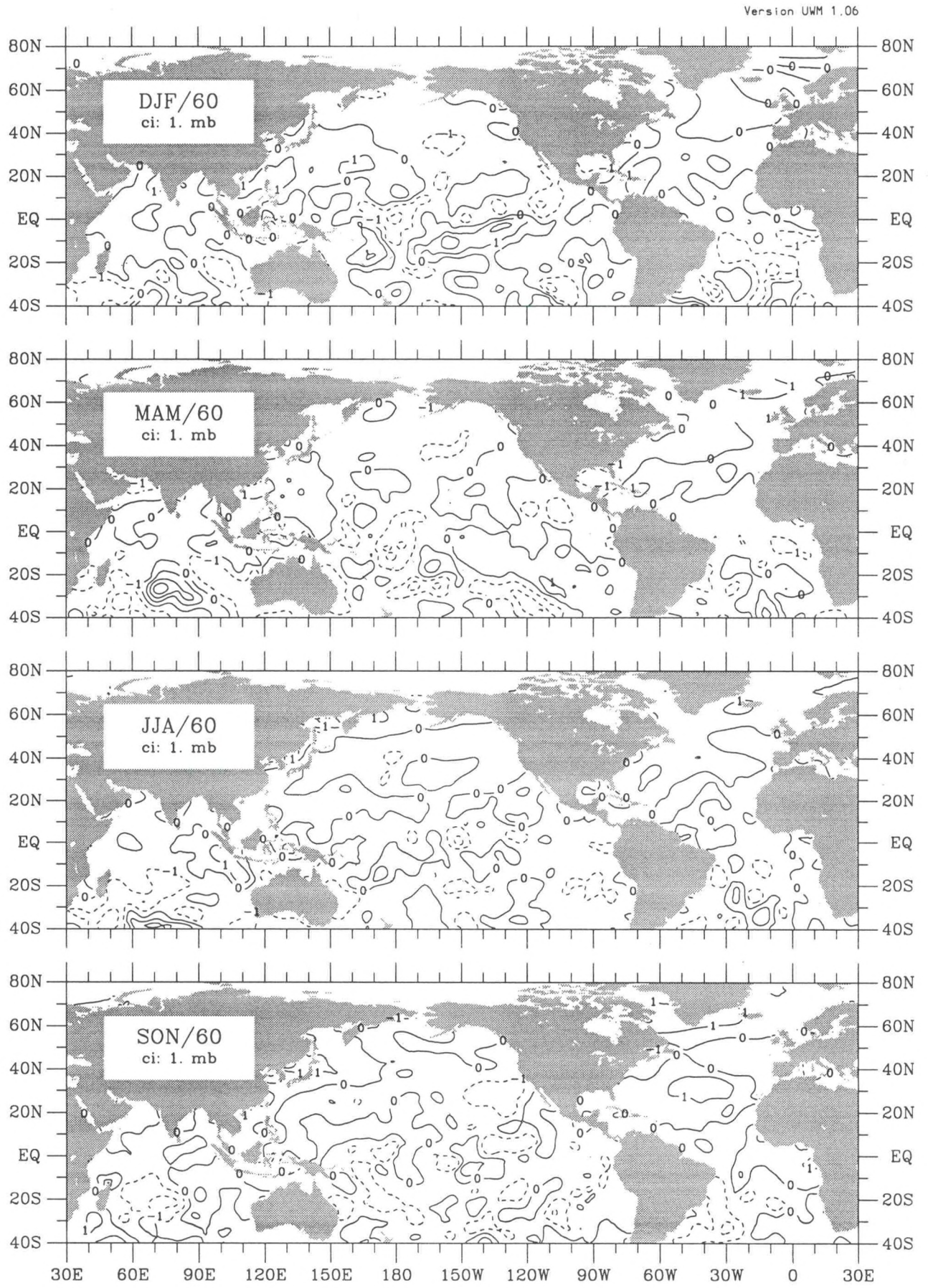

Figure e-21. Vapor pressure seasonal anomaly for 1960.

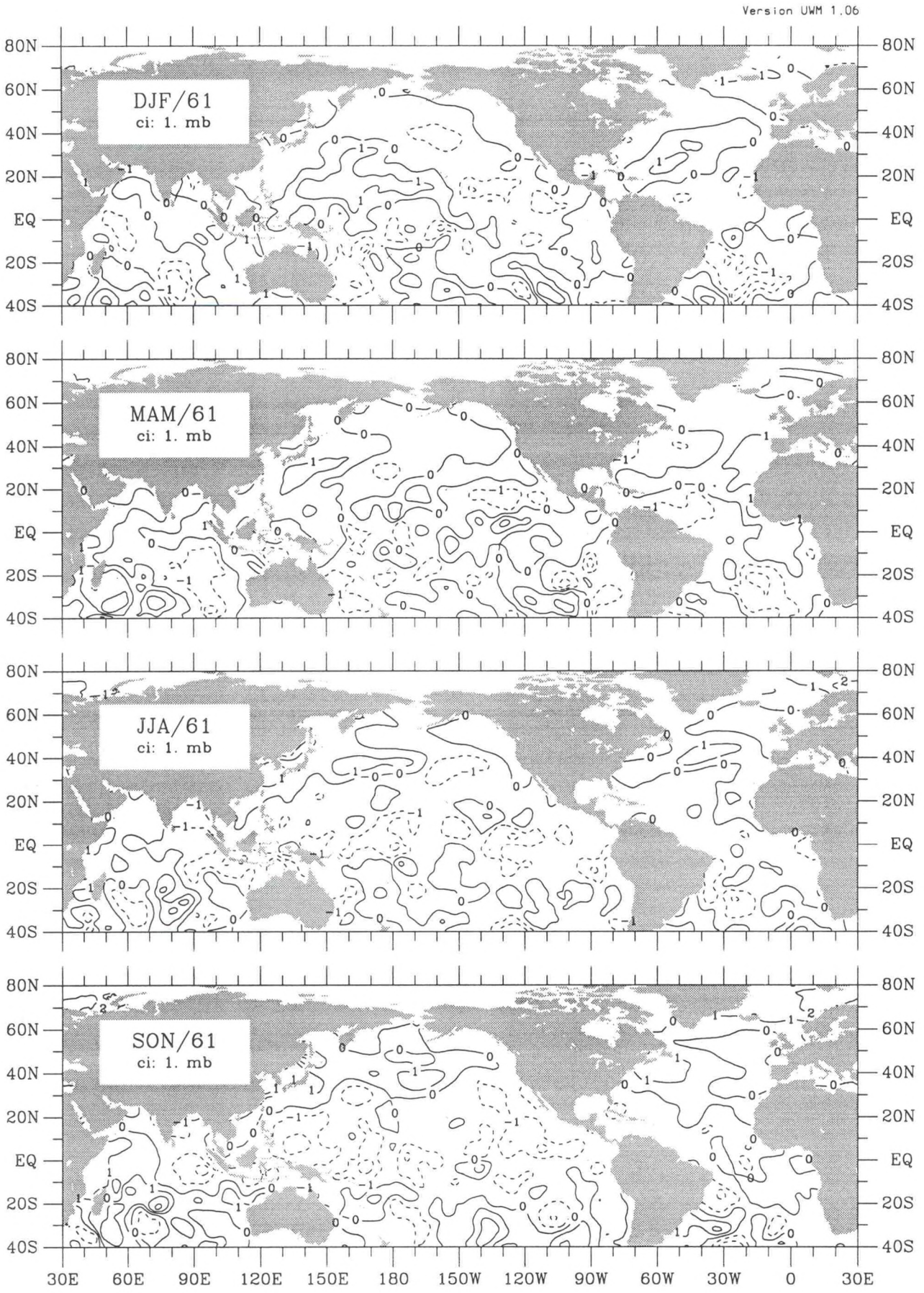

Figure e-22. Vapor pressure seasonal anomaly for 1961.

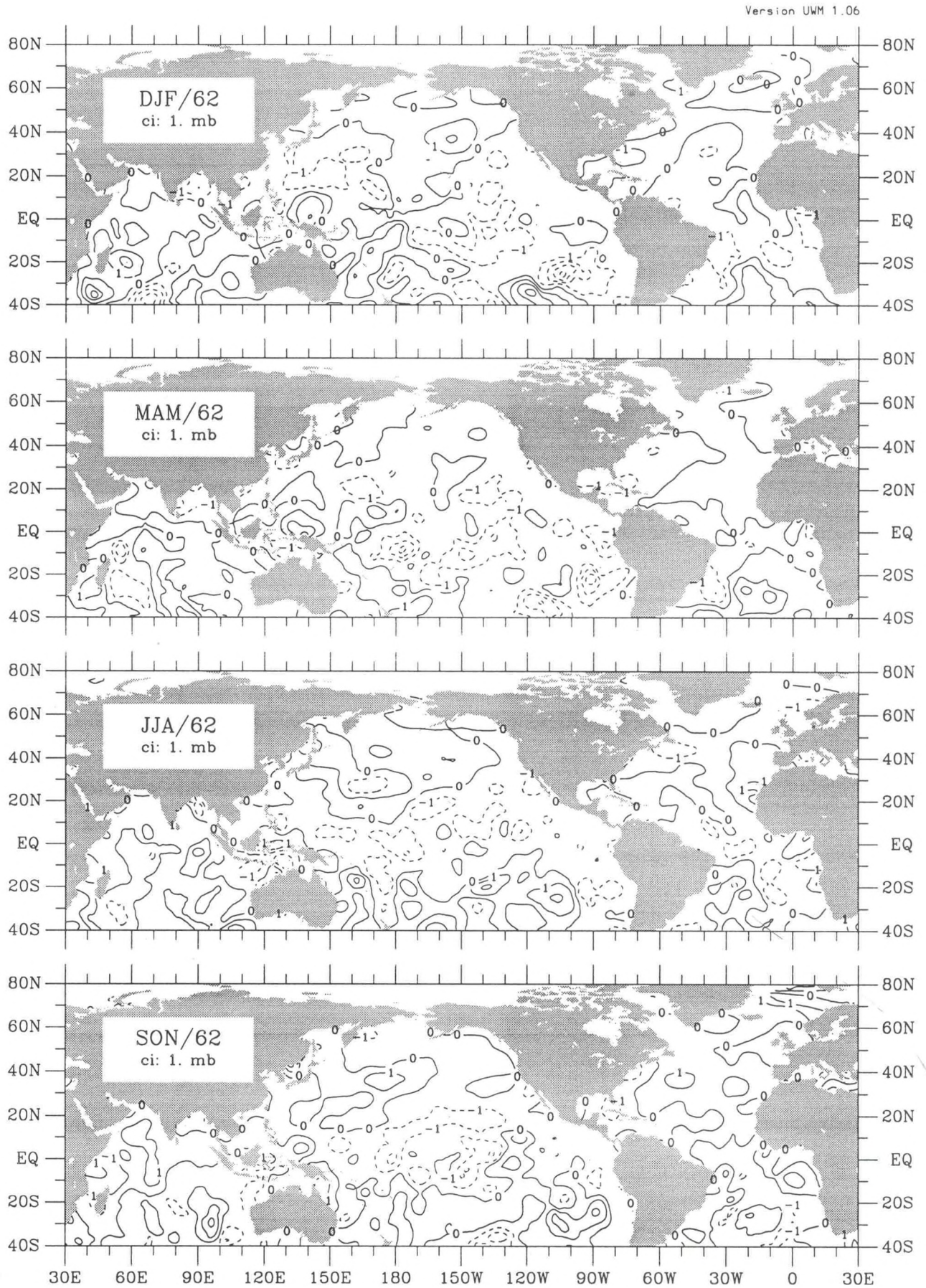

Figure e-23. Vapor pressure seasonal anomaly for 1962.

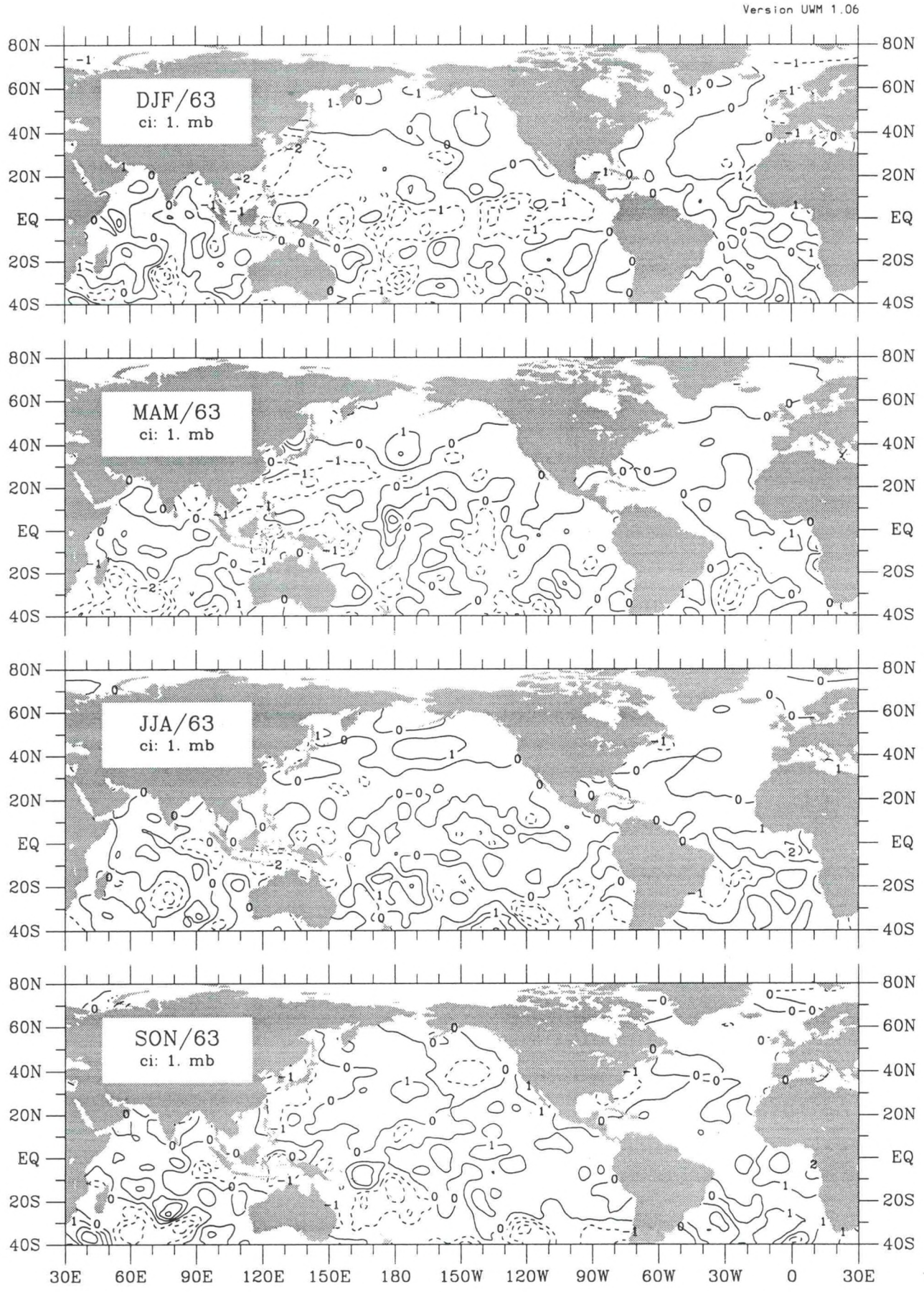

Figure e-24. Vapor pressure seasonal anomaly for 1963.

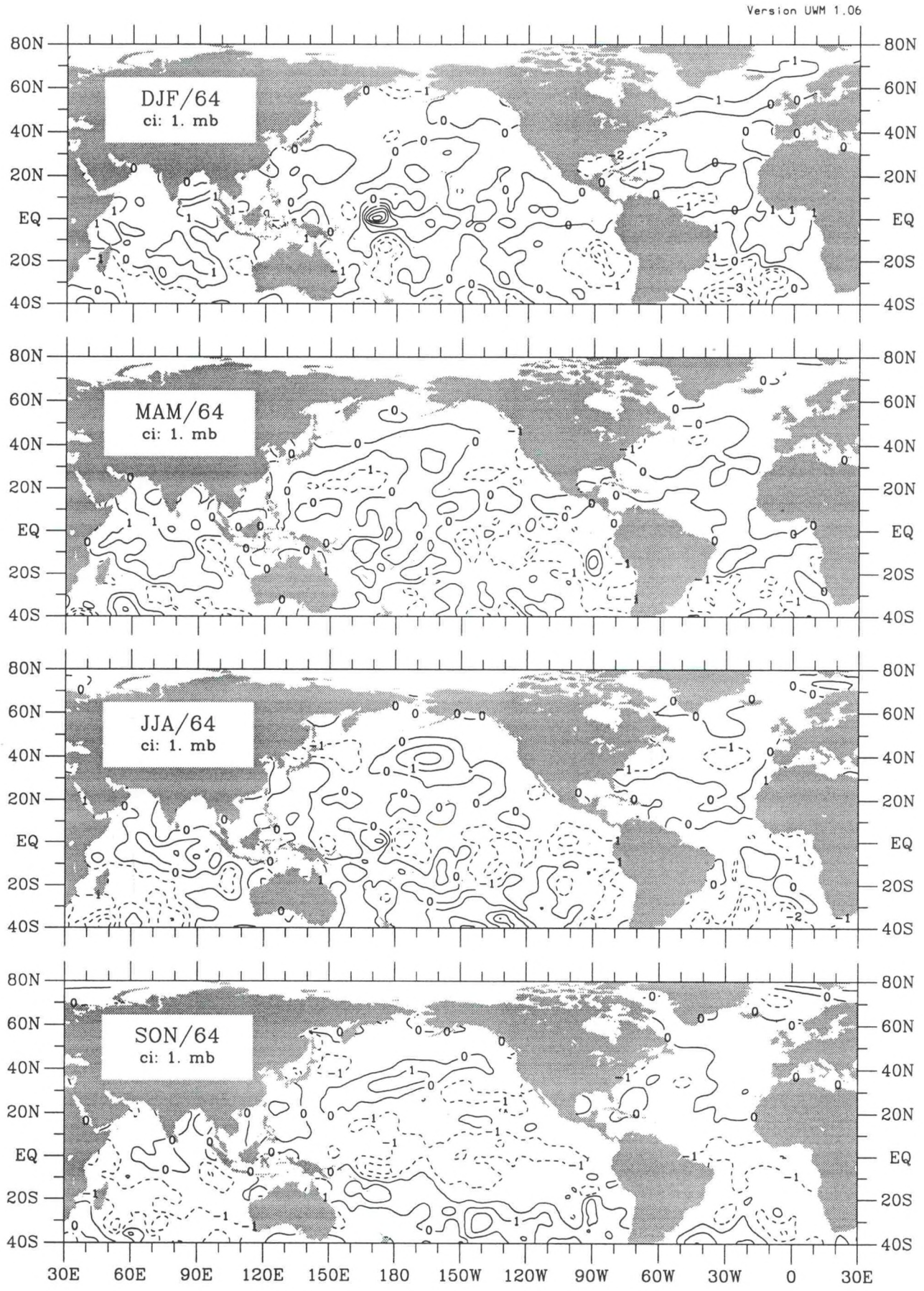

Figure e-25. Vapor pressure seasonal anomaly for 1964.

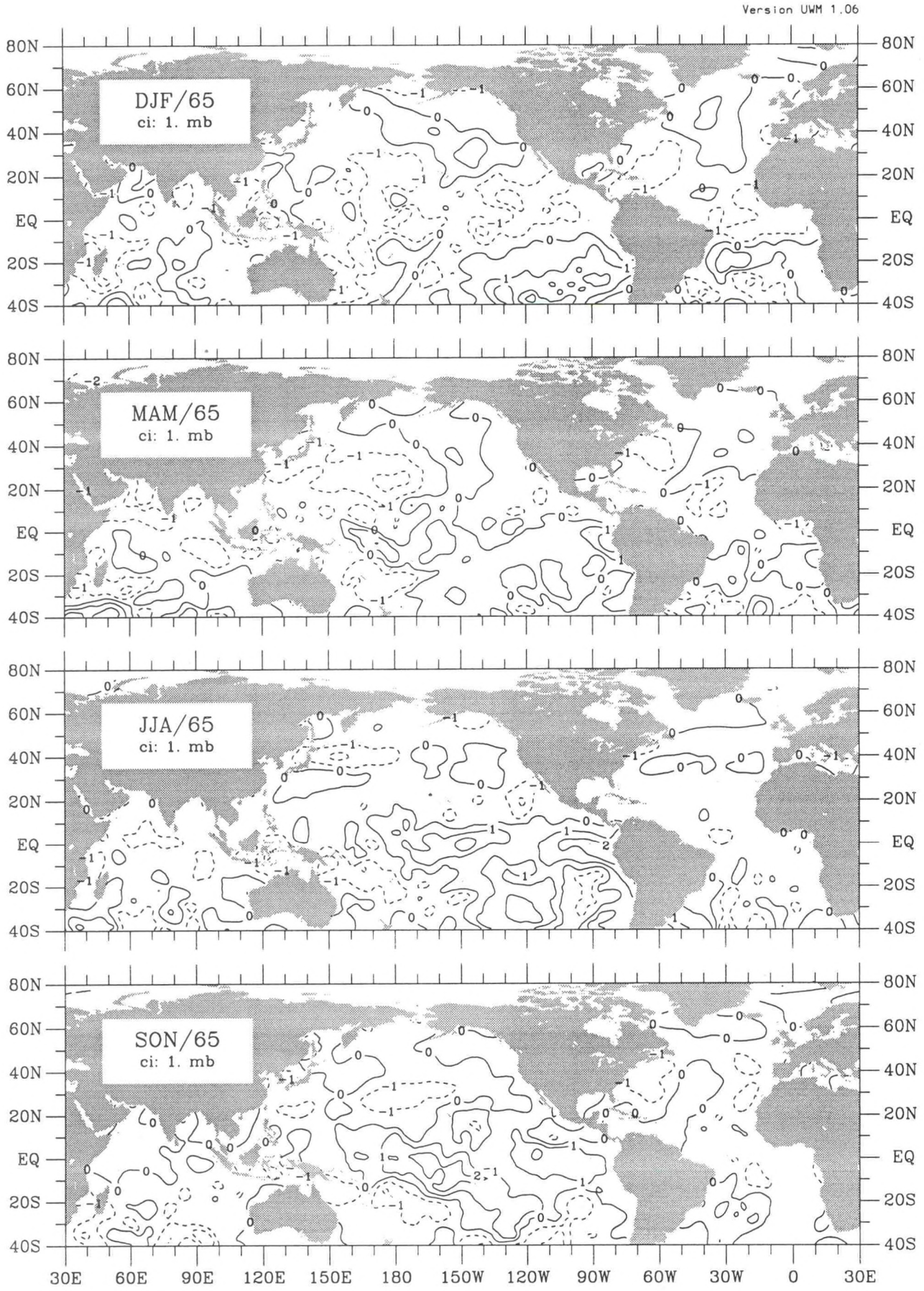

Figure e-26. Vapor pressure seasonal anomaly for 1965.

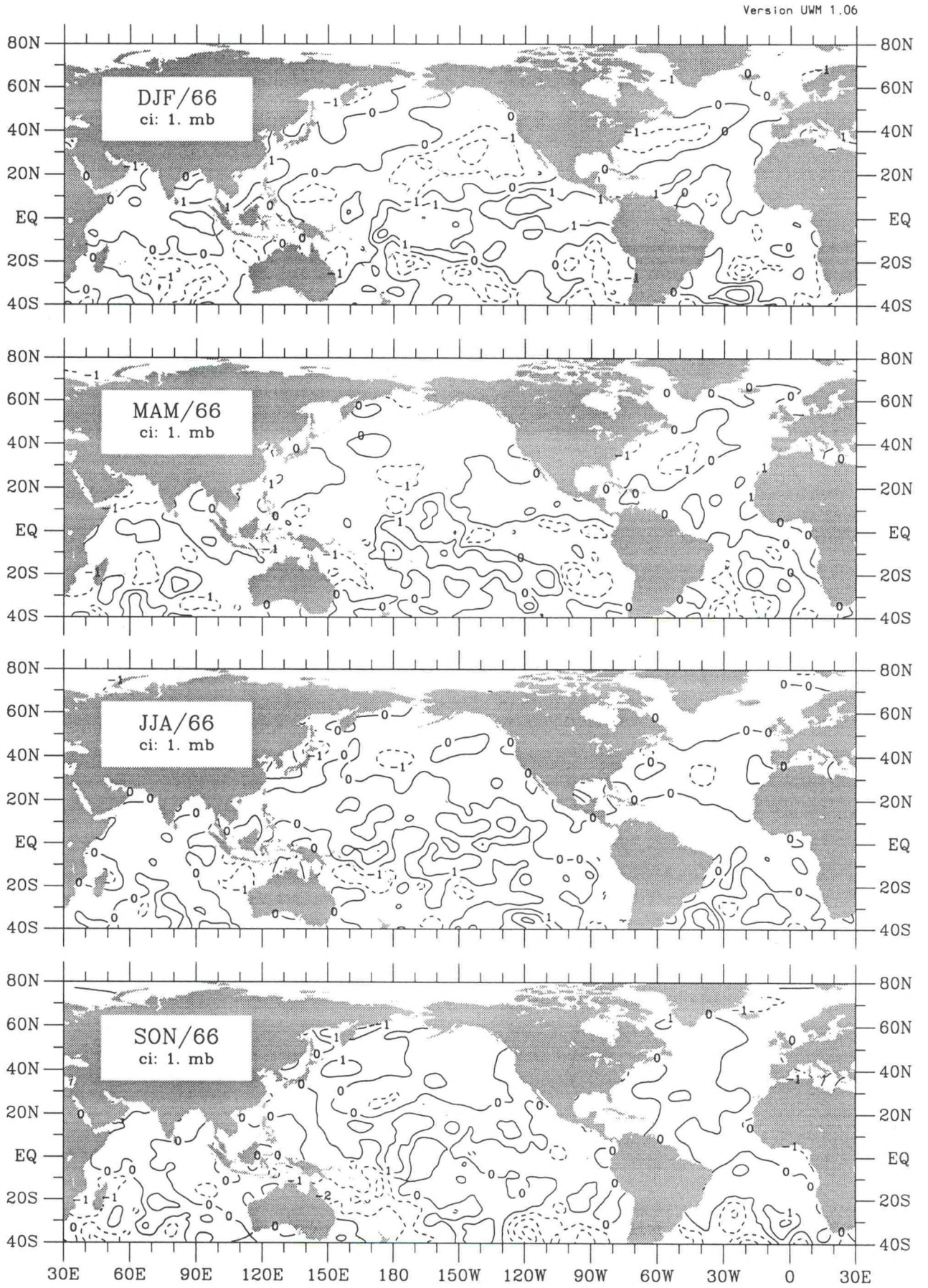

Figure e-27. Vapor pressure seasonal anomaly for 1966.

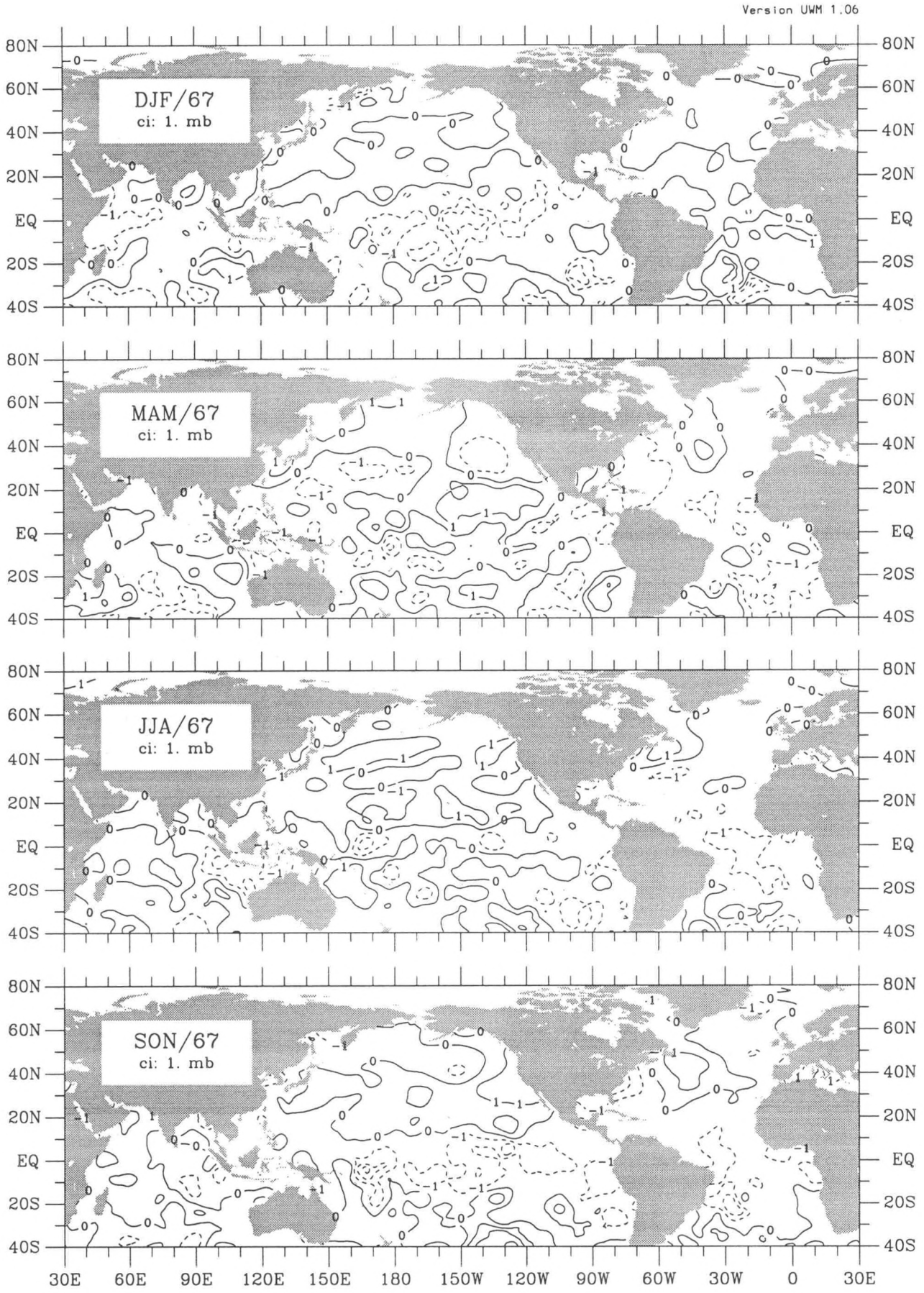

Figure e-28. Vapor pressure seasonal anomaly for 1967.

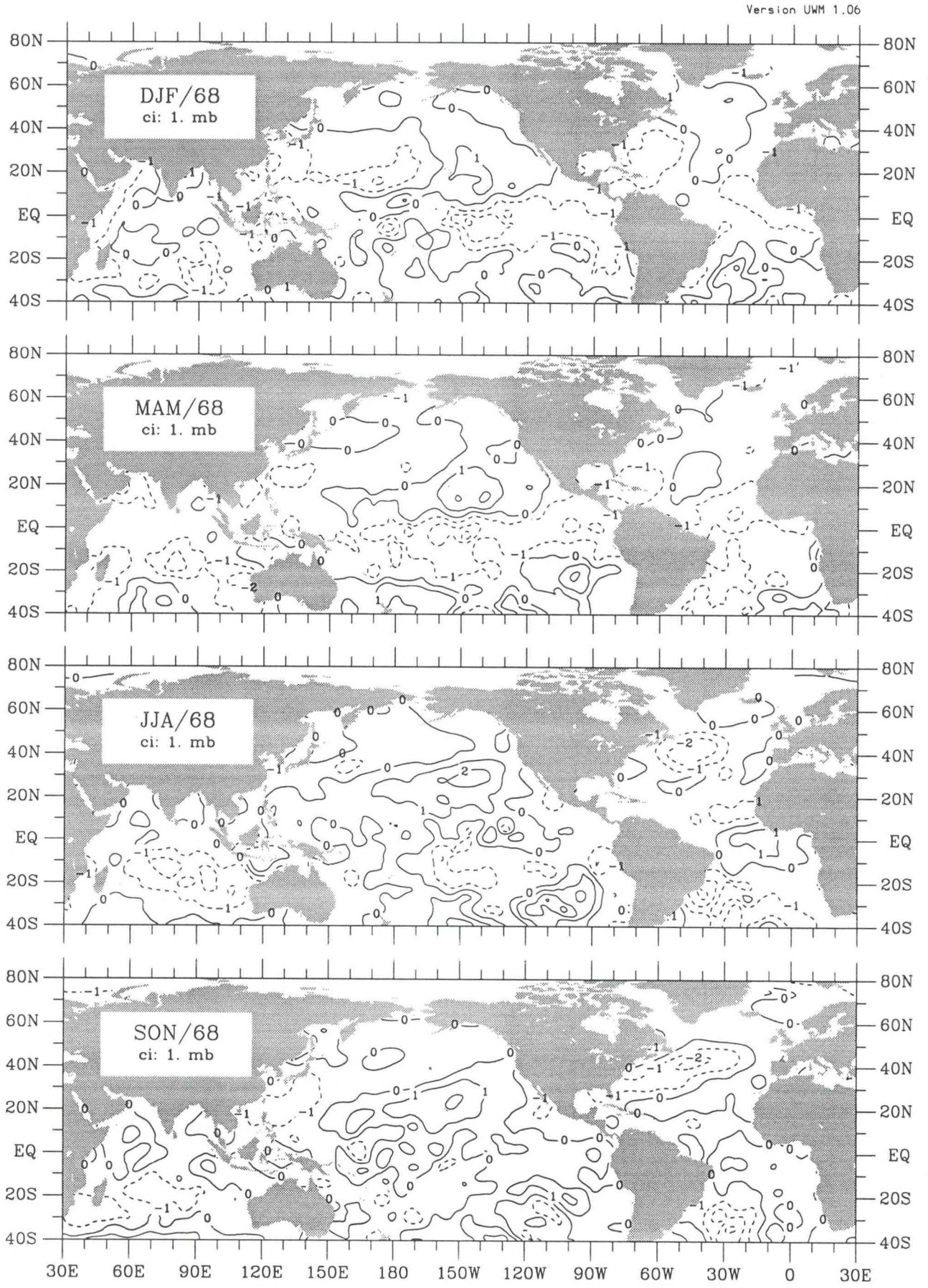

Figure e-29. Vapor pressure seasonal anomaly for 1968.

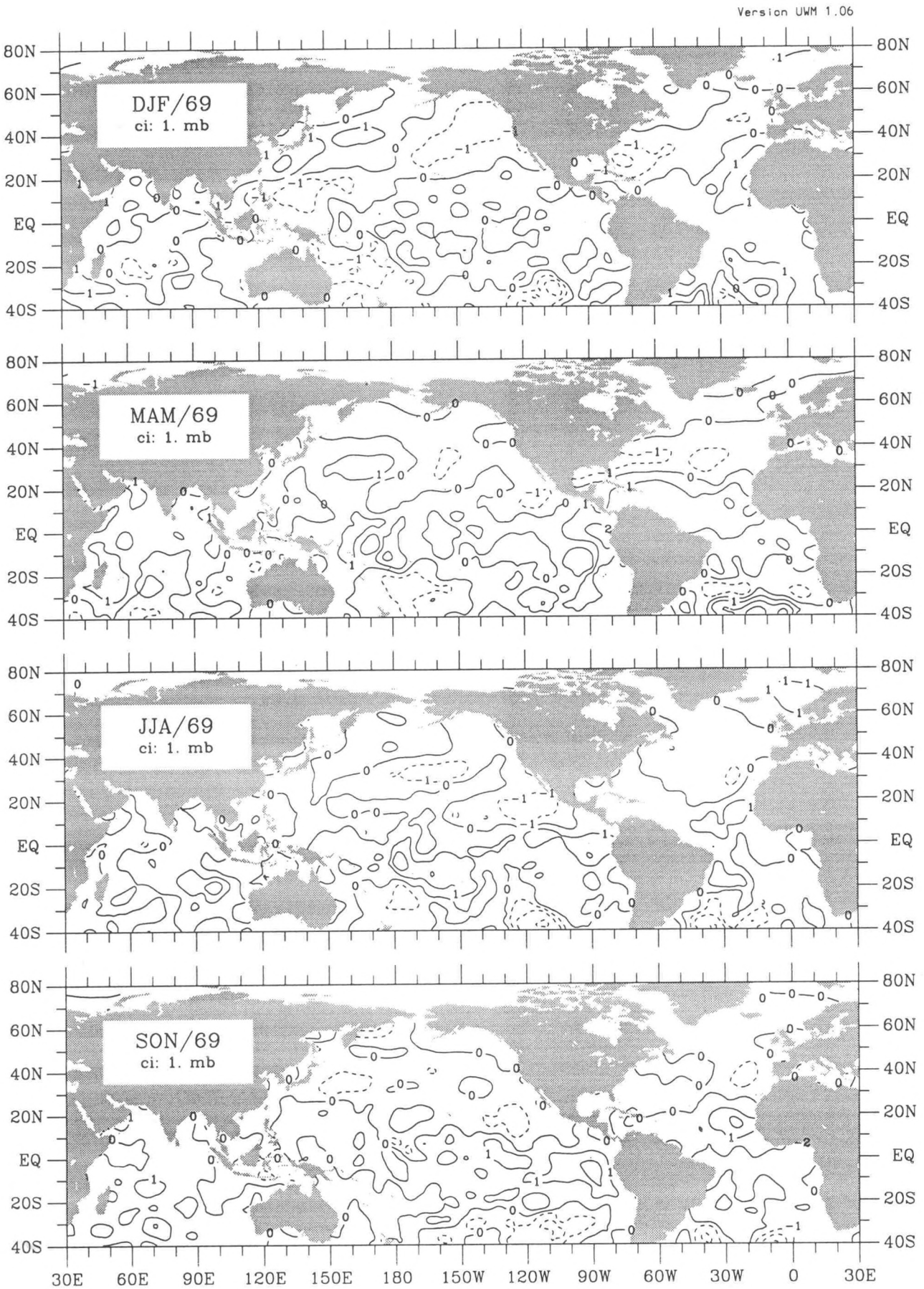

Figure e-30. Vapor pressure seasonal anomaly for 1969.

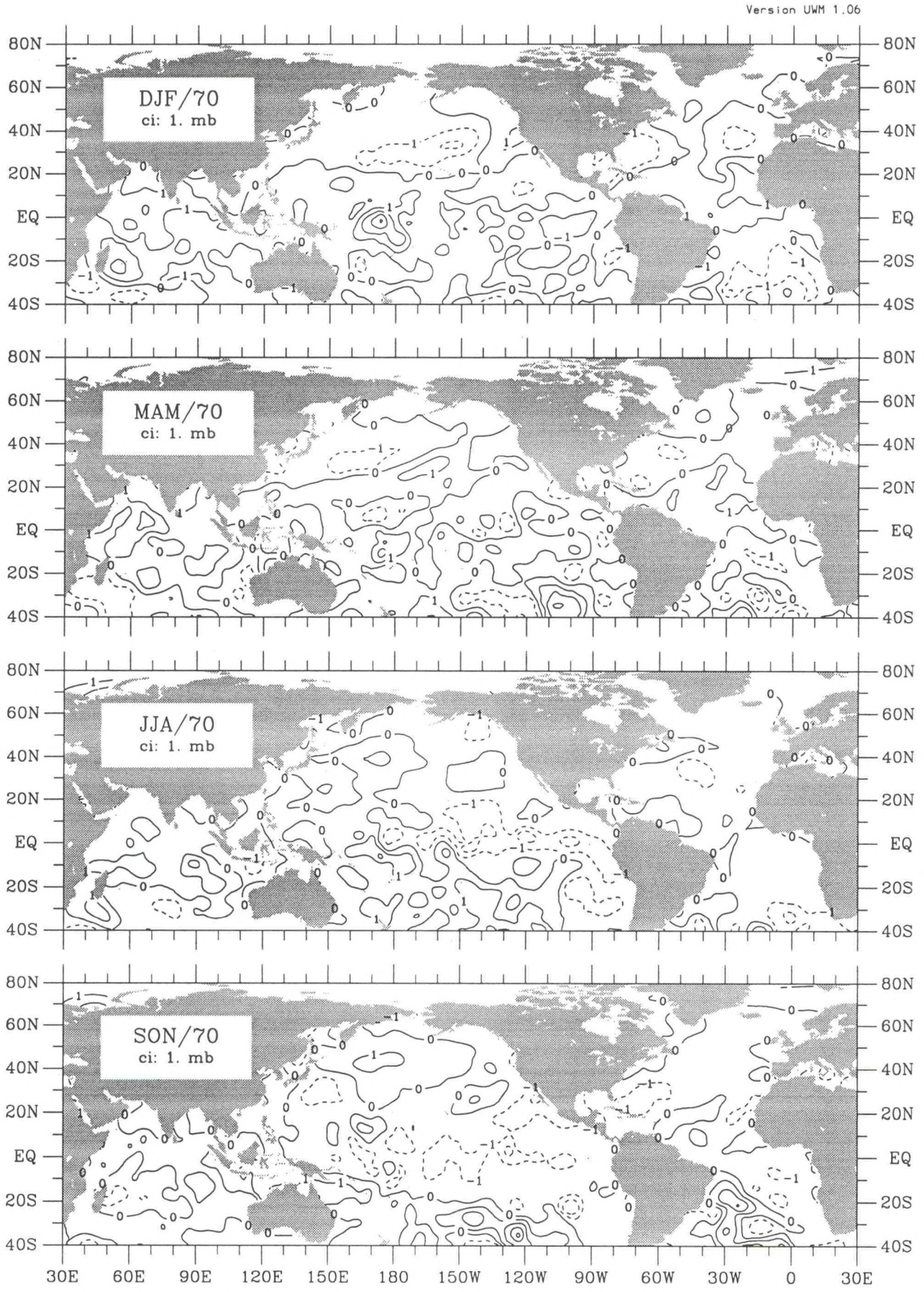

Figure e-31. Vapor pressure seasonal anomaly for 1970.

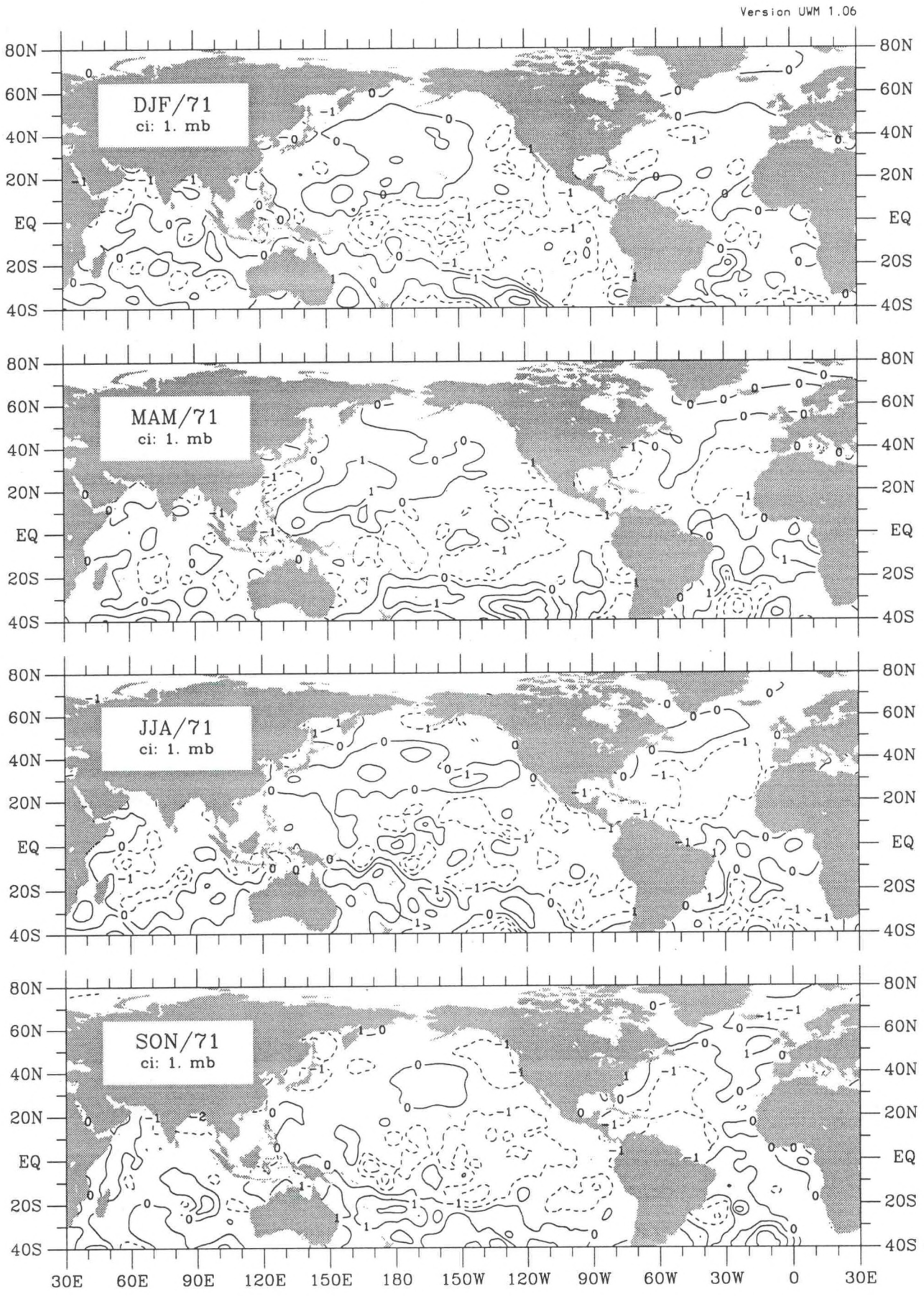

Figure e-32. Vapor pressure seasonal anomaly for 1971.

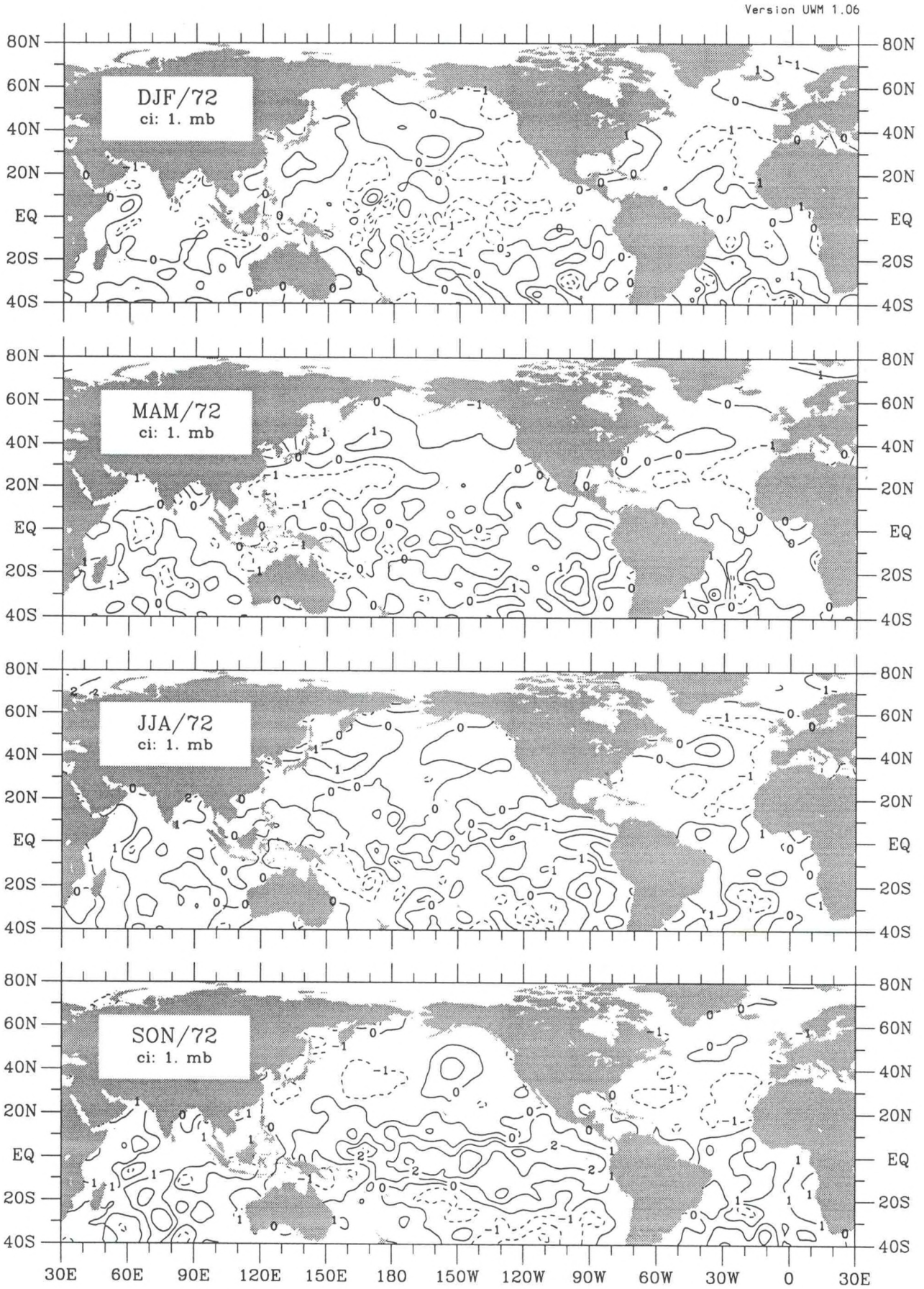

Figure e-33. Vapor pressure seasonal anomaly for 1972.

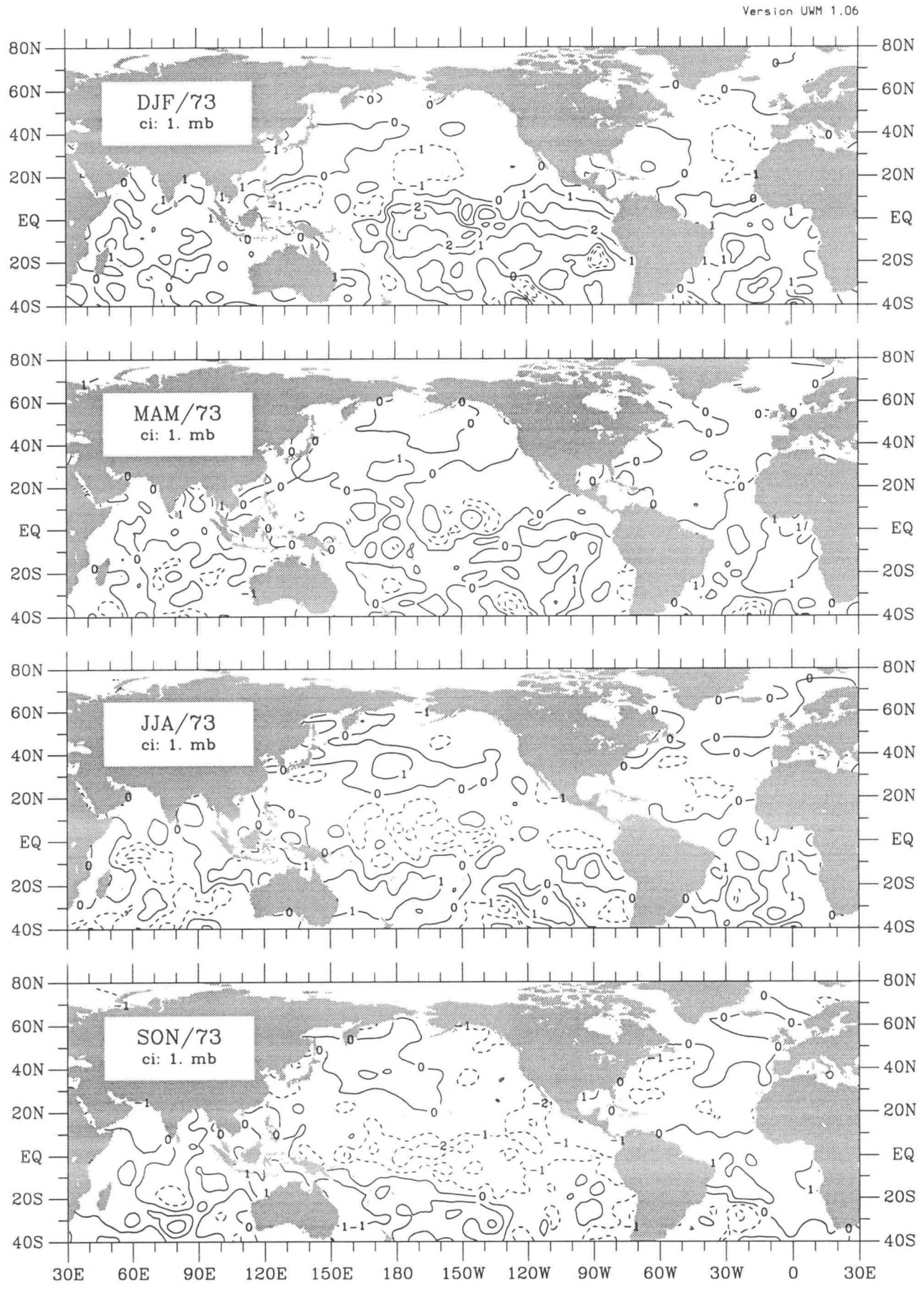

Figure e-34. Vapor pressure seasonal anomaly for 1973.

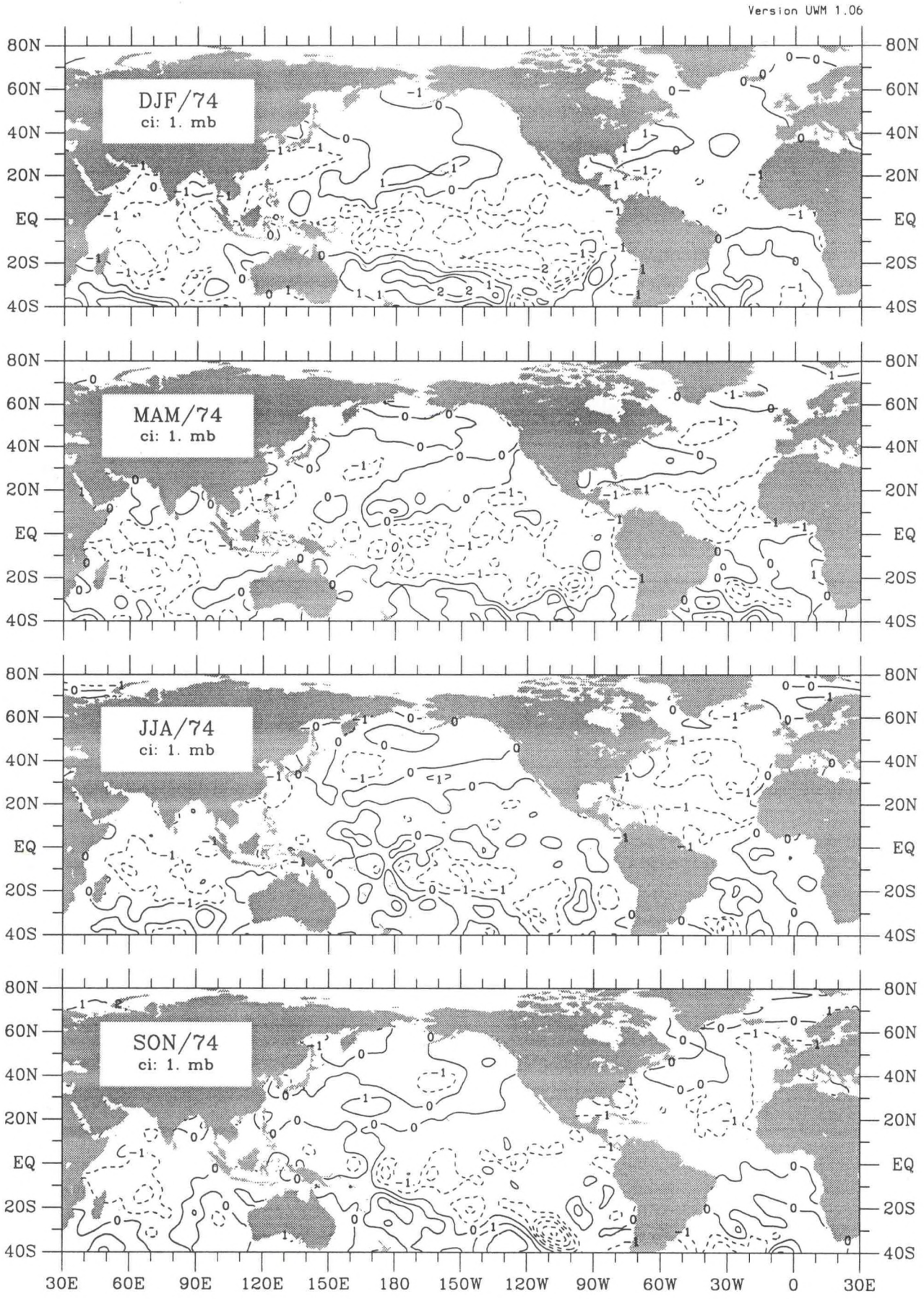

Figure e-35. Vapor pressure seasonal anomaly for 1974.

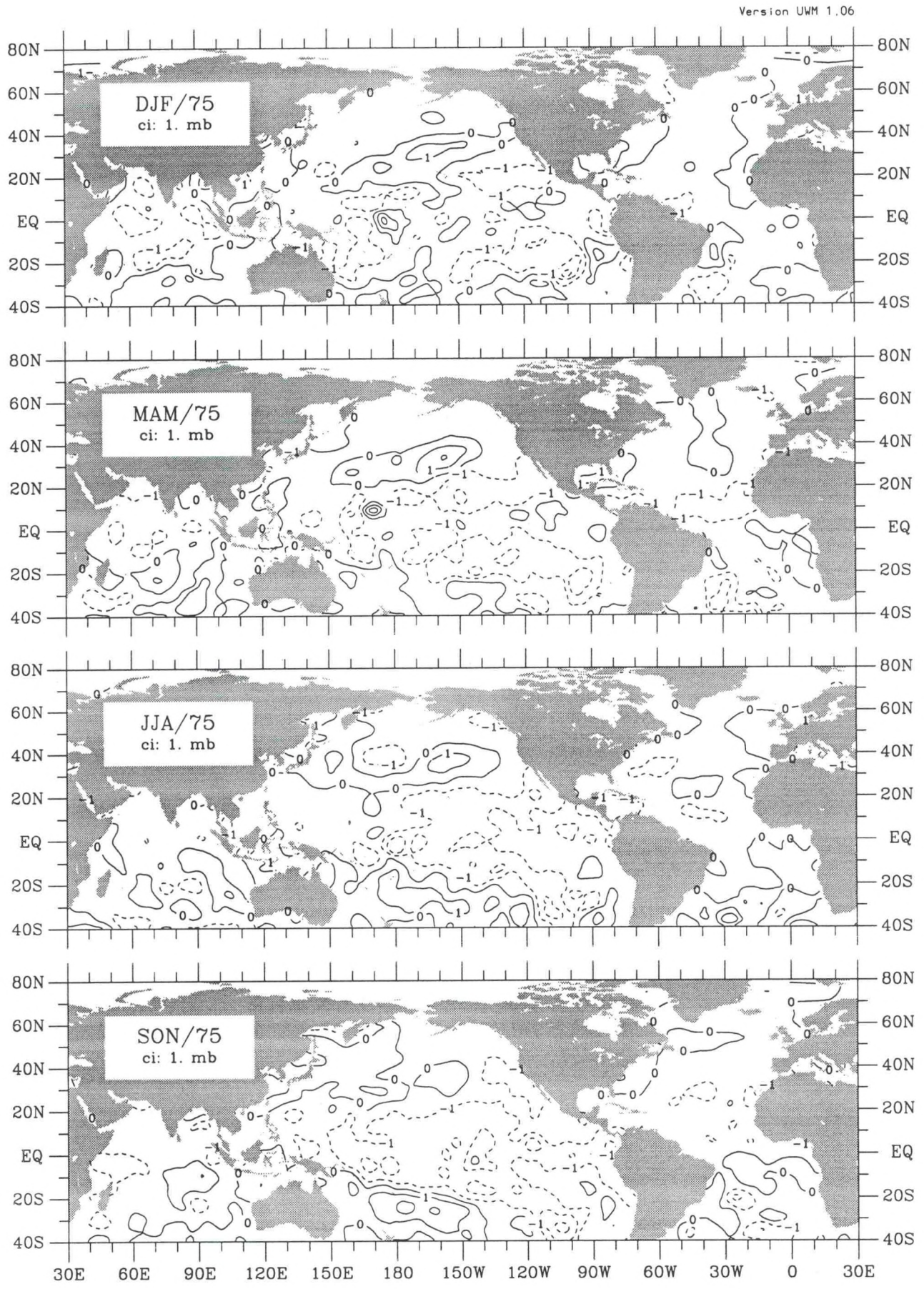

Figure e-36. Vapor pressure seasonal anomaly for 1975.

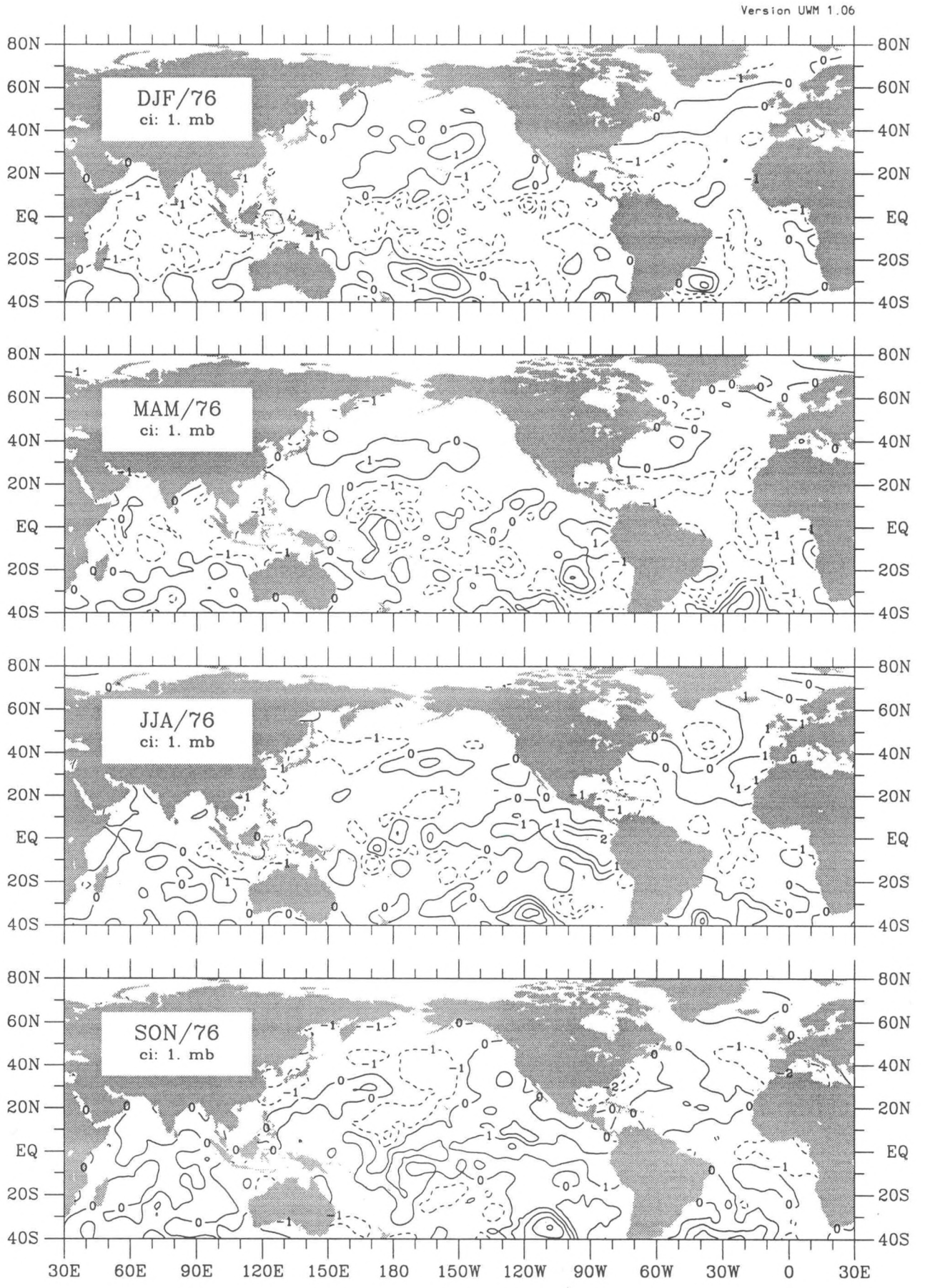

Figure e-37. Vapor pressure seasonal anomaly for 1976.

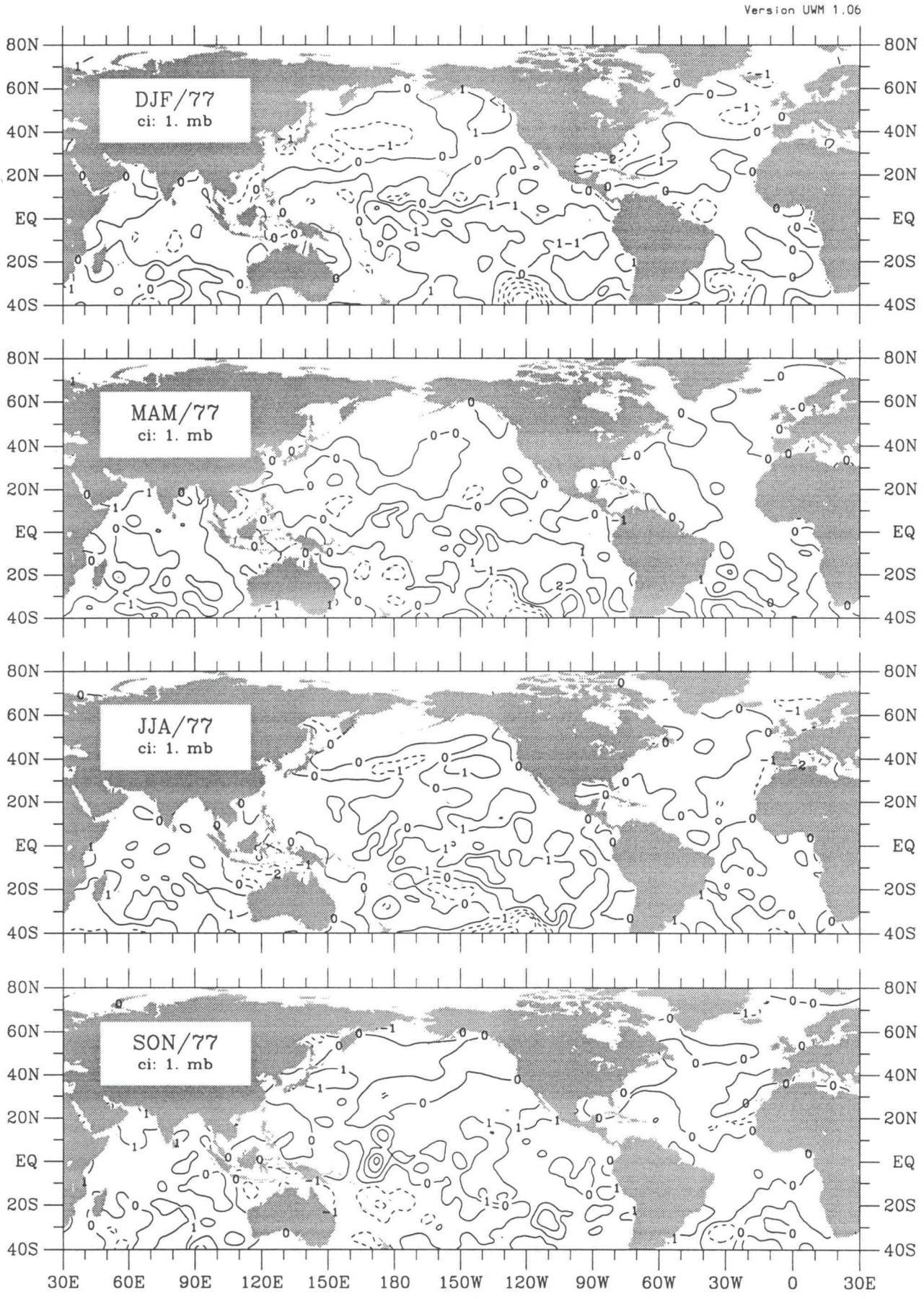

Figure e-38. Vapor pressure seasonal anomaly for 1977.

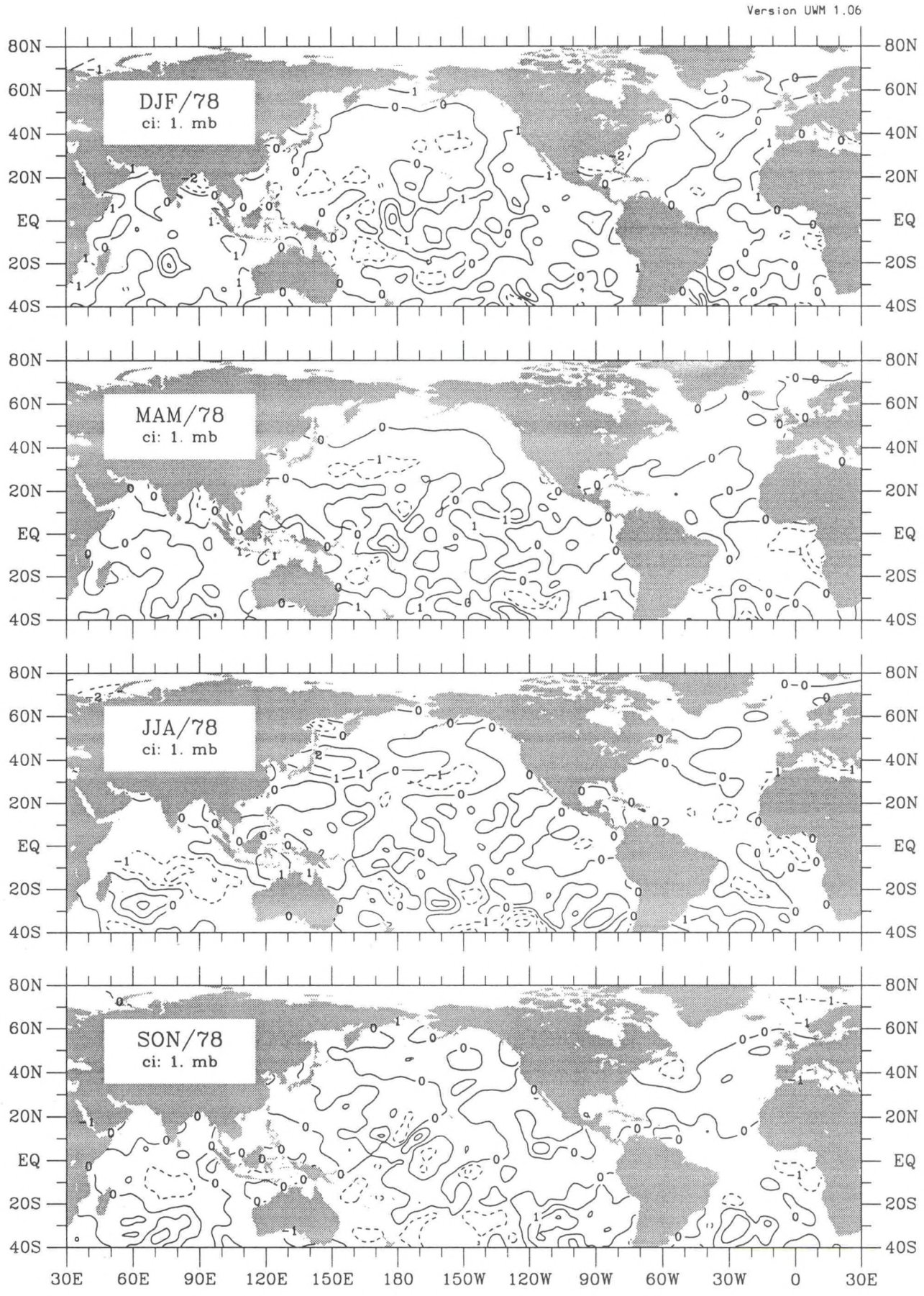

Figure e-39. Vapor pressure seasonal anomaly for 1978.

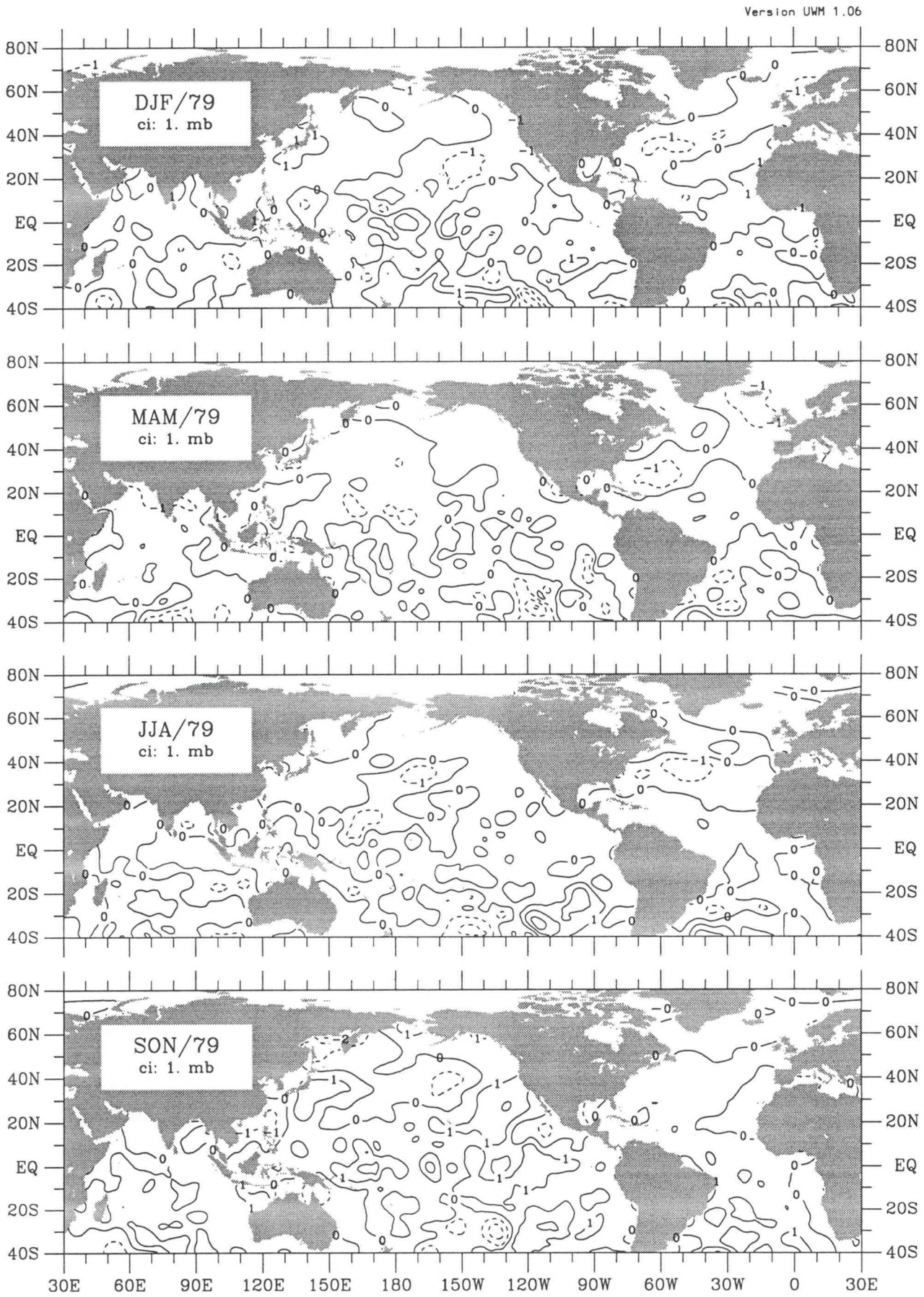

Figure e-40. Vapor pressure seasonal anomaly for 1979.

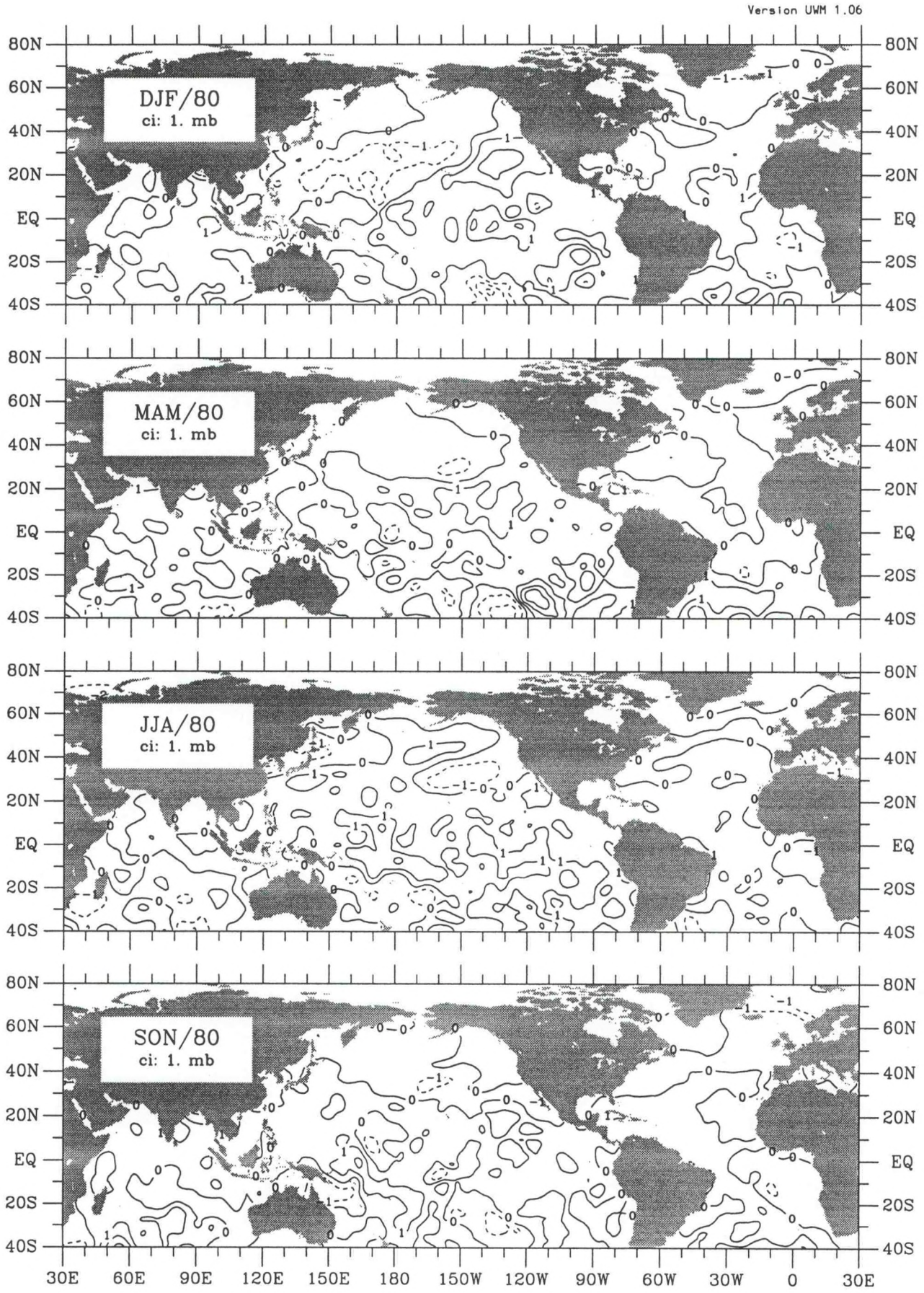

Figure e-41. Vapor pressure seasonal anomaly for 1980.

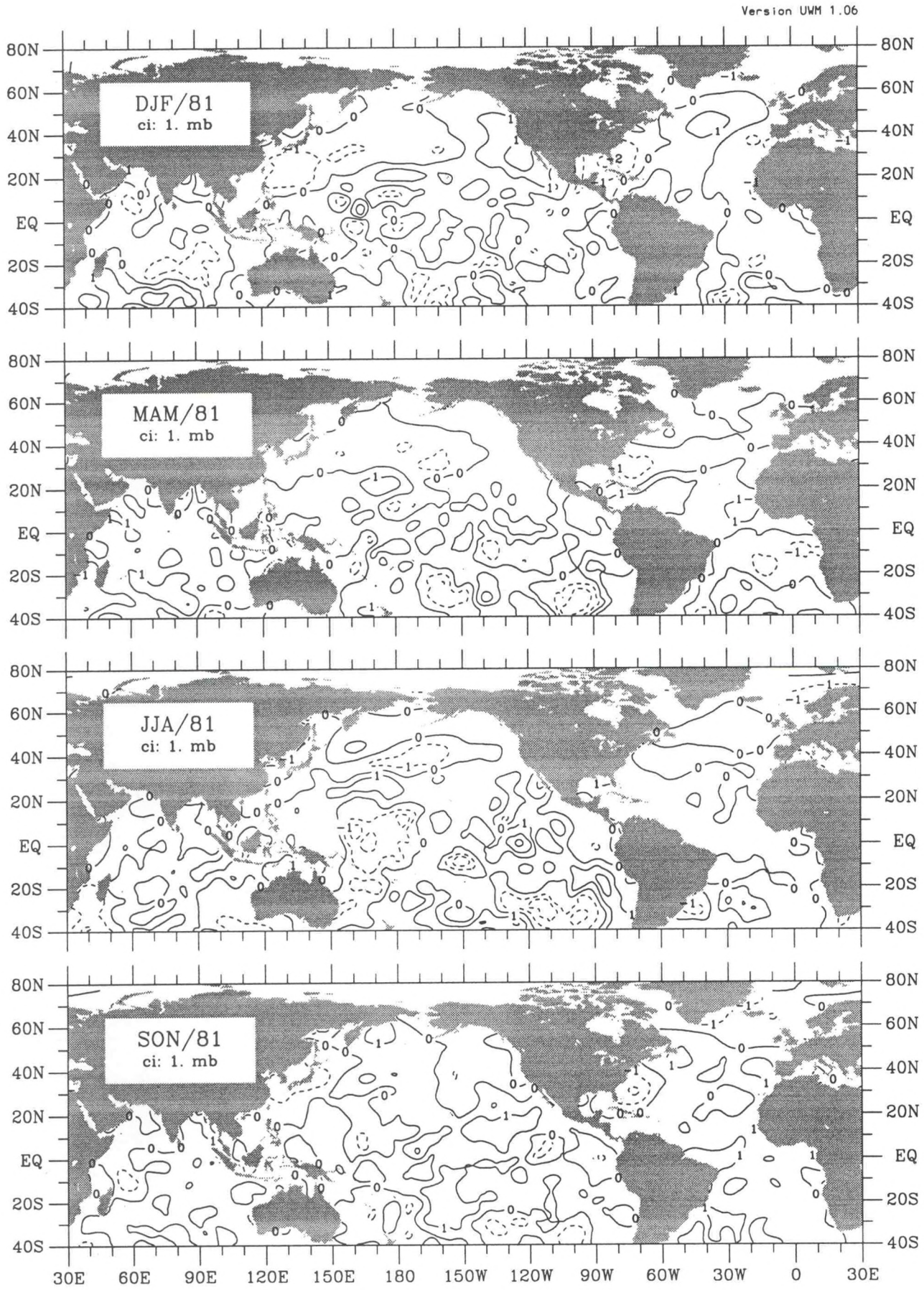

Figure e-42. Vapor pressure seasonal anomaly for 1981.

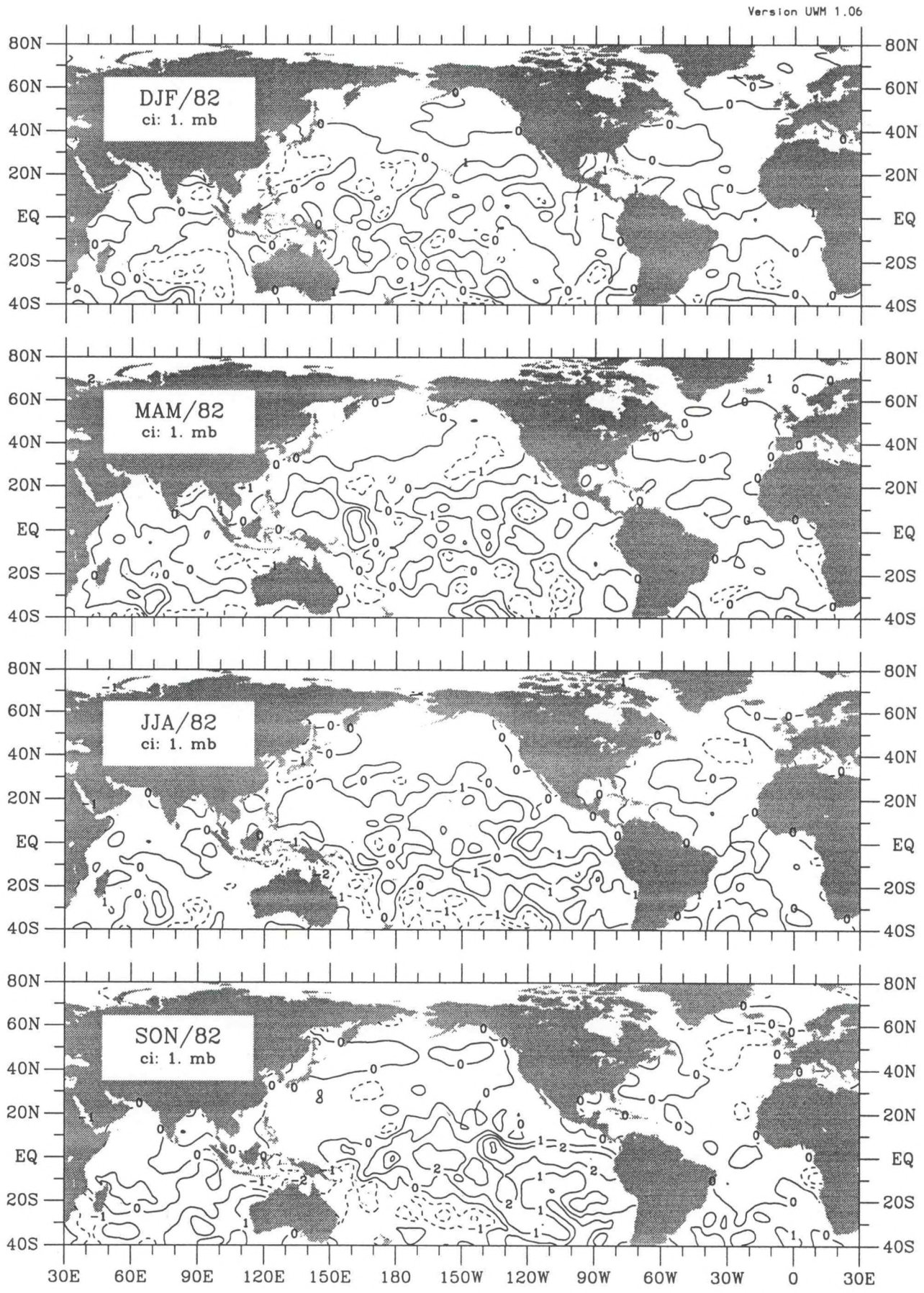

Figure e-43. Vapor pressure seasonal anomaly for 1982.

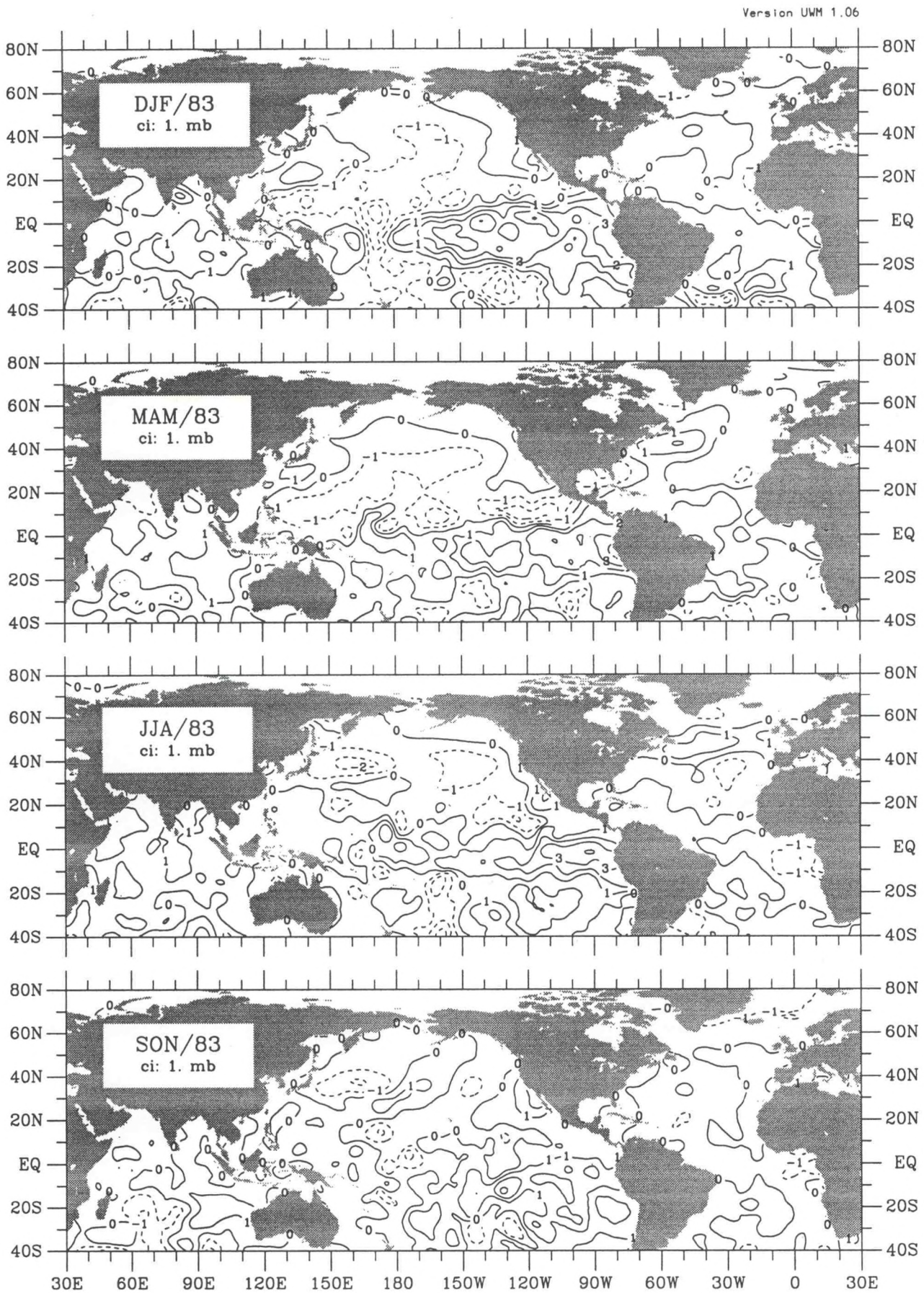

Figure e-44. Vapor pressure seasonal anomaly for 1983.

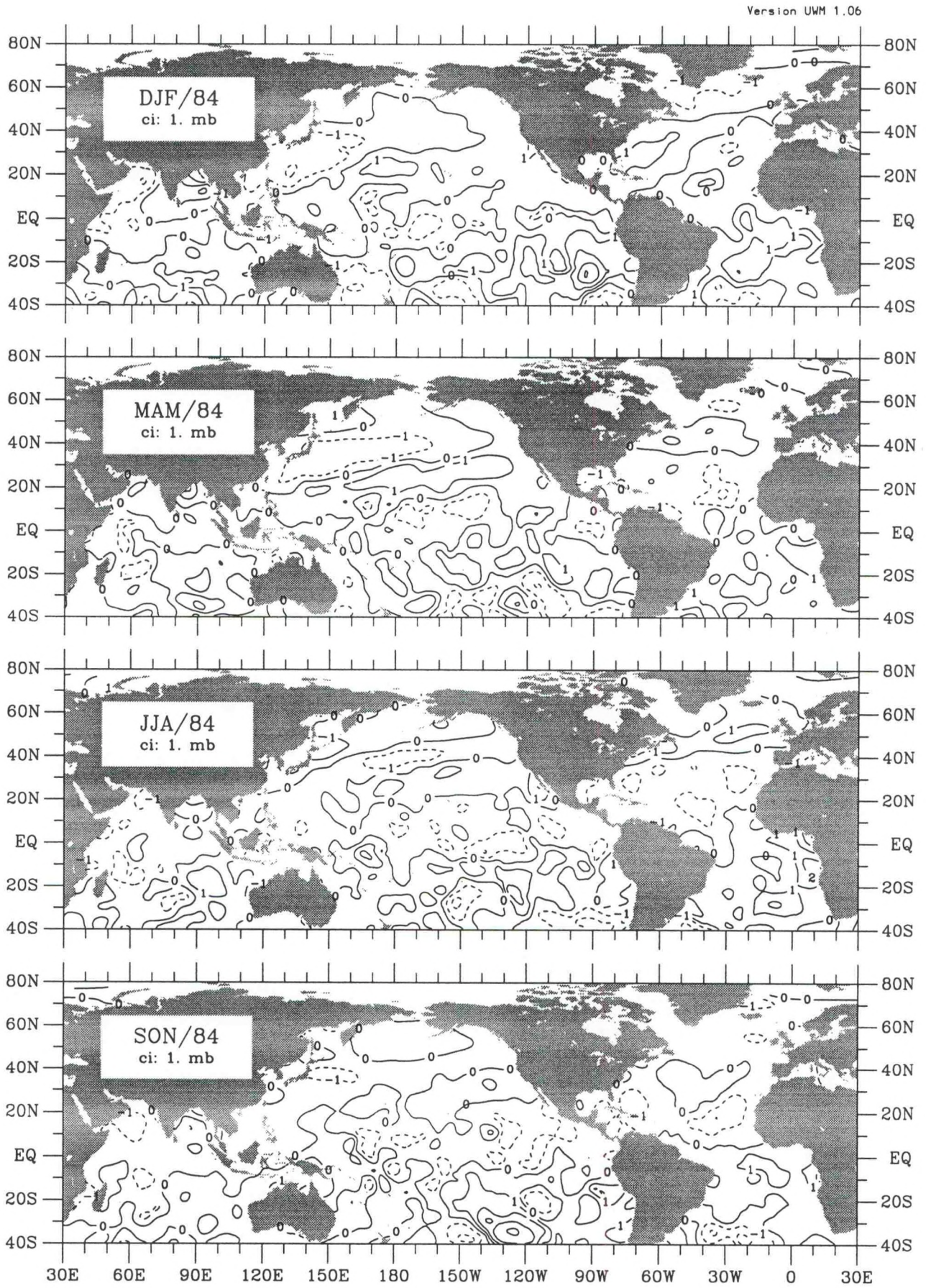

Figure e-45. Vapor pressure seasonal anomaly for 1984.

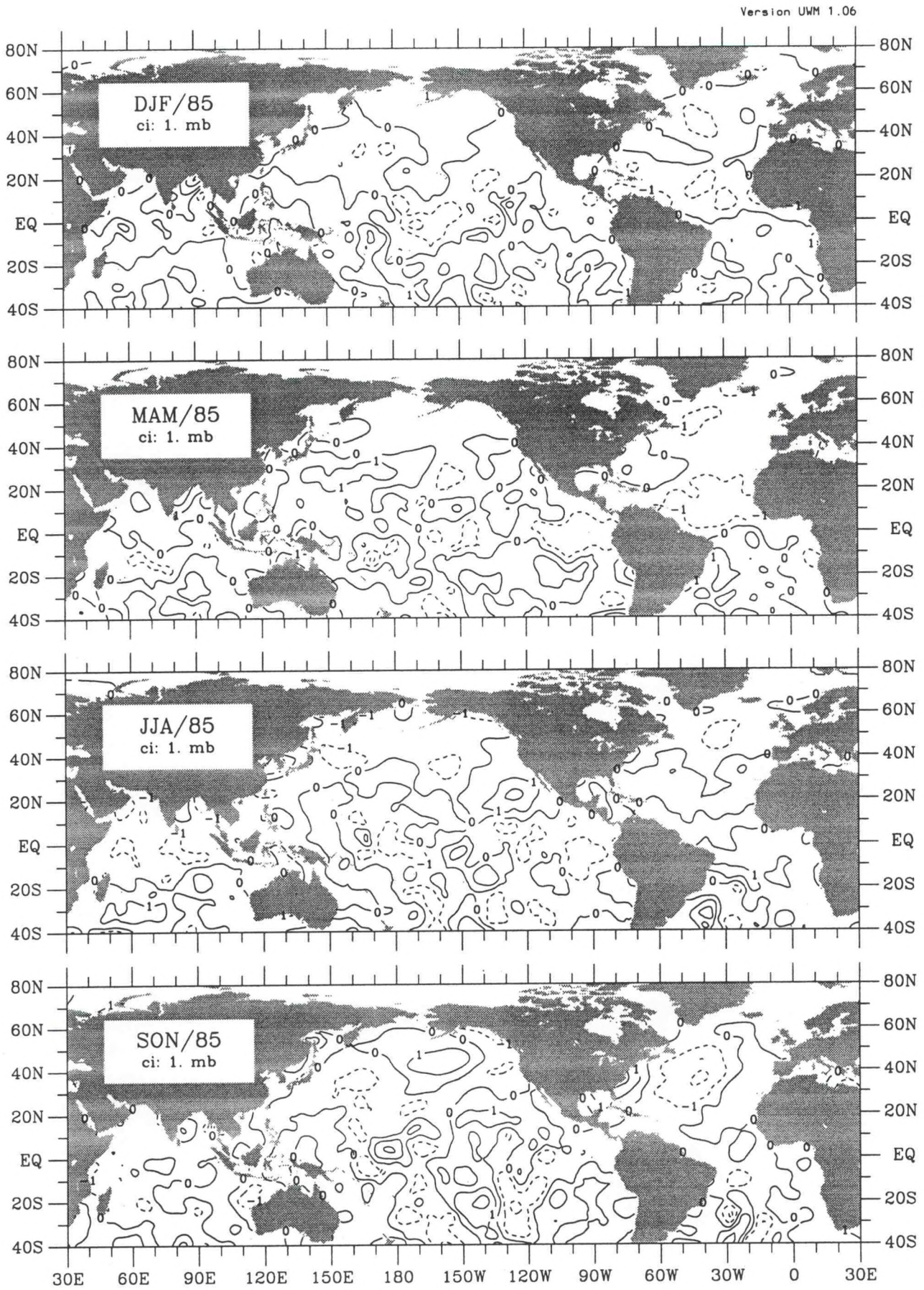

Figure e-46. Vapor pressure seasonal anomaly for 1985.

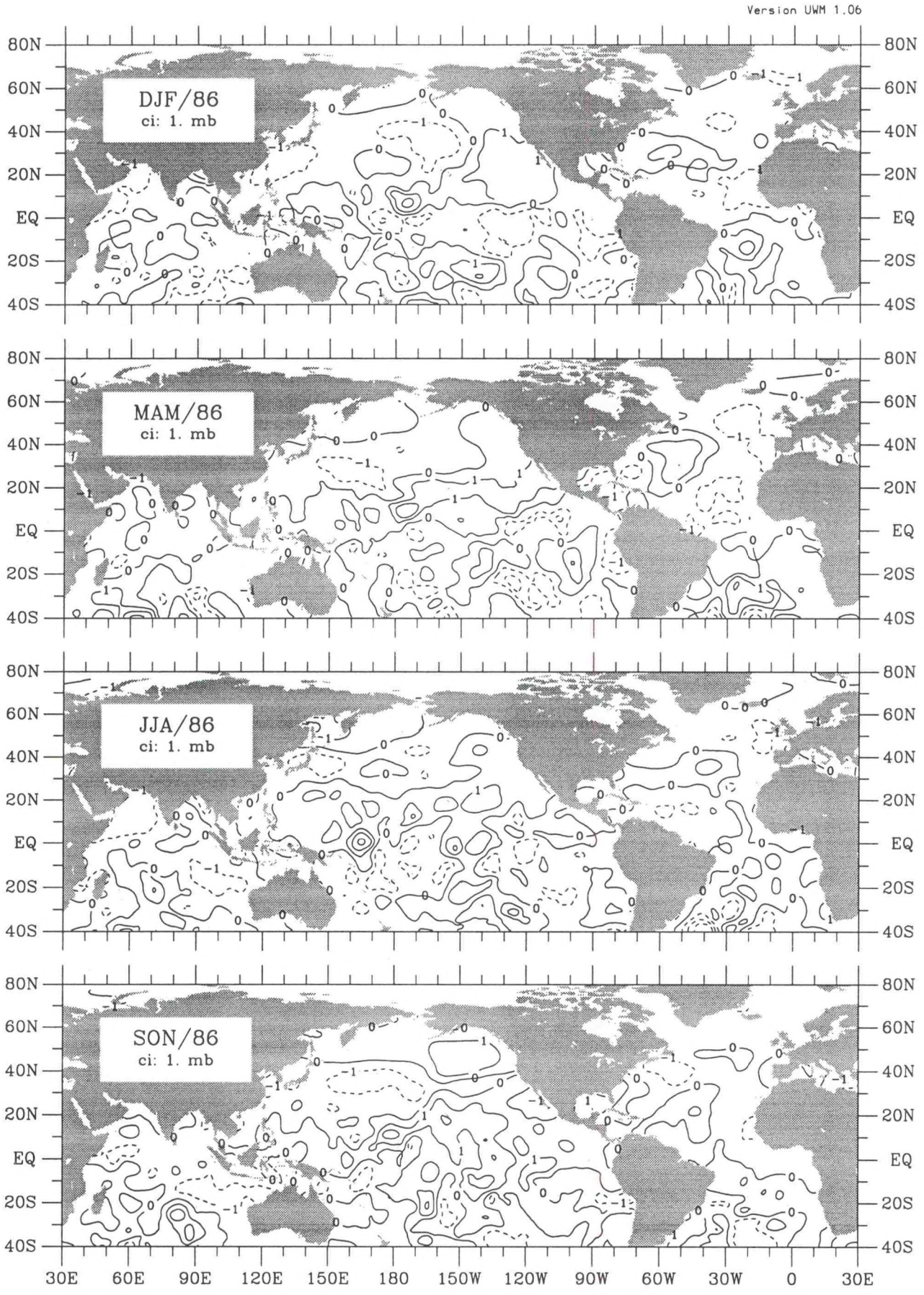

Figure e-47. Vapor pressure seasonal anomaly for 1986.

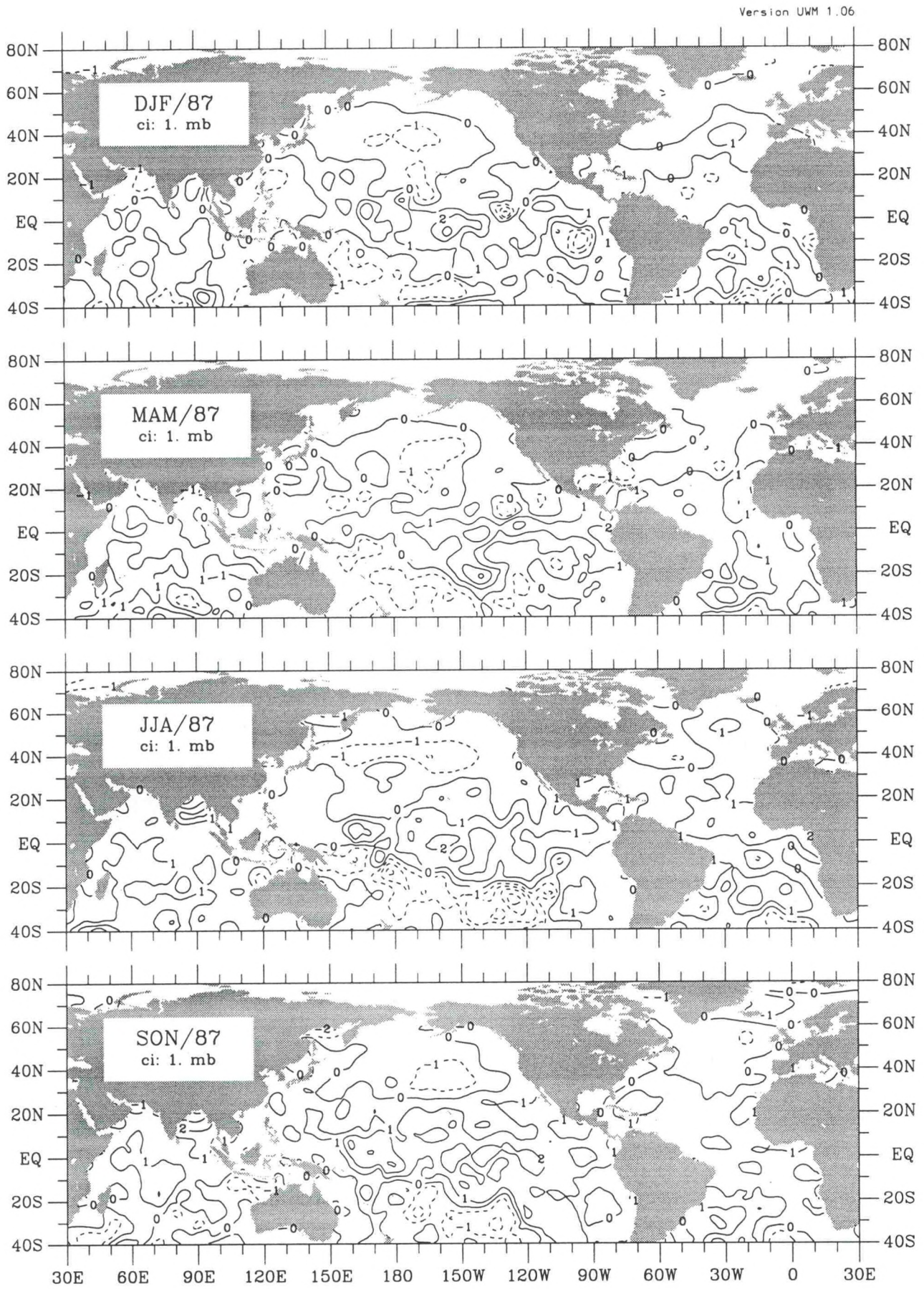

Figure e-48. Vapor pressure seasonal anomaly for 1987.

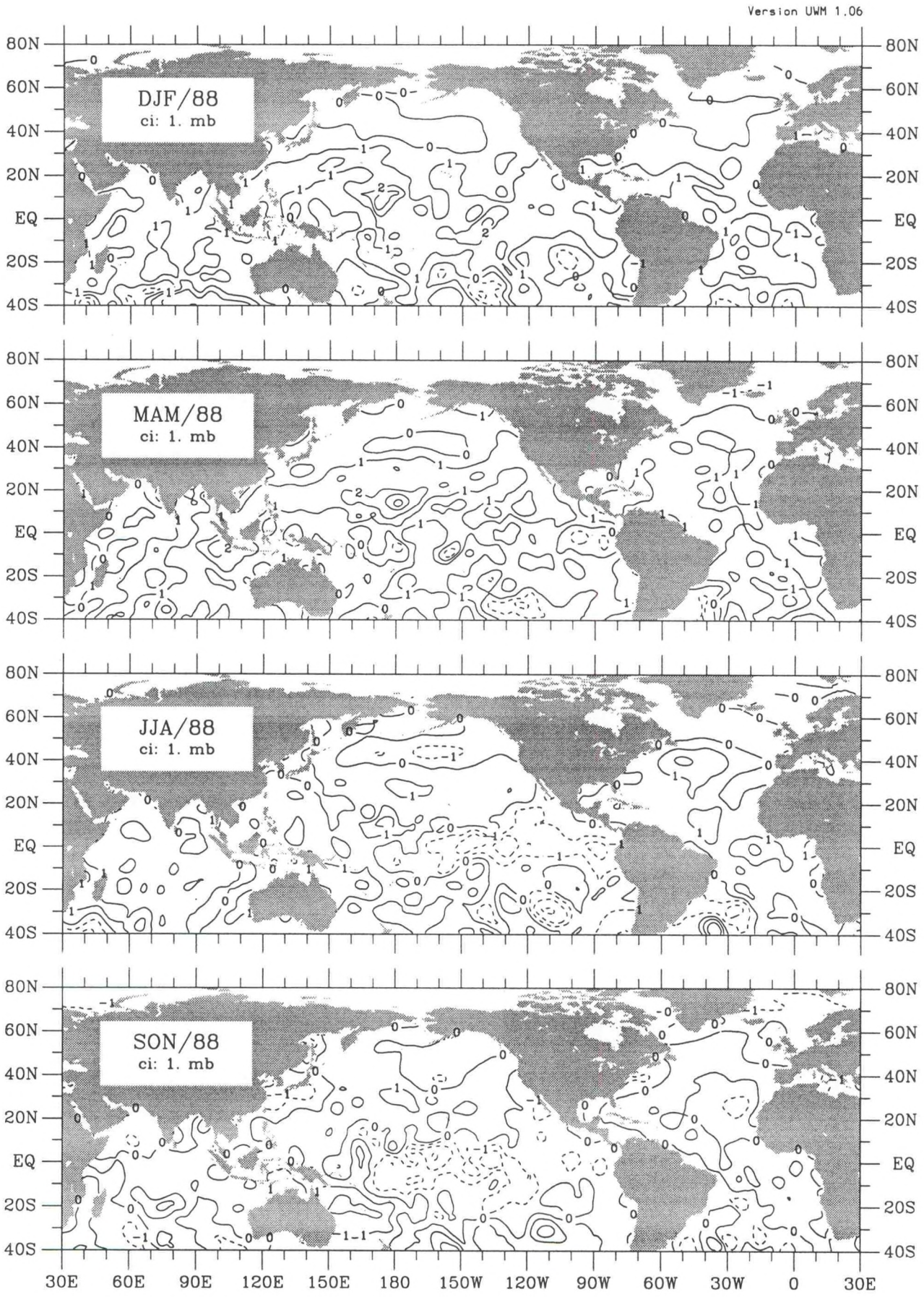

Figure e-49. Vapor pressure seasonal anomaly for 1988.

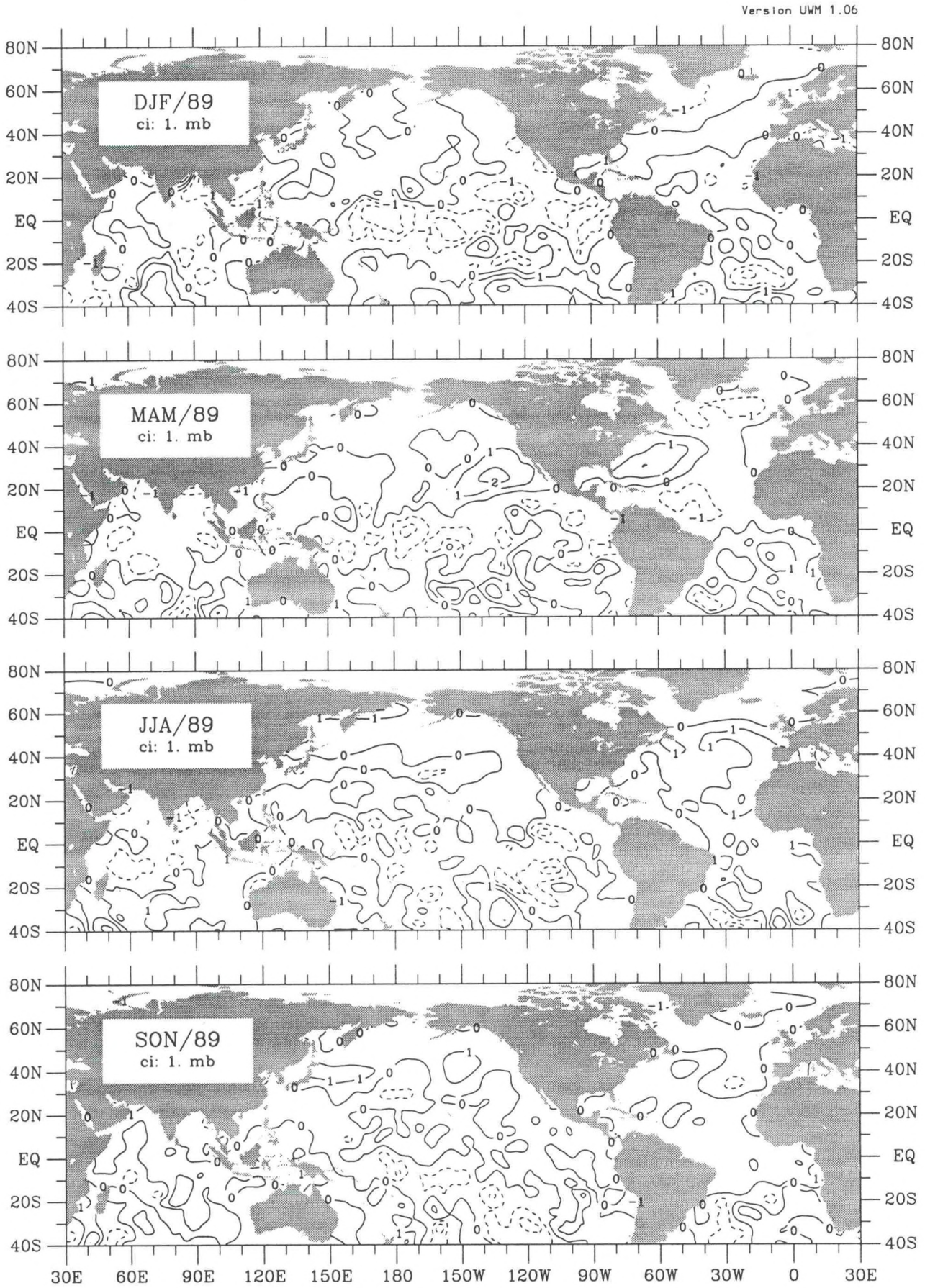

Figure e-50. Vapor pressure seasonal anomaly for 1989.

15 Zonal heat flux

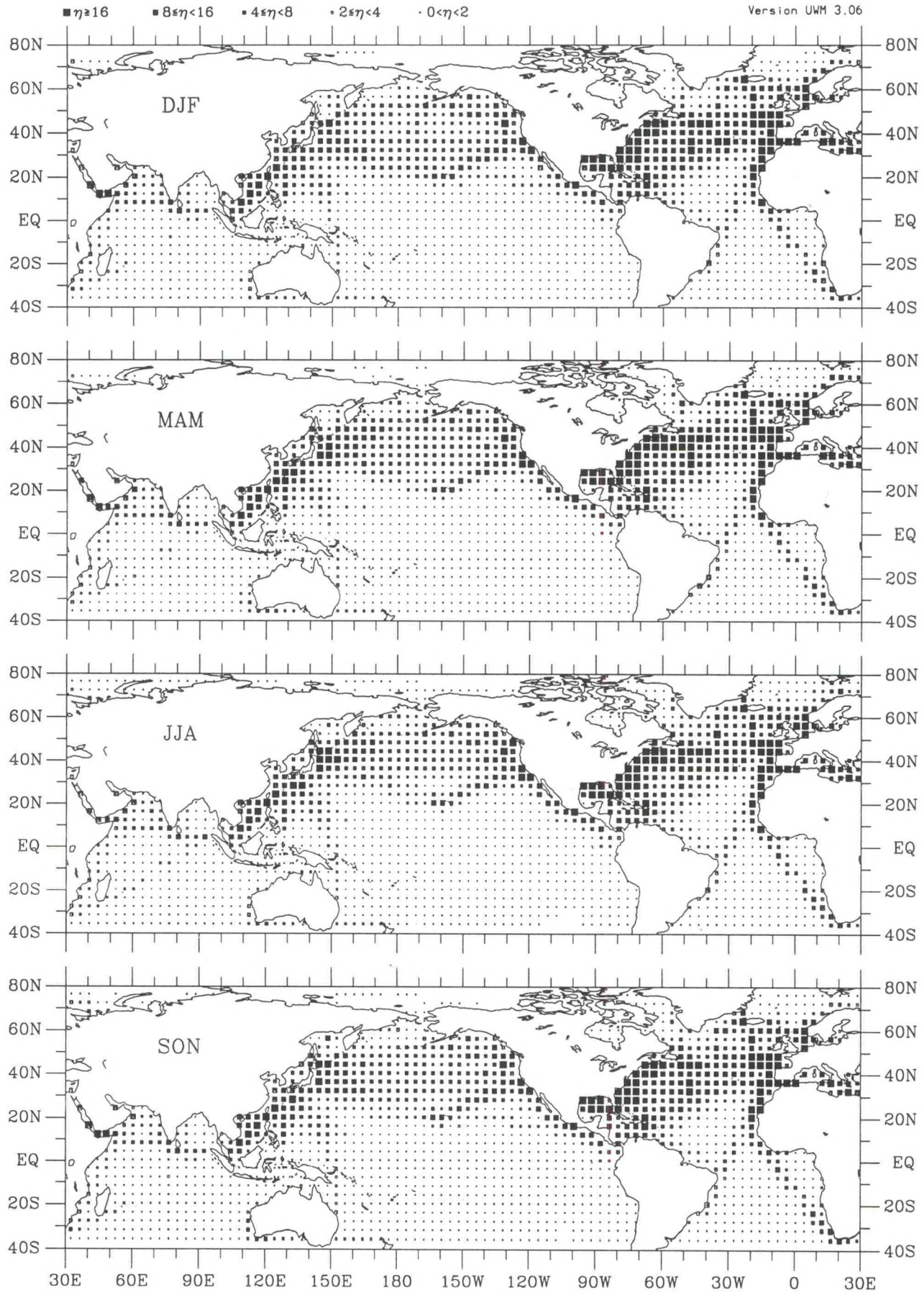

Figure ua-1. Zonal heat flux seasonal observation density (1945-89).

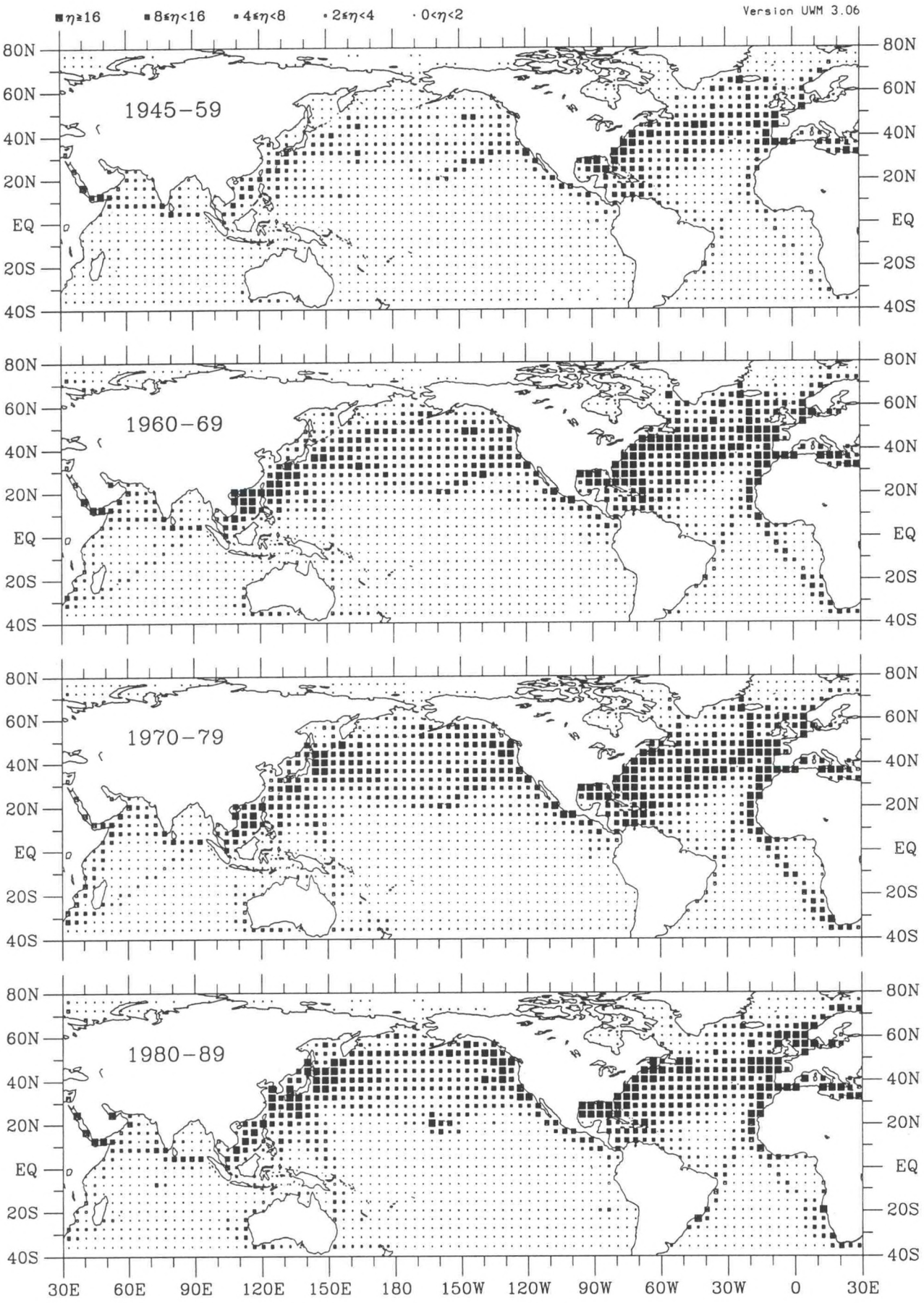

Figure ua-2. Zonal heat flux decadal observation density.

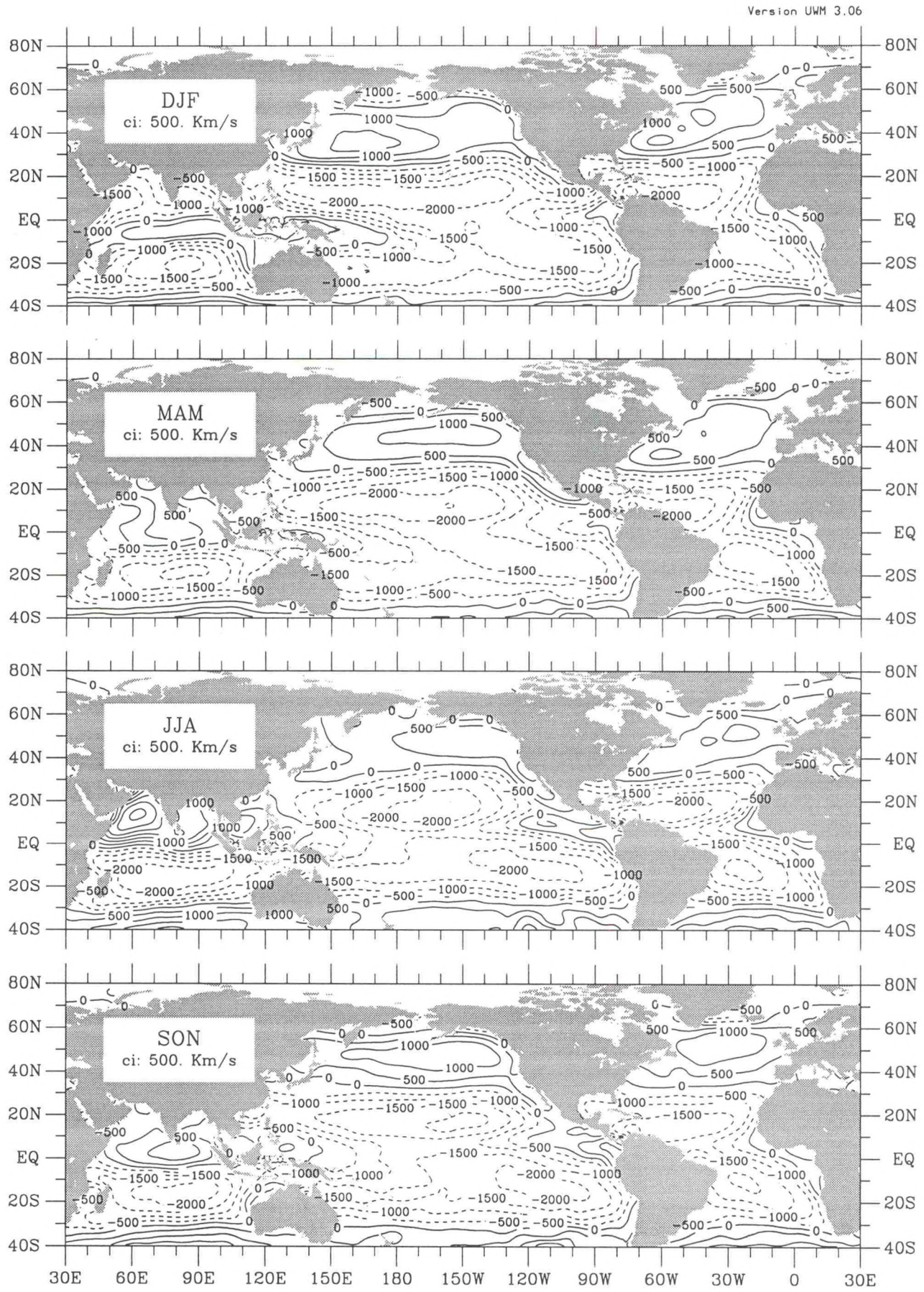

Figure ua-3. Zonal heat flux seasonal climatology (1945-89).

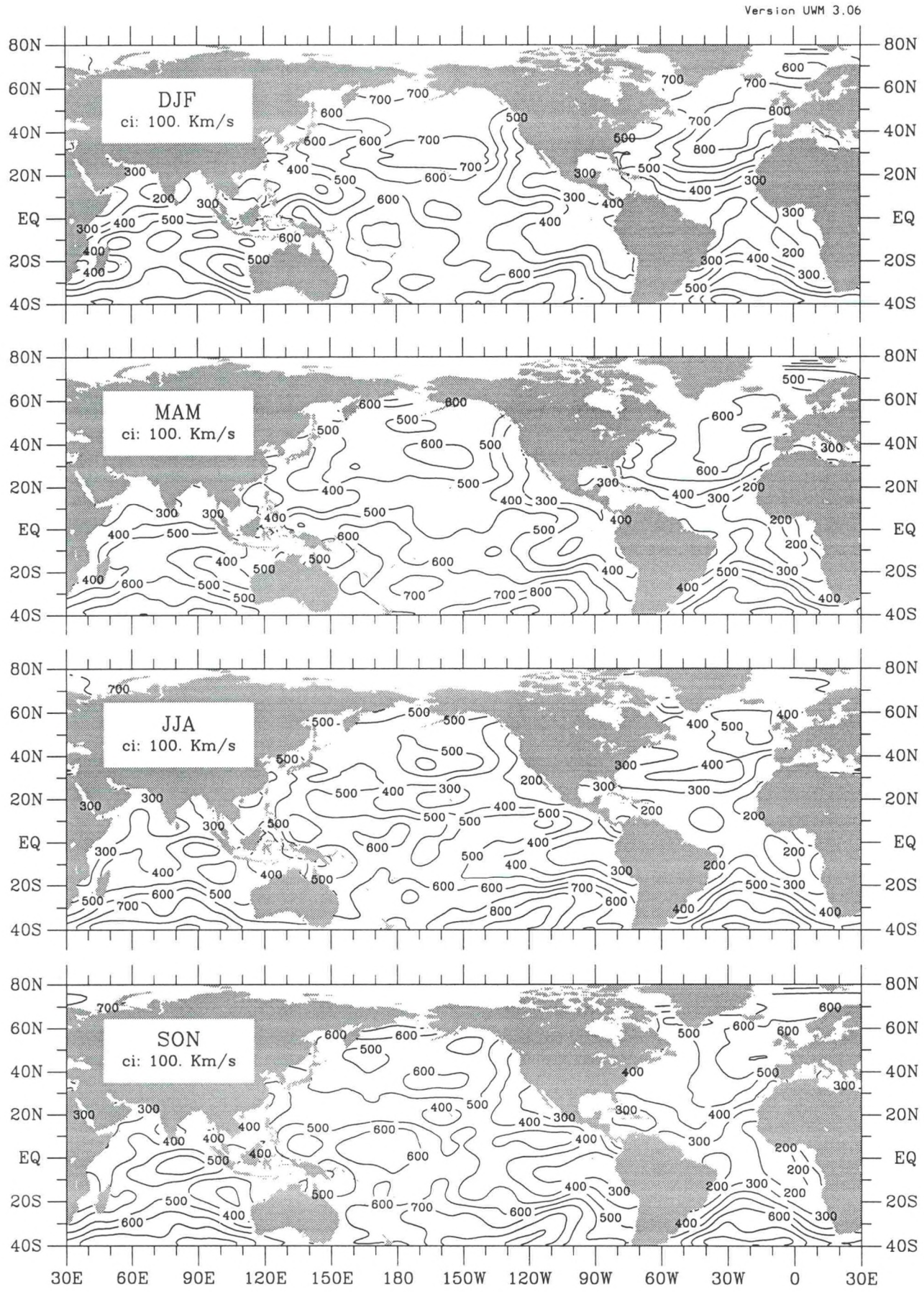

Figure ua-4. Zonal heat flux seasonal interannual std dev (1945-89).

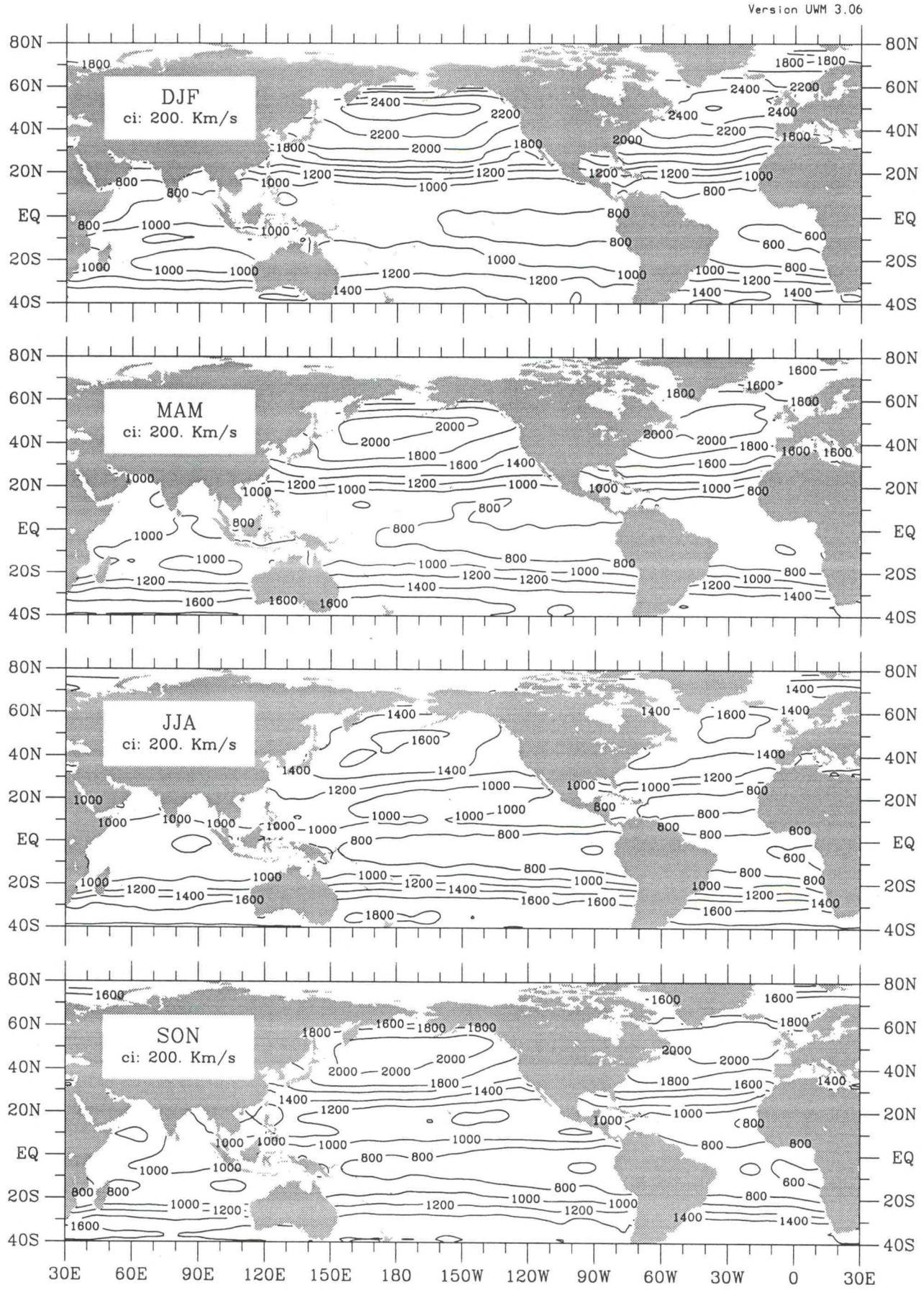

Figure ua-5. Zonal heat flux seasonal standard deviation (1945-89).

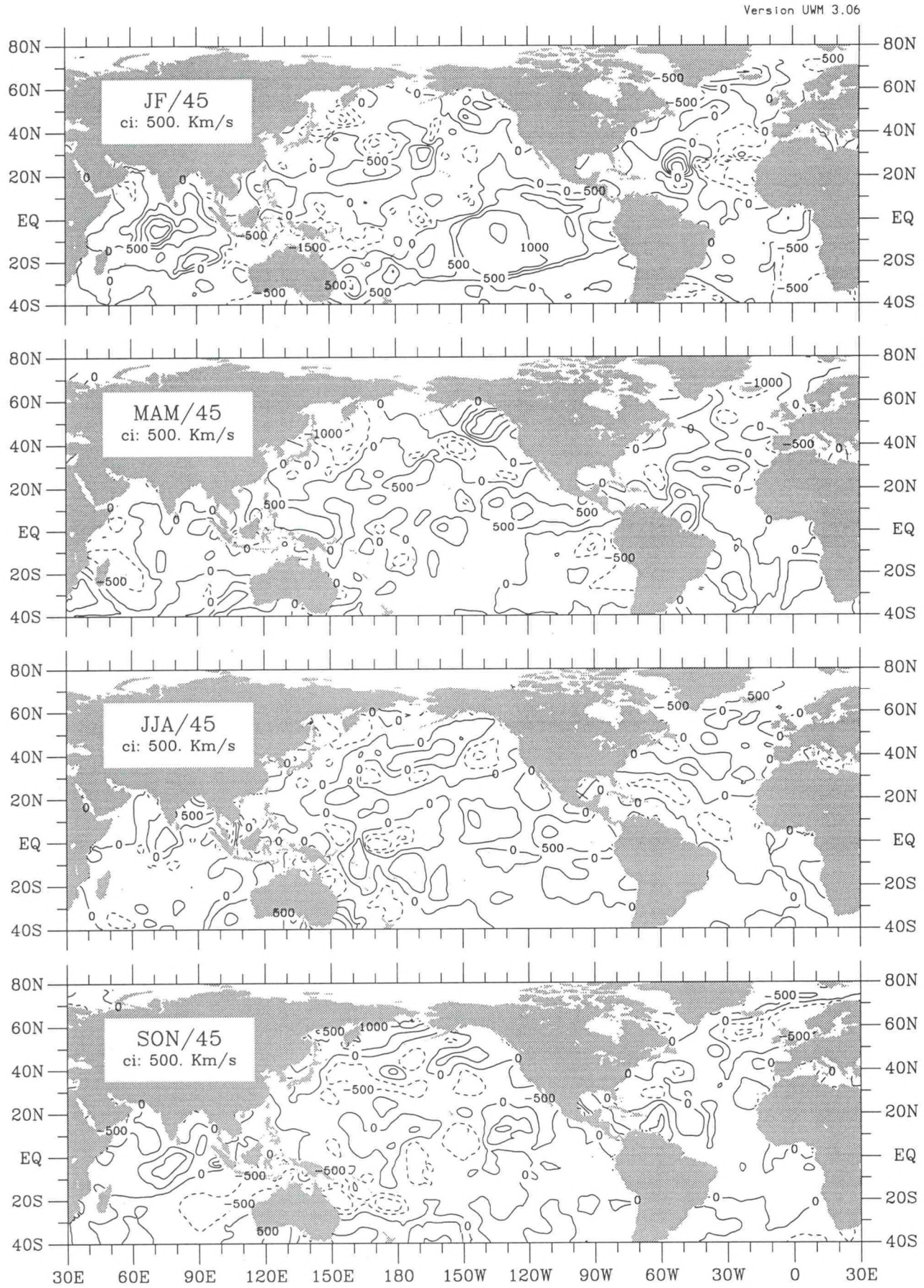

Figure ua-6. Zonal heat flux seasonal anomaly for 1945.

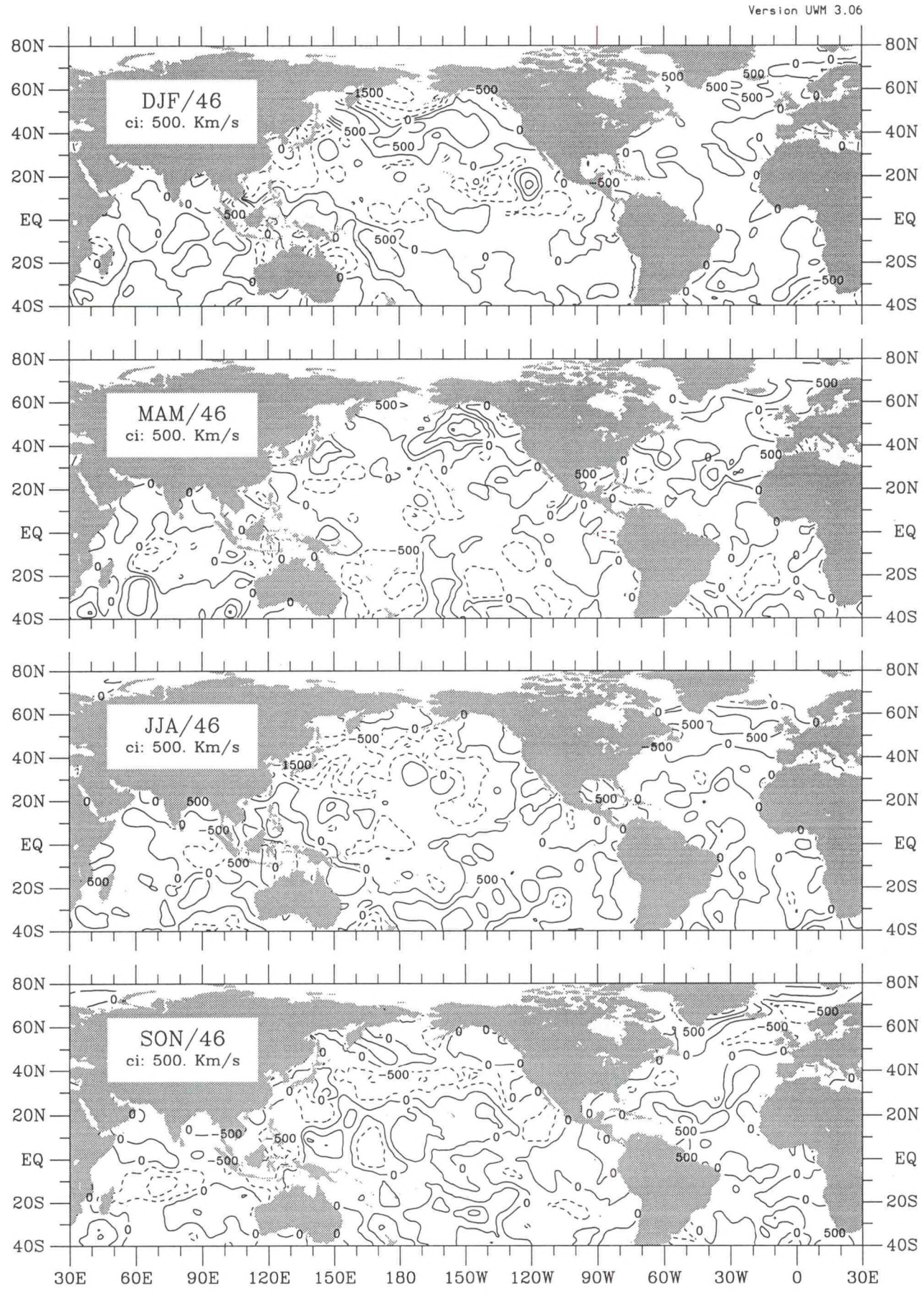

Figure ua-7. Zonal heat flux seasonal anomaly for 1946.

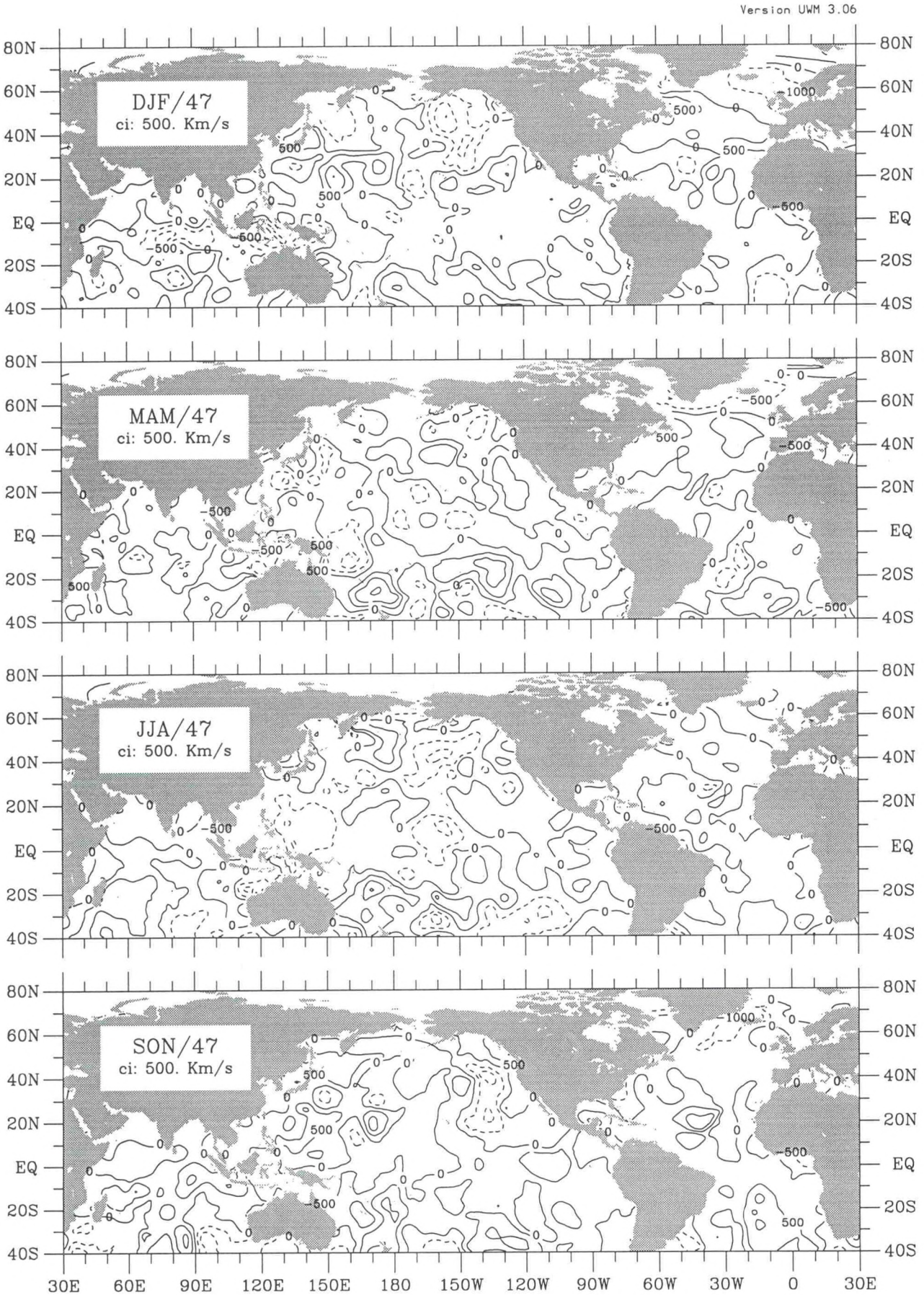

Figure ua-8. Zonal heat flux seasonal anomaly for 1947.

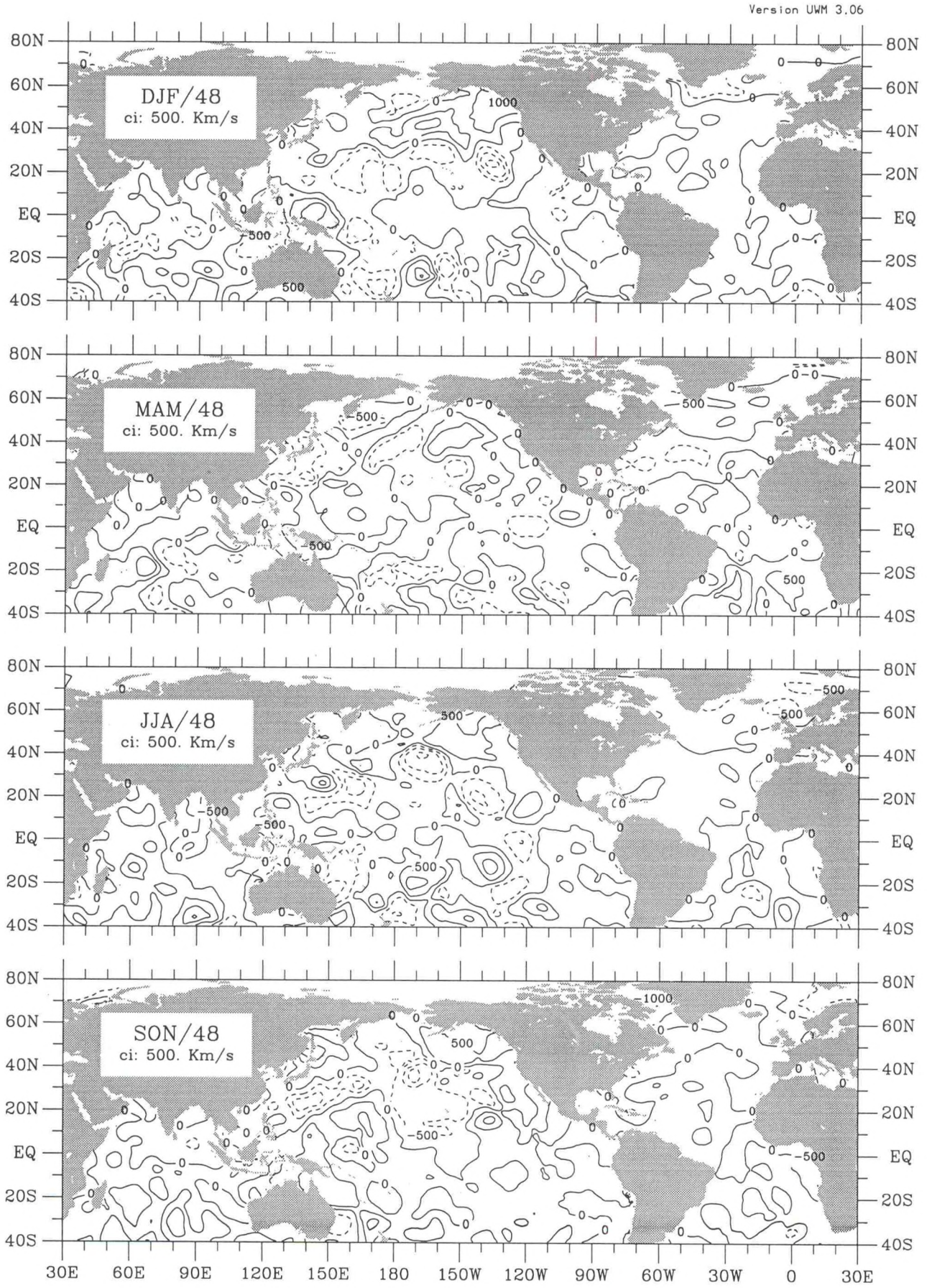

Figure ua-9. Zonal heat flux seasonal anomaly for 1948.

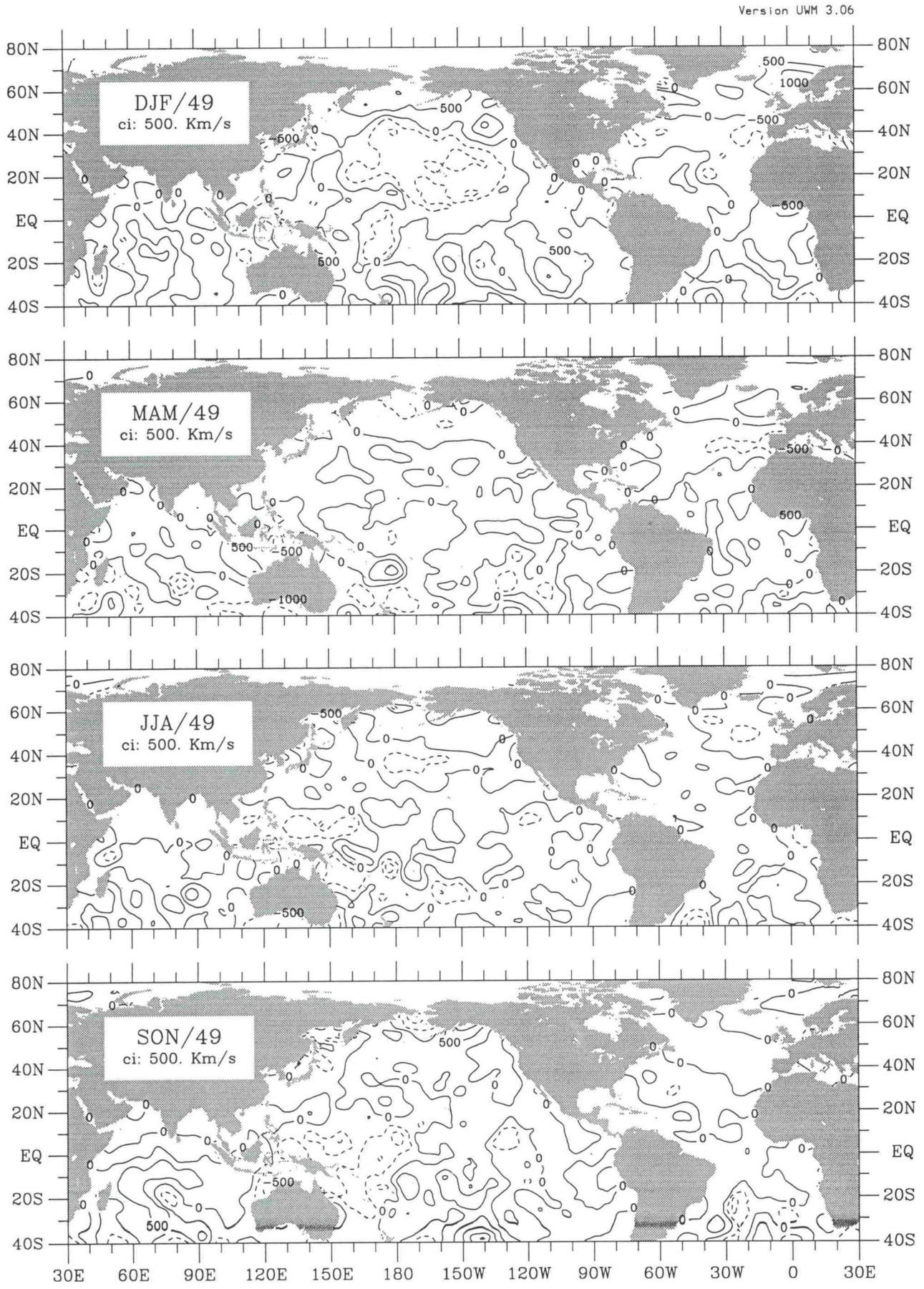

Figure ua-10. Zonal heat flux seasonal anomaly for 1949.

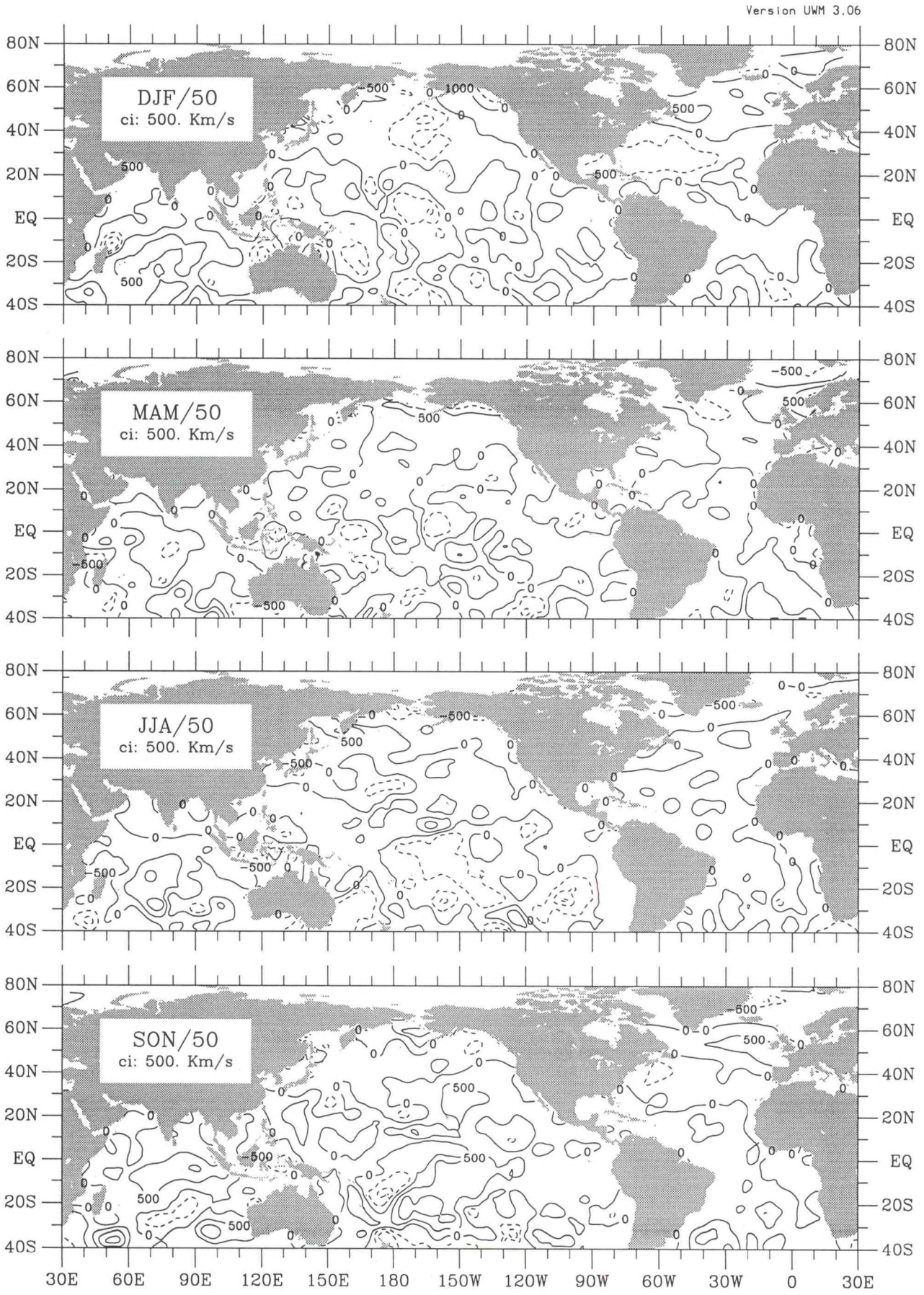

Figure ua-11. Zonal heat flux seasonal anomaly for 1950.

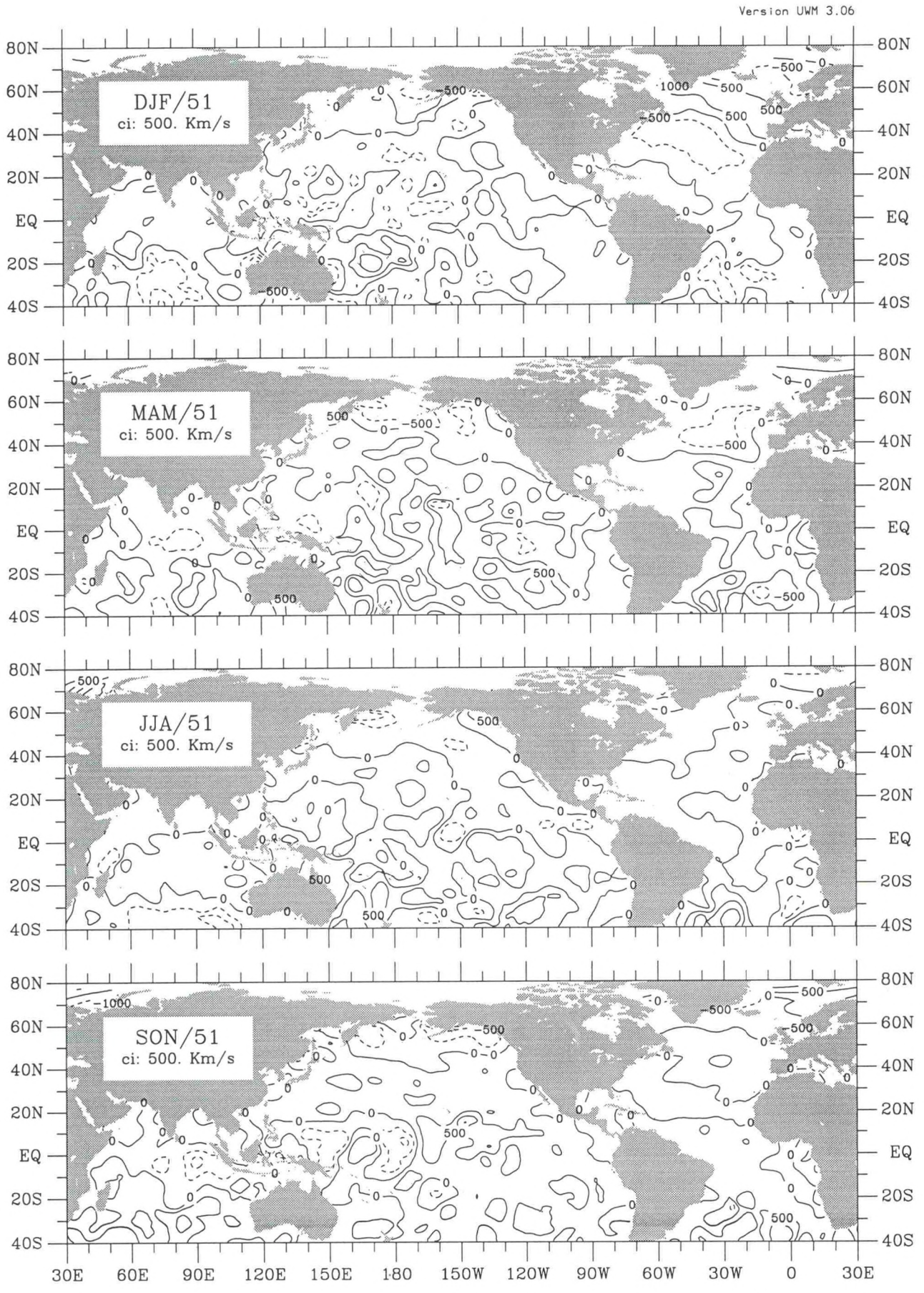

Figure ua-12. Zonal heat flux seasonal anomaly for 1951.

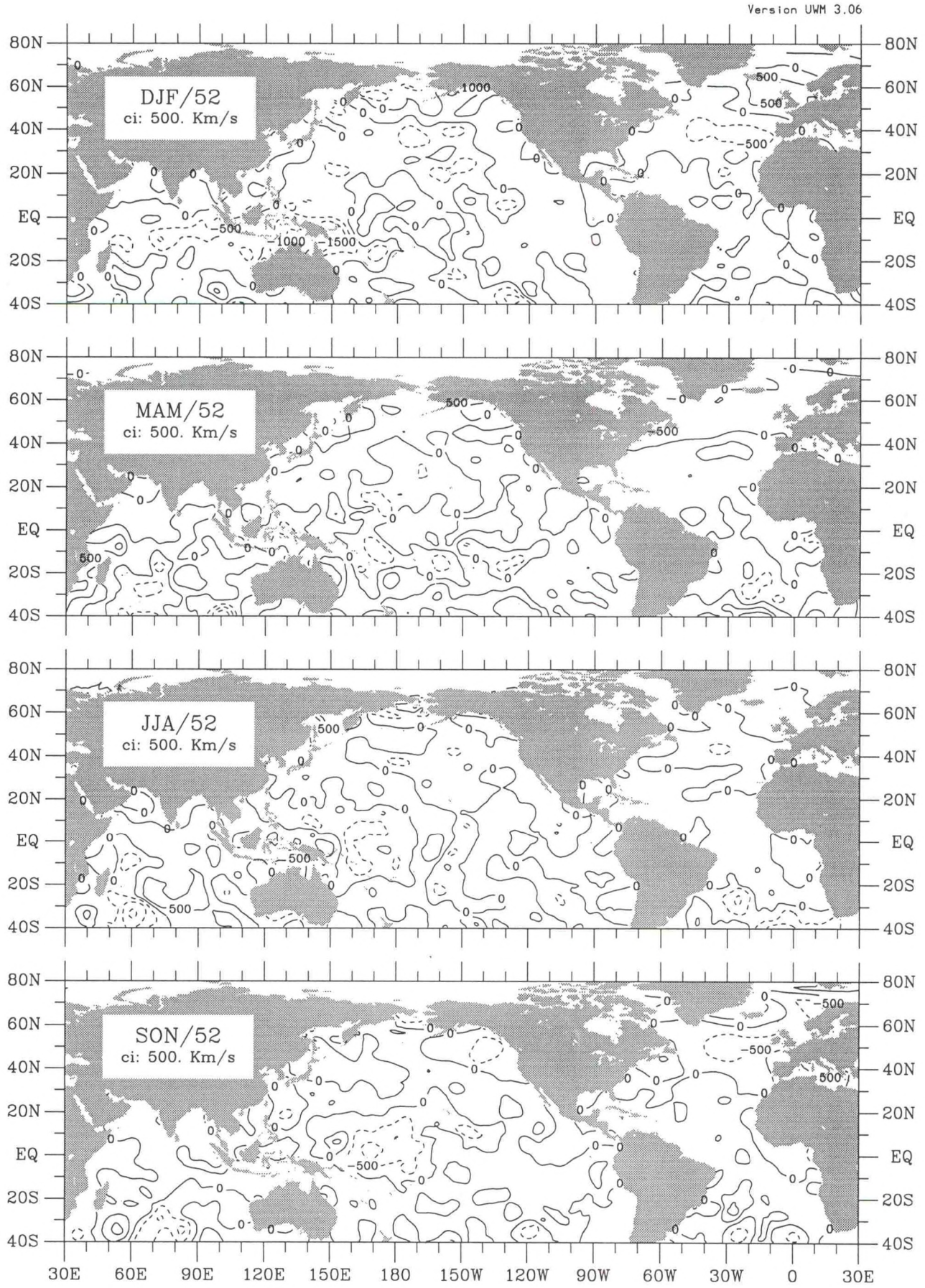

Figure ua-13. Zonal heat flux seasonal anomaly for 1952.

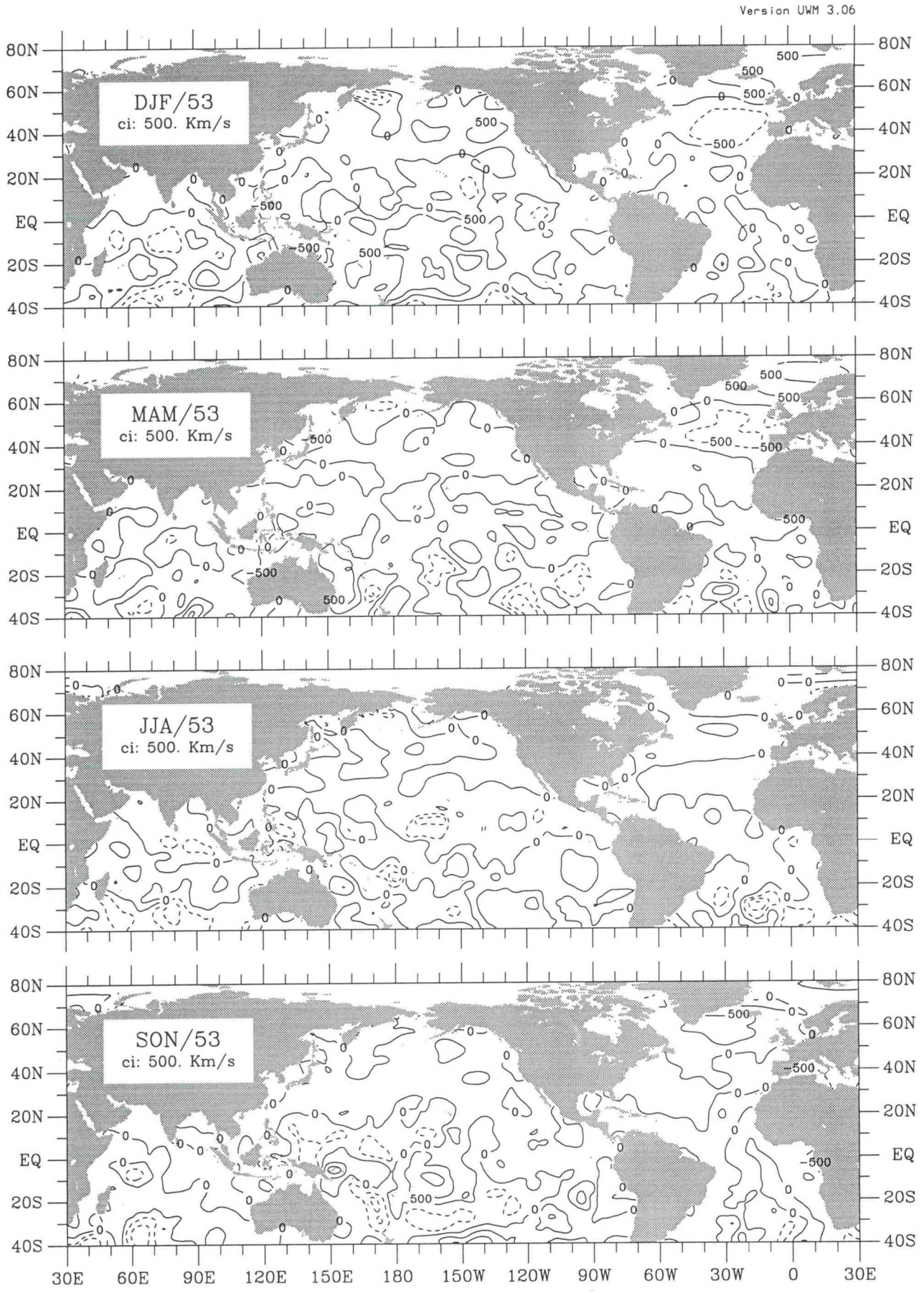

Figure ua-14. Zonal heat flux seasonal anomaly for 1953.

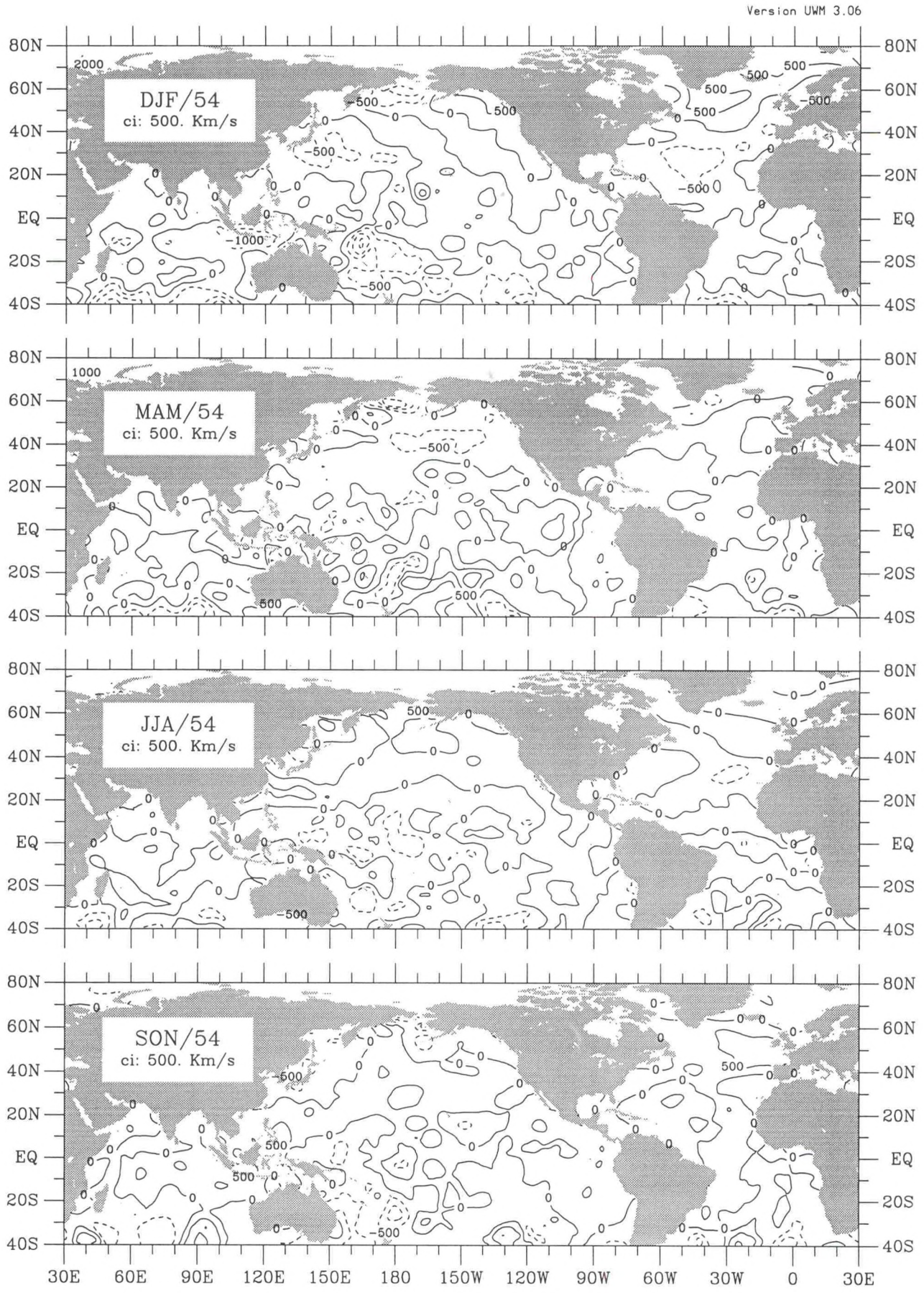

Figure ua-15. Zonal heat flux seasonal anomaly for 1954.

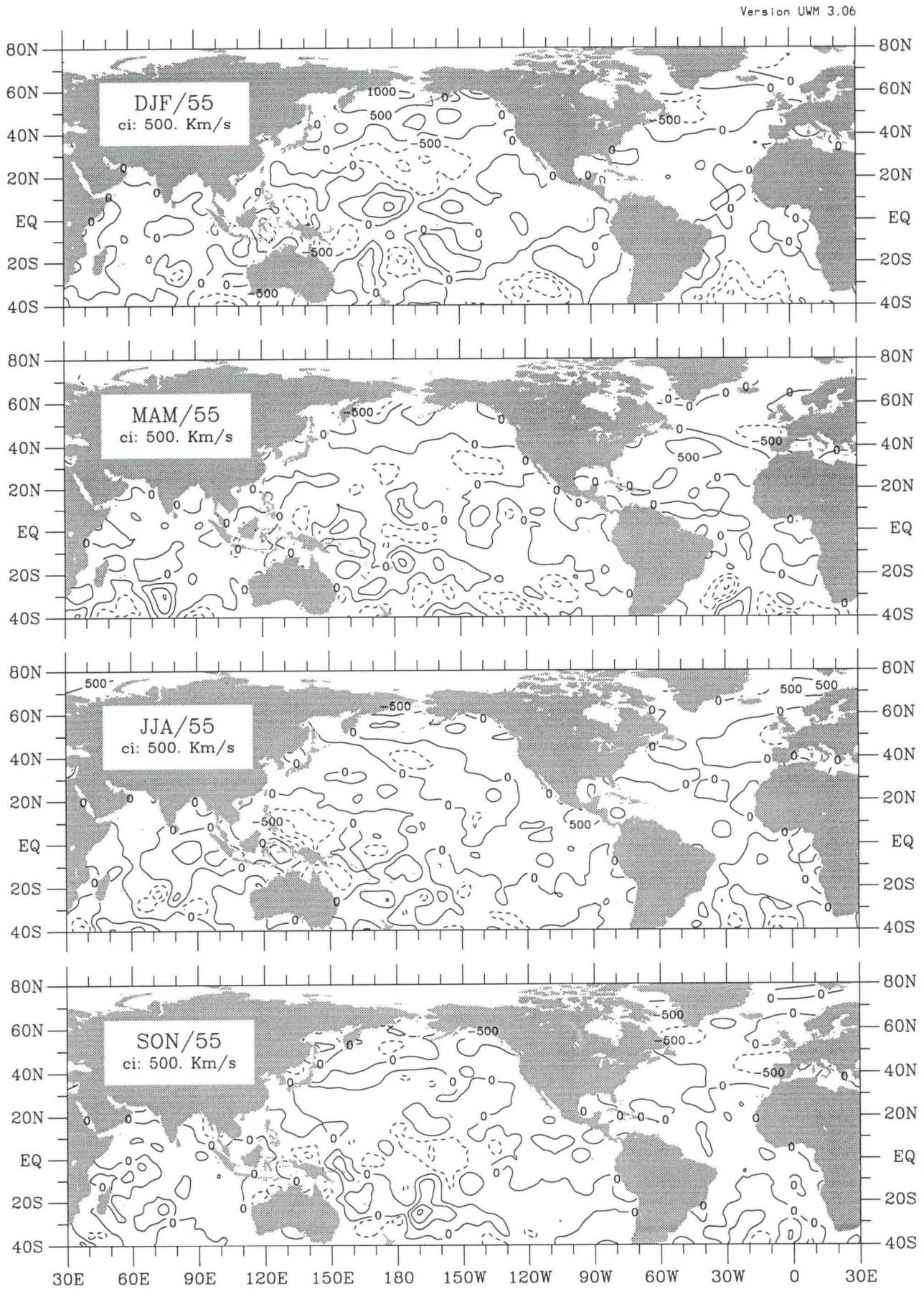

Figure ua-16. Zonal heat flux seasonal anomaly for 1955.

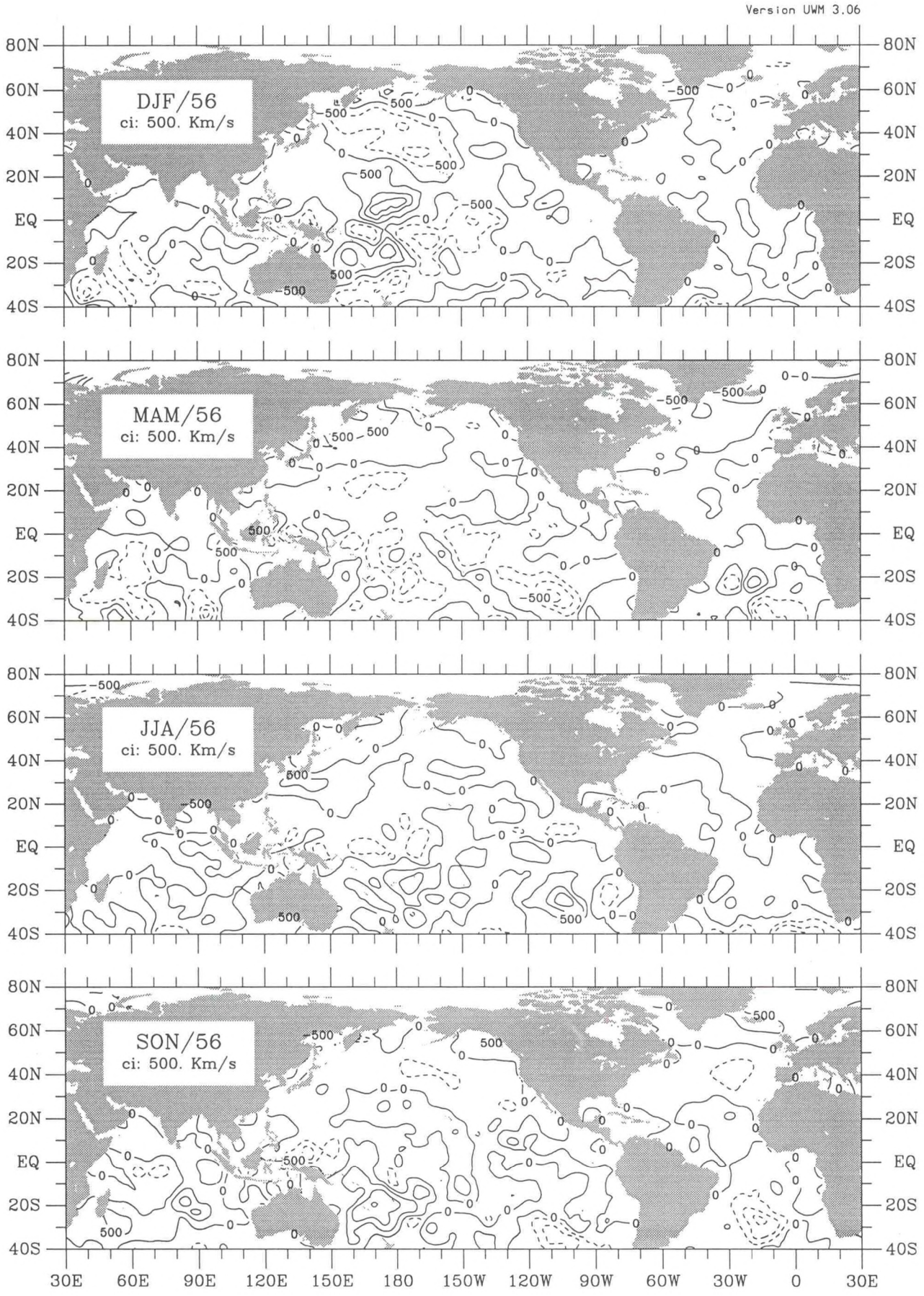

Figure ua-17. Zonal heat flux seasonal anomaly for 1956.

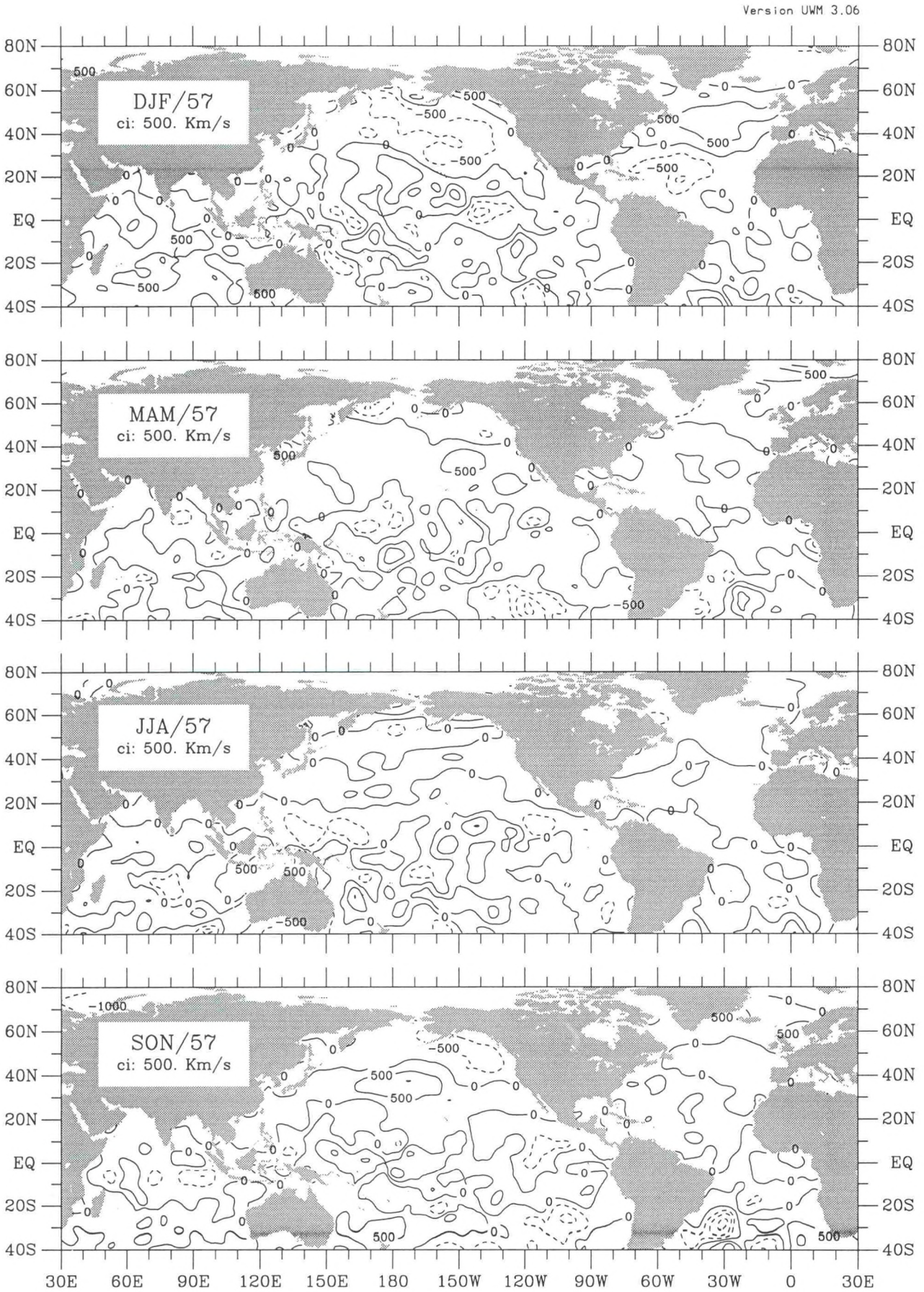

Figure ua-18. Zonal heat flux seasonal anomaly for 1957.

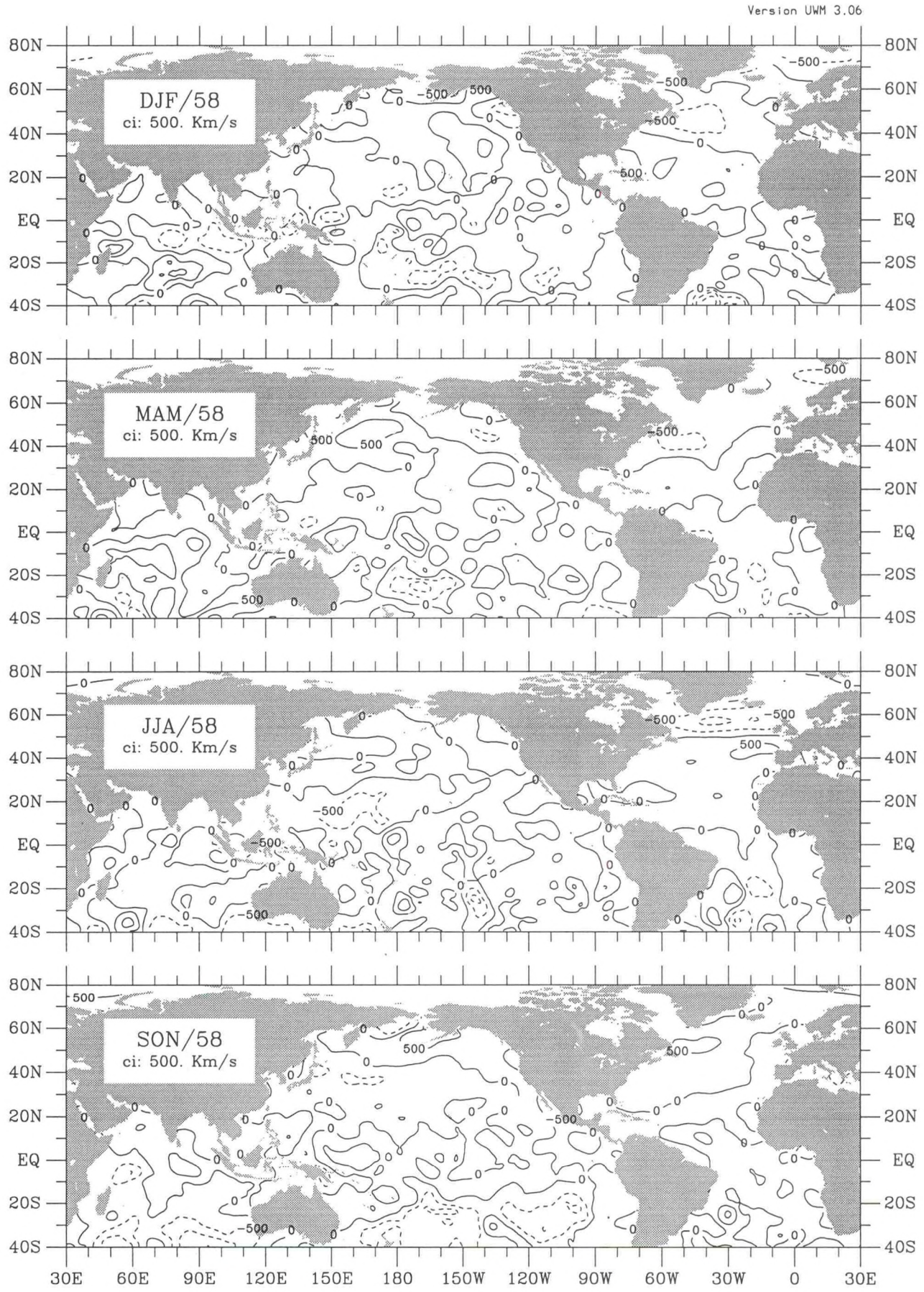

Figure ua-19. Zonal heat flux seasonal anomaly for 1958.

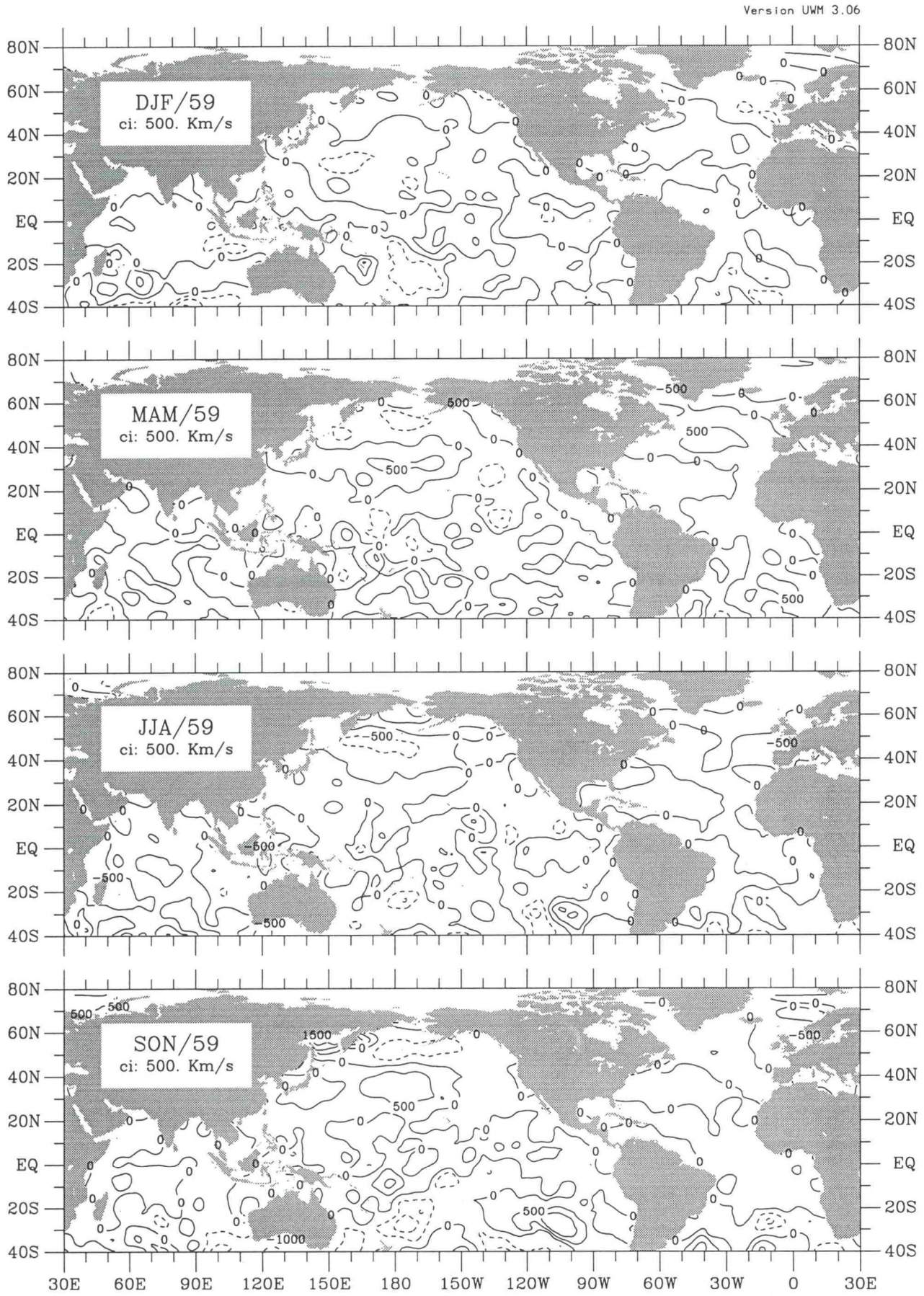

Figure ua-20. Zonal heat flux seasonal anomaly for 1959.

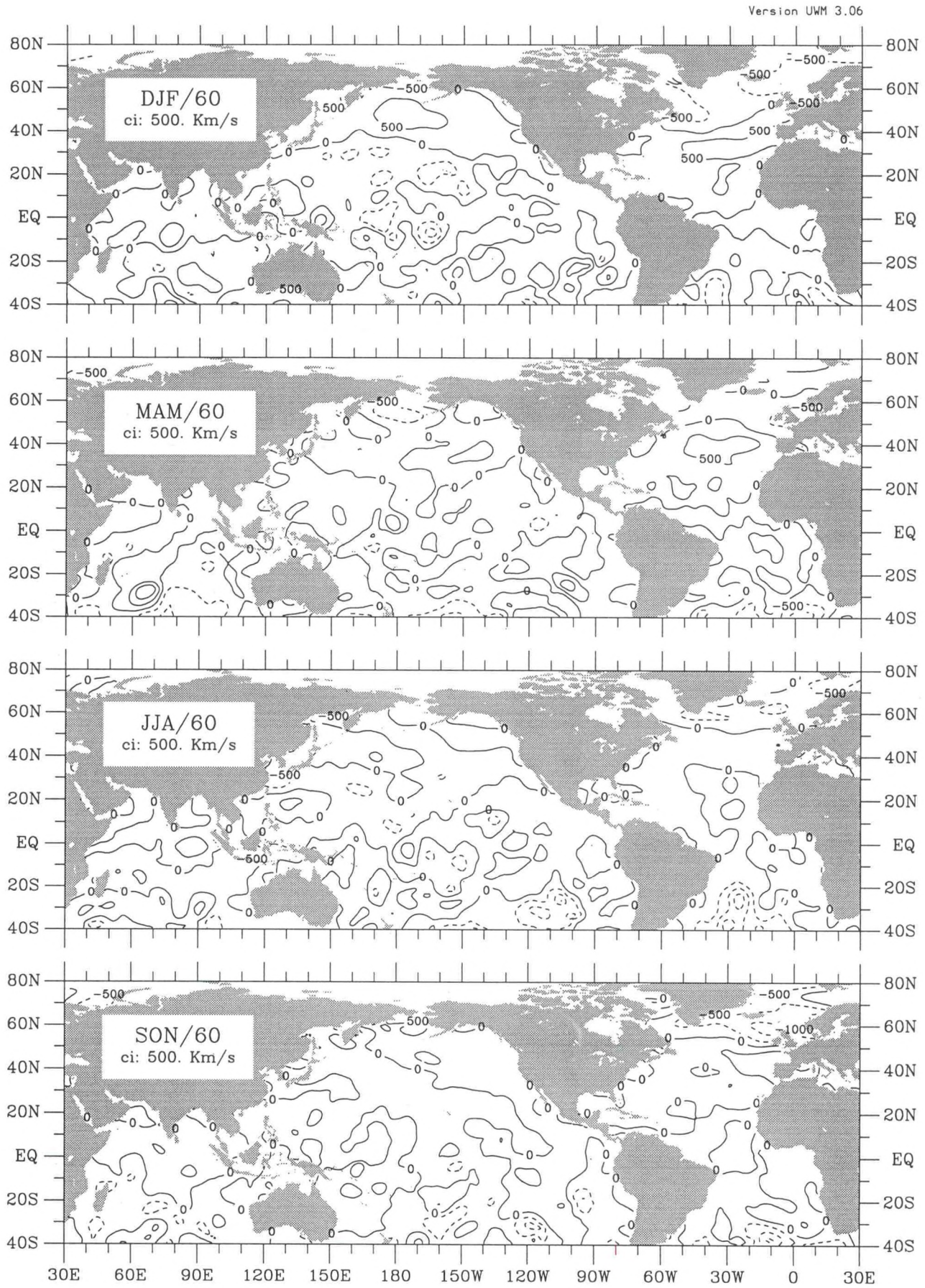

Figure ua-21. Zonal heat flux seasonal anomaly for 1960.

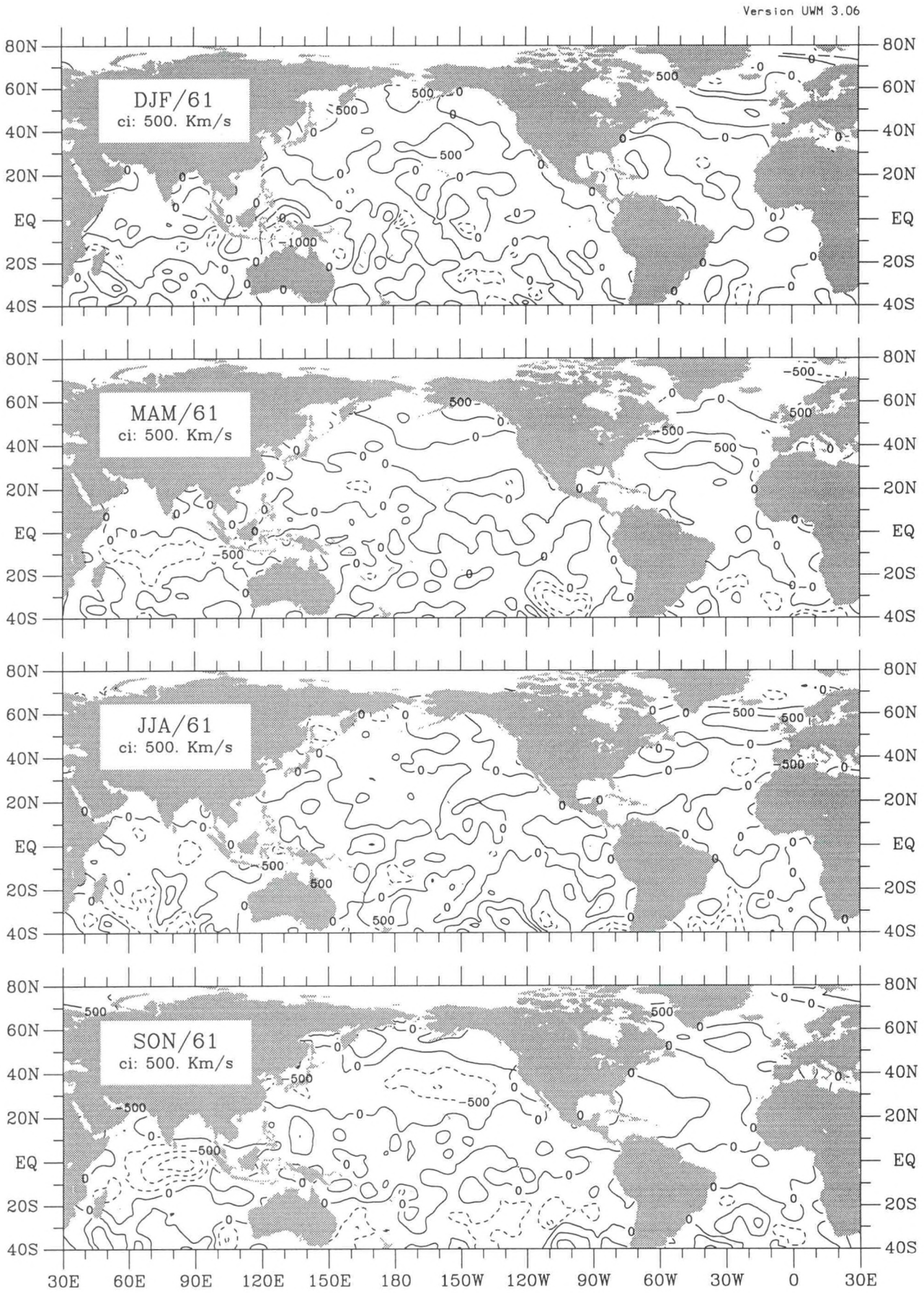

Figure ua-22. Zonal heat flux seasonal anomaly for 1961.

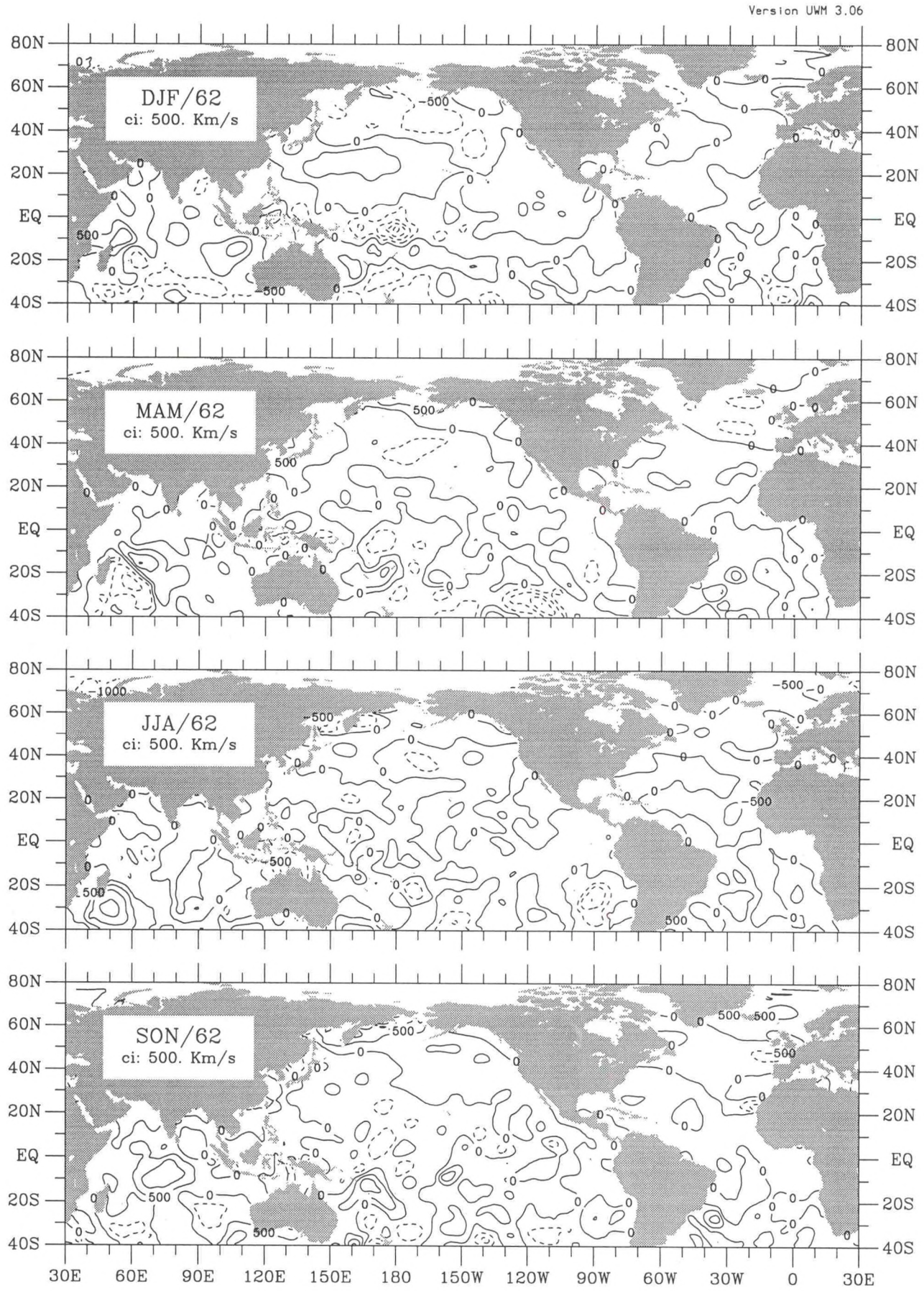

Figure ua-23. Zonal heat flux seasonal anomaly for 1962.

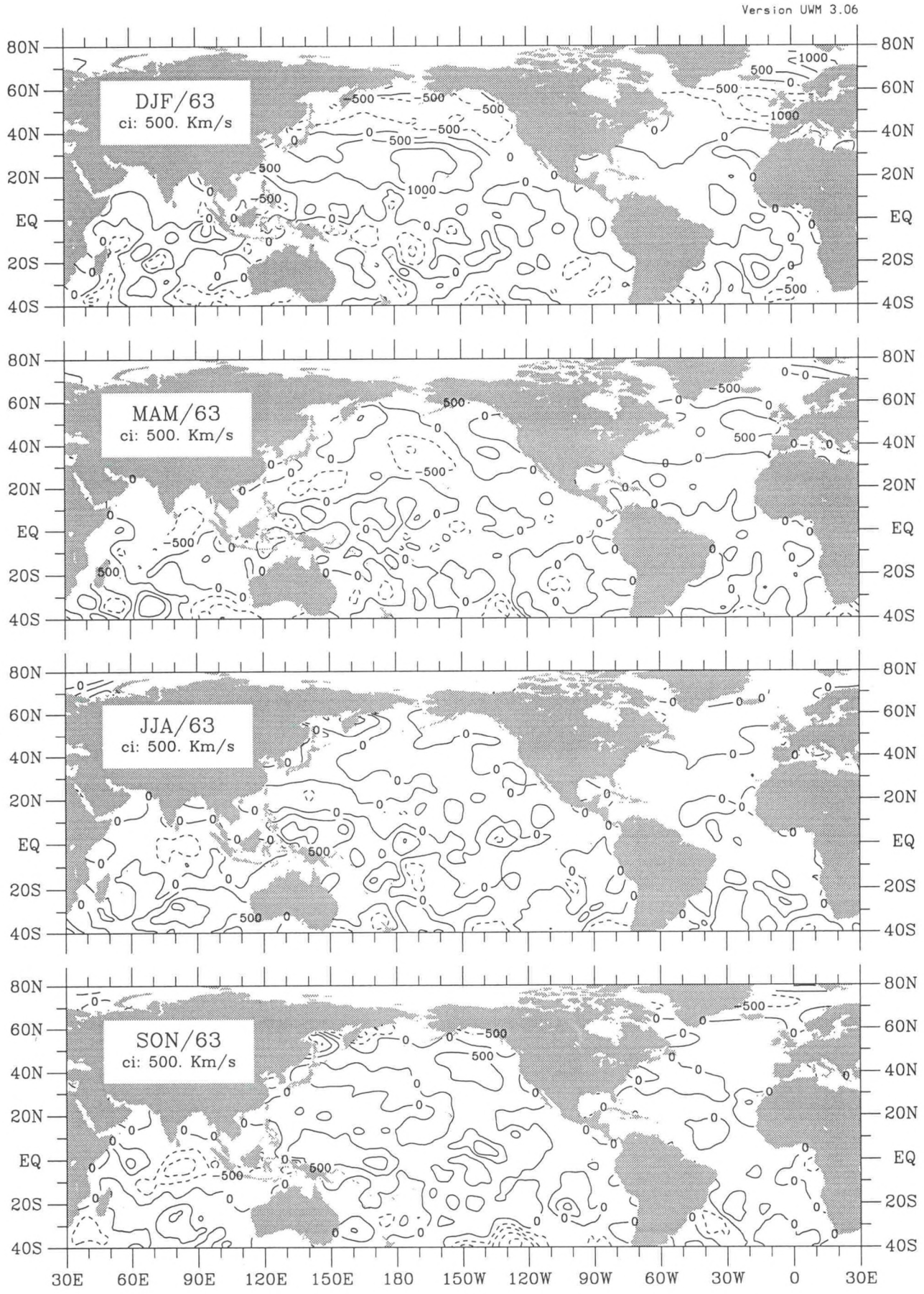

Figure ua-24. Zonal heat flux seasonal anomaly for 1963.

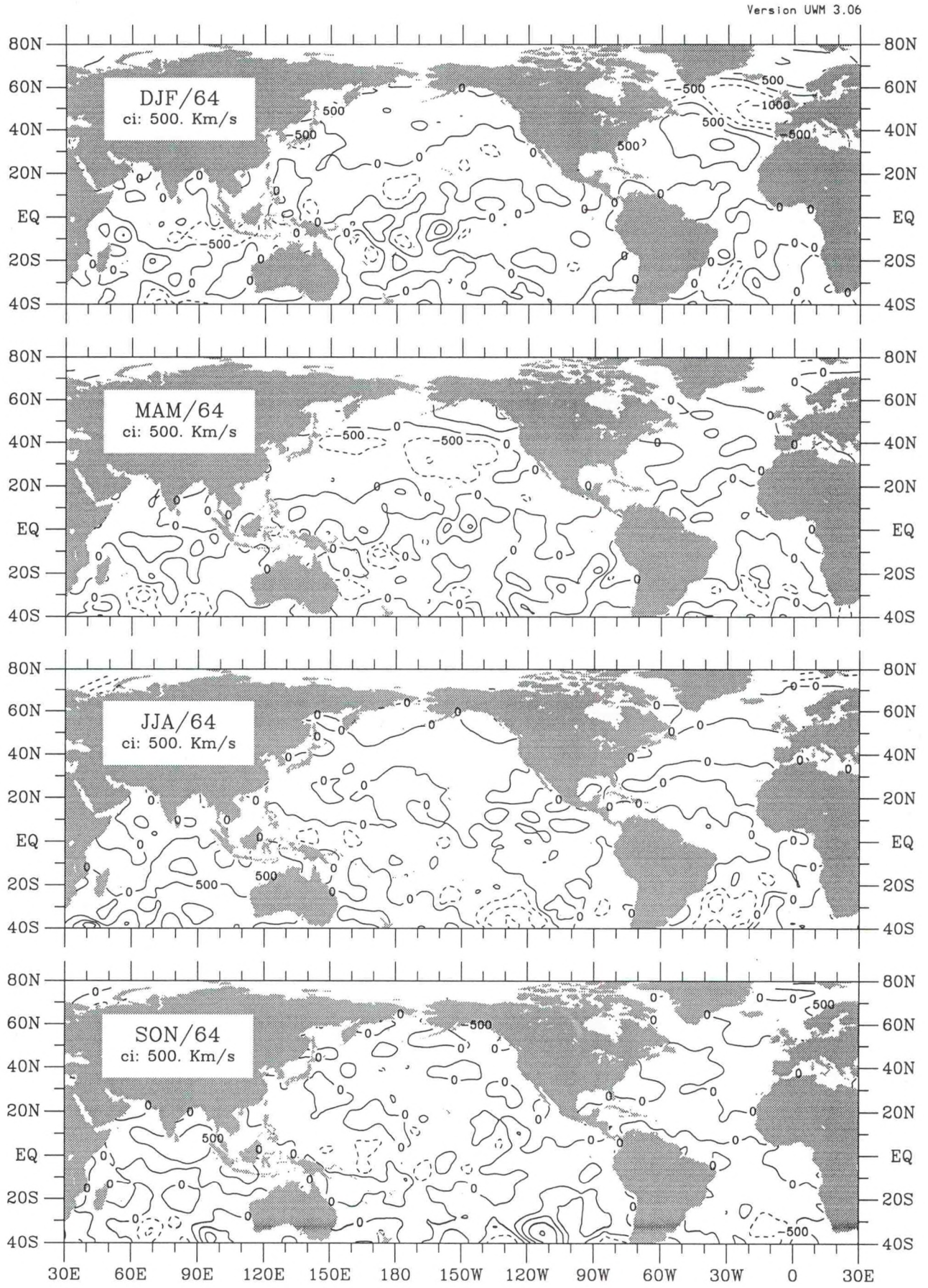

Figure ua-25. Zonal heat flux seasonal anomaly for 1964.

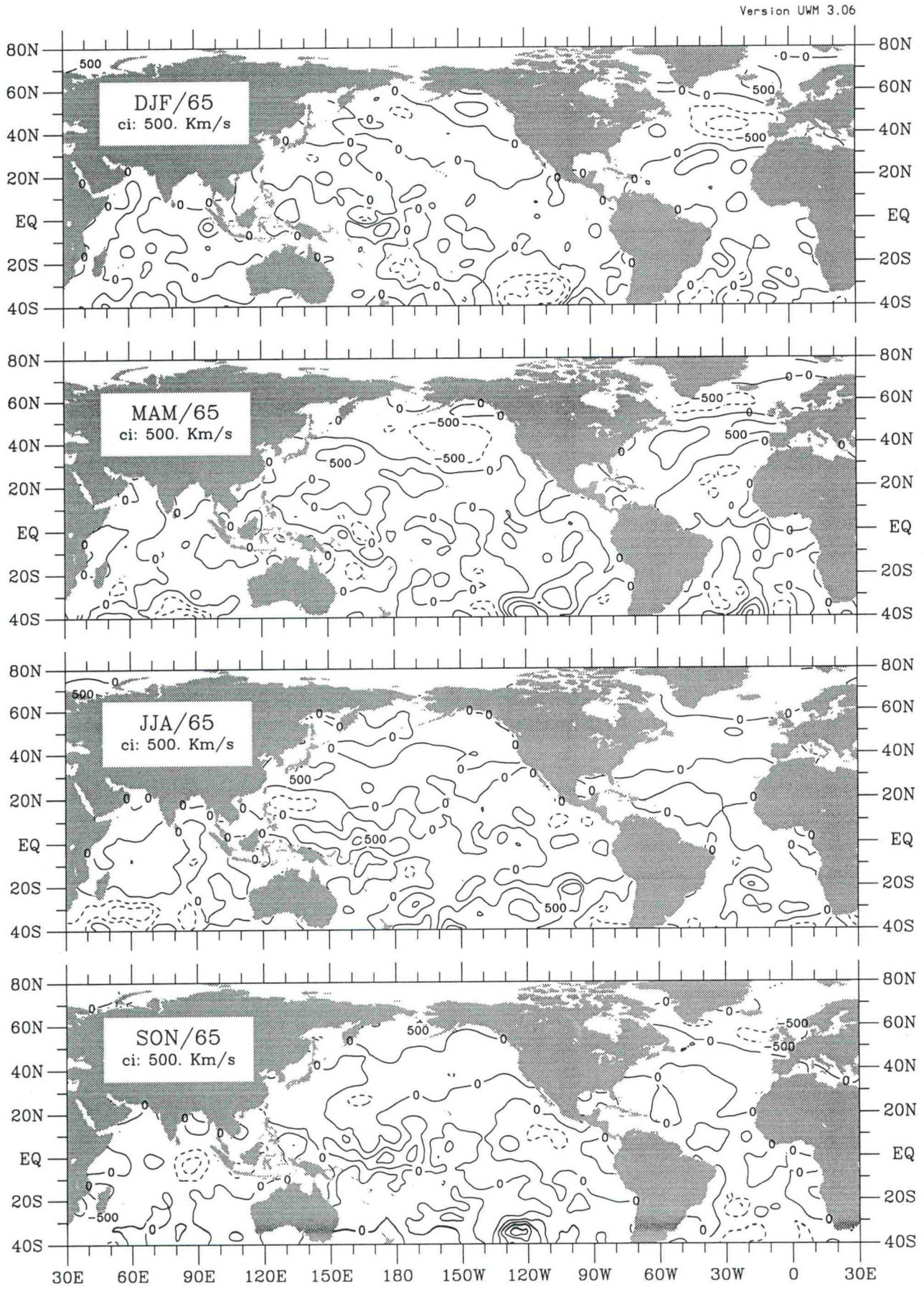

Figure ua-26. Zonal heat flux seasonal anomaly for 1965.

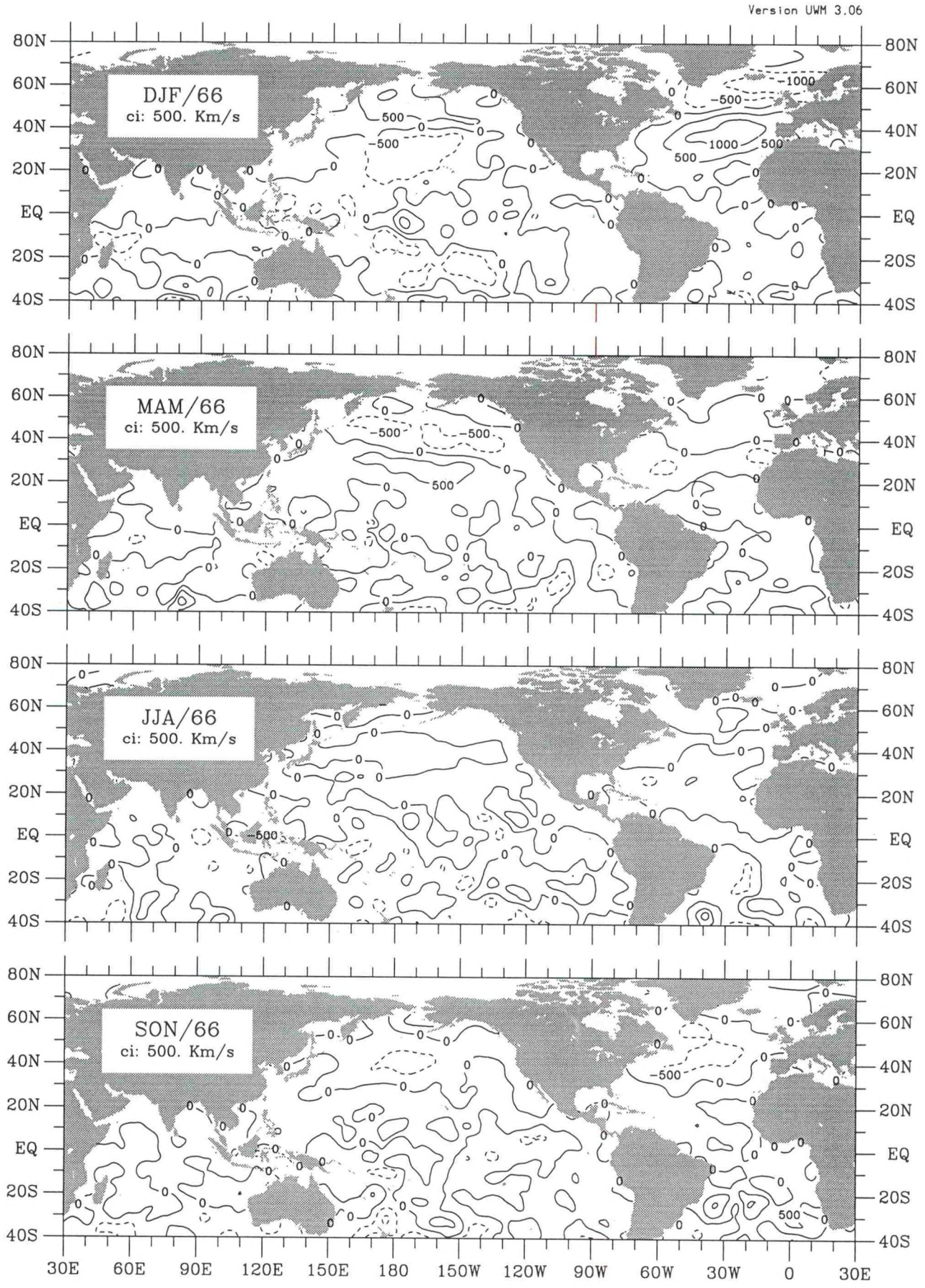

Figure ua-27. Zonal heat flux seasonal anomaly for 1966.

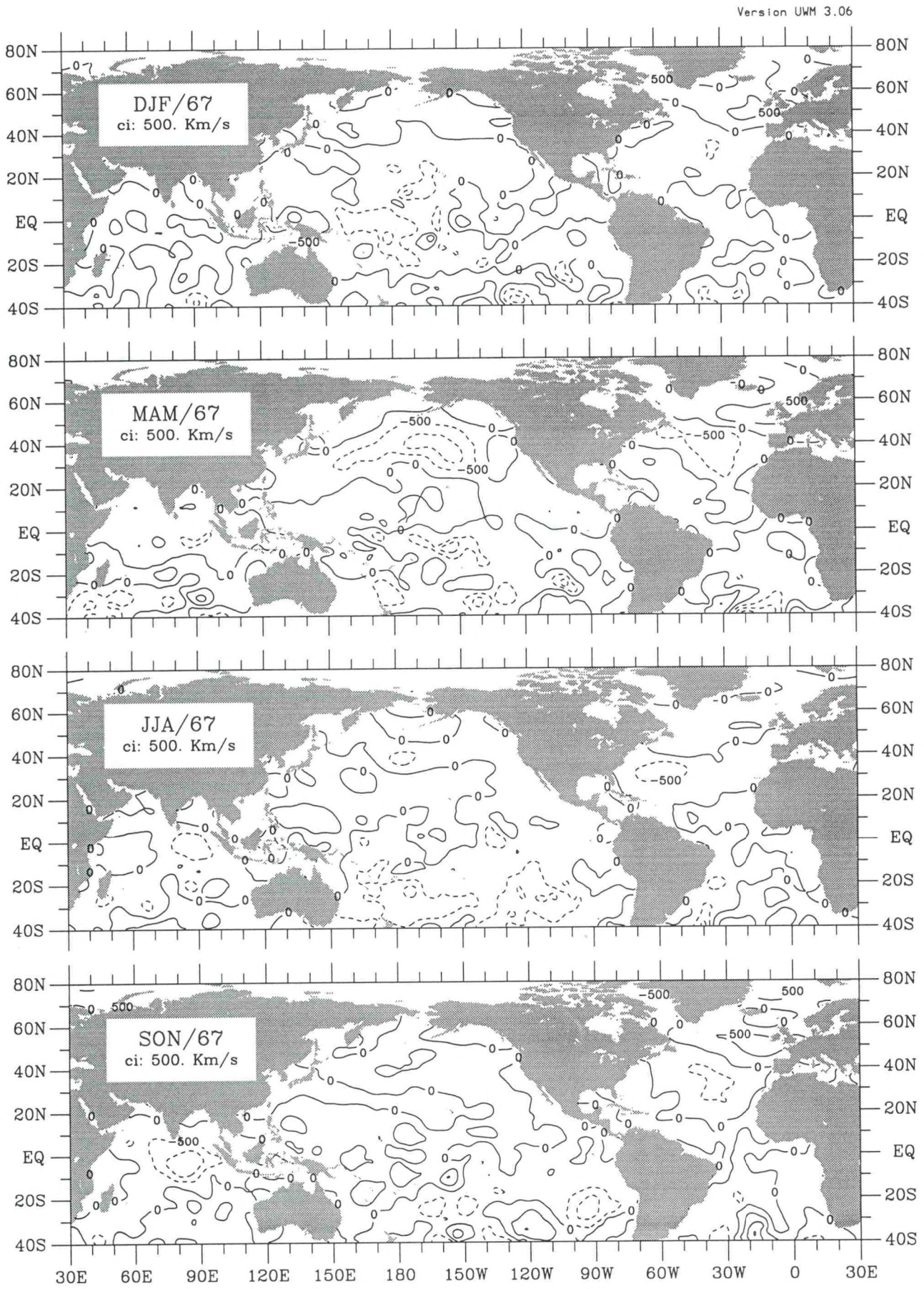

Figure ua-28. Zonal heat flux seasonal anomaly for 1967.

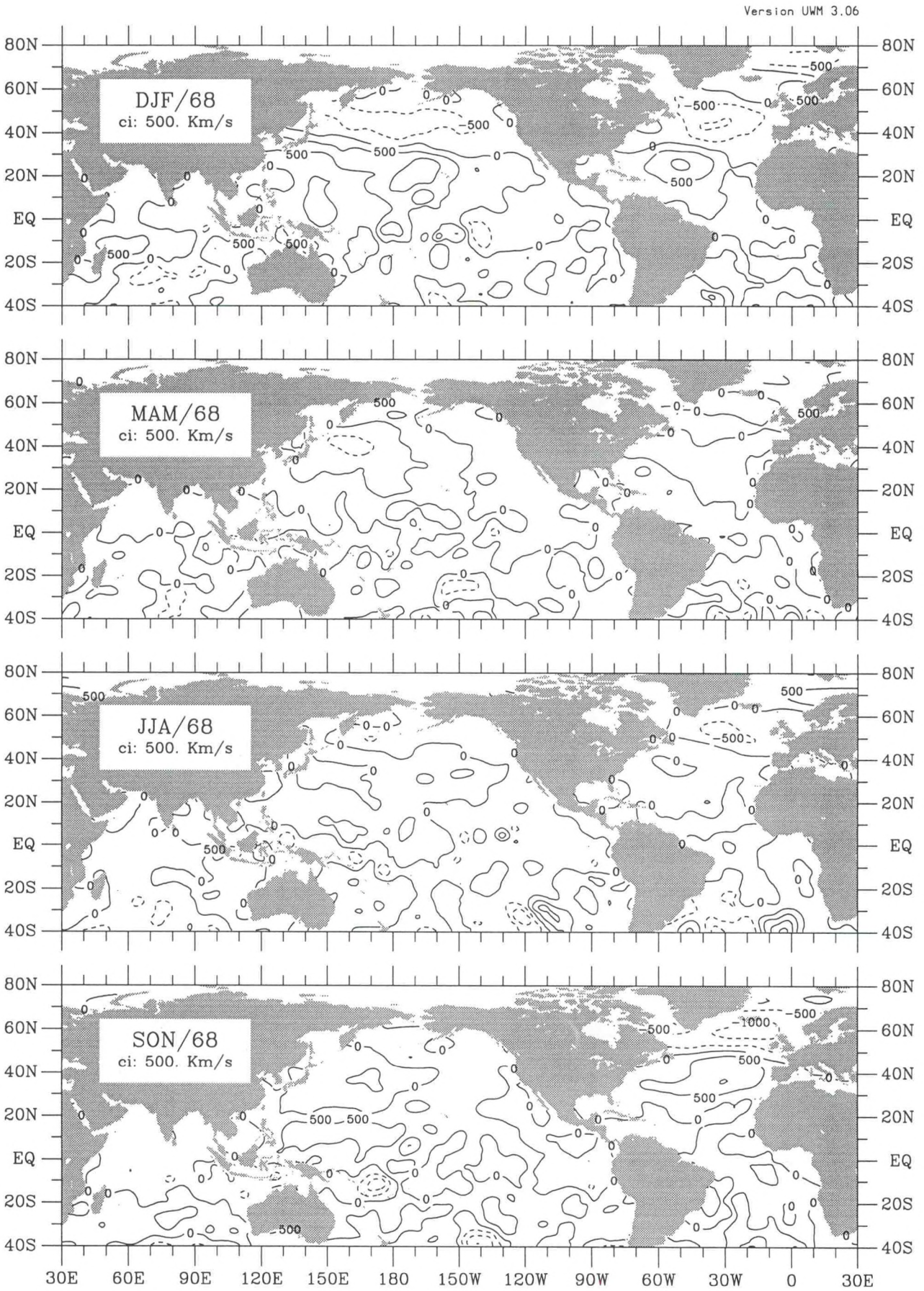

Figure ua-29. Zonal heat flux seasonal anomaly for 1968.

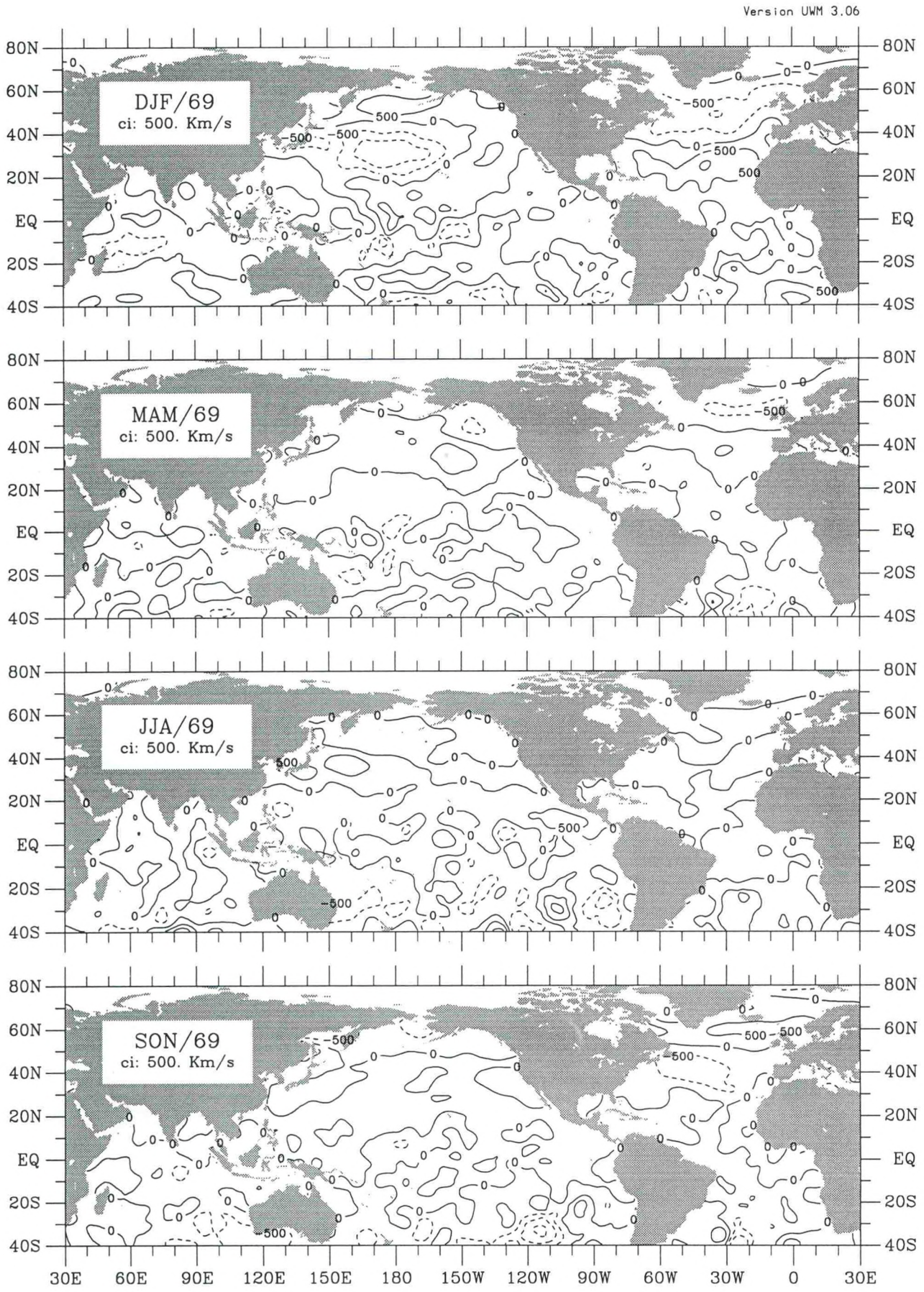

Figure ua-30. Zonal heat flux seasonal anomaly for 1969.

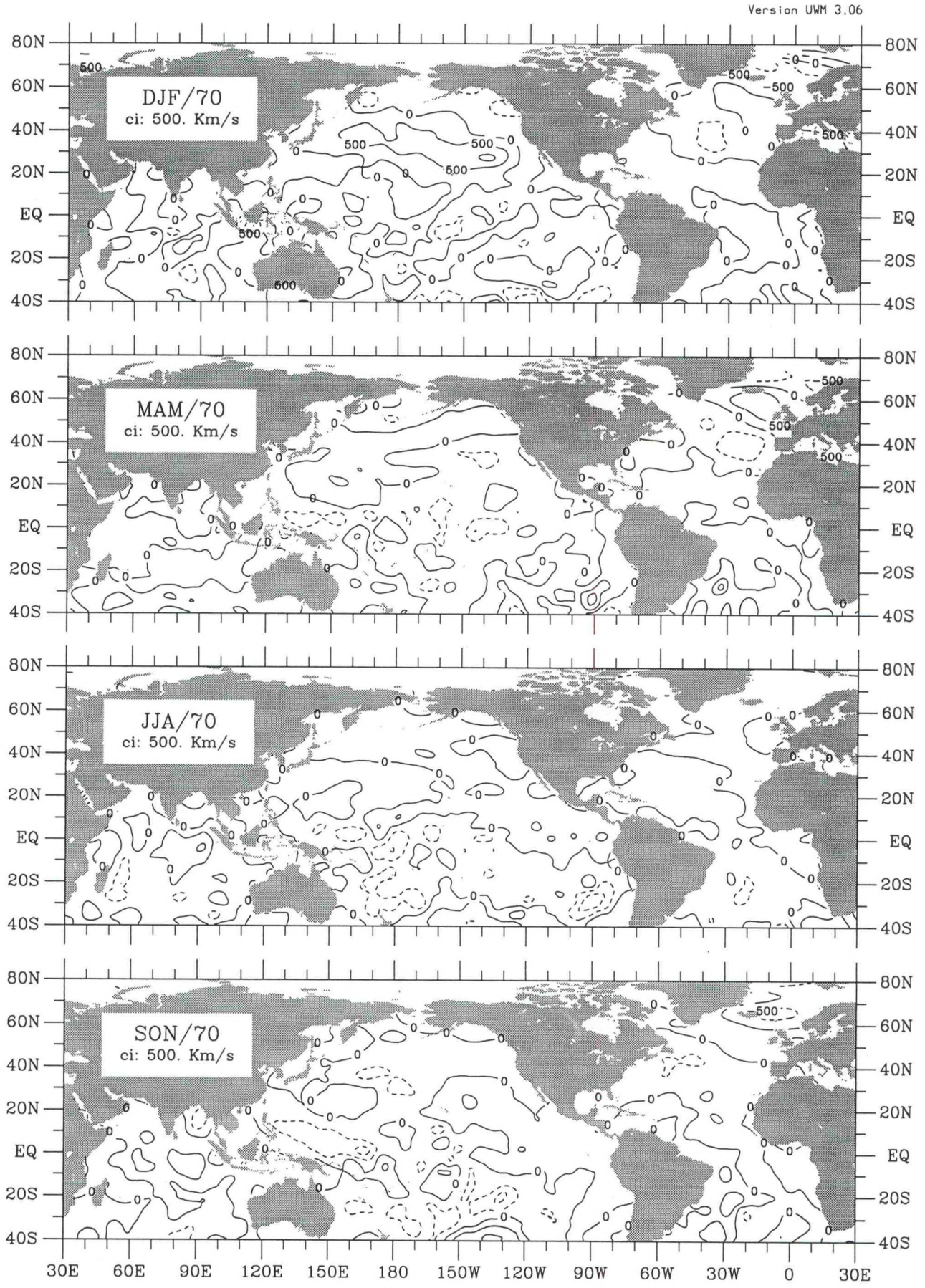

Figure ua-31. Zonal heat flux seasonal anomaly for 1970.

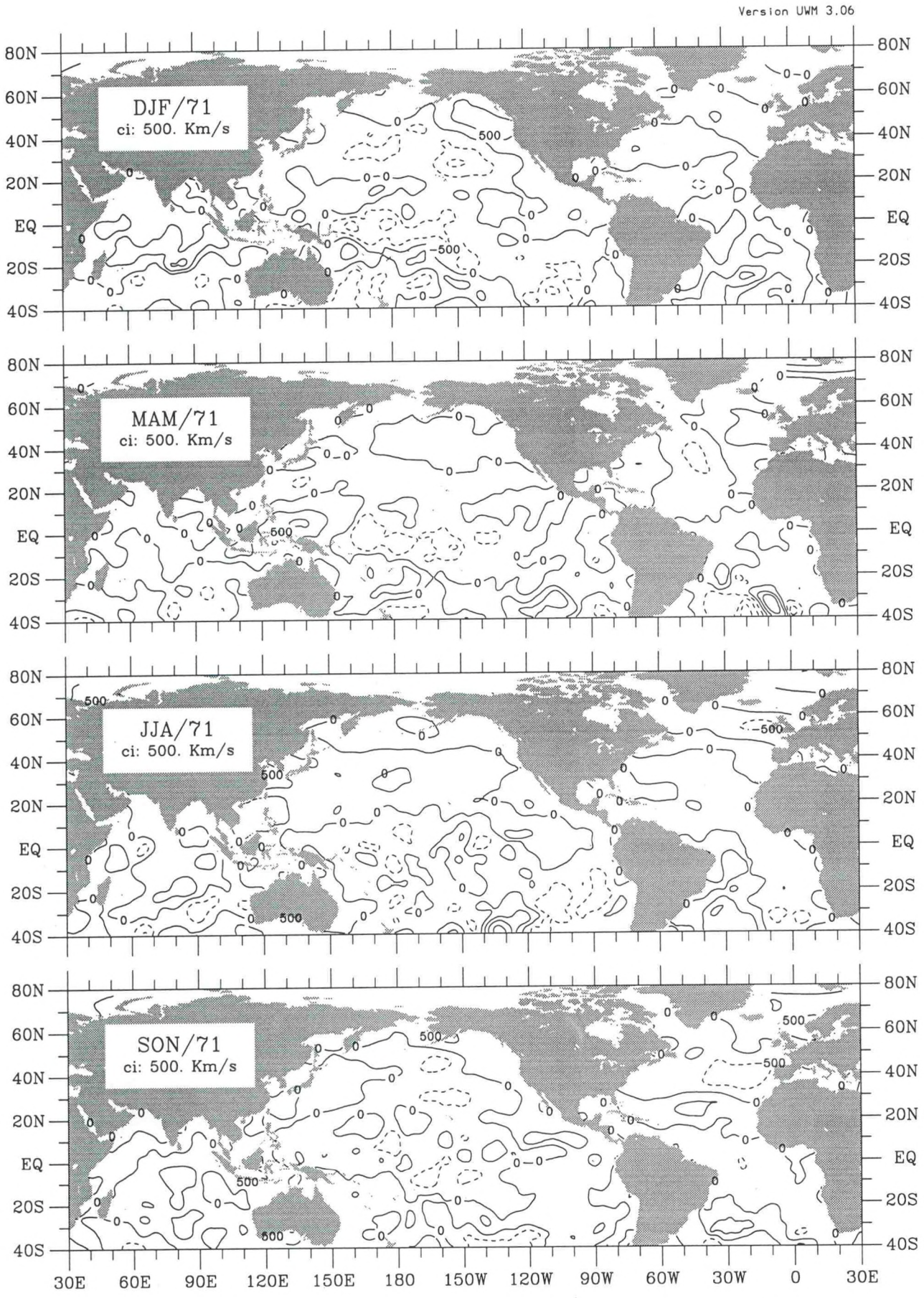

Figure ua-32. Zonal heat flux seasonal anomaly for 1971.

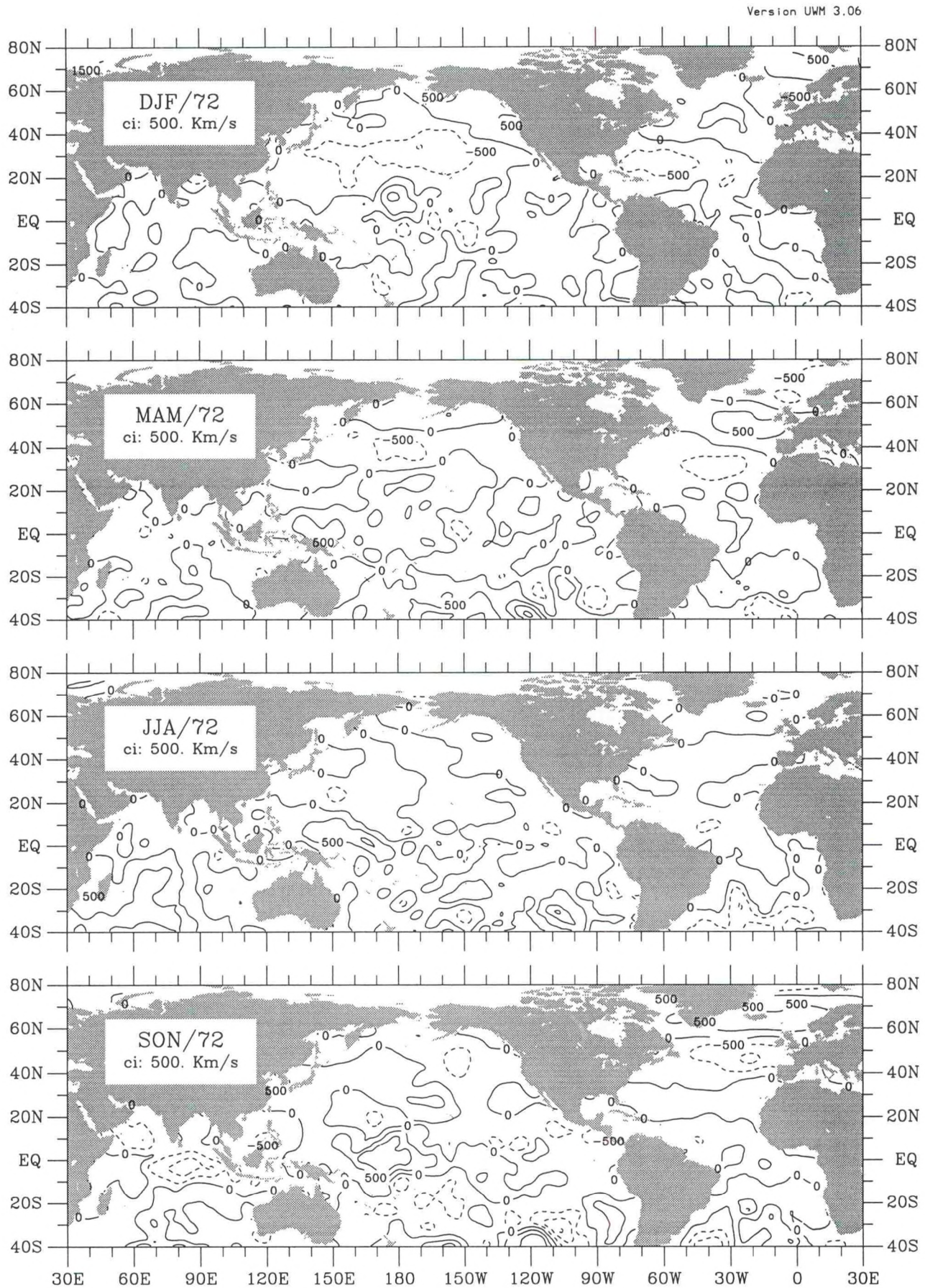

Figure ua-33. Zonal heat flux seasonal anomaly for 1972.

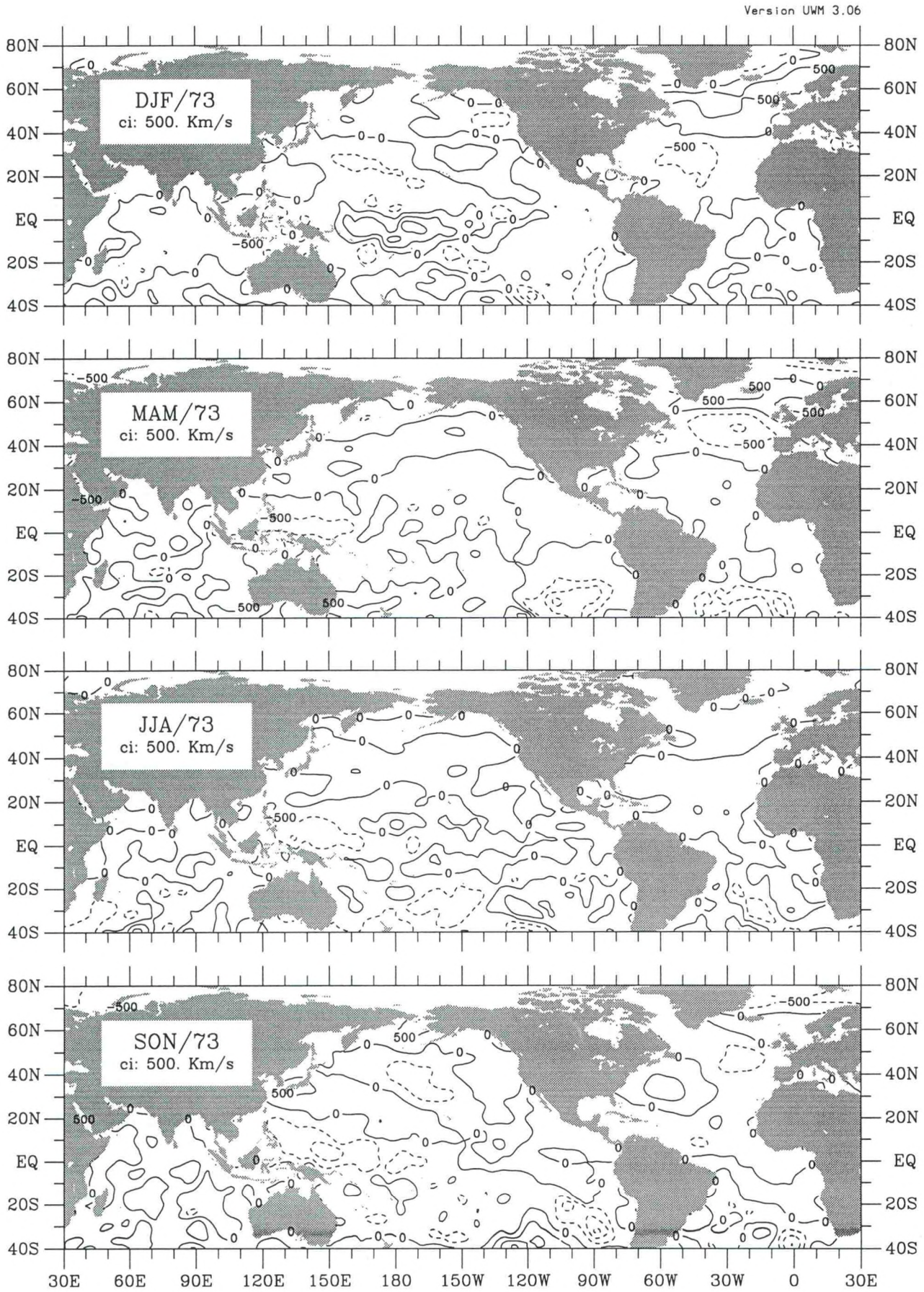

Figure ua-34. Zonal heat flux seasonal anomaly for 1973.

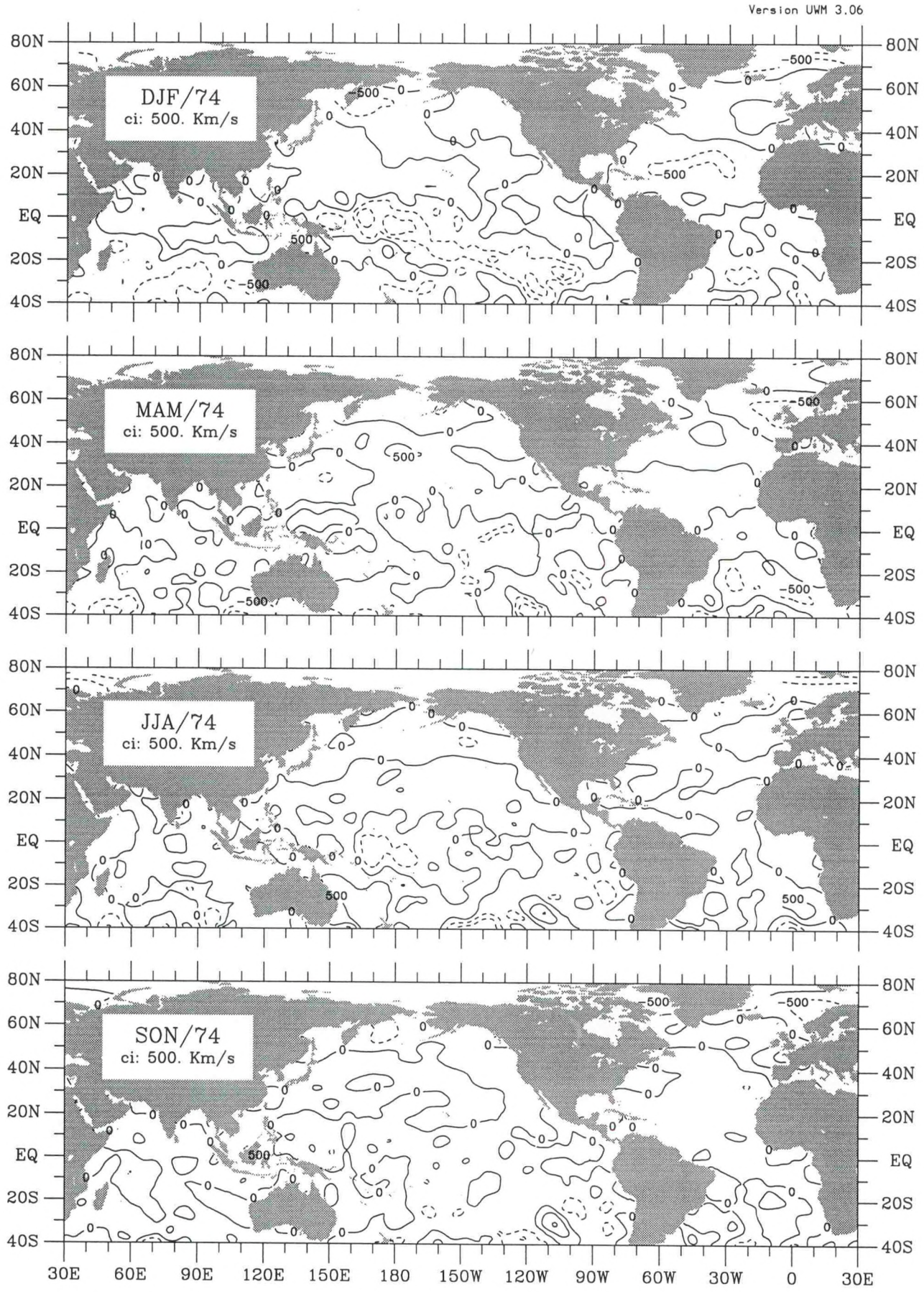

Figure ua-35. Zonal heat flux seasonal anomaly for 1974.

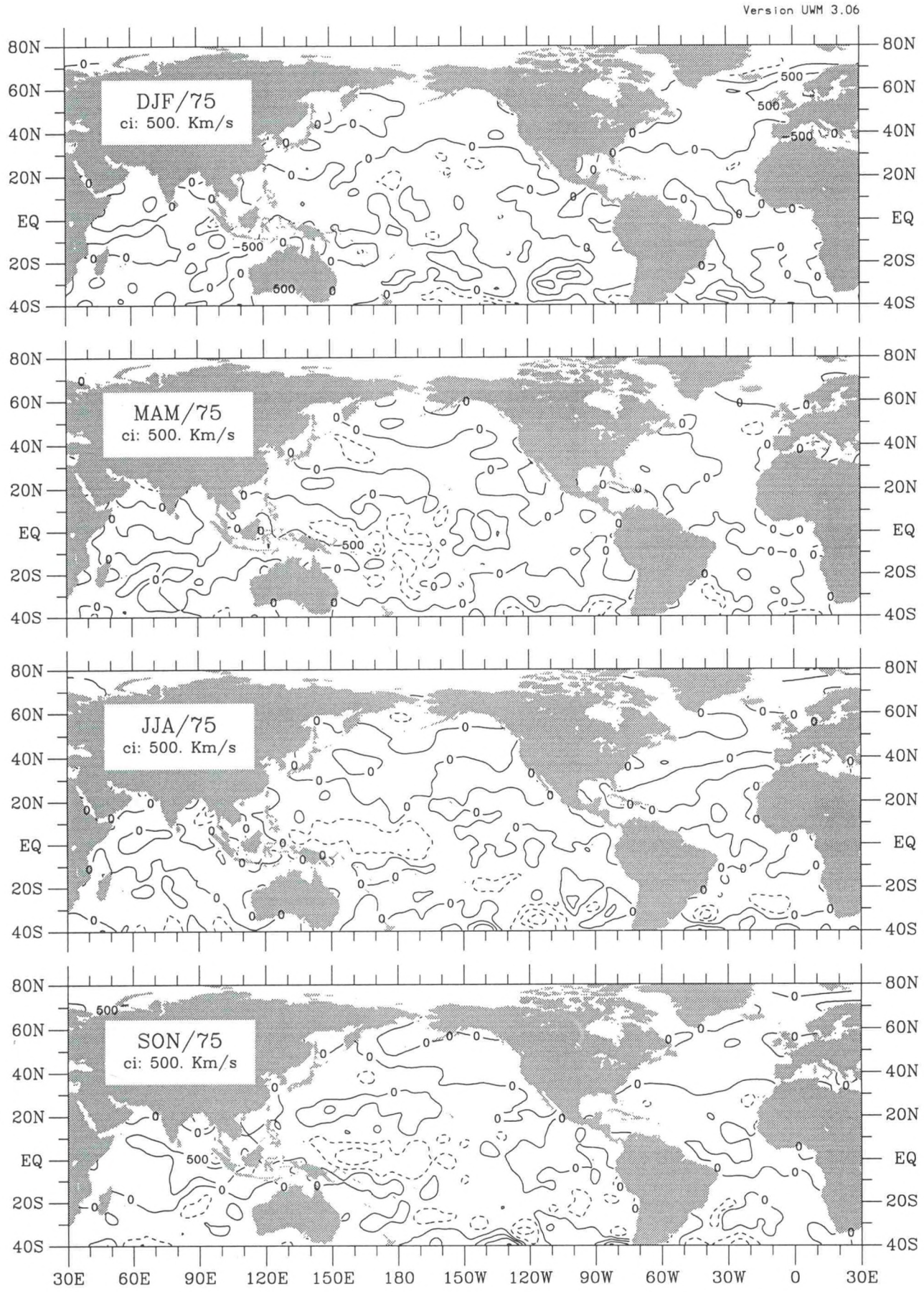

Figure ua-36. Zonal heat flux seasonal anomaly for 1975.

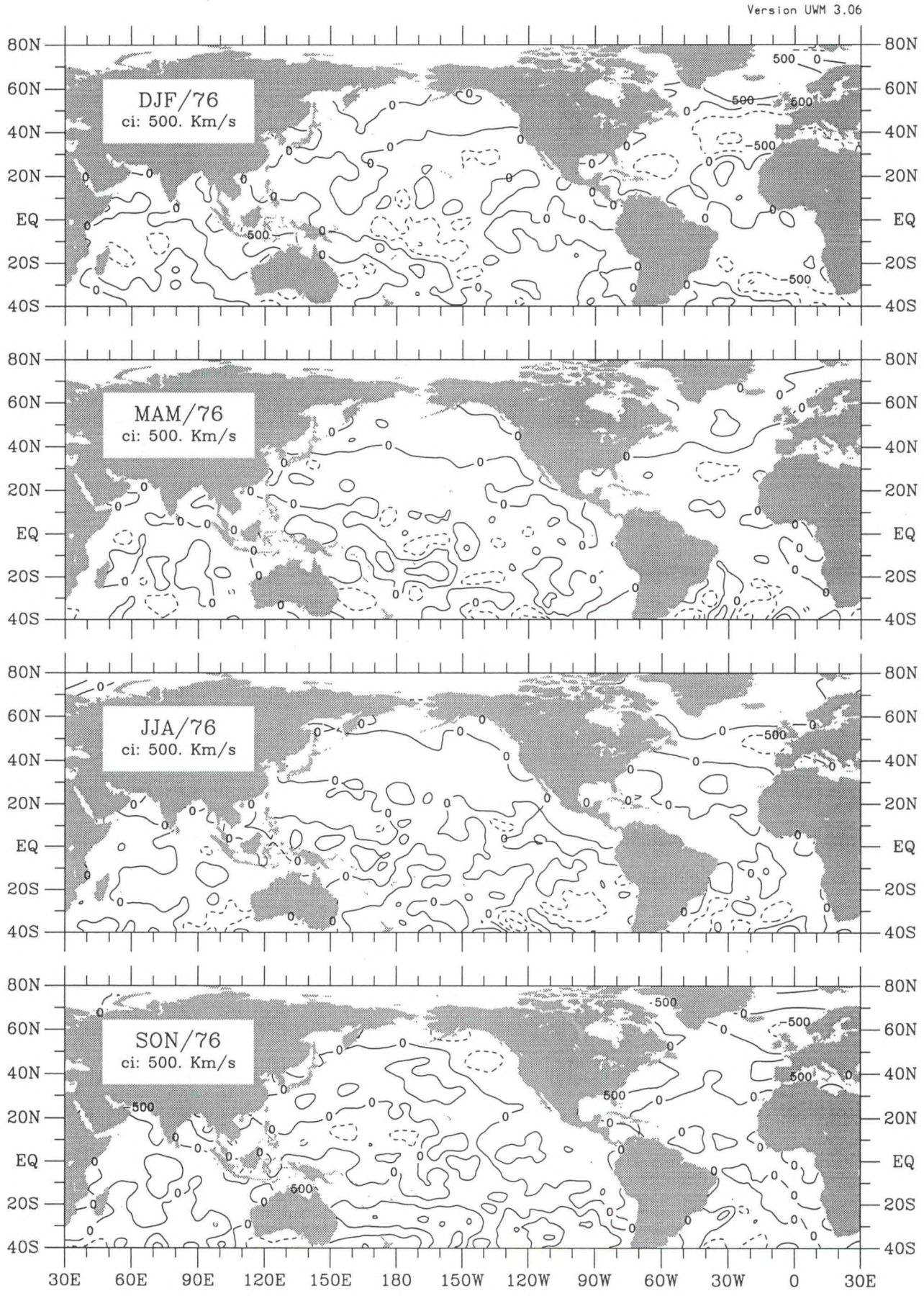

Figure ua-37. Zonal heat flux seasonal anomaly for 1976.

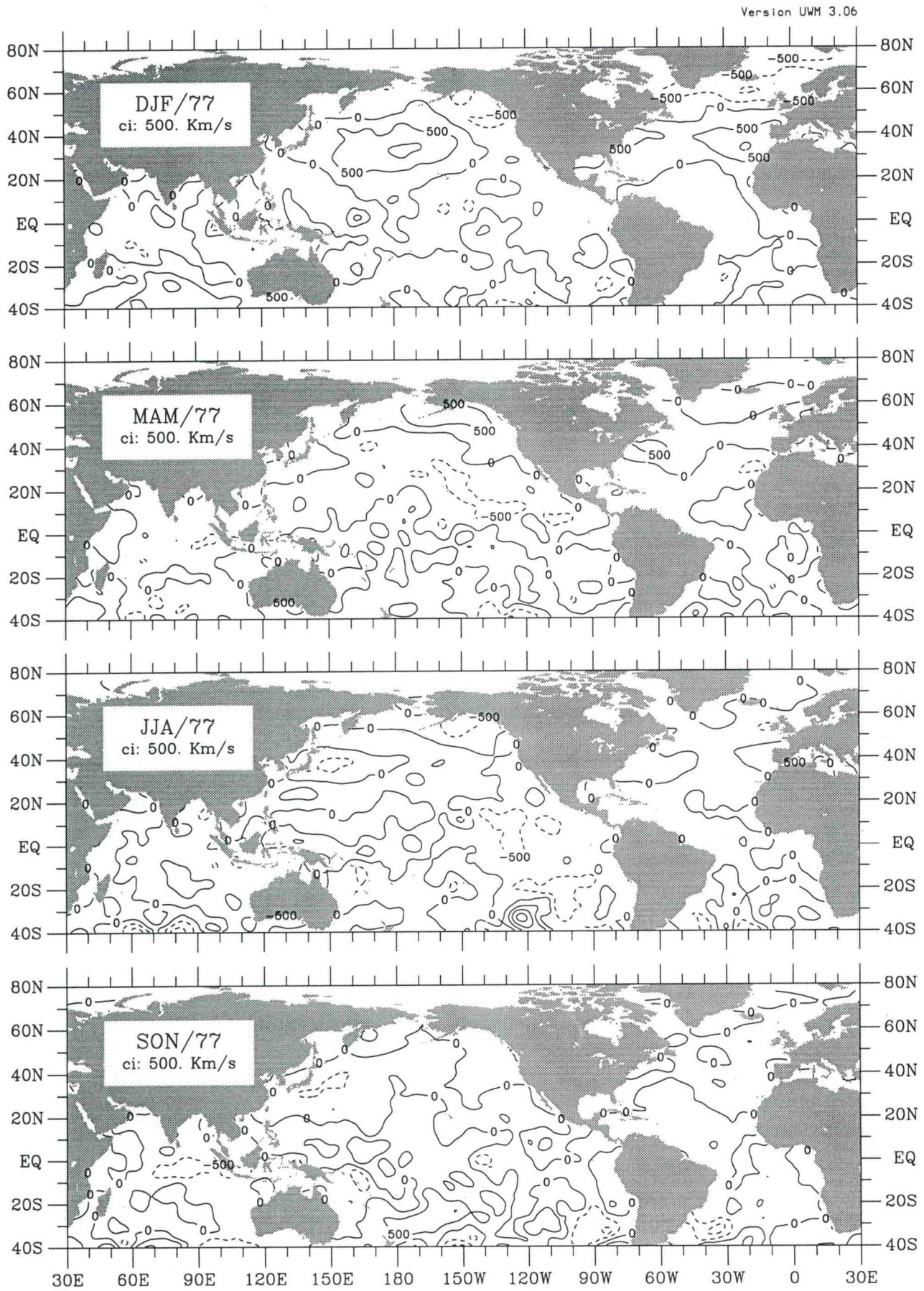

Figure ua-38. Zonal heat flux seasonal anomaly for 1977.

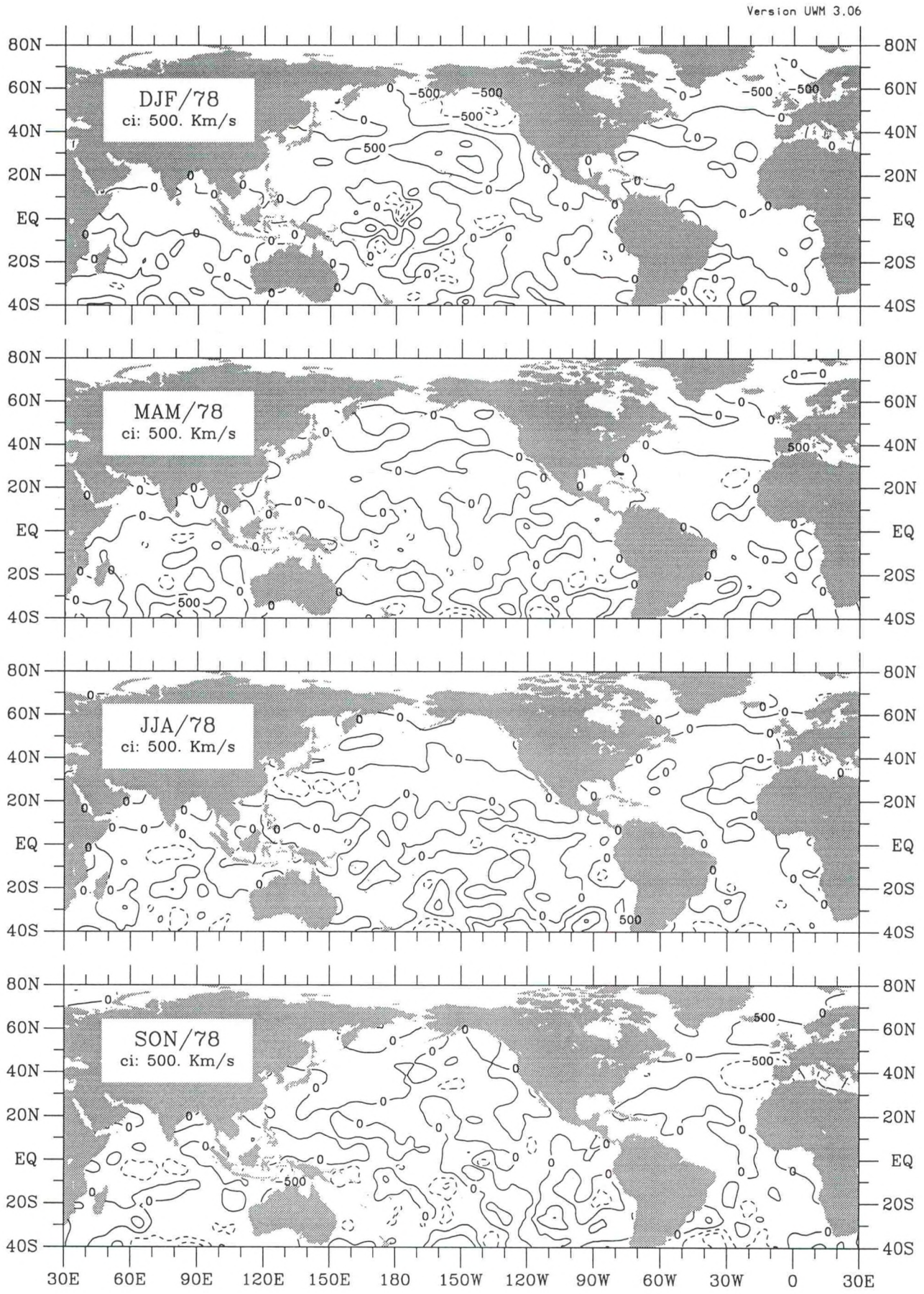

Figure ua-39. Zonal heat flux seasonal anomaly for 1978.

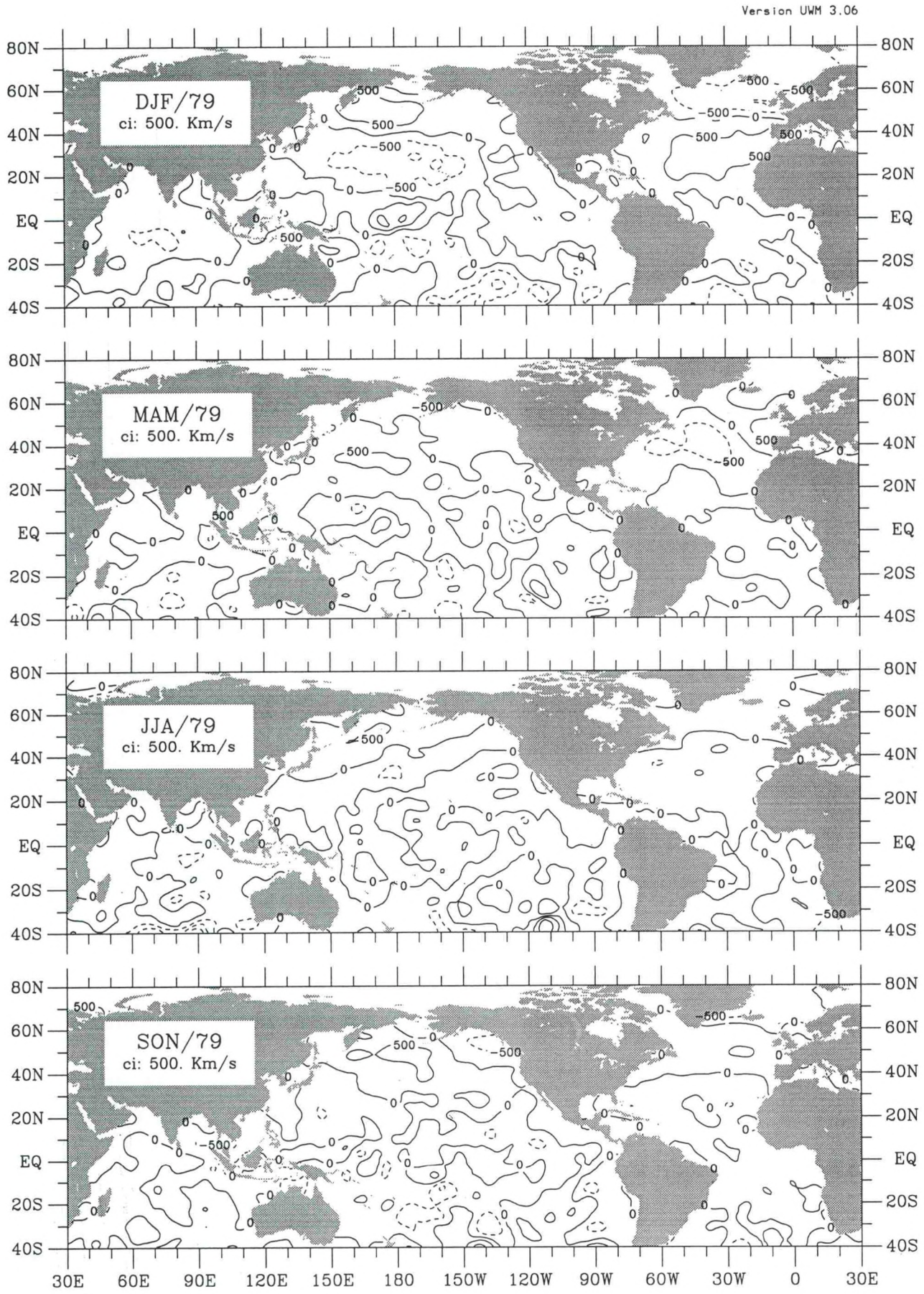

Figure ua-40. Zonal heat flux seasonal anomaly for 1979.

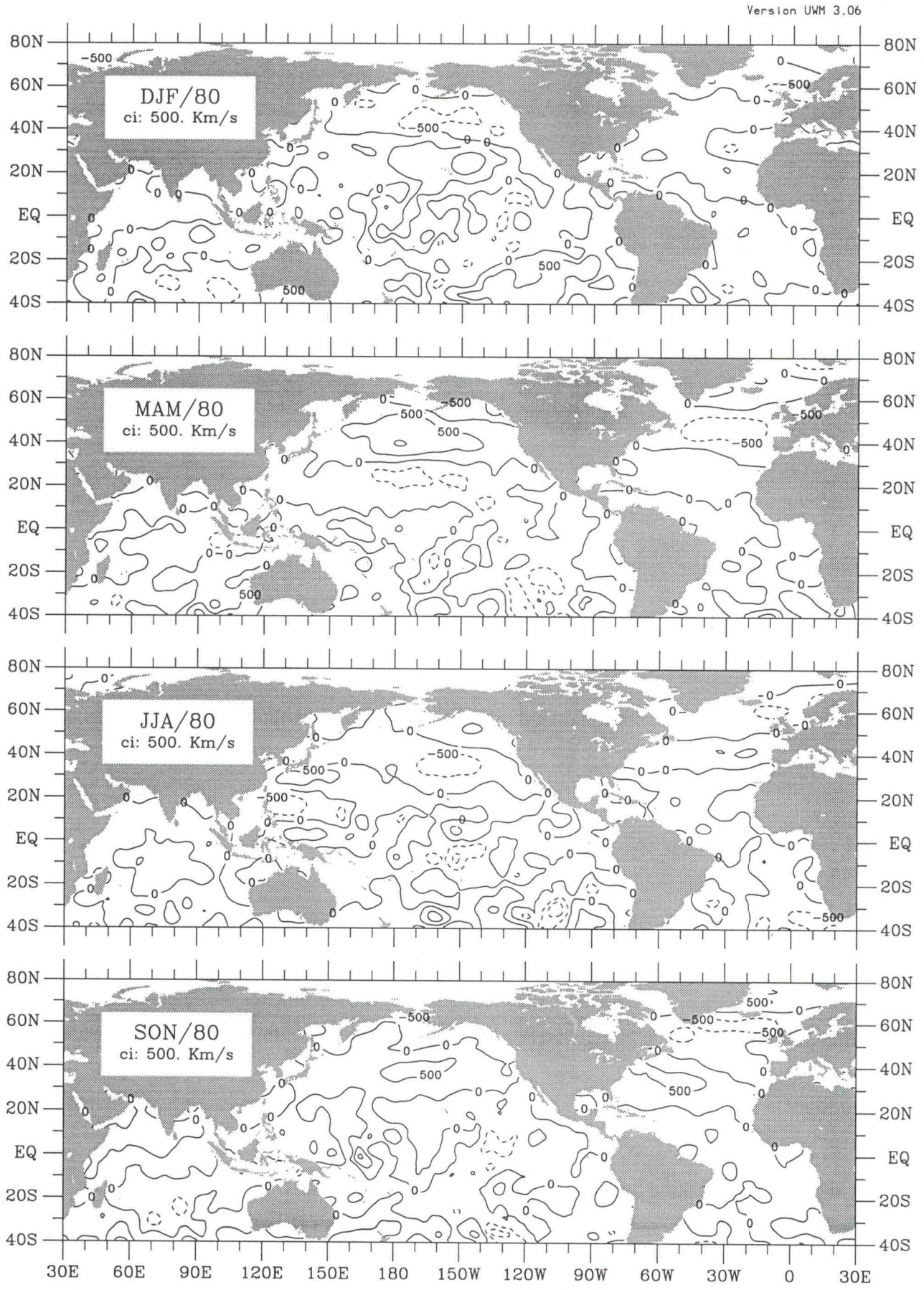

Figure ua-41. Zonal heat flux seasonal anomaly for 1980.

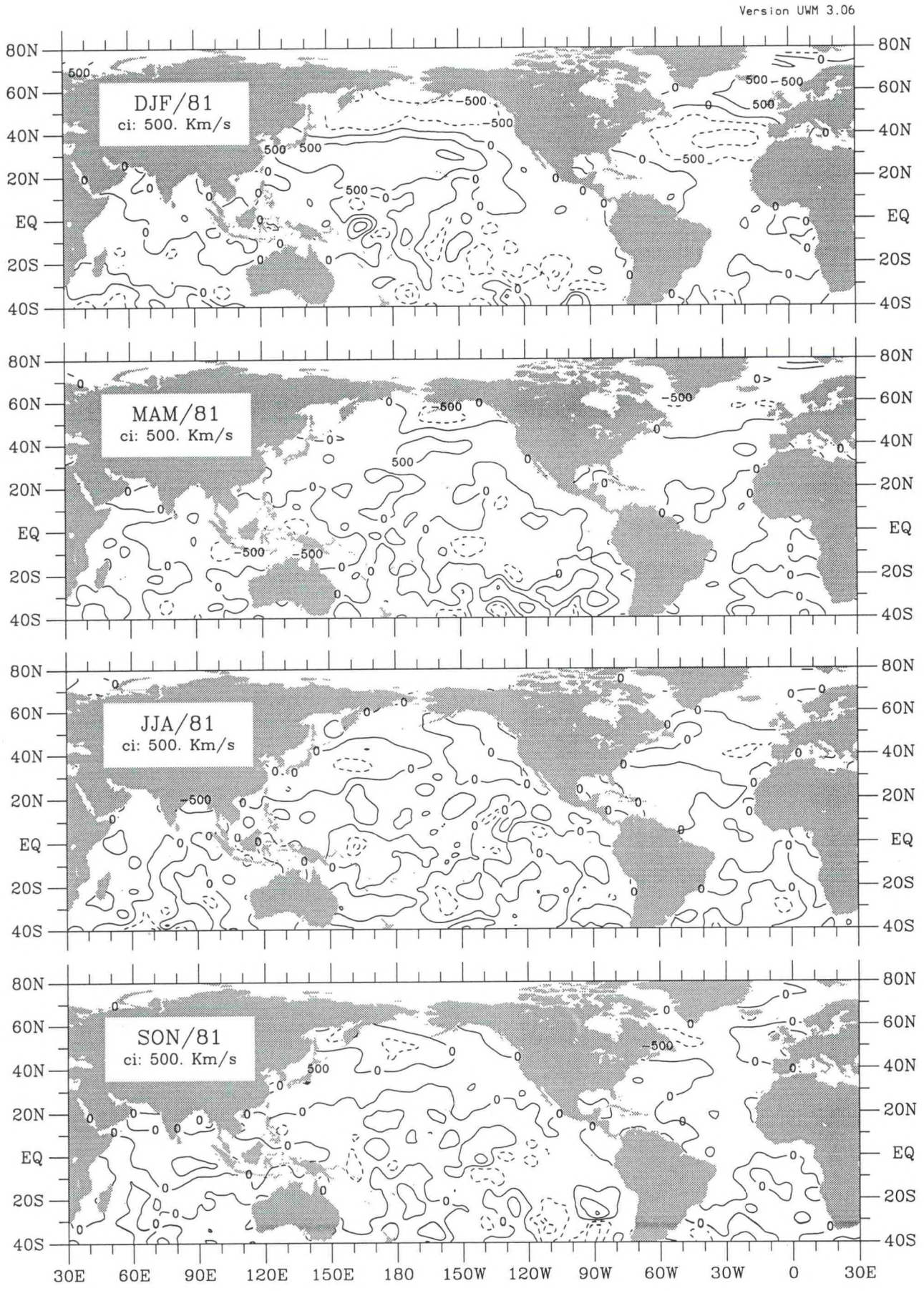

Figure ua-42. Zonal heat flux seasonal anomaly for 1981.

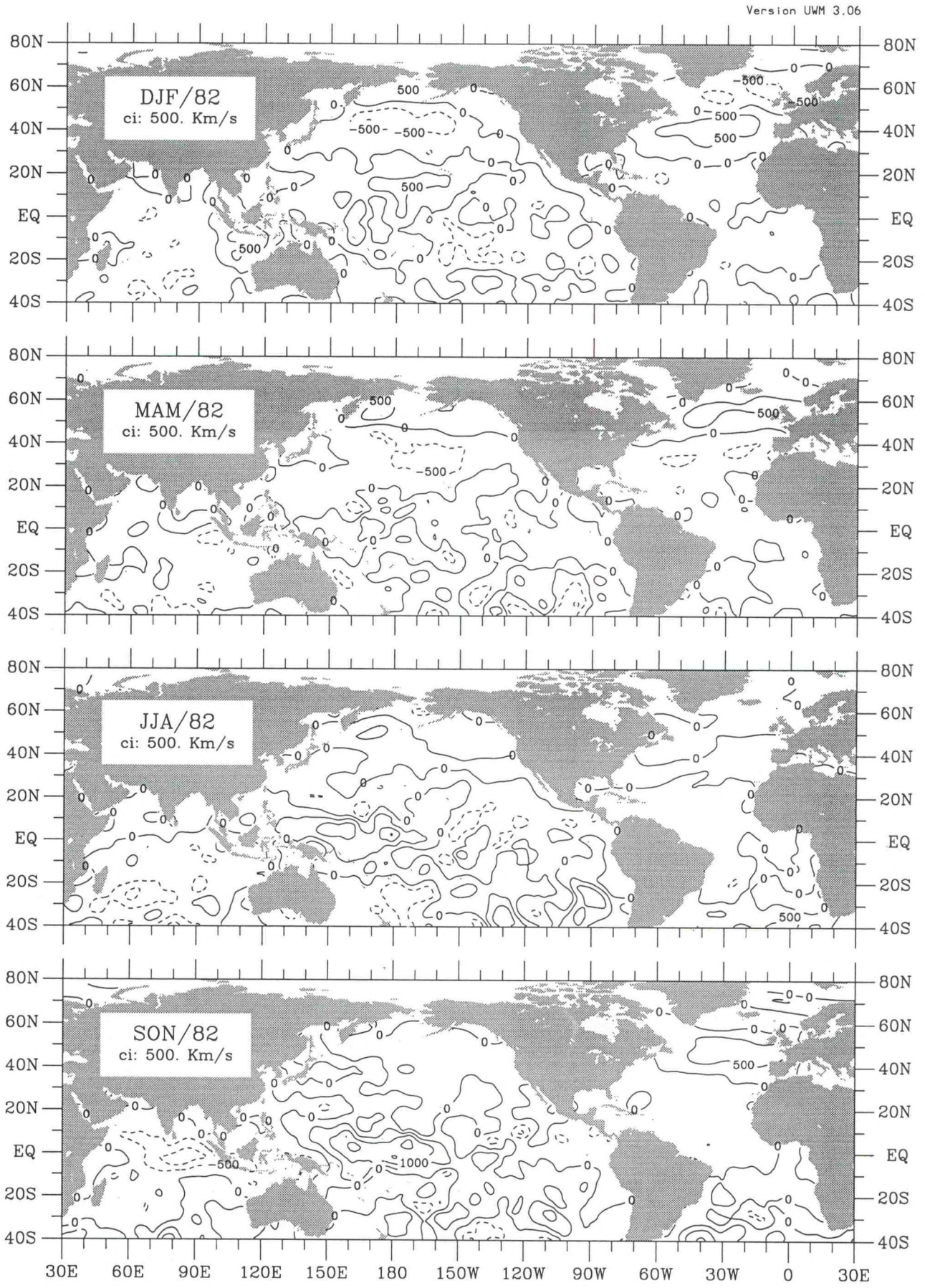

Figure ua-43. Zonal heat flux seasonal anomaly for 1982.

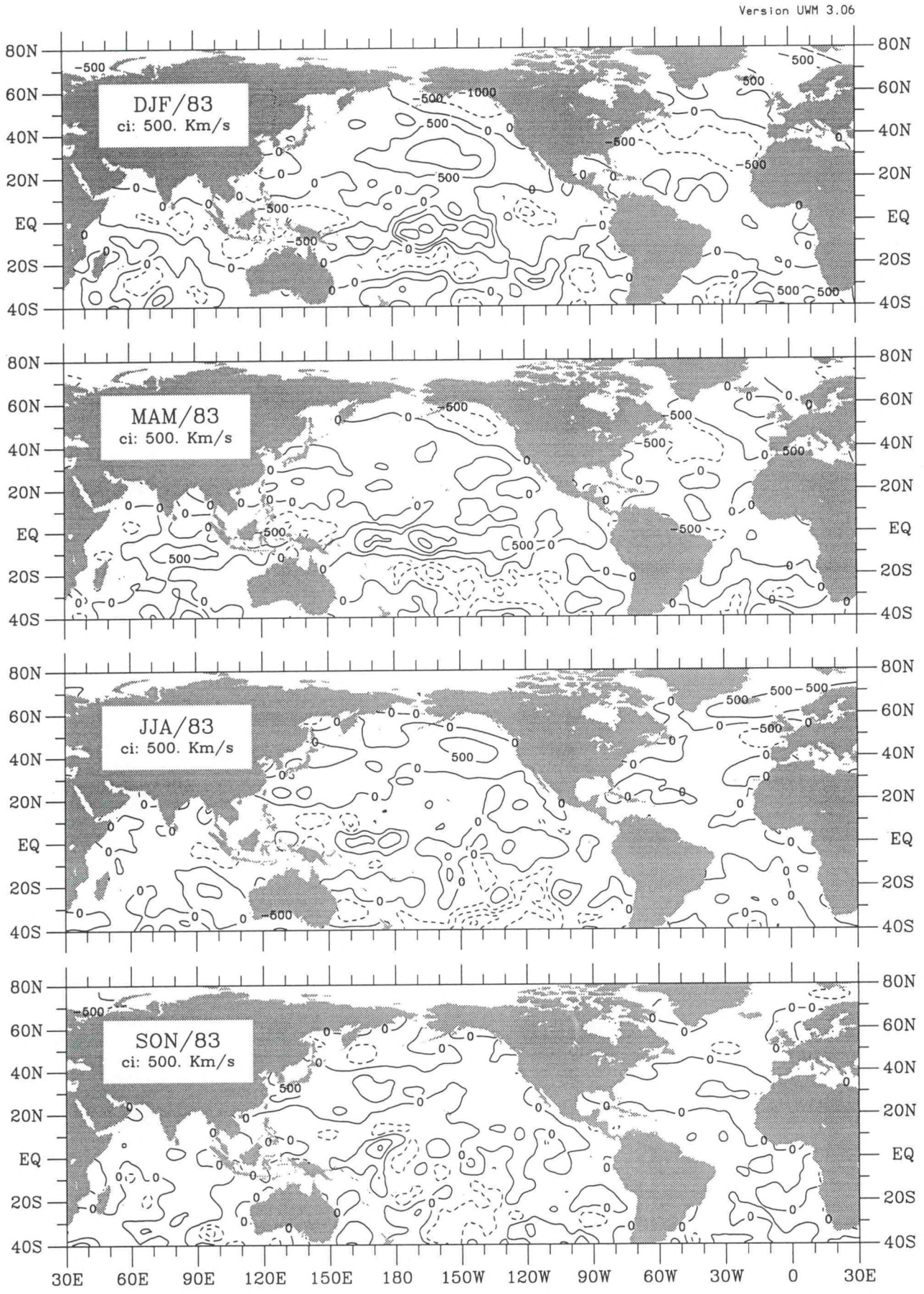

Figure ua-44. Zonal heat flux seasonal anomaly for 1983.

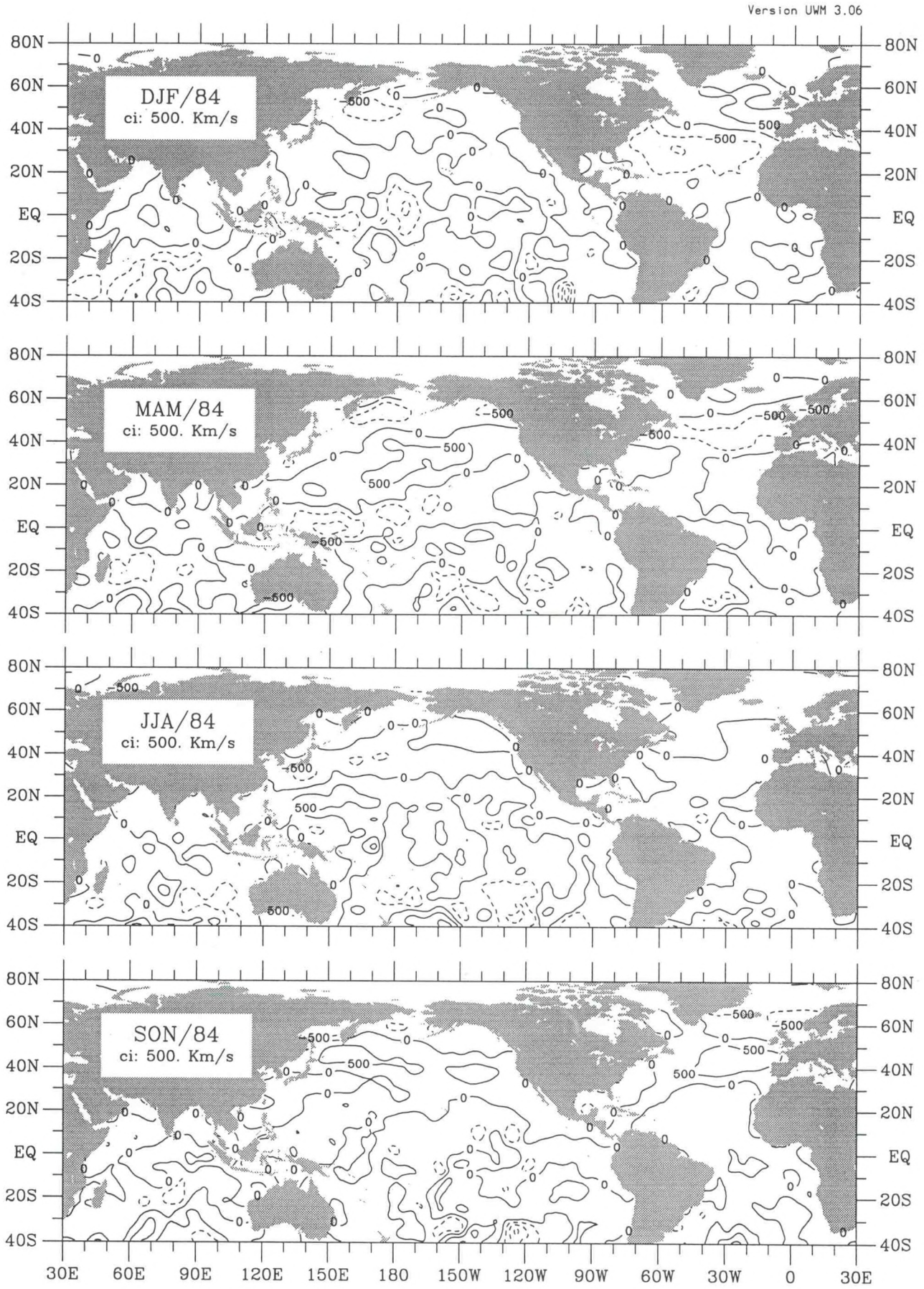

Figure ua-45. Zonal heat flux seasonal anomaly for 1984.

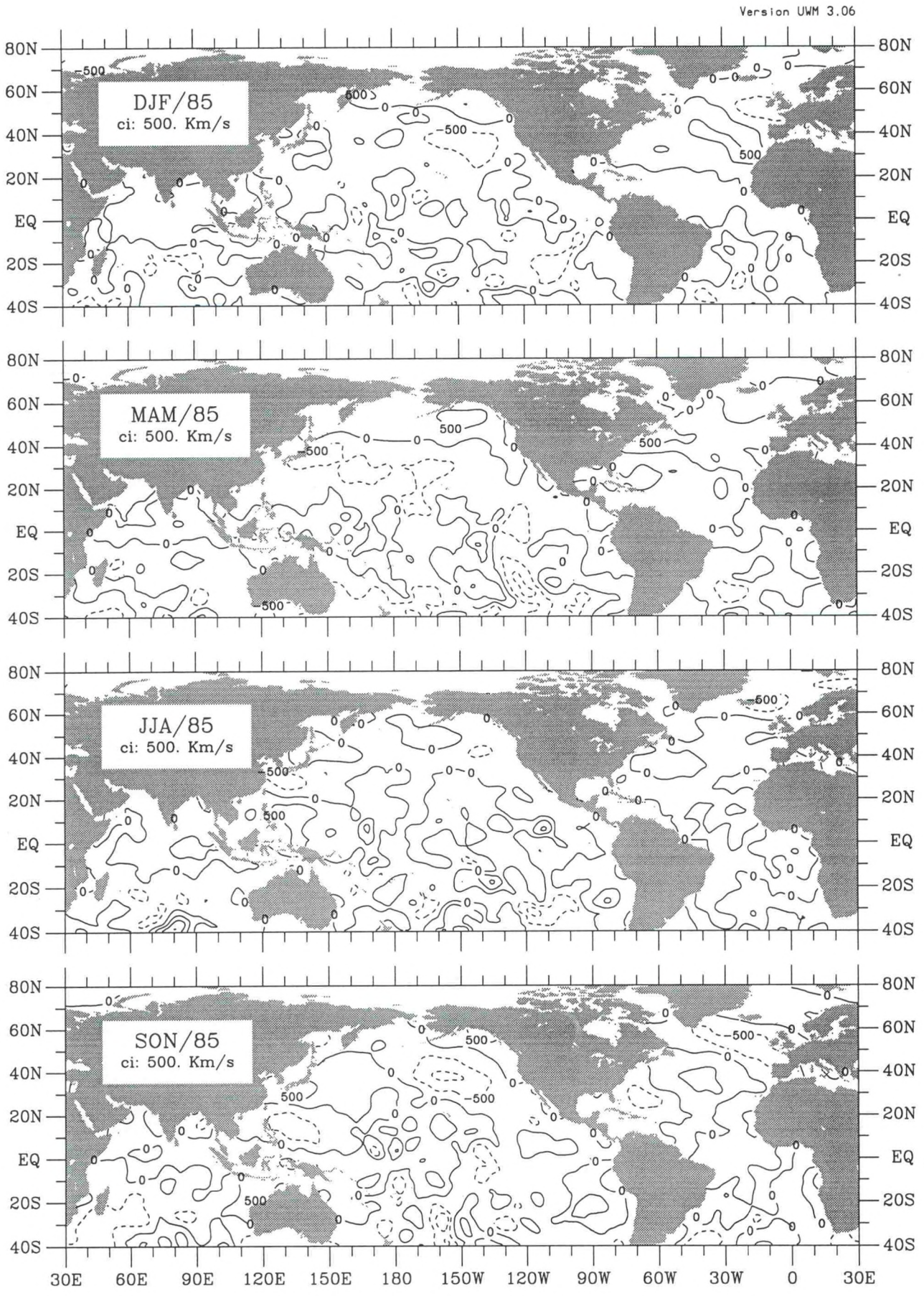

Figure ua-46. Zonal heat flux seasonal anomaly for 1985.

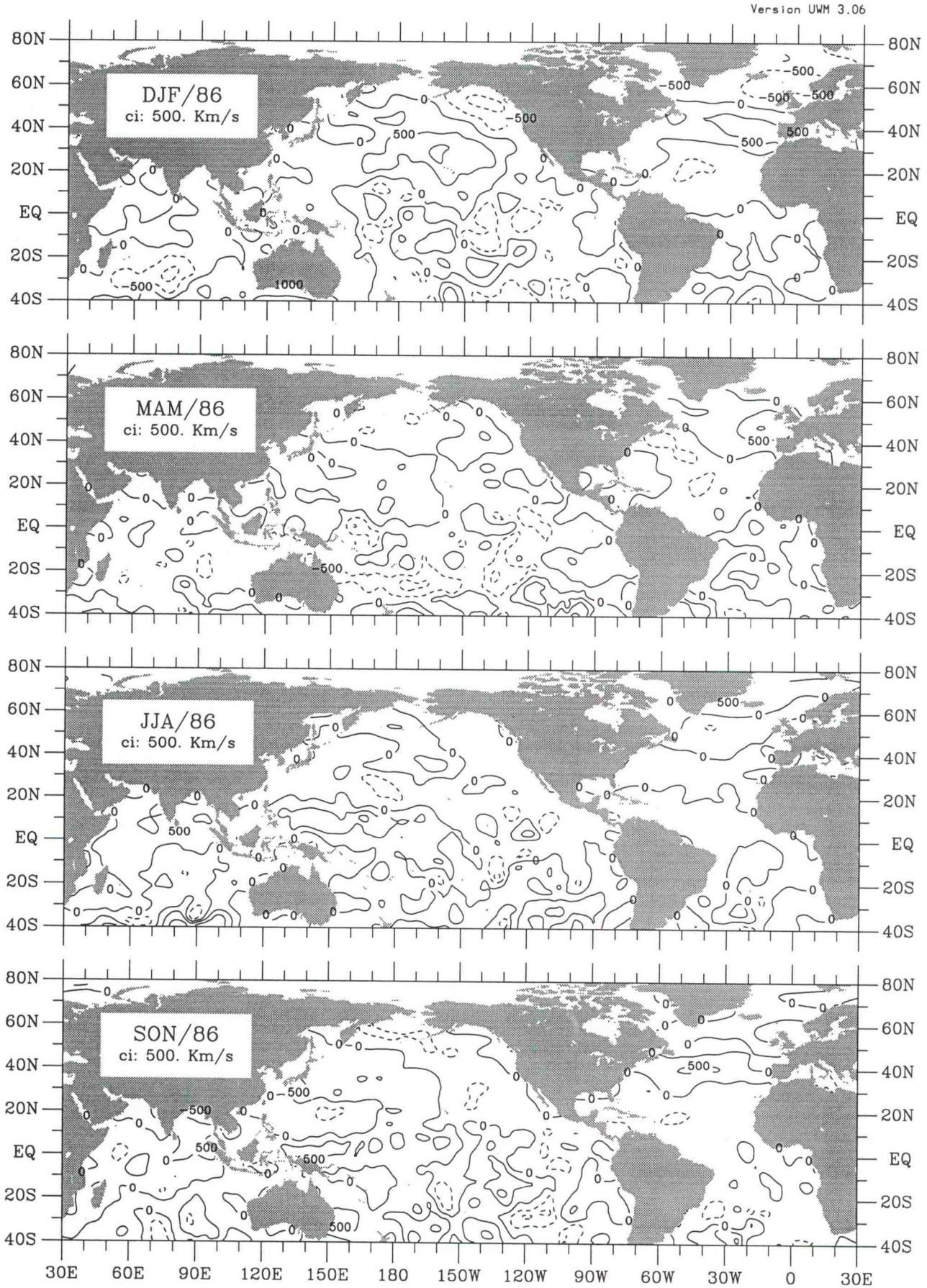

Figure ua-47. Zonal heat flux seasonal anomaly for 1986.

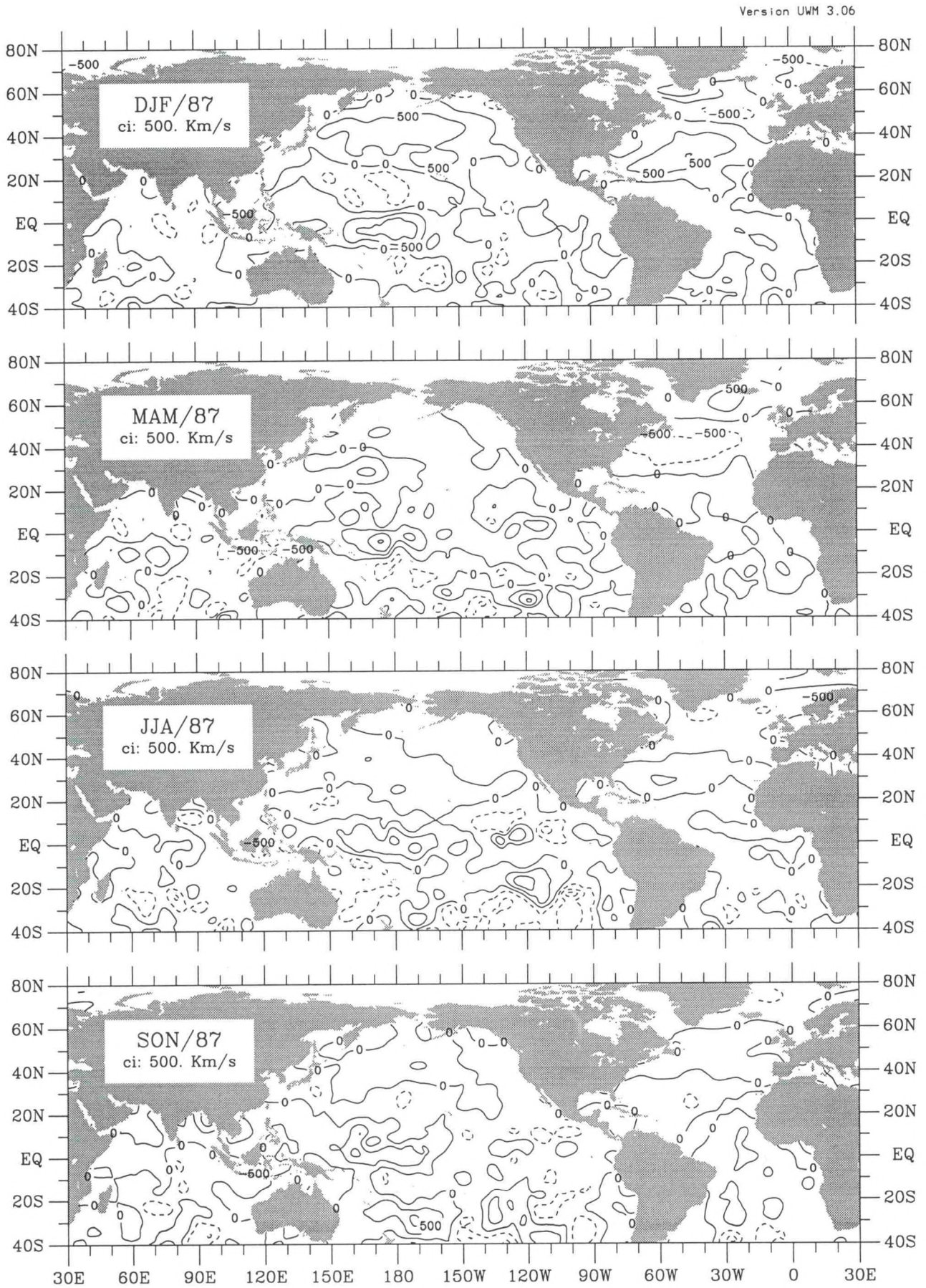

Figure ua-48. Zonal heat flux seasonal anomaly for 1987.

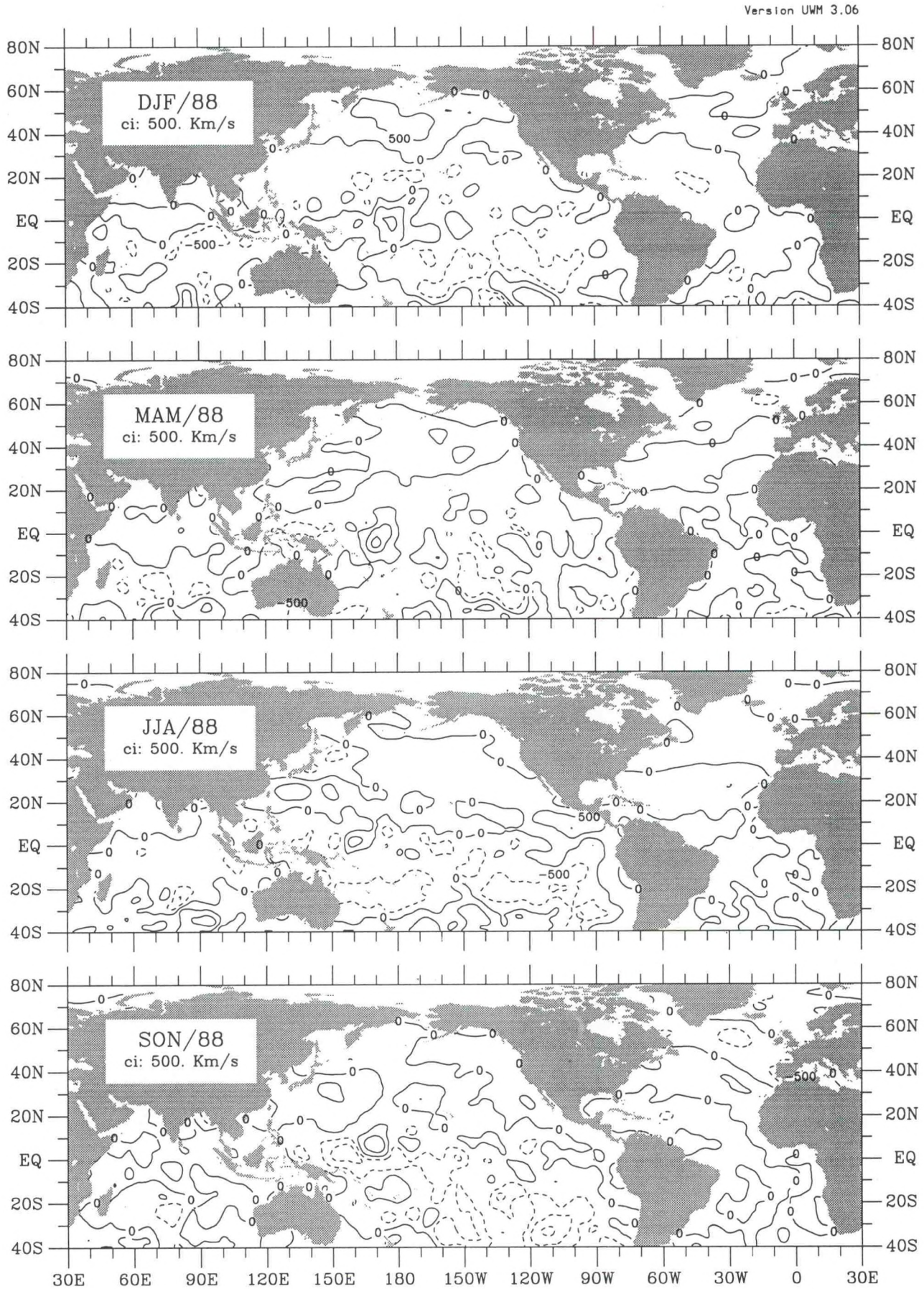

Figure ua-49. Zonal heat flux seasonal anomaly for 1988.

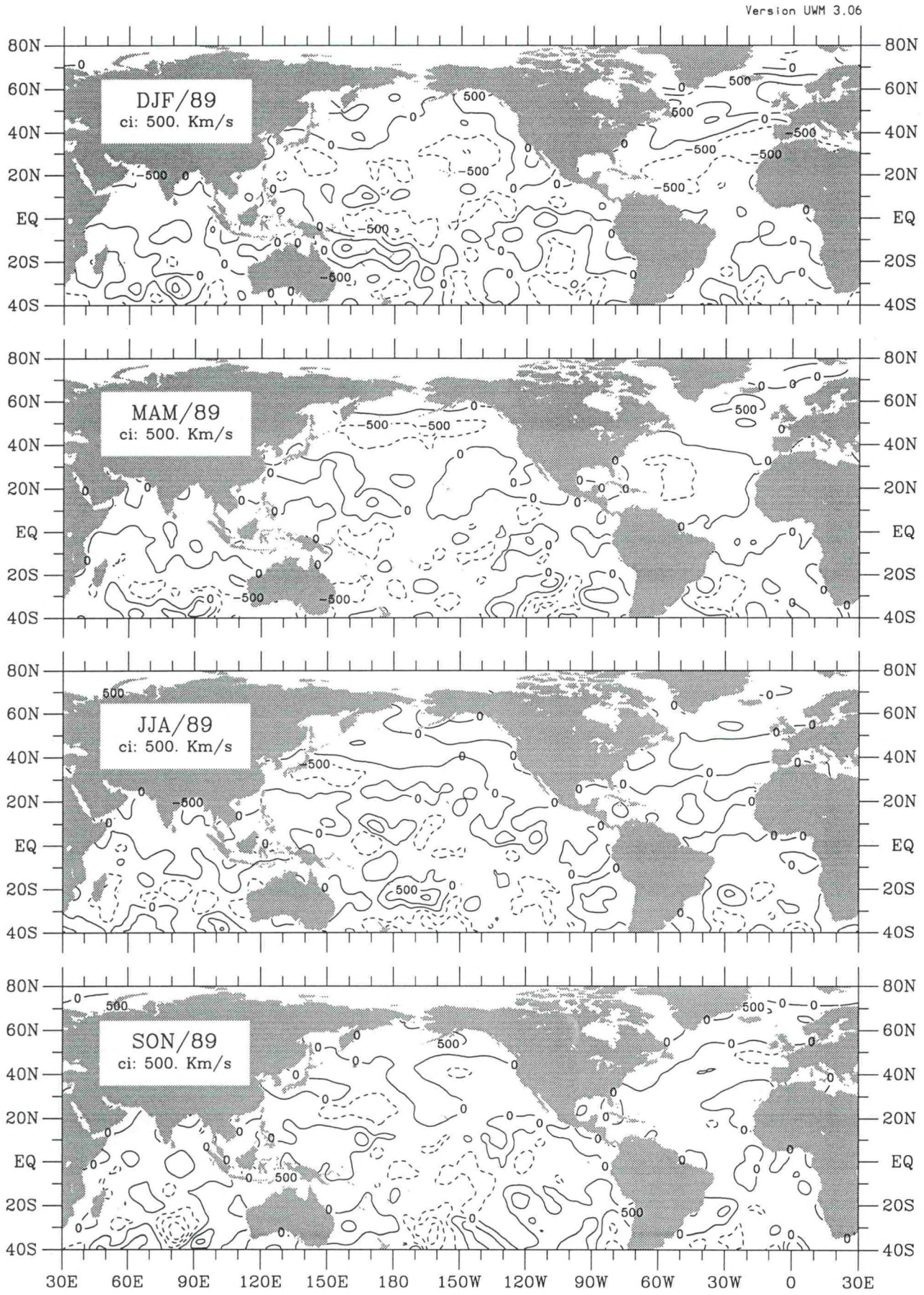

Figure ua-50. Zonal heat flux seasonal anomaly for 1989.

16 Meridional heat flux

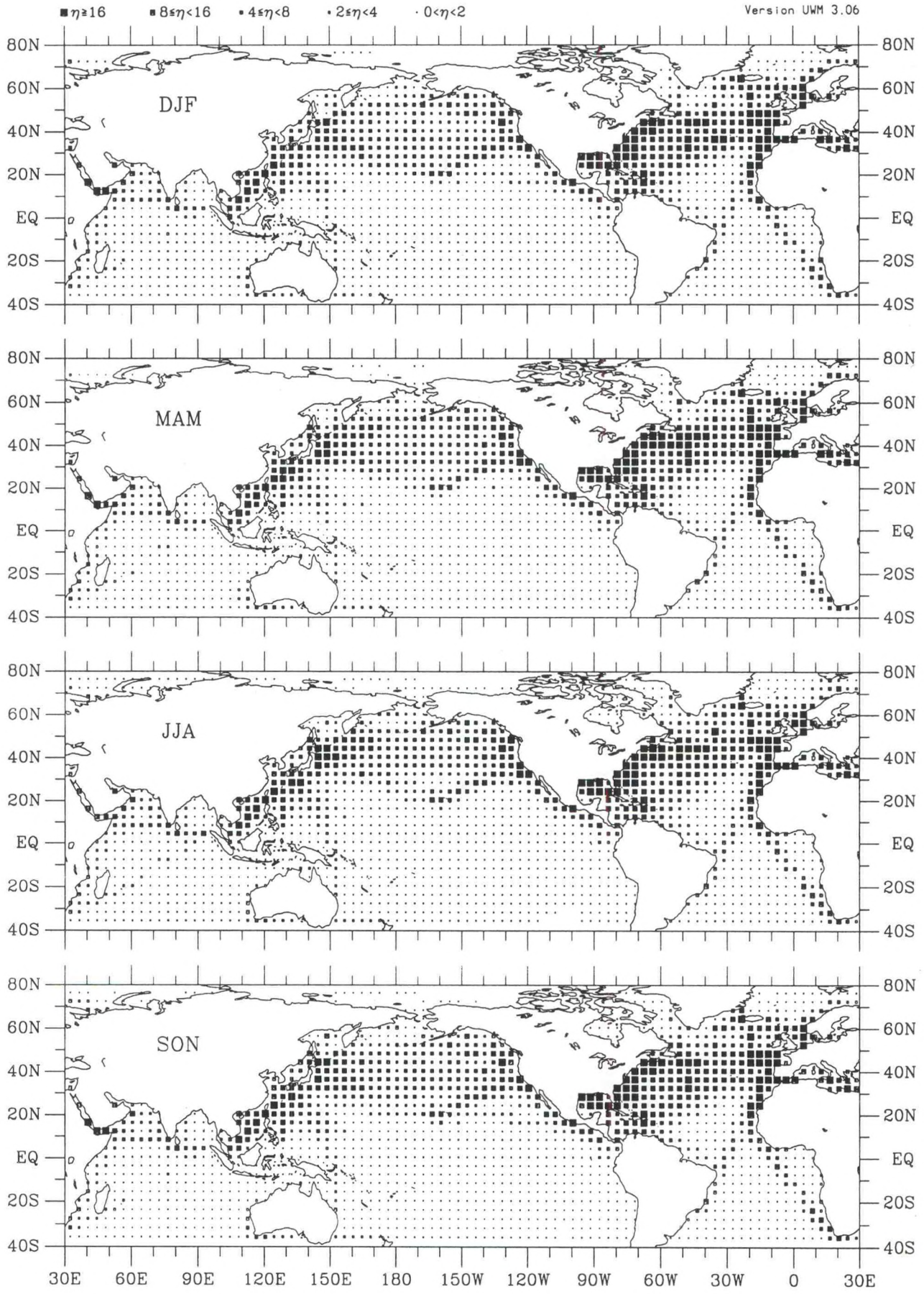

Figure va-1. Meridional heat flux seasonal observation density (1945-89).

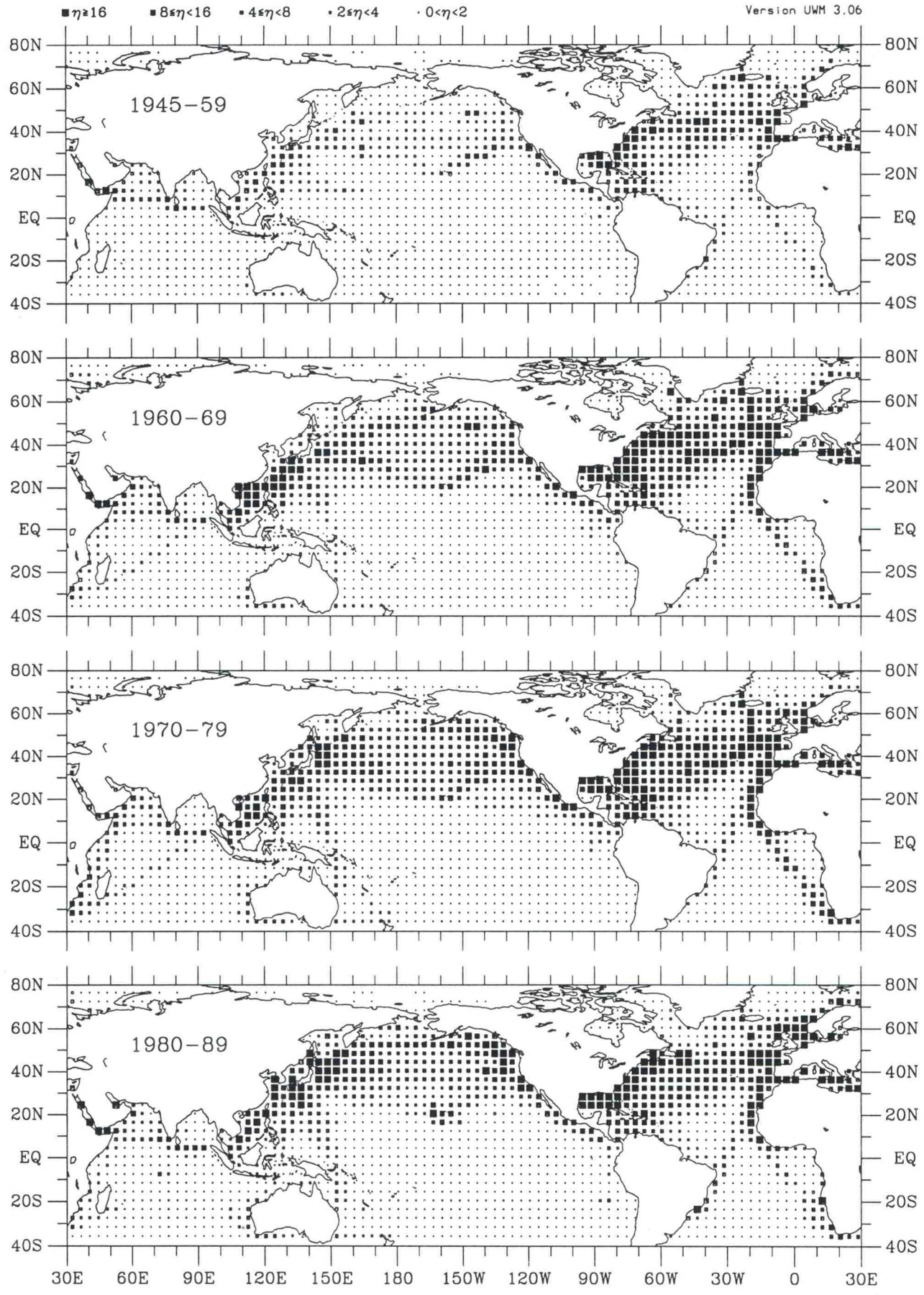

Figure va-2. Meridional heat flux decadal observation density.

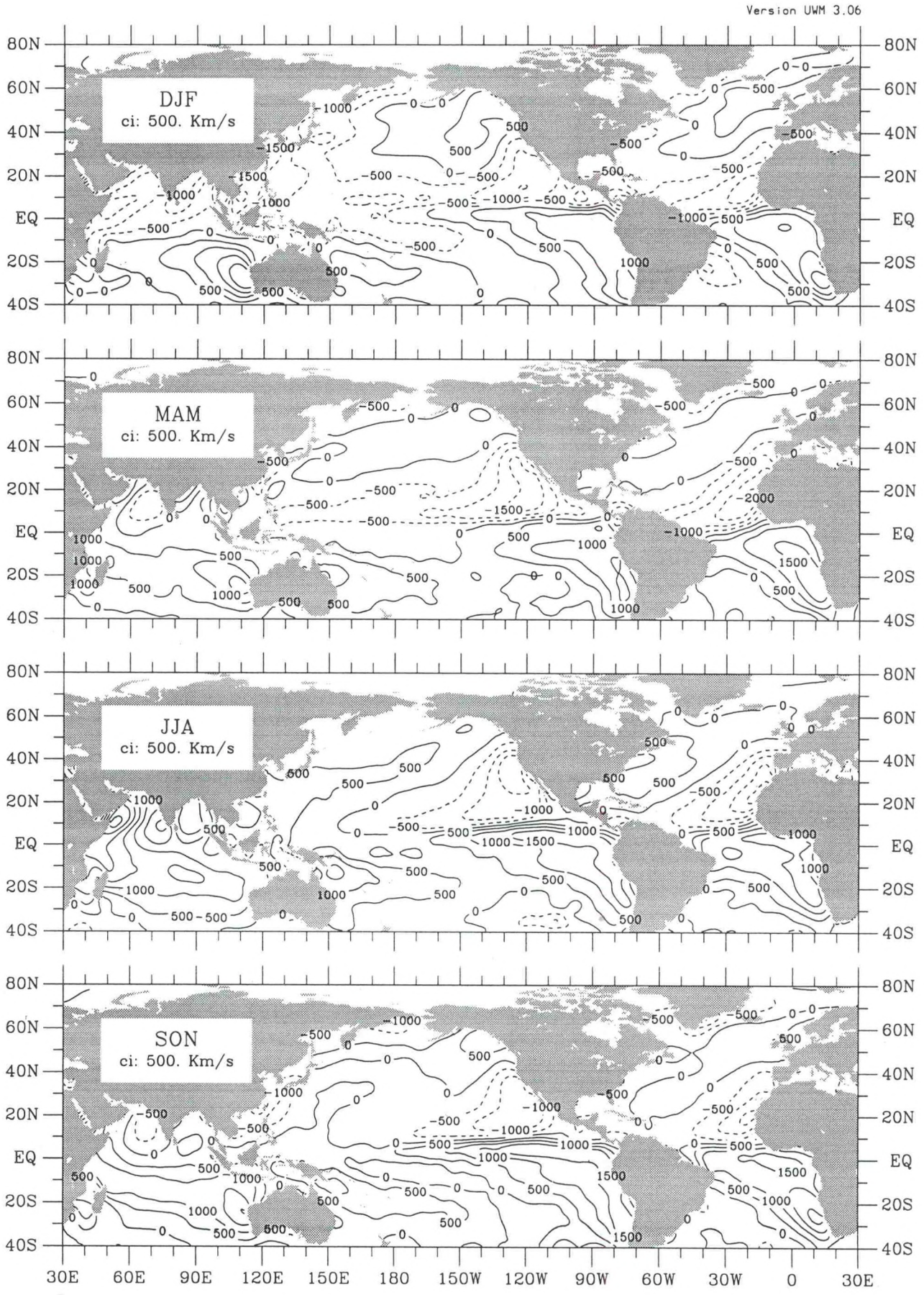

Figure va-3. Meridional heat flux seasonal climatology (1945-89).

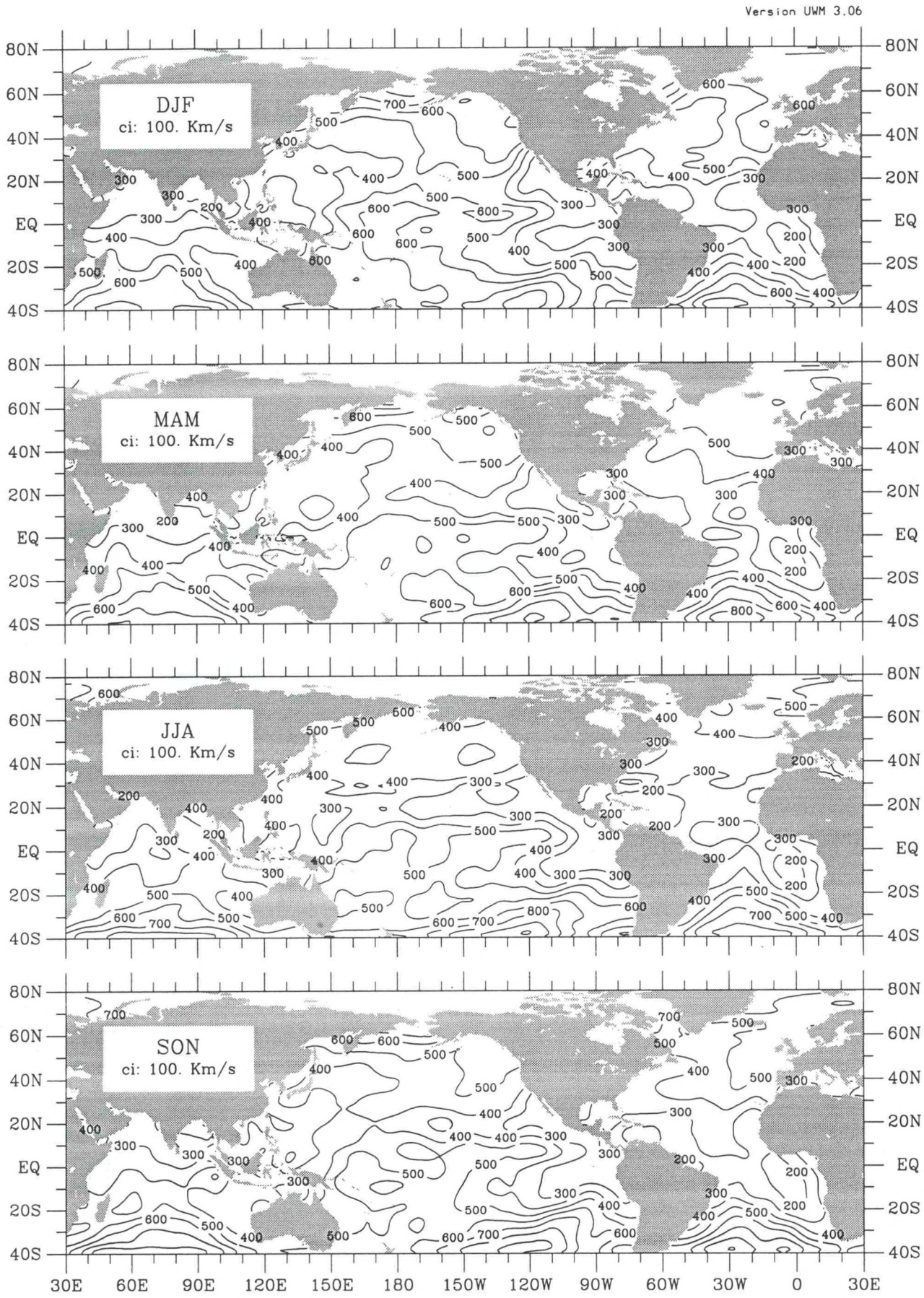

Figure va-4. Meridional heat flux seasonal interannual std dev (1945-89).

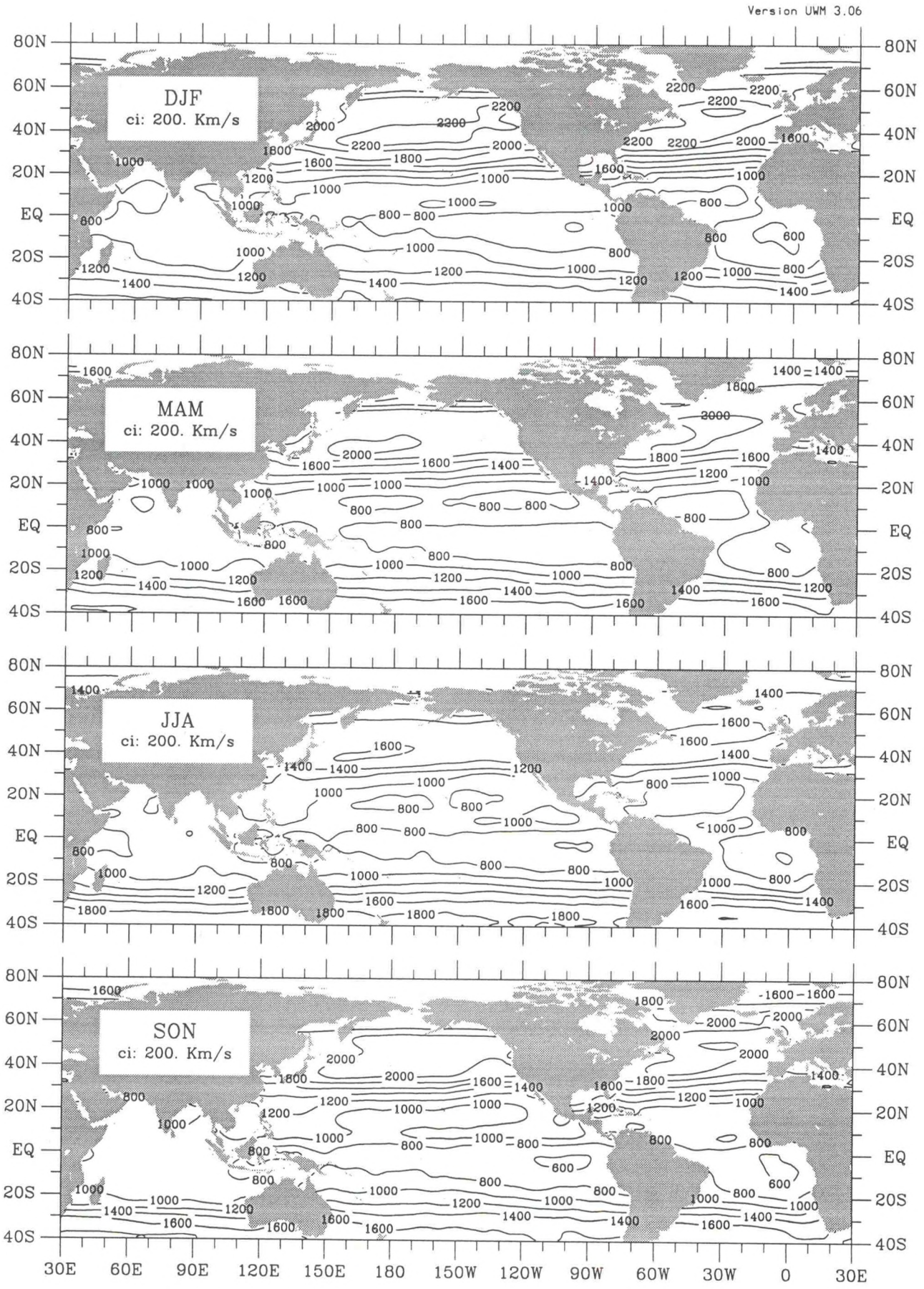

Figure va-5. Meridional heat flux seasonal standard deviation (1945-89).

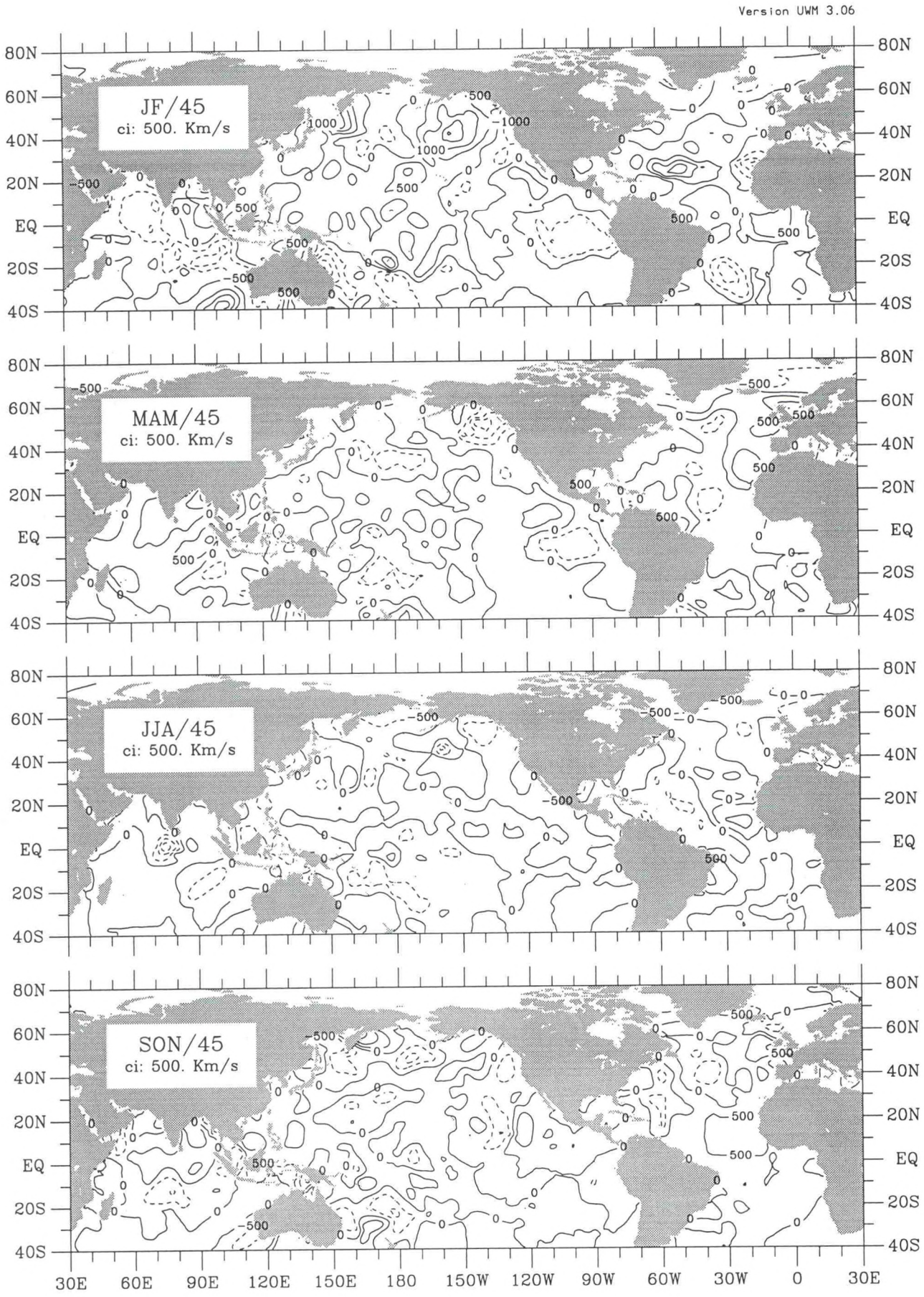

Figure va-6. Meridional heat flux seasonal anomaly for 1945.

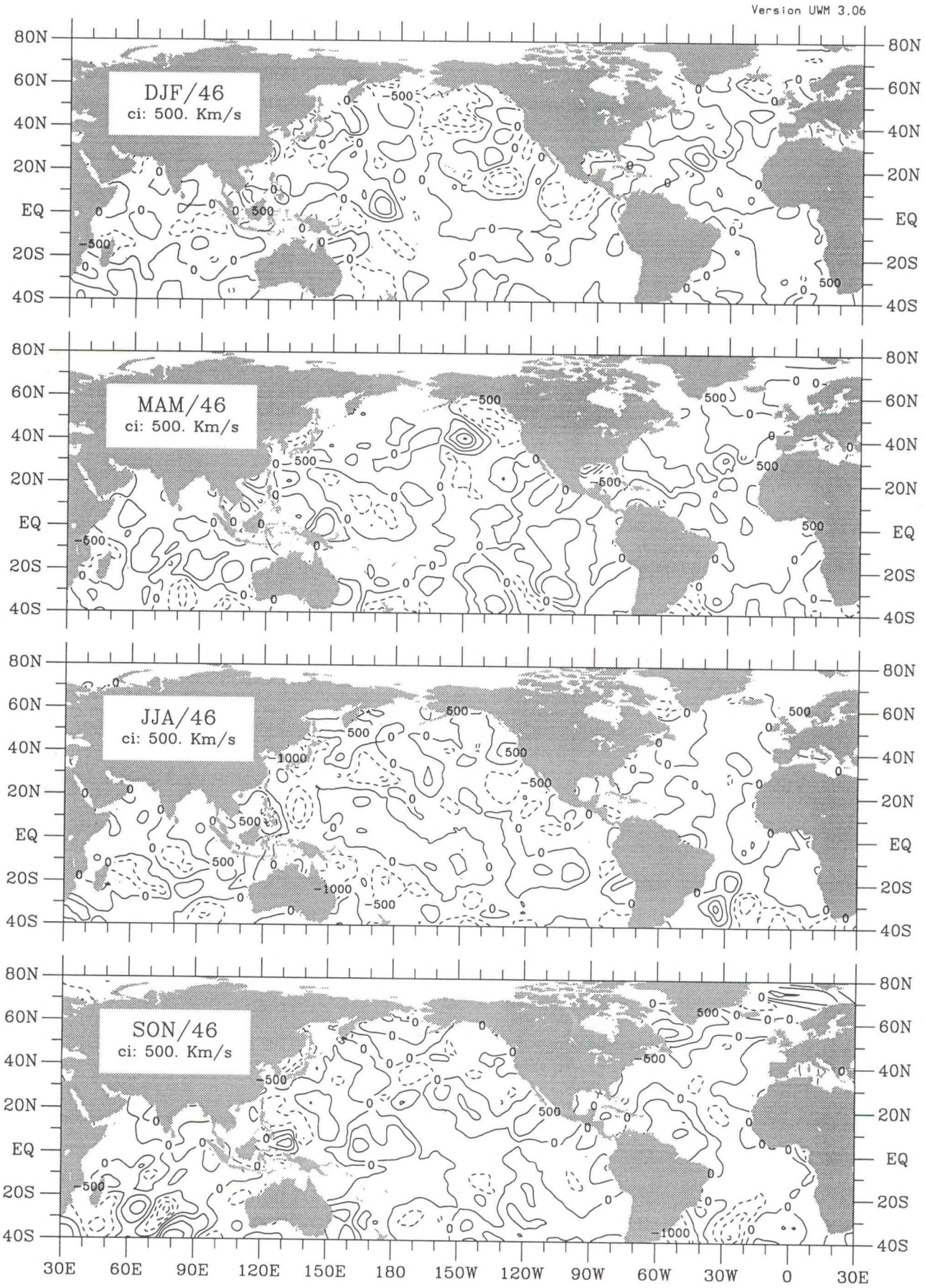

Figure va-7. Meridional heat flux seasonal anomaly for 1946.

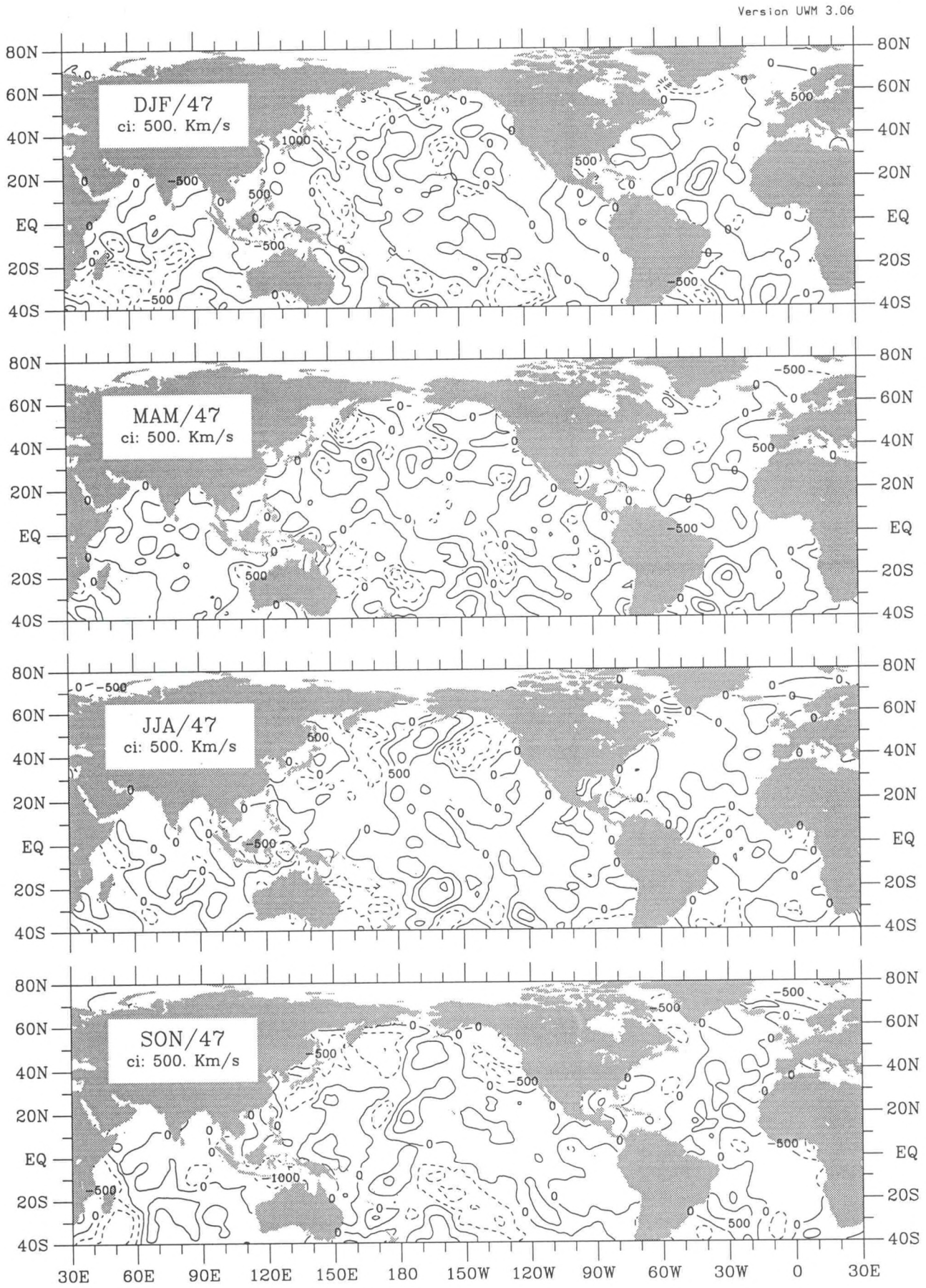

Figure va-8. Meridional heat flux seasonal anomaly for 1947.

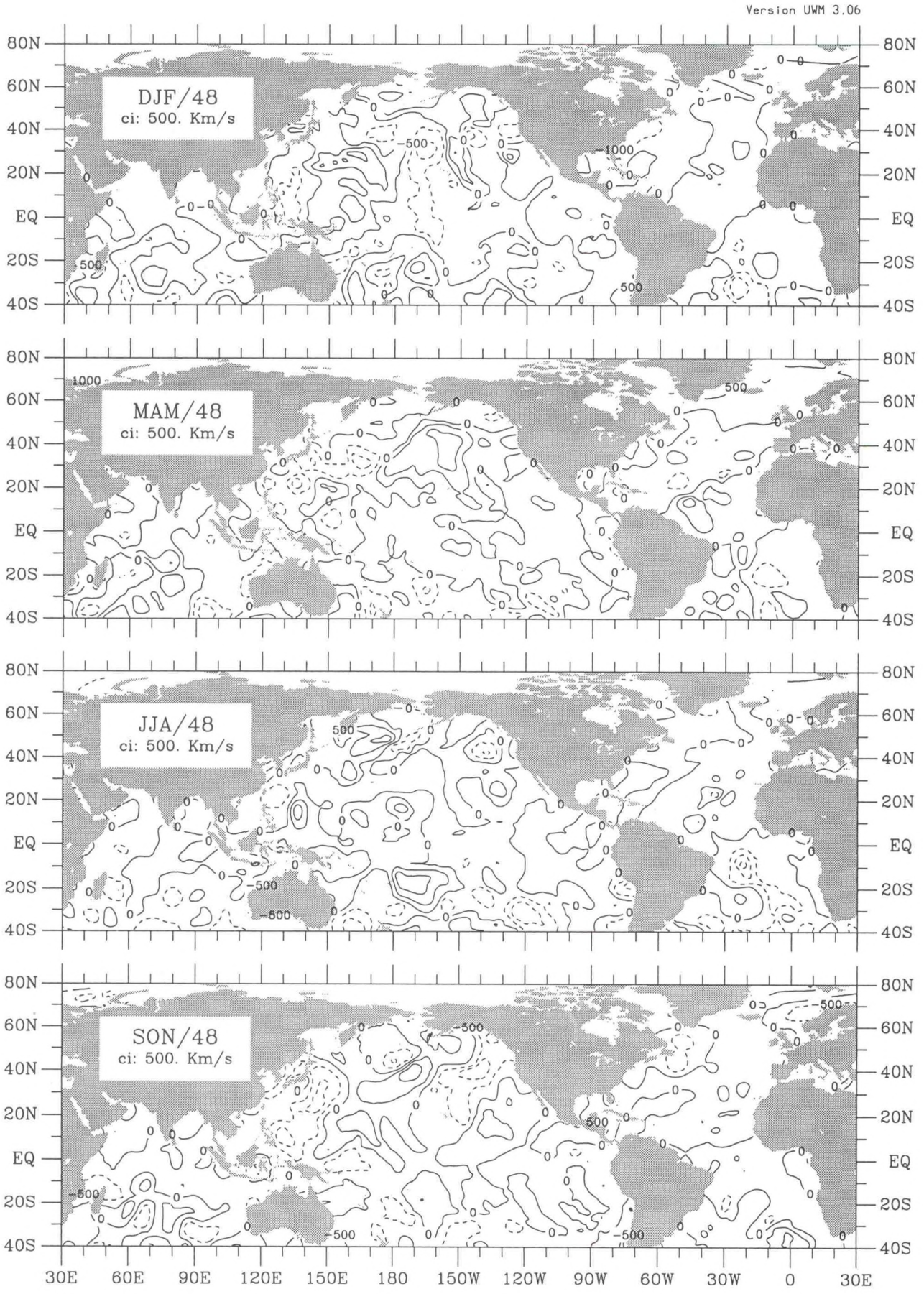

Figure va-9. Meridional heat flux seasonal anomaly for 1948.

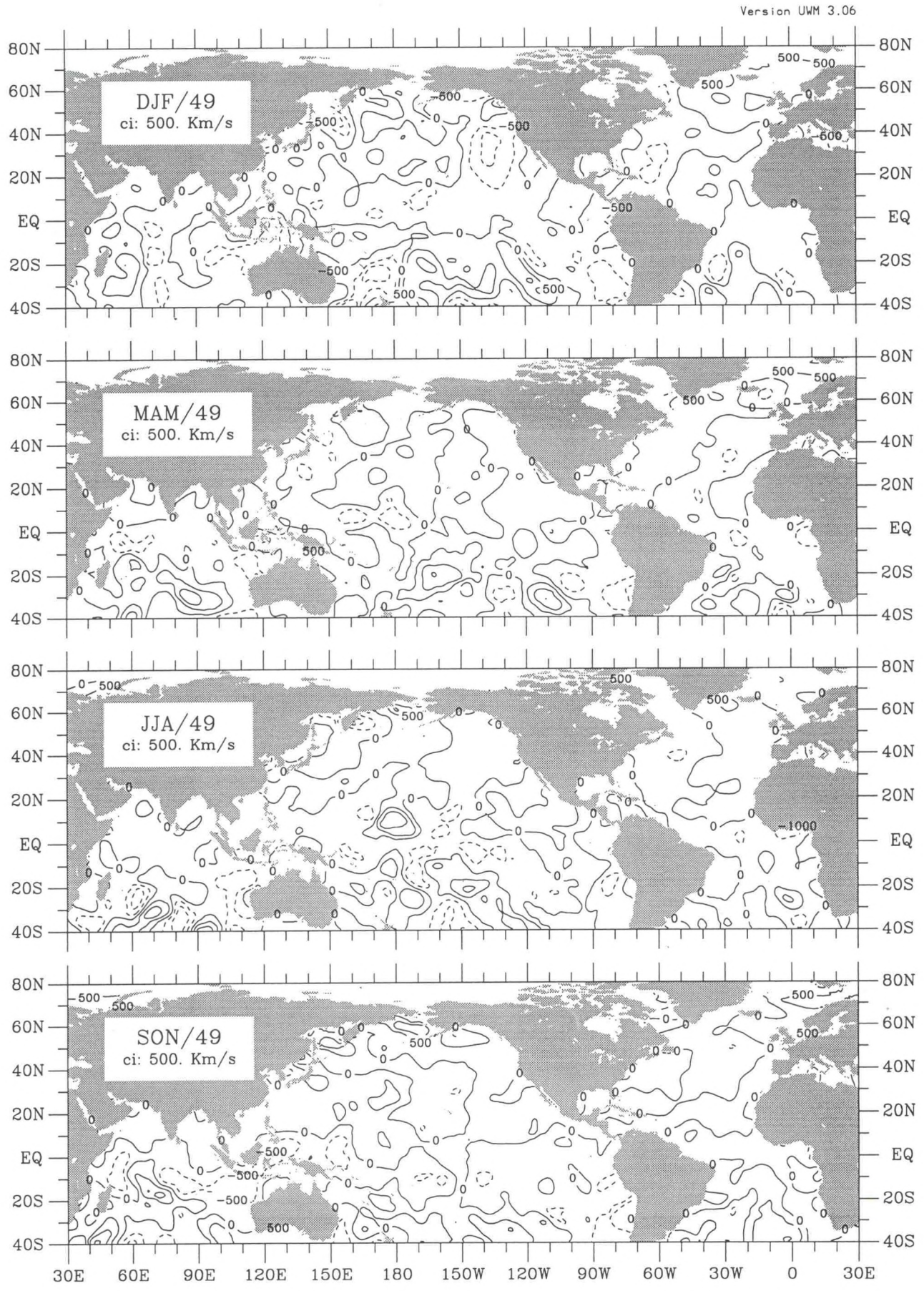

Figure va-10. Meridional heat flux seasonal anomaly for 1949.

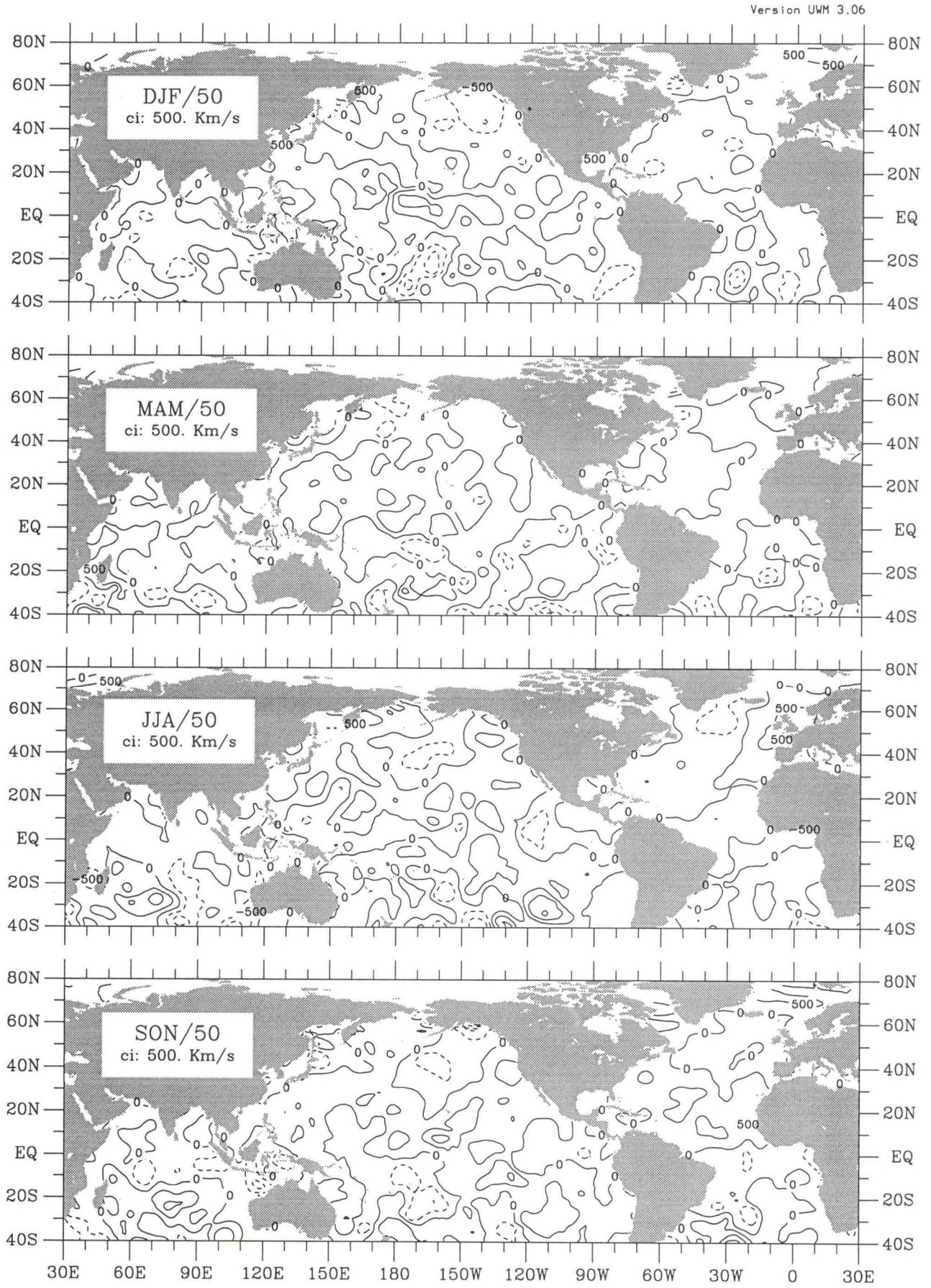

Figure va-11. Meridional heat flux seasonal anomaly for 1950.

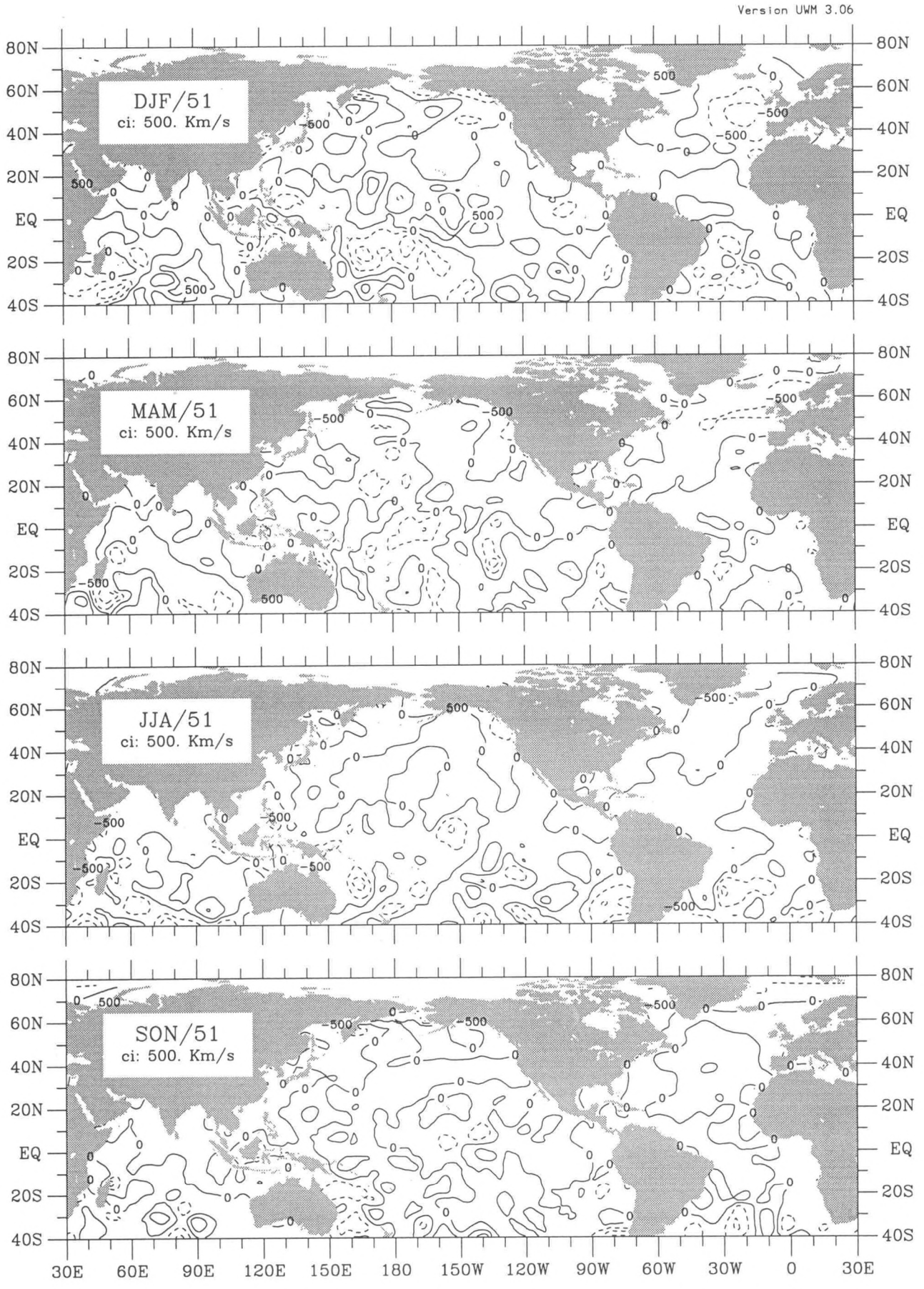

Figure va-12. Meridional heat flux seasonal anomaly for 1951.

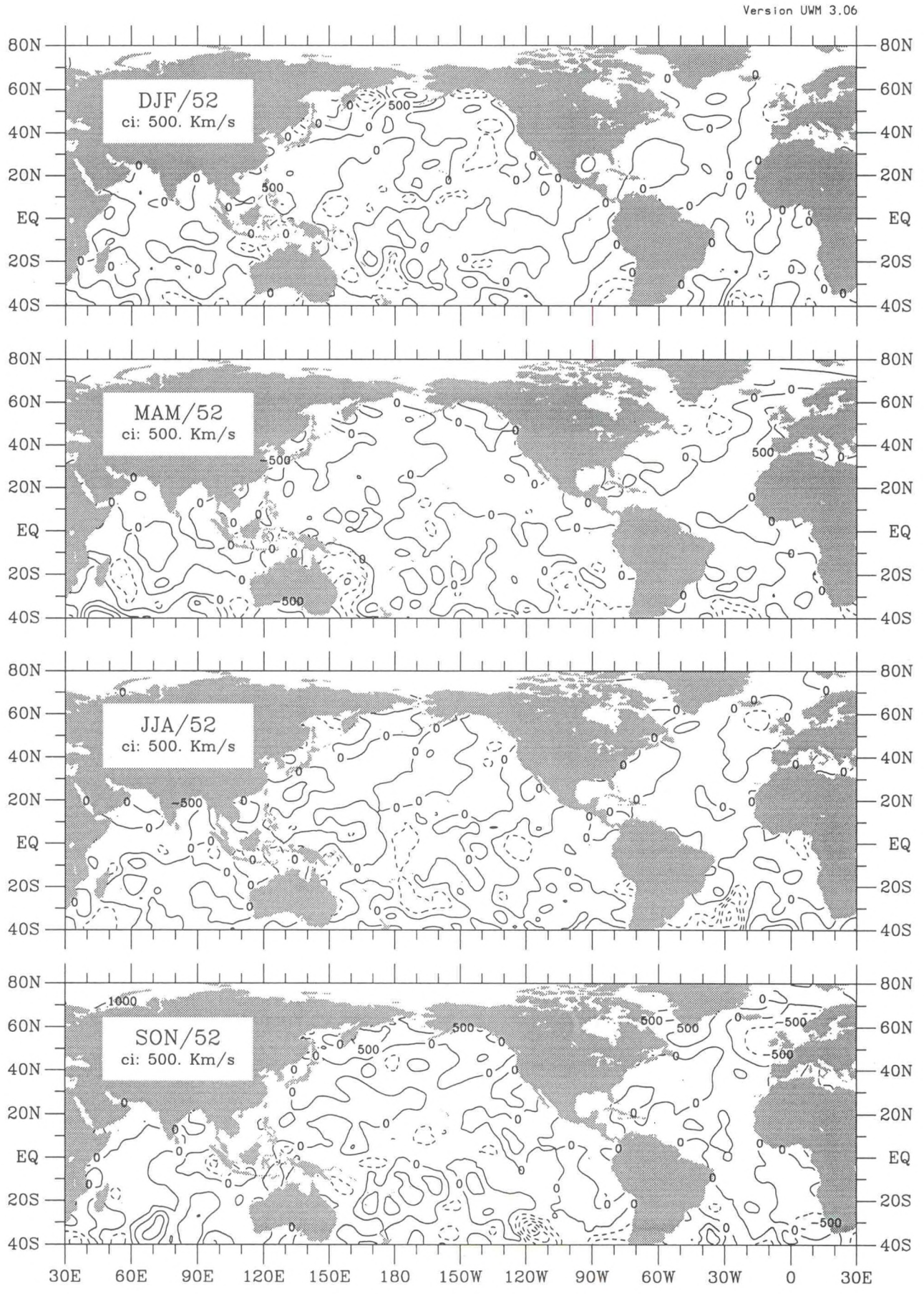

Figure va-13. Meridional heat flux seasonal anomaly for 1952.

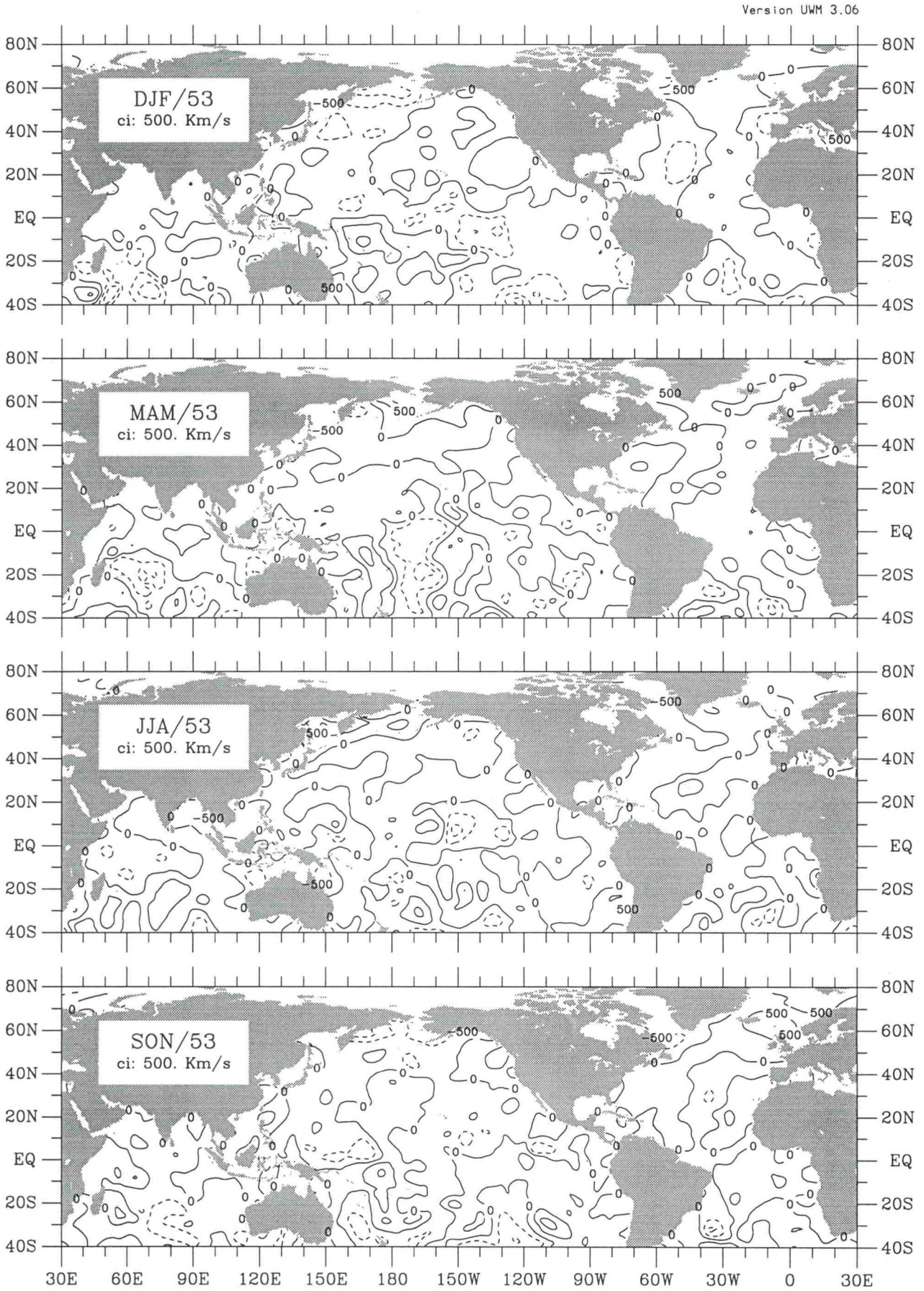

Figure va-14. Meridional heat flux seasonal anomaly for 1953.

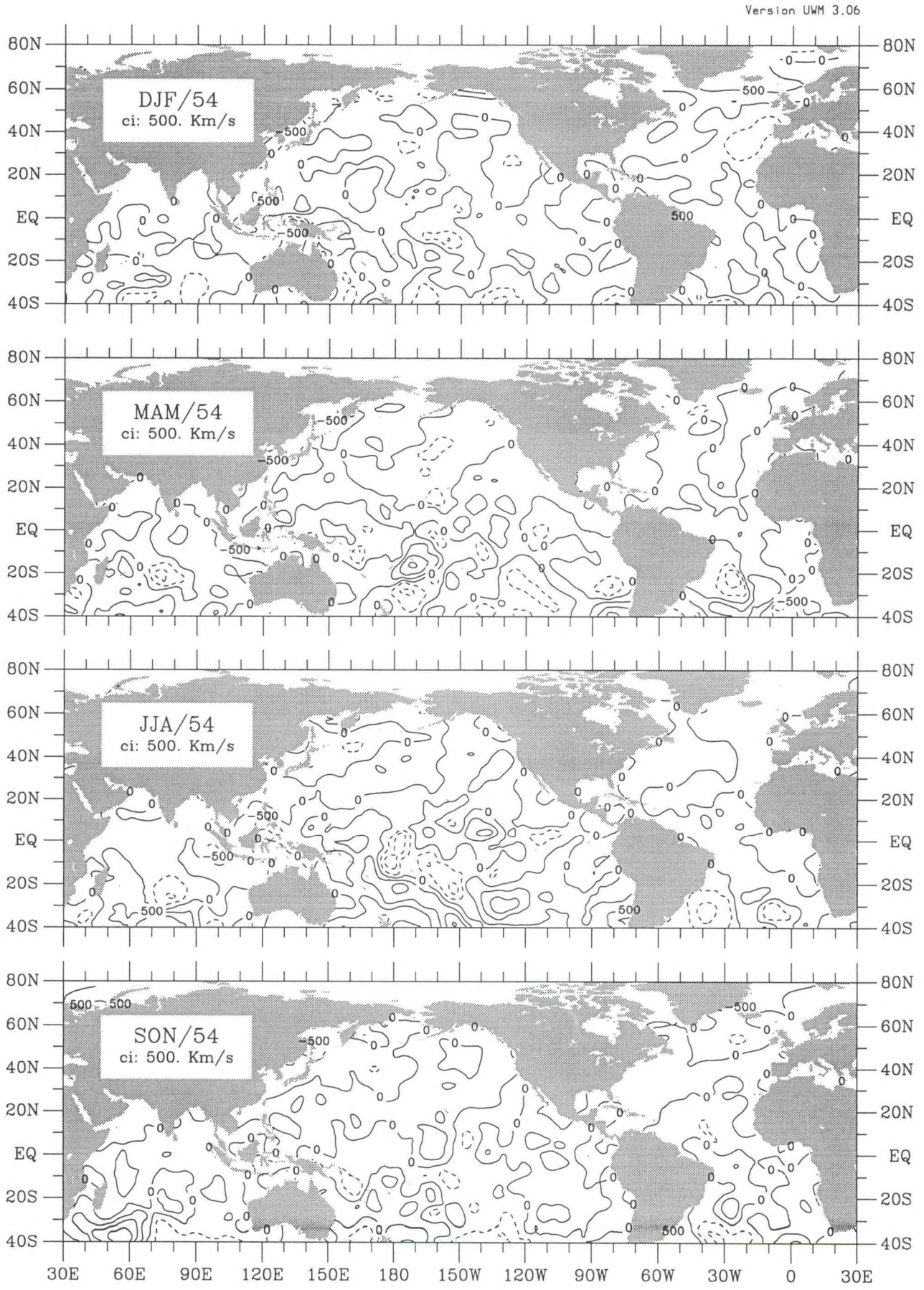

Figure va-15. Meridional heat flux seasonal anomaly for 1954.

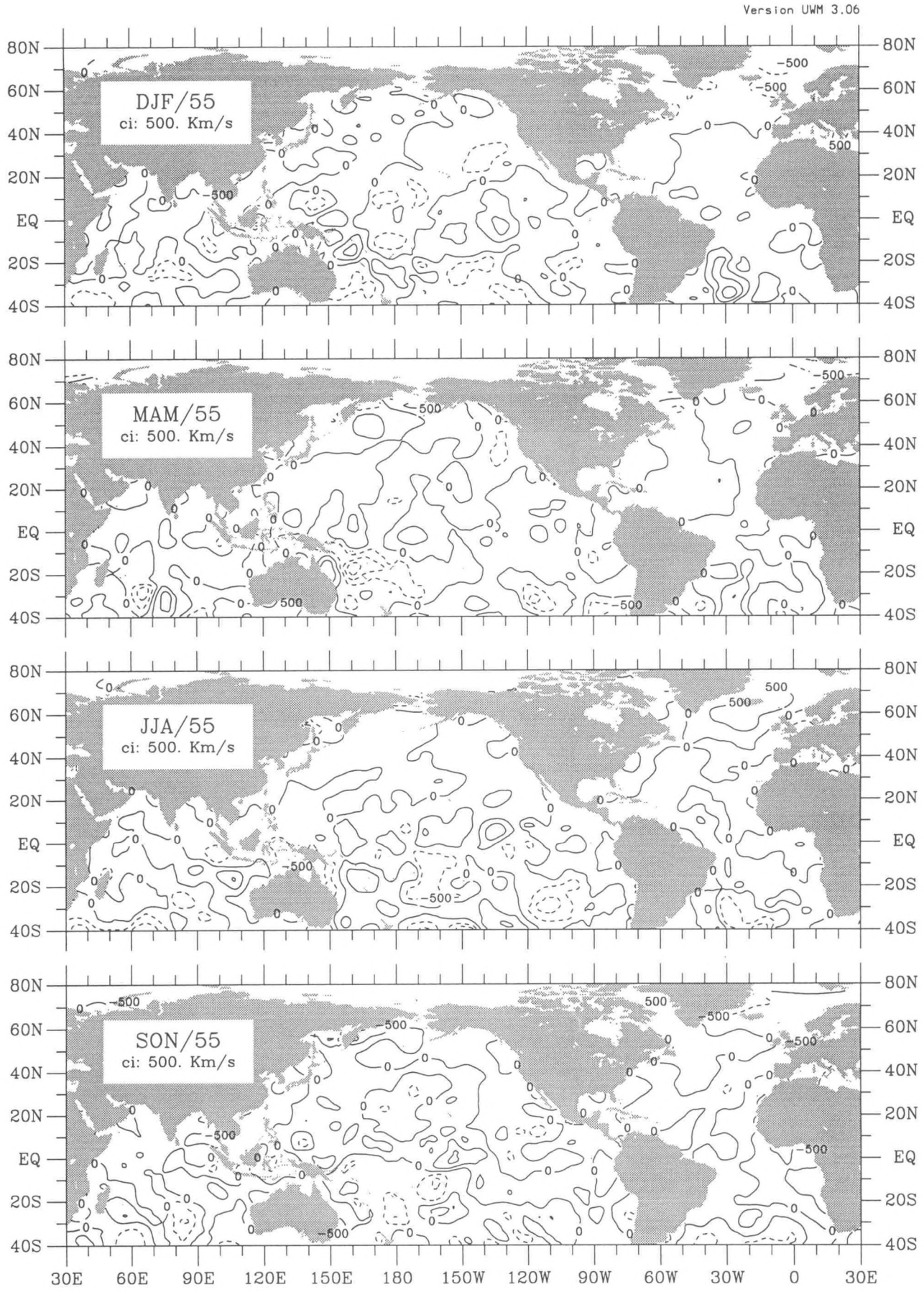

Figure va-16. Meridional heat flux seasonal anomaly for 1955.

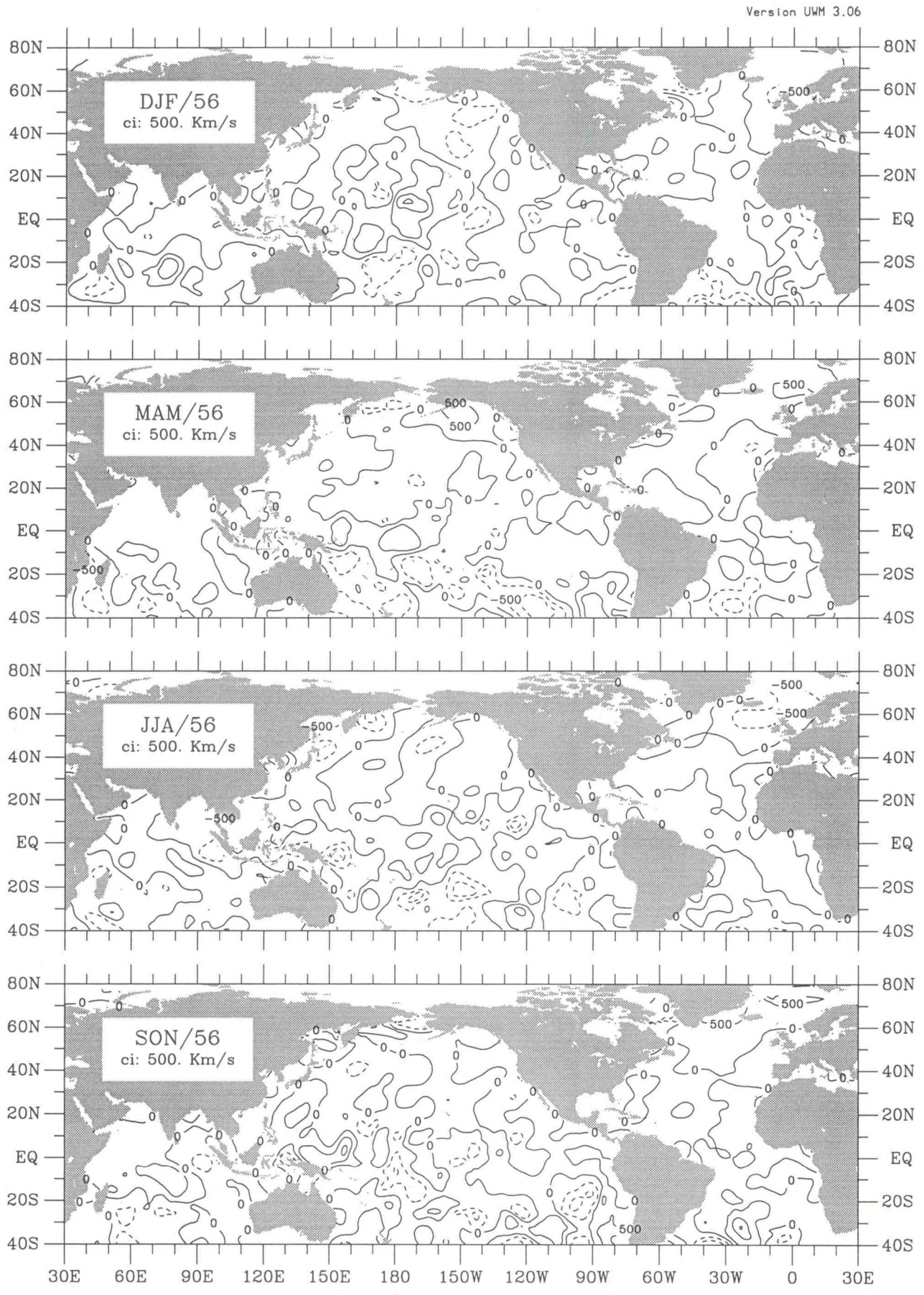

Figure va-17. Meridional heat flux seasonal anomaly for 1956.

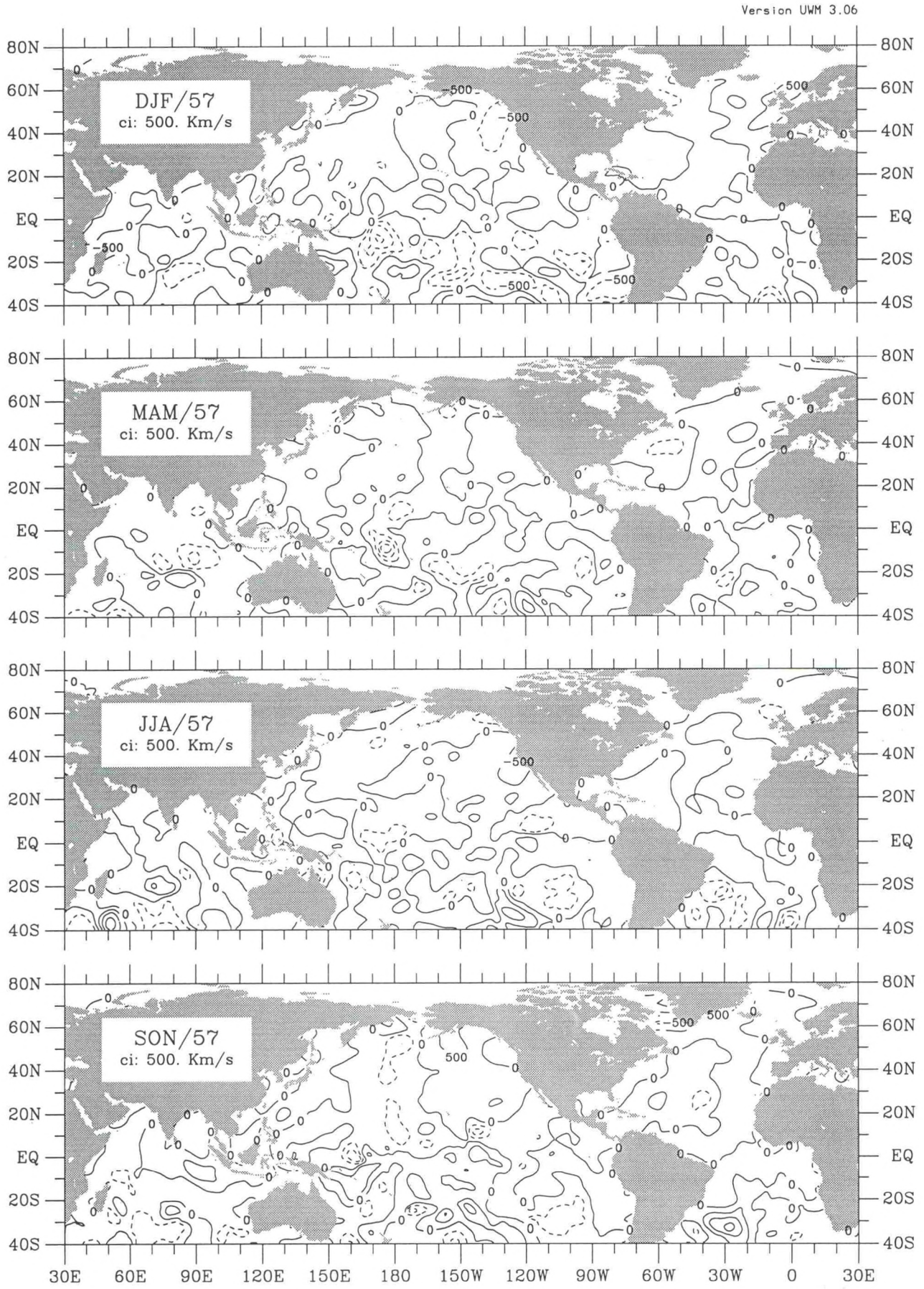

Figure va-18. Meridional heat flux seasonal anomaly for 1957.

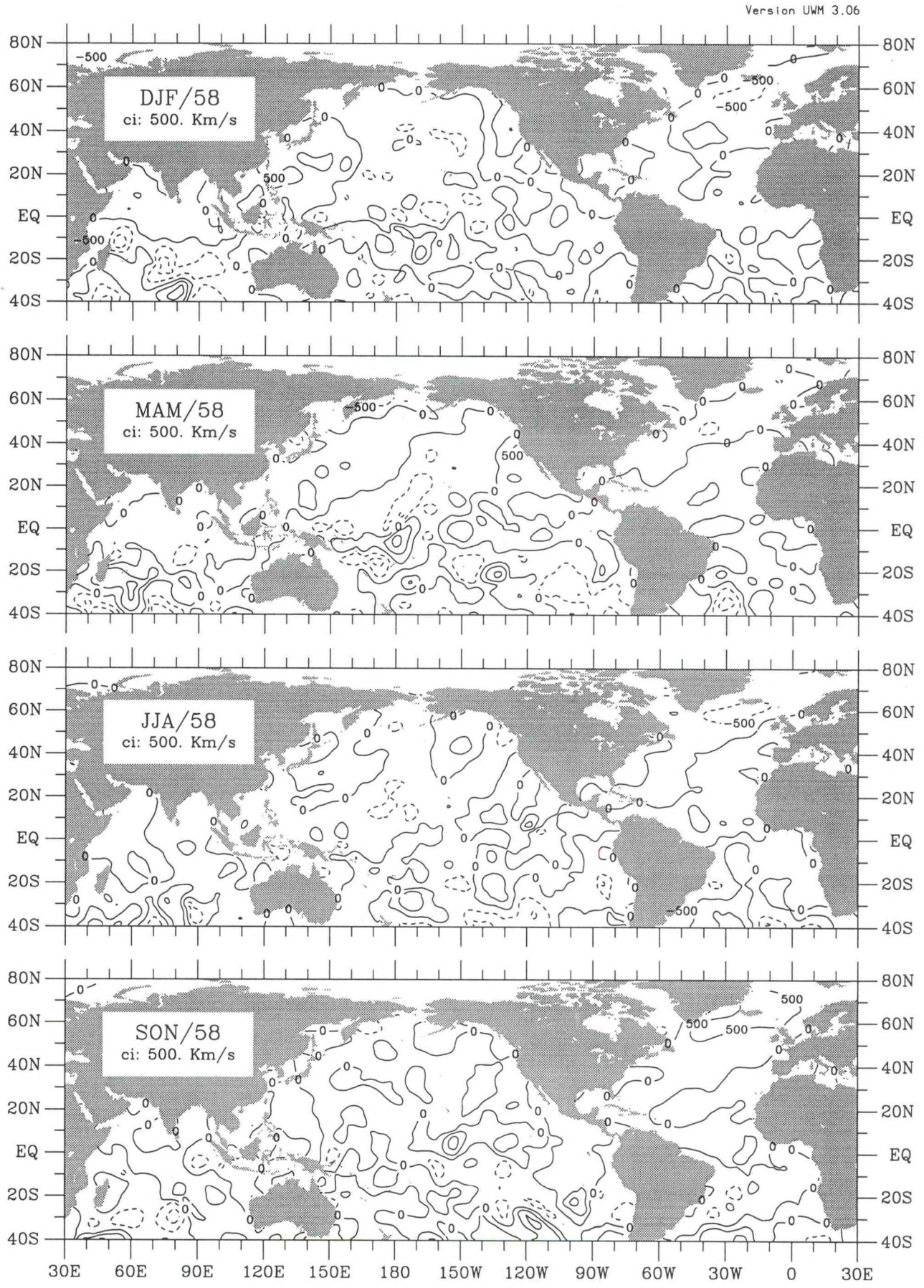

Figure va-19. Meridional heat flux seasonal anomaly for 1958.

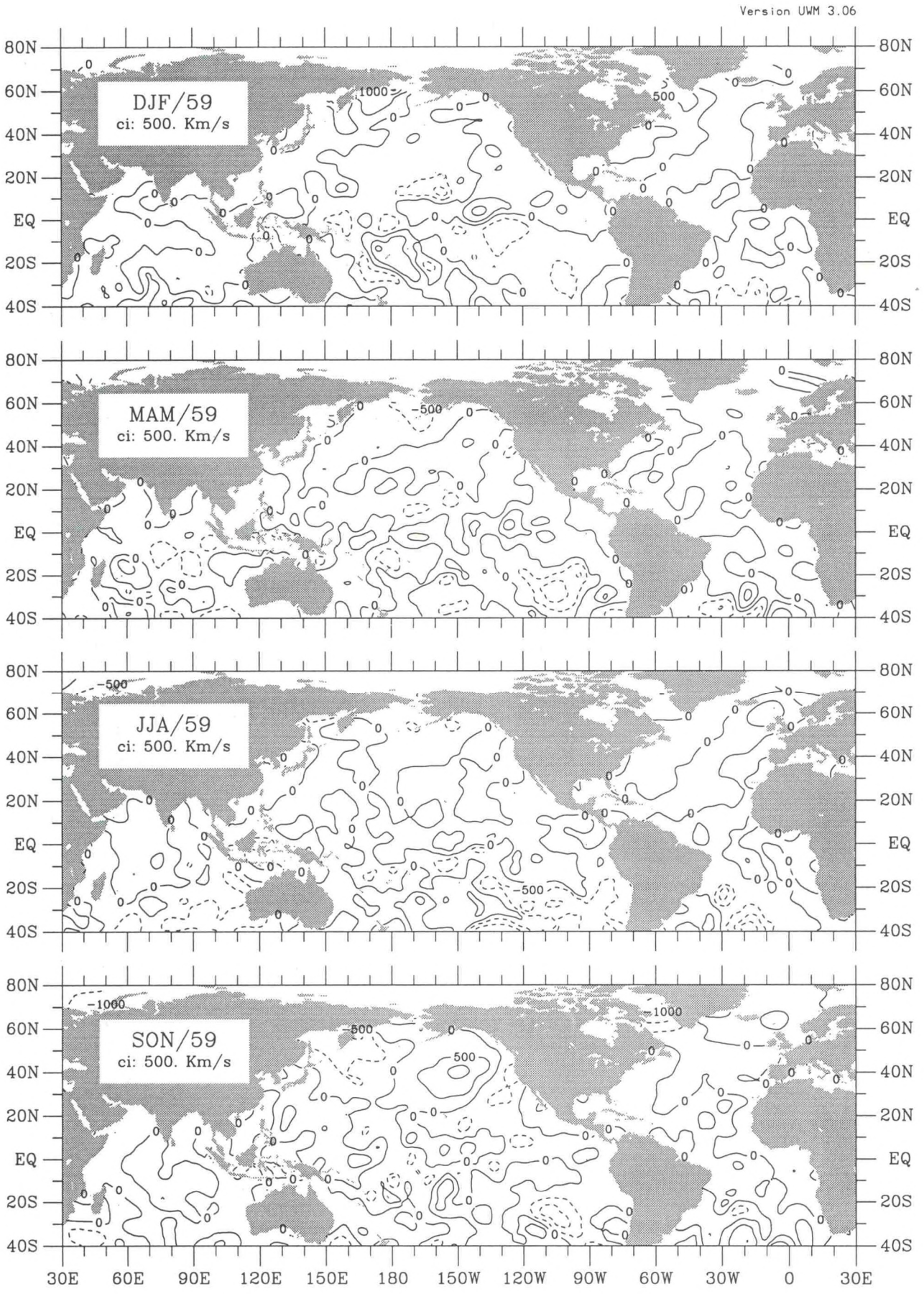

Figure va-20. Meridional heat flux seasonal anomaly for 1959.

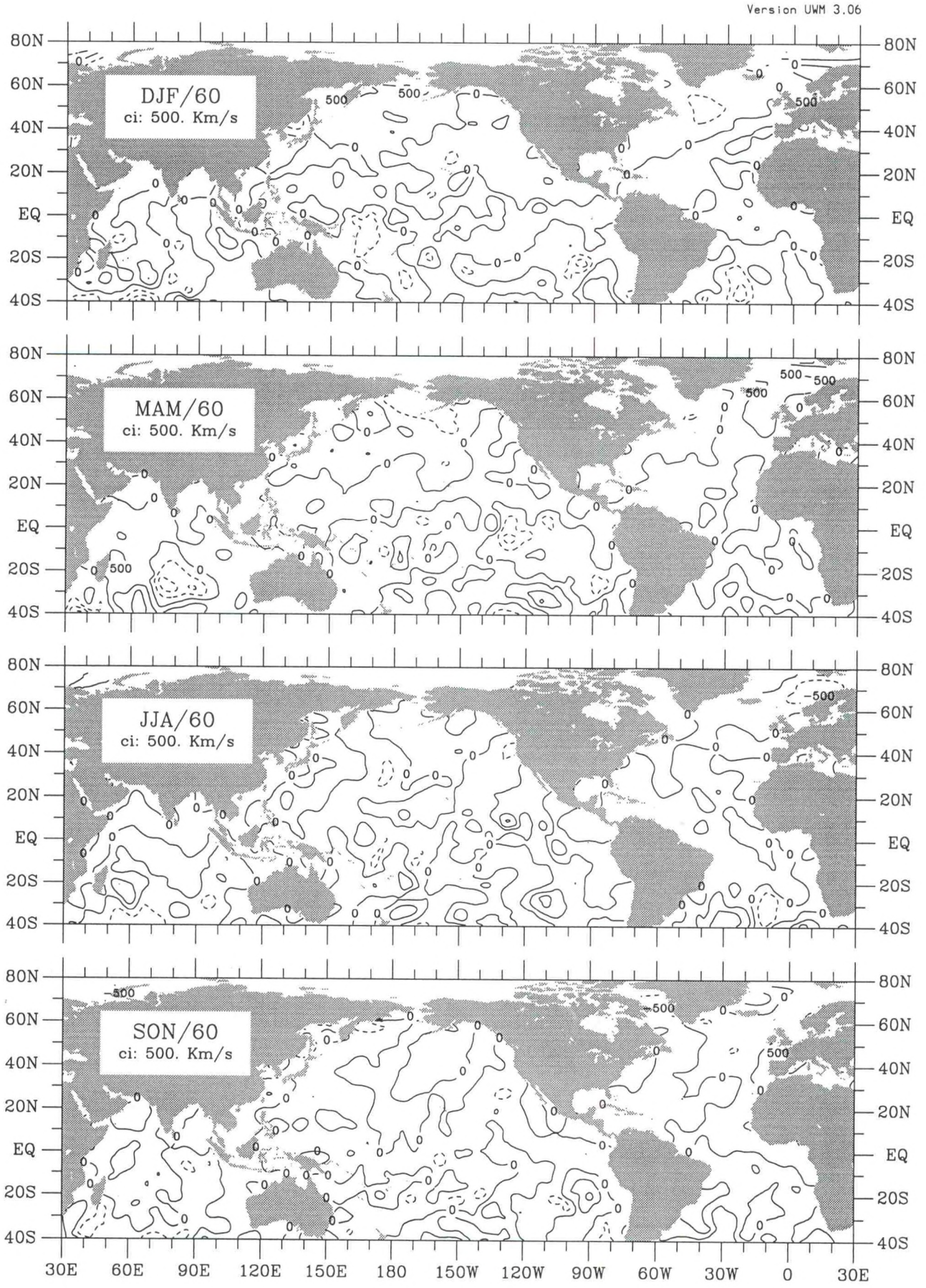

Figure va-21. Meridional heat flux seasonal anomaly for 1960.

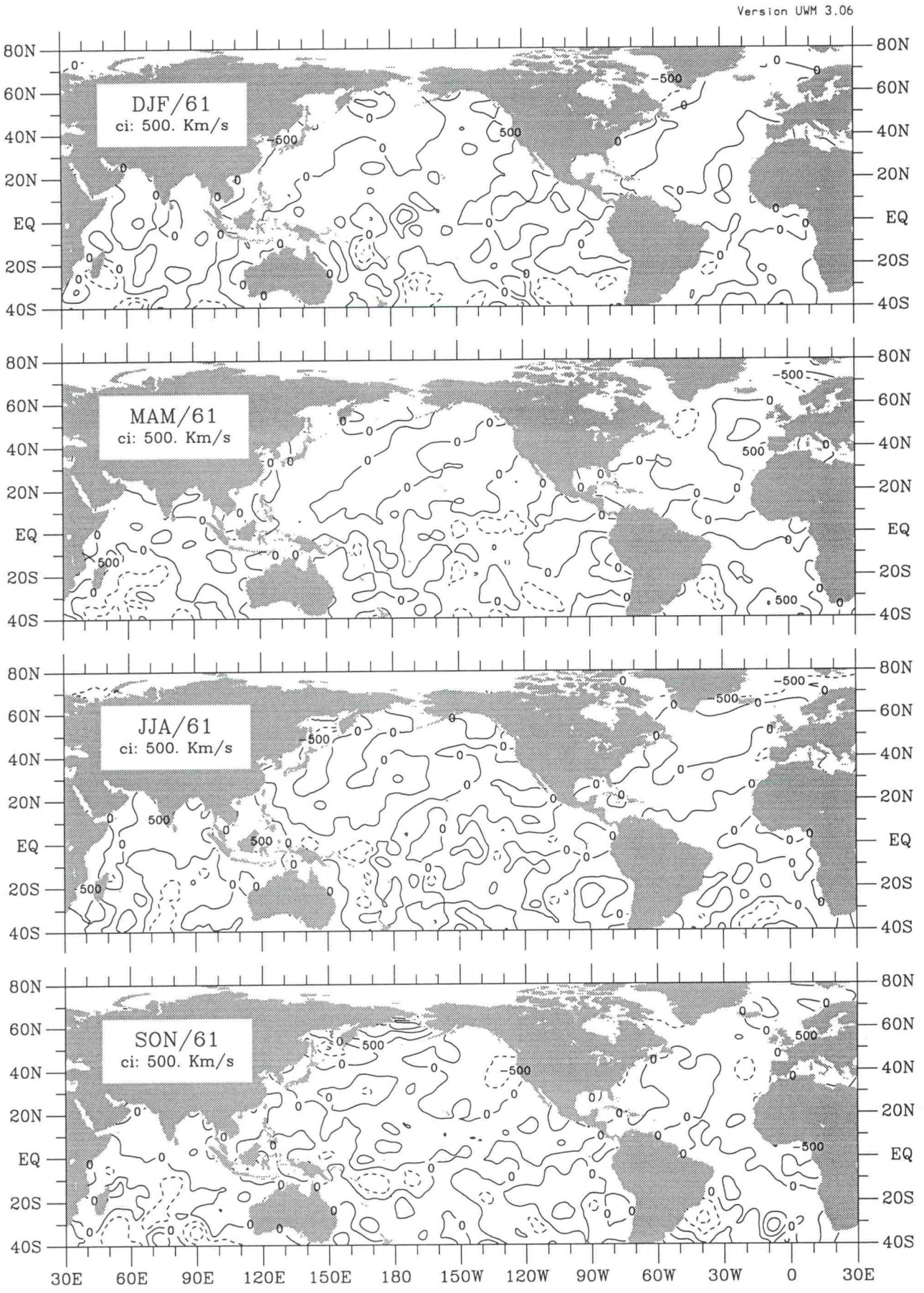

Figure va-22. Meridional heat flux seasonal anomaly for 1961.

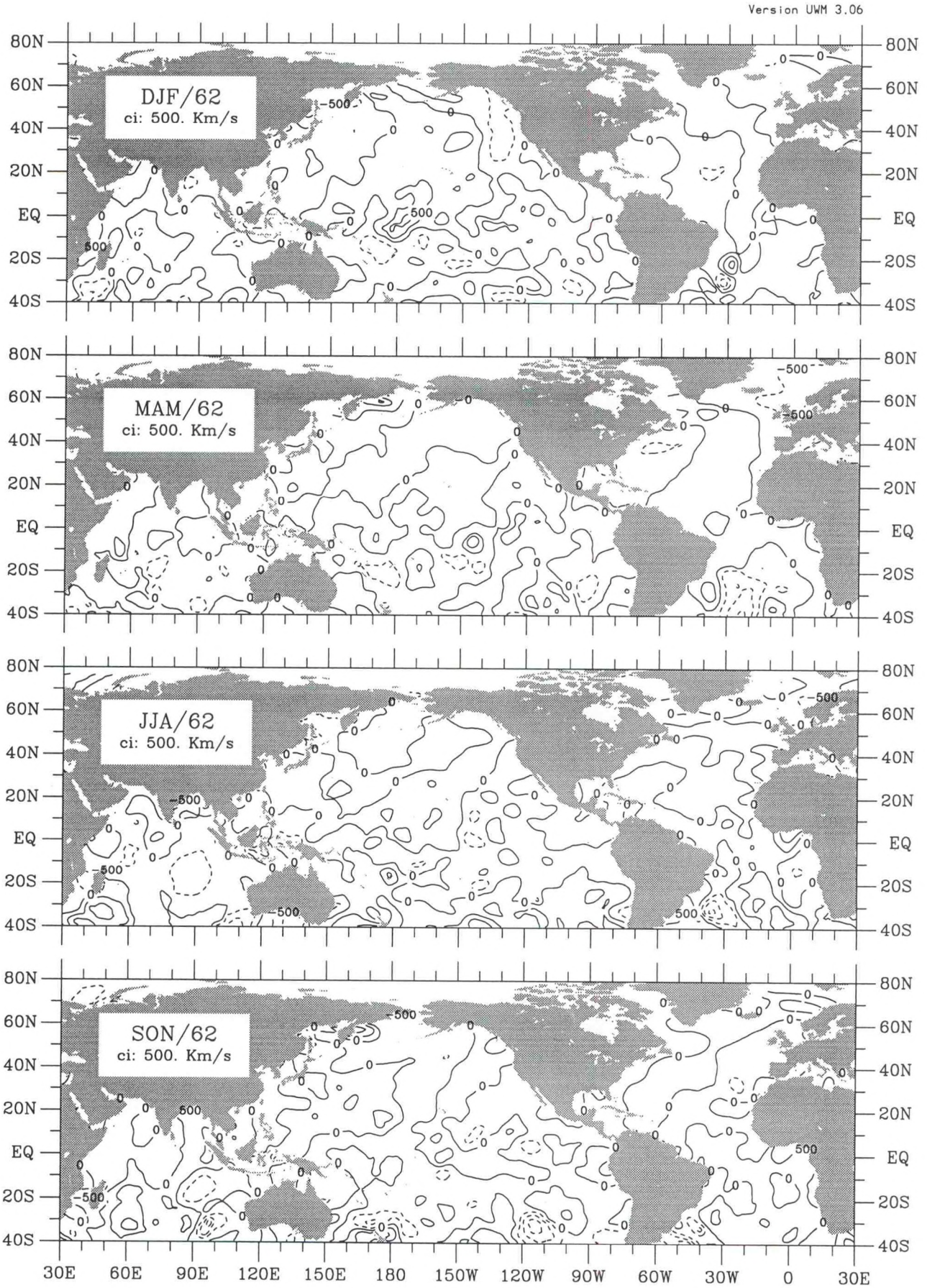

Figure va-23. Meridional heat flux seasonal anomaly for 1962.

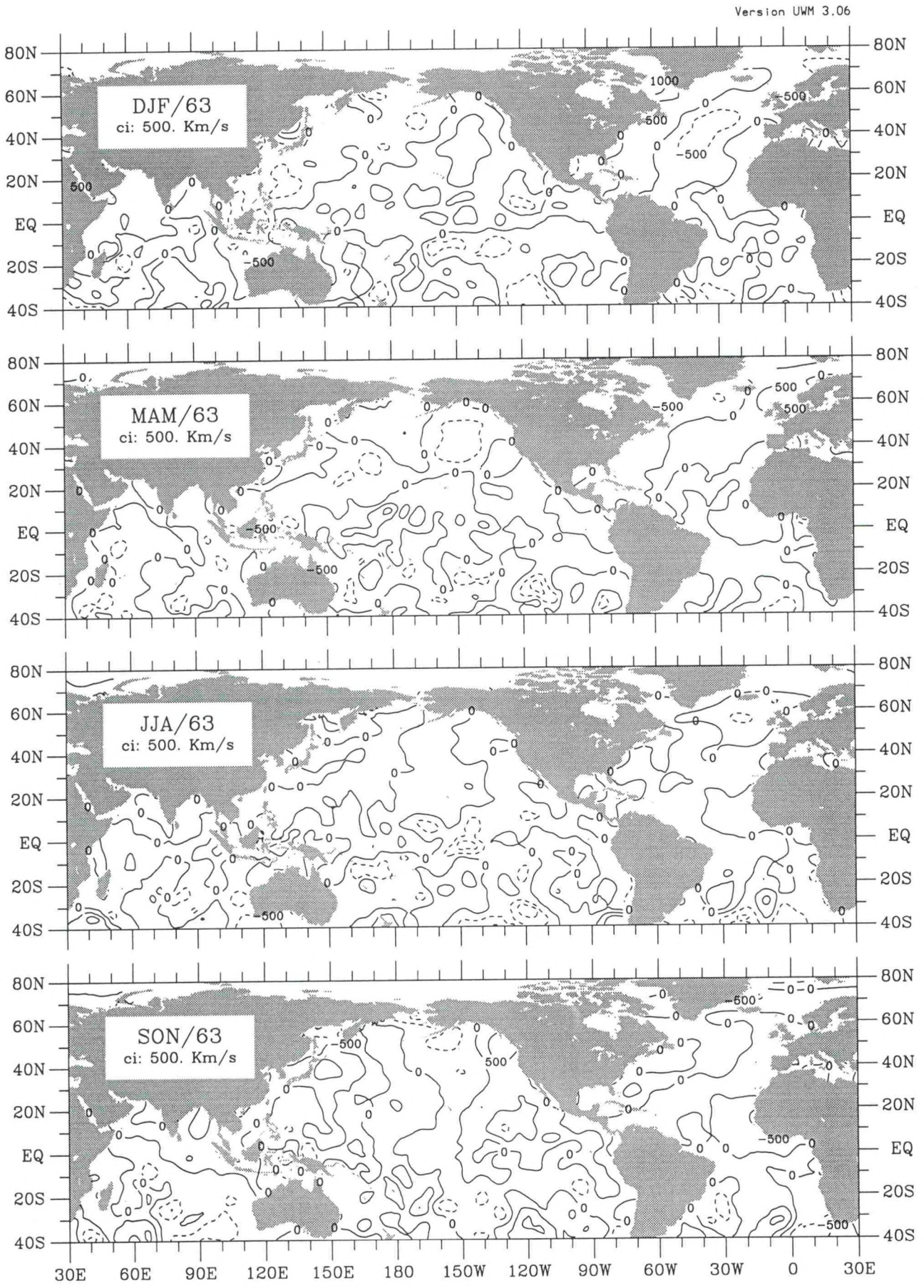

Figure va-24. Meridional heat flux seasonal anomaly for 1963.

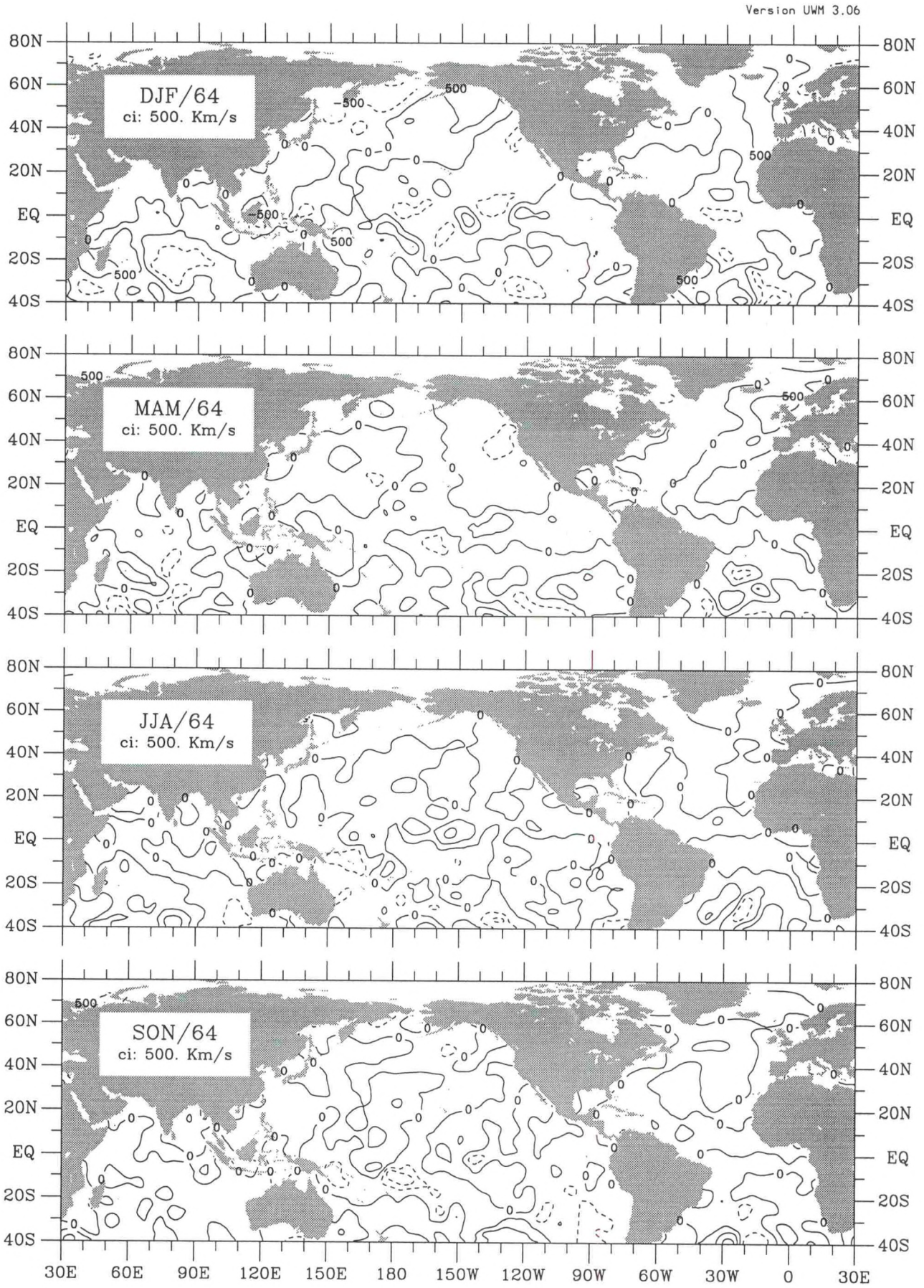

Figure va–25. Meridional heat flux seasonal anomaly for 1964.

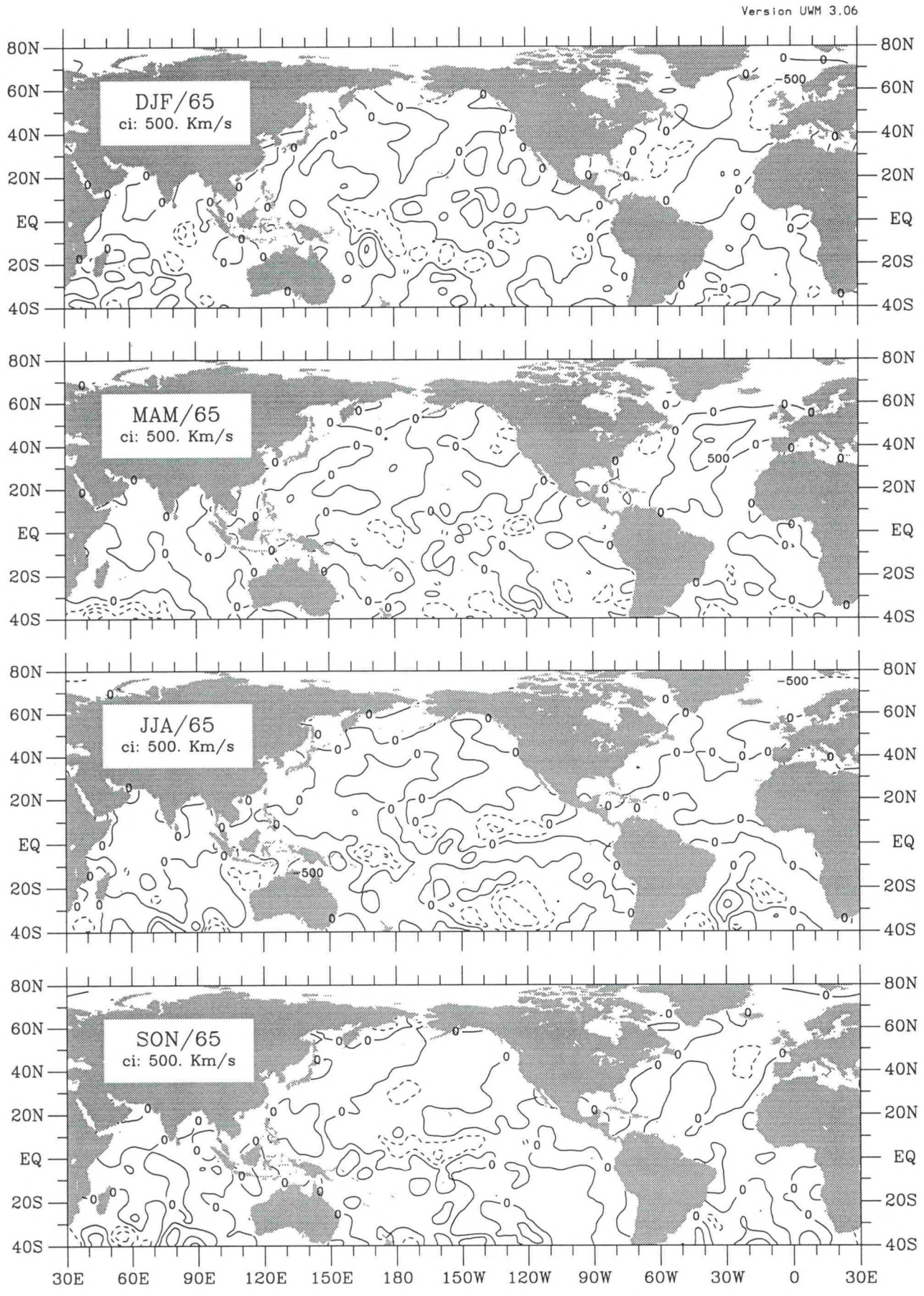

Figure va-26. Meridional heat flux seasonal anomaly for 1965.

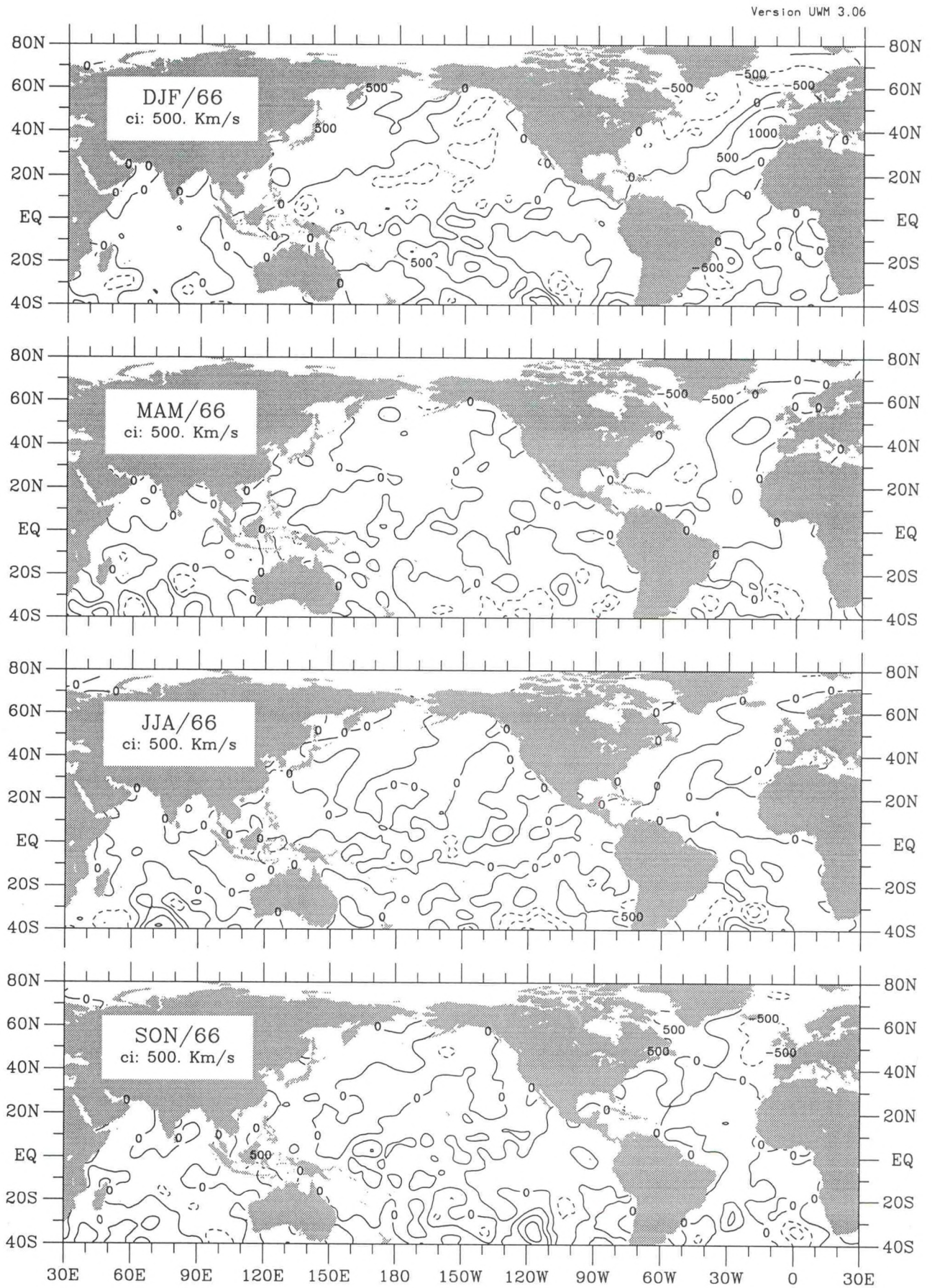

Figure va-27. Meridional heat flux seasonal anomaly for 1966.

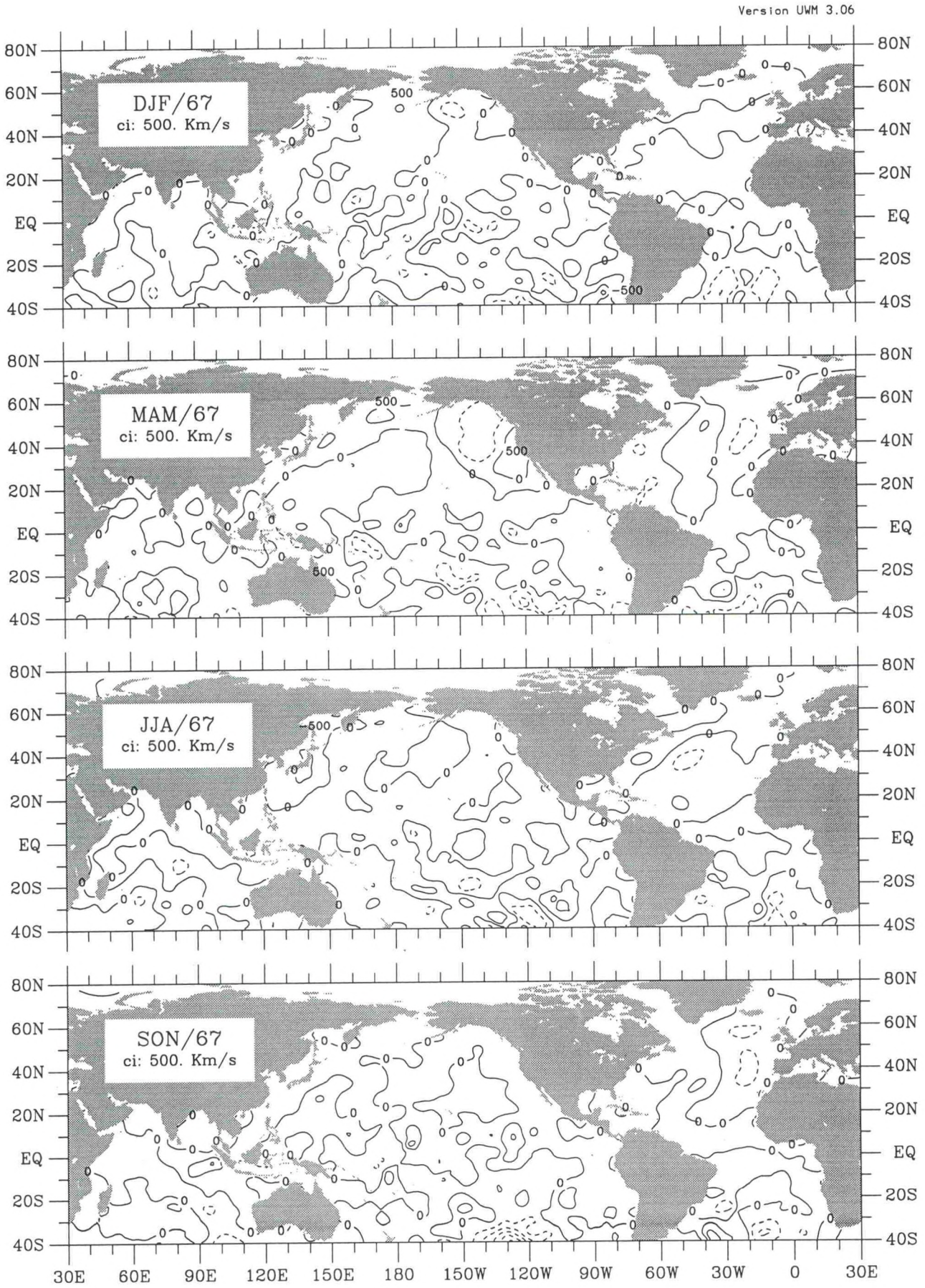

Figure va-28. Meridional heat flux seasonal anomaly for 1967.

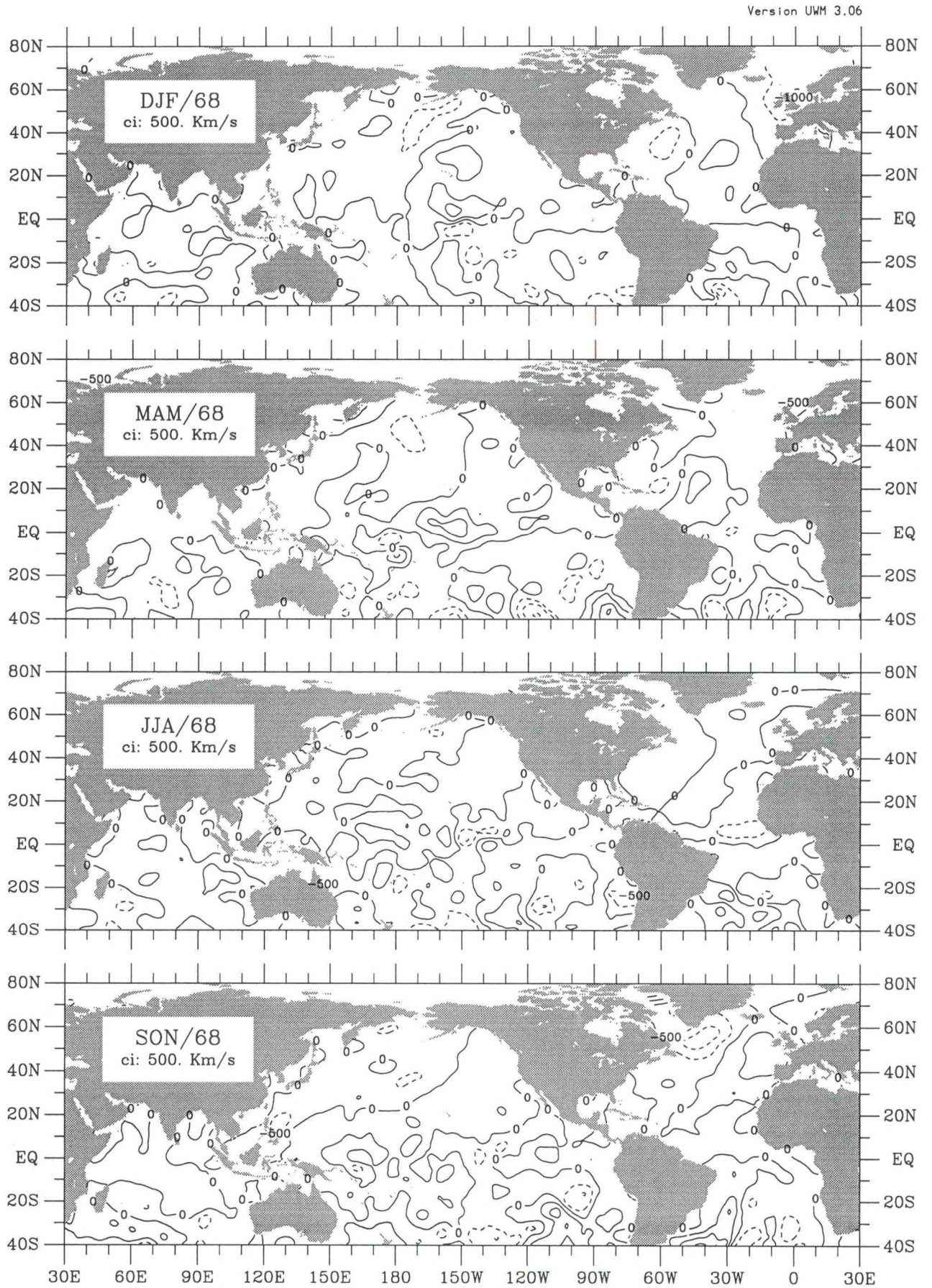

Figure va–29. Meridional heat flux seasonal anomaly for 1968.

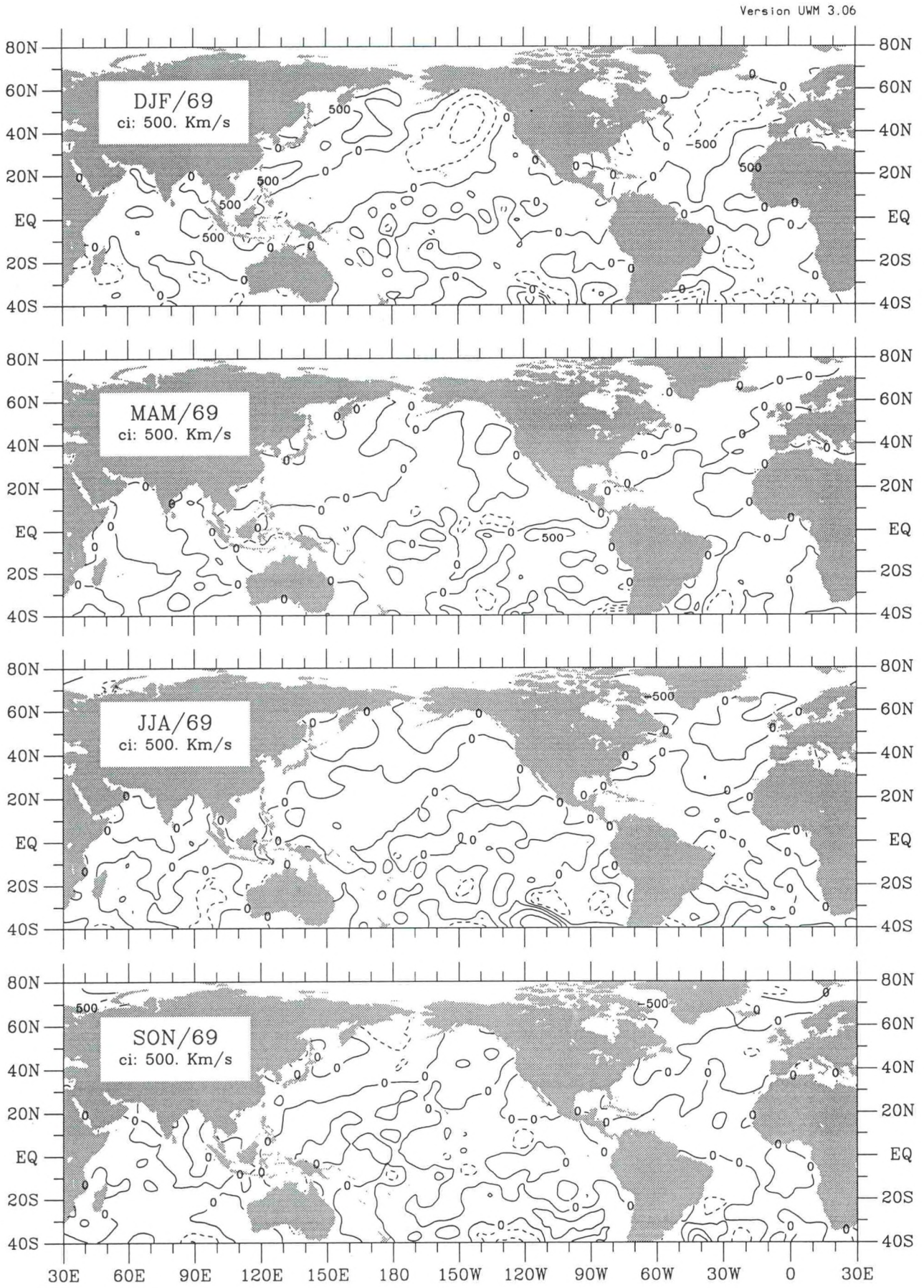

Figure va-30. Meridional heat flux seasonal anomaly for 1969.

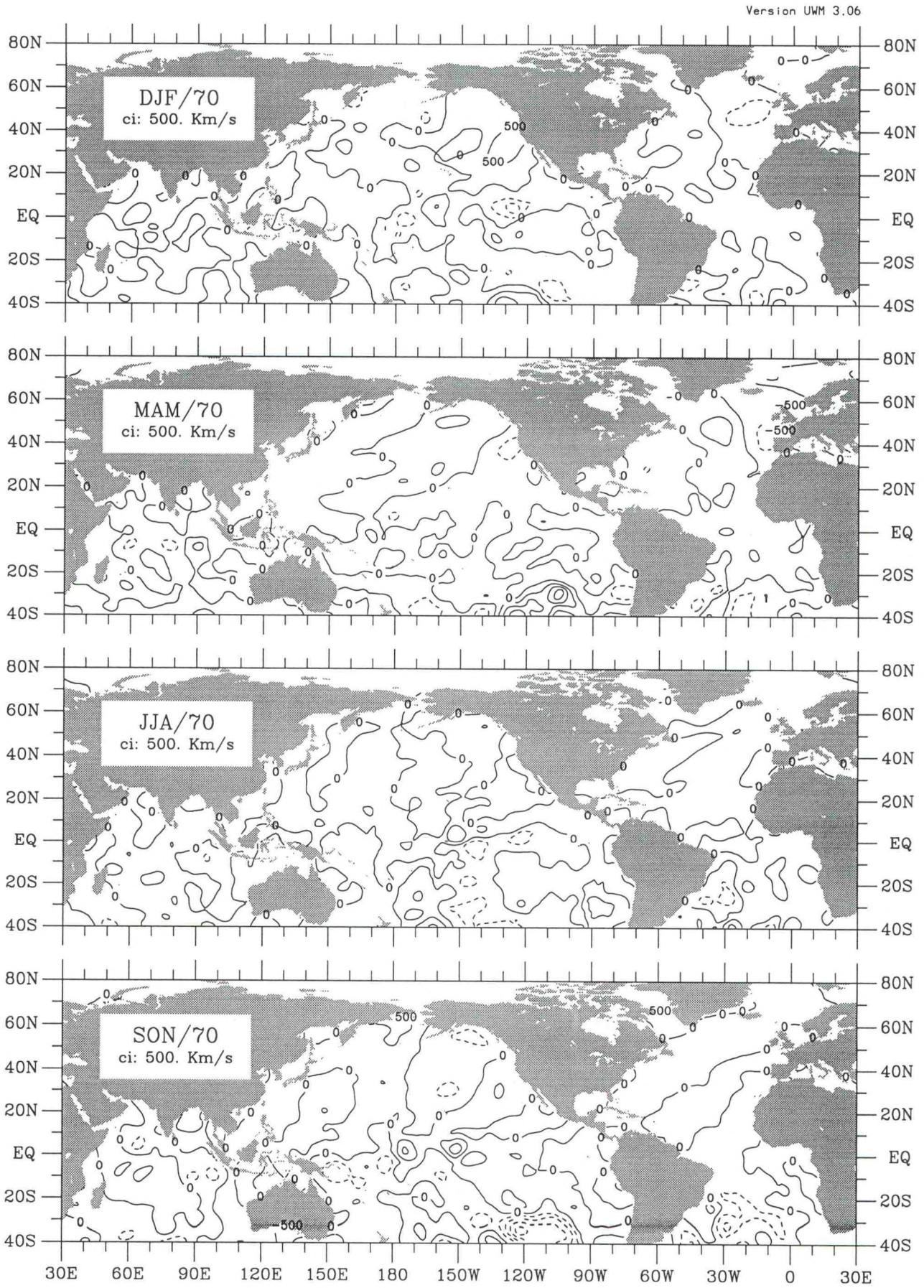

Figure va-31. Meridional heat flux seasonal anomaly for 1970.

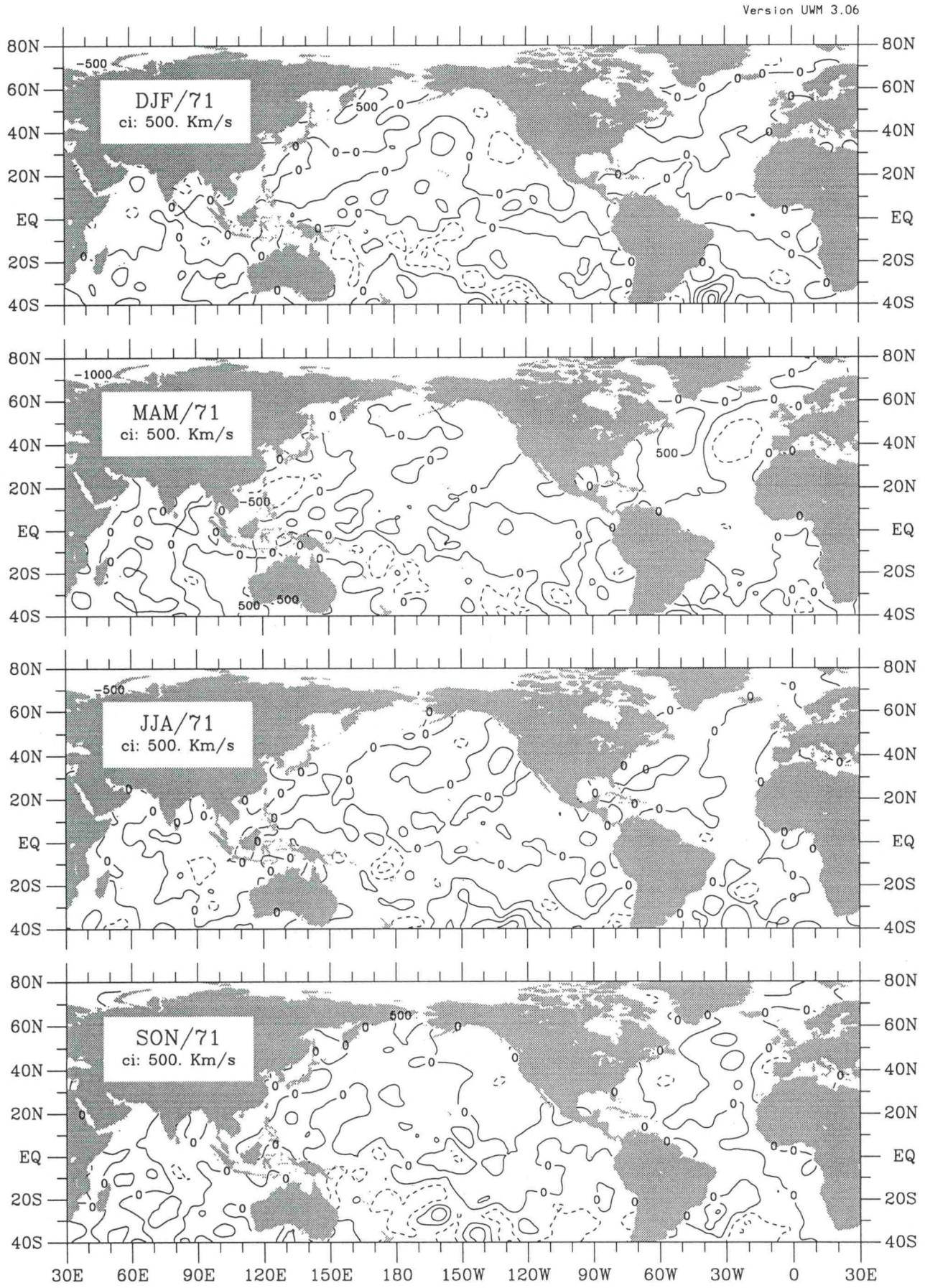

Figure va-32. Meridional heat flux seasonal anomaly for 1971.

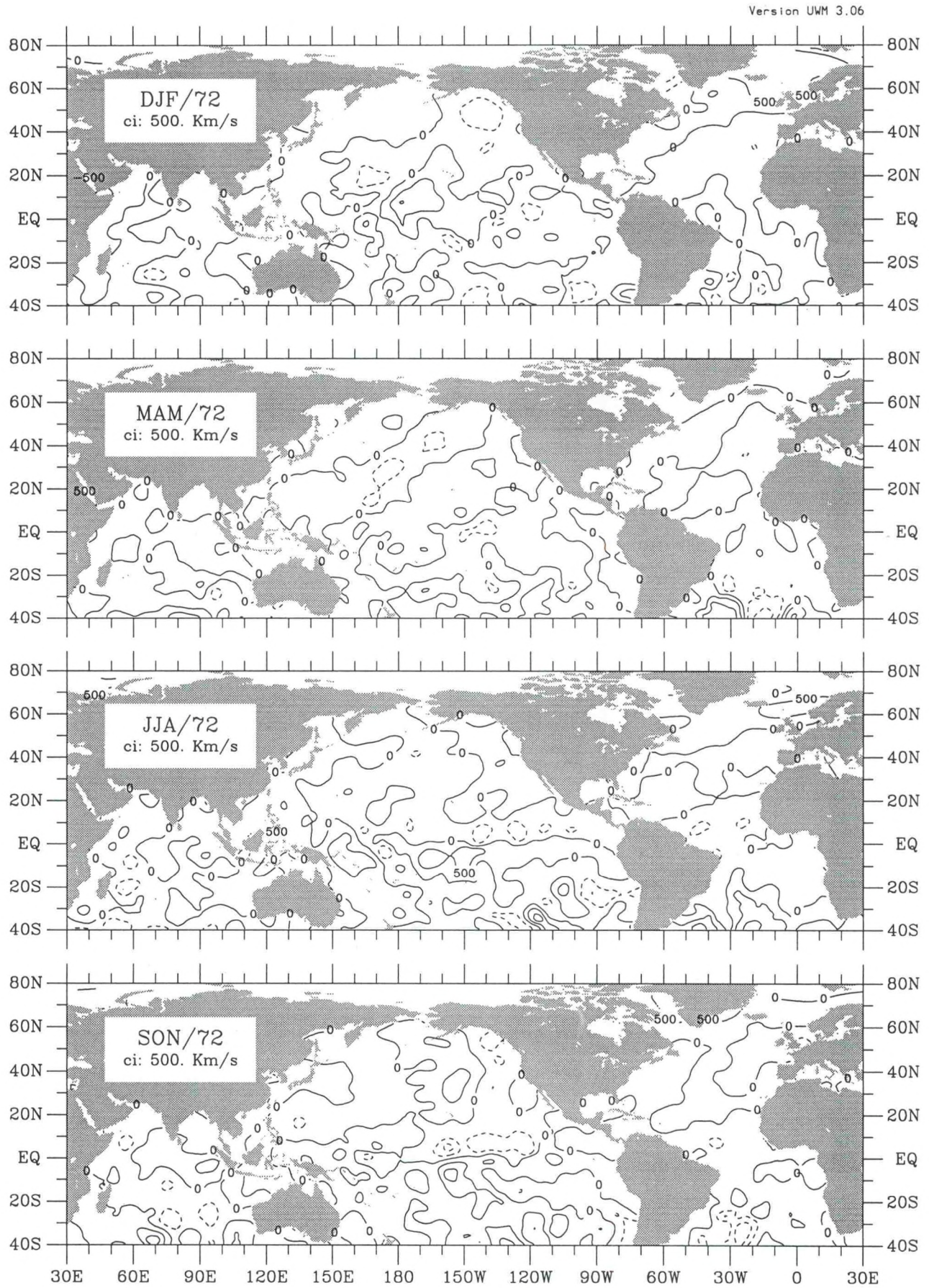

Figure va-33. Meridional heat flux seasonal anomaly for 1972.

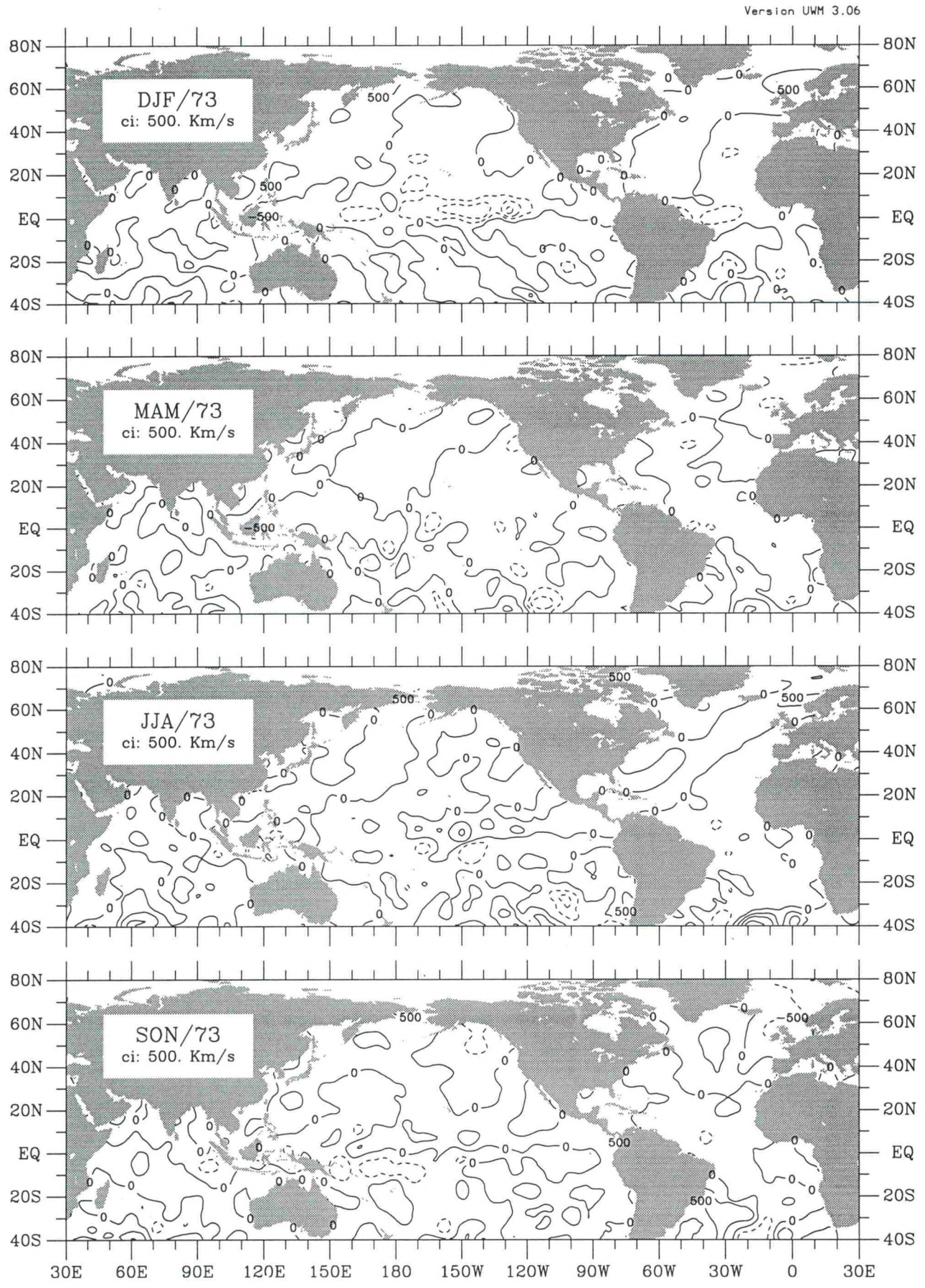

Figure va-34. Meridional heat flux seasonal anomaly for 1973.

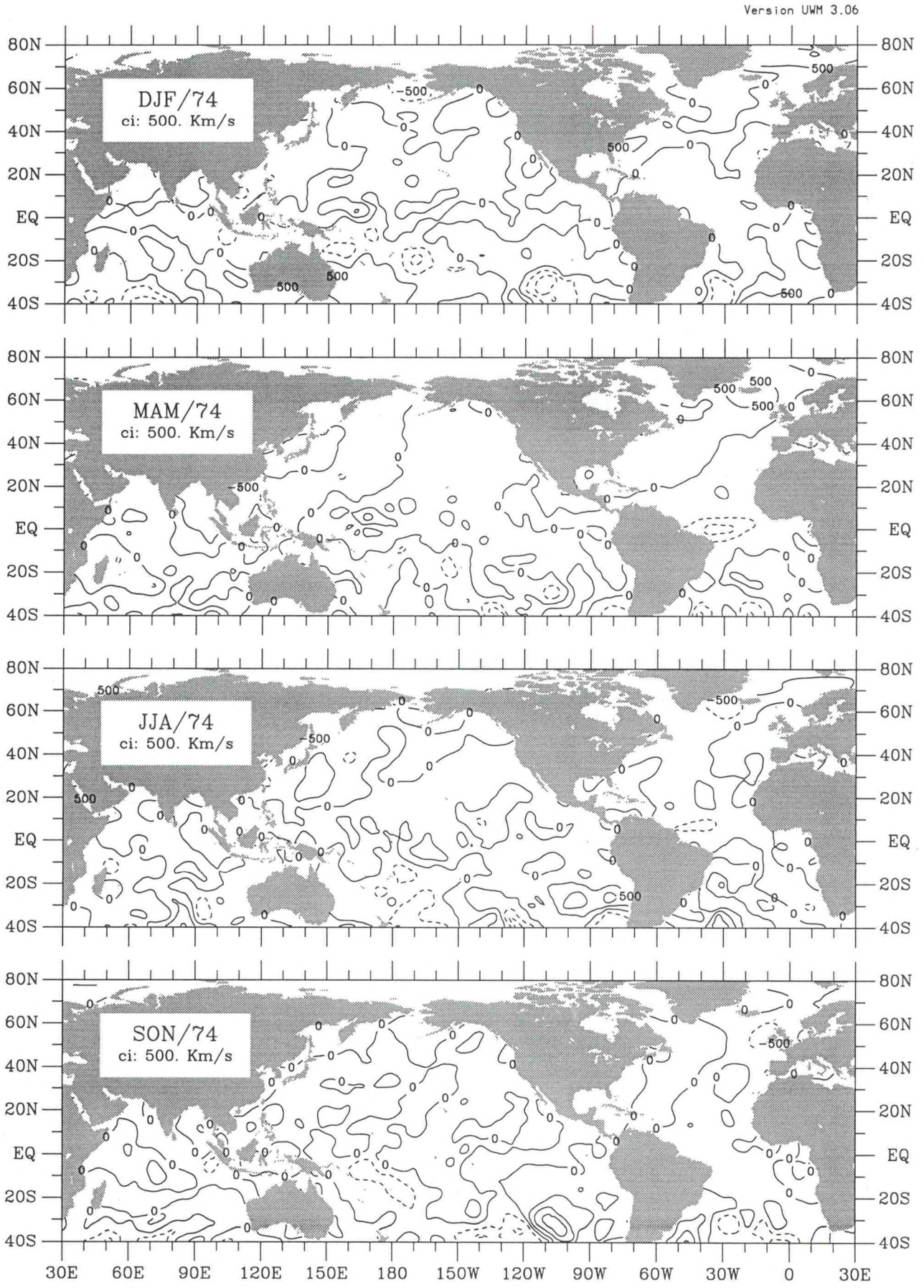

Figure va-35. Meridional heat flux seasonal anomaly for 1974.

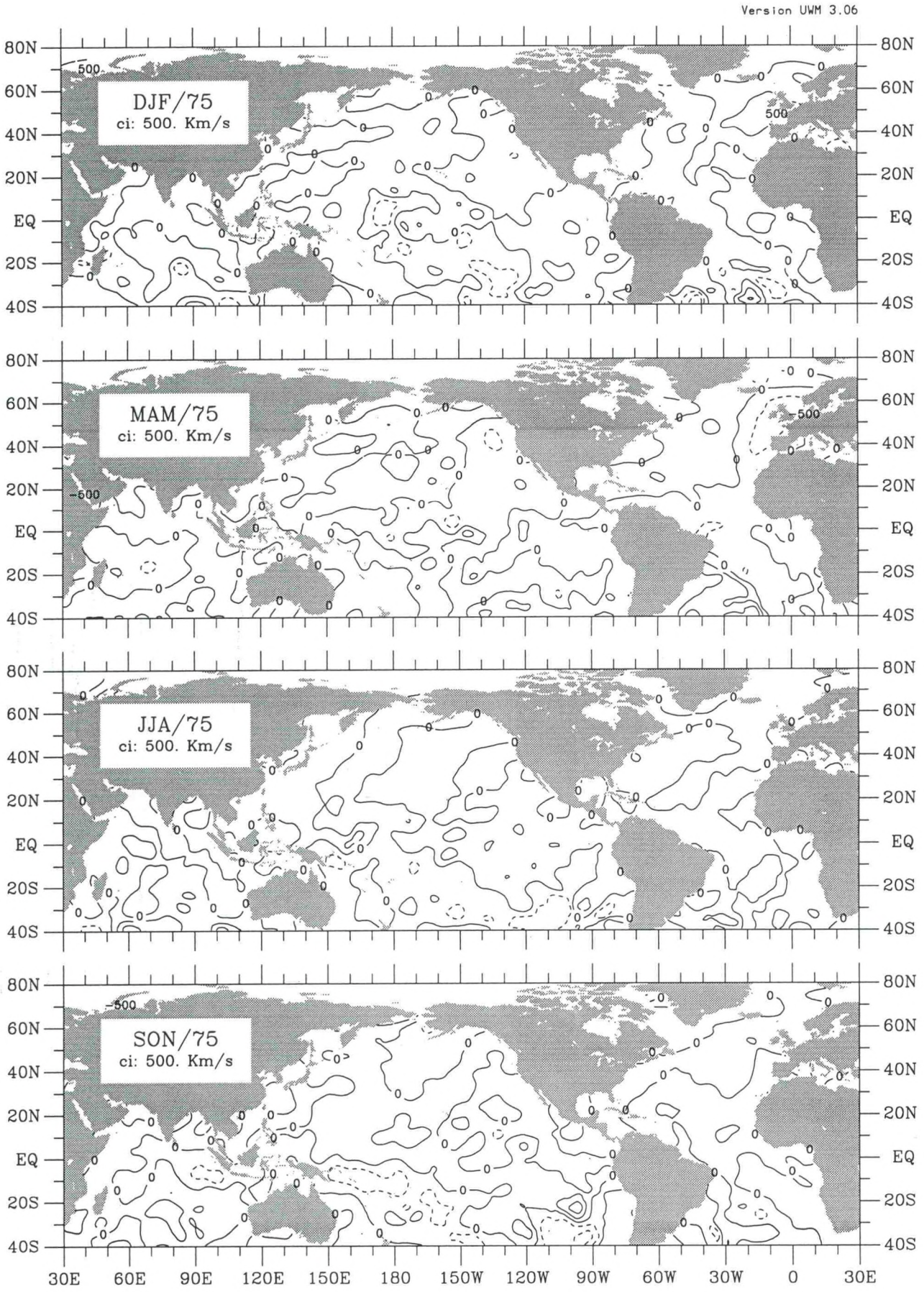

Figure va-36. Meridional heat flux seasonal anomaly for 1975.

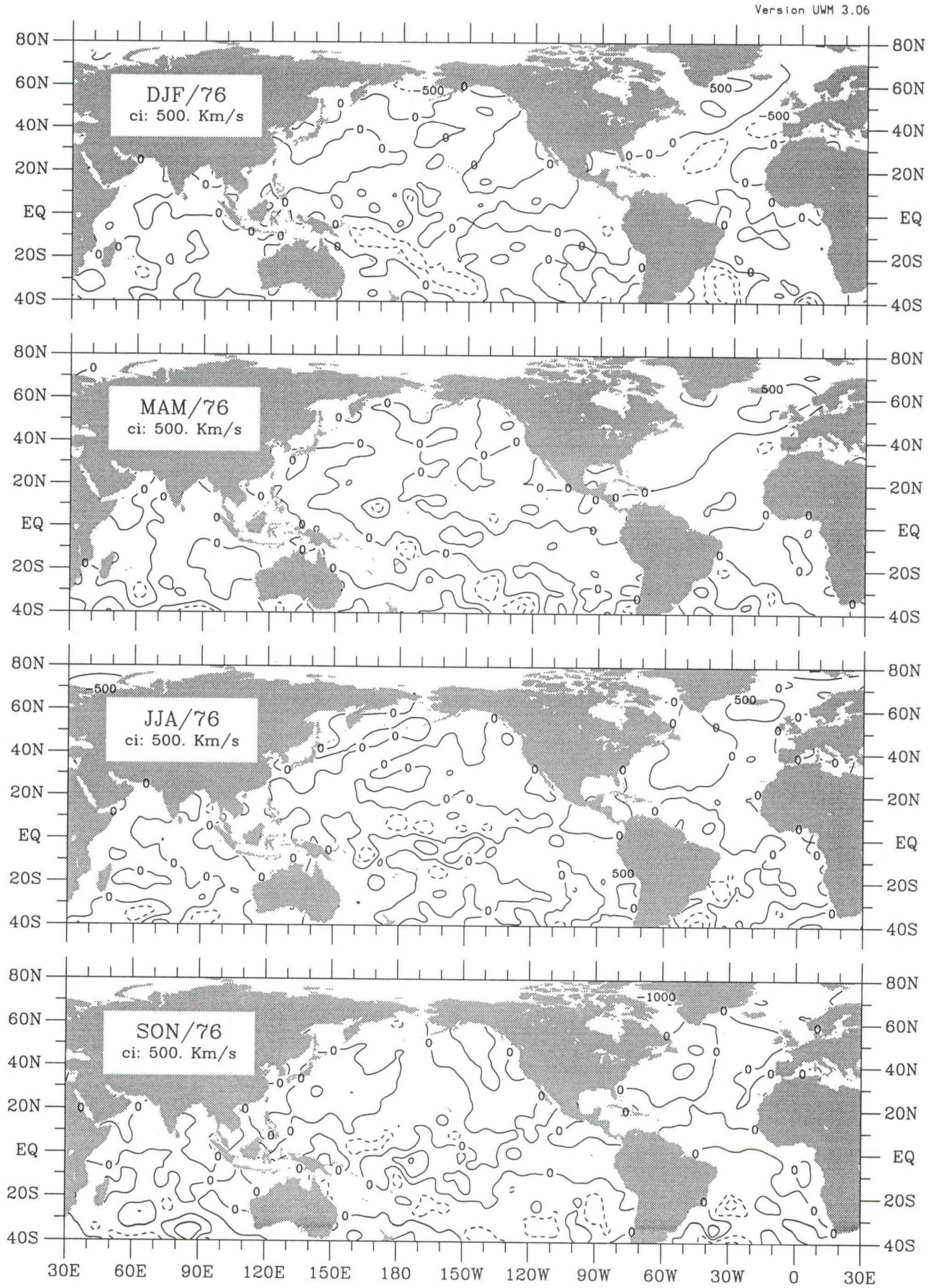

Figure va-37. Meridional heat flux seasonal anomaly for 1976.

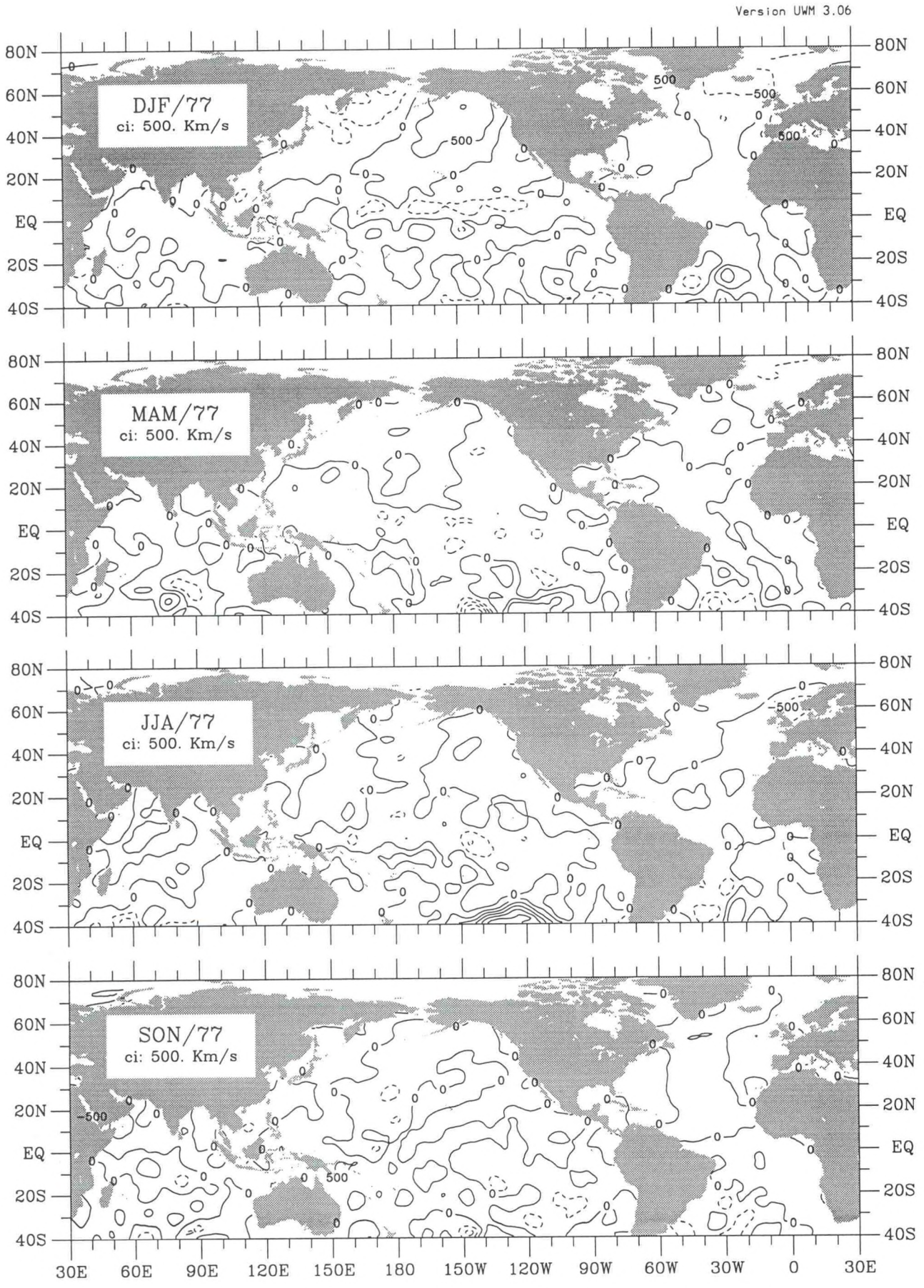

Figure va-38. Meridional heat flux seasonal anomaly for 1977.

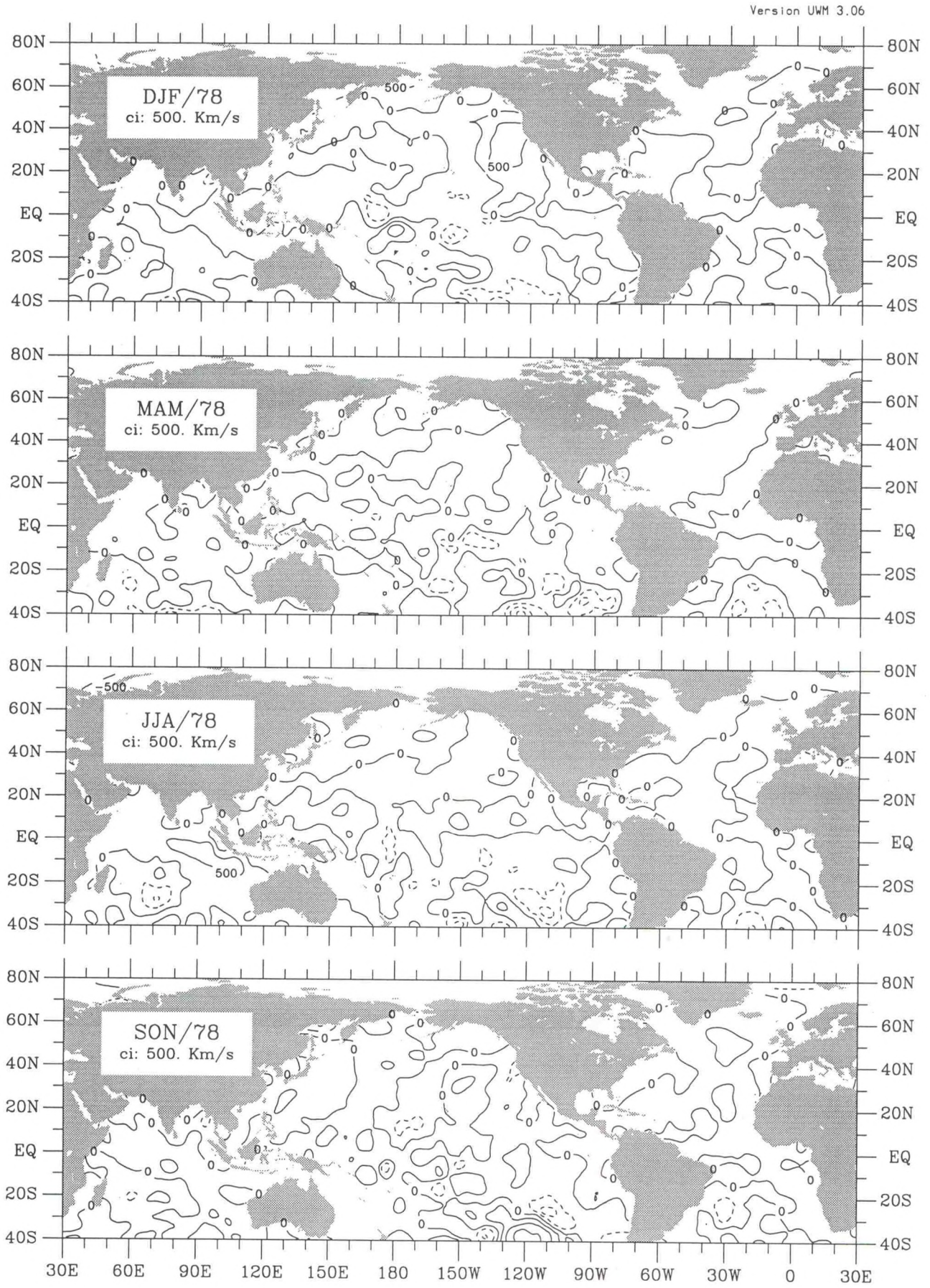

Figure va-39. Meridional heat flux seasonal anomaly for 1978.

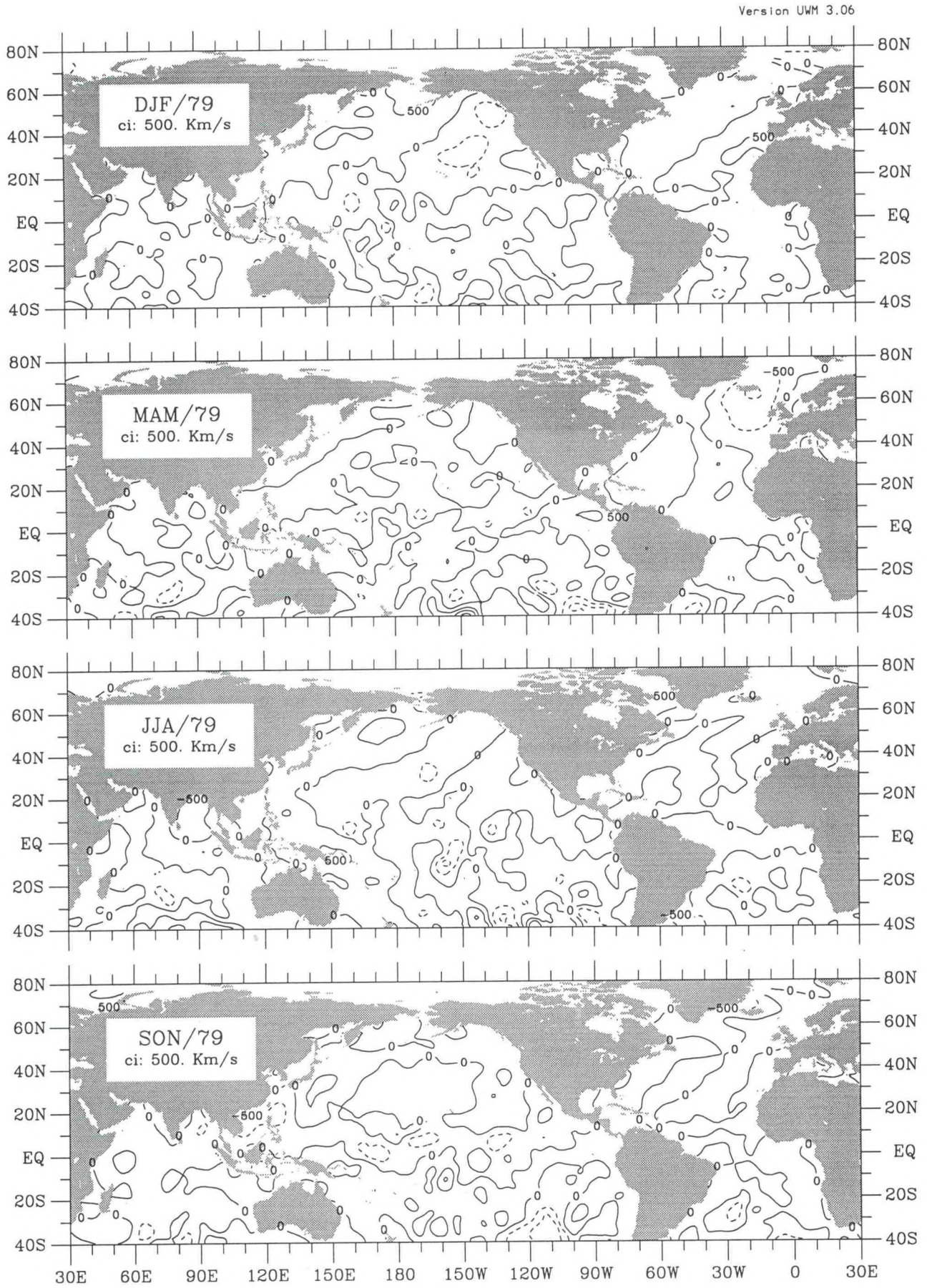

Figure va-40. Meridional heat flux seasonal anomaly for 1979.

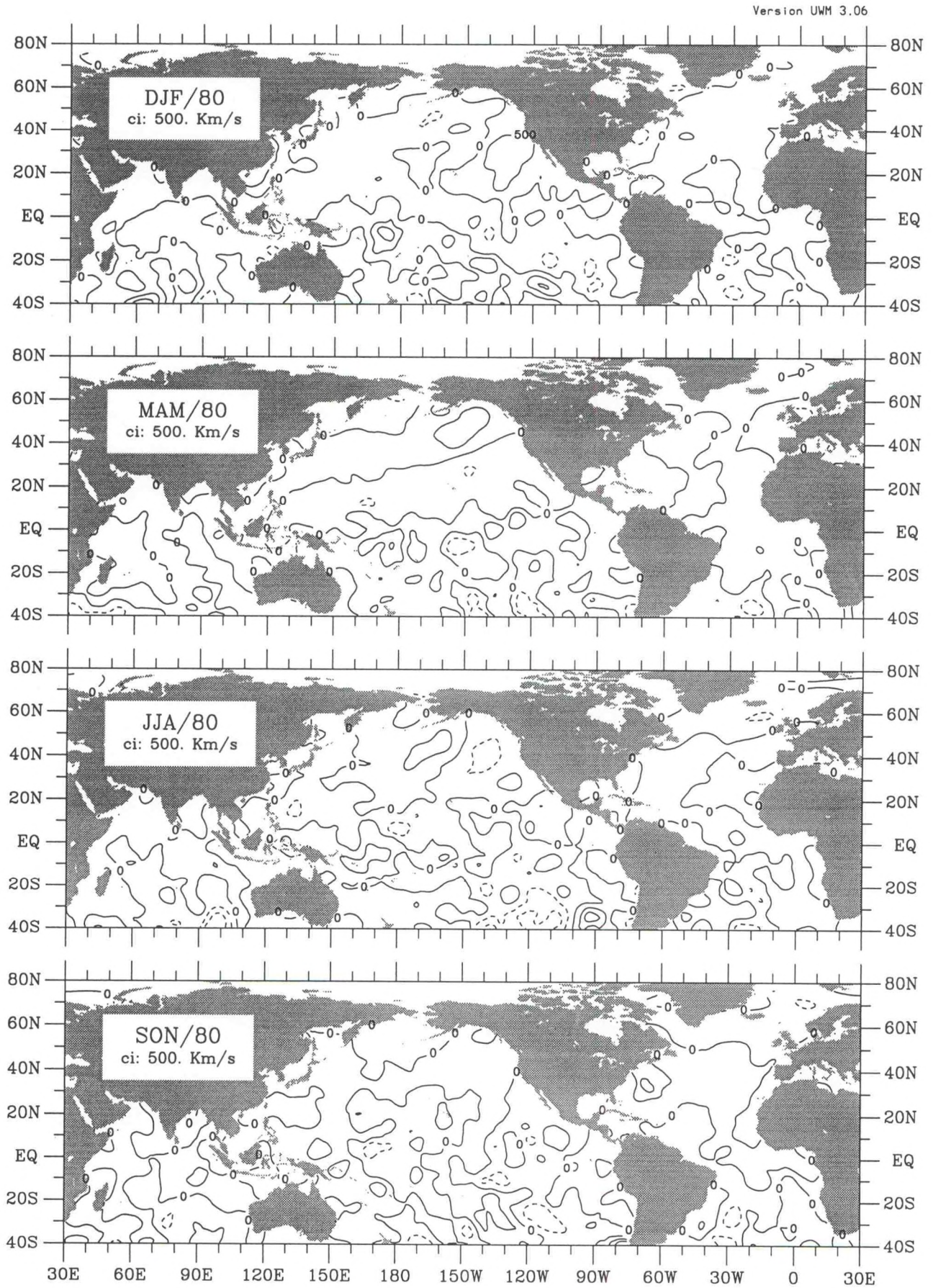

Figure va-41. Meridional heat flux seasonal anomaly for 1980.

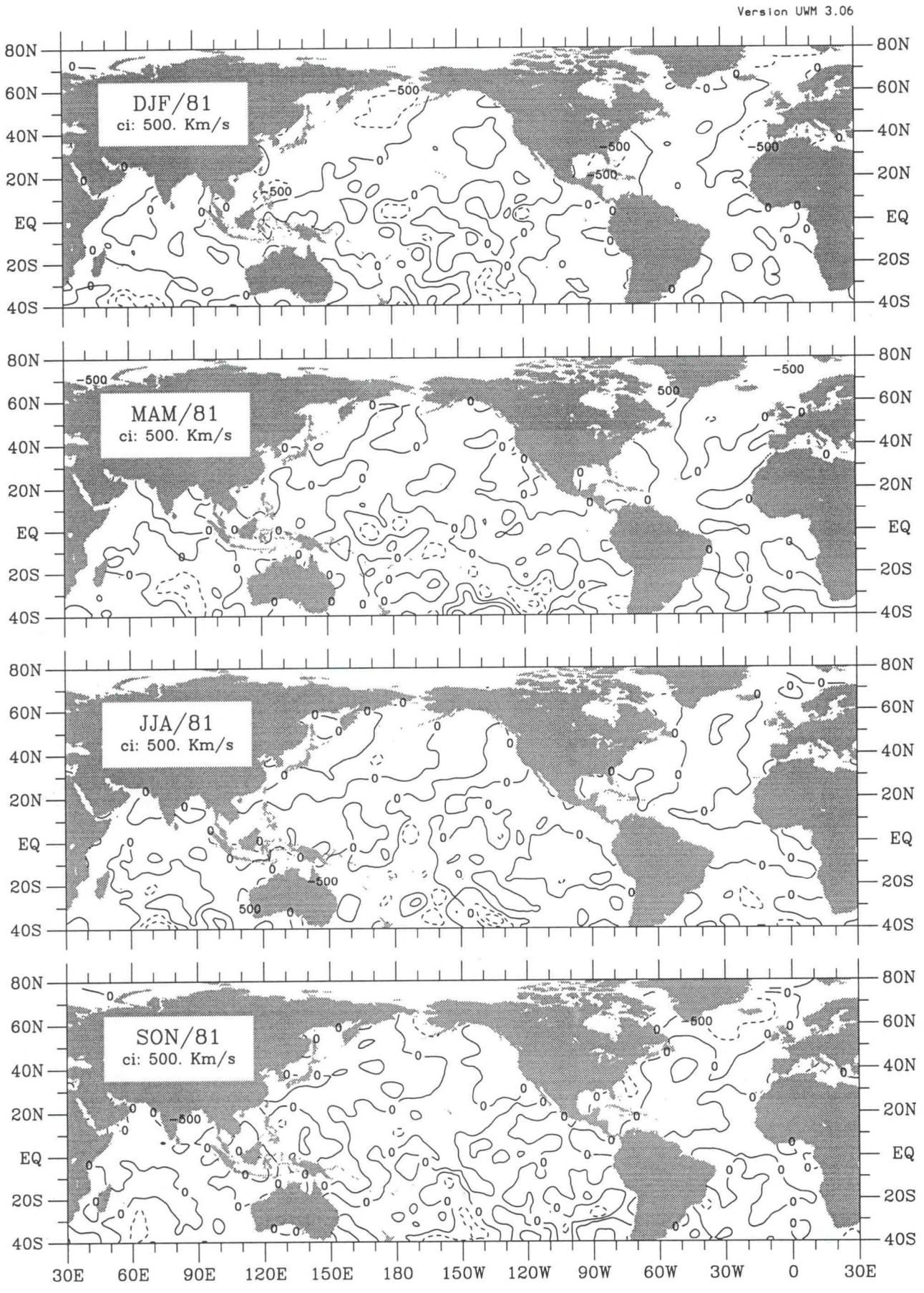

Figure va-42. Meridional heat flux seasonal anomaly for 1981.

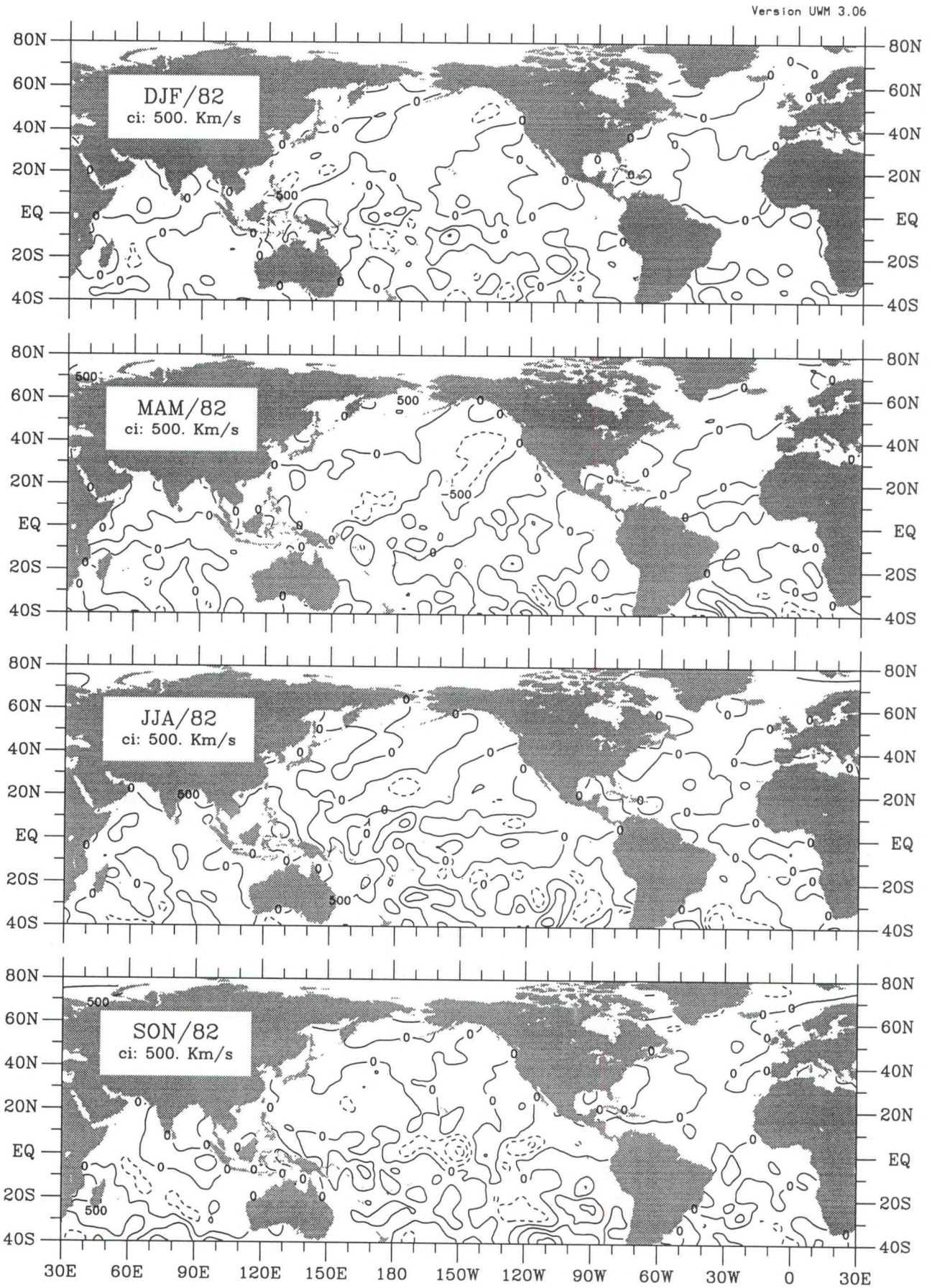

Figure va-43. Meridional heat flux seasonal anomaly for 1982.

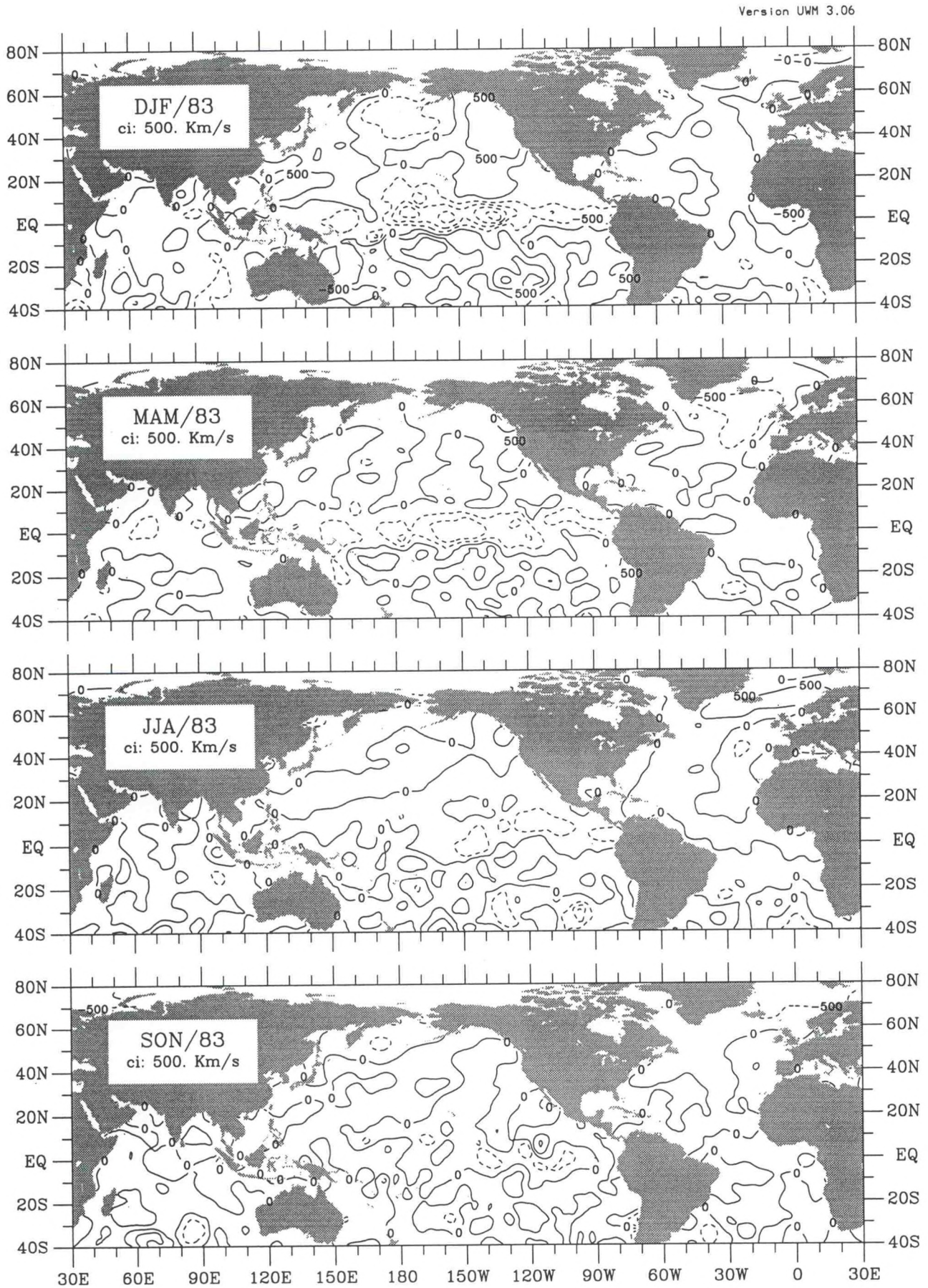

Figure va-44. Meridional heat flux seasonal anomaly for 1983.

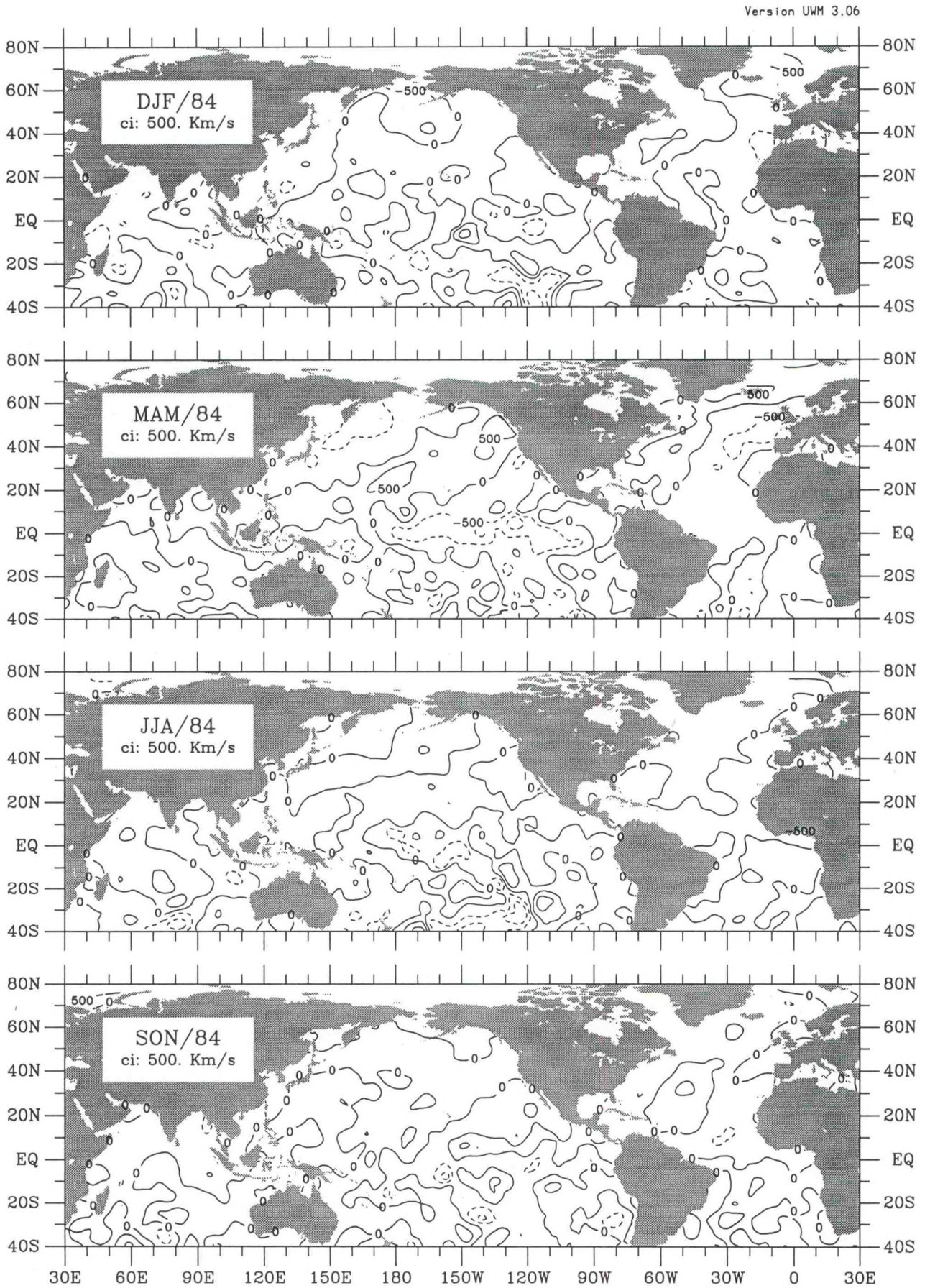

Figure va-45. Meridional heat flux seasonal anomaly for 1984.

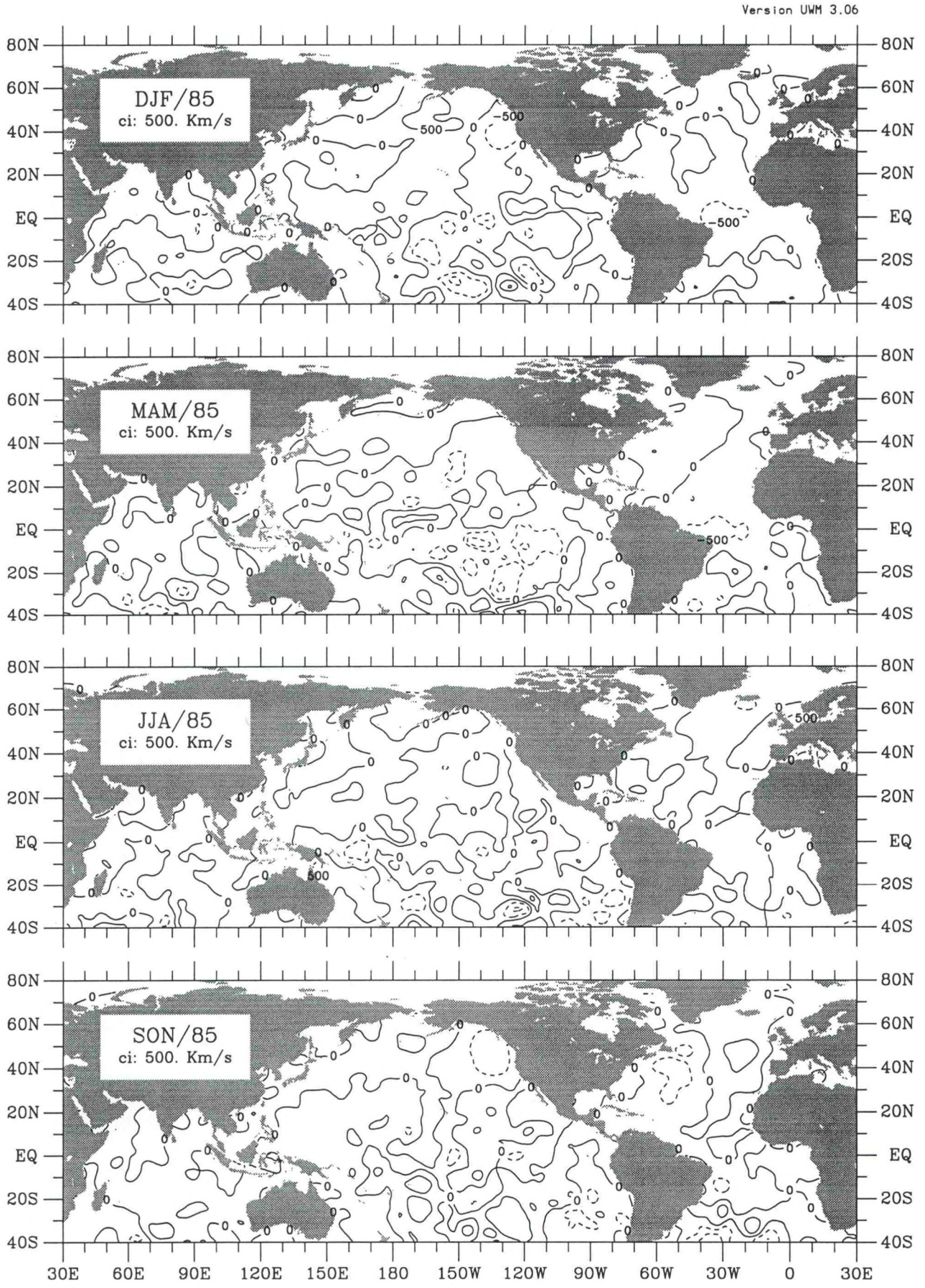

Figure va-46. Meridional heat flux seasonal anomaly for 1985.

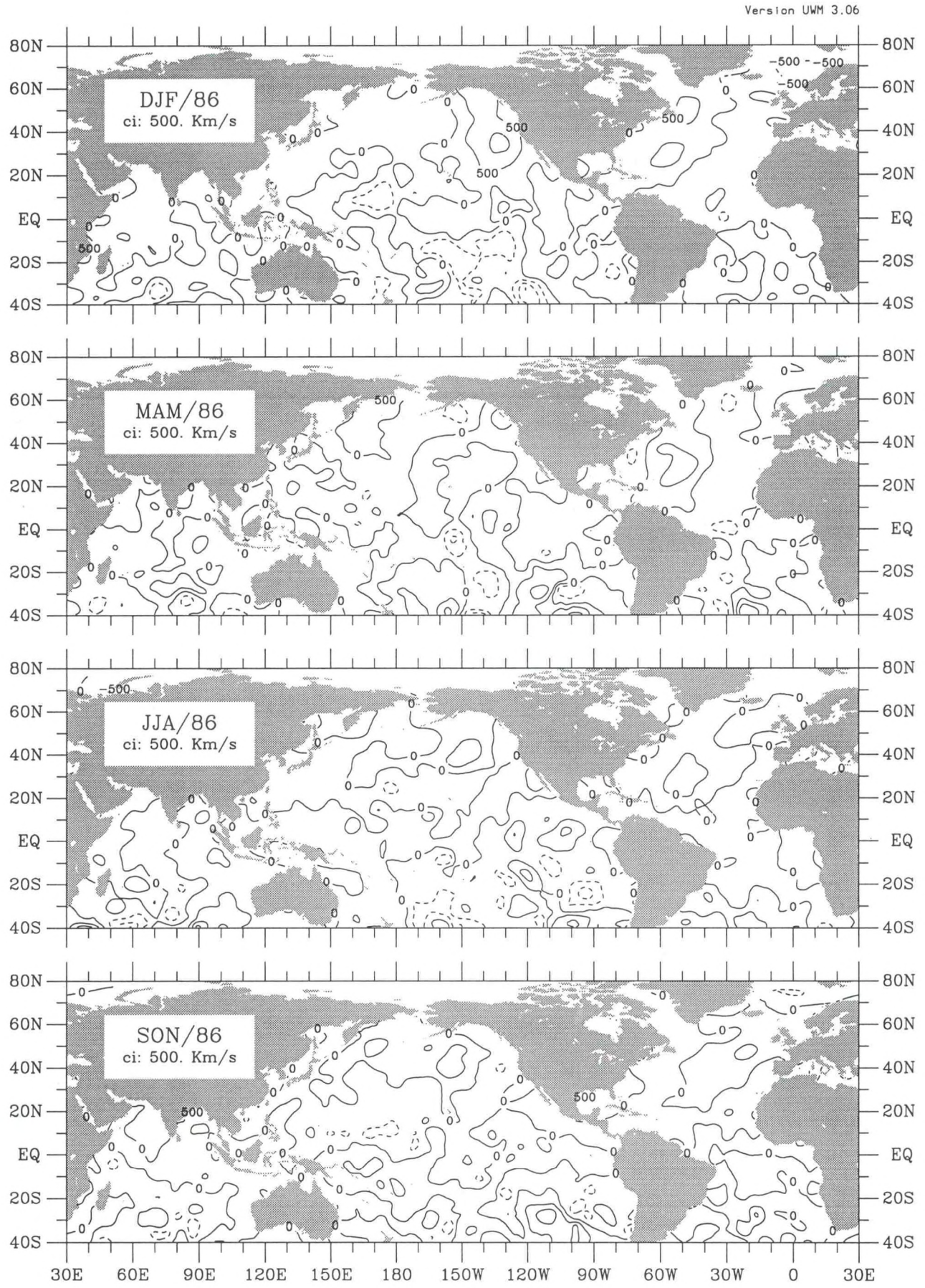

Figure va-47. Meridional heat flux seasonal anomaly for 1986.

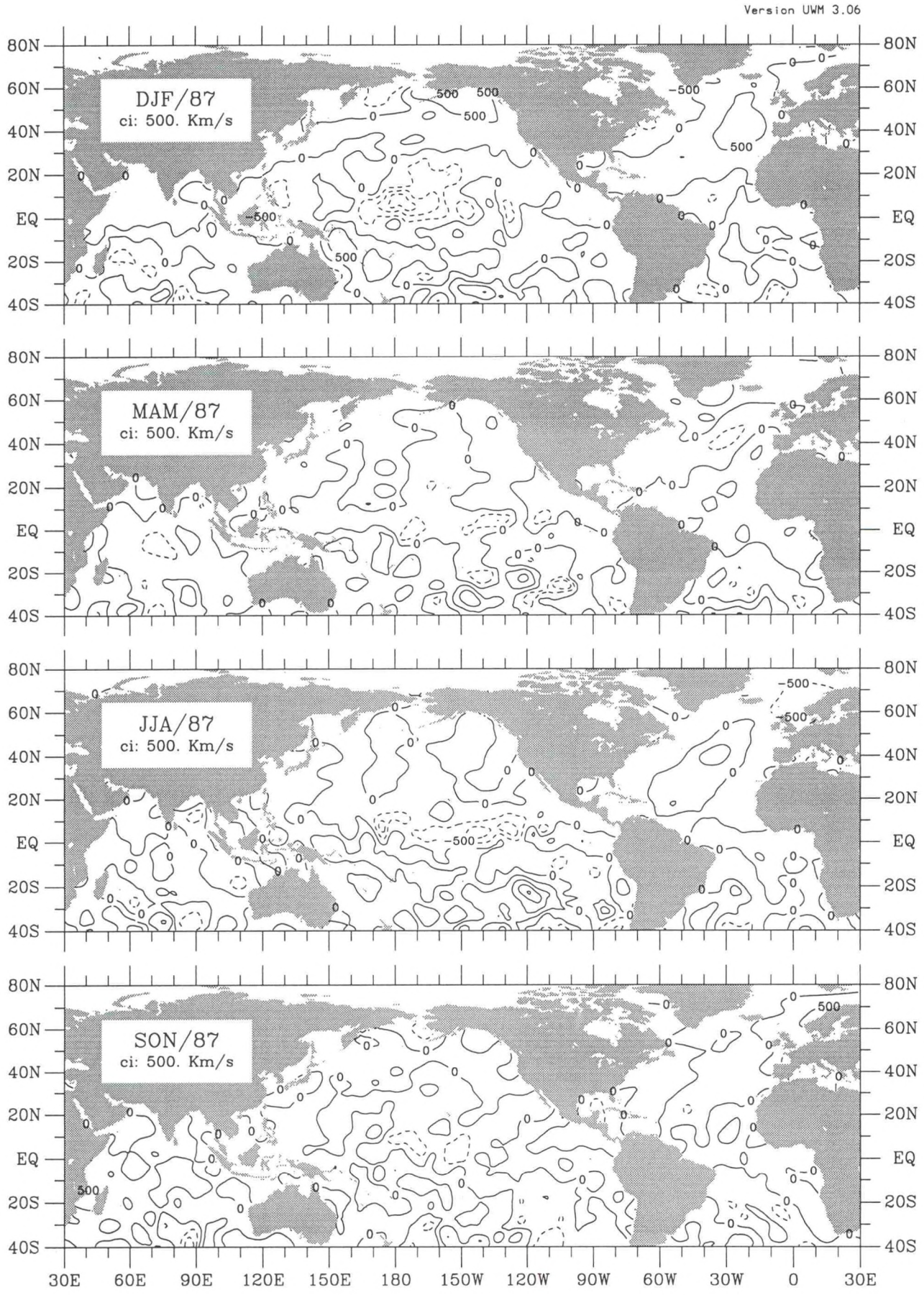

Figure va-48. Meridional heat flux seasonal anomaly for 1987.

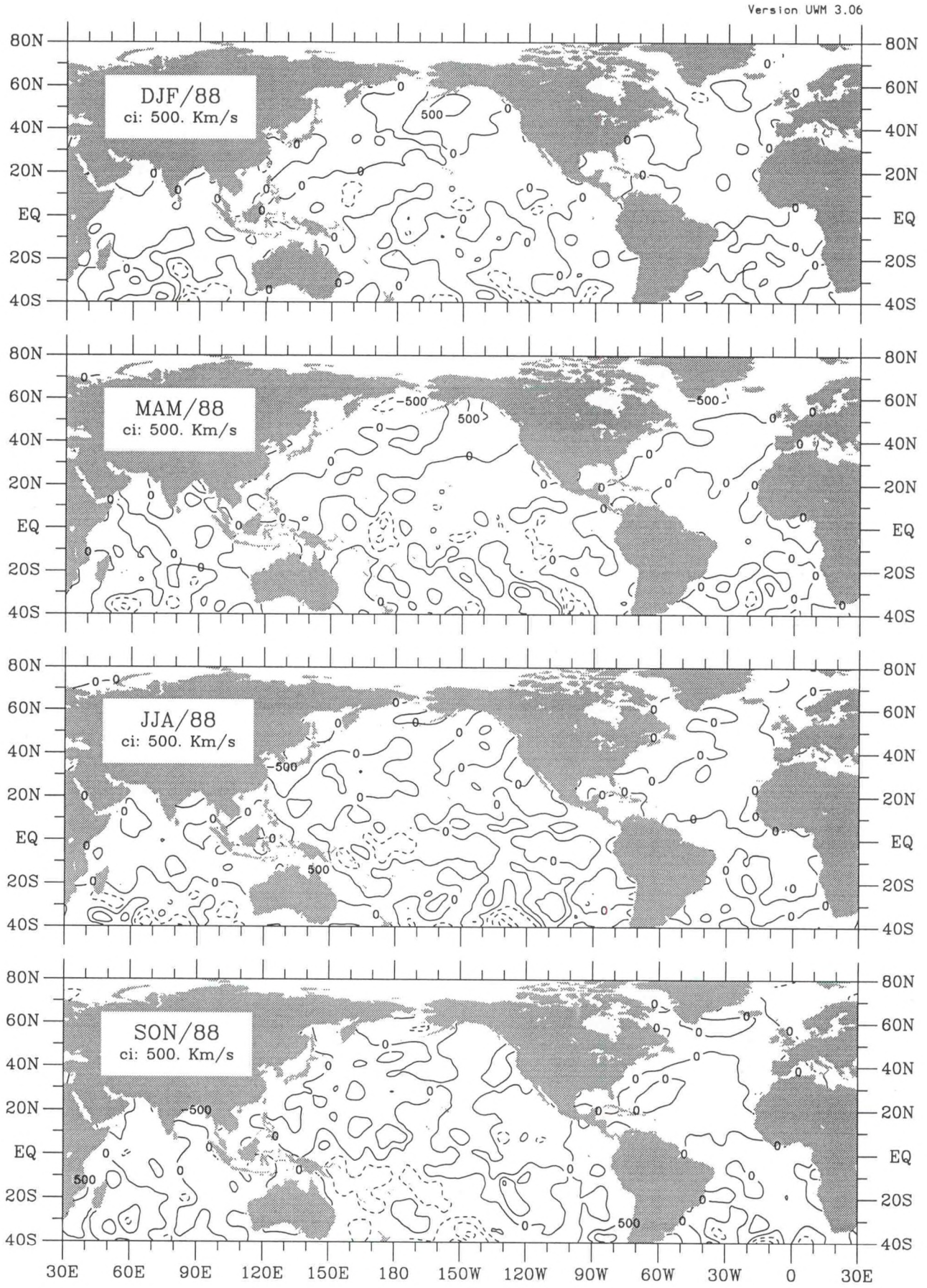

Figure va-49. Meridional heat flux seasonal anomaly for 1988.

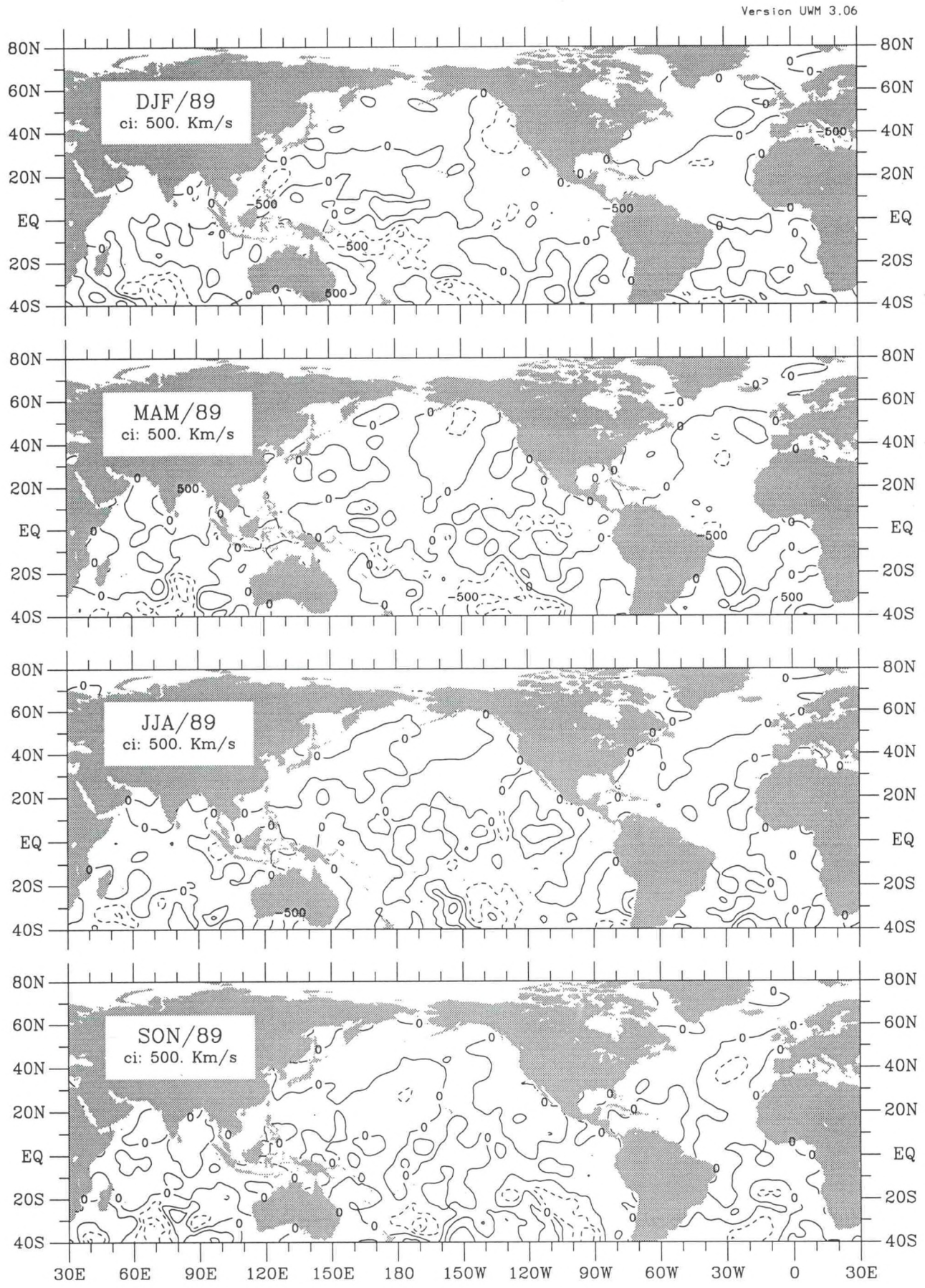

Figure va-50. Meridional heat flux seasonal anomaly for 1989.

17 Z/L (10m/Monin Obukov length)

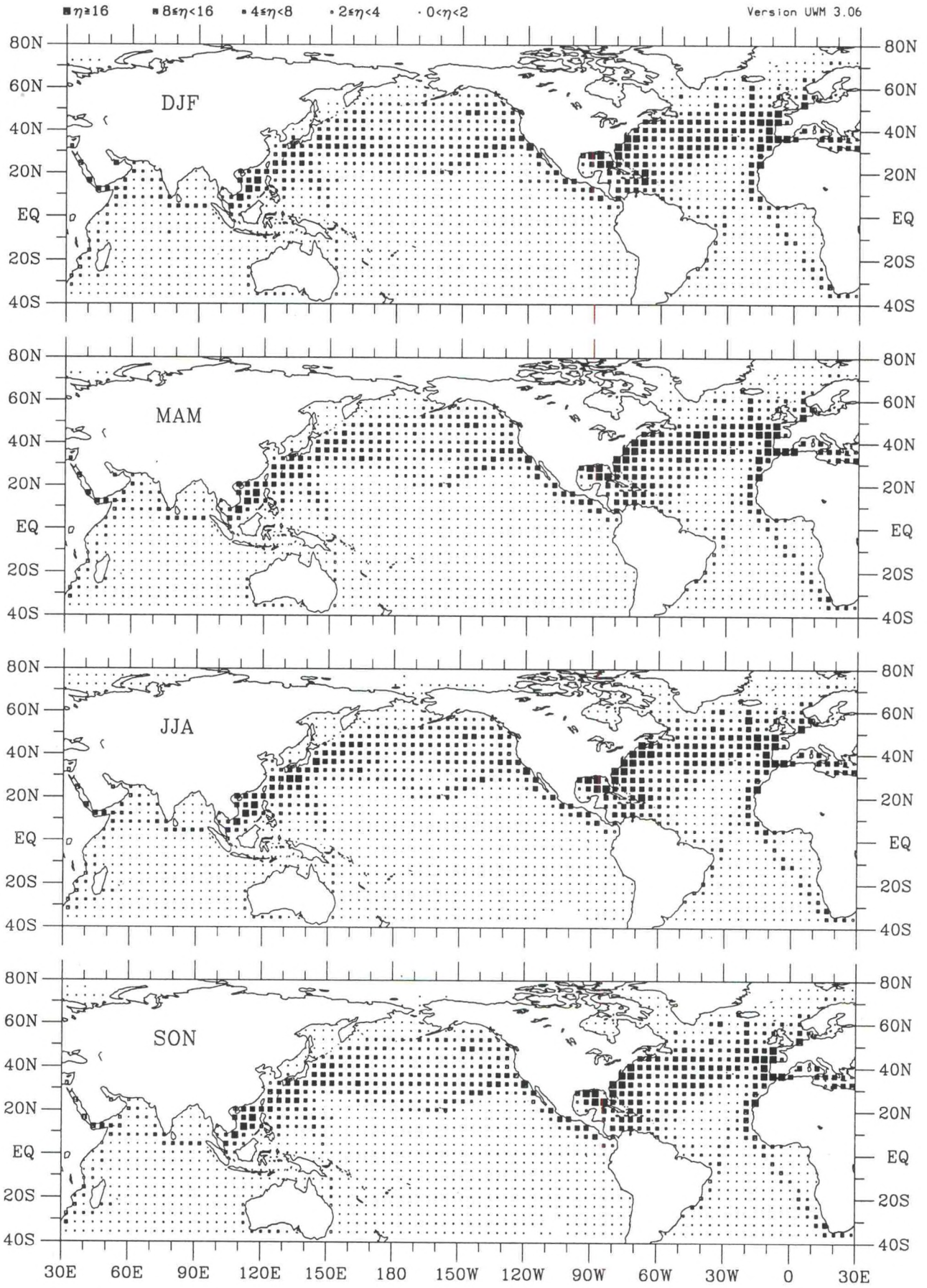

Figure Z/L–1. Stability parameter seasonal observation density (1945–89).

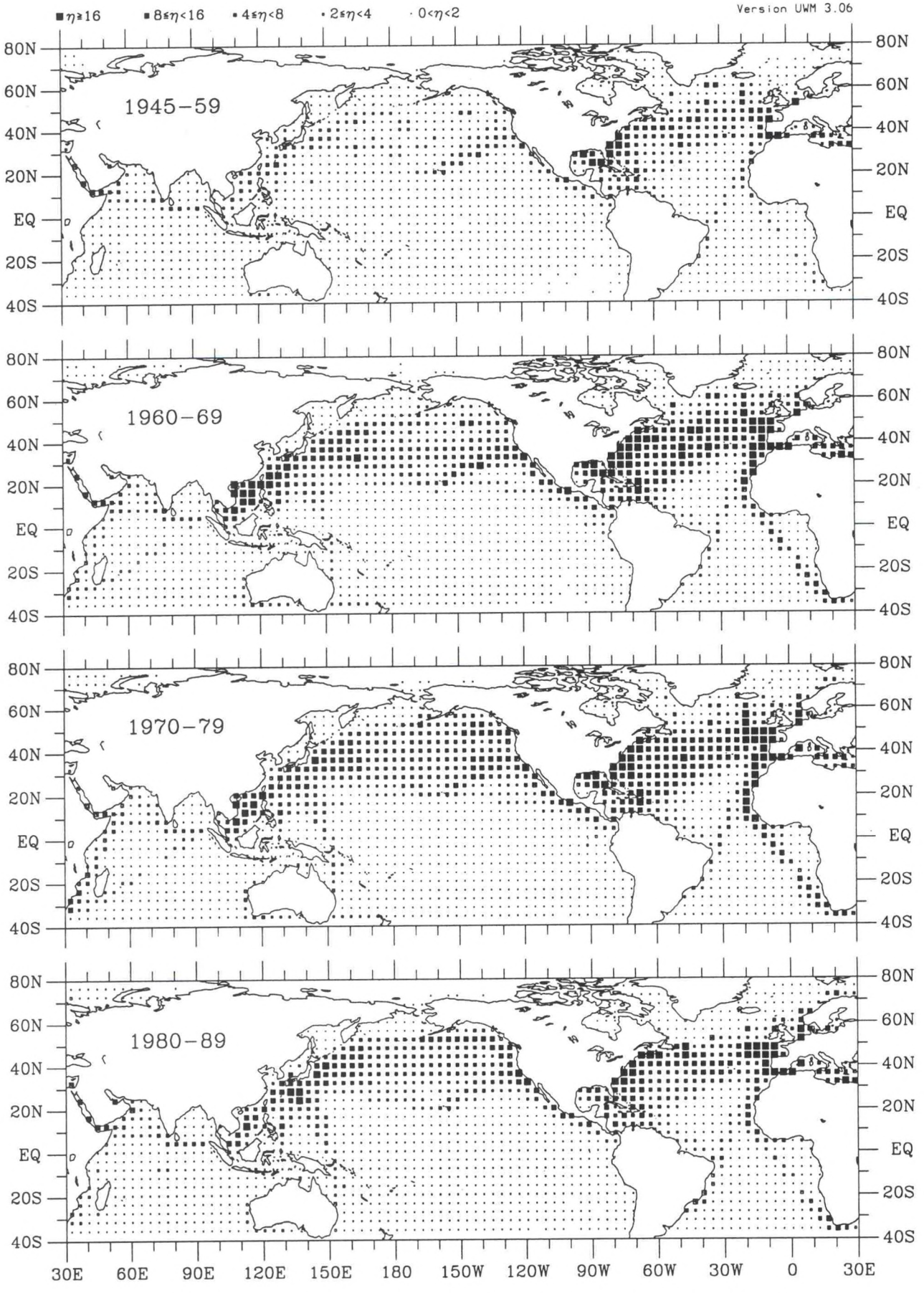

Figure Z/L-2. Stability parameter decadal observation density.

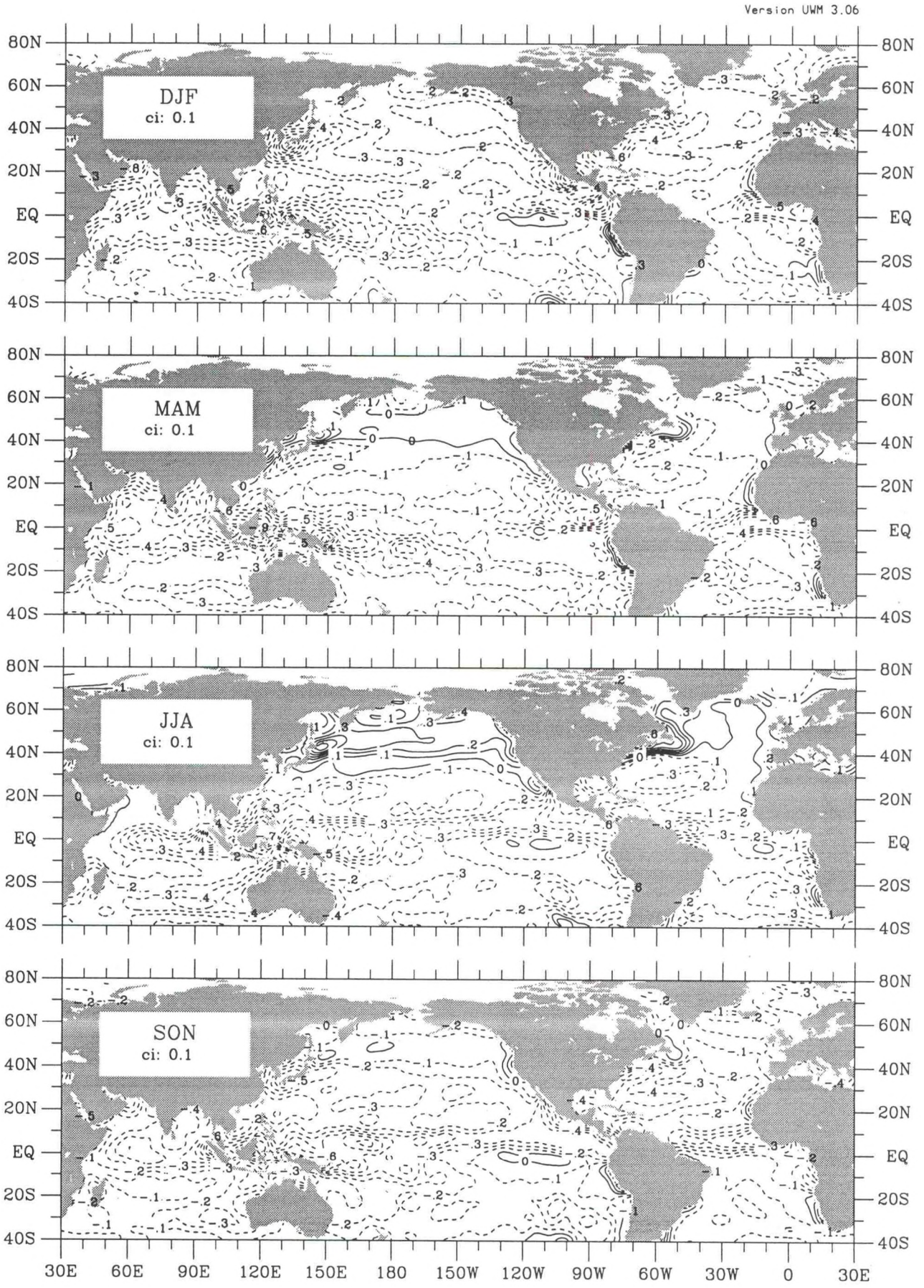

Figure Z/L-3. Stability parameter seasonal climatology (1945-89).

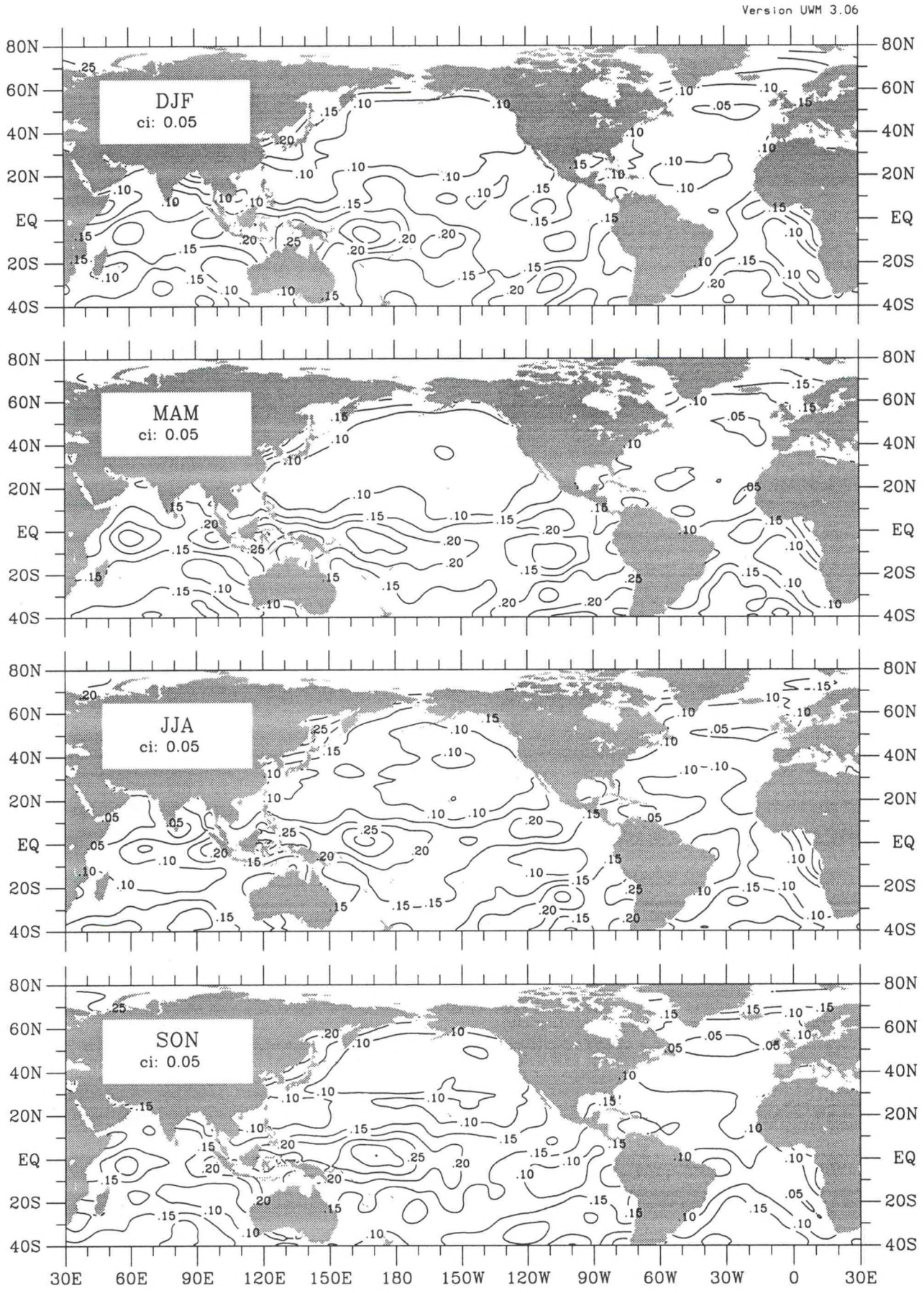

Figure Z/L-4. Stability parameter seasonal interannual std dev (1945-89).

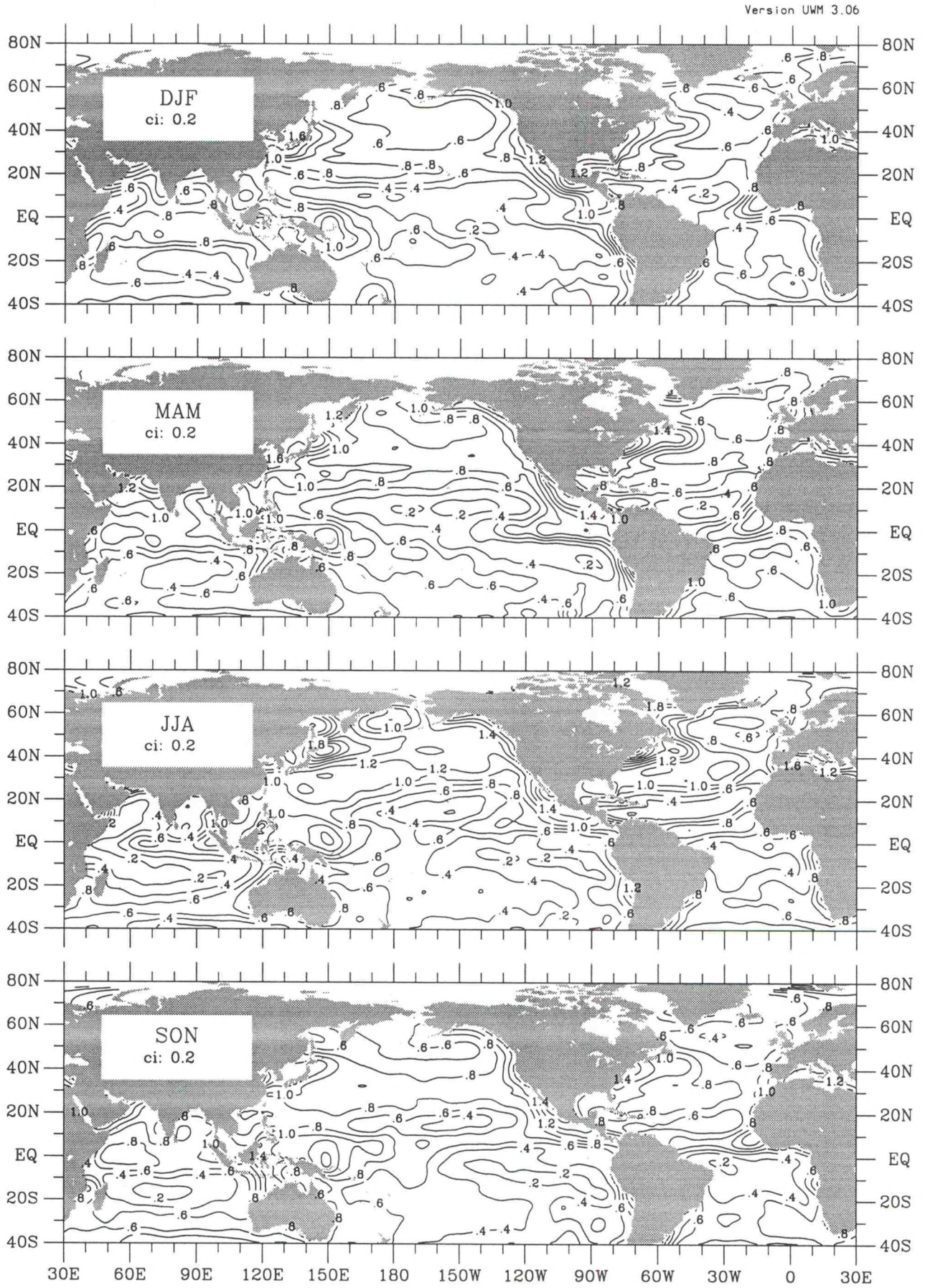

Figure Z/L-5. Stability parameter seasonal standard deviation (1945-89).

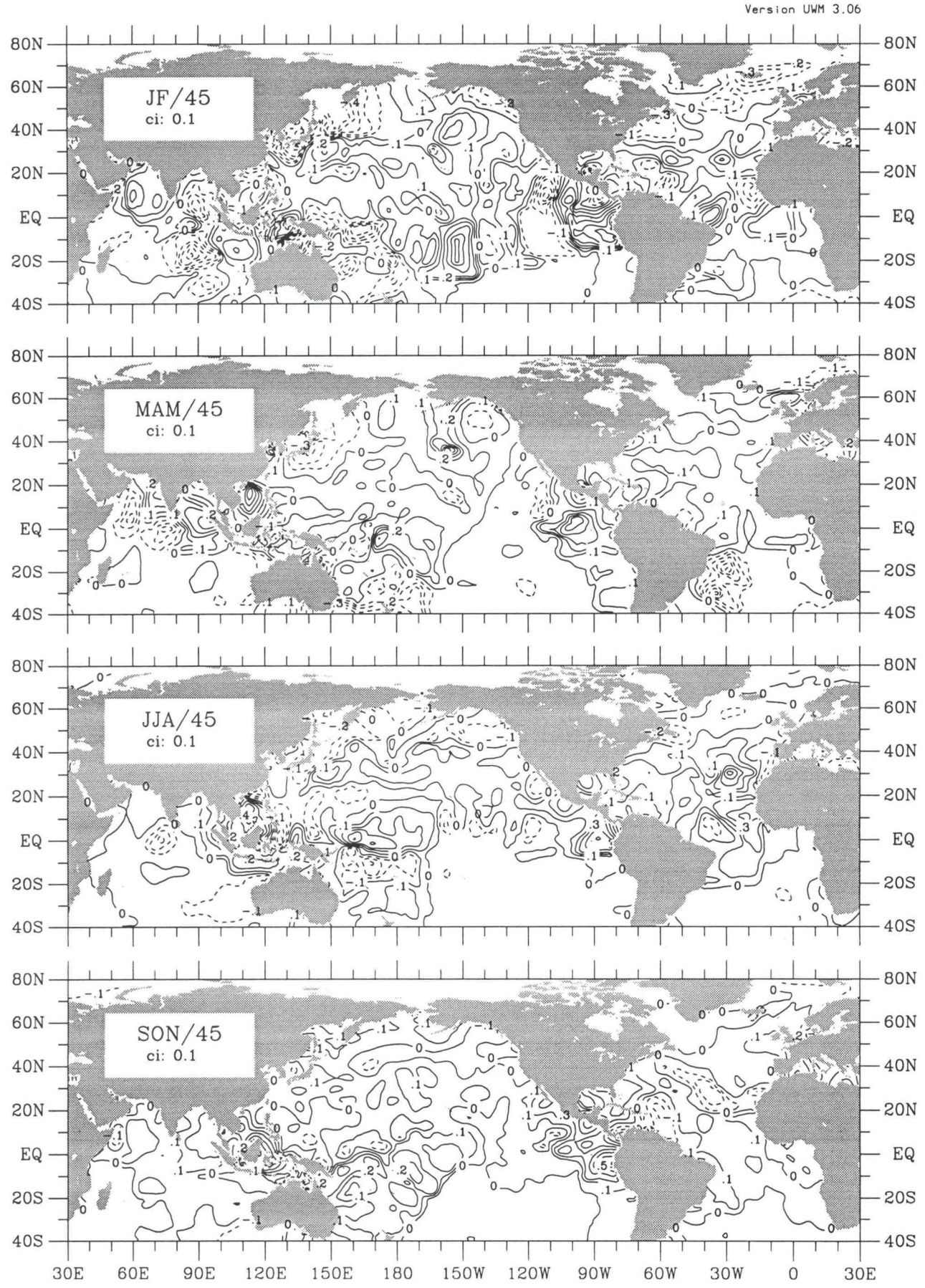

Figure Z/L-6. Stability parameter seasonal anomaly for 1945.

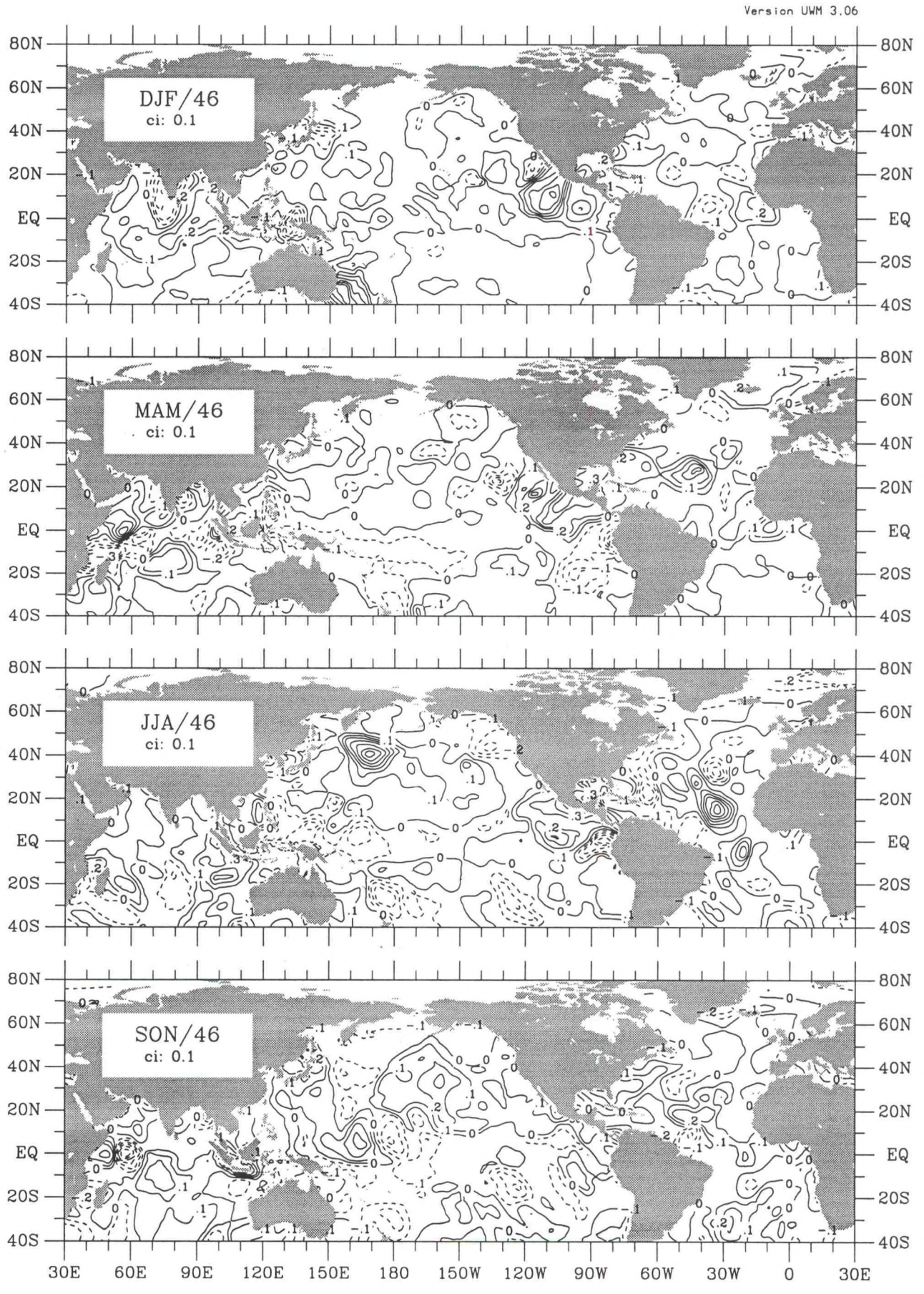

Figure Z/L-7. Stability parameter seasonal anomaly for 1946.

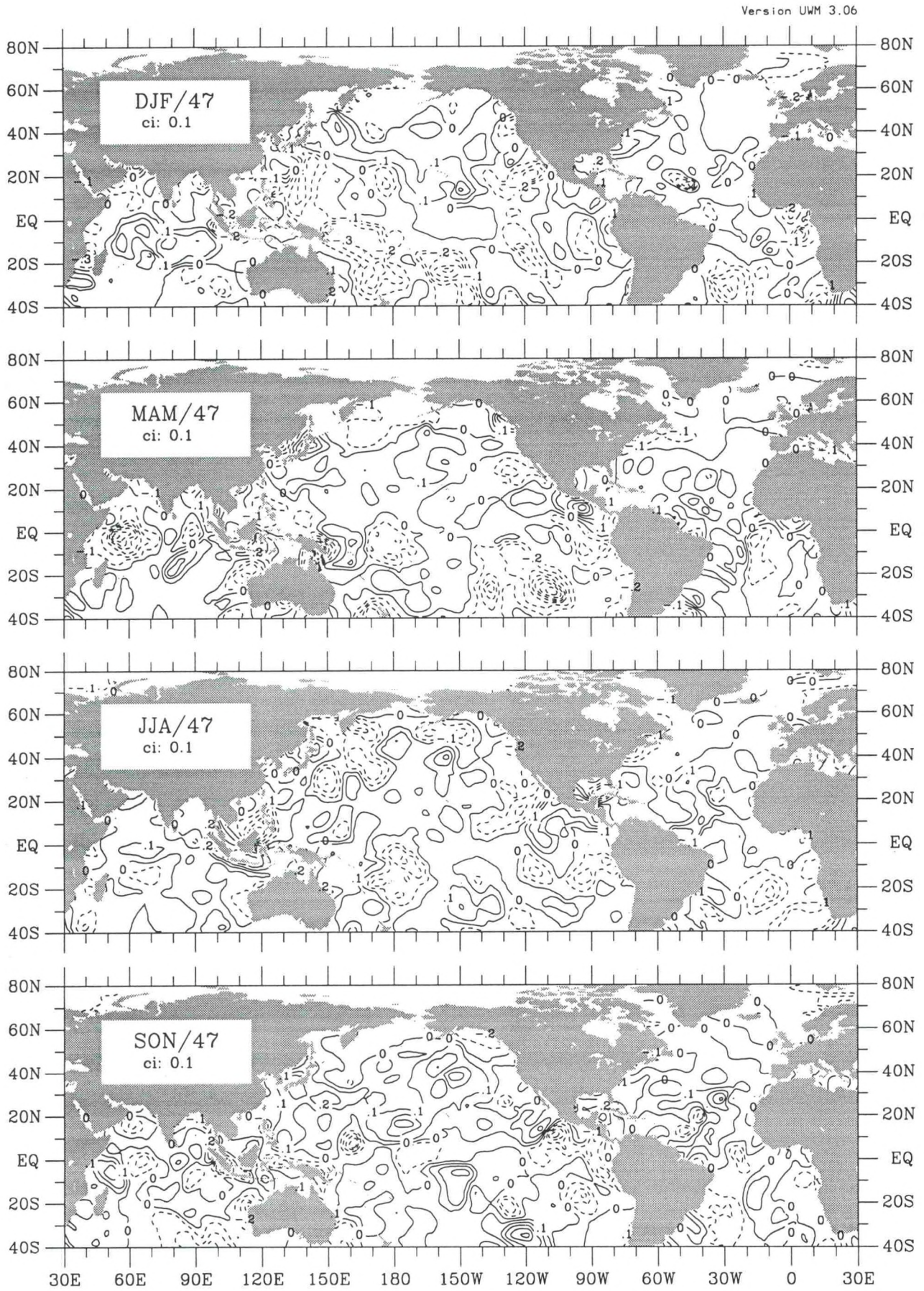

Figure Z/L-8. Stability parameter seasonal anomaly for 1947.

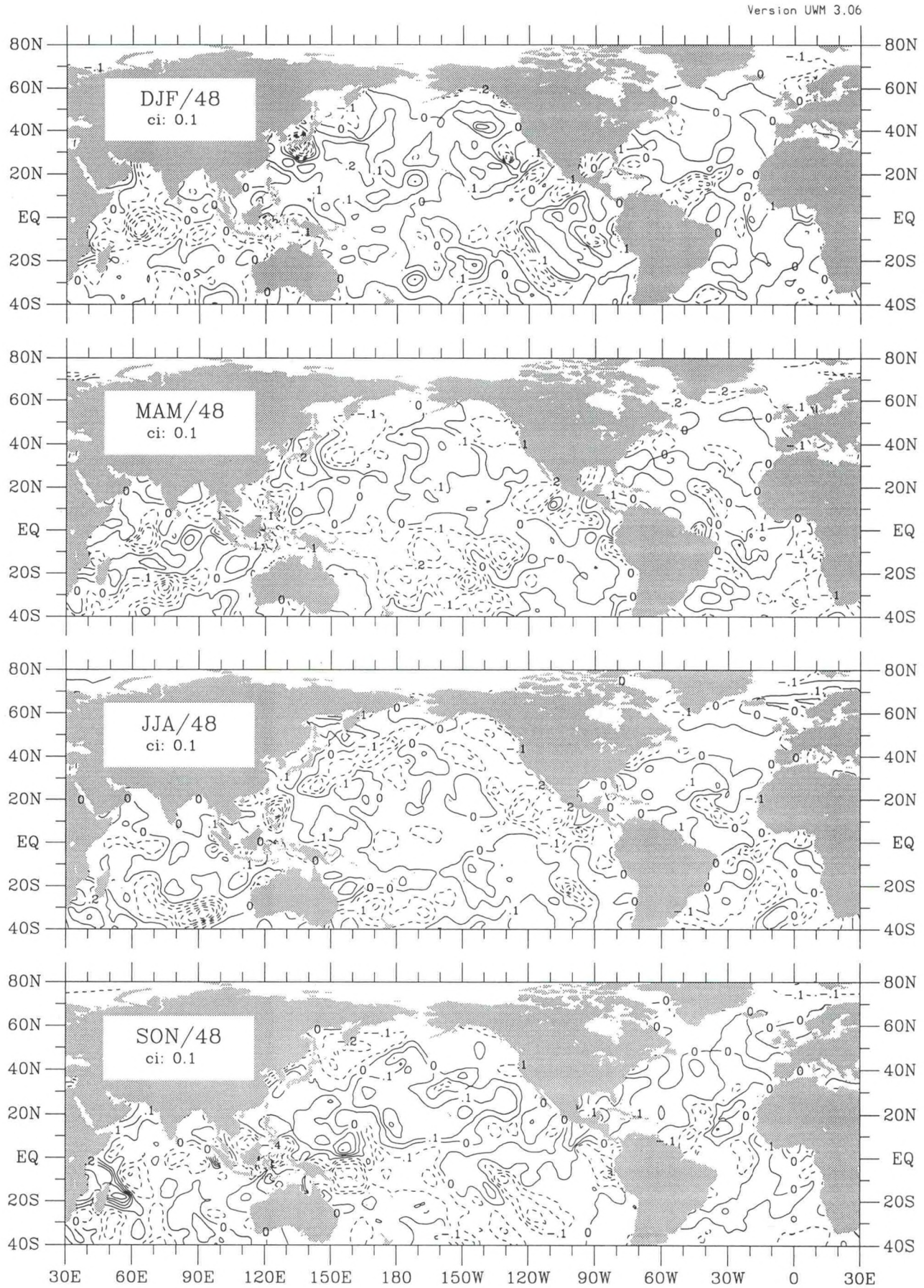

Figure Z/L-9. Stability parameter seasonal anomaly for 1948.

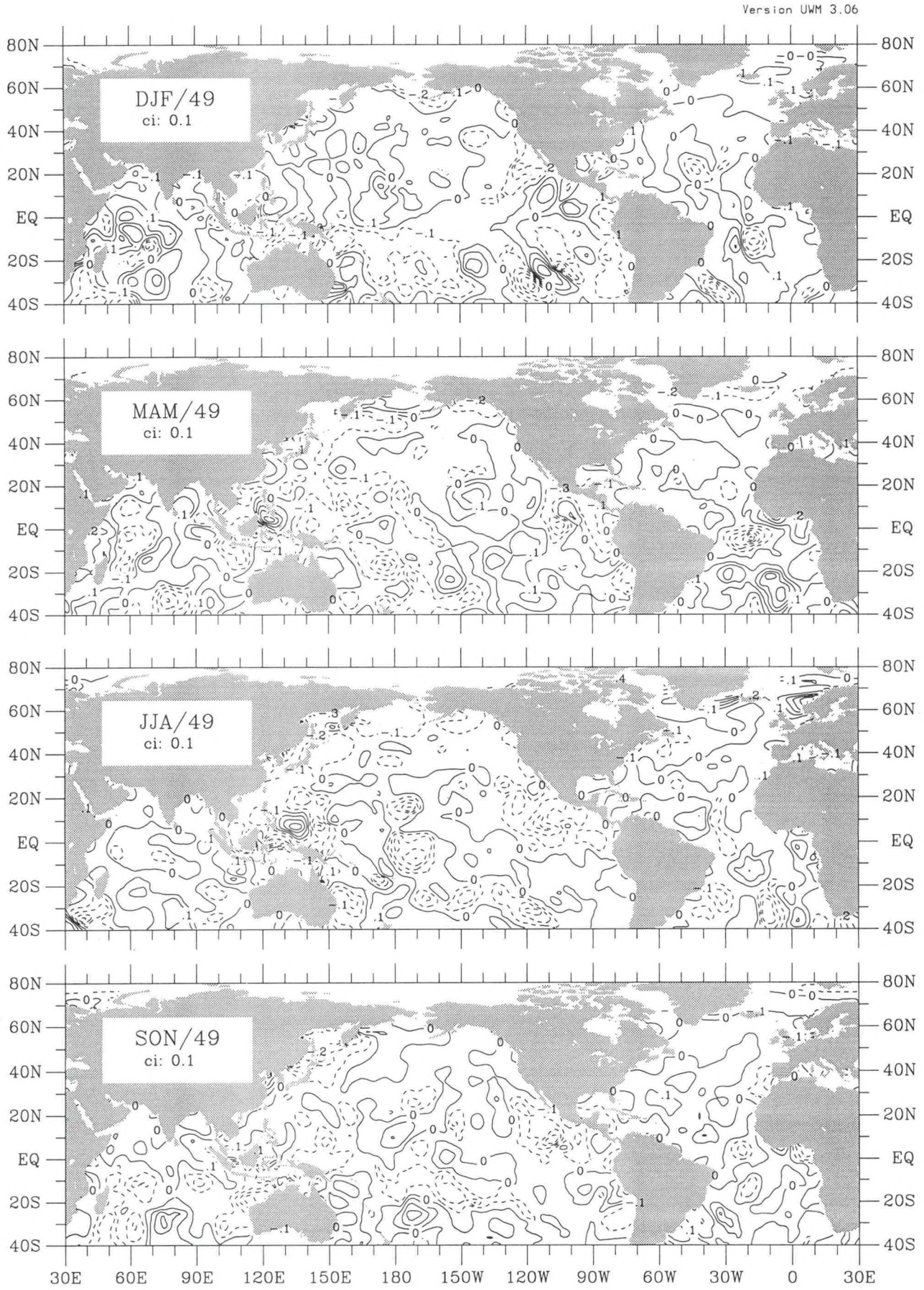

Figure Z/L-10. Stability parameter seasonal anomaly for 1949.

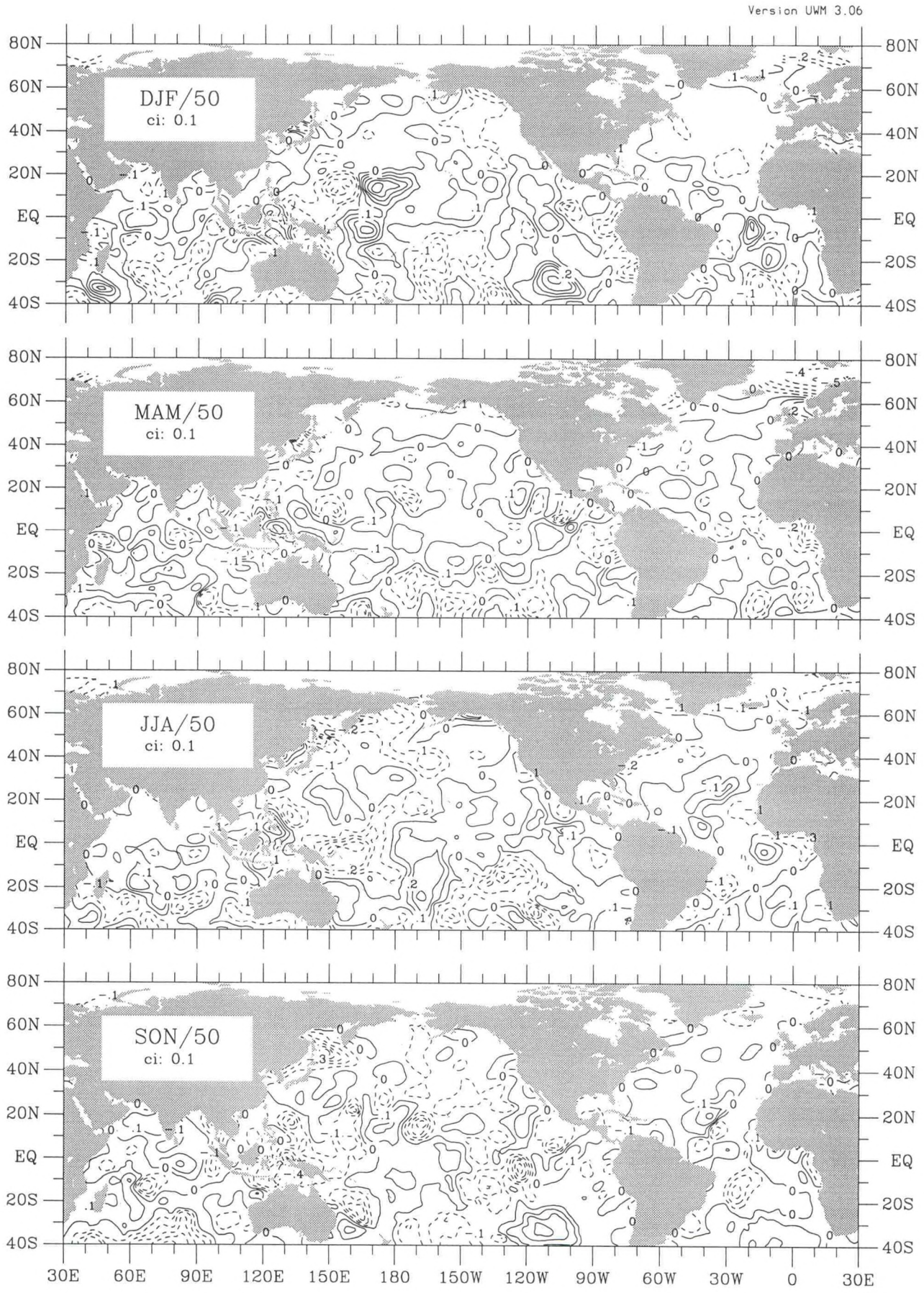

Figure Z/L-11. Stability parameter seasonal anomaly for 1950.

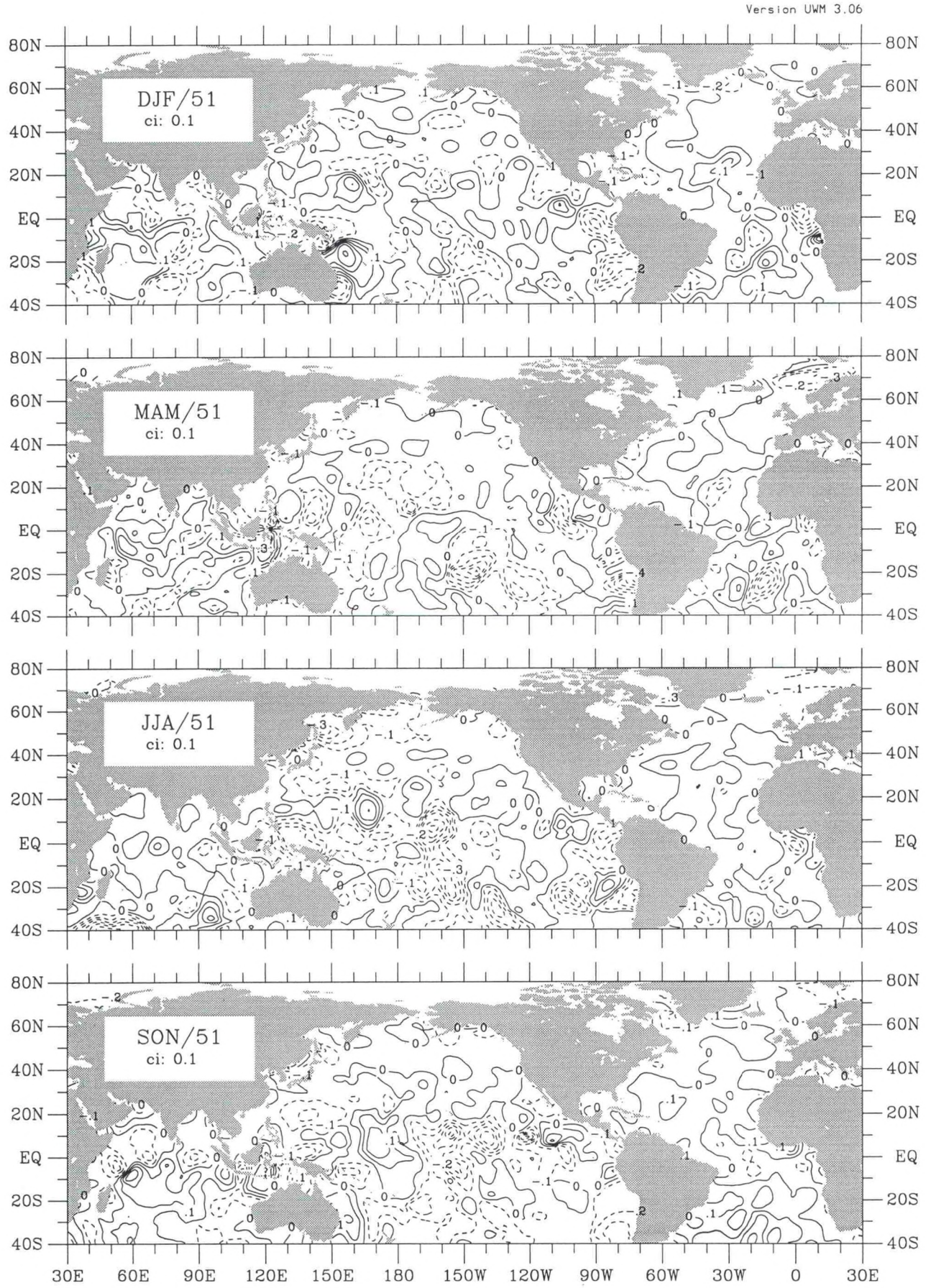

Figure Z/L-12. Stability parameter seasonal anomaly for 1951.

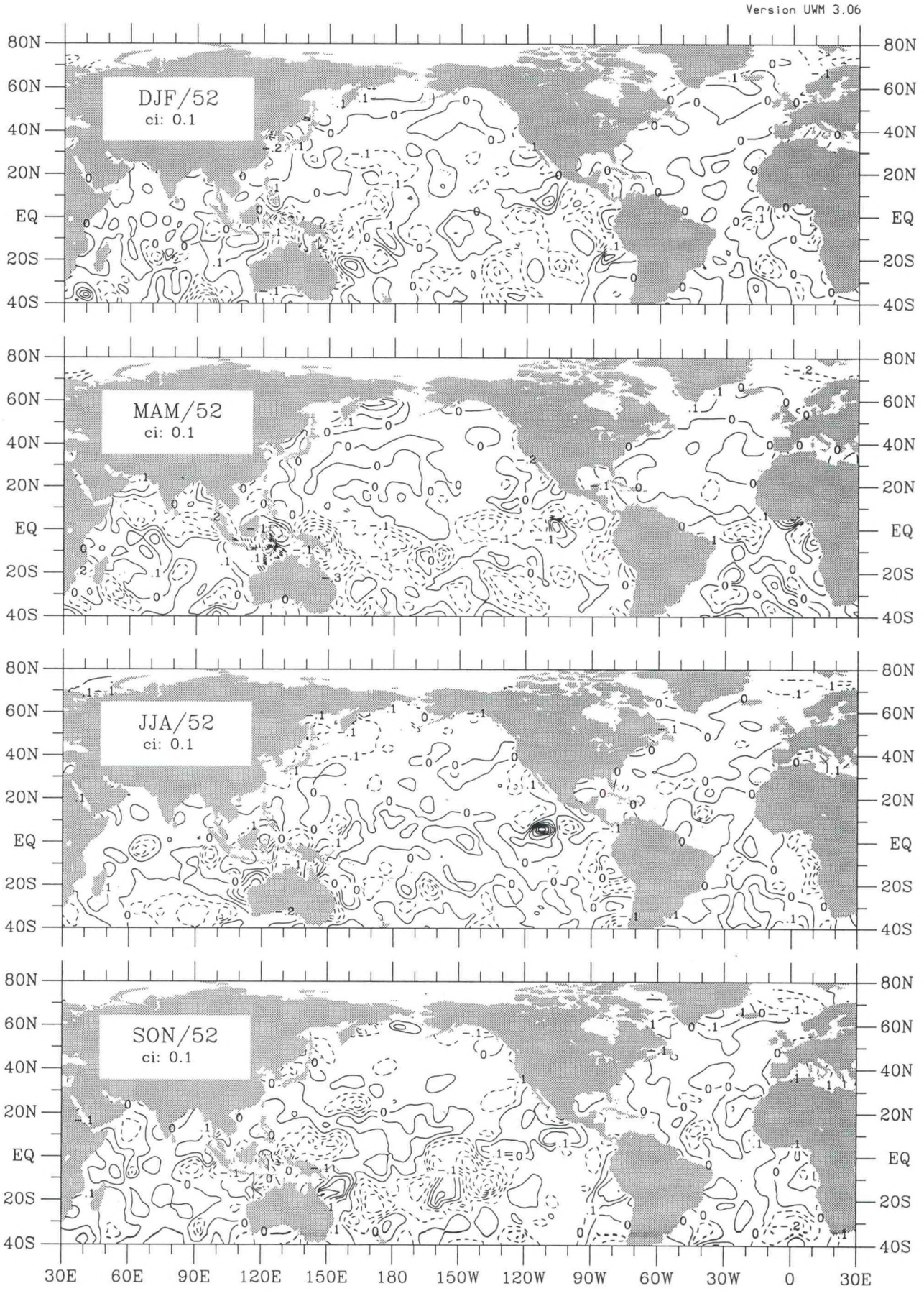

Figure Z/L-13. Stability parameter seasonal anomaly for 1952.

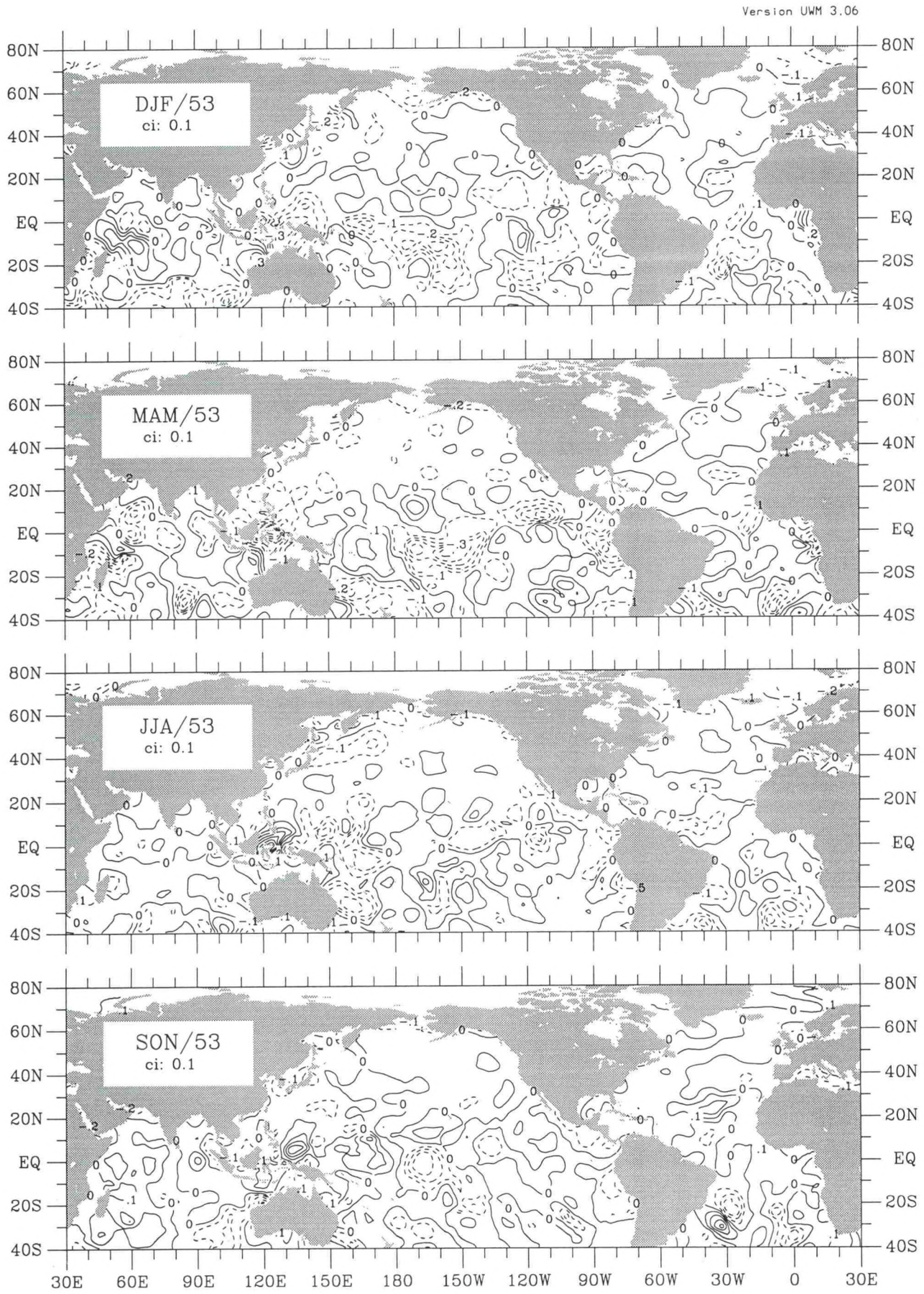

Figure Z/L-14. Stability parameter seasonal anomaly for 1953.

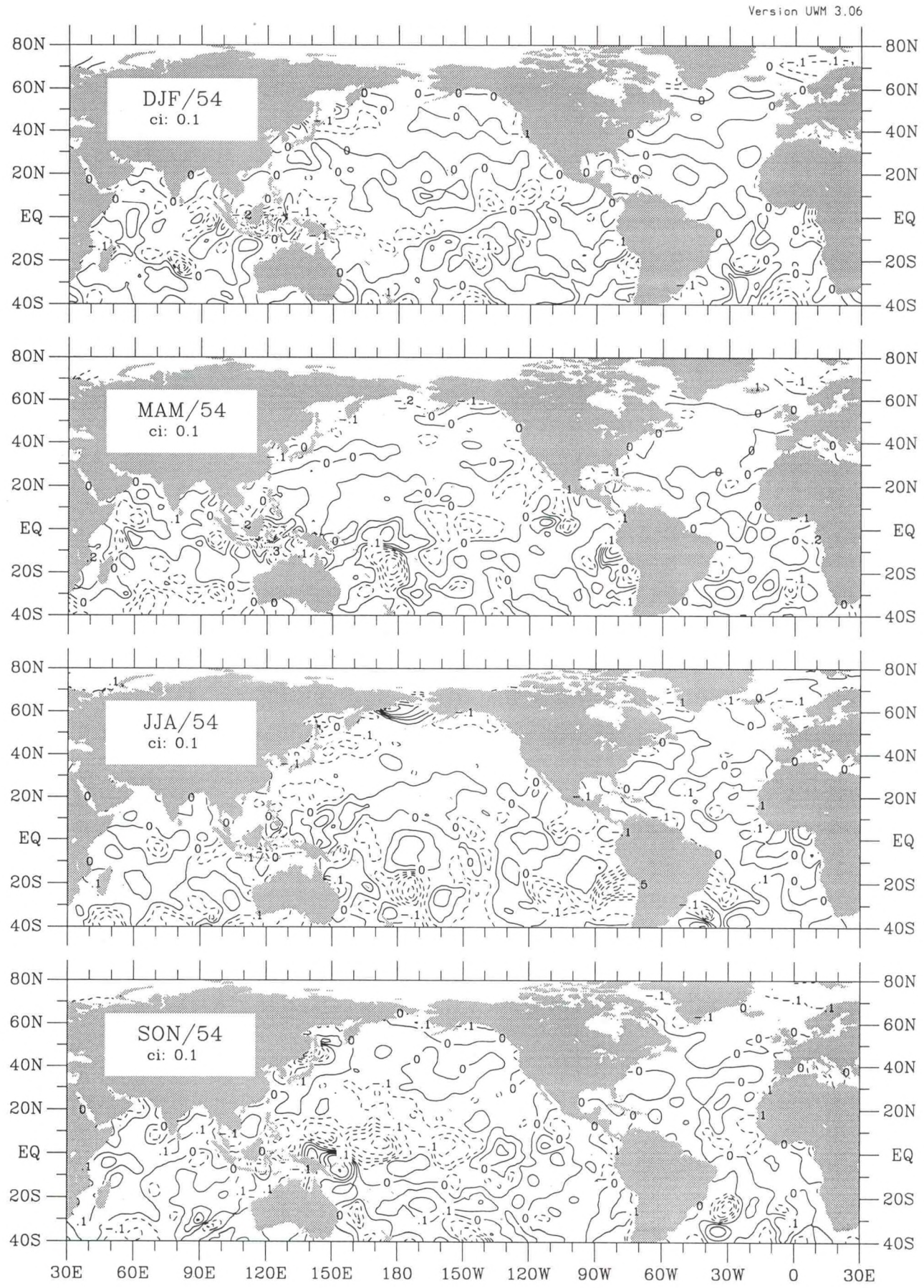

Figure Z/L–15. Stability parameter seasonal anomaly for 1954.

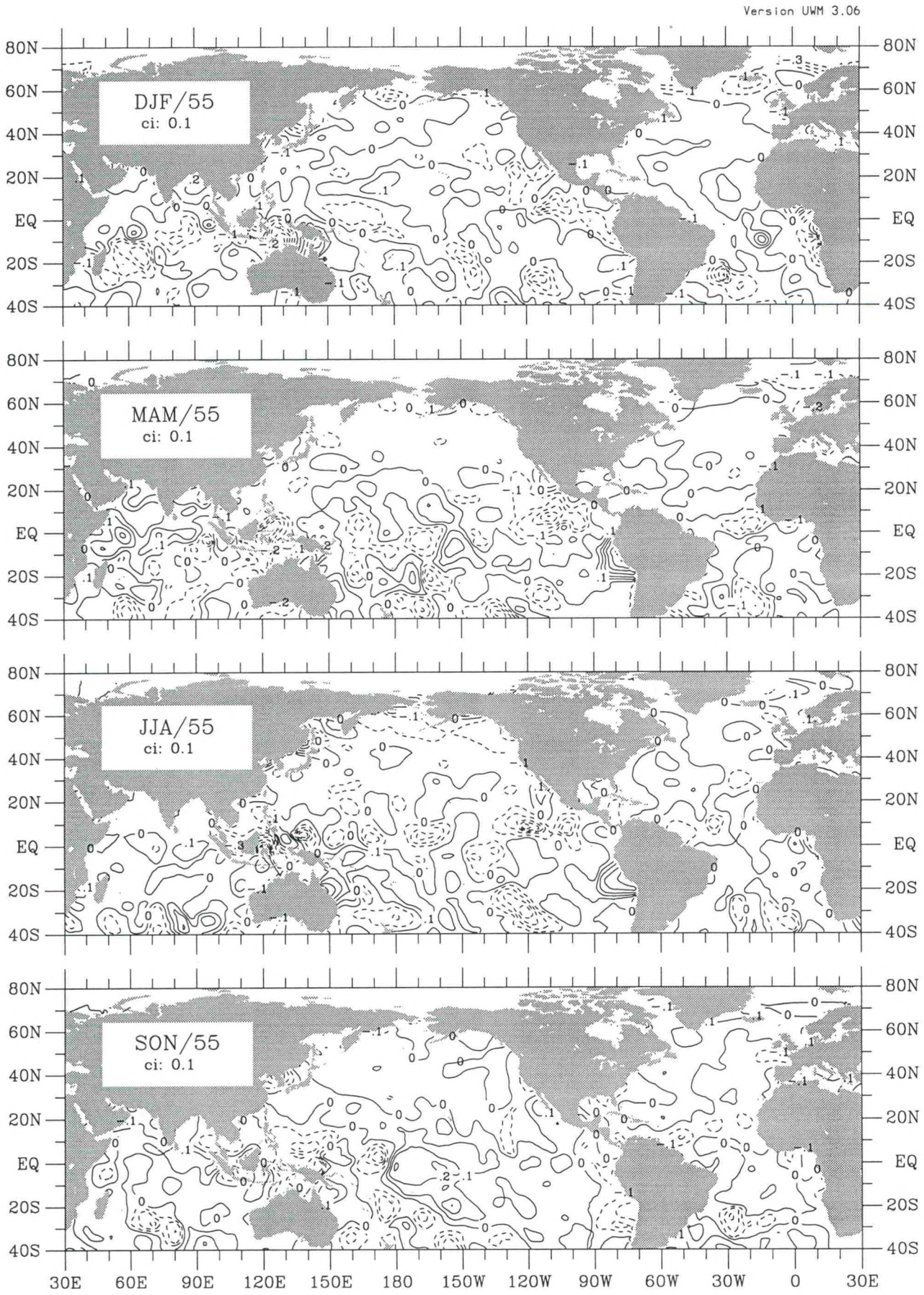

Figure Z/L-16. Stability parameter seasonal anomaly for 1955.

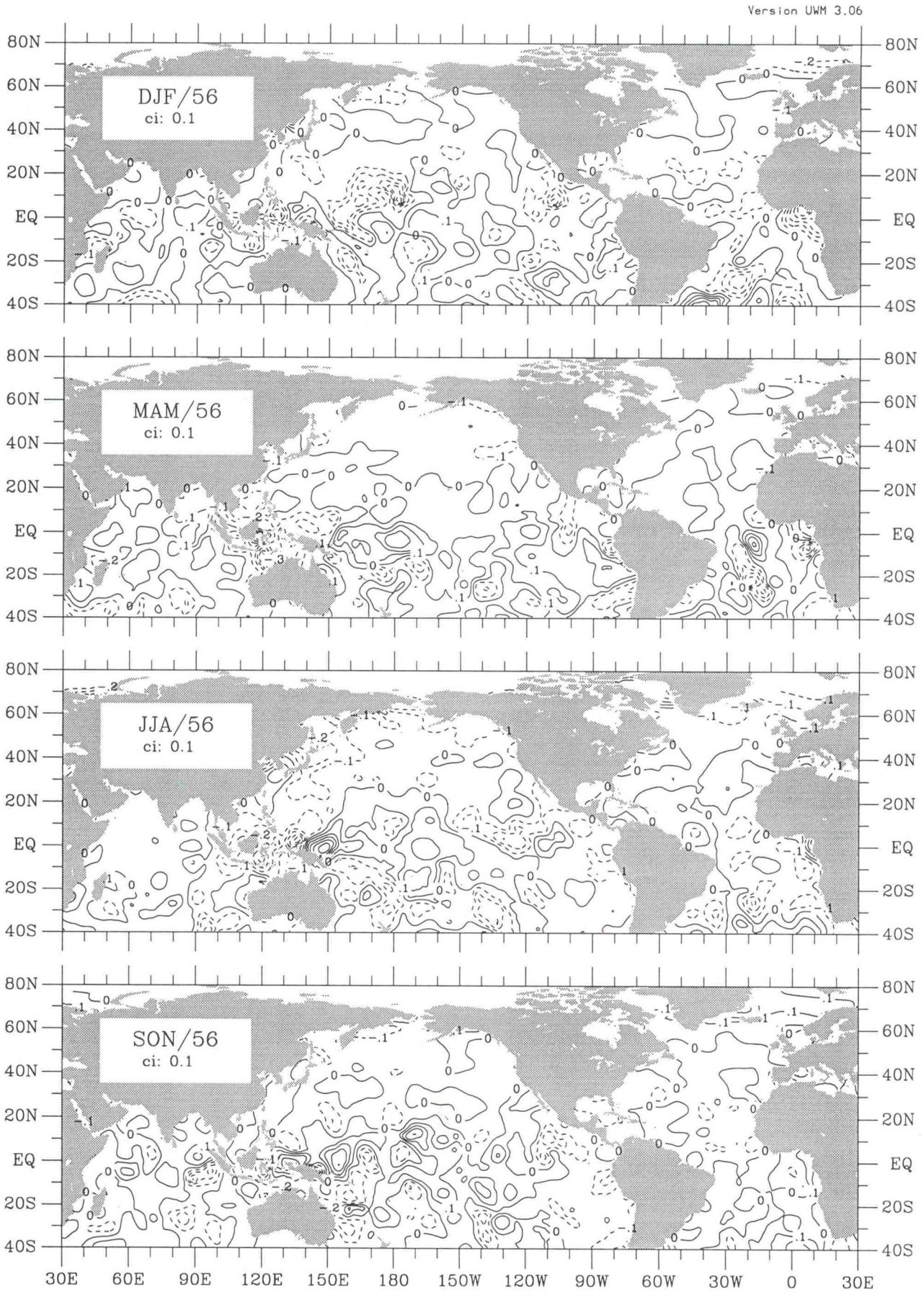

Figure Z/L-17. Stability parameter seasonal anomaly for 1956.

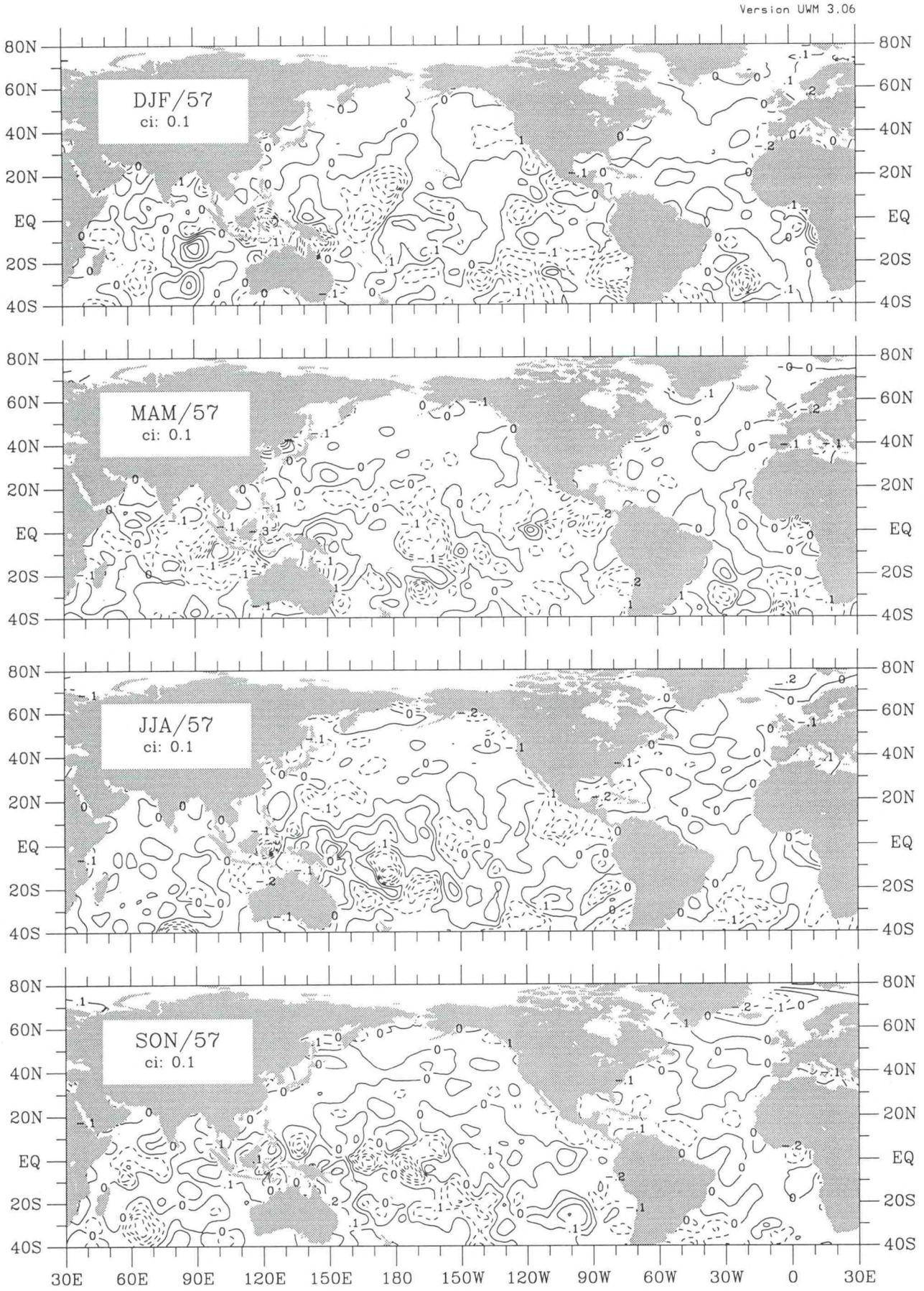

Figure Z/L-18. Stability parameter seasonal anomaly for 1957.

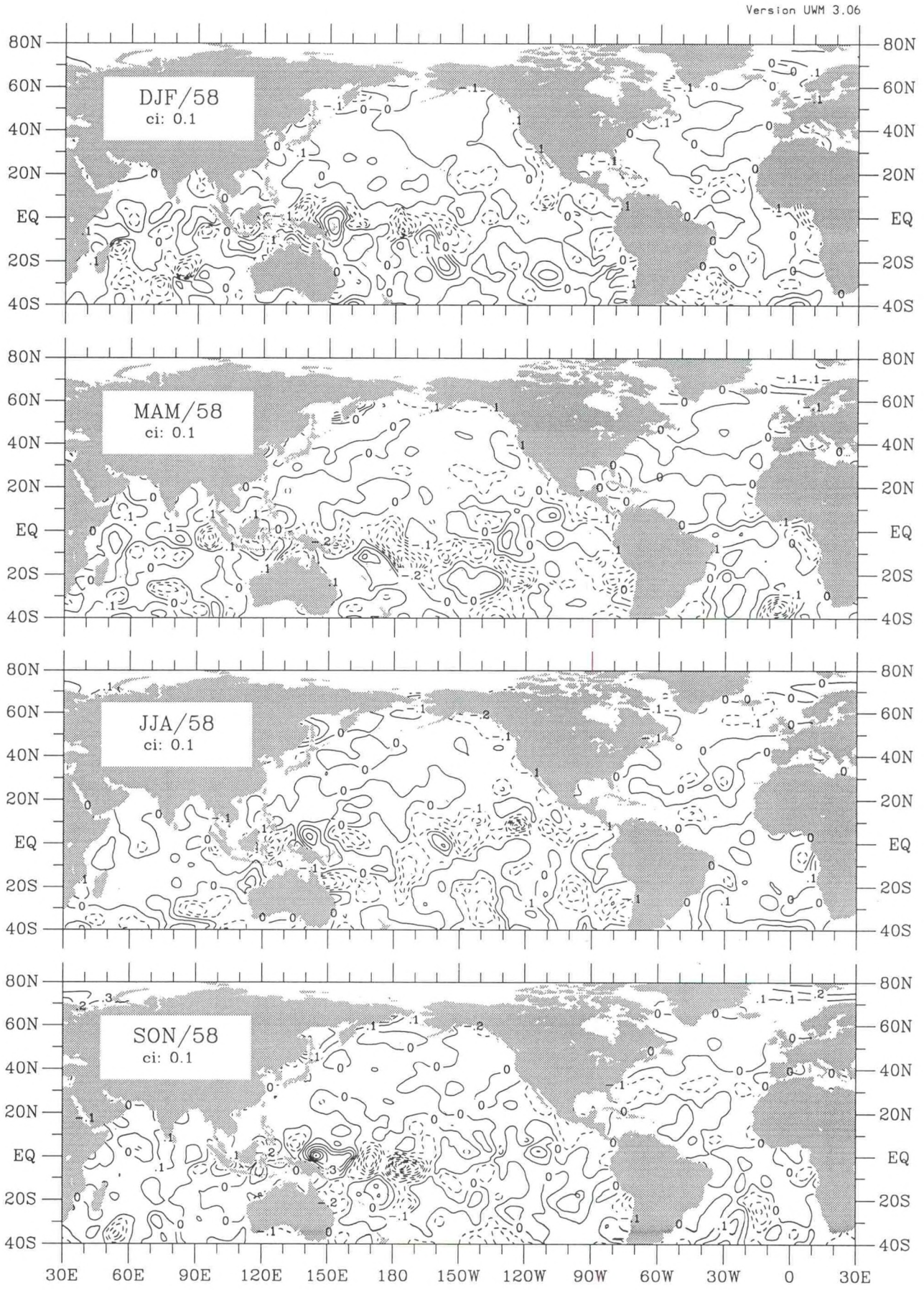

Figure Z/L-19. Stability parameter seasonal anomaly for 1958.

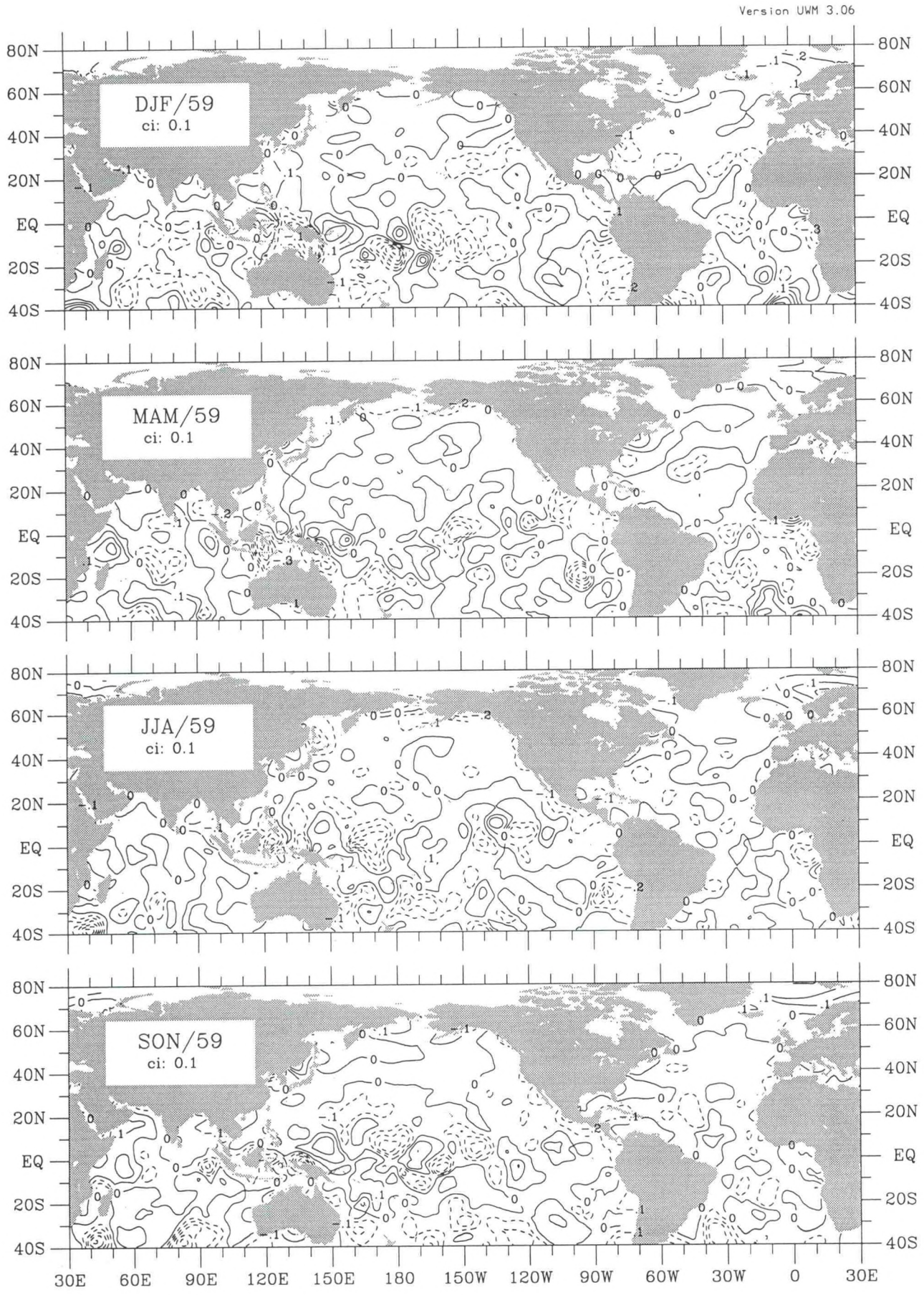

Figure Z/L-20. Stability parameter seasonal anomaly for 1959.

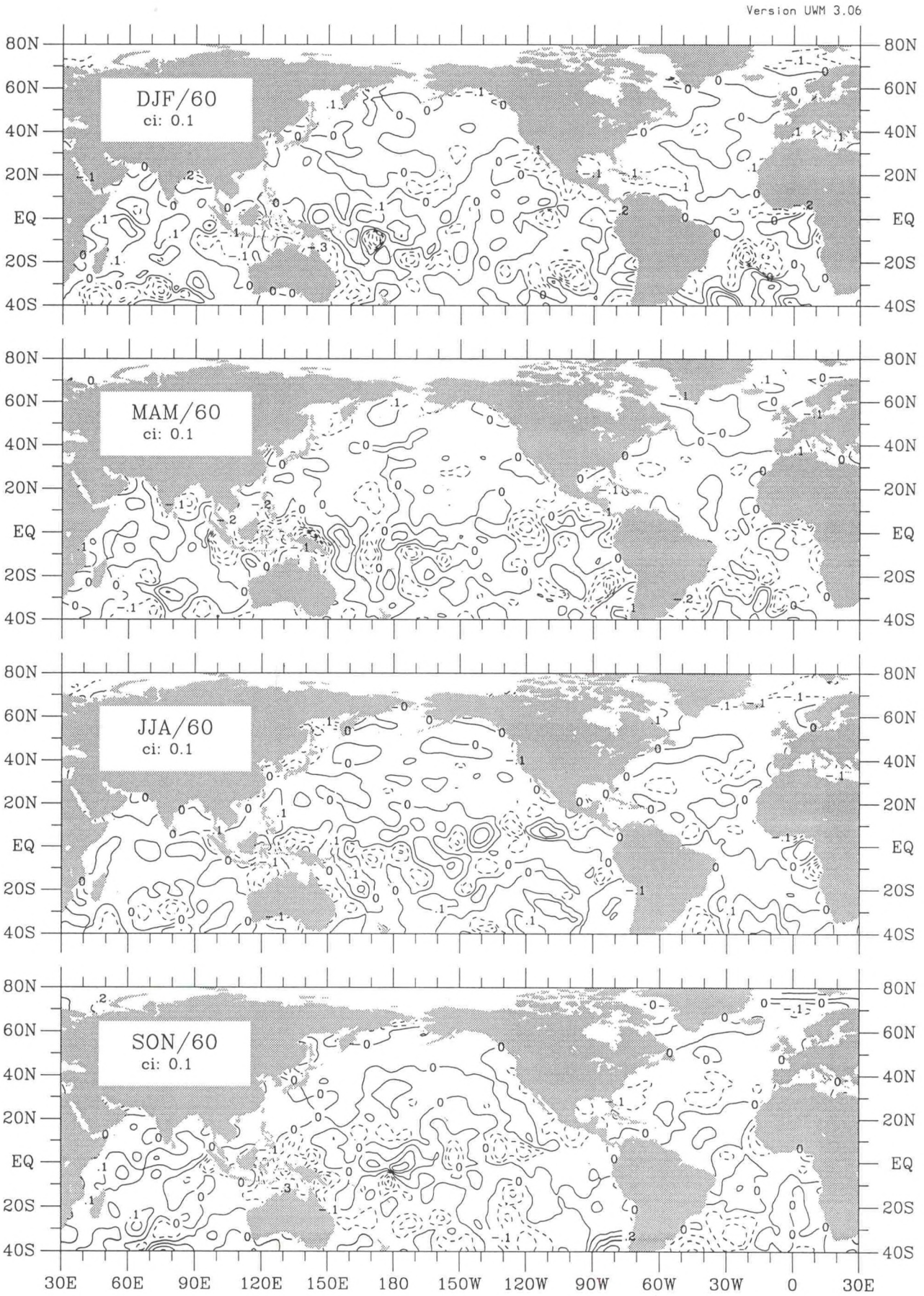

Figure Z/L-21. Stability parameter seasonal anomaly for 1960.

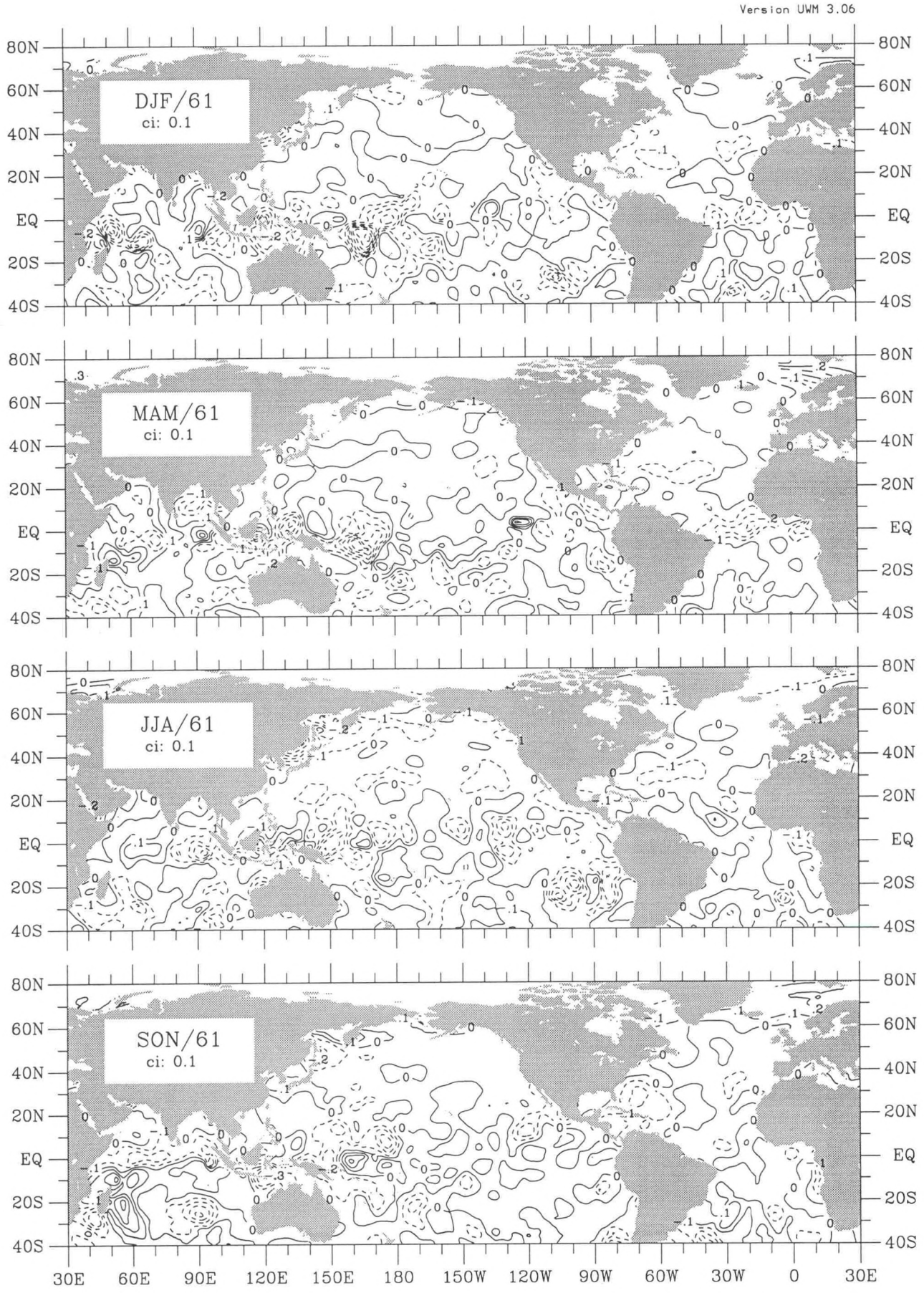

Figure Z/L-22. Stability parameter seasonal anomaly for 1961.

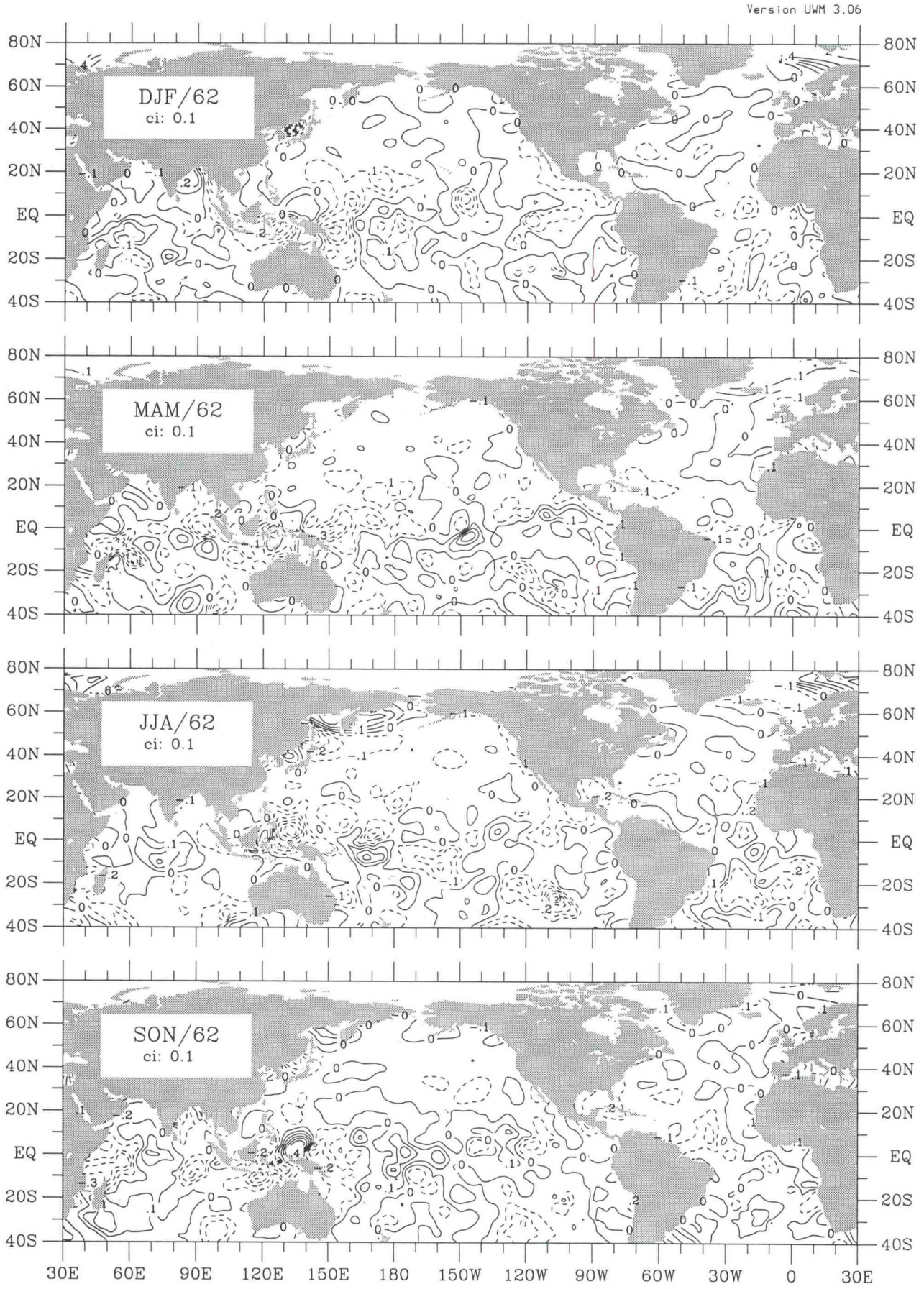

Figure Z/L-23. Stability parameter seasonal anomaly for 1962.

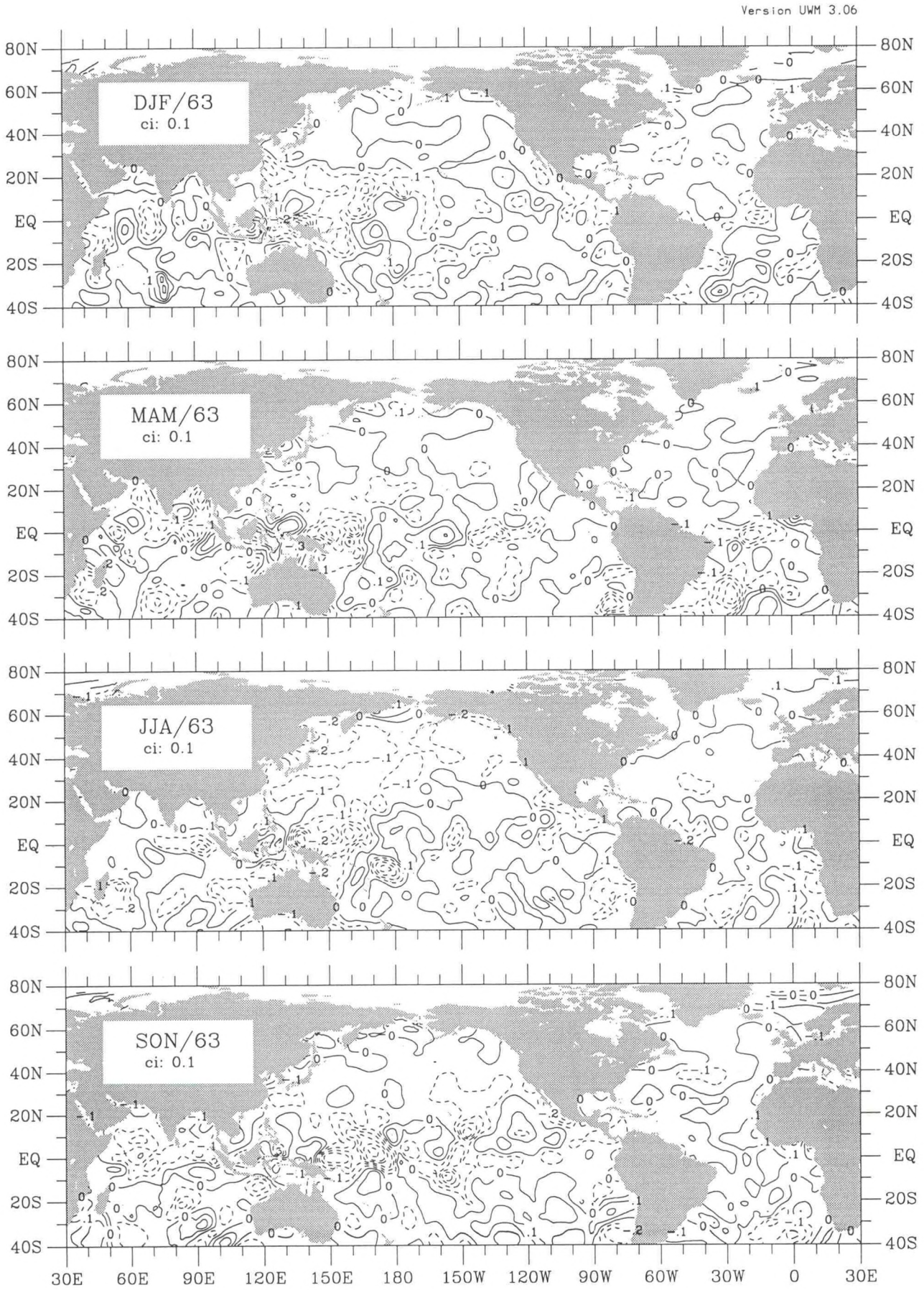

Figure Z/L-24. Stability parameter seasonal anomaly for 1963.

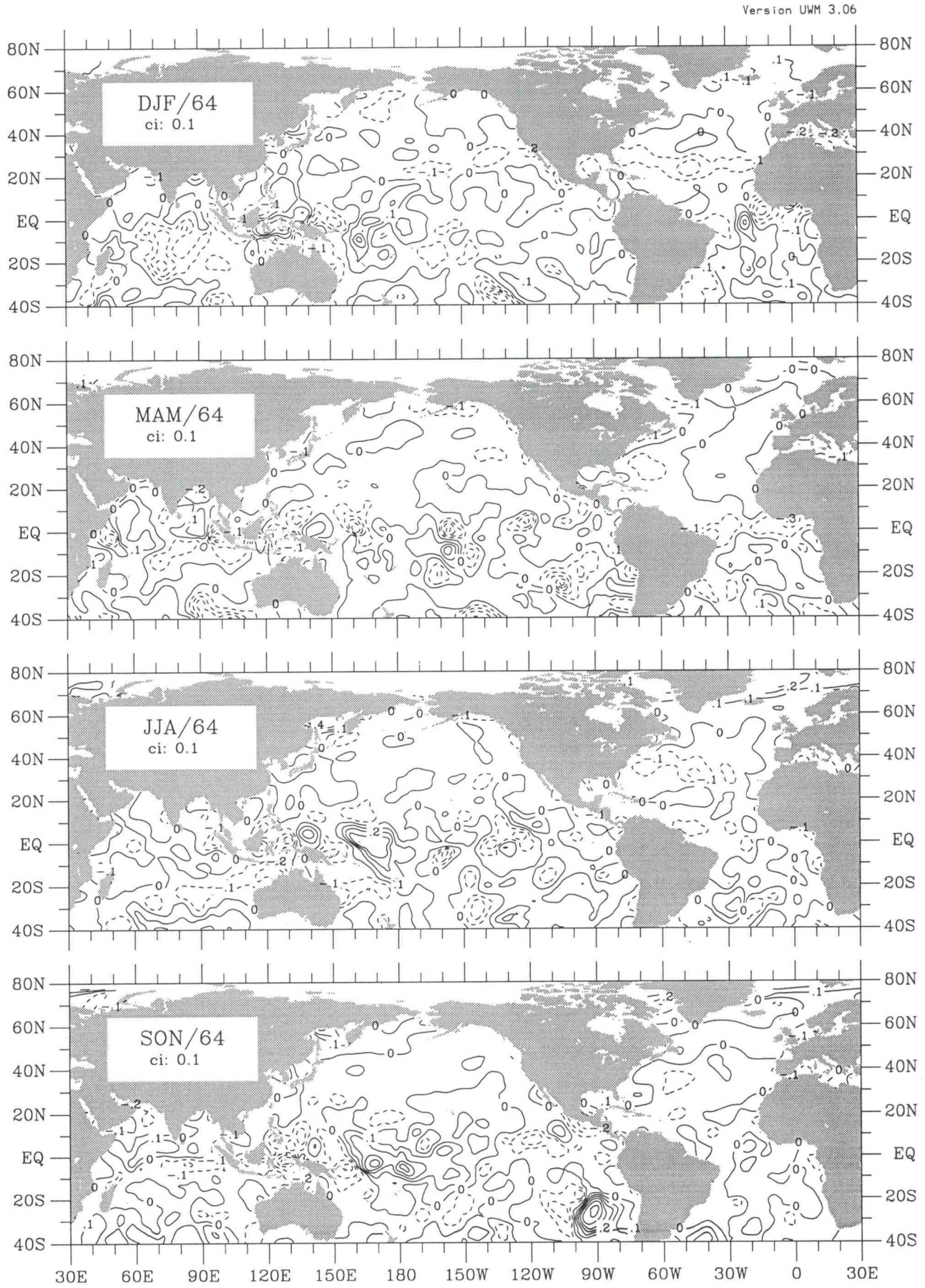

Figure Z/L-25. Stability parameter seasonal anomaly for 1964.

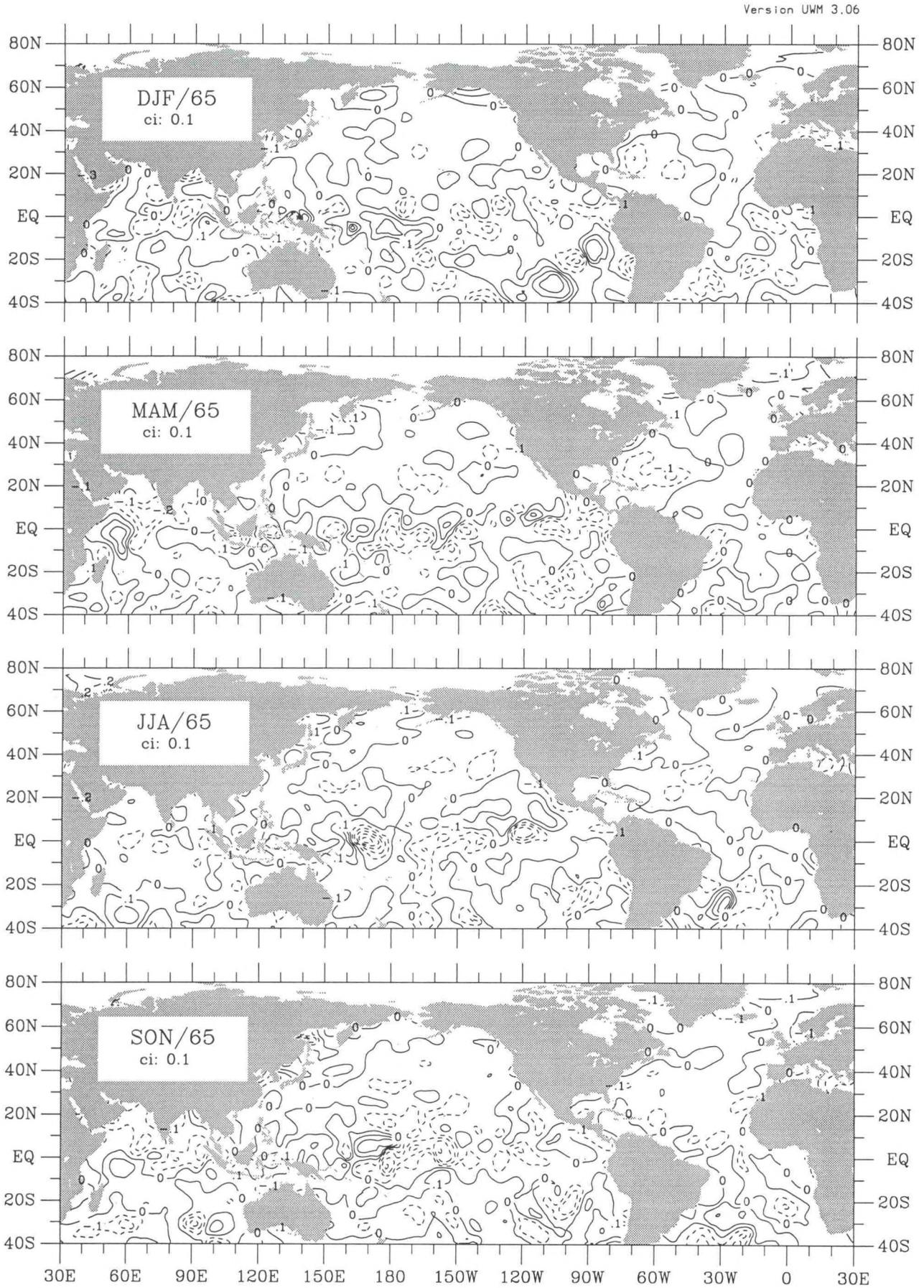

Figure Z/L-26. Stability parameter seasonal anomaly for 1965.

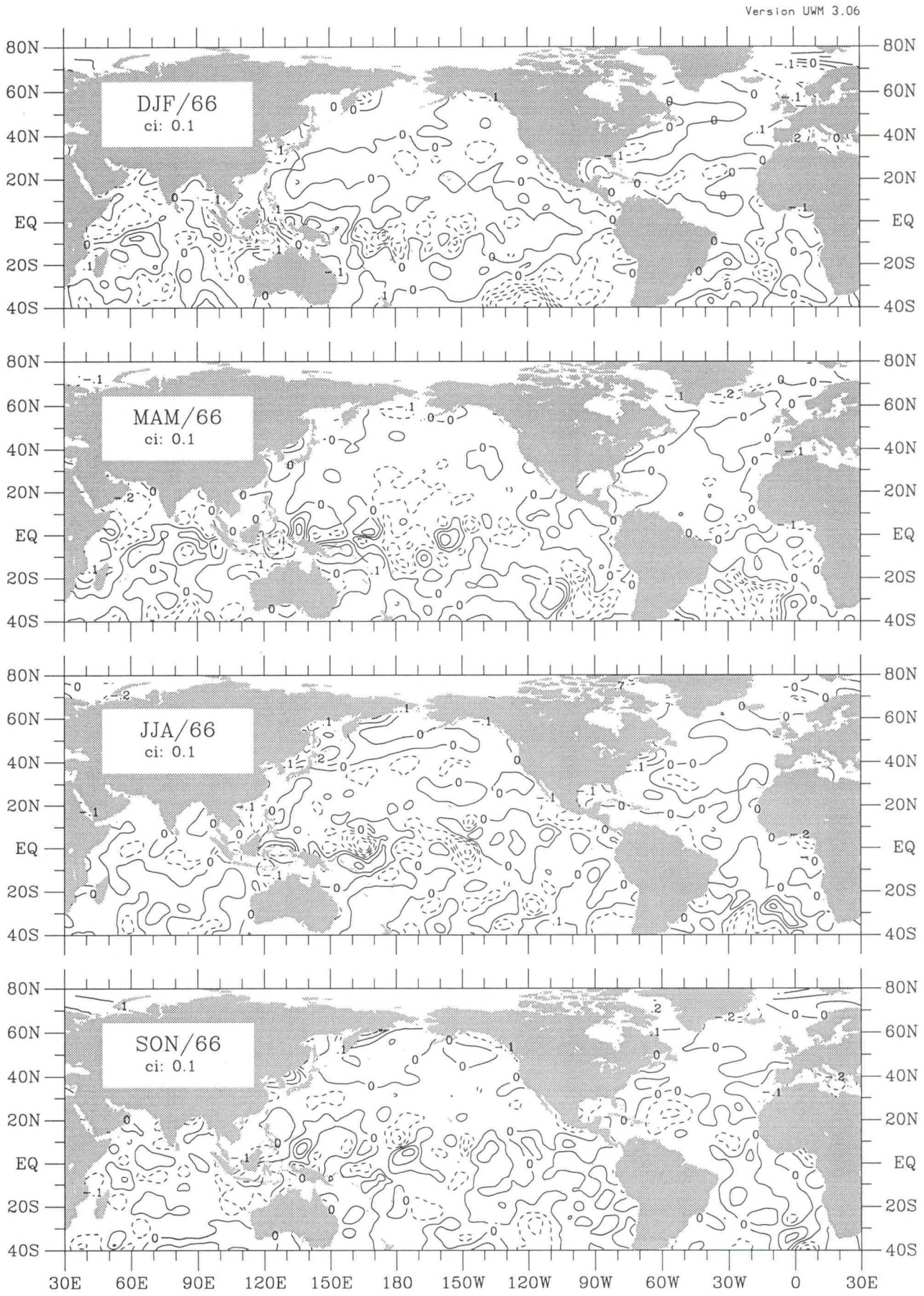

Figure Z/L-27. Stability parameter seasonal anomaly for 1966.

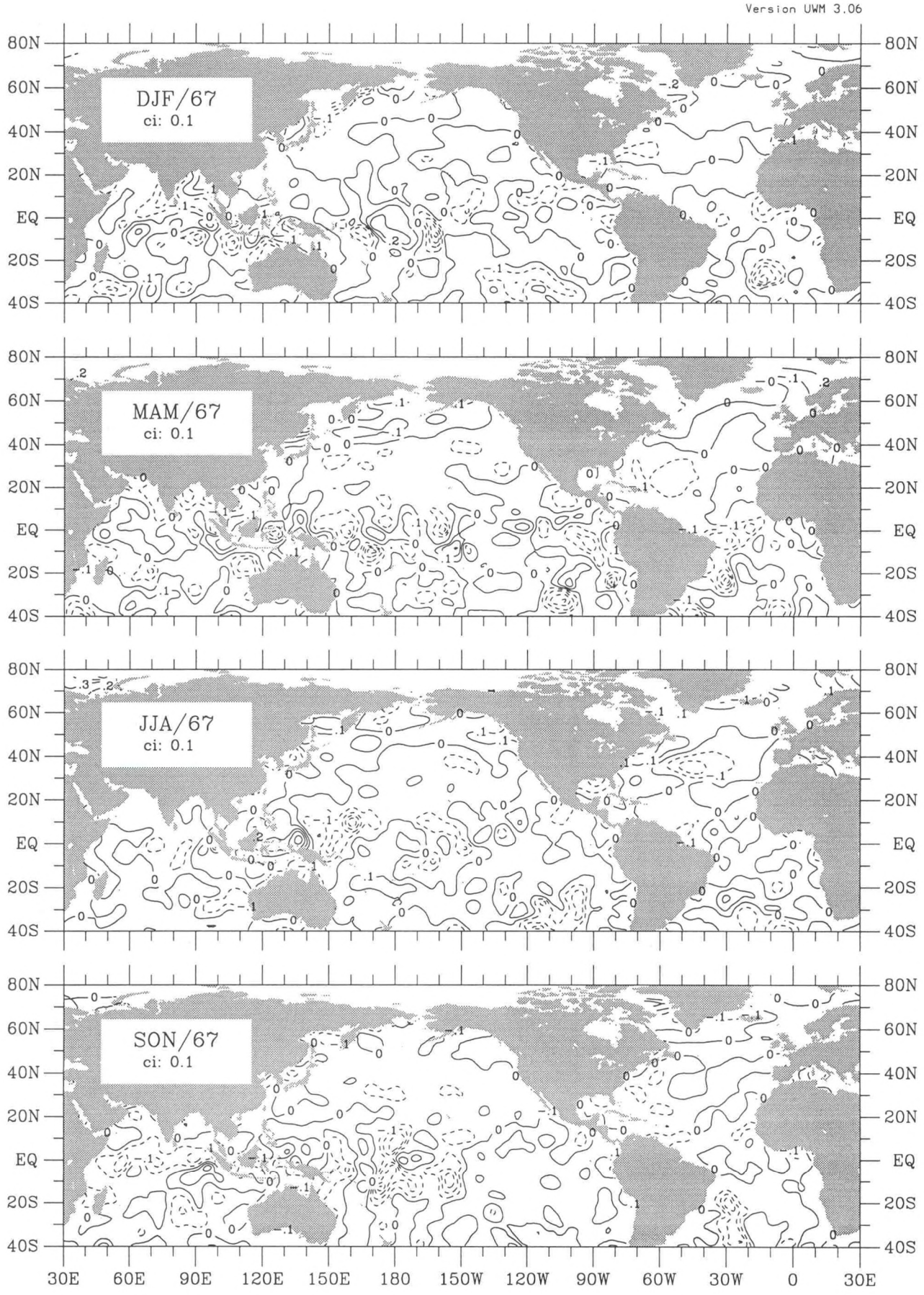

Figure Z/L-28. Stability parameter seasonal anomaly for 1967.

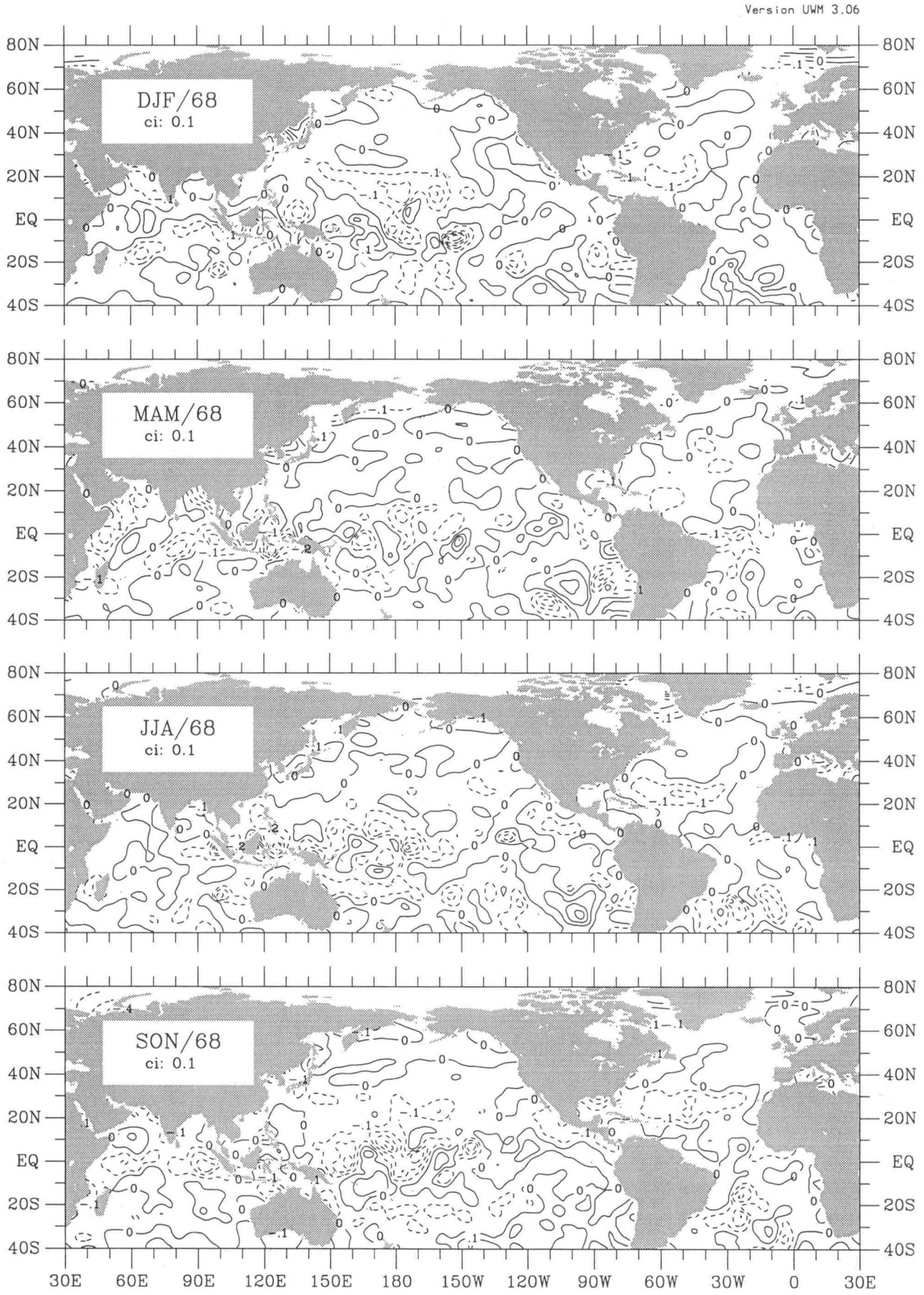

Figure Z/L-29. Stability parameter seasonal anomaly for 1968.

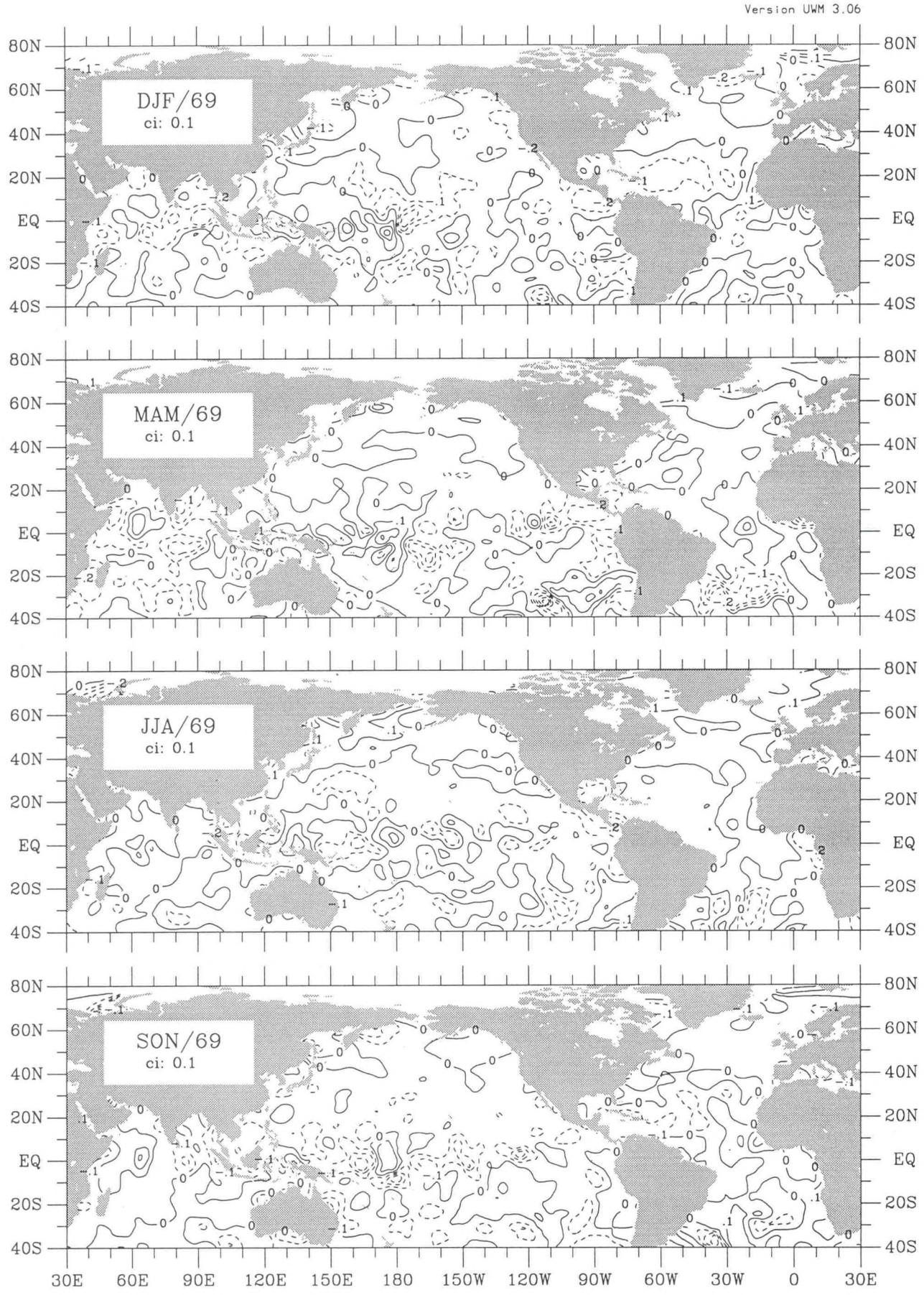

Figure Z/L-30. Stability parameter seasonal anomaly for 1969.

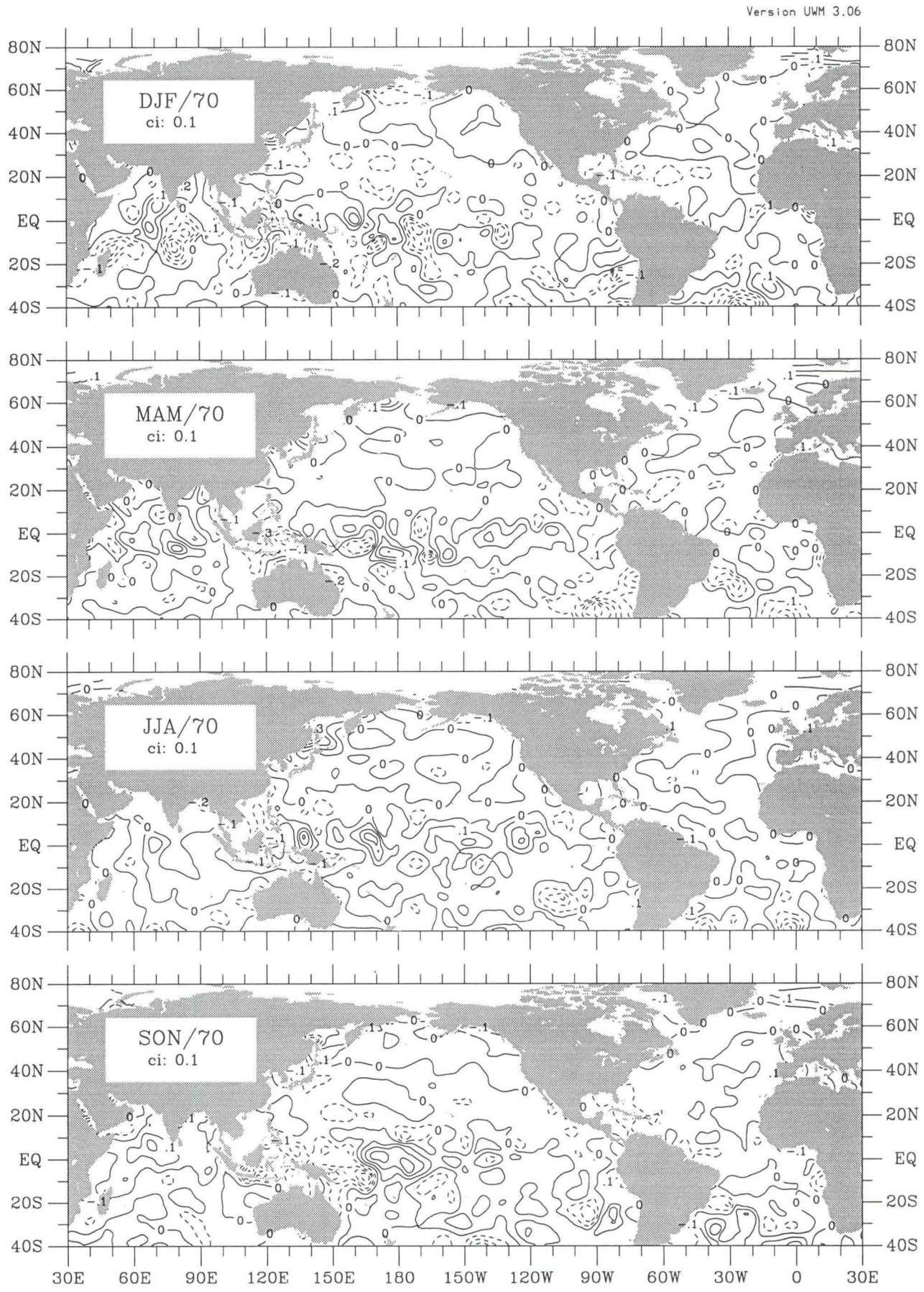

Figure Z/L-31. Stability parameter seasonal anomaly for 1970.

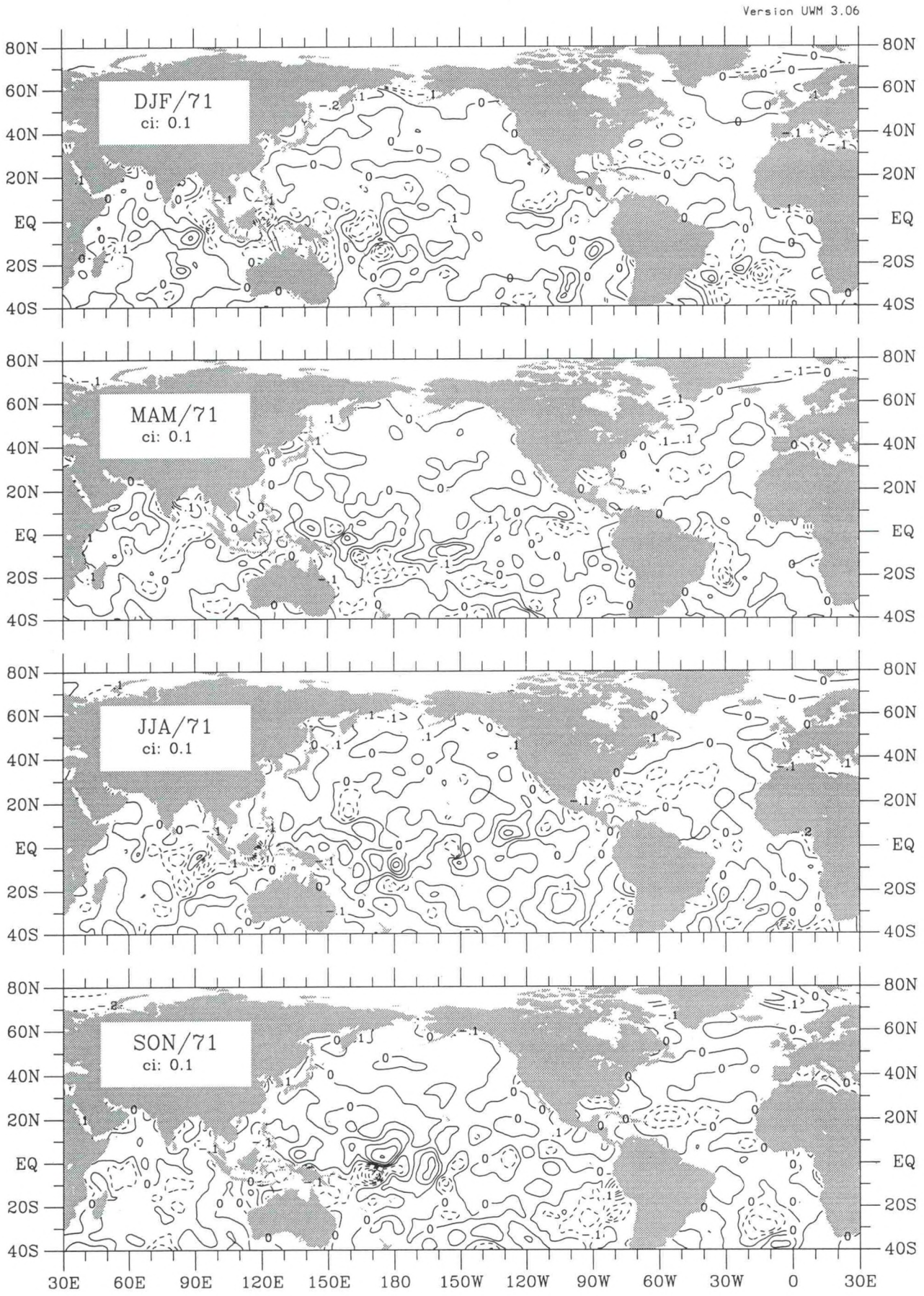

Figure Z/L-32. Stability parameter seasonal anomaly for 1971.

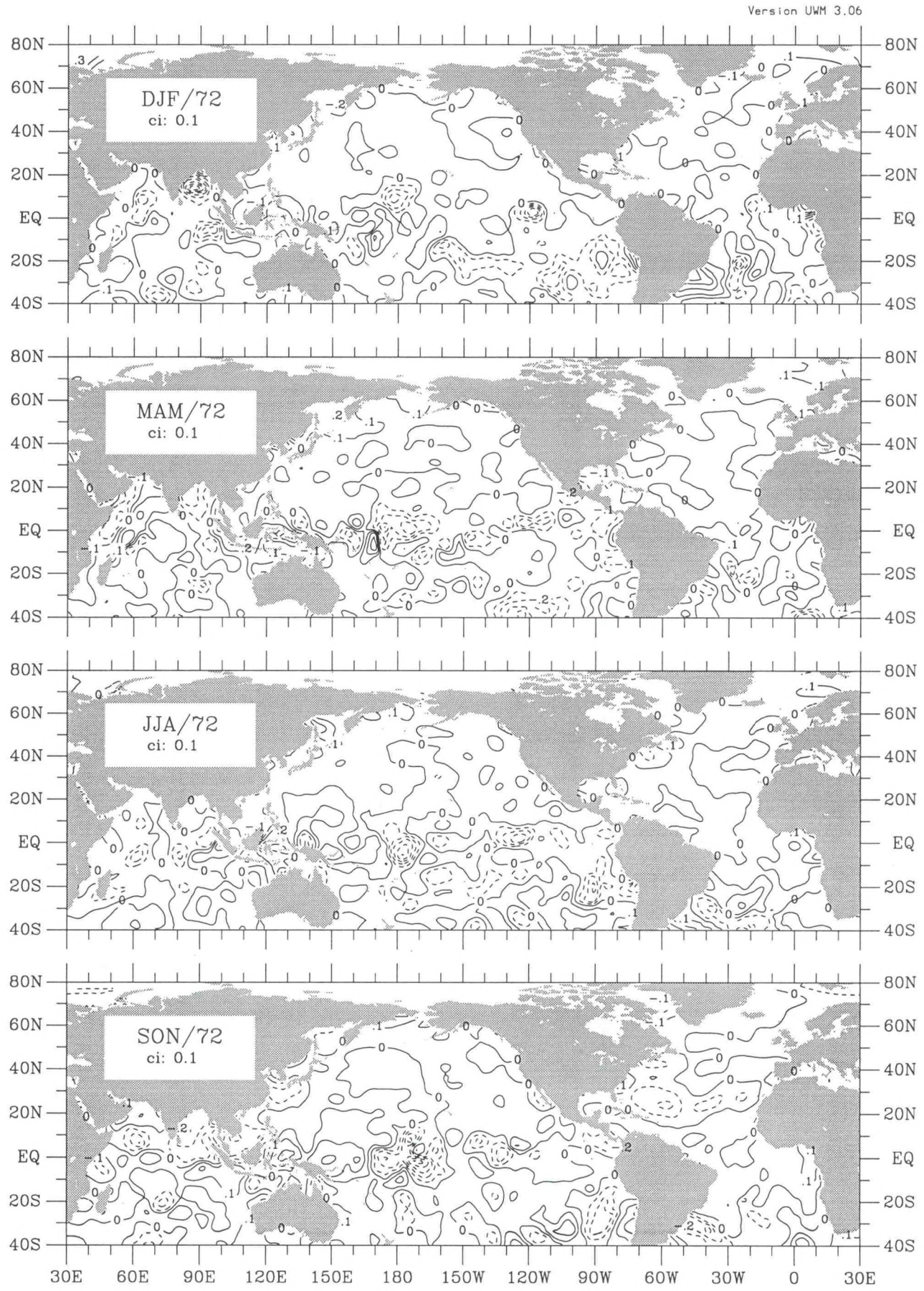

Figure Z/L-33. Stability parameter seasonal anomaly for 1972.

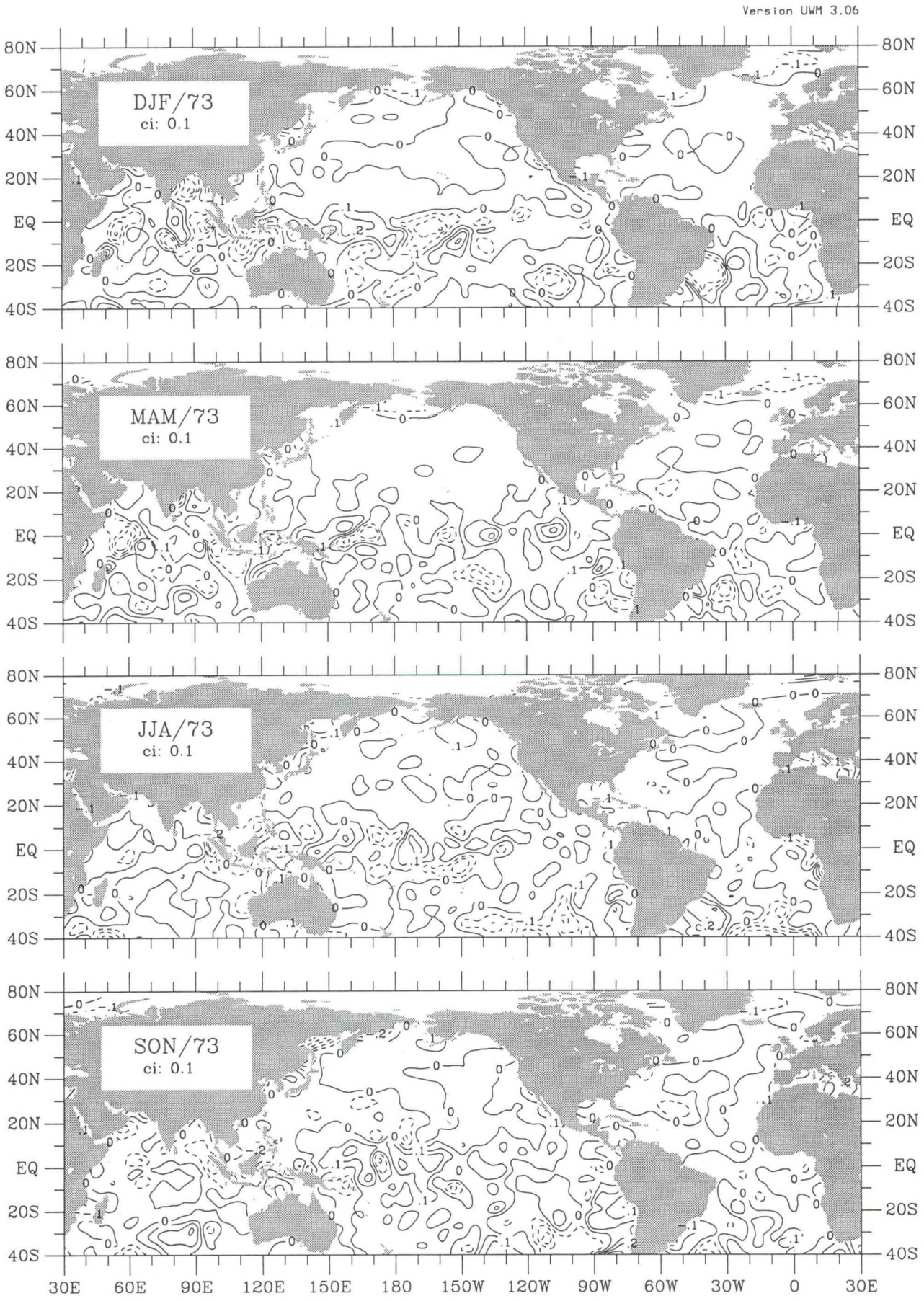

Figure Z/L-34. Stability parameter seasonal anomaly for 1973.

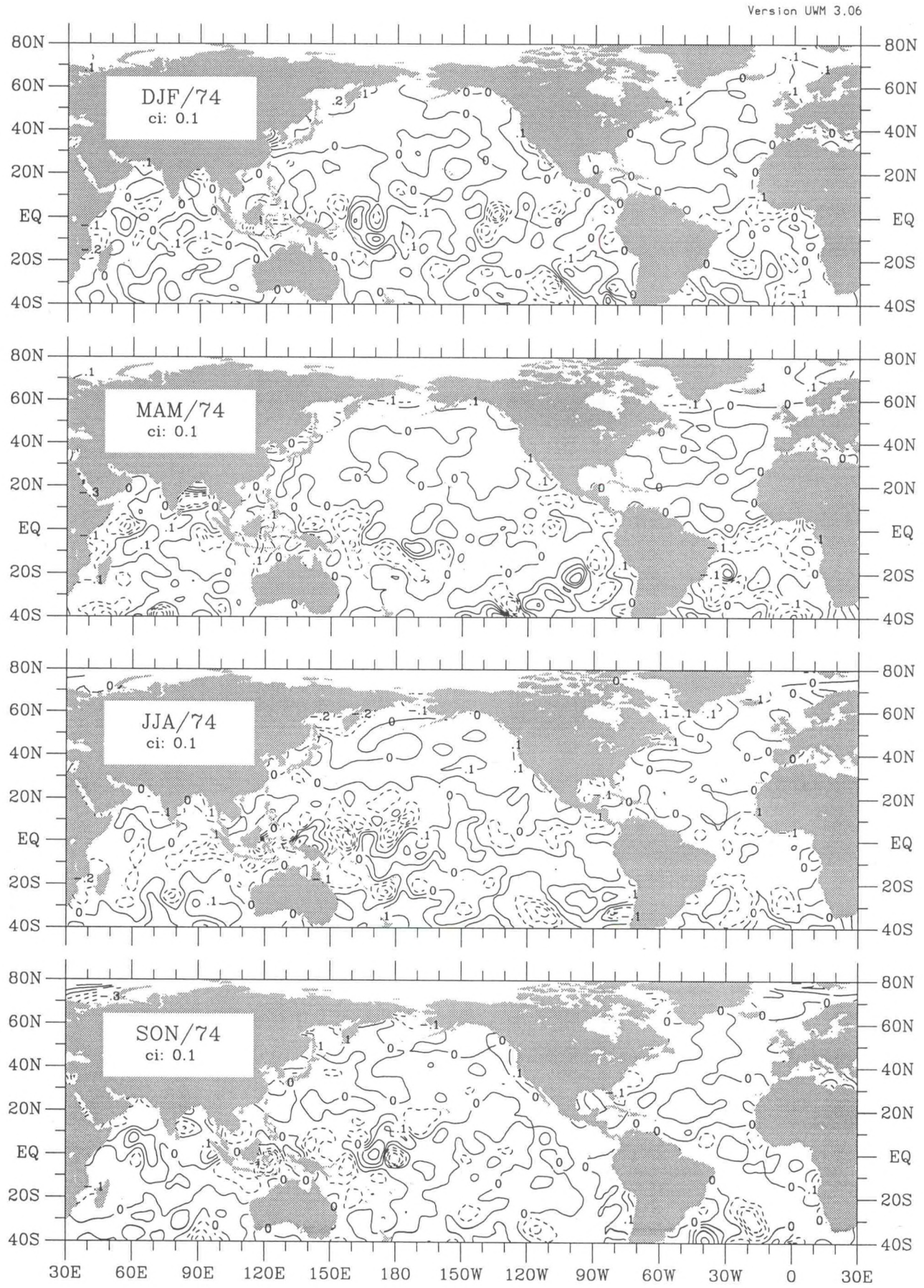

Figure Z/L-35. Stability parameter seasonal anomaly for 1974.

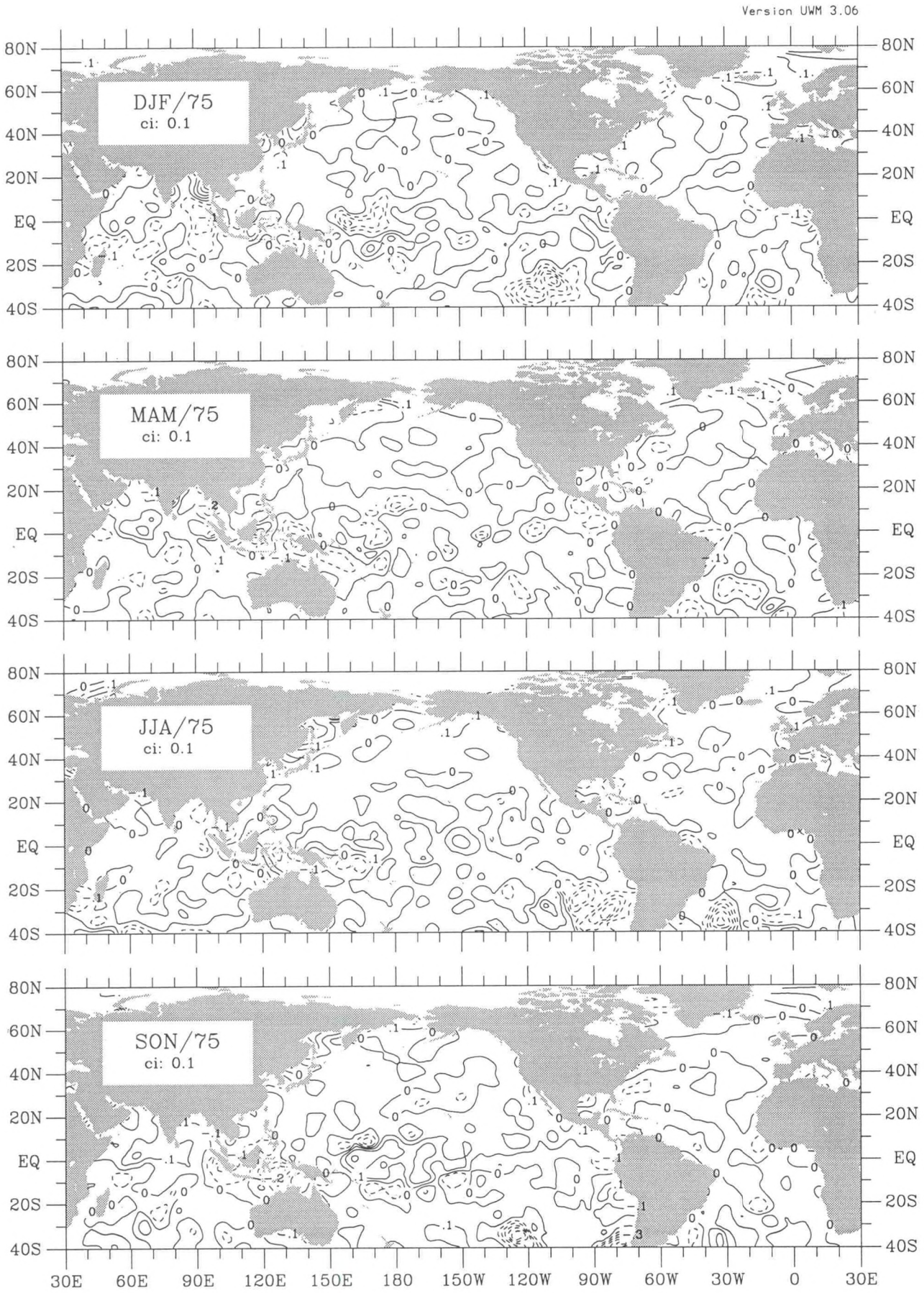

Figure Z/L-36. Stability parameter seasonal anomaly for 1975.

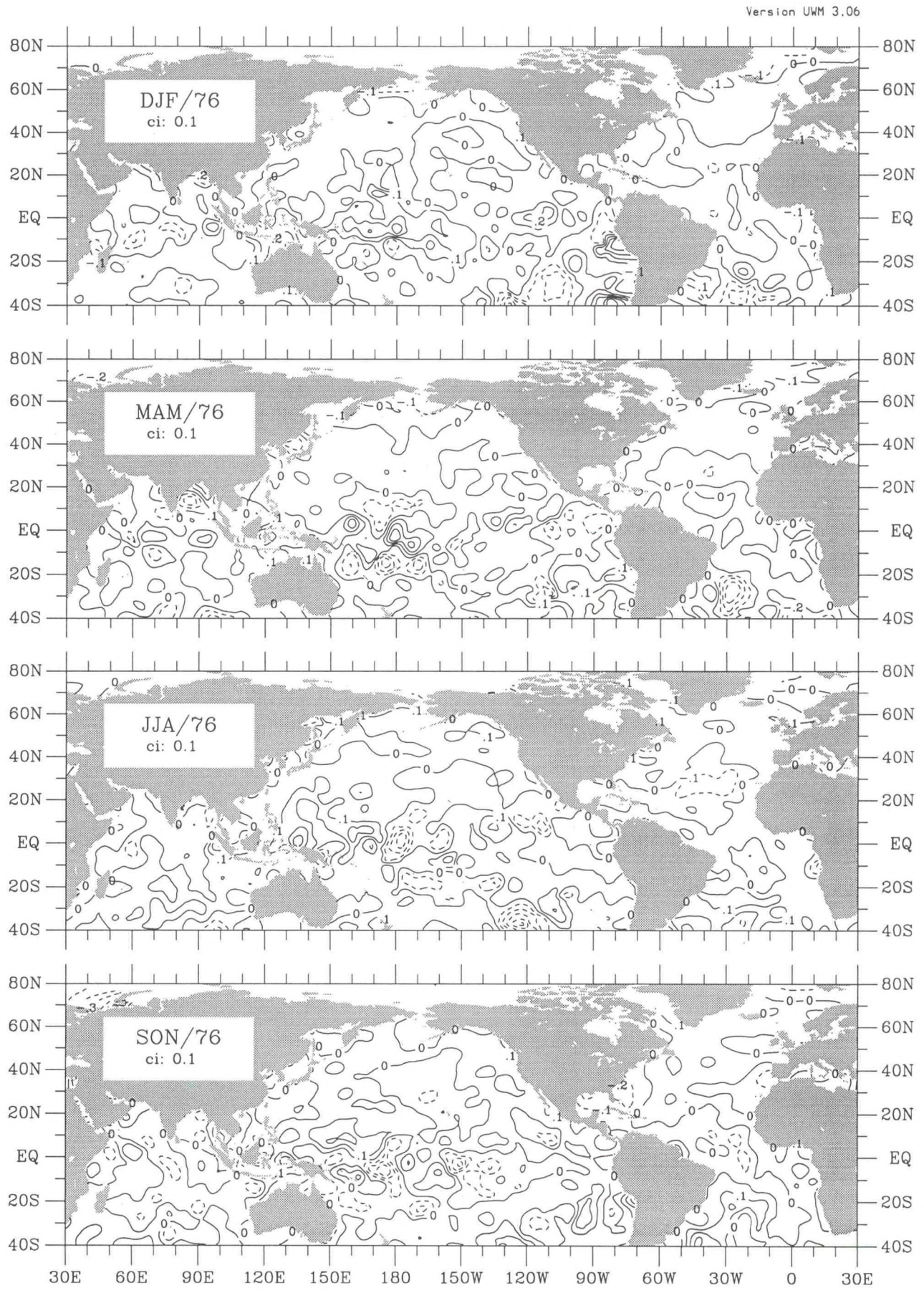

Figure Z/L-37. Stability parameter seasonal anomaly for 1976.

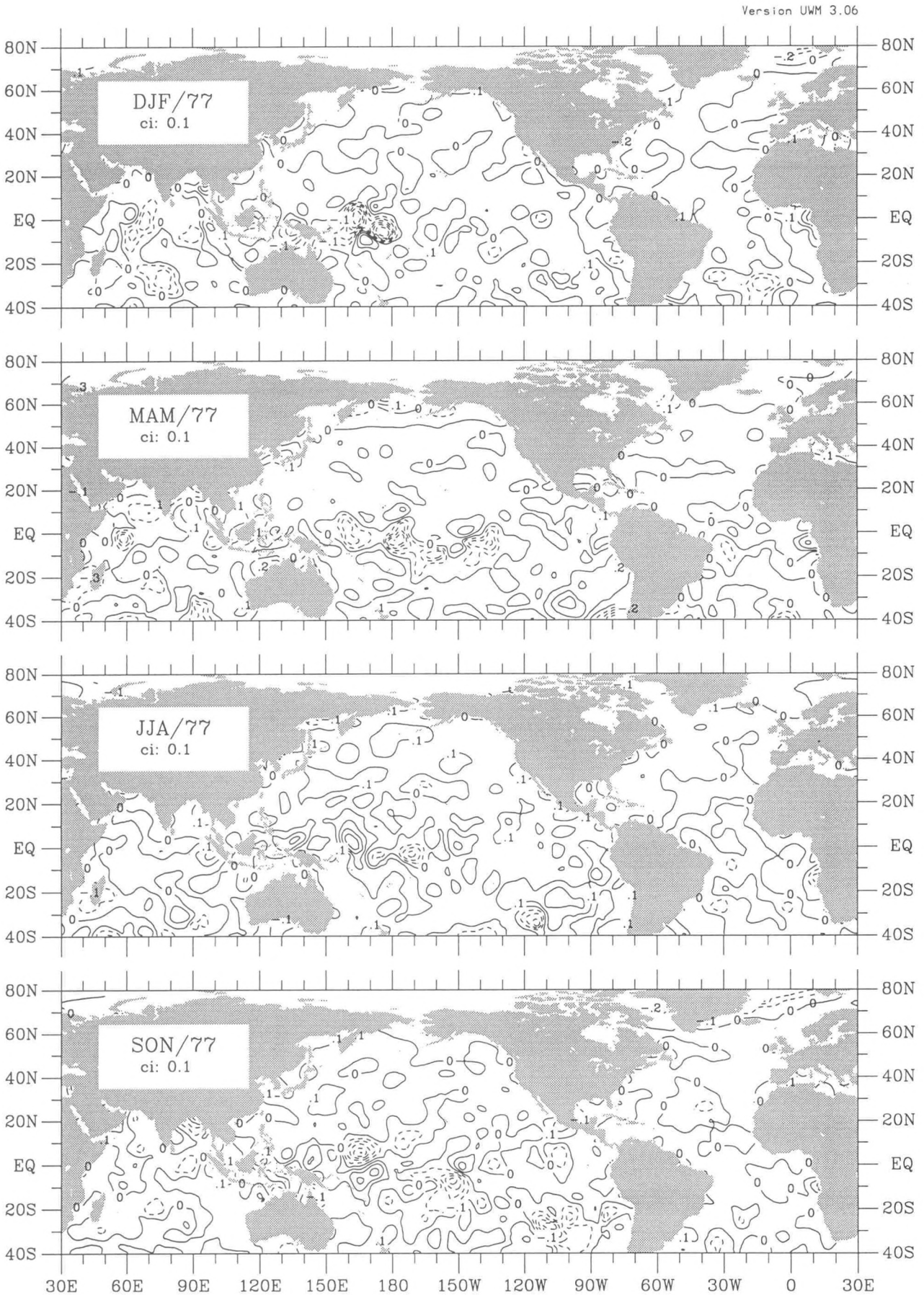

Figure Z/L-38. Stability parameter seasonal anomaly for 1977.

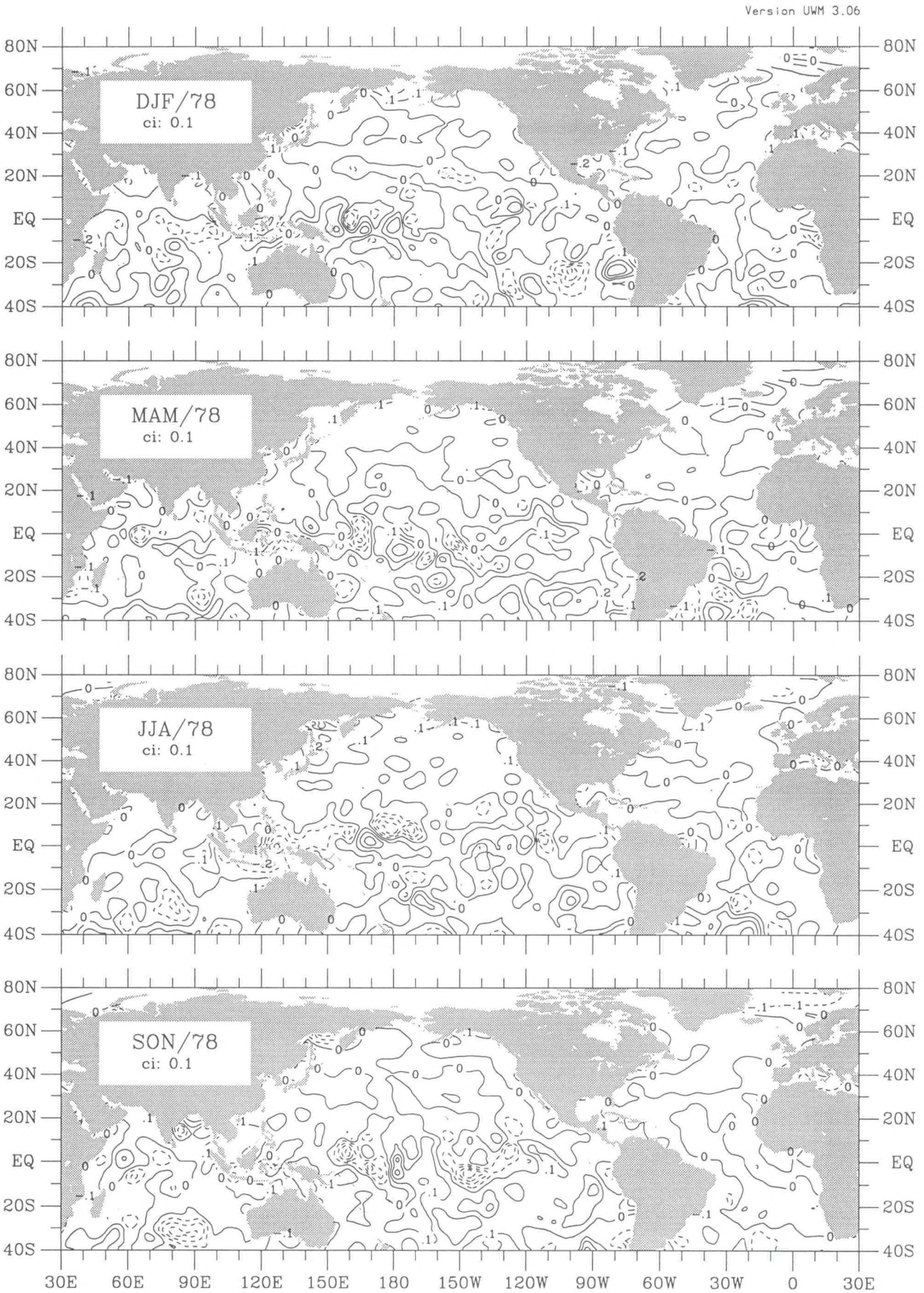

Figure Z/L-39. Stability parameter seasonal anomaly for 1978.

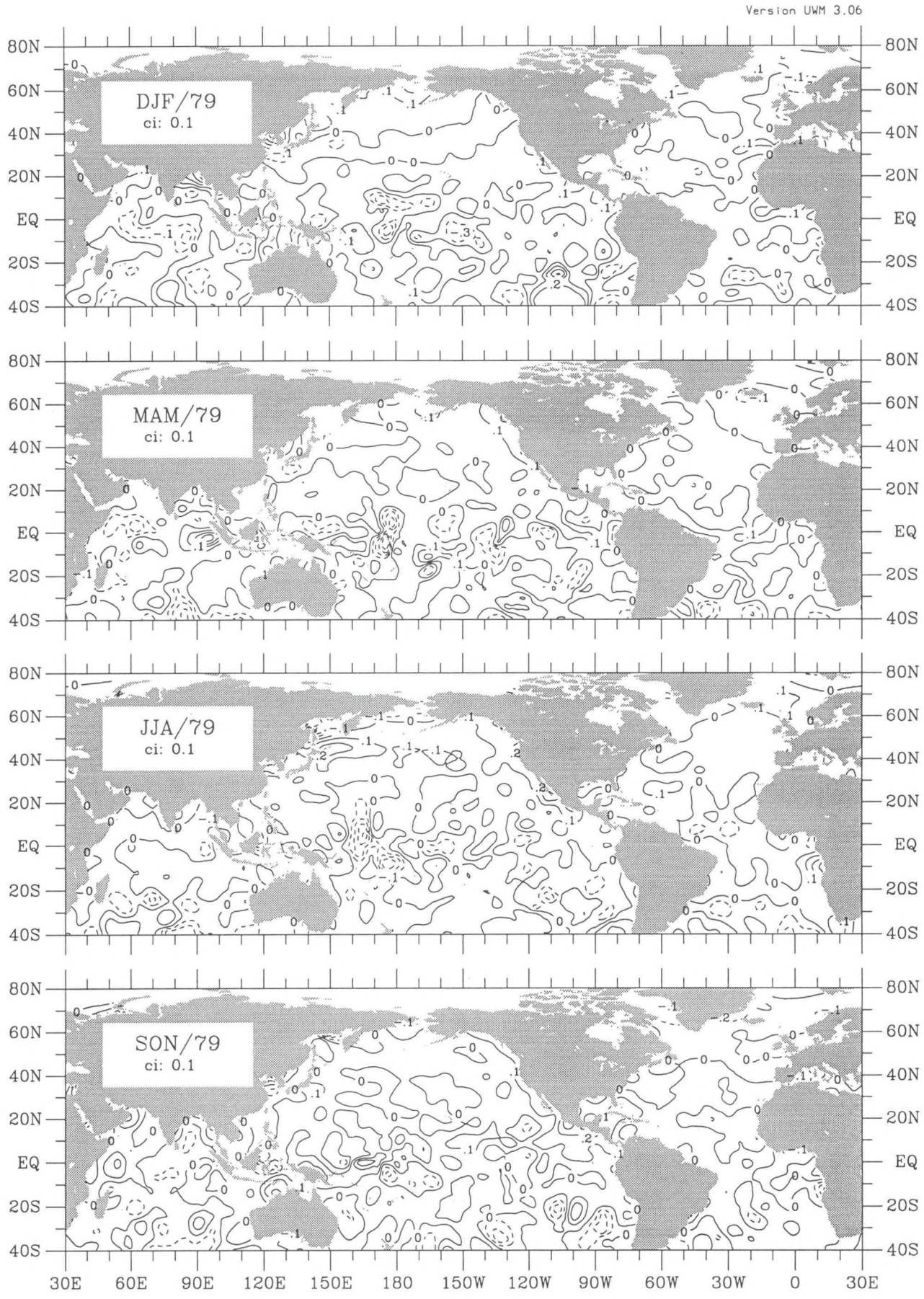

Figure Z/L-40. Stability parameter seasonal anomaly for 1979.

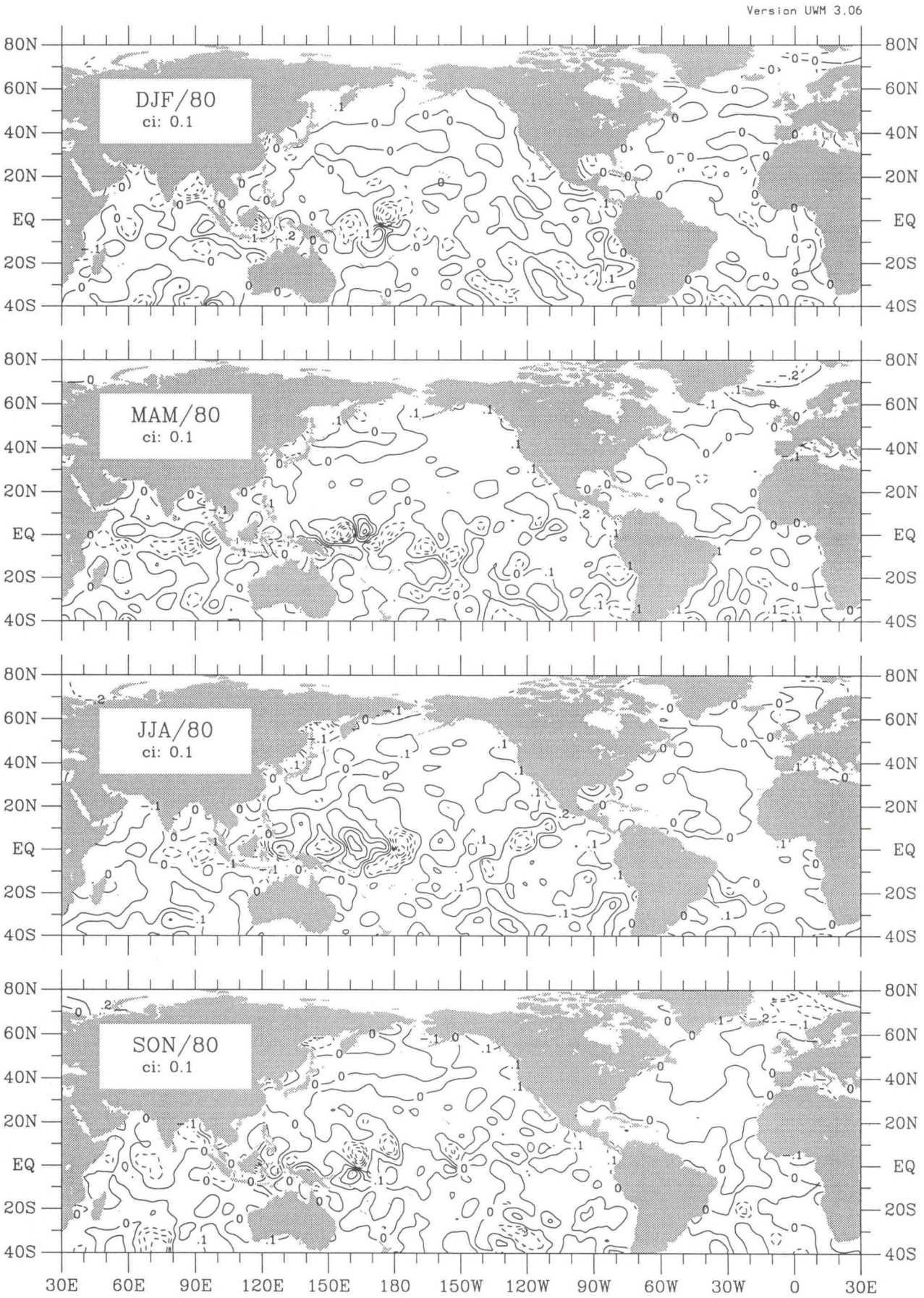

Figure Z/L–41. Stability parameter seasonal anomaly for 1980.

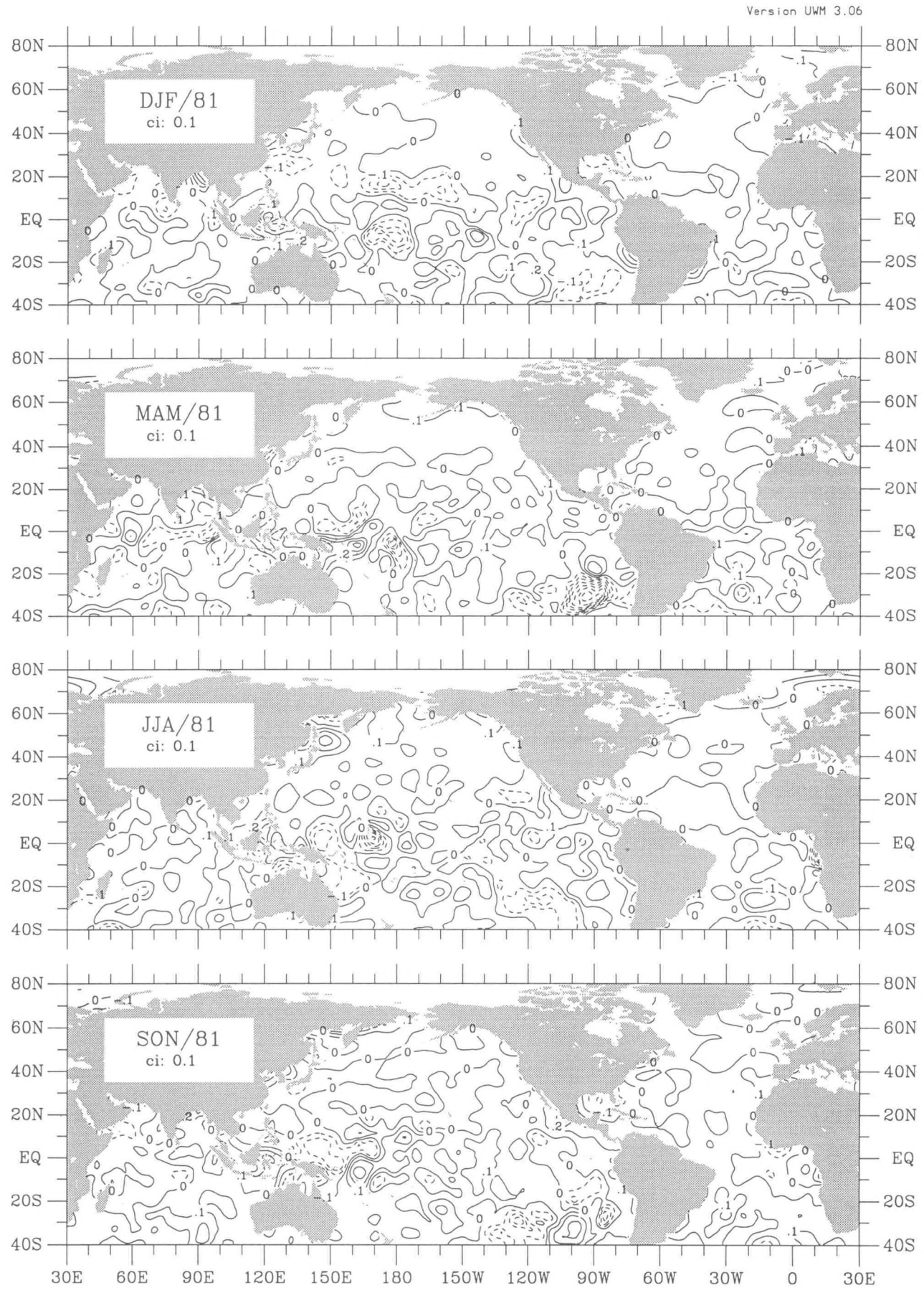

Figure Z/L-42. Stability parameter seasonal anomaly for 1981.

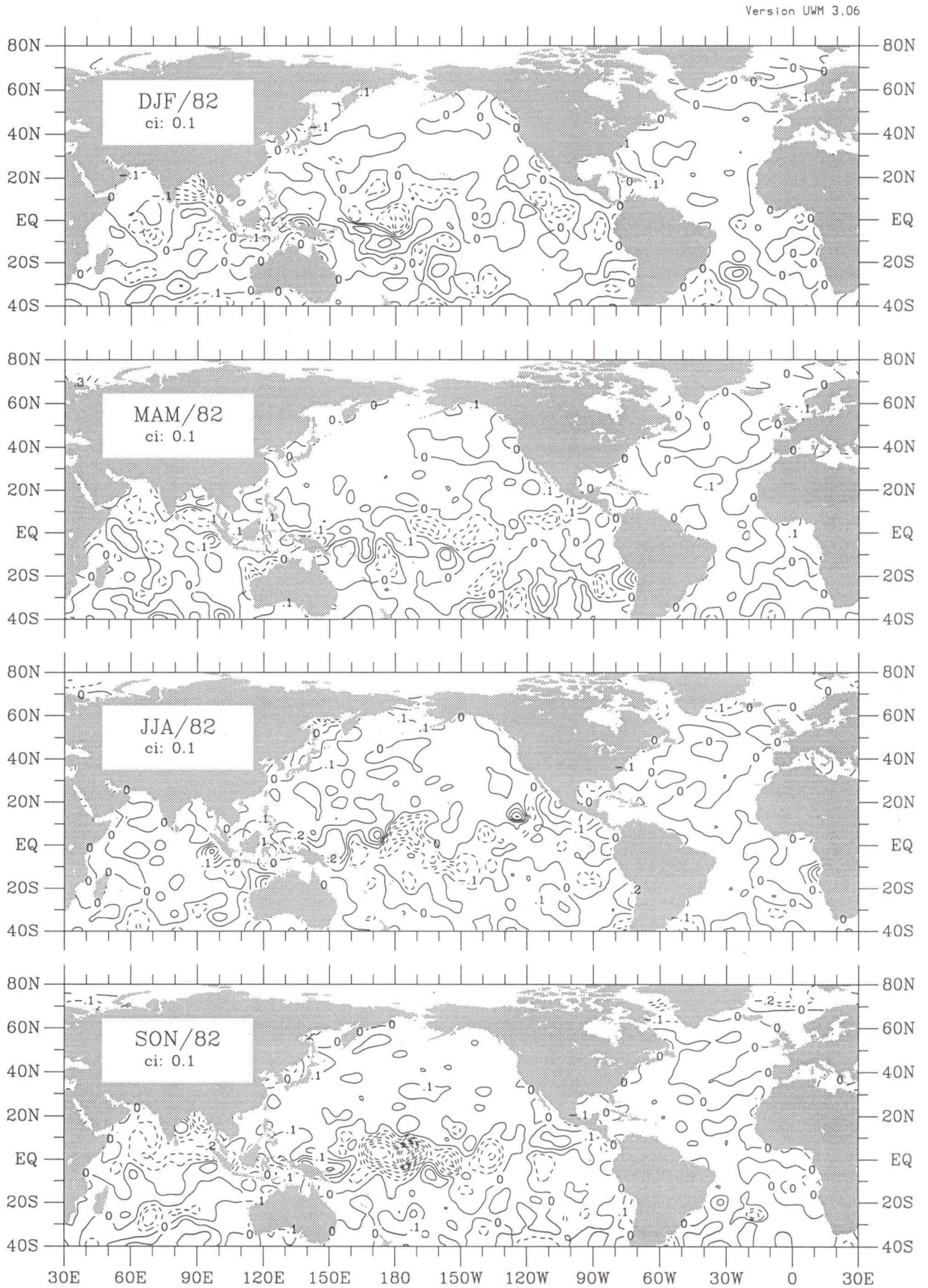

Figure Z/L-43. Stability parameter seasonal anomaly for 1982.

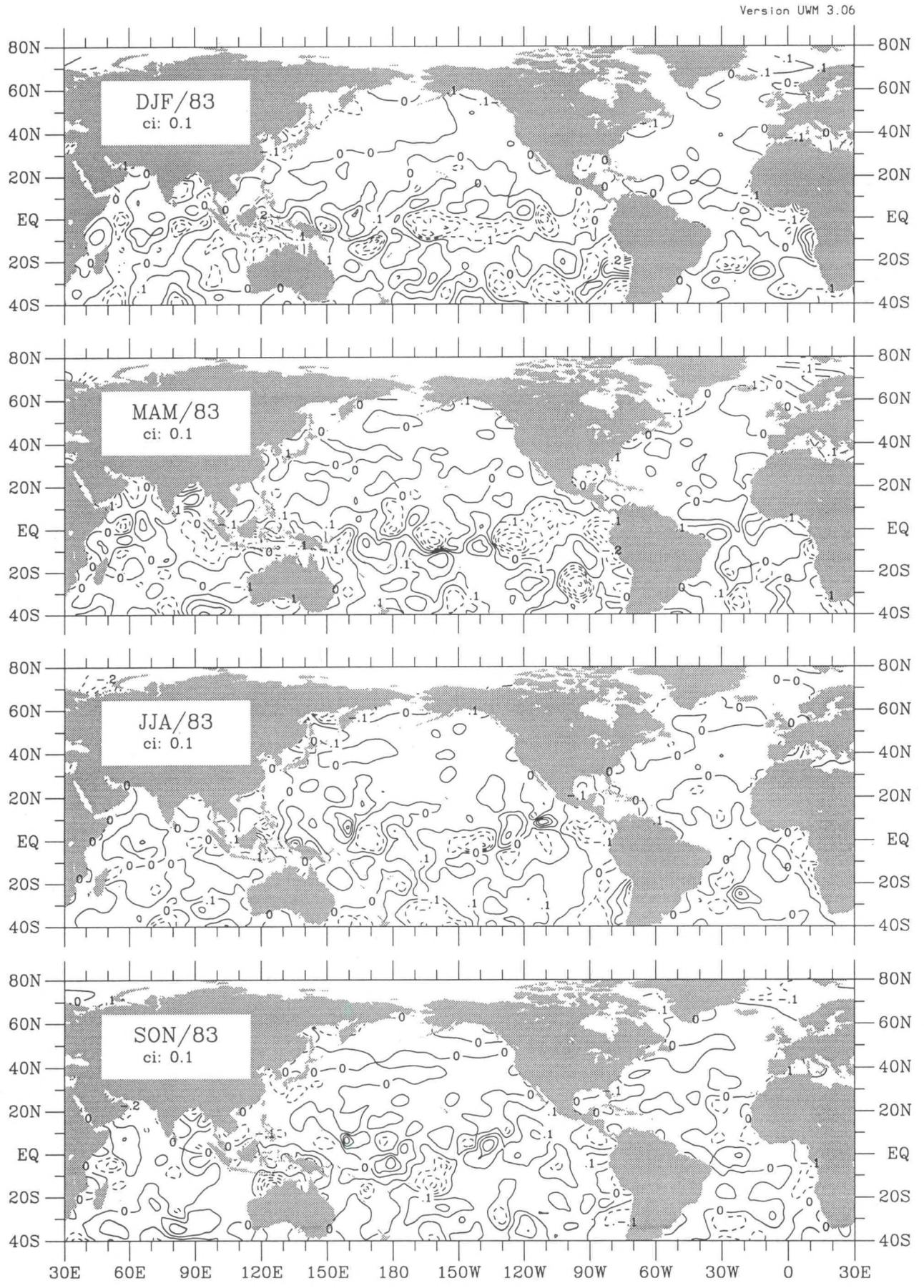

Figure Z/L-44. Stability parameter seasonal anomaly for 1983.

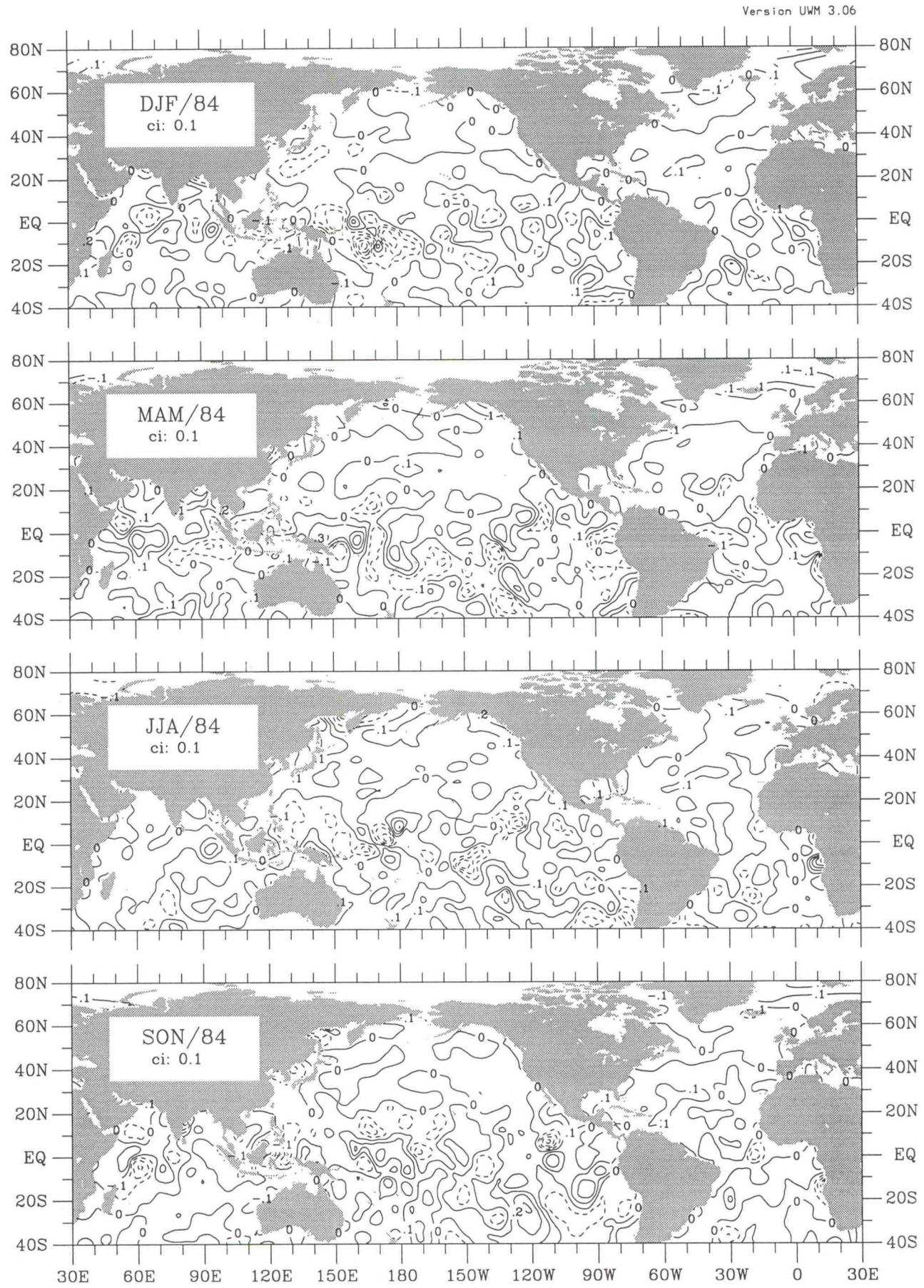

Figure Z/L-45. Stability parameter seasonal anomaly for 1984.

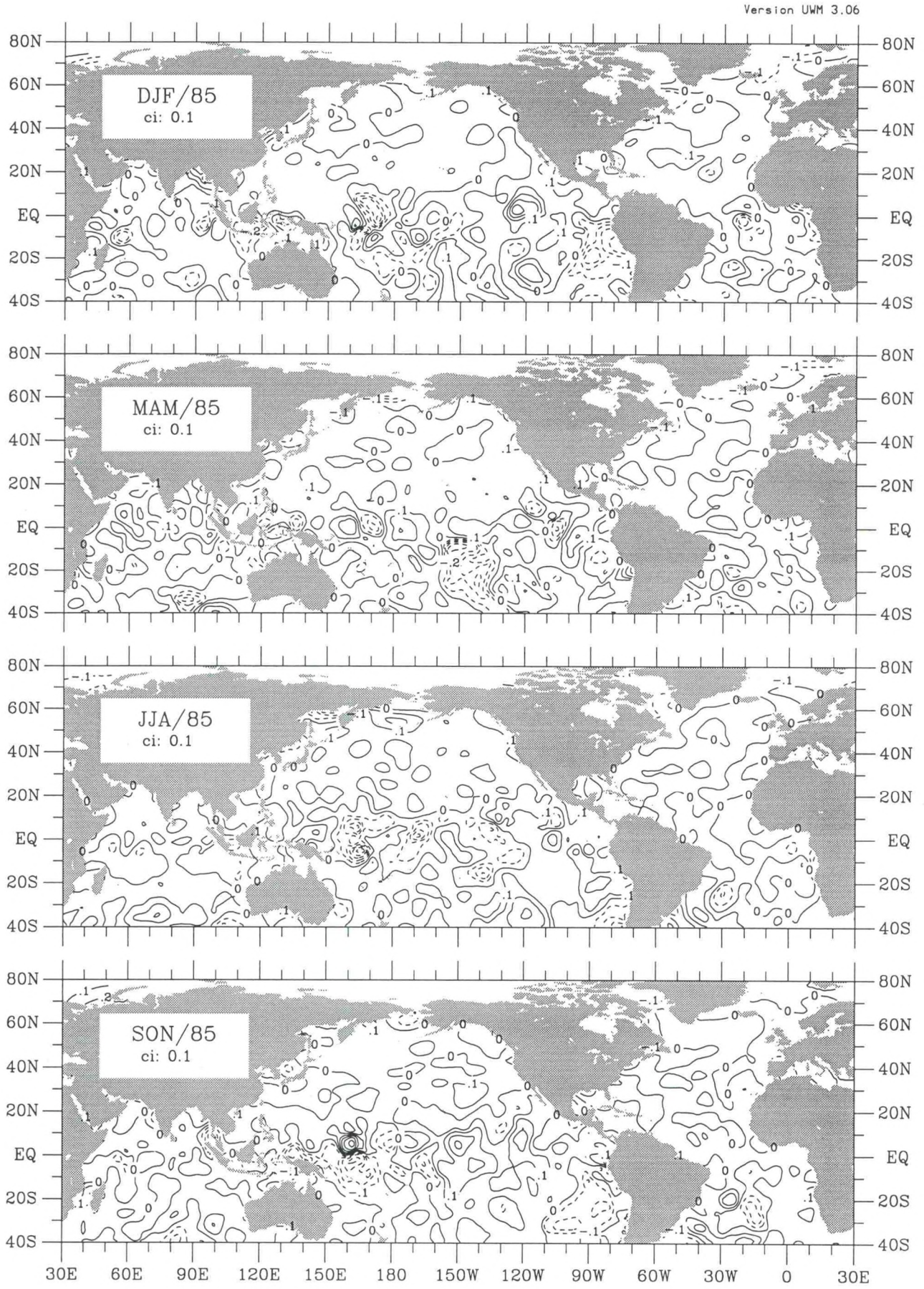

Figure Z/L-46. Stability parameter seasonal anomaly for 1985.

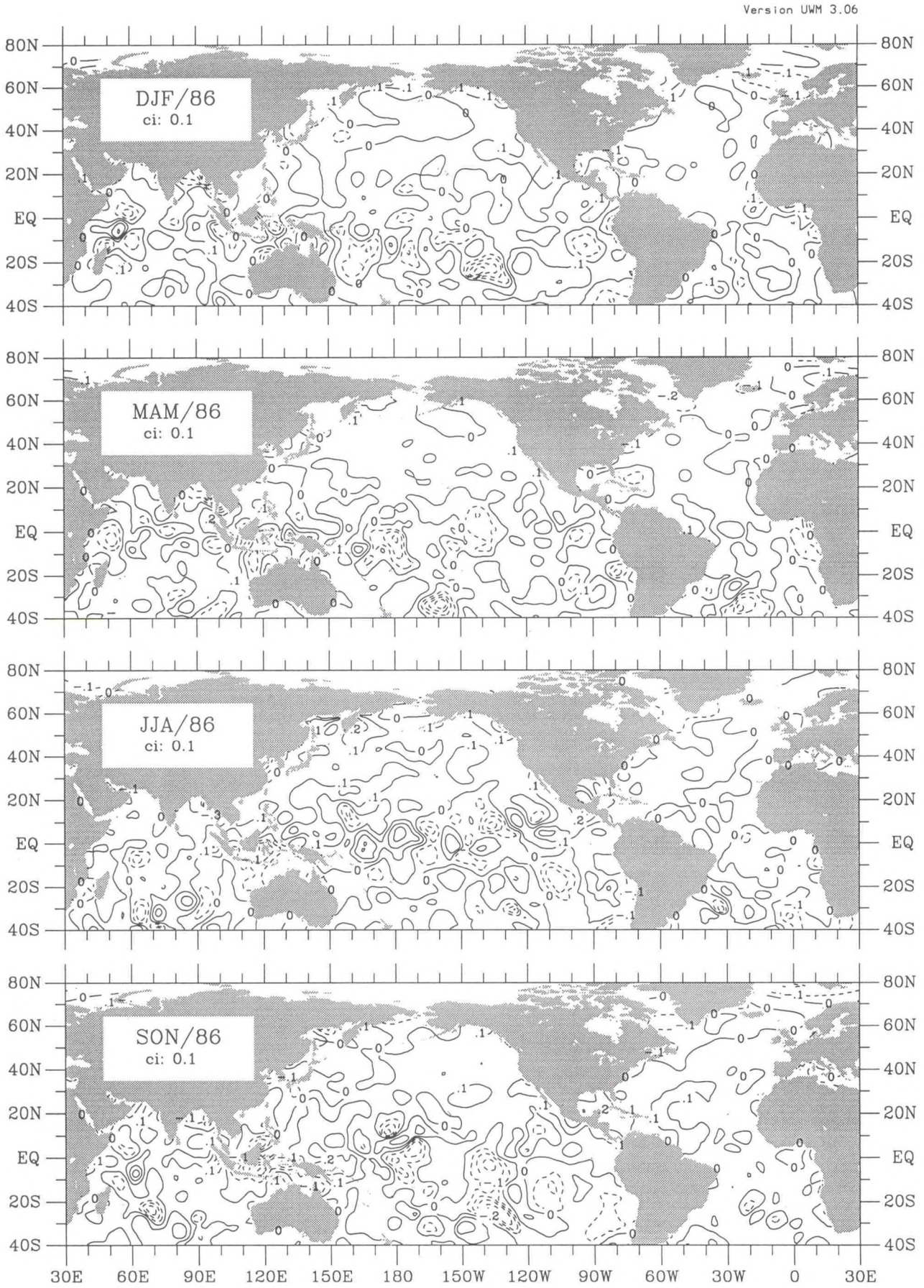

Figure Z/L-47. Stability parameter seasonal anomaly for 1986.

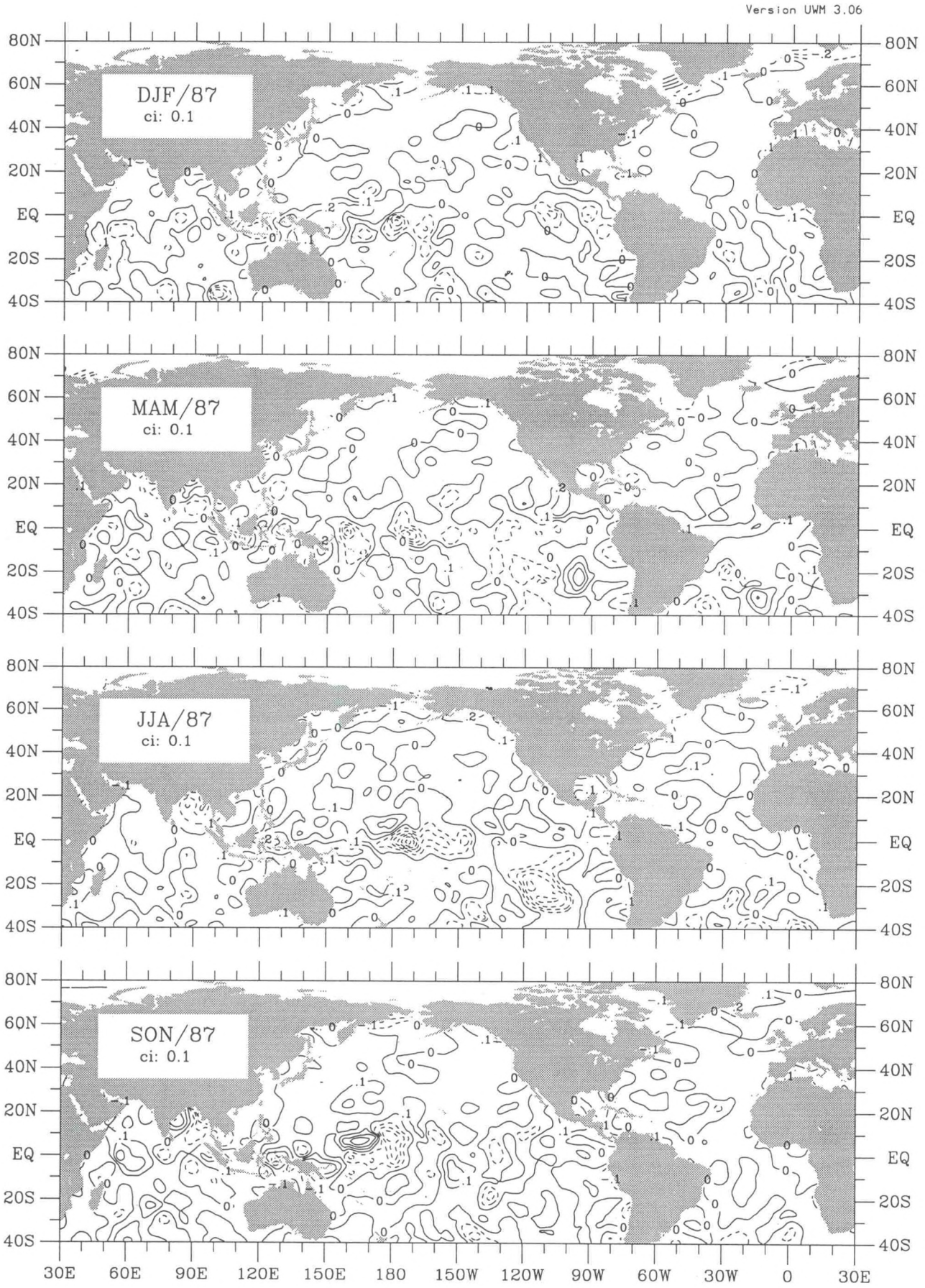

Figure Z/L-48. Stability parameter seasonal anomaly for 1987.

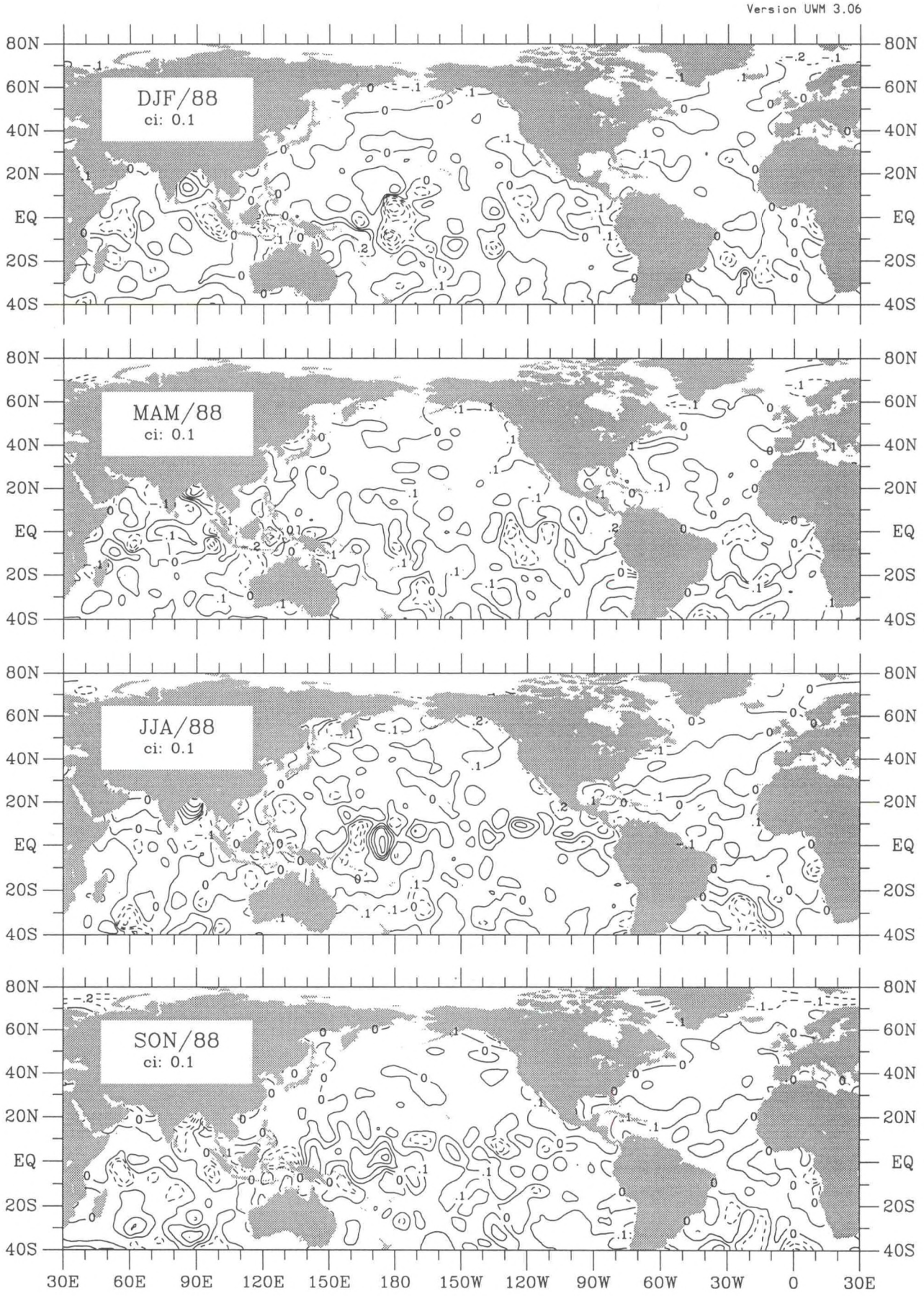

Figure Z/L-49. Stability parameter seasonal anomaly for 1988.

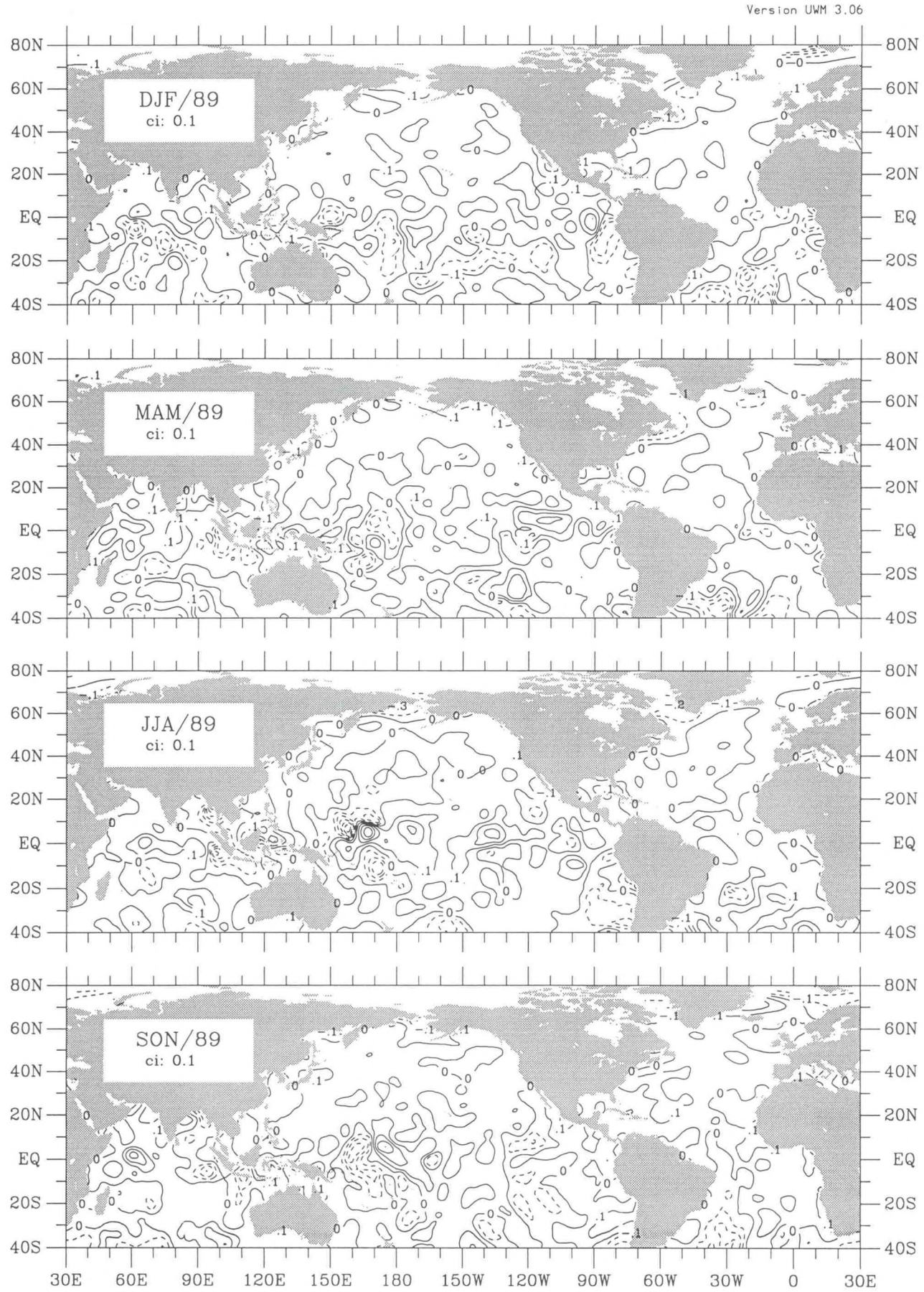

Figure Z/L-50. Stability parameter seasonal anomaly for 1989.

3 8398 1004 3684 3
N.O.A.A. CENTRAL LIBRARY

NOAA SCIENTIFIC AND TECHNICAL PUBLICATIONS

The National Oceanic and Atmospheric Administration was established as part of the Department of Commerce on October 3, 1970. The mission responsibilities of NOAA are to assess the socioeconomic impact of natural and technological changes in the environment and to monitor and predict the state of the solid Earth, the oceans and their living resources, the atmosphere, and the space environment of the Earth.

The major components of NOAA regularly produce various types of scientific and technical information in the following kinds of publications:

PROFESSIONAL PAPERS - Important definitive research results, major techniques, and special investigations.

CONTRACT AND GRANT REPORTS - Reports prepared by contractors or grantees under NOAA sponsorship.

ATLAS - Presentation of analyzed data generally in the form of maps showing distribution of rainfall, chemical and physical conditions of oceans and atmosphere, distribution of fishes and marine mammals, ionospheric conditions, etc.

TECHNICAL SERVICE PUBLICATIONS - Reports containing data, observations, instructions, etc. A partial listing includes data serials; prediction and outlook periodicals; technical manuals, training papers, planning reports, and information serials; and miscellaneous technical publications.

TECHNICAL REPORTS - Journal quality with extensive details, mathematical developments, or data listings.

TECHNICAL MEMORANDUMS - Reports of preliminary, partial, or negative research or technology results, interim instructions, and the like.

U.S. DEPARTMENT OF COMMERCE
National Oceanic and Atmospheric Administration
National Environmental Satellite, Data, and Information Service
Washington, D.C. 20233